35

MONOGRAPH ON GIS VERY FAST TRANSIENTS

Working Group 33/13.09

cigré

Monograph on GIS Very Fast Transients

Presented by Working Group 33/13.09
consisting of members from Study Committees

12/13/15/21/23/33/36

TABLE OF CONTENTS

* short description of the topics of each paper

4. GROUP 23 / PREFERENTIAL SUBJECT 2 : GROUNDING AND EARTHING IN SUBSTATIONS. EFFECTIVE AVOIDANCE OF IMPERMISSIBLE INDUCTION VOLTAGE OF LOW AN HIGH FREQUENCY ON PRIMARY COMPONENTS AND AUXILIARY SYSTEMS. SYSTEM NEUTRAL GROUNDING TECHNIQUES.

Paper 23-00 SPECIAL REPORT (partly).

Paper 23-06 SUBSTATION EARTHING WITH SPECIAL REGARD TO TRANSIENT GROUND POTENTIAL RISE. DESIGN AIMS TO REDUCE ASSOTIATED EFFECTS. (TEV, EMC, shielding, secondary equipment, test procedure)

Paper 23-10 ATTENUATION OF FAST TRANSIENTS IN GIS EARTHING SYSTEMS. (TEV, EMC, shielding)

Paper 23-11 DEVELOPMENTS IN IMPROVED RELIABILITY FOR GAS INSULATED SUBSTATIONS. (Pref. Subj. 3, but dealing with VFTO, TEV, disconnector, testing)

GROUP 23 : MEETING DISCUSSIONS (11 contributions).

5. GROUP 36 / PREFERENTIAL SUBJECT 3 : ELECTROMAGNETIC COMPATIBILITY PROBLEMS AND PROTECTION METHODS ESPECIALLY WITH REGARD TO LOCAL INTRUMENTATION NETWORKS (INCLUDING OPTICAL FIBER TRANSMISSION) IN POWER PLANTS AND SUBSTATIONS.

Paper 36-00 SPECIAL REPORT (partly).

Paper 36-05 PROTECTION OF MICROPROCESSOR BASED DISTRIBUTED CONTROL UNITS IN GAS INSULATED SUBSTATIONS AGAINST ELECTROMAGNETIC INTERFERENCES. (TEV, EMC radiated and induced, computer, shielding)

Paper 36-07 PROTECTION OF DATA COMMUNICATION SYSTEMS AGAINST ELECTROMAGNETIC INTERFERENCE IN HIGH VOLTAGE STATIONS. (EMC, optical fiber, immunity tests, general protection methods)

Paper 36-10 EVALUATION OF THE ELECTROMAGNETIC INTERFERENCES ON THE POWER PLANT AND SUBSTATION AUXILIARY EQUIPMENT. (EMC, general protection methods)

Paper 36-01 EXPERIENCES IN THE INFLUENCE OF PRIMARY PLANT OPERATION ON SECONDARY PLANT AND PROCEDURES TO MINIMISE ITS EFFECT. (EMC, general protection methods)

GROUP 36 : MEETING DISCUSSIONS (11 contributions).

6. CLOSING REMARKS

FOREWORD

During the 1988 CIGRE session half a day of the discussion meeting of group 33 (Overvoltages and Insulation Coordination) dealt with the multiple aspects of the Very Fast Transient Overvoltages (VFTO) due to disconnector switching or line to enclosure fault in Gas Insulated Substation. These VFTO stress the GIS itself but also all the equipments connected to it, over a frequency range reaching unexpectedly high values. Therefore, this half day discussion meeting was a joint discussion sponsored also by groups 12 (Transformers), 13 (Switching Equipment), 15 (Insulating Materials), 21 (HV Insulated Cables), 23 (Substations) and 36 (Interference). During this joint half day meeting the various aspects involved were discussed such as:

- generation mechanisms, characteristics and measurement of VFTO,

- effects of VFTO on the insulation of GIS and other power components,

- effects of VFTO on low voltage components: relaying and control systems (Electro-Magnetic Compatibility).

In addition to this joint discussion, as the matter is very broad, a lot of experience and knowledge, dealing with more specific aspects, were exchanged during the discussion meetings of Groups 15, 23 and 36.

Therefore it was decided to publish, under the sponsorship of these Study Committees, a monograph on the VFTO subject, gathering all the reports and discussions of 1988 CIGRE session on its various aspects.

The task of preparing this special CIGRE publication was assigned to CIGRE WG 33/13-09*, which was asked to write closing remarks on the state of present knowledge, showing the points of agreement and the remaining unclear aspects, taking into account all the contribution of the CIGRE 1988 session.

To achieve this target, it was necessary to choose an order for the presentation of the reports and of the related discussions. It was decided that the best solution was to keep the session reports and discussions within their groups. For the introduction the text of the related preferential subject of the special report of the discussion meeting of each group was chosen.
In this monograph, the order of the Groups was chosen according to the following order of subjects: generation of VFTO, effects on the HV insulation, effects on LV equipments. Therefore, the sequence of reports and discussions is : Group 33, 15, 23 and 36.

Within a Group first come the reports then the discussions with the order chosen during the Group discussion of the 1988 CIGRE session. For the reports within a Group, the order was choosen according to the following: large scope reports first then reports on more specific aspects.

*Members: R. ALVINSSON (SE), A. ARDITO (IT), W. BOECK (DE), K. FESER (DE), N. FUJIMOTO (CA), J. GRANDL (CH), D. KOENIG (DE), D. LIGHTLE (GB), G. LUONI (IT), G. LUXA (DE), W. MULLER (DE), S. ROWE (FR), A. SABOT (FR, convener), S. YANABU (JP).

1. INTRODUCTION

Very Fast Transient Overvoltages (VFTO) in Gas Insulated Substation (GIS) is the general class of transient overvoltage phenomena generated primarly by the operation of disconnectors. These transients are characterised by their short duration and very high frquency nature. Their rise times are often in the 10 nanosecond range, with dominant frequency components up to 40 MHz. The peak magnitude is always lower than equipment rated Lightning Insulation Withstand Level (LIWL). Nevertheless, many problems in the past have been attributed, rightly or not, to VFTO, because at the time this new kind of stress was poorly understood. However, VFTO have been directly implicated in some GIS failures. VFTO are also responsible for the momentary high voltage transient overvoltages which appear on the enclosure and earthed components of the GIS (Transient Enclosure Voltage: TEV).

VFTO present a new class of stress on GIS and other power system components directly connected to the GIS. With increased understanding, the phenomenon can be put into perspective. For instance, from an insulation coordination point of view, disconnector induced VFTO are apparently not dangerous for GIS, except in presence of certain defects occurring in the GIS, and for inadequately designed componants.

TEV phenomena, which are VFTO affecting the earthing system, present two additional aspects: personnel safety and the Electro-Magnetic Compatibility (EMC) of auxilliary and control circuits. Understanding the phenomena enables the characteristic of GIS design and possible mitigation measures to be assessed.

VFTO are also incident on externally connected power system components such as transformers , bushings, etc, but there is not even the smallest evidence suggesting that such equipment is harmed by VFTO.

VFTO therefore represent a new class of stress which should not be ignored but understood so that problems linked to design and operating pratice changes may be avoided.

The following papers and discussion describe all aspects of VFTO phenomena including generation mechanism, measurement and calculation. The effect of VFTO on GIS insulation, on other components and the resultant interference with control circuits are discussed.

VFTO are primarily generated by the operation of disconnectors. Each spark which occurs across the contacts of the disconnector generates a short rise time travelling wave which leads to the development of VFTO. VFTO characteristics are determined by operating conditions, disconnector design and GIS configuration [papers 33-13, 33-15, 33-09]. Because of the high frequency nature of the VFTO special techniques for computer calculations are necessary. As discussed in papers 33-13, 33-09, 33-12, distributed component models are an absolute necessity. Special measurements techniques are also necessary to measure VFTO. Despite the wide bandwidth (100 MHz at least) measurements are relatively easy [papers 33-13, 33-12].

The general calculation approach for VFTO can be extended to include TEV. Although TEV modelling is somewhat more difficult, order of magnitude calculations can be made to assess a given situation on a quantitative basis and to evaluate mitigation schemes [papers 33-13, 33-06, 23-11].

TEV have raised questions regarding personnel safety although there were no reported accidents relating directly to TEV.
The EMC aspects of TEV can be adequately addressed by proper high frequency shielding and several guidelines are given in papers 23-06, 23-10, 36-05, 36-07.

VFTO have brought into question the dielectric integrity of GIS. VFTO-influenced failures of disconnector switches during operation occurred in the past, but the greater understanding of VFTO and disconnector phenomena resulted in reliable designs [papers 33-13, 33-09, 15-06, 15-05].

This increased understanding has led to an industry consensus that VFTO do not present an excessive stress to GIS arranged in a "proper" condition. However some experimental evidence [papers 33-13, 15-06] suggests that the breakdown voltage for GIS with some defects might be greatly reduced. For this reason a good understanding of VFTO induced breakdown mechanisms is important in the insulation coordination of GIS and in assessing the effectivness of high voltage testing techniques [discussion Group 33 and 15].

The influence of VFTO on conventionally insulated (i.e. oil/paper) components connected to GIS is also of interest and is discussed in paper 33-13.

33-00

PART OF SPECIAL REPORT FOR GROUP 33

(Overvoltage and Insulation Co-ordination)

by

K.H. WECK*
(Special Reporter)

With the introduction of GIS a new type of overvoltages called "fast transients" was created. They contain frequencies far above those arising in conventional open-air substations and have thus caused unexpected problems for the GIS insulation or the insulation of other equipment connected to it. Owing to the effects of such fast transient voltages on many equipment several CIGRE Study Committees are dealing with them. Attention is drawn to the this year's discussions within Group 15 concerning the dielectric strength of SF_6, Group 23 concerning the substation grounding and Group 36 for interference problems. Although the activity of SC 33 in this topic is restricted in the description of the overvoltages and a relevant testing technique, overlapping discussions may not only be unavoidable but also be desirable considering the common interest. The convener of WG 13/33-09 "Fast Transients", a common Working Group of the Study Committees 13 and 33, was the expert in the preparation of the Special Report.

Preferential Subject 3
M. A. SABOT (Subject Reporter)

FAST TRANSIENTS

- -origin in service of fast transients. Problems involved in the measurement of the relevant currents and voltages.
- -expected distribution of current and of voltage characteristics influencing the dielectric behaviour of equipment. Accuracy of calculations.
- -relevant testing of equipment both in laboratory and on site.

Five reports have been submitted to this subject: 33-06, 33-09, 33-12 and 33-15. Beyond these report 33-13 is presented at the request of the Study Committees 13 and 33 by WG 13/33-09 "Fast Transients" common to both Committees. Additionally, two reports of Subject 1 deal partially with the subject: 33-01 and 33-04. Furthermore, parts of the report 23-11 are within this subject and will be considered.

Although fast transient overvoltages of the GIS enclosure apart from the measurement technique problems involved do not necessarily belong to the scope of SC 33, they shall be also addressed owing to the general interest in this subject. Attention is drawn to the reports 33-06 and 33-13 as well as on the reports 23-06, 23-10 and 23-11 submitted to Group 23. The impact of these overvoltages on secondary systems shall not be discussed here, but left to the corresponding subjects in Group 23 (Substations) and Group 36 (Interference).

A similar remark applies to the reports 15-05 and 15-06 submitted to Group 15 (Insulating Materials). They contain important information on the dielectric strength of SF_6 under these overvoltages, which is necessary for the classification of fast transient overvoltages, but the discussion to this topic belongs exclusively to this Group.

In Gas Insulated Stations, disconnector operation or faults generate voltage transients with steep fronts (voltage steps). Transmissions and reflections of these initial voltage steps superimpose to build up the so-called "Very fast Transient (VFT) Overvoltage". Contrary to that mentioned in the preferential subject, this term is proposed in report 33-13 to clearly distinguish between this type of overvoltages and the so-called fast-front overvoltages describing overvoltages with much lower front steepnesses as for example, lightning overvoltages. The VFT overvoltages occur not only inside the GIS between phase conductors and enclosure, but also outside between the enclosure and earth or between different parts of the enclosure (Transient Enclosure Voltage: TEV).

As the rise-time of the voltage step is very short compared to the travelling time within the GIS, the VFT overvoltages are not the same at the different points of the locations inside the GIS, or in the vicinity of it, with special reference to equipment location and reflection points.

Failures have already occurred during disconnector switching. These failures were attributed to the VFT overvoltages generated by disconnector switching, in spite of the fact that the estimated levels were lower than the lightning impulse withstand level of the GIS. These failures

*FGH eV, Postfach 810 169, 6800 Mannheim 81, Fed. Rep. of Germany

occurred not only at the disconnector itself, but also within busbar sections. Failures of transformers and capacitive bushings were also reported and attributed to disconnector operations.

Very fast transient overvoltages

Reports 33-01, 33-04, 33-09, 33-12, 33-15 and 23-11 deal with the calculation of VFT overvoltages within GIS of different configuration. Comparisons with actual measurements show sufficient agreement, when correct assumptions for the voltage collapse are made. Concerning disconnector operations the assumed value for this collapse vary considerably, reaching from 1.15 p.u. (33-01) over 1.4 p.u. and 1.5 p.u. (33-13, 33-15, 23-11) up to 2.7 p.u. (33-09).

QUESTION 7: Can a single value for the voltage collapse across disconnectors during opening be recommended or does it depend on the disconnector design or even on the GIS configuration to such an extent that it has to be established in tests?

QUESTION 8: Have VFT overvoltages due to faults with values of the voltage collapse close to the relevant rated withstand voltages of the GIS any importance for the insulation co-ordination of equipment connected to it?

QUESTION 9: Are the parameters maximum rate-of-rise of the front, time-to-crest, frequency of the main oscillation and peak value sufficient to fully describe the VFT overvoltage with respect to its stress on the equipment? Can values be given for these parameters, e.g. for a voltage collapse across the disconnector of 2 p.u.?
Is the measuring technique sufficiently developed to record all parameters of interest?

Equipment testing

Up to now the insulation level of the equipment is determined by the rated lightning or switching impulse withstand voltage. For transformers a chopped lightning impulse test is required in some national standards. It is up to now uncertain, whether these tests can cover all cases of VFT overvoltages, in particular in the higher voltage range where the ratio between the rated lightning impulse withstand voltage to the operating voltage is decreased compared to that in the lower range.

Concerning the GIS insulation report 33-15 stresses the importance of a DC prestress simulating the trapped charge on the load side of the disconnector, whereas report 33-13 states equal strength for VFT overvoltages and lightning impulses irrespective of the geometry of the GIS insulations. As regards the insulation of transformers report 33-13 states an extremely high overvoltage at a selected tap of the regulating winding, however, derived from measurements with steady state high frequency voltages. Others assume that the VFT stresses can be covered by a suitable chopped impulse test.

The necessity to test disconnectors during operation seems to be agreed upon (33-13). Alternatives under discussion are the disconnection of unloaded GIS sections or the synthetic test with two out-of-phase AC voltages.

QUESTION 10: Is a test with an aperiodic impulse adequate to assure a withstand of the GIS insulation against VFT overvoltages or is it necessary to consider additional parameters as prestress or oscillations?
What are the consequences for the on-site testing?

QUESTION 11: Has a special test to be developed for transformers or can the traditional chopped-wave test be used to check their ability to withstand VFT overvoltages in service?

QUESTION 12: What type of test of disconnectors is considered suitable for both the determination of the voltage collapse and the disconnector withstand during operation?

Transient enclosure voltages

Reports 33-06, 33-13, 23-06 and 23-10 are addressing the so-called transient enclosure voltage of GIS, all with special reference to means of reduction as low inductance earthing, improved shielding especially at discontinuity points, or damping by non-linear resistors. As this topic is not fully within the scope of SC 33, the discussions should be restricted to the overvoltage phenomena themselves.

QUESTION 13: Is there a principal difference in shapes, rates-of-rise or frequencies between transient enclosure voltages and VFT overvoltages, or can similar calculation procedures and measuring techniques be applied to both?

International Conference on Large High Voltage Electric Systems

112, boulevard Haussmann — 75008 Paris

1988 Session — 28th August - 3rd September

O

33-13

Pref. Subj. 3

VERY FAST TRANSIENT PHENOMENA ASSOCIATED WITH GAS INSULATED SUBSTATIONS

Paper presented at the request of Study Committees 33 and 13

by

Working Group 33/13-09 *

Summary

Gas Insulated Substation (GIS) insulation is subjected to Very Fast Transient Overvoltage (VFTO). This paper presents firstly the origins of VFTO : disconnector switching and fault to ground. Then the characteristics of VFTO inside and outside the equipment are presented.

As far as possible the effects of VFTO on equipment are discussed : the effets on transformers, disconnectors and circuit-breaker, insulation, enclosure, cables, arrestors, bushings and secondary equipments.

Different test procedures for disconnectors are presented and on site testing of the GIS discussed.

Finally modelling and measuring techniques are presented in appendices.

Key words

Overvoltage , GIS, disconnector, transformer , EMC, testing, measurement .

1 - INTRODUCTION

In the past twenty years, Gas Insulated Substation (GIS) have been more and more generally installed in power networks. The development of this technology began with the 123 kV voltage level and now GIS up to 765 kV voltage level are in service, having reliabilities at least as good if not better than that of open air substations.

So long as the voltage level remained lower than 300 kV, no one had to pay very much attention to the Very Fast Transients Overvoltages (VFTO) generated during switching operations performed within GIS (disconnectors, circuit-breakers or load switches). This lack of interest for these VFTO was supported by the fact that for voltages lower than 300 kV no problem correlated with operating switches has occurred.

Despite the excellent service record of this equipment, at 420 kV and above some problems including a few failures and sparking between earthed parts have been encountered simultaneously with disconnector or circuit-breaker switchings within GIS. These problems arose at various locations : disconnector itself, in the gas, along spacer, in bushing and transformer. These are attributed to the VFT voltages generated during the switchings.

To clarify as far as possible these problems, it is necessary to characterize more precisely on one hand the VFTO and on the other hand the behavior of the different types of insulation with respect to these VFTO.

In the first part of the paper, the origin of the VFT phenomena and the build up mechanism leading to the VFTO are described. Then the range of the main characteristics of the VFTO are given related when possible to their frequency of appearance. These characteristics are given for both the internal and external VFTO.

In the second part of the paper, the behavior of the different types of insulation and equipment with respect to the VFTO is discussed. Consequently for equipments which can be affected by the VFTO, tests are proposed to assure the high reliability of these equipments in service.

*Members:
ALVINSON (SE), ARDITO (IT), BOECK (DE), FESER (DE), FUJIMOTO (CA), GRANDL (CH), KOENIG (DE), LIGHTLE (GB) LUONI (IT), LUXA (DE), MULLER (DE), ROWE (FR), SABOT*(FR, convener).

* ELECTRICITE DE FRANCE, DER, 1 avenue du Général de Gaulle, 92141 Clamart Cédex, France

2 - ORIGINS OF THE VFTO

2.1 - Voltage collapse time during SF_6 breakdown

In case of a line to earth fault the voltage collapse at the fault location occurs in a similar way as in the disconnector gap during striking. The voltage just preceding the collapse is defined as Δu. By this event step shaped travelling surges are injected to all GIS lines directly connected to the collapse location. For such a surge source inside a GIS bus duct, two surges travelling in opposite directions are generated but there will be only one surge if the collapse occurs at the open end of a GIS bus duct. Even more than two surges are created in case of a surge source in a multiple bus junction.

For all cases considered the risetime t_r of these surges can be obtained by:

$$t_r = 13{,}3 \frac{k_T}{\Delta u/s}$$

with the Toepler spark constant k_T = 50 kV ns/cm and the spark length s [1,2]. Therefore, short risetimes are obtained for high medium breakdown fields $\Delta u/s$ in the case of almost homogeneous field distributions of a faultless GIS insulation system. By the approximation:

$$\Delta u/s = (E/p)_0 \; p \cdot \eta$$

with $(E/p)_0$ = 860 kV/cm MPa, the gas pressure p and the field utilization factor $E_{mean}/E_{max} = \eta$ = 0,5 ... 0,8 of a normal GIS design the lower limit $t_{r\ min}$ of the expected risetimes can be gained by:

$$t_{r\ min} = (1 \ldots 1{,}5) \frac{1}{p} \quad [ns, MPa]$$

Protrusions, excessive roughness and particles lead to longer risetimes. Extraordinarily long risetimes up to 200 ns are obtained for extremely inhomogeneous fields, caused for instance by long needle shaped protrusions in case of a VFT-breakdown where the medium breakdown field strengths $\Delta u/s$ is considerably reduced (fig. 12 C).

2.2 - Disconnector and circuit-breaker or load break switch operations

The transient overvoltages generated during GIS Disconnector (DS) operation are a consequence of the propagation of voltage steps created by the voltage collapse across the inter-contact gap at striking. However the specific overvoltage shape is formed by the multiple reflections and refractions of these steps at all points where they encounter impedance changes inside the GIS. As might be expected both the rise time and amplitude of the initial steps are instrumental in giving the transient its particular form and peak value, as is the configuration of the GIS in question. In practice however the highest frequency component which can exist and the peak transient voltage will be limited by the finite voltage collapse time which depends on gas pressure and can be estimated to be 15 ns for 0,1 MPa but only 3 ns for 0,5 MPa [3].

Furthermore the step heights will be fixed by the actual conditions prevailing on each side of the DS at the instant of striking. This in turn will determine the overall crest value of the transient overvoltage. Although very steep fronted steps may be generated, transmission line effects will rapidly change the waveshape, such that the very high frequency content is notably reduced a short distance from the disconnector.

In order to understand the general switching behaviour of a DS consider one closing on a pure, uncharged capacitive load (fig. 1a). R_s is added as a fictional lumped element to help the comprehension of the phenomenon.

As the contacts approach the electric field between them will rise until sparking occurs. This first strike will almost inevitably occur at the crest of the power frequency voltage, due to the slow operating speed ; the voltage across the DS contacts, just preceding striking is defined as Δu. Thereafter current will flow through the spark and charge the capacitive load to the source voltage. As it does so, the potential difference across the contacts falls and the spark will eventually extinguish (fig. 1b).

This having occurred the source side of the DS will continue to follow the power frequency, falling from the peak value, leaving the load charged. The potential difference across the DS will therefore rise again, but now with the opposite polarity, and a second strike will occur when the source voltage is near zero.

The intercontact breakdown voltage of a DS is always higher in one polarity than in the other, due to the asymmetrical contact design, and the first strike will often take place when the moving contact has a negative polarity. Consequently, the second strike will mostly take place for a greater potential difference than the first and will occur when the source voltage has crossed zero.

The gradual approach of the contacts engenders a steady reduction of intercontact breakdown voltage difference which in turn causes a corresponding increase of the number of restrikes per cycle and the amplitude of individual voltage steps becomes smaller and smaller. The severity of the overvoltages generated hence falls rapidly as closing proceeds.

The behavior on opening is very nearly a complete reversal of the above description except that the non polarity-asymmetrical breakdown characteristics causes the last few strikes to occur in such a manner as to leave a trapped charge on the busbar, following the last restrike (fig. 1c). The level of this trapped charge is statistical and depends on the asymmetry of the contacts and the speed of operation.

In practice each intercontact restrike arc burns for times far in excess of those predicted by the charging of the load through the surge impedance of a GIS Bus (R_s) (see fig. 1a). This is because the step induced transients are accompanied by high frequency arc cur-

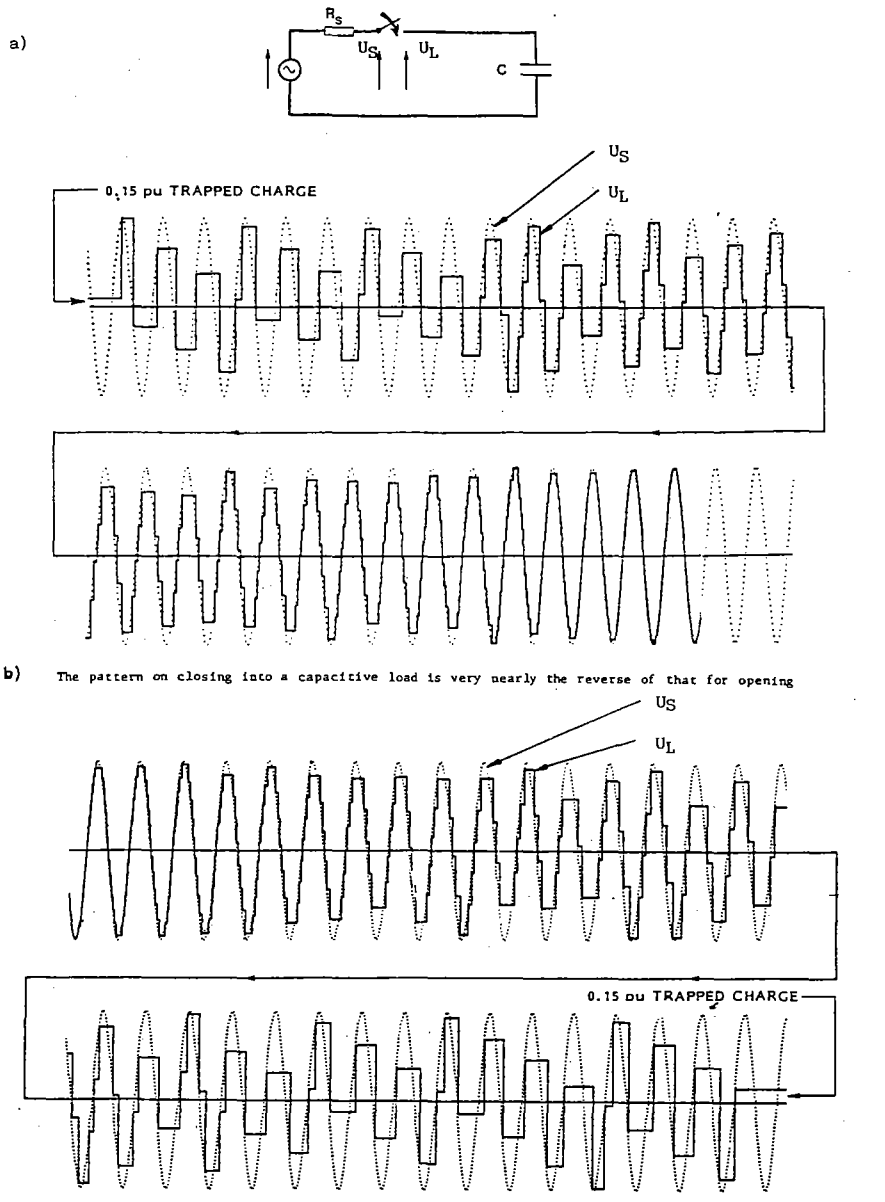

Fig. 1 — Variation of load and source side voltages during D.S. switching [3].

rents which keep the latter burning until they are damped out : this can take several tens of micro-seconds.

The precise number and amplitude distribution of steps during a typical switching will depend firstly on the specific DS design and operating speed, secondly on the behaviour of the GIS after each restrike spark extinction and thirdly on specific GIS functional procedures. The third case is only important in rare cases where a specific operational mode, involving the opening of a circuit-breaker, can leave a floating busbar charged to a level near maximum (1 p.u.). Generally one talks of trapped charge but, of course, the important parameter is the remaining voltage (U = Q/C). This can create particularly severe conditions because the first strike will occur on the peak of the power frequency source voltage giving a Δu of 2 p.u. On striking the voltages on each side of the DS will collapse initialy to zero hence creating two 1 p.u. voltage steps of opposite polarities which will begin propagating outwards. This assumes the common situation where the surge impedance is equal on both sides of the DS.

Fortunately, however, for low speed DS of conventional design, the trapped charge left when opening a pure capacitive load (busbar) gives remaining voltages ranging from 0.1 to 0.5 p.u. peaked around 0.3 p.u. This produces values of Δu at first strike of 1.1 to 1.5 p.u. once again peaked around 1.3 p.u. Fast operating DS on the other hand can leave trapped charge levels corresponding to 1.0 p.u. in a non-negligiable number of cases, giving rise to Δu values up to 2 p.u. However, no matter what the actual design, on extinction of an intercontact arc, the circuit on each side

of the DS can oscillate at the corresponding natural frequencies.

These frequencies will be in the range of a few tens to several thousands hertz and, if time is sufficient between strikes, they can be clearly seen. This has the inconvenience of creating conditions under which the phase differences between the two sides of the opening DS can trigger the final restrikes at $\Delta u = 2$ p.u.

A practical example of this would be the opening of a GIS bus containing a saturable magnetic voltage transformer [4]. Circuit-breakers and load-break switches may also generate transients in GIS but due to their very rapid operation only a few strikes occur.

A larger number of strikes may occur for the special case of switching small inductive currents, eg. shunt reactor switching.

The case of single enclosure three phase GIS is considerably complicated with respect to single phase ones. This is because voltage steps are not only generated between the striking phase and enclosure but also between the phases. The steps will have largely differing amplitudes and will propagate such as to build up phase-enclosure and phase-phase voltages. The form of which will depend on GIS structure, coupling between phases and on the presence or absence of a burning spark between the contacts of the other two DS.

Furthermore overvoltages generated by one phase and coupled to the others may promote or retard sparking of the latter hence totally modifying the restriking behaviour of all phases.

This subject has received little or no published attention to the knowledge of the WG due to the complexity of the calculations and experimental set ups required.

2.3 - Propagation and mechanism of VFT

As described in the previous sections, breakdown phenomena in the compressed gas insulation of GIS, whether across the contacts of a DS during operation or a line-to-earth fault, generate nanosecond-risetime travelling wave voltages which propagate in either direction from the disturbance source. As coaxial GIS forms an excellent low-loss high frequency distribution network, the travelling waves propagate throughout the GIS and to other connected equipment.

2.3.1 - Transients internal to the GIS

For VFT phenomena internal to the GIS, the formation of overvoltage waveshapes can be analyzed conveniently by treating each section of GIS (bus and other components) as a transmission line characterized by a surge impedance and electrical length (transit time). As the initial travelling waves encounter transmission line discontinuities, such as formed by open disconnectors, "T" junctions, and other connections, the travelling waves are reflected and refracted (transmitted) with magnitudes according to basic transmission line theory. The superposition of all the various component travelling waves generated in the GIS network results in the waveshape of the VFT. Because of this travelling wave nature and the short risetime, the VFT waveshape can be significantly different at points within the GIS separated by only a few meters [5]. Another consequence of the travelling wave nature is that the oscillation frequencies of the VFT are determined by electrical lengths of GIS bus. Generally, the primary oscillation frequency tends to be in the 5-10 MHz range, although in view of the short initial risetime, higher frequency components exist in the range of 100 MHz. In some cases, the ~100 MHz high frequency oscillations have been observed to be more prominent or perhaps to dominate the VFT waveform in the vicinity of the DS [6].

The concept that GIS is a network of interconnected transmission lines can be demonstrated with simulations using simple travelling wave computer programs or the well-known EMTP. Figure 2 demonstrates the accuracy of such techniques by comparing a computer simulation with a direct measurement of a transient waveform in an actual GIS [7]. Computer calculation and measurement techniques are described in the appendix.

The simulation of figure 2 neglects the presence of propagation losses (skin effect, etc.) which results in less damping of the high frequency detail of the waveform. In addition, the effect of spacers, flanges, elbows, corona shields, and other connection hardware, were included by adjusting the propagation velocity to 0.95 times the velocity of light. With these assumptions, the fine detail of the waveform is not precisely reproduced but the overall agreement between simulation and measurement can be quite good. With more precise attention to detail, such as modelling each individual spacer as a capacitance, many of the fine details in the waveform can be explained [8]. However a poor modelling of the operated disconnector and its vicimity may lead to extreme deviations [6,39].

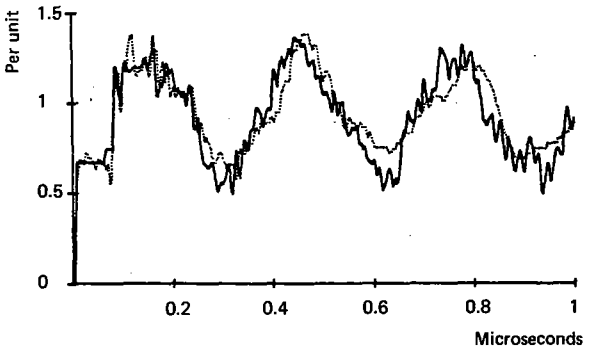

Fig. 2 — A comparison of a computer simulation and an actual measurement of a DS induced transient overvoltage waveform in a 138 kV GIS. The details of the configuration and computer model are given in [7]. The measured data are plotted with the dotted line and the computed data are plotted with a solid line.

2.3.2 - Transients enclosures voltage

Transient enclosure voltage (TEV - also known as transient groundrise) is a special case of VFT which merits special attention and has been thoroughly studied and surveyed [9,10]. The phenomena refers to short risetime, short duration high voltage transients which appear on the external of the "earthed" enclosure of the GIS through the coupling of internal transients to the enclosure at enclosure discontinuities. TEV occurs because the normal earthing connections, which were designed on the basis of power frequency considerations, are too long (i.e. too inductive) to provide effective grounding for the short risetime VFT.

As high frequency currents are restricted to the surface of conductors by the skin effect, VFT currents in GIS are restricted to the internal surface of the GIS until a discontinuity in the enclosure is encountered. Thus TEV does not emerge onto the external enclosure surface at the point of the initial disturbance (DS operation or breakdown to the enclosure). Transients couple onto the exterior surface of the enclosure at physical discontinuities, such as at air terminations. Although visual inspection ports and other openings are also apertures through which transients could emerge, the SF_6-air bushing is normally the most significant source of TEV. Insulated flanges at GIS/cable interfaces and at some current transformers can also allow the emergence of TEV.

The mechanism of TEV generation at the air termination can be analyzed by considering the GIS-air interface to be a connection of three transmission lines, viz., (1) the coaxial GIS transmission line, (2) the transmission line formed by the bushing conductor and overhead line, and (3) the GIS enclosure-to-ground transmission line. These three transmission lines, with surge impedances Z_1, Z_2 and Z_3 respectively, and the manner of their connection are shown in figure 3. When an internal travelling wave propagates to the gas-to-air bushing, a portion of the transient is coupled onto the overhead line-to-ground transmission line (2) and a portion is coupled onto the GIS enclosure-to-ground transmission line (3). The latter constitutes TEV.

The TEV wave which couples onto the enclosure encounters earthing connections which form transmission line discontinuities and attenuate TEV. Earthing leads can also be analyzed with transmission line approximations. For instance, the point of connection of the earthing lead to the GIS enclosure is an impedance discontinuity. A fraction of the TEV is transmitted through, some is reflected, and some is transmitted down along the earthing lead. When the portion which was coupled onto the earthing lead encounters the groundplane, a negative reflection occurs which propagates up the earthing lead and tends to cancel the original TEV (fig. 4). This analysis indicates that earthing leads are effective in reducing TEV if their surge impedance is low and their electrical length, which determines the time required for the negative reflection from the earthing lead to return to the enclosure, is short compared to the typical VFT risetime.

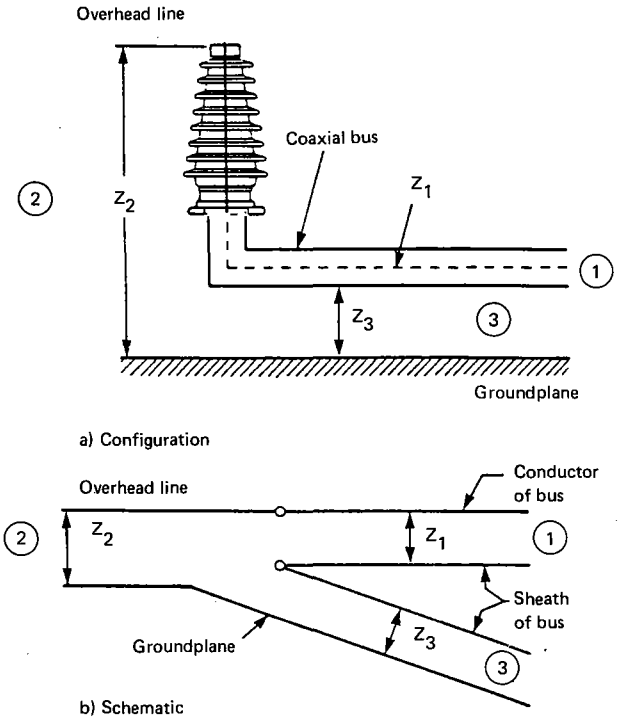

Fig. 3 — The GIS air termination modelled as a connection of three transmission lines. The portion which couples from the internal GIS (1) to the transmission line formed by the GIS enclosure and the groundplane (3) is the primary mechanism for TEV at the air termination.

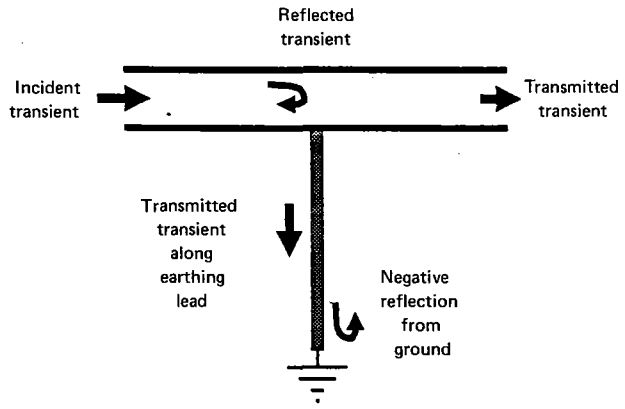

Fig. 4 — The influence of earthing leads based on transmission line analysis. The negative reflection which propagates back from the groundplane along the earthing lead tends to negate the original waveform. By reducing the electrical length, earthing connections become more effective by reducing the time required for the negative reflection to have an effect [9].

By assuming transmission line equivalents of the various earthing connections, proper treatment of the transmission line model of the air termination, and with knowledge of internal VFT characteristics, TEV magnitudes can be estimated [11].

In general, TEV waveforms have at least two components. The first component has a short initial risetime and is followed by high frequency oscillations determined by the lengths of various sections (bus duct and earthing connections) of the GIS. The precise

frequency components depend on the details of the GIS, but the bulk of the transient energy is concentrated in the 5-10 MHz range for typical arrangements. The second component is of lower frequency (hundreds of kHz) and is often associated with the discharge of large capacitive devices (e.g. capacitive voltage dividers) with the earthing system. Both waveform components are damped quickly as a result of the lossy nature of the enclosure-to-groundplane transmission mode; TEV voltages generally persist for only a few microseconds.

2.3.3 - Transients on overhead connections

As discussed above, a portion of a VFT travelling wave incident at an air termination is coupled onto the overhead connections and propagates to other power system components. As a general rule, propagation of VFT on air-insulated lines and bus is lossy and results in some increase of the waveform risetime. However, measurements indicate that if the air connections are relatively short, VFT with risetimes in the range of 10-20 ns can propagate from GIS over short air connections to connected components, such as power transformers [12]. In general, external VFT waveforms have two distinct characteristics. The overall waveshape is dictated by lumped circuit parameters, such as the capacitance of voltage transformers, line and earthing inductance, etc. As a result, the overall risetime is in the range of a few hundred nanoseconds. However, waveforms also include a fast front portion which is dictated by transmission line effects. This portion has a risetime in the range of 20 ns and, because of numerous discontinuities in the transmission path, is usually reduced in magnitude (to about 20-40% of the incident magnitude). The fast risetime of the initial portion is possible as capacitive components, such as bushings, are physically long and distributed (with respect to the VFT risetime) and cannot be treated as lumped elements. Lumped parameter approximations inevitably lead to erroneous risetime information, although the overall waveshape may be similar.

3 - CHARACTERISTICS OF THE VFTO AND TEV

3.1 - Internal VFTO

3.1.1 - VFTO due to disconnector operation

The circuits involved including the GIS and connected apparatus like transformers can be considered as linear for the phenomena under consideration with oscillation frequencies of more than 20 kHz. Therefore, the superposition principle can be applied for the two main phenomena involved.

a) Travelling wave phenomena

Caused by the two injected step shaped surge voltages travelling in opposite direction from the disconnector into the GIS VFT overvoltages are generated. These surges will be superimposed at the beginning to the actual supply or load voltage respectively at the considered location. But the final stationary value will be 1 p.u. for the most unfavourable case which has to be taken into account. The maximum values of the local VFT overvoltage is dependent on the voltage drop Δu at the disconnector just before striking, the location considered and the remaining voltage. Theoretical considerations, computer simulations of a broad variety of GIS layouts and measurements in laboratories and in actual GIS led to the following results [13-23].

Δu = 2 p.u. should be taken into account as the most unfavourable case corresponding to a remaining voltage of -1 p.u. due to trapped charges on the load side in case of high speed disconnectors or phase opposition conditions. For this case the maximum VFTO peak has a typical value between 1.5 and 2.0 p.u. for most configurations. However, values up to 2.5 p.u. had been found for very specific cases. But for normal switching conditions of most disconnector designs a voltage collapse of Δu = 1.5 p.u. is not exceeded resulting in lower peak values of the VFT overvoltage (up to 1.7 p.u. for most configurations and 2 p.u. for very specific cases).

Some important points of interest with regard to shape and frequency of VFTO are the following.

1) Sometimes close to the disconnector superimposed additional VFTs with oscillation frequencies up to 100 MHz are observed created by reflections at adjacent internal GIS components in short distance or within the disconnector itself [19,22].

2) The main frequency of the dominating VFTO component is given by the total length of the GIS bus switched by the disconnector. By refraction and damping effects the superimposed VFTs of high frequency are decaying leading to mainly monofrequent oscillations in the range of 1 ... 40 MHz after some microseconds normally. An example for a typical travelling wave pattern measured in an actual GIS is shown in fig. 5 A and B [16].

3) The maximum value is usually reached at the second or even a later peak [22].

b) Overall transients

In case of power transformers feeding the GIS overall transients with frequencies in the range of 20 ... 100 Hz were observed caused by oscillations of the whole system consisting of the GIS and the transformer. The amplitude of these oscillations however is smaller than that of the VFT oscillation. An example for such an overall transient measured in an actual GIS fed by a power transformer is given in fig. 5 C and D [16].

3.1.2 - Line to enclosure fault

According to para 2.2 step shaped surges with magnitudes equal to the instantaneous value of the applied voltage at the moment of breakdown are generated in the GIS by a line to enclosure fault at the fault location. Calculations have shown that VFT overvoltages up to twice this magnitude may be caused in

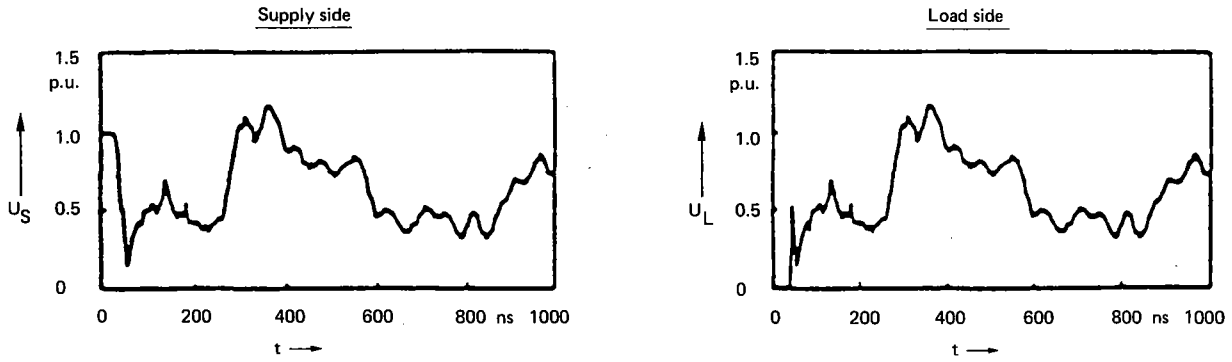

a) Steep voltage transients (travelling waves) - Typical risetime 5 - 10 ns.

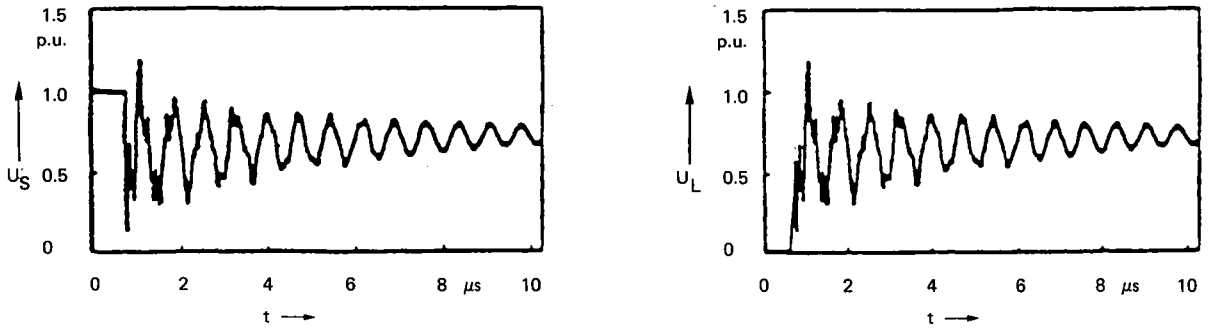

b) Mainly monofrequent oscillation after some μs - Frequency range : MHz.

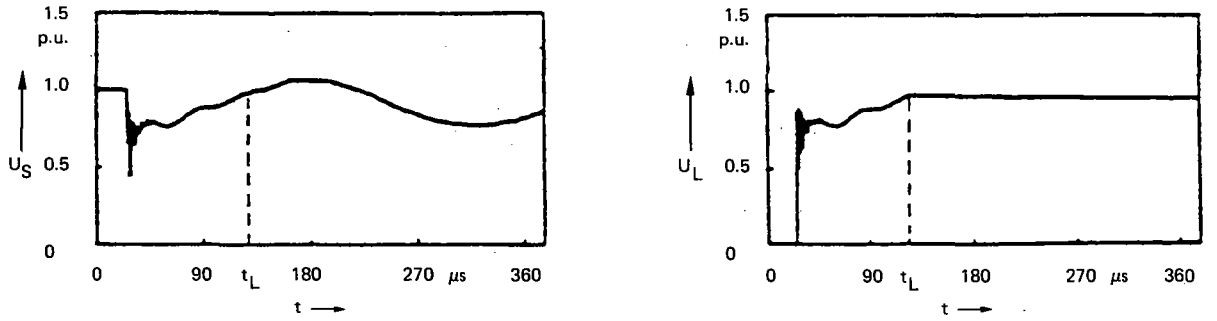

c) Overall transients by oscillation of the power transformer and the GIS - Frequency range : 20 ... 100 kHz.

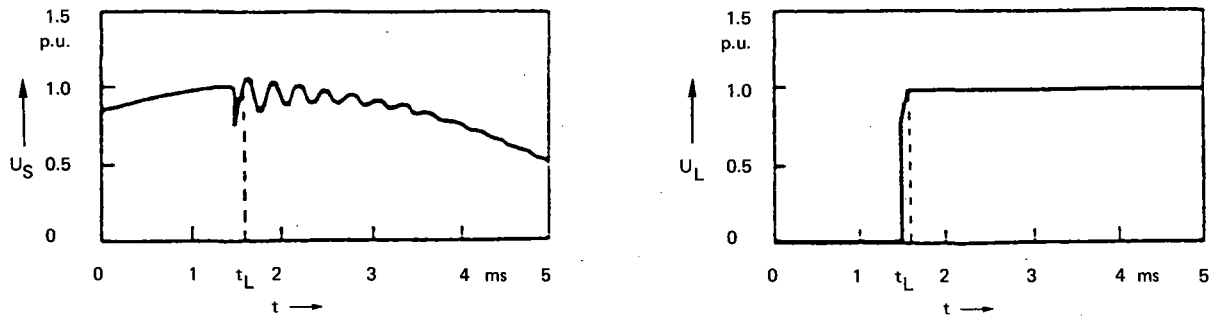

d) Low frequency transient and steady state condition.

Fig. 5 — Transients on the supply and load side of a GIS due to disconnector switching at different time resolutions (measurements in an actual GIS) t_L arc extinguish.

special locations. This is of special concern during tests on site [23].

3.2 - External VFT voltages

As previously mentioned in paragraph 2.3.2 at the air SF_6 termination, there is a change of impedance where the internal VFTO are partly reflected inside GIS and partly transmitted between the overhead line and earth and between the GIS enclosure and earth.

This sharing is performed according to the surge impedances of the three part transmission line system.

3.2.1 - Transient on overhead connections

Although the magnitude of the fast risetime portion of external transients is generally less than that of internal VFT, the voltage rate-of-rise can be in the range of 10-30 MV/µs [12], which is a stress similar to that of a chopped waveform. However, as VFT occur during normal conditions in GIS and each DS operation may generate tens to hundreds of individual transients, the possible ageing effect on the insulation of external components needs to be considered.

3.2.2 - Transient Enclosure Voltage

TEV although not unique to GIS probably manifests itself more visibly in this type of substation than in the conventional air insulated type by the appearance of sparks between metallic components of the enclosures and between enclosures and other earthed components or structures. The magnitude of the transient can vary according to the location of the measurement point on the enclosure. On simple arrangements it can vary between. 0.1-0.25 p.u. [24] for the GIS generally but can reach an order of magnitude higher near the SF_6 to air terminations [9,10].

TEV has caused a concern for personnel safety but is in itself a low energy phenomenon [10] and there is no recorded evidence available to suggest that it is directly dangerous to the health of personnel performing normal duties within the substation. The element of surprise which may be occasioned at the appearance of sparking, however, is of greater concern for the safety of personnel and in some cases has brought about the introduction of appropriate operating procedures (e.g. warning signals, limited access, etc.) [10].

TEV can also cause interference with or even damage to the substation control, protection and other secondary equipment [10].

In 1983 an international enquiry instituted by WG3 of Study Committee 23 attempted by means of a questionnaire to assemble manufacturers and users experience of the TEV phenomenon in GIS and thereby set out to examine and classify measures taken to ameliorate the effects on equipment.

More than half the respondants, in themselves responsible for over 50% of the Gas Insulated Substations in service reported having had problems with sparking between earthed enclosures, components and structures and interference with secondary equipment.

It became apparent when analysing the responses to the survey that the various methods employed for earthing the substation equipment, although adequate for the safe discharge of power frequency current in the enclosure, were not all effective in handling the very fast transient currents resulting from disconnector switching and similar breakdown phenomena.

The report of the Working Group [10] therefore recommended further study of earthing systems in GIS. In 1986 the Chairman of SC23 set up a team from Working Groups 3 and 4 under the leadership of the Convenor of WG4 and charged it with formulating recommendations for the earthing of Gas Insulated and conventional substations which would minimise the effects of Transient Ground Potential Rise.

The study is complete and the results will be published in time for discussion at the 1988 CIGRE Conference [25].

3.2.3 - Radiations

Electromagnetic fields associated with the external VFTO are radiated from the enclosure and the overhead line. Any electronic cubicle even at some distance from the enclosure will therefore be subjected to a transient electromagnetic field which may induce voltages or currents within an electronic circuit. The amplitude of the electric field is typical some 10 kV/m near the enclosure. The frequency of the electromagnetic field depends on the arrangement of the GIS, but is typically in the range of 10 to 20 MHz. Figure 6 shows the measured electric field in a 420 kV-GIS, at different distances from the enclosure during the operation of a disconnector [24]. Near the enclosure, the electric field decreases with the distance (fig. 6). There are multiple reflections in the earthing system, resulting in higher frequencies in the electric field near the earth side. The electric fields were measured with a spherical electric field sensor (see Appendix). The magnetic field can be estimated to be in the range of some 10 A/m having the same frequencies as the electric field.

4 - EFFECTS OF VFTO ON EQUIPMENT

4.1 - Effects on transformers

Transformers are either directly connected through SF_6-bushings or indirectly by SF_6-air-bushings, overhead lines and air-oil-bushings.

Two different effects have been observed on the windings of direct connected transformers:

- Steep fronted wave impulses create an extremely non linear voltage distribution along the high voltage winding connected to the oil-SF_6-bushing. If the winding is composed of interleaved coils, at least in the entrance region, for steep-fronted impulses each interleaved coil can for example be represented

by surge impedance and earth capacity as shown in fig. 7a-d with the theoretical impulse form 7e compared to measured ones 7f [26].
For directly connected transformers the loop formed by two bushings and an overhead line smoothes the steep front to values comparable to chopped waves, which are well established and covered by impulse testing. For directly connected transformers experience with hundreds of transformers installed worldwide shows that transformers withstand the stresses built up by steep fronts.

- Transient oscillations within the GIS can develop extremely high part winding-resonance voltages in the transformer windings.

  For directly connected transformers frequencies up to several MHz can be transmitted through the SF_6-oil- bushing. For indirectly connected transformers the highest frequency transmitted through two bushings and an overhead line is about 1 MHz. In both cases part winding resonances also perferably could occur near the connection points e.g. the entrance coils and the selected tap of a step winding connected to a neutral point on load tap changer.

Fig. 8 shows the voltage ratio between one step of the tapped winding and the high-voltage side of a 420 kV transformer directly connected to a GIS as a function of frequency. Extremely high values develop in the Megahertz range. The q-factors (defined as peak transient voltage divided by peak power frequency voltage at the point of interest) can amount up to 200 due to transient potential rise of the neutral point.

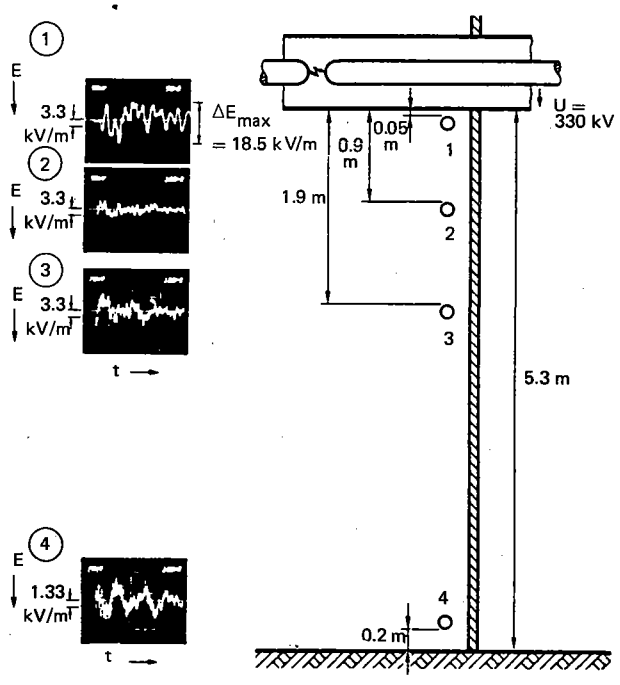

Fig. 6 — Radiated electric field from the enclosure in a 420 kV-GIS during a disconnector operation in the GIS [24]. (1 : 50 ns/div ; 2, 3, 4 : 100 ns/div).

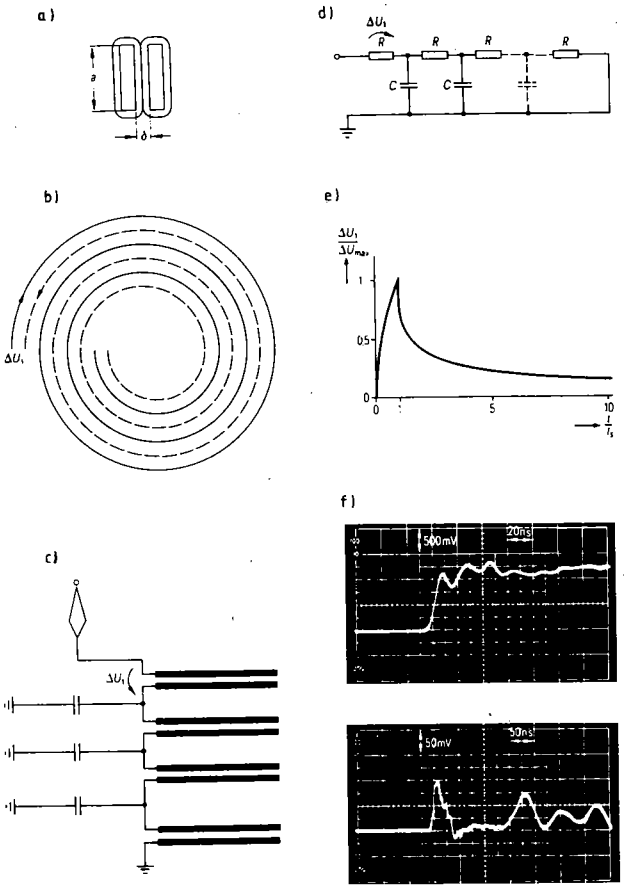

Fig. 7 — Voltage Distribution of Steep-Fronted Input Waves.

a) Geometrical dimensions of flat conductors for determining the surge impedance.

b) Top view of a two-strand spiral

c) Coil connections.

d) RC equivalent circuit.

e) Voltage or current wave set up at the first coil by a ramp-shaded impulse voltage.

f) Measured input voltage and partial voltage applied to the first coil.

Relevant measurements and investigations showed, that the damping decrement of the transient oscillations within the GIS determines as well the amplitudes developed by part resonance as the oil insulation strength under high frequency voltage stress [27].

The smaller the quotient of two subsequent amplitudes of same polarity, the smaller are the developed resonance amplitudes and the higher the insulation strength.

In critical cases it may be necessary to take measures as e.g. to protect the tap changer with varistors connected between the selected and preselected tap.

4.2 - Effect on disconnectors and breakers

According to the relevant IEC-standards dielectric tests of switching equipment have to be done with

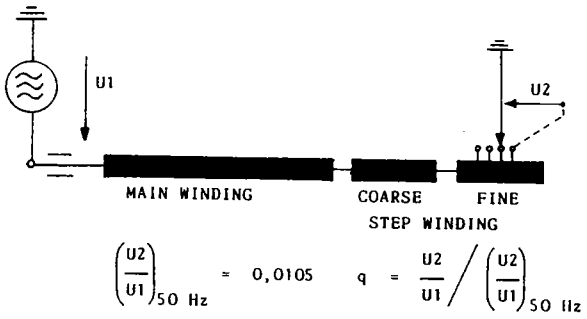

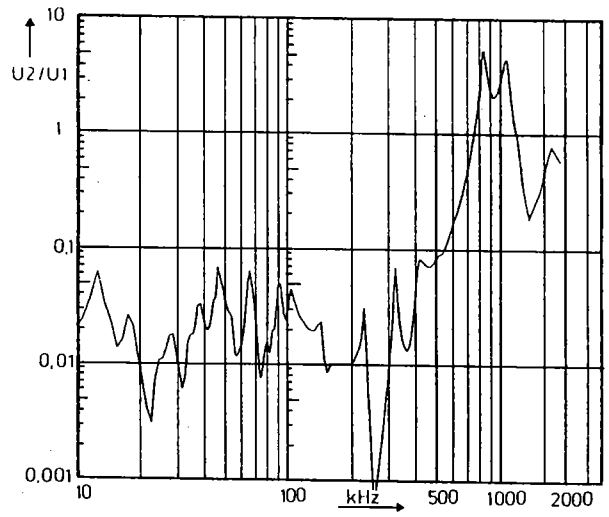

Fig. 8 – Voltage ratio between one step of tapped winding and HV-side versus frequency.

specified impulse or ac withstand-voltages in the closed and open position of the contact system, while intermediate positions have not to be taken into account. However, striking takes place in the intermediate position of the contact system. Depending on the dielectric stress, which is determined by the design parameters of the switching equipment such as service voltage, gap distance, electrode geometry, gas pressure, a discharge to the earthed enclosure leading to an internal arc may develop.

Due to the specific design parameters of circuit-breakers and loadbreak switches no earth faults during operation induced by self generated VFT overvoltages have been observed either in the breakers and switches themselves or in adjacent GIS-components. Since the contact system of this type of equipment is generally working in a gaseous atmosphere with a comparatively high overpressure, the striking distances between the contacts are very small compared to the distance between the contacts and the enclosure, thus resulting in a dielectric stress, which is too small for a discharge propagation in the direction of the enclosure. Furthermore, as shown by experience the insulation system of circuit-breakers and loadbreak switches seems not to be essentially endangered by VFT overvoltages, which are generated in adjacent GIS-components.

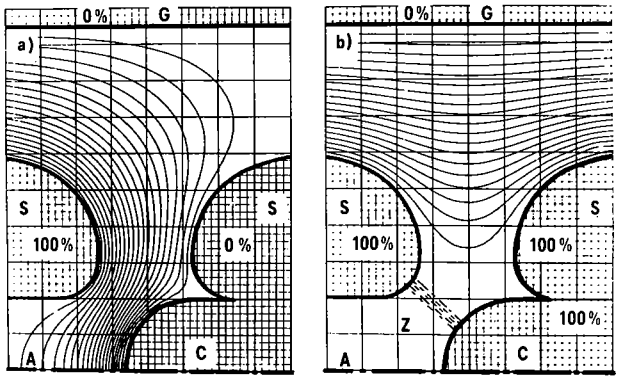

Fig. 9 – Electric field distribution of a disconnector.
a) Before striking b) During striking.
S Shielding electrode
C Moving contact
G Grounded enclosure
A Axis of disconnector
Z Striking zone.

VFT overvoltage induced earth faults, however, have been observed in case of disconnector switching operations. Depending on the relevant disconnector design the change of the electrical field gradient from a longitudinal to a radial direction as a consequence of a restrike or prestrike may be essential. The change of the field gradient for a well designed disconnector before (a) and during (b) striking is illustrated by fig. 9 [14].

In case of service voltages ≧ 300 kV the design parameters of disconnectors are in general such that a leader - type discharge, which tends to branching, becomes probable (fig. 10). After the bridging of the contact gap the propagation of residual leader branches directed to the enclosure may be supported as well by the change of the main electrical field direction towards a strong radial gradient and by simultaneously generated travelling wave patterns (VFT overvoltages) due to reflections inside the GIS.

Under this point of view the earth fault of a disconnector immediately after striking is basically a problem of activating residual leader branches by means of an enhanced field gradient to earth and by feeding them with VFT overvoltages generated in the attached GIS-configuration [21,28,29,14,16]. Though various questions on details of the described breakdown mechanism are still open and research activities in this field are going on, necessary design measures for GIS- disconnectors have already identified to prevent failures during switching operations. Appropriate designed GIS- disconnectors have proved to be reliable.

It is meanwhile generally agreed that switching tests on GIS-disconnectors have to be established with the purpose to check their switching capability and to verify their behaviour [29] (see chapter 5.1).

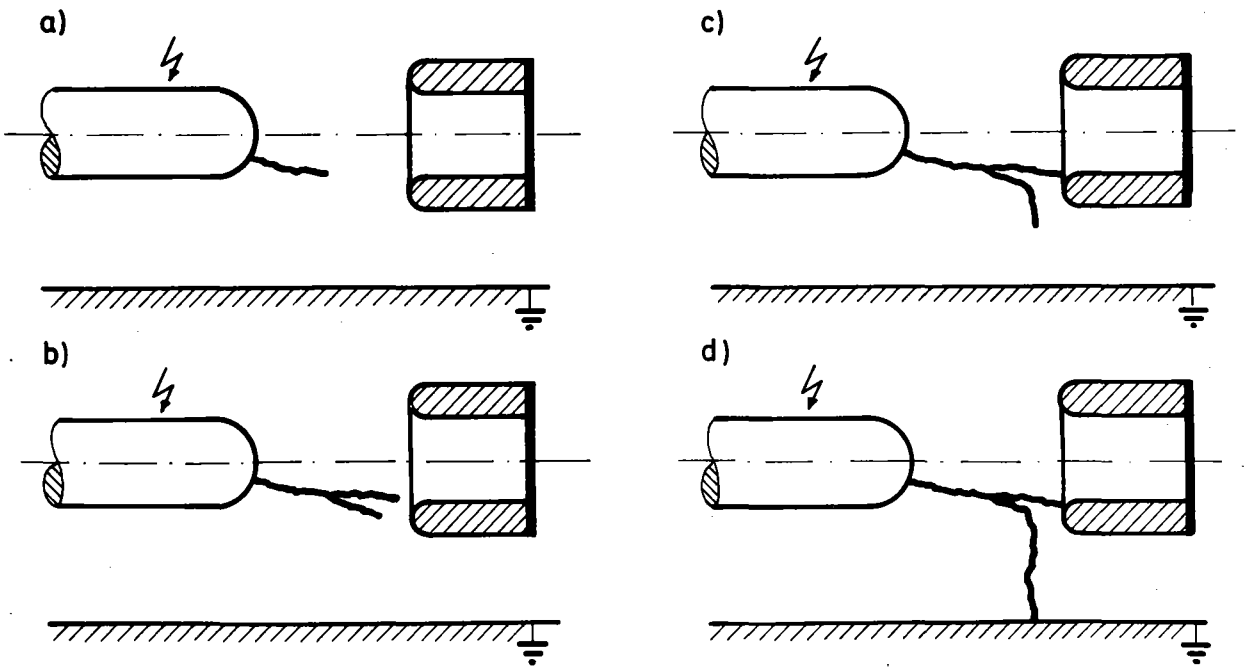

Fig. 10 — Development of an earth fault by branching of the leader-discharge during disconnector operation (principle)
Remark : Although branching commonly occurs, the development of a single branch to an earth fault can be avoided by a proper disconnector design.

4.3 - Effect on SF_6 insulation: gas and spacer

In correct GIS insulation system, the pure gas breakdown and spacer flashover behaviour is principally similar due to the insignificant field enhancement of modern spacer designs and the low influence of surface effects on the discharge development [30,31,32,33]. In accordance with the upturning trend of the Lightning Impulse (LI) voltage-time curves B in fig. 11 for increasing front steepnesses mainly caused by the formative time lag for the break-down channel all VFTO breakdown or VFTO flashover values are above the Lightning Impulse Withstand Level (LIWL) within the area A in fig. 11. Due to the longer formation time lag the negative polarity VFTO breakdowns (fig. 12 B) occur delayed for some hundred nanoseconds in the oscillating tail and at slightly higher values in comparison with positive breakdowns in the initial front or close to the primary peak (fig. 12 A). A big scatter range is typical for both polarities. Nevertheless all VFTO breakdown values for both polarities with and without spacer are comparatively close together within the frame A in fig. 11. Therefore, a VFTO breakdown is improbable in a correct GIS insulation system during normal operation.

Regarding extremely inhomogeneous fields caused by irregularities of the insulation system like needle shaped protrusions the VFTO breakdown values within the area C in fig. 11 are considerably reduced in accordance with the downturning trend of the corresponding LI voltage-time curve D in fig. 11 for increasing front steepness [31,32]. Both effects are mainly caused by the decreasing corona stabilization and changing leader inception conditions. The breakdowns occur late on the oscillation tail (fig. 12 C) with a big scatter. The positive breakdown values are somewhat lower than those for negative polarity as in a correct GIS insulating system. Due to the big scatter the breakdown probability is very low for low VFTO amplitudes and increases with the oscillation frequency and the degree of the field inhomogenity. For 40 MHz and a needle length of 15 mm a breakdown probability of 1% had been found during disconnector switching operation at rated service voltage in a 420 kV GIS which was successfully tested beforehand on site with Oscillating Switching Impulse (OSI) of 100% Switching Impulse Withstand Level (SIWL). Such VFTO breakdowns had been observed very rarely and only in the neighbourhood of disconnectors, where the breakdown level is extremely reduced by high VFTO oscillation frequencies. A similar but much less pronounced decrease of the breakdown voltage has to be expected for more conceivable irregularities like particles, edges and fissures with lower field distortion effects [33]. The behaviour of the insulation stressed by VFTO can be covered by standard lightning impulse stress [31]. Recent research results are compiled in a CIGRE paper [40].

4.4 - Effects on enclosure

With insulating flanges the build up of transient enclosure voltage causes sparking across flanges which established high frequency continuity in the enclosure and limits the magnitude of the TEV coupled onto the enclosure to about 10 kV [9] whereas TEV near SF_6 to air connections can be within the range of several tens of kV to 100 kV in magnitude [9-10].

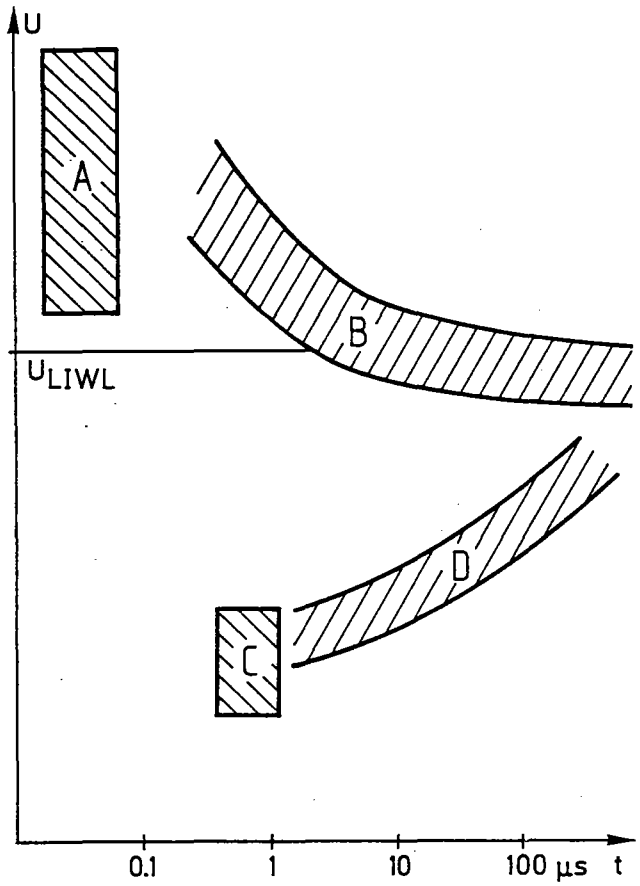

Fig. 11 – Principal voltage-time characteristic.

A VFT voltage, B Impulse voltage } Insulation system in correct condition

C VFT voltage, D Impulse voltage } Insulation system with a long needle shaped protrusion.

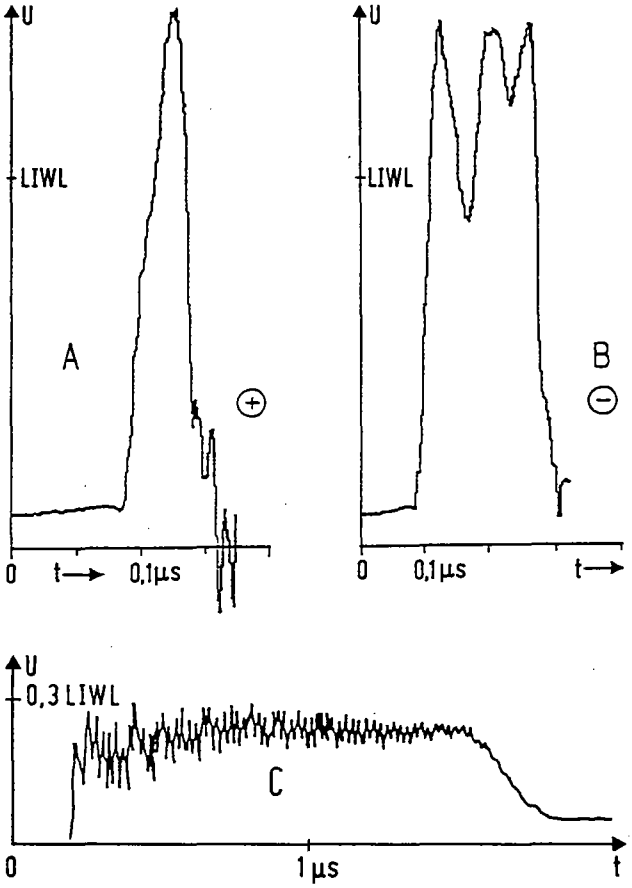

Fig. 12 – VFT breakdown development.

A positive polarity, B negative polarity } Insulation system in correct condition

C positive polarity } Insulation system with a long needle shaped protrusion.

The sparks may also cause damage to insulating material in the vicinity and impair its service life. Damage to insulating bushes in the housings of externally mounted current transformer may give rise to the development of short-circuited turns around the current transformers and hence interference with the correct operation of these devices. Equally, puncture of insulation intended to limit the spread of circulating currents within the enclosure, due to the passage of normal load current in the main conductor, may have harmful effects particularly under short-circuit conditions.

Probably of most consequences however are the cases where TEV interferes with the operation of control, protection and metering equipment.

Transient Enclosure Voltage effects in Gas Insulated Substations can be mitigated by the following means:

1) The design and arrangement of the substation earthing mat to provide effective attachment of the various earthing connections.

2) To minimise the surge impedance and the electrical length of the earthing straps. By keeping these leads as straight and as short as possible these objectives are achieved and thus low profile switchgear constructions are advantageous. Increasing the number of connections is also beneficial. Relatively massive earthed support structures will also reduce TEV.

3) To introduce shielding to prevent the Very Fast Transients generated internally from reaching the outside of the enclosure.

4) Where insulated spacers must be employed, to introduce voltage limiting varistors, of suitable rating.

4.5 - Effect on secondary equipment

TEV may interfere with secondary equipment by raising the housing potential of such equipment in case it is connected directly or via cable shields to the GIS enclosure, and by emitting free radiation which may induce voltages or currents in adjacent equipment. Though intermittent and of short duration, these effects may interfere with the normal functioning of electronic equipment or even damage sensitive circuits.

To minimize interference, correct cable connection procedures should be followed [25]. The coupling of radiated energy may be reduced by mounting control cables closely along enclosures, supports and other grounded structures, and by grounding cable shields at both ends by leads as short as possible or alternatively by the application of optical coupling devices. In the secondary equipment, voltage limiting devices may have to be added.

To ensure the integrity of electronic equipment, interference tests on such equipment are necessary. Suitable tests are:

- fast transient test (5 ns, 2 kV) on processing cables acc. to IEC 801-4,

- electrostatic discharge (ESD, 1 ns, 8 kV) test on housings acc. to IEC 801-2.

A radio test with continuous-wave radiation (10-30 V/m, 25-1000 MHz) acc. to IEC 801-3 or IEC 255 is less relevant due to the intermittent character of the radiation caused by GIS VFT.

4.6 - Effects on cables

Reported effects of VFTO on cable lines appear all to be located in earthed circuits and to be originated by Transient Enclosure Voltages so that reference can be made to section 4.4. In fact the earthing connections had to be modified in order to eliminate the troubles.

No problems have been experienced on the main insulation; as can be expected since characteristic impedance of cables is lower or at most equal to that of GIS.

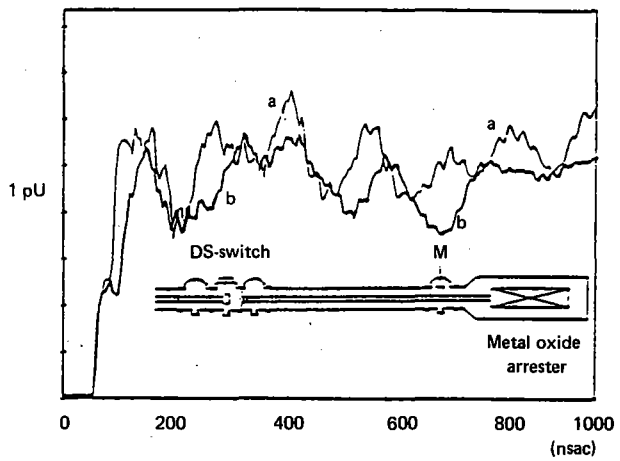

Fig. 13 — Capacitive behaviour of a metal oxide arrester. Influence on the shape of VFT voltages.
(a) Measured VFT in a test configuration without arrester
(b) Measured VFT in the same test configuration with arrester.

4.7 - Influence of a metal oxide arrester on VFTO

VFTO can appear at an arrester theoretically under two conditions, the conducting and non-conducting state.

The amplitudes of VFT events, according to measurements in gas insulated substations, are below the protection level of installed metal oxide arresters. So, under usual conditions VFT will appear at the arrester in the non-conducting state.

To investigate the behavior for that case, tests were performed in a high voltage laboratory. An enclosed metal oxide arrester for a 550 kV system was connected to a section of SF_6-insulated busbar, where high-voltage-VFTO were produced by a disconnector gap. The transient voltage was measured close to the arrester. Measurements for comparison were made for the same configuration but without the arrester.

The results are shown in fig. 13. The two curves represent the voltages in the busbar measured with and without the arrester connected. The arrester in the non-conducting state acts as a capacitance. Steep voltage fronts are sloped as shown in fig. 13.

4.8 - Effects on bushings

Bushings are needed at the interfaces between SF_6 insulated apparatus of GIS and air insulated equipment like overhead lines or links to transformers etc.

These SF_6/air bushings can have different design principles: SF_6 insulated or capacitively graded by multiple conductive layers.

The transformer bushings generally are capacitively graded, for air/oil application or for SF_6/oil in case of direct connections to GIS.

Bushings with mainly SF_6 insulation can be treated similar to the other GIS components. Therefore, interest is focussed on the influence of VFT on capacitively graded bushings with their main insulation formed by oil or epoxy impregnated foils.

Service experience for all designs and applications of bushings for voltages up to 800 kV has shown very few problems.

In one incident with an air/SF_6 bushing (525 kV system) the failure might have been accelerated by VFT effects. The main reason, however, was a bad contact design for a grading electrode.

Attention has to be paid also to avoid a too high inductance in the connections of the last grading layer to the enclosure.

5 - TESTING PROCEDURE OF EQUIPMENT

5.1 - Disconnectors

Up to now no disconnector switching tests have been standardised by IEC.

Such tests have been studied by CIGRE SC13 WG04 and their recommendations have been publicised [29]. The tests described are adequate to cover the general switching duties of disconnectors but it is recognised that they do not cover some special switching conditions under which disconnectors intended for application at voltages above 300 kV can operate.

For exemple the conditions which apply when a disconnector closes onto an off-load busbar on which a 1 p.u. remaining voltage has been left by the previous opening of a circuit-breaker are not covered nor are those in which the interruption of circuits which contain inductive voltage transformers takes place.

It should also be noted that recent investigations have shown that the presence in the network of different types of voltage source such as high voltage test transformers or power transformers can influence the behaviour of the arc in the disconnector switching gap.

To prove the satisfactory operation of disconnectors under these special conditions a number of test procedures have been proposed. Those that have been published are mentioned below.

A "one minute arcing test" intended to test the integrity of the phase to enclosure insulation under repeated striking at the disconnector gap has been proposed [4]. However this test is no longer considerate an adequate one.

A procedure using a synthetic test circuit has also been described [36]. This circuit is intended to correctly reproduce the transient peek overvoltage, which have been predicted, in the presence of the normal power frequency voltage.

The results of measurements of actual overvoltages occuring during disconnector switching in 110 kV networks have been reported and from these circuits designed to reproduce these overvoltages during laboratory tests have been described [35].

Finally a group of french manufacturers and users have described an analysis of the stresses occurring in disconnectors during switching under conditions of full phase opposition and have derived from this a test circuit and conditions to ensure impeccable [21] operation even in the most severe service conditions.

From the above it would seem that a further review of disconnector test methods would be appropriate when any other methods hitherto unpublished could be taken into consideration.

5.2 - On site testing

As described in section 4.3, the dielectric integrity of GIS stressed by VFTO can be adversely affected by the presence of defects such as particles and sharp protrusions, which might result during the shipping and assembly process. As a result, some form of additional testing might be necessary, especially for higher voltage classes which have smaller safety margins in the dielectric design. The purpose of testing is to prove the absence of defects which might cause problems in the presence of VFT overvoltages. Although there is a general consensus that power frequency tests are best for dealing with particles, the "best" testing approach for other defects is, however, subject of much discussion.

The use of short risetime impulses (such as the lightning impulse) is often suggested as a test waveform, as shorter risetimes are generally more sensitive to the presence of fixed defects [38], for which impulse testing, in general, is considered to be a good approach. The selection of waveform parameters requires standardization. Although short risetimes are best for detection, too short a risetime can lead to testing problems associated with travelling wave effects within the GIS. Some have suggested that a longer risetime waveform (such as a switching impulse) might be more practical, despite the reduction in sensitivity to certain types of defects. In some cases, both lightning and switching impulse voltages have been performed for the same GIS.

Despite the benefits of impulse testing, alternate test philosophies have been developed. For instance, under power frequency excitation supplied during the usual conditioning and AC test procedure, harmful defects as for instance free particles could result in detectable partial discharge or accoustic emissions. As a result, sensitive partial discharge measurements, based on electrical and acoustic techniques, have been suggested [39]. Such testing can be performed in lieu of impulse testing, although on occasion, both tests have been specified for the same GIS.

A third approach, supported by some manufacturers, involves no specialized testing on site. Instead, a greater emphasis is placed on quality control during manufacture and assembly, reducing the need for elaborate site tests. In this case, simple power frequency tests at 1.2 p.u. are thought adequate to detect assembly errors.

6 - CONCLUSION

In Gas Insulated Substation (GIS), disconnectors (DS) operations and line to enclosure faults generate short rise time travelling step voltages. The initial amplitude of these steps depends on the voltage Δu accross the DS at the instant of restrike or on the line to ground voltage before the fault. Reflections and transmissions of these initial travelling waves superimpose to build up the so called Very Fast Transient Overvoltages (VFTO). Their peak values are proportional to the amplitudes of the initial steps and depend on the GIS layout (bus bar lengths, location of the changes of impedance). The time-to-peak of the VFT voltages are lower than the conventional 1.2 μs and their rates of rise are greater than those of lightning impulse. The faster rise times of the initial steps have been estimated to be in the region of 5 ns and so due to the build up mechanism the VFTO have not the same shape and the same amplitude all throughout the GIS.

The VFT voltage appear within the GIS but also outside: between overhead lines and earth but also between the enclosure of the GIS and earth. So both inside and outside the GIS components are subjected to such stresses for which they have to be designed.

For the VFTO due to line to enclosure fault their amplitude can be dangerous for insulation only during on site testing and can reach twice the applied voltage at the instant of the failure.

For disconnector switchings when Δu at restrike is 2 p.u. the peak value of the VFT voltages can reach 2,5 p.u. for very severe case of GIS lay out but generally the peak value remains in the range of 1.5 to 2 p.u. For most cases the value of Δu is lower, the peak value of VFTO are below 1.5 p.u.

From an insulation point of view the main following conclusion can be drawn:

1) For disconnector switching the peak amplitude of the VFTO remains even in the worst case much lower than the lightning impulse withstand level of the equipment for all rated voltage level.

2) Nevertheless for GIS insulation, it has been shown that defects of the HV bars can greatly decrease the insulation level and in this case the VFTO produced at the strikes of the disconnector can cause failure especially for upper voltage level for which the LIWL is reduced compare to the rated voltage. So additional on site testing is required to detect defects which are sensitive to VFTO. Appropriate test procedures are currently under discussion.

3) For disconnector, a type test is necessary to ensure that there will not be any flashover between the arc between contacts and the enclosure during switching.

4) Regarding the GIS insulation the VFTO amplitude in normal configurations is lower than the protective level of arresters and therefore it cannot be significantly influenced by them.

5) A chopped lightning impulse test may be useful in assessing the reliability of transformers and bushing subjected to VFTO.

6) For equipment (transformers, bushings...) care must be taken in designing the links which must insure the limitation of the voltage between screens and earth. Such links must not have a too high inductance because for VFTO these links due to the voltage rise cannot ensure their task. Sparks between different "earthed" parts of the system can then occur.

7) For reducing the external VFTO between enclosures and earth, GIS designers must take care at each interruption of the enclosure. At the bushing the grounding leads can be coaxially mounted and the surge impedance of these leads should be as low as possible (low earth impedance). At the junction between enclosures or at the junction of the enclosure and the screen of a cable the straps or any non linear resistors can be also coaxially installed.

Some failures have been attributed to the VFT voltages sometimes wrongly sometimes truly. The levels of the VFTO are much lower than the LIWL and the dielectric strength of most of the equipment for VFTO exceeds the dielectric strength for lightning impulse (LI) voltages.

REFERENCES

[1] PFEIFFER W.: Impulstechnik, Carl Hansa Verlag München Wien, (1976), p. 44.

[2] PFEIFFER W.: Gesetzmäßigkeit beim Durchschlag von Funkenstrecken in komprimiertem Schwefelhexafluorid, ETZ-A Vol. 95 (1974), p. 405.

[3] BOGGS S.A., CHU F.Y., FUJIMOTO N.: "Disconnect switch induced transients and trapped charge in GIS". I.E.E.E. Trans. Vol. PAS-101, N° 10, October 1982.

[4] LALOT J., SABOT A., KIEFFER J., ROWE S.W.: Preventing earth faulting during switching of disconnectors in GIS including voltage transformer, IEEE Trans. Vol. PWRD-1, 1986, P. 203.

[5] BOGGS S.A., FUJIMOTO N., COLLOD M. and THURIES E.: "The modeling of statistical operating parameters and the computation of operation-induced surge waveforms for GIS disconnectors". 1984 CIGRE, paper 13-15.

[6] BOECK W. and WITZMANN R.: "Main Influences on the Fast Transient Development in Gas-Insulated Substations (GIS)". 5th ISH, Braunschweig, FRG, 1987. Paper 12-01.

[7] FUJIMOTO N., STUCKLESS H.A. and BOGGS H.A.: "Calculation of disconnector induced overvoltages in gas- insulated substations". In L.G. Christophorou and M.O. Pace (Eds.) *Gaseous Dielectrics IV*, Pergamon Press, New York, 1984.

[8] WITZMANN R.: "Fast Transients in Gas Insulated Substations (GIS). Modeling of Different GIS Components". 5th ISH, Braunschweig, FRG, 1987. Paper 12-06.

[9] FUJIMOTO N., DICK E.P., BOGGS S.A. and FORD G.L.: "Transient ground potential rise in gas-insulated substations - Experimental studies". IEEE Trans. on PAS, PAS-101, N° 10, October 1982.

[10] BOERSMA R.: "Transient Ground Potential Rises in Gas-Insulated Substations with respect to earthing systems". Electra N° 110, January 1987, p. 47.

[11] DICK E.P., FUJIMOTO N., FORD G.L. and HARVEY S.: "Transient ground potential rise in gas-insulated substations - Problem Identification and Mitigation". IEEE Trans. on PAS, *PAS-101*, N° 10, October 1982.

[12] FUJIMOTO N. and BOGGS S.A.: "Characteristics of GIS disconnector-induced short risetime transients incident on externally connected power system components". IEEE PES Winter Meeting, New Orleans, 1987. Paper 87WM185-2.

[13] LUHRMANN H.: "Ausgleichsvorgänge beim Schalten von Trennschaltern in SF_6-isolierten Schaltanlagen, ETZ-Archiv, Vol. 3 (1981), p. 209.

[14] BOSOTTI O., MOSCA W., RIZZI G., HASKOFF L., KYNAST E., LUHRMANN H.: "Phenomena associated with switching capacitive currents by disconnectors in metal enclosed SF_6-insulated switchgear, CIGRE 13-06, 1982.

[15] BOGGS S.A., CHU F.Y., FUJIMOTO N.: "Disconnect switch induced transients and trapped charge in gas-insulated substations. IEEE Trans. Vol. PAS-101, (1982), p. 3593.

[16] KYNAST E., GOROBLENKOW J., LUXA G., PATRUNKY H., MORITZ G., HENNINGSEN C.: "Investigation concerning the switching of disconnectors in an SF_6-insulated 380 kV substation, CIGRE 33-02, 1984.

[17] KONIG D., IMGRUND G., NEUMANN C., MAATZ K., SCHIWECK L.: "Vorgänge beim Schalten kleiner kapazitiver Strome mit SF_6-isolierten metallgekapselten Trennschaltern im 110-kV-Netz und ihre Simulation im Hochspannungslaboratorium. Elektrizitätswirtschaft, Vol. 85 (1986), p. 131.

[18] OGAWA S., HAGINOMORO E., NISHIWAKI S., YOSHIDA T., TERESAKA K.: "Estimation of restriking transient overvoltage on disconnecting switch for GIS. IEEE Trans. Vol. PWRD-1, (1986), p. 95.

[19] FUJIMOTO S.A., BOGGS S.A., STONE G.C.: "Mechanism and Analysis of short risetime GIS transients, CIGRE SC 15 Symp. Vienna 1987.

[20] FREISINGER F., MUHR M., DIESSNER A., SCHENNER H.: "Field measurement of fast transient voltages in the 420 kV Wien Sued. CIGRE SC 15 Symp. Vienna, 1987.

[21] LALOT J., SABOT A., KIEFFER J.: "Dielectric behaviour of GIS switching disconnectors comparison of possible phase opposition tests. IEEE SUMMER MEETING 1986 PAPER 86 SM 387-5

[22] BOECK W., WITZMANN R.: "Main influences on the fast transient development in gas-insulated substations (GIS), Int. Symp. on High Voltage Engineering (ISH), Braunschweig, 1987, paper 12-01.

[23] FESER K., KULIK P., MENTEN L.: "Dielectric field testing of GIS". CIGRE-Report 33-09, 1986.

[24] Meppelink et al: "Very Fast Transients in GIS". IEEE winter meeting 1988 PAPER 88 WM 114-1

[25] Aanestad et al: Substation Earthing with special regard to Transient Ground Potential Rise - Design Aims to Reduce Associated Effects - CIGRE 1988 paper 23.06.

[26] MULLER W., STEIN W.: "Behaviour of High-Voltage Transformer Windings on Steep-fronted Input Waves of Nanosecond Duration". Siemens Power Engineering V, N° 5, pp. 259-262 (1983).

[27] BREITFELDER D., BUCKOW E., KNORR W., PESCHKE W.: "Dielectric Strength of Transformer Oil Under Impuls and High Frequency Stress". 5. ISH, Braunschweig, 1987.

[28] EDLINGER A., MAUTHE G., PINNEKAMP F., SCHLICHT D. SCHMIDT W.: "Disconnector switching of charging currents in metal-enclosed SF_6-gas insulated switchgear at EHV. CIGRE-Report 13-14, Paris, 1984.

[29] CIGRE WG 13-04: "Requirements for switching tests of metal-enclosed switchgear. Electra, N° 110 (1987), First part pp. 7-23
Second part pp. 26-46.

[30] TASCHNER W.: "Voltage-time curves ov SF_6 insulation for steep fronted impulse voltages below 1 µs 8th Intern. Conf. on Gas-discharges and their Application. Oxford, 1985, p. 259.

[31] BOECK W., TASCHNER W., GORABLENKOW J., LUXA G.F., MENTEN L.: "Insulating behaviour of SF6 with and without solid insulation in case of Past Transients. CIGRE-Report 15-07, (1986).

[32] LUXA G., KYNAST E., BOECK W., HIESINGER W., PIGNI A., BARGIGIA A., SCHLICHT D., WIGART H., ULLRICH L.: "Recent research activity on the dielectric performance of SF_6, with special reference to very fast transients". CIGRE-Report 15-.., (1988).

[33] REYNDERS J.P., MODRY R., MEPPELINK J.: "Volt-time curves of disconnector generated fast transients in GIS". 5th Inter. Symp. on Gaseous Dielectrics, Koxville, (1987).

[34] CIGRE WG 13-04: "Requirements for switching tests of metal enclosed switchgear". Electra, N° 110, First part pp. 7-23
Second part pp. 26-46.

[35] KONIG D., IMGRUND G., NEUMANN C., MAATZ K., SCHIWECK L.: "Phenomena occuring during switching small capacitive currents with SF_6-insulated metalenclosed disconnectors in 110 kV-networks and their simulation in a high voltage laboratory (in German)". Elektrizitätswirtschaft Vol. 85 (1986), pp. 131-138.

[36] NISHIWAKI S., KANNO Y., SATO S., HAGINOMORI E., YAMASHITA S., YANABU S.: "Ground fault by restriking surge of SF_6 gas-insulated disconnecting switch and its synthetic tests". IEEE/PES-Conference paper 82 WM 187-3, Winter Meeting, New York, January/February 1982.

[37] DIESSNER A., LUXA G.F., MOSCA W., PAGINI A.: "High Voltage Testing of SF_6-Insulated Substations on Site". CIGRE, 1986 Session, Paper 33-06.

[38] LALOT J.: "On-Site Acoustic Detection of Abnormalities in Metal-Clad Substations". In BOGGS S.A., CHU F.Y. and FUJIMOTO N. (Eds.). *Gas-Insulated Substations - Technology & Practice.* Pergamon Press, 1986, pp. 322.

[39] OZAWA J., YAMAGIWA T., HOSOKAWA M., TAKEUCKI S., KOZOWA H.: "Suppresion of Fast Transient Overvoltages During Gas Disconnector Swintching in GIS" IEEE Trans. Vol. PWRD-1, N° 4, 1986, p. 174.

[40] LUXA, KYNAST, BOECK, HIESINGER, PIGINI, BARGIGIA, SCHLICHT, WIEGART, ULLRICH: "RECENT research activity on the dielectric performance of SF_6, with special reference to very fast transients" CIGRE 1988 paper 15-06.

APPENDIX 1 - GIS COMPONENT MODELLING

The most adopted modelling of GIS components, to simulate Very Fast Transients by digital programs, makes use of electrical equivalent circuits composed by lumped elements (capacitances, inductances and resistances) and distributed parameter lines, defined by their own surge impedance and travel time. The disconnector spark itself has to be taken into account by a transient spark resistance according to the Toepler (see 2.1) and the subsequent arc resistance of a few ohms.

Component	Equivalent circuit	Notes
Bus duct	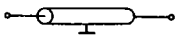	Loss-free distributed parameter transmission lines
Spacer		(c ≃ 20 ÷ 30 pF)
Elbow	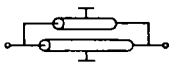	
Spherical shield	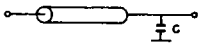	(c ≃ some pF)
Surge arrester	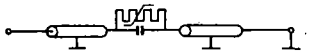	
Closed switch	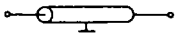	
Open switch	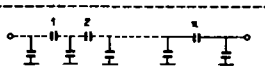	n = number of breaking chambers
Closed disconnector	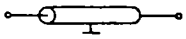	
Open disconnector		
Disconnector during sparking	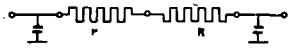	r = r(t) ; R = a few Ω c = a few tens pF
Bushing (capacitive type)	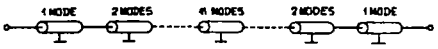	n = number of equivalent shields (5 ÷ 8) simulated
Bushing (gas filled)	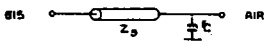	c = a few tens pF $z_s \simeq 250\,\Omega$
Power transformer (termination)	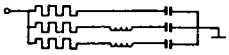	parameters evaluated from the frequency response of the transformer
Current transformer		sometime negligible
Capacitive voltage transformer		
Earth connection	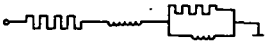	
Aerial line or long cable (termination)	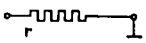	r = surge impedance

Series resistances or shunt conductances have to be included if Joule losses in the conductor or, respectively, dielectric losses cannot be neglected. Because of the high frequencies involved during VFT, in some GIS components only the dielectric losses need be taken into account (in the coaxial bushings, for instance).

The calculation of the parameters of the equivalent circuit is carried out from the electromagnetic field relevant to the particular components to be modelled. This approach is easy when the plane of the electric and magnetic field vectors is normal to the surge direction of propagation. On the contrary, when strong field distortions appear, such as in spherical arrangements or elbows (normally existing in GIS configurations), the evaluation of the parameters of the equivalent circuit is questionable. However, when studying phenomena with frequencies below 50 MHz, practical modelling experience teaches that a satisfactory agreement with the real behaviour of the GIS is reached even if such distortions are neglected; slight empiric corrections to the parameter calculation should be necessary at the most.

The next table shows the electrical equivalent circuits commonly adopted to represent the main components of a typical GIS; other solutions are sometimes adopted particularly for elbows and spherical shields -see the difficulties just mentioned- and for bushings, dependent on the accuracy to be reached and the frequencies of interest.

It is important to note that, in the table, all the distributed parameter lines take into account the internal mode (conductor-enclosure) only, supposing the external enclosure perfectly earthed. If Transient Enclosure Voltage has to be considered, it is necessary to add one more mode (enclosure-ground) since at high frequencies the earth connections assume significant impedance values.

REFERENCE

[1] "Guide for representation of network elements when calculating transients" in preparation by CIGRE WG 33.02.

[2] ARDITO A., SANTAGOSTINO G.: "A review of digital and analog methods of calculation of overvoltages in electric systems".
CIGRE SC 33 Colloquium 1985 Budapest.

[3] FUJIMOTO N., BOGGS S.A.: "Characteristics of GIS disconnector induced short risetime transients incident on externally connected power system components".
IEEE 87 WM 185-2.

[4] WITZMANN R.: "Fast transients in gas insulated substation (GIS) - Modelling of different gis components".
Fifth international symposium on high voltage engineering - Braunschweig, August 87.

APPENDIX 2 - MEASUREMENT

The measurement of the different VFTO's is performed with electric field sensors [1],[4]. Generally an electric field sensor consists of a measuring electrode connected via a measuring impedance to a reference area often at earth potential. The principle of all capacitive field sensors can be deduced from the first Maxwell equation [9]:

$$\int_{\vec{H}} \vec{H}\vec{dl} = \int_{\vec{A}} \vec{g}\vec{dA} + \varepsilon \int_{\vec{A}} \frac{\vec{dE}}{dt}\, dA$$

In an equivalent circuit the $\int_{\vec{H}} \vec{H}\vec{dl}$ can be replaced by a current source $i_0(t)$. The conduction current $\int_{\vec{A}} \vec{g}\vec{dA}$ is normally negligible in this application. With these assumptions the equivalent simplified circuit is given in Fig. 1. The equation for this circuit is then:

$$\varepsilon \int_{\vec{A}} \frac{\vec{dE}}{dt}\, \vec{dA} = i_0(t) = C_2 \frac{du}{dt} + \frac{U}{R} = i_C + i_R$$

Two possibilities exist to measure a voltage with an electric field sensor in a given electric field:

1) The sensor is terminated with the characteristic impedance of a measuring cable (e.g. $R = R_M = 50\Omega$). In this case the capacitive current i_C is much lower than the ohmic current I_R and therefore

$$u_M = R \cdot \varepsilon \cdot A_{eff} \cdot \frac{dE}{dt}$$

Thus the measuring voltage is porportional to the derivative of the electric field. To get the electric field (or the voltage) the signal has to be integrated. The upper frequency limit of such a sensor is proportional to $f_0 \sim 1/R.C_2$. To get a high upper bandwidth the capacitance C_2 has to be small (< 20 pF). This leads to a poor sensitivity at lower frequencies e.g. by a sensitivity of 10 V at 100 MHz, the sensitivity at 100 Hz is 120 dB lower and therefore the signal to noise ratio will be critical.

2) The sensor is terminated with a high impedance ($R > 1\ M\Omega$). This leads to ($i_C \gg i_R$):

$$u_M = \frac{A_{eff}}{C_2} \cdot \varepsilon \cdot E$$

The measured voltage is proportional to the electric field. If a TEM-mode can be assumed the electric field at the earth sides is proportional to the voltage at the inner bus. The capacitance C_2 includes any additional measuring capacitance C_M. Thus the voltage ratio U_1/U_2 can be adjusted. The lower cut-off frequency is proportional to $1/R.C_2$. The higher the capacitance C_2 the lower the lower cut-off frequency. In

addition the voltage ratio is increased by C_2. The limitatons of this sensor principle are the signal to noise ratio (gets smaller with increasing C_2), the cable length (as short as possible, depending on C_2) and the oscillations introduced by the inductance of any measuring circuit with concentrated C_2. This gives the upper frequency limitation.

Both principles are used in practical applications. In most cases the high ohmic termination is used with an enlarged sensor area [5] or with additional capacitances C_2 [3] or terminating networks [5],[6],[7] to get an adequate voltage ratio or with an impedance converter to increase R and to allow the connection of a long measuring cable [7].

Instead of considering the device as an electric field sensor (the general theory) the measuring device can also be treated as a capacitive voltage divider [1], [5]. In that case the current source i_0 in the equivalent circuit (Fig. 1) is replaced by the high voltage capacitance C_1. Applying a voltage to C_1 results in a current i_0 to the low voltage part.

The construction of the sensor area is adapted to the measuring problem (Fig. 2). In case of the measurement of VFT's inside the SF_6-enclosure the sensor area is mounted in a hole in the enclosure (Fig. 2a) or as a cylinder near the enclosure (Fig. 2b). Care has to be taken that the dielectric of the low voltage capacitancies has the same behaviour as the high voltage gas capacitance in respect to temperature and frequency.

To measure external transient voltages, e.g. at the enclosure, the spherical electric field sensor [8], [10] was developed. The sensor has also the high ohmic termination, but the transmission of the signal from the sensor to the instrument is done by an optical link (Fig. 2c).

One of the main problems of all these sensors is their calibration. This calibration has to be performed in the final field arrangement [10], e.g. for the flat sensor in the coaxial arrangement. The dimension of the sensor gives the sensitivity, but on the other hand the dimension should be small against the travel times of the transient field across the sensor compared to the rise time of the transient.

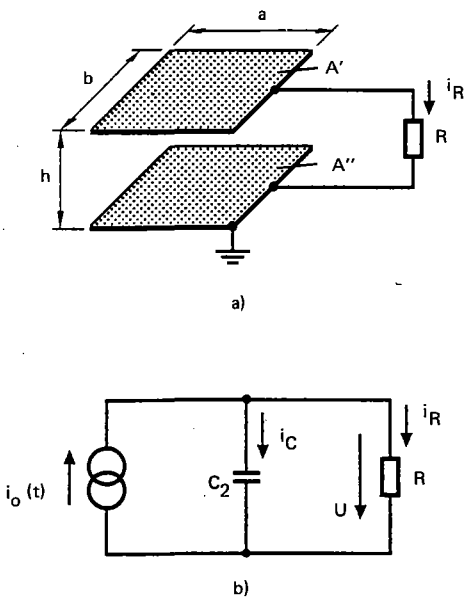

Fig. A1 — Principal diagram of electric field sensor.
a) Arrangement.
b) Equivalent simplified circuit (C_2 - capacitance between plates A).

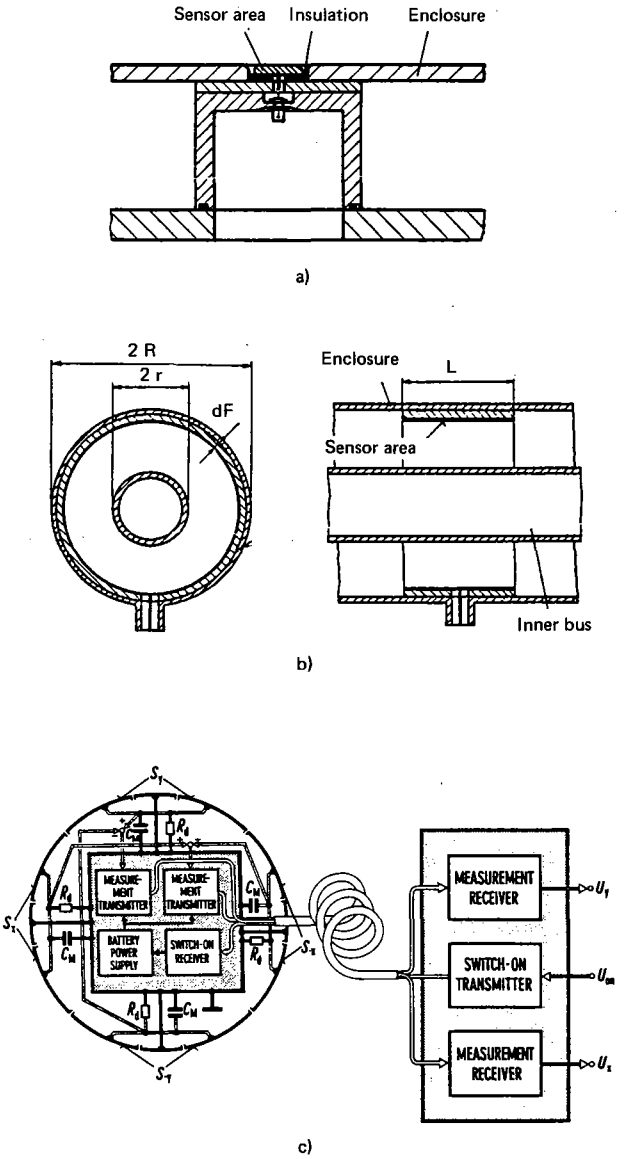

Fig. A2 — Examples of electric field sensors.
a) Sensor with circular area in the encapsulation /7/.
b) Sensor with enlarged cylindric area /5/.
c) Spherical electric field sensor /8/ (complete system).

All the built sensors have an upper bandwidth of at least 100 MHz ([1]...[8]), limited by resonances in the input circuits. The sensors differ in the lower cut-off frequency, depending on the input resistance R and the used capacitance C_2. Typical values are some Hz (C_2 > 20 nF, R > 1 MΩ [8],[5]) to some kHz [7]. With a cut-off frequency below 50 Hz the sensor can be calibrated with 50 Hz.

REFERENCE

[1] BOGGS S.A., FUJIMOTO N.: "Technique and Instrumentation For Measurement of Transients in Gas-Insulated Substations". IEEE Trans. on El. Insulation Vol. EI-19, N° 2. 1984, pp. 87-92.

[2] BOLOGNESI F., ELLI E., RIZZI G., THIONE L.: "A capacitive Probe Device for Fast Transient Measurements in SF_6-insulated Installations". 4 Int. Symp. on High Volt. Engineering, Athens, 1983.

[3] FREISINGER F., MUHR M., DIESSNER A., SCHENNER H.: "Field Measurements of Fast Transient Voltages in the 420 kV-GIS Wien Sued". CIGRE Symp. Vienna (1987).

[4] PFEIFFER W.: "Fast Measurement Technique for Research in Dielectrics". IEEE Trans. on El. Insulation Volt. EI-21 N° 5, 1986, pp. 763-780.

[5] KÖNIG D., IMGRUND G.: "Transiente Ausgleichsvorgänge beim Schalten von Trennschaltern in SF_6-isolierten Anlagen". PTB-Bericht-E-28 Dez. 1986, S. 65-71.

[6] LALOT J.: "Generation and Measurement of Fast Transient Over-voltages with Special Reference to Disconnector Operations in GIS". CIGRE 33-86 (WG 03) 35 IWD.

[7] WITZMANN R.: "Ein Meßsystem zu Erfassung von schnellen transienten Vorgängen in metallgekapselten SF_6-isolierten Schaltanlagen". To be published in etzArchiv (1987).

[8] FESER K., PFAFF W.: "A potential Free Spherical Sensor for the Measurement of Transient Electric Fields". IEEE Trans. on PAS Vol.-103, N° 10, 1984, pp. 2904-2911.

[9] FESER K.: "Fast High Voltage Measuring Systems". Colloquium of IEEE, London, April 1986.

[10] FESER K., PFAFF W., WEYRETER G., GOCKENBACH E.: "Distortion-Free Measurement of High Impulse Voltages". IEEE on PAS 87 WM 177-9, 1987 New Orleans.

PERFORMANCE OF METAL-CLAD DISCONNECTOR AND ITS IMPACT ON THE INSULATION DESIGN OF GAS INSULATED SUBSTATIONS

by

A. BARGIGIA *, A. PORRINO
ENEL

B. MAZZOLENI
Nuova Magrini Galileo

W. MOSCA, G. RIZZI
CESI

(Italy)

Summary

Fast transients, originated in a GIS when operating disconnectors, may be responsible for insulation failures on substation components. The most important factors that determine these failures are both the behaviour of the disconnector during its operation and the insulation withstand under these particular overvoltage shapes. In order to define adequate technical specifications both for the disconnectors and for the insulation design of the metal-clad components, a series of investigations and laboratory tests were performed that are described in this paper.
Tests were performed on disconnectors by means of different testing arrangements to simulate different GIS configurations. The influence of the test parameters, such as the ratio between surge and load capacitances and the amplitude of the switched currents, were investigated to identify the behaviour characteristics of disconnectors of different design and operating voltage.
The insulation withstand of GIS components was investigated by reproducing the overvoltages due to disconnectors that are characterized by a fast oscillation superimposed on a prestressing direct voltage.
On the base of these experimental investigations, the test arrangement and procedure were established together with the quantities to be measured that are suitable to better characterize the disconnector behaviour. The test results are given and explained on the base of a mathematical model of the disconnector during switching.
It was also found that the insulation strength under fast transients is remarkably influenced by the presence and the amplitude of the prestressing direct voltage. This can help to explain the insulation flashovers occurred in laboratory and in field.
Some indications on the impact of fast transients on insulation co-ordination are given.

Keywords

Composite insulation stresse., Insulation co-ordination, Metal-clad disconnector , Testing procedure , Transient overvoltage .

* ENEL Centro di Ricerca Elettrica, via Volta 1, 20093 Cologno Monzese (MI), Italy.

1. Introduction

The performance of a metal-clad disconnector during switching operation of capacitive currents has been widely studied due to its impact on the reliability of the gas insulated substations [1], [2], [3].
The investigation of the behaviour of the disconnectors during operation under different service conditions aims to determine the dielectric withstand capability of the disconnector itself and of the metal enclosed equipment under the overvoltages generated in the different location of the gas insulated substation.
Particular attention must be paid to the characterization of the disconnector due to its statistic behaviour. Special testing procedure has been defined to this pourpose.
The insulation strength of the equipment under the non standard wave shapes generated by disconnector operation (fast transients superimposed to direct voltage components), must be taken into account.
Finally, the insulation coordination strategy has to face the problems connected to decreasing of the margins between Lightning Impulse Withstand Voltage (LIWV) with the system voltage levels.

2. Switching overvoltages caused by disconnector operations

The operation of a disconnector occurs through several restrikes leading to a succession of overvoltages, characterized by a fast transient component superimposed to a direct voltage component (Figure 1). These overvoltages depend on the substation configuration, on the operating conditions and on the design of the disconnector.
The transient caused by a single restrike extinguishes in a few microseconds, well before a subsequent restrike occurs, so that each transient can be evaluated independently from the others.
The overvoltage U(t) to earth, caused by a single restrike, at a given location P in the substation, can be expressed, as reported in [1], as:

$$U(t) = Uo + k(t) * DU \qquad (1)$$

where:

- Uo is the preexisting voltage at the point considered and DU is the voltage difference at the disconnector terminals before the restrike.

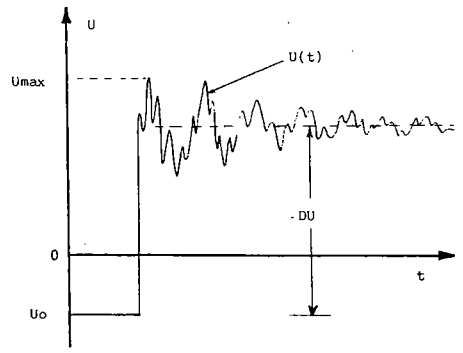

Figure 1 :Typical overvoltage due to disconnector operation. Uo is the preexisting voltage, DU the voltage difference at the disconnector terminals before restrike. Umax = Uo + K * DU where K is invariant from one restrike to another.

- k(t) is the overvoltage factor that depends only on the point considered and on the substation layout at the moment of the disconnector operation and does not change from one restrike to the other.

The maximum peak overvoltage Umax caused by the operation of the disconnector corresponds to the peak K of k (t) and depends on the combination of Uo and DU; the maximum overvoltage in the substation is reached in the point where the maximum value K (Kmax) occurs. Kmax depends on the substation layout but not on the type of disconnector.
Uo and DU are statistical variables, depending mainly on the characteristics of the disconnector and on switching conditions.
Thus, the evaluation of the overvoltage caused by disconnector operations can be performed by a two steps process:

- evaluation, by means of computer simulation (EMTP), of the response characteristic of the substation, Kmax;
- identification, on the basis of experimental measurements, of a statistical model of the disconnector that provides the distributions of Uo and DU.

3. Switching conditions

Disconnectors may operate in service, when opening or closing capacitive currents of bus-bar sections, under different substation switching conditions. These conditions are summarized in the following:

- opening and closing with only one terminal fed at AC phase voltage;
- closing and opening with two terminals fed at AC voltage out of phase;
- closing with one terminal fed at AC voltage and the other with a DC voltage.

The voltage conditions at the beginning of the closing and opening operations where analyzed in [1]. The voltage values depend on the presence of grading capacitors on Circuit-Breakers (CB), on the characteristics of the disconnectors and on the operation conditions and sequences.
The cases of CB with and without grading capacitors are here analysed when opening a no load line or cable both in the case of discharge and no discharge of the charge trapped on the line before the operation of the disconnector.
In the Table I the voltage conditions before operation of the disconnector are given under the following assumptions: trapped charge left by the CB or the disconnector equal to 1.3 or 0.4 p.u. of the peak of the phase to earth voltage respectively; ratio between capacitance to ground of the bus bar section between disconnector and CB and capacitance across the CB equal to 0.2. It results that, with CB equipped with grading capacitors, voltage differences across disconnector terminals may reach values up to 2.5 p.u.. Lower values are obtained if, before switching, a sufficient time to discharge the line elapses.

TABLE I: Voltage at disconnector terminals before its closing operation

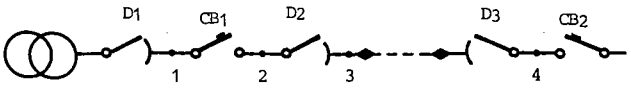

a): CB with grading capacitors

CB WITH GRADING CAPACITOR	NO DISCHARGE OF THE LINE BETWEEN CB1 AND D2 OPERATION			DISCHARGE OF THE LINE BETWEEN CB1 AND D2 OPERATION		
OPERATION SEQUENCE D1 CB1 D2 D3 CB2	VOLTAGE AT POINTS 1 2 3		VOLTAGE ACROSS D2	VOLTAGE AT POINTS 1 2 3		VOLTAGE ACROSS D2
C C C O O	1 AC	1 AC 1 AC	-	1 AC	1 AC 1 AC	-
C O C O O	1 AC	1.3 DC 1.3 DC	-	1 AC	1.3 DC 1.3 DC	-
C O O O O	1 AC	1.3 DC 0 + 0.8 AC	1.3 DC + 0.8 AC	1 AC	0.8 AC 0	0.8 AC
O O O O O	-0.4 DC	1.6 DC 0	1.6 DC	-0.4 DC	0.3 DC 0	0.3 DC
O O O C O	-0.4 DC	1.6 DC 0	1.6 DC	-0.4 DC	0.3 DC 0	0.3 DC
O O O C C	-0.4 DC	1.6 DC 1 AC	1.6 DC + 1 AC	-0.4 DC	0.3 DC 1 AC	0.3 DC + 1 AC

b): CB without grading capacitors

CB WITHOUT GRADING CAPACITOR	NO DISCHARGE OF THE LINE BETWEEN CB1 AND D2 OPERATION			DISCHARGE OF THE LINE BETWEEN CB1 AND D2 OPERATION		
OPERATION SEQUENCE D1 CB1 D2 D3 CB2	VOLTAGE AT POINTS 1 2 3		VOLTAGE ACROSS D2	VOLTAGE AT POINTS 1 2 3		VOLTAGE ACROSS D2
C C C O O	1 AC	1 AC 1 AC	-	1 AC	1 AC 1 AC	-
C O C O O	1 AC	1.3 DC 1.3 DC	-	1 AC	1.3 DC 1.3 DC	-
C O O O O	1 AC	1.3 DC 0	1.3 DC	1 AC	0 0	-
O O O O O	-0.4 DC	1.3 DC 0	1.3 DC	-0.4 DC	0 0	-
O O O C O	-0.4 DC	1.3 DC 0	1.3 DC	-0.4 DC	0 0	-
O O O C C	-0.4 DC	1.3 DC 1 AC	1.3 DC + 1 AC	-0.4 DC	0 1 AC	1

O= Opening C=Closing
Voltage in p.u. of the peak value of the phase to earth voltage

4. Disconnector behaviour

The disconnector should be submitted to laboratory tests to determine whether, during operation, the arc between contacts involves the earth or not and to determine the distributions of the values Uo, DU and Ur (residual voltage at the end of each opening operation) which depend in principle on the design of contacts and on their speed. The possibility of evolution of the arc to earth is related to the maximum length of the arc between contacts and thus to the total arcing time At which is peculiar of the disconnector design.
As the operating conditions may in principle influence the disconnector behaviour, the tests should be performed in order to cover all the worst actual service conditions. These quantities which

may influence the disconnector behaviour are:

- amplitude of the switched current;
- ratio between the source side and the load side capacitance (Cs/Cl);
- type, amplitudes and combinations of supply voltages at both terminals of the disconnector in the switching condition.

The switched current and the ratio Cs/Cl depend on the rated voltage of the substation and its layout. The switched currents are in the range 0.01-0.5 A. The ratio Cs/Cl, which has an influence on the distributions of trapped charges Uo and thus on voltage collapses DU, may vary in a wide range under operating conditions. Normally Cs is much higher than Cl.
To evaluate the influence of the amplitude of the switched current and of the ratio Cs/Cl tests have been performed feeding one terminal of the disconnector with AC at 1 p.u..
Figure 2 reports At, DU and Ur as a function of the switched current. The tests were performed varying the switched current between 0.02 and 0.5 A and keeping constant the ratio (Cs/Cl). The figure does not show any evident dependence on the current of the above parameters at least within the range of currents considered.

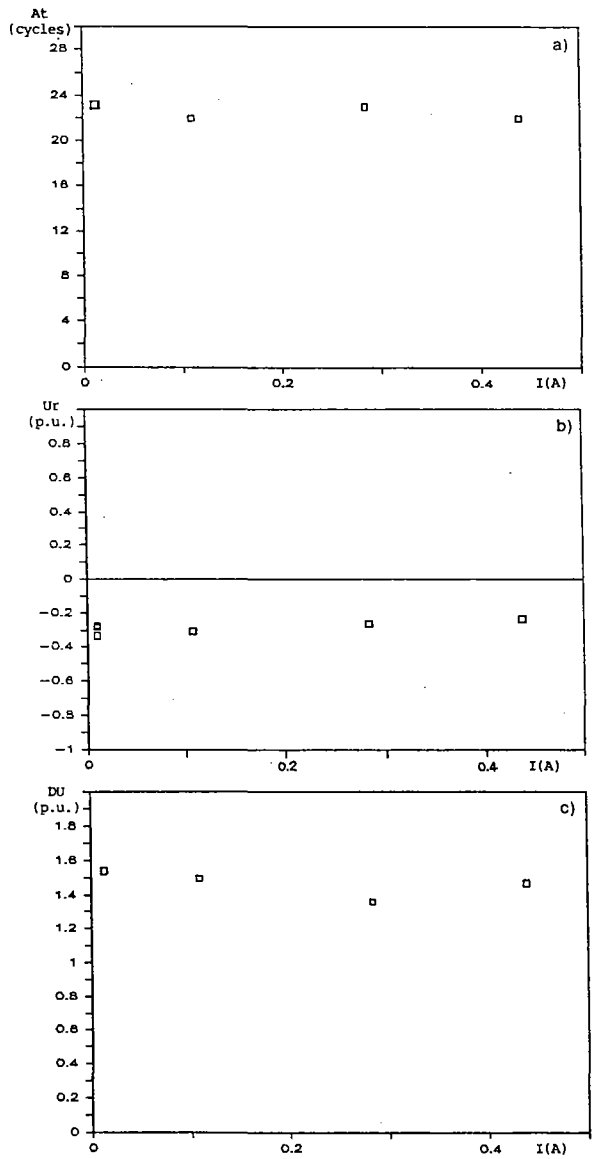

Figure 2 :Influence of the switched current on the arcing time At, on the residual voltage after opening operations Ur and on the maximum voltage difference at disconnector terminals before restrike DU.

Figure 3 reports At, DU, and Ur as a function of Cs/Cl. Tests were performed varying Cs/Cl between 10 and 90. The Figure 3 shows a dependence of At and DU on Cs/Cl while the residual voltage Ur does not.
The overvoltage factor K depends on the testing circuit, and thus on the ratio Cs/Cl being maximum for the highest values of the ratio. Figure 4 reports the maximum overvoltage to ground obtained in laboratory as a function of Cs/Cl.
It can be said that, for the characterization in laboratory of the disconnector performance, the value of Cs/Cl should be of the order of at least 15 while, if it is needed to maximize the dielectric stress on the tested bus-bar arrangement, even higher values should be adopted.

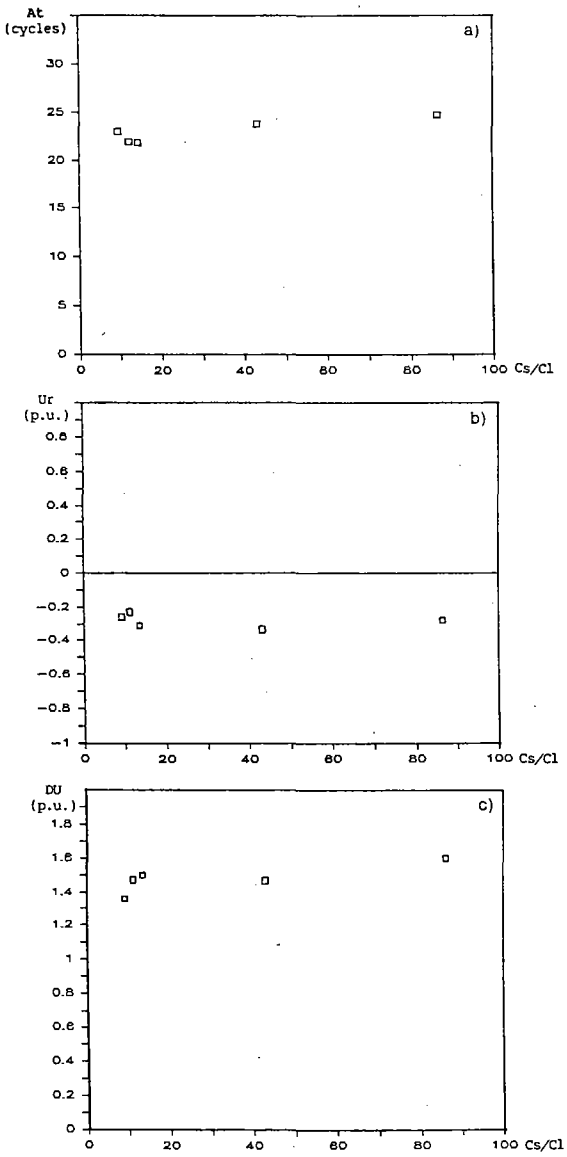

Figure 3 :Influence of the ratio between source and load side capacitances (Cs/Cl) on the arcing time At, on the residual voltage after opening operations Ur and on the maximum voltage difference at disconnector terminals before restrike DU.

To find the maximum interrupting distance and its dependence on the feeding conditions, several tests have been performed. The breakdown voltages between disconnector contacts in a fixed position at variuos distances ("static" dielectric characteristic) were

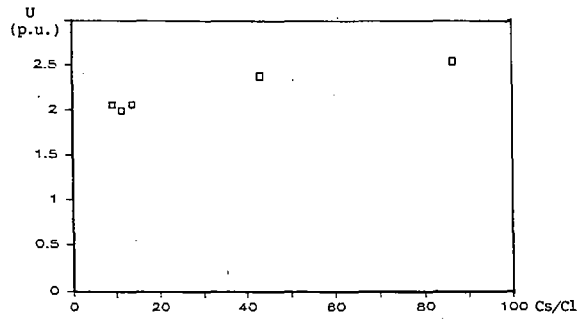

Figure 4 :Maximum overvoltage to earth obtained in laboratory as a function of the ratio between source and load side capacitances Cs/Cl.

determined. Figure 5 gives an example of the breakdown voltages of a disconnector when fed from only one terminal the other being earthed; while Figure 6 gives an example of the characteristics of the same disconnector when fed from the two terminals [4]. The figure shows that:

- the total strength is higher when energizing the two contacts than when energizing a single contact;
- breakdown voltage with AC-AC supply (out of phase) is equal or slightly lower than with AC-DC supply;
- the well known non symmetrical breakdown voltage of the gap is evident.

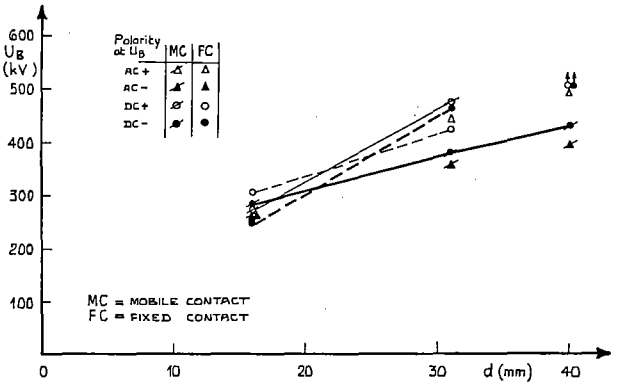

Figure 5 :Typical dielectric characteristic of the longitudinal insulation of a disconnector, when fed from one terminal, the other terminal being earthed. Average breakdown voltage versus the distance between contacts (distance measured from contact parting). Test with DC and AC voltages.

Figure 7 gives an example of the comparison between "static" and "dynamic" discharge characteristics of a disconnector. The figure reports the time of closing operation (proportional to the distance between the contacts for the same disconnector) as a function of the total strength between the contacts; for AC-AC out of phase supply all the avaible cases were considered while for AC-DC supply only the most critical polarity combinations were considered. The figure confirms that the AC-AC supply is equal or slightly more critical than AC-DC at least from the point of view of the maximum length of the arc between the contacts.
From the above considerations it derives that, to verify correctly the maximum arcing time At (which is related to the possibility of an evolution of the arc to the enclosure) both for opening and closing it is required to apply between the contacts the maximum voltage stress combination foreseen in service conditions; in addition the highest voltage value has to be applied at the terminal which gives the maximum voltage gradient.

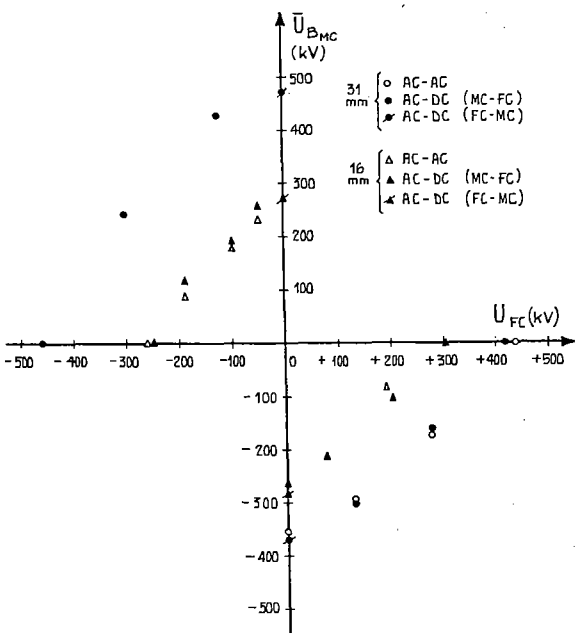

Figure 6 :Typical dielectric characteristics of the longitudinal insulation of a disconnector when fed from both terminals (AC on one terminal and AC or DC on the other terminal). Average breakdown voltage (value on the mobile contact) versus the corresponding value on the fixed contact.

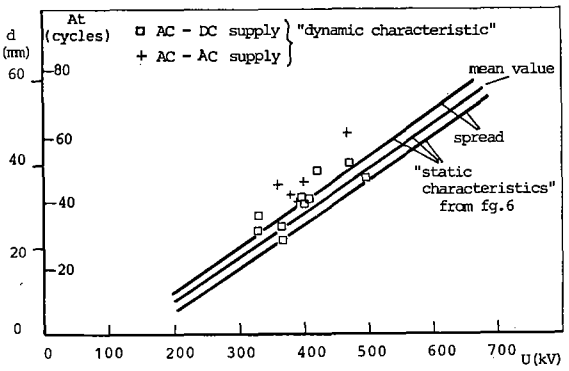

Figure 7 :Maximum arcing distance when closing disconnectors as a function of the total strength between the contacts. The "dynamic" characteristic is compared with the "static" one.

5. Analysis of disconnector behaviour

As it was said in chapter 2, the disconnector should be characterized also by the voltage left on the load side after each restrike, Uo, by the voltage difference at its terminals when restiking, DU, and by the residual voltage after opening, Ur. These quantities can easily be measured in laboratory and recorded. An example of the records obtained during an operation is given in Figure 8 where the voltage drop at each restrike is plotted versus the time.
As Uo, DU and Ur are statistical variables, a sufficient number of disconnector operations should be performed. To establish this, a mathematical model of the disconnector was set up. The model allows the simulation of a disconnector operation whose main characteristics (e.g. the speed of the contacts, the asymmetry of the withstand between terminals and the dispersion of the withstand) are known. It can fairly well reproduce the sequence of the voltage collapses of the restrikes during operation as it is shown in Figure 8. The model allows also an analysis of the influence of the

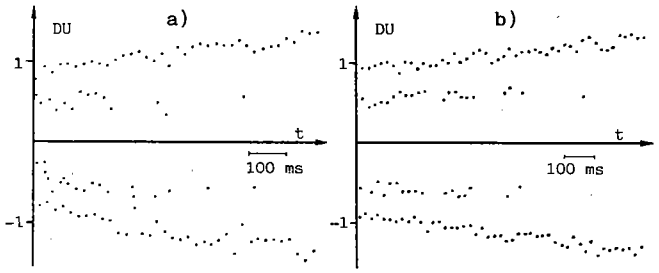

Figure 8 :Example of sequences of voltages across terminals of a disconnector during opening.
a) measurements from laboratory tests.
b) mathematical model.

various parameters characterizing the disconnector on the distributions of the values Uo, DU and Ur.
Figure 9 shows the maximum DU and Ur obtained by simulating 8 times groups of a fixed number N of disconnector operations ranging between 13 and 800. It results that the average value increases with N, while the dispersion decreases. 200 operations in laboratory seem the minimum acceptable number to characterize with a certain accuracy the disconnector.
The overvoltage due to a certain restrike characterized by a couple of values Uo and DU (voltage before restrike and voltage between contacts respectively) can be evaluated by means of the formula (1) U = Uo + K * DU. Generally the maximum overvoltage during an opening or closing operation of a disconnector does not correspond to the last restrike or the first one respectively but to an unfavourable couple of values Uo and DU. From the simulations with the model it resulted that it is possible to calculate with a sufficient accuracy the maximum overvoltage due to a certain type of disconnector by using the couple of values Uo=1-DUmax and DUmax (where DUmax is the maximum voltage drop measured in laboratory), instead of the worst couple Uo and DU. This procedure leads to a very little overestimation of the maximum overvoltage (less than 5%). The maximum value of DU seems thus sufficient to characterize a disconnector from this point of view.
Figure 10 shows the maximum values 1 - DU and Ur, obtained by several groups of 200 simulations each, for different types of disconnectors. The correlation between 1 - DU and Ur seems insufficient to allow the estimation of the maximum Ur from the maximum DU only. Both maximum DU and Ur have thus to be measured and recorded in laboratory to identify a disconnector.
The model was also extensively used to investigate the effects of the different design characteristics of a disconnector on the parameters DU and Ur that identify its behaviour from the point of view of overvoltages.

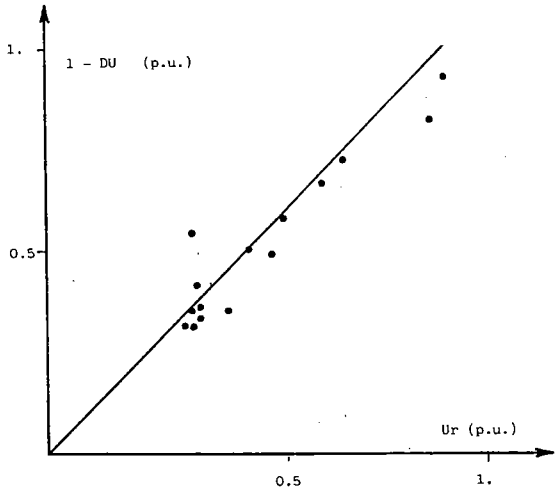

Figure 10 :Couples of the maximum values 1-DU and Ur obtained by several groups of 200 simulations each of disconnector operations of different design characteristics. (DU = maximum voltage across disconnector terminals at restrike, Ur = maximum residual voltage left by opening operations).

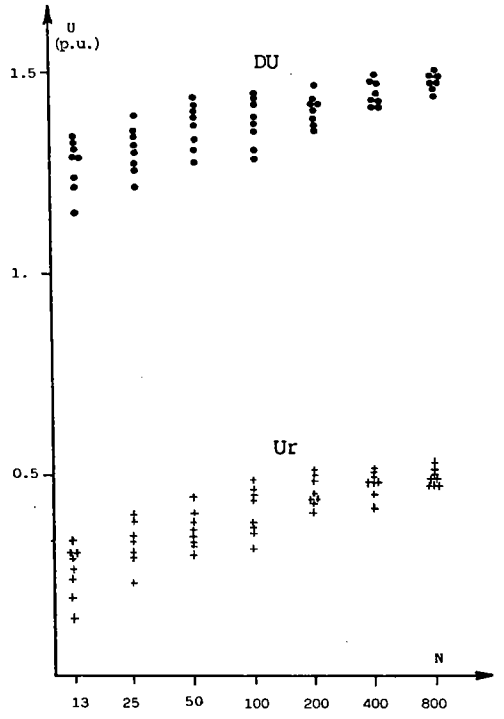

Figure 9 :Maximum values of DU (voltage collapse between disconnector terminals) and Ur (residual voltage after opening) obtained by simulating 8 times groups of the given number N of disconnector operations.

As the dispersion of the withstand between contacts resulted of the order of 4, 5% for all the disconnectors tested (from 245 kV to 1050 kV), the analysis was performed mainly to see the effect of the asymmetry and of the speed of contacts. Figures 11 and 12 show the effect on the maximum DU of these two parameters. Both appear to have a great impact on the behaviour of the disconnector.

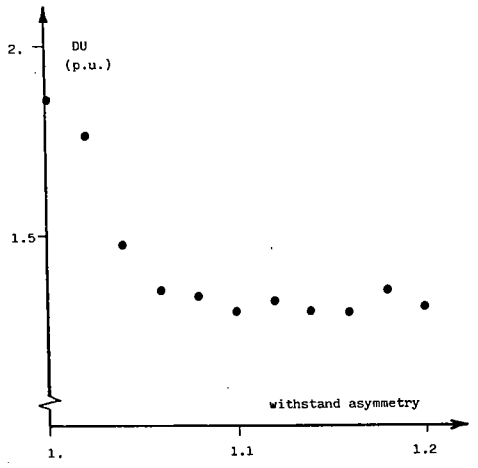

Figure 11 :Maximum value DU (voltage collapse between disconnector terminals) obtained by simulating groups of 1000 disconnector operations, for different asymmetry degrees of the withstand between contacts. The disconnector simulated reaches 1 p.u. positive withstand voltage between contacts in 1500 ms.

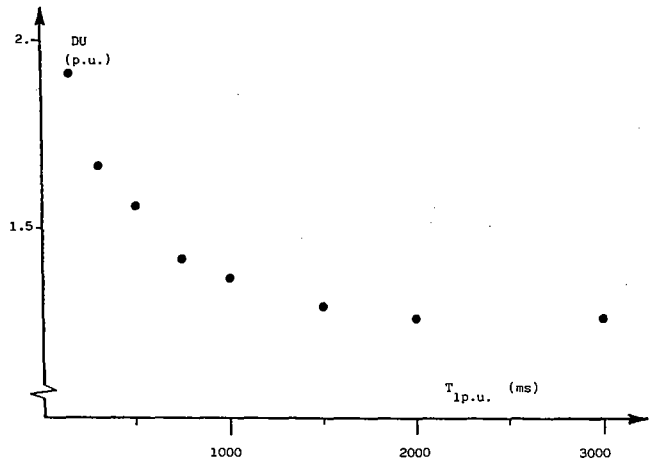

Figure 12 :Maximum value DU (Voltage collapse between disconnector terminals) obtained by simulating groups of 1000 disconnector operations for different speeds of the contacts. The speed of the contacts is expressed through T1p.u. that is the time needed to reach a U50% positive withstand voltage between contacts equal to 1 p.u.. The disconnectors simulated have a withstand asymmetry equal to 1.1.

As regards the asymmetry it has to be said that the plots of the values DU obtained in laboratory on the different disconnectors tested (see Figure 8) show that the actual "dynamic" asymmetry is lower than 1.1, while the dielectric asymmetry that could be expected from the asymmetry of the electric fields due to the electrode shapes is much higher.

6. Insulation strength under disconnector overvoltages

As already said, the stress to ground on the load side of the disconnector is a fast transient superimposed to a DC voltage. Systematic research was carried out to determine the strength of real configurations with different gas pressures under composite stresses [5], [6].
The Figure 13 gives the lowest strength limit curve obtained during the tests. It appears the great influence of the presence of the DC component on the withstand that can explain some insulation breakdowns occurred in service.
The limit curve was obtained with a duration of the DC prestress sufficiently long to be at least comparable to the duration occurring when closing a disconnector in presence of a trapped charge left by a previous opening operation. Under these conditions the value of DU at the first restrike is equal to the phase voltage plus the trapped charge Ur and the maximum overvoltage in p.u. is thus

$$Umax = (1 - Ur) * Kmax + Ur. \qquad (2)$$

This overvoltage, due to the weakening of the withstand caused by the long permanence of the DC component, results more critical than the overvoltages generated by the subsequent restrikes in closing and opening operations.

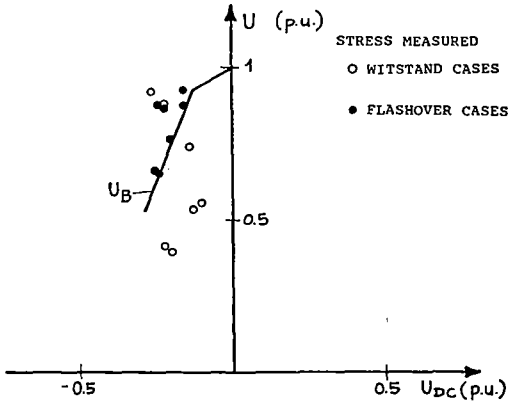

Figure 13 :Tests with composite stresses (LI + DC). Minimum observed breakdown voltages (total voltage to ground at breakdown) obtained after a large number of test repetitions versus the value of the applied DC component (1 p.u. = minimum observed breakdown voltage under negative LI without DC prestress at the examined pressure).

7. Application to the insulation design

An example of the application of the above results to the insulation design is given in figure 14. In the figure the limit withstand curves under composite stresses (derived from figure 13 assuming the minimum breakdown voltage under negative lightning impulse equal to the LIWV) are reported together with some curves representing the overvoltages calculated with formula (2) for constant values of the overvoltage factor (Kmax = 2, 1.5 and 1.2).
Three different voltage systems were considered:

- 245 kV having a LIWV of 850kV and characterized by a ratio B between the LIWV and the peak value of phase to earth voltage equal to 4.25
- 420 kV having a LIWV of 1300 kV (B=3.79)
- 1050 kV having a LIWV of 2250 kV (B=2.62)

It is worth noticing that the considerations that can be derived from the figure can be applied to systems having different voltage levels but the same ratio B.
The following remarks can be made:

- for systems having a ratio B=4.25 practically all the situations examined are below the limit curve except for some particular situations with very high trapped charges (greater than 0.9 for K = 2)
- for systems having value of B=2.62 critical values

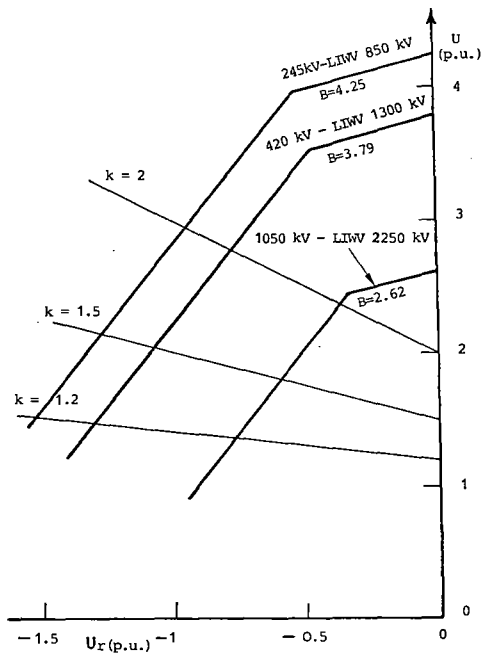

Figure 14 :Comparison between limit withstand curves under composite stresses, for different system ratios B between LIWV and system voltage levels, and overvoltage levels due to disconnector operations for different disconnector characteristics (maximum residual voltage Ur after opening) and overvoltage factors Kmax.

are obtained with Ur = 0.35 and K=2 or Ur = 0.6 an K = 1.5.
- for systems having B values between 2.62 and 4.25 intermediate situations will result.

A first general indication is that, as a good rule, the trapped charges should be limited to those left by the operation of the disconnector itself avoiding those left by the operation of circuit-breakers. If this would result insufficient, the overvoltage factor K should be reduced by means of a proper overvoltage control for example with closing and opening resistors. As an example the figure 15 reports the K values calculated for a 1050 kV substation as function of the resistor value. It can be seen that the overvoltage factor can be reduced down to 1.2 with a resistance of about 100 OHM. In such a case the overvoltages are acceptable with values of Ur up to 0.75.

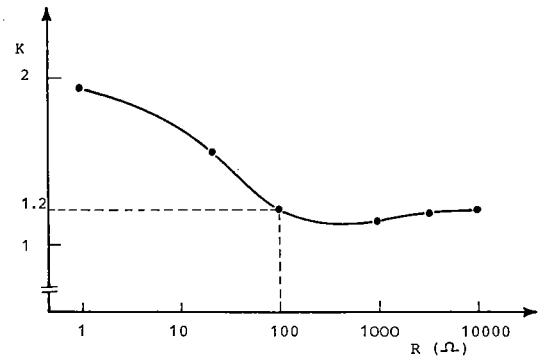

Figure 15 :Example of the dependence of overvoltage factor K on the value of the opening and closing resistor in case of a 1050 kV metal-clad substation.

8. Conclusions

The nature of the overvoltages generated by disconnector operations in a GIS allow to separate the problem of their evaluation into two independent steps: the evaluation of the transient response of the substation through computer simulations and the identification of the behaviour of the disconnector through laboratory tests.

Extensive laboratory investigations allowed the assessment of the main test conditions suitable to identify the parameters that characterize the disconnector behaviour (arcing time At, maximum voltage difference between contacts DU, and maximum residual voltage Ur). In particular it was found that the ratio between the capacitances on the source side and on the load side (Cs/Cl) should be at least 15 and even greater to maximize the generated overvoltages if the withstand of the gas insulated equipment has to be checked.

To investigate the possibility of evolution of the arc between contacts towards the enclosure, it is required to apply at two terminals of the disconnector the stress combination which gives:
- the maximum voltage difference independently of the type of stress (AC or DC) in a closing operation
- the maximum AC voltage difference in an opening operation.

A mathematical model of the disconnector was set up and used to investigate the variation of the parameters that identify its behaviour (DU and Ur). The model confirmed the need to perform a sufficient number of closing and opening operations (at least 200) to cope with the dispersion of the parameters. The same model can be used to investigate the influence of some design features (asymmetry and speed of contacts) on the disconnector behaviour.

The investigations on strength of GIS components under the composite overvoltages generated by disconnector operation put into evidence a high influence of the DC component (trapped charge). Trapped charges are lower when CB are not equipped with grading capacitors and are greatly influenced by switching sequences and timing of operations. The results were used to give indications on the problem of the insulation design for GIS when considering overvoltages generated by disconnectors. Resistors appear the most effective means to reduce the overvoltage down to acceptable values.

9. Acknowledgments

The authors are greatful to Mr A. Cattaneo of CESI for his valuable contribution for the co-ordination of the laboratory activity and for the evaluation of the results.

10. References

[1] A. Bargigia, A. Porrino,G. Rizzi, G. Santagostino, B. Mazzoleni: "Contribution to the choice of the dielectric withstand levels of SF6 Gas Insulated Substations". CIGRE 1984, 33-13.

[2] J. Lalot, A. Sabot, J. Kieffer, S.W. Rowe: "Preventing earth faulting during switching of disconnectors in GIS including voltage transformers". IEEE Trans. Vol. PWRD-1, 1986.

[3] A.A. Boggs, F.Y. Chu, N. Fujimoto: "Disconnect switch induced transients and trapped charges in gas insulated substations". IEEE Trans. Vol. PAS-101, 1982.

[4] A. Bargigia, G. Mazza, A. Pigini, G. Rizzi: "Strength of typical GIS configurations with special reference to composite and combined stresses". 5th Int. Symp. on Gas. Diel., Knoxville, 1987.

[5] G. Luxa, E. Kynast, W. Boeck, H. Hiesinger, A. Pigini, A. Bargigia, D. Schlicht, N. Wiegart, L. Ullrich: " Recent research activity on the dielectric performance of SF6 with special reference to very fast transients". CIGRE 1988, 15-...

[6] A. Bargigia, G. Mazza, A. Bertazzi, W. Mosca, A. Pigini: "The dielectric strength of SF6 configurations under impulses superimposed to DC voltages. Impact on the design of AC insulated substations". IEEE Int. Conf. on Prop. and Appl. of Diel. Mater., Xi'an China, 1985.

International Conference on Large High Voltage Electric Systems

112, boulevard Haussmann — 75008 Paris

1988 Session — 28th August - 3rd September

O

33-09

Pref. Subj. 3

DISCONNECTOR OPERATIONS IN GAS INSULATED SUBSTATIONS OVERVOLTAGE STUDIES AND TESTS ASSOCIATED WITH A 420 kV INSTALLATION

by

J. LEWIS*, B.M. PRYOR
South of Scotland Electricity Board

C.J. JONES, T. IRWIN
NEI Reyrolle Ltd

L.C. CAMPBELL, A. AKED
University of Strathclyde
(United Kingdom)

SUMMARY

The first part of the paper describes extensive computer studies undertaken to evaluate the overvoltages arising from a range of disconnector operations on a 420kV, 8 circuit-breaker mesh substation which will control the output of a nuclear generating station. The results are analysed in a number of ways showing maximum voltage changes; maximum peak voltages and maximum voltage reversals as well as the rates of change of these values. The maximum computed value of voltage change was 3.58pu and was associated with a rate of change of 3.3MV/μs. These may not necessarily be the characteristics which impose the severest stress on the insulation and other characteristics are analysed in some detail.

All the computed waveforms indicate that the overvoltages have three predominant frequencies in the 0-3MHz, 5-17MHz and 30-100MHz ranges respectively.

A series of tests, on the same type of disconnector, in the more onerous out-of-phase mode were undertaken in order to verify adequate capability during certain synchronising operations. These are described in the latter part of the paper. Overvoltage studies carried out using a transient network analyser (TNA) to ensure that the test circuit adequately represented the actual installation are also presented.

Key Words Gas insulated substations; disconnector operation; overvoltages; out-of-phase tests; SF_6.

INTRODUCTION

Gas insulated substations (GIS) have now been in operation for a number of years and their reliability continues to improve. Phenomena arising from the operation of disconnectors, particularly at higher voltages, continue to occupy a great deal of investigational time. Increasing emphasis is now being placed on the need for careful design of the disconnector contacts, to ensure that 'break-out' of the arc does not take place within the disconnector.

Equally important, from the point of view of the overall integrity of the GIS, are the overvoltages set up at other points, possibly remote from the disconnector but resulting from its operation. The characteristicts of these overvoltages have been described in a number of reports but in most cases they have been related to comparatively simple test arrangements (1).

In view of the electrical and physical complexity of the substation layout, it was considered essential to verify that the overvoltages generated were unlikely to overstress the dielectric.

In addition, a switching procedure involving the operation of a disconnector in an 'out-of-phase' mode needed to be studied in order to ensure that there was no arc break out and also that the consequential overvoltages were not excessive.

DESCRIPTION OF EQUIPMENT

The installation involved is an 8 circuit-breaker 420kV gas insulated, mesh configured substation controlling the output of a nuclear power station, Fig 1.

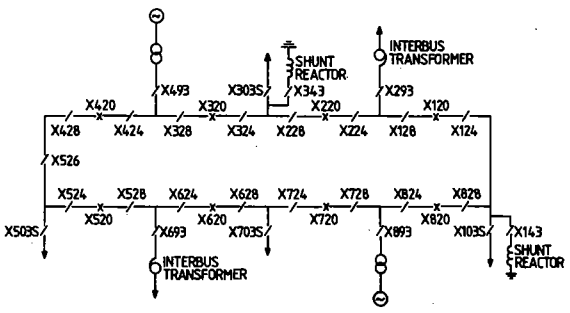

Figure 1 Schematic Diagram of System as Studied

The outgoing circuits are:-

2 - generator transformers connected to the 420kV switchgear via 400kV underground cable.

2 - interbus 400/132kV transformers connected directly to the 420kV switchgear through SF6/oil bushings.

2 - cable/overhead line circuits each 'teed' with a shunt reactor.

2 - cable/overhead line circuits.

The shunt reactors are connected to the switchgear via SF6/oil bushings and the cable circuits via SF6/oil sealing ends.

The design incorporates the normal operational requirements i.e. there is a disconnector in each arm of a junction and on either side of a circuit-breaker.

Each phase is segregated and, in order to minimise the overall size of the substation, the chambers are arranged on several levels in a complex physical layout. Such a layout results in a large number of reflecting nodes and an attempt was made in these studies to model the physical arrangement as closely as possible, physical corners however were ignored.

PART I

DESIGN REQUIREMENTS

The withstand strength of the equipment under standard lightning and switching impulses was, of course, known. In addition, insulation co-ordination studies had been carried out and measures taken, using surge arresters, to limit the lightning and switching overvoltages to within the capability of the substation insulation.

It is known, however, that disconnector operations in GIS can give rise to lower magnitude, but still substantial, overvoltages which are characterised by very short rise times. A number of factors made it essential that the consequences of disconnector operations be closely studied. These were the physical and electrical complexity of the installation together with the expected frequent operation of the disconnectors, especially during the commissioning stages.

The most frequent disconnector operations are those associated with the disconnection and reconnection of a circuit, or a part-circuit, from the substation for operational purposes. Examples are:

(a) circuit disconnection e.g. the opening of X103S with X120, X820 and X143 open.

(b) mesh corner disconnection e.g. the opening of X828 with X120 and X820 open.

(c) circuit breaker maintenance e.g. the opening of X128 with X120 and X124 open.

It was necessary, therefore, to assess the magnitude and rise times of the most onerous overvoltages resulting from a complete range of disconnector operations, especially those likely to occur during normal day to day service. It was also necessary to determine the points in the substation configuration where these maximum overvoltages occurred.

PROGRAMME DESCRIPTION

Calculating the transient overvoltages produced by the operation of disconnectors installed in GIS equipment is not simple. This is because the installation consists of GIS busbar sections and cables having distributed parameters whereas the associated generators, transformers and capacitors are considered as lumped elements. As a consequence, the method employed to determine these switching overvoltages must be capable of satisfactorily representing both lumped and distributed parameters.

One method, which has been successfully applied, is that known as the 'Bewley Lattice' and this method has been adapted by Bickford and Doepel (1) for digital computation. Although the method is strictly applicable only to distributed parameter elements, the lumped elements can be satisfactorily represented by short stub lines.

SYSTEM ELEMENT REPRESENTATION

In the lattice method all circuits are represented basically by distributed lines, specified in terms of surge impedance, length and attenuation. The propagation times of the lines and cables comprising the system are determined from a knowledge of their lengths and propagation velocities.

The time constant T, associated with a shunt capacitance C connected at a node, where the effective surge impedance is Z_e, is expressed by Z_eC. Such a shunt capacitance can be represented by a stub line, open circuited at its remote end. The surge impedance of this line, Zo, is equal to $\theta/2C$ where θ is the maximum permissible time step. The value of θ must be such that the travel time of each GIS busbar section is an integral number. Additionally, θ must be less than $T_{min}/3$, where T_{min} is the maximum time constant in the network.

In the GIS system studied, it was considered appropriate to represent the mesh and the circuits, as shown in Figure 1, with a dimensional resolution of 0.5m. This resolution required a basic time interval for the calculations of 1.67ns based on a propagation velocity of 300m/μs. Therefore, all lengths were rounded up or down to the nearest 0.5m.

The GIS busbar sections were assumed to have zero attenuation and the only damping considered was that provided by two 17Ω resistors connected in series with two grading capacitors across each circuit-breaker's series gaps. In the program each lumped resistance produced an attenuation factor = $2Zo/(2Zo + R)$ where Zo is the surge impedance of the GIS busbar section in ohms and R = 17Ω.

PROGRAMME DATA MANAGEMENT

The data set required for each of the 100 plus switching operations studied was produced by appending, to the "branch time table" of the complete 129 node system, the requisite data modifications.

In this way the integrity of the complete system data block, containing over 450 lines of data, was maintained.

SWITCHING CONDITIONS

It was assumed in each study that the voltage across the disconnector was 2pu. This resulted from the peak system voltage of +1pu being applied to one side of the disconnector with a voltage of -1pu, due to trapped charge remaining from a previous opening of the disconnector on the other side.

In practice, the trapped charge remaining is

dependent on a number of factors including the capacitance of the busbar section; the design of the disconnector contacts; the capacitance across the circuit breaker contacts, etc. In the present study it was decided, for comparison purposes, to keep the initial switching conditions constant at 2pu.

GIS AND PLANT REPRESENTATION

The short duration of the switching process allows the various items of plant connected to the GIS system to be represented by lumped capacitances to earth. The values of these capacitances, together with the appropriate GIS busbar and cable surge impedances used in the study, are presented in Table 1.

TABLE 1

GIS Busbar	
Large diameter section	Zo = 97Ω
Small diameter section	Zo = 75Ω
Circuit Breaker	Capacitance/gap 2800pF Resistance/ gap 17Ω Lumped earth cap. 200pF
Disconnector (closed)	Lumped earth cap. 88pF
Disconnector (open)	Lumped earth cap. 52pF
Surge Arrester	Lumped earth cap. 50pF
Voltage Transformer	Lumped earth cap. 400pF
Supergrid Trans. and Bushing	Lumped earth cap.1250pF
Reactor and Bushing	Lumped earth cap.1175pF
Generator Trans. Cable	Zo = 20Ω
Circuit Cable	Zo = 15Ω

ANALYSIS OF RESULTS

Each overvoltage trace obtained was analysed to determine the maximum voltage change; the peak voltage and the largest voltage reversal. The way in which each of these values was derived is shown in Figs 2 which also explains how the rise time for each of the values was determined.

The values of voltage change; peak voltage and maximum voltage reversal were subsequently plotted against rise times for each disconnector operation (Figs 3, 4 and 5) and a number of conclusions can be drawn from these curves:-

(a) Voltage Change (See Fig 3)

- the largest voltage changes tended to occur with slower 'rates of change'.
- larger voltage changes occurred when operating 'off-mesh' circuit disconnectors associated with transformers and shunt reactors.
- smaller voltage changes occurred when operating 'off-mesh' circuit disconnectors associated with cables.
- the maximum computed voltage change was 3.58p.u. with a rate of change of 3.3MV/μs.
- the maximum computed rate of voltage change was 38MV/μs. This was associated with a voltage change of 2pu and occurred during a 'mesh corner' operation.

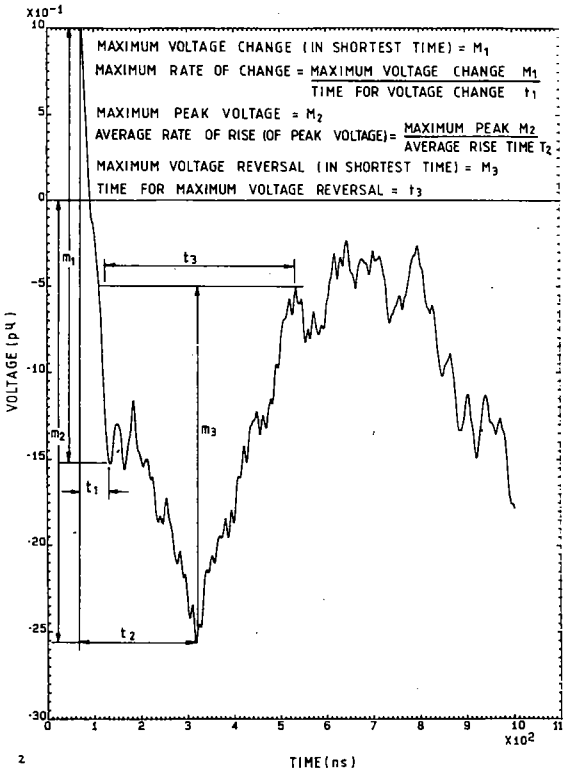

Figure 2 Typical Voltage Measurements

(b) Peak Voltage (See Fig 4)

- the maximum computed peak voltage relative to earth was 2.58pu with an average rate of rise of 1.92MV/μs. It occurred during the operation of an 'off-mesh' circuit disconnector associated with a transformer.
- the maximum average rate of rise of peak voltage was 7MV/μs with a peak voltage of 2.15pu. It occurred during the operation of a circuit-breaker disconnector.

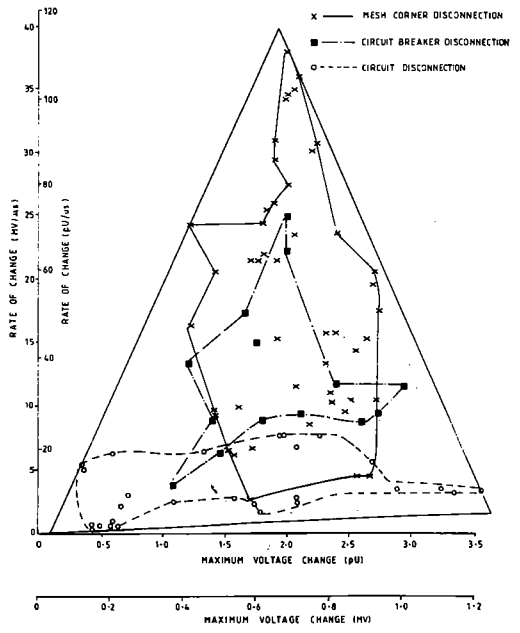

Figure 3 Relationship Between Maximum Voltage Change and Rate-of-Change of Steepest Surges

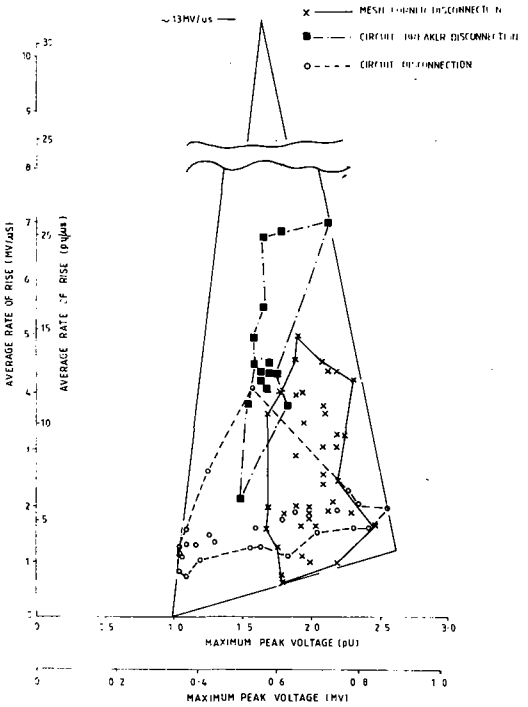

Figure 4 Relationship Between Maximum Peak Voltage and Rate of Rise

- the lower maximum peak voltages tended to occur when operating 'off-mesh' circuit disconnectors associated with cables.

(c) Voltage Reversals (See Fig. 5)

- the maximum computed voltage reversal was 2.3pu and the time for the reversal was 750ns.

- the larger maximum voltage reversals are associated with lower frequencies.

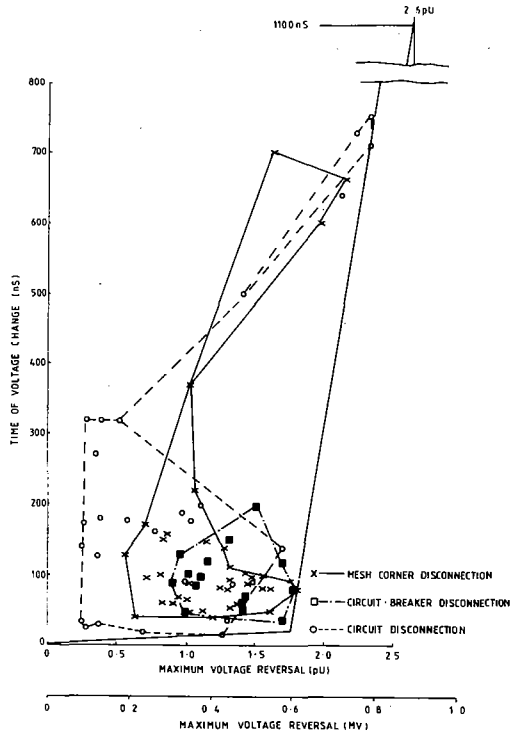

Figure 5 Relationship Between Maximum Voltage Reversal and Time of Voltage Change

Extrapolation of these maxima would suggest an ultimate maximum of approximately 2.6pu with a change time of around 1100ns, a figure in keeping with the natural frequency of the complete mesh.

The computed results of the overvoltage studies confirm that the over-voltages, whilst extremely complex, do have fairly well defined patterns. It is not clear whether the overvoltage magnitude or the rate of change of voltage has the severer stressing effect on the insulation. Information from research in this field could be extremely important to future developments in GIS design.

It is clear that the over-voltages produced by disconnector operations differ completely in character from those to which GIS equipment is presently tested i.e. lightning and switching impulses. It is suggested that the form and magnitude of the overvoltages need to be studied further in order to determine whether current testing practices are adequate.

PREDOMINANT FREQUENCIES

An interesting feature of all the traces analysed was the existence of three predominant frequencies. The way in which these frequencies f_1, f_2 and f_3 were derived is explained in Fig 6. The incidence of the three frequencies which are in the ranges 0-3MHz; 5-17MHz and 30-100MHz respectively are shown in the form of histograms in Fig 7.

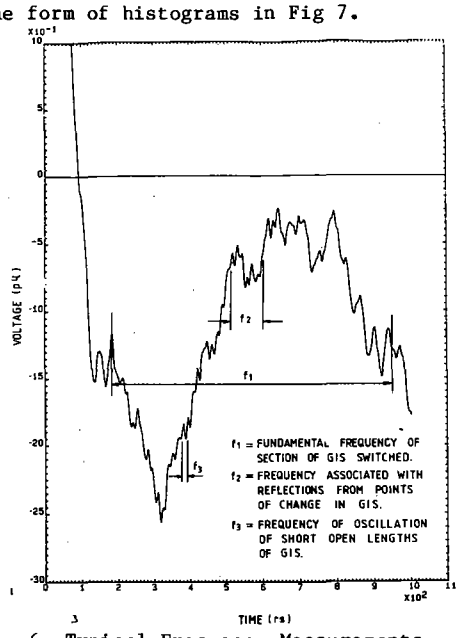

Figure 6 Typical Frequency Measurements

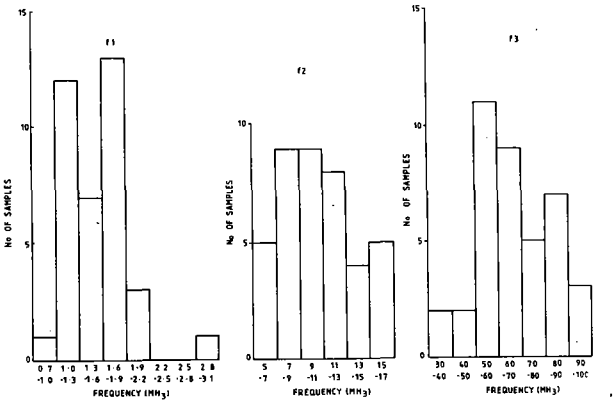

Figure 7 Histograms of Predominant Frequencies for Mesh Corner Disconnectors

OFF-MESH CIRCUIT SWITCHING

The operation of a disconnector produces a transient overvoltage which contains a range of frequencies. These frequencies are propagated through the circuit being switched and any discontinuities and lumped capacitances affect their amplitudes.

In the case of an 'off-mesh' disconnector operation the low frequency component of the waveform has been found to be a function of the complete mesh, whereas the higher frequencies are derived from the various bus-section lengths. The case of a supergrid transformer circuit, where the transformer is connected to the GIS via a bushing, has been studied in detail. The transient voltages obtained at several nodes are shown alongside the diagram of the GIS circuit. (See Fig. 8).

Switching took place at node E and the transient propagated in both directions from this node. The circuit breakers at A and C were open.

At the supergrid transformer node 'G' the lumped capacitance of the bushing, etc. eliminated high frequency components from the waveform. The high frequencies were generated as a result of the change of GIS section surge impedance from 97Ω to 75Ω . The variation of the transient amplitude along the switched circuit can be seen from the voltage-time plots at the selected nodes (Fig 8).

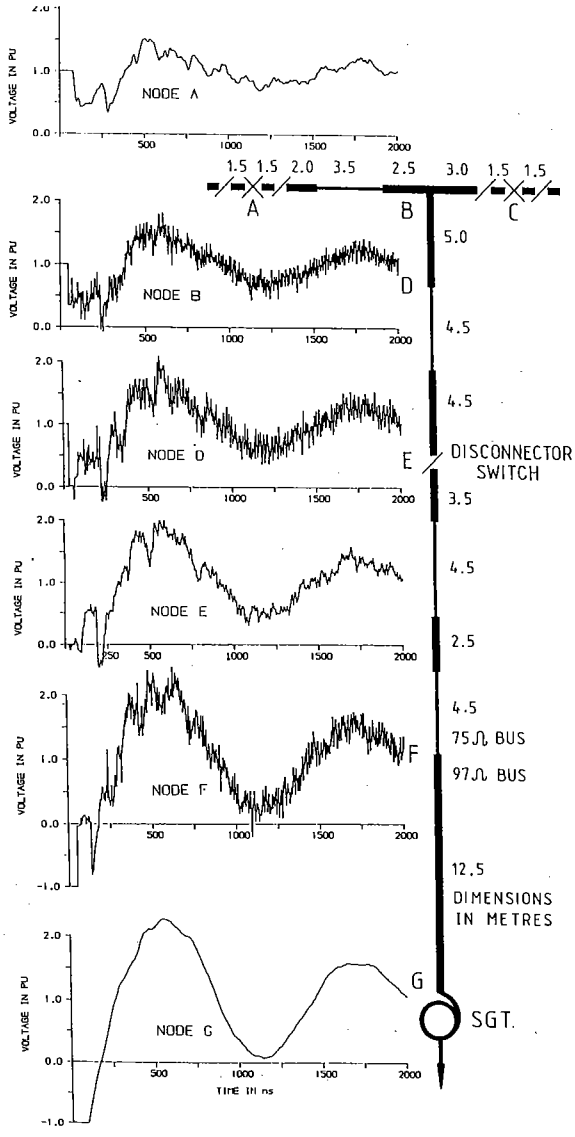

Figure 8 Voltage-Time Plots for Off-Mesh Circuit Switching

In a simplified representation, the mesh was replaced by 97Ω resistors at each of the circuit-breaker nodes. In this representation the 1MHz low frequency oscillation of Fig 8 was not present thus indicating the influence of the complete mesh on the form of the 'off-mesh' transients.

CONCLUSIONS

The switching conditions studied indicate that the largest overvoltage is likely to be less than 3pu and to be associated with transformer/reactor circuits. These terminations are represented by lumped capacitance of a value which is dependent on the size and type of the equipment. Studies on other systems have indicated a dependence of overvoltage magnitude on the value of terminating capacitance.

In general the GIS is arranged such that 'on mesh' switching is associated with a 'T' configuration. This results in the reflected transients always being less than +1pu in magnitude because of the impedance mismatch. This has been found to limit the maximum overvoltage produced and the 'worst case' conditions are confined to 'off-mesh' disconnector operations.

PART II

'OUT OF PHASE' DISCONNECTOR OPERATION

BACKGROUND

The capability of disconnectors performing switching operations under 'out-of-phase' conditions has been investigated by CIGRE Working Group 13-04 (3).

The 'out-of-phase' condition is brought about when the disconnector on a generator feeder is required to be closed whilst 'running-up' the generator before synchronising with the system. Although the circuit-breaker(s) would be open, the grading capacitors across the open contacts would allow power frequency voltage feed-through. Typically this voltage can be in the range 70% - 95% of normal system volts depending on the amount of capacitance i.e. length of GIS busbar; VTs; barriers etc on the 'dead' side of the circuit-breaker. Thus with the generator voltage on one side of the disconnector and part-system voltage via the grading capacitors on the other, an 'out-of-phase' closing operation can result.

The configuration adopted at the nuclear installation meant that the operational advantages of being able to carry out the above switching, on occasion, justified further investigation. Whilst the design of GIS disconnector proposed for the installation had previously been tested under normally specified off-load switching duties it had not been applied in circumstances which required the 'out-of-phase' duty.

Some GIS users (4), (5) have reported experiences of flashovers to earth on their equipment caused by a 'breaking out' of the across-gap discharge (6) (7) (8). As it was believed that the 'out-of-phase duty would increase the chances of arc breakout, it was decided to carry out tests on the

proposed design of disconnector under such conditions.

SYSTEM STUDY

Since the magnitude and waveshape of the transient voltage generated during a disconnector operation determine its performance, and that of the associated equipment, it was important to represent the actual service conditions with a reasonable degree of accuracy.

As the complete disconnector circuit existing at the installation could not be assembled in the laboratory, it was decided to assess, by means of computer and TNA studies, the transient over-voltages produced when switching the disconnector under actual service conditions. These studies identified the critical parameters that would have to be reproduced by the test circuit and so determined the test-circuit specification. Validation of the test circuits, prior to actual testing, was also required and again the TNA was used to model the test-circuit and obtain results that were compared with those obtained from the system studies.

SYSTEM MODEL

That part of the GIS substation for which a detailed single phase model was required is shown in Fig 9. This section of the mesh was selected for study as it gave the maximum a.c. feed through the open circuit-breakers.

A simplified version of the transient network analyser model is shown in Fig. 9. The TNA techniques applied in this model have been well proved over a number of years (9), however it was decided that, for the purpose of comparison, the system would also be modelled, using the electro-magnetic transient program (EMTP) for selected switching operations. The switching operations studied included single-end-fed as well as double-end-fed i.e. 'out-of-phase' configurations.

The TNA results were also compared with computed results obtained from the EMTP and the Strathclyde University (Bewley Lattice) programme. The extremely close matches obtained gave further verification of the TNA techniques.

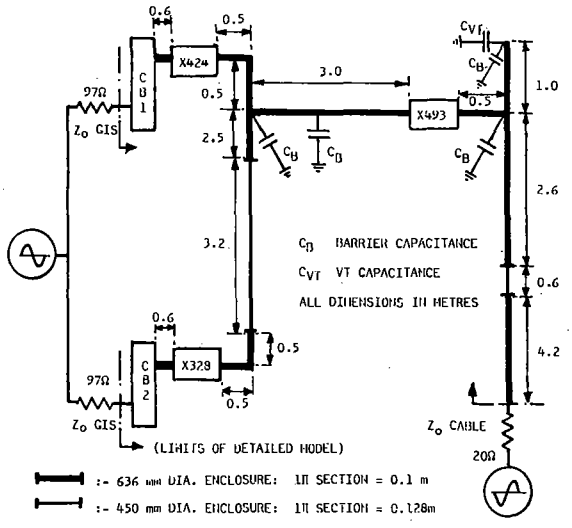

Figure 9 System Model Studied by TNA

The results indicated the type of transient produced when energising from a cable feeder with the GIS precharged to 1pu i.e. with trapped charge present and closing at the negative peak of the system voltage.

TEST RIG MODEL

The response of the system model was used as the basis for the design of a test arrangement which represented the service conditions whilst complying with practical constraints.

Fig 10 shows the final test circuit arrangement which was considered to provide the 'best fit' that could be achieved. A full reproduction of all phenomena was not possible and was not considered necessary (3).

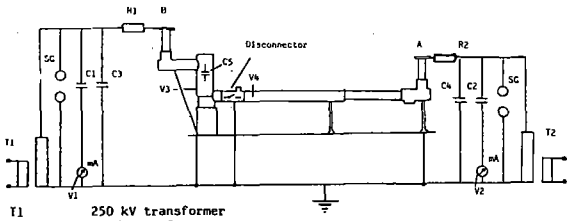

T1	250 kV transformer
T2	2 MV transformer
C1, C2	Standard capacitors for 50 Hz voltage measurement
C3	Equivalent GIS side capacitance (1290 pF)
C4	Equivalent cable source side capacitance (7000 pF)
C5	Circuit breaker capacitance
R1	54 ohm resistor
R2	20.4 ohm resistor
SG	Spark gap
V1, V2	50 Hz voltage measurement points
V3, V4	Disconnector voltage measurement points

Figure 10 Schematic of Test Arrangement

The main points arising from the out-of-phase switching study on the test rig were:

(I) - the high frequency transient recorded at the disconnector was similar in shape and magnitude to that determined in the studies of the actual system.

(II) - representing the two circuit-breakers in the system by a single circuit-breaker in the test rig did not significantly affect the initial portion of the transient overvoltage.

(III) - the 50Hz voltage across the disconnector contacts was slightly higher in the test rig than in the computed case. This results from the larger voltage coupled across the test rig circuit-breaker due to the short bus length between this circuit-breaker and the test disconnector.

It was considered that for those parameters which were significant in determining the performance of a disconnector during out-of-phase switching, the test rig shown in Fig 10, provided a reasonable representation of the duty which would be imposed at the actual site installation.

PROCEDURE AND OBJECTIVES

In order to prove satisfactory performance of the disconnector various measurements were performed.

Measurements of voltage on the GIS primary conductors were made using capacitive coupler devices positioned at the GIS inspection cover points. The locations at which V_3 and V_4 were measured in the test rig are shown in Fig 10. Low

frequency measurements were made directly whilst high frequency measurements were made using a fibre optic link, to overcome problems associated with transient ground potential rise,(10).

The GIS enclosures of the test rig were filled with SF_6 gas to minimum operating pressures and earthing connections were similar to service conditions.

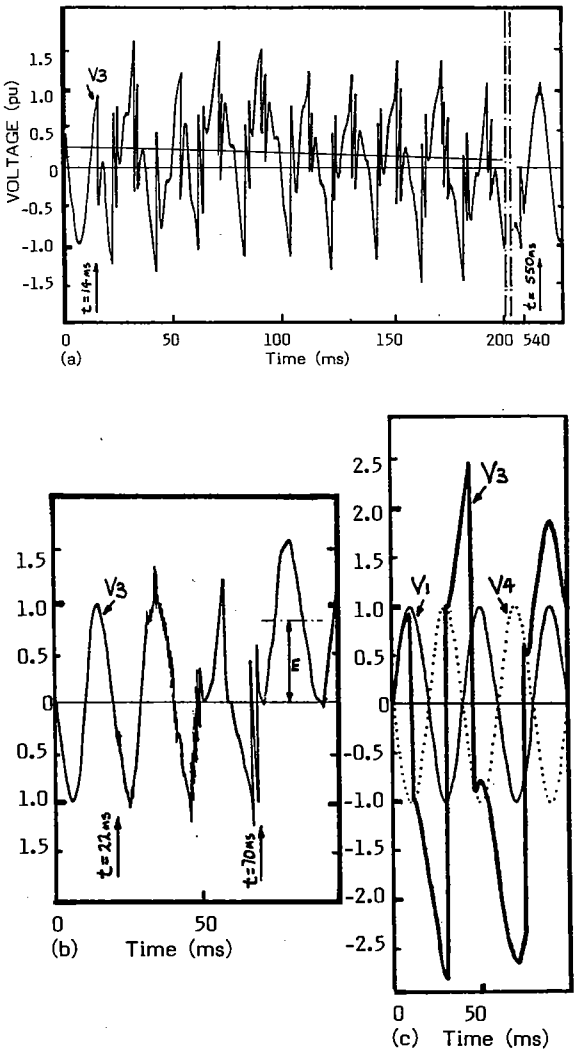

Figure 11 Low Frequency Transients Resulting from Out-of-Phase Switching

TEST PROCEDURE

With the test circuit arranged as in Fig 9 and with the circuit-breaker contacts open test voltages 180° out-of-phase were applied to the terminals of the test rig. Normal phase voltage for a 420kV system was applied to one test bushing (i.e. 242kV rms) and a reduced voltage of 200kV rms was applied to the other bushing to represent system conditions in terms of a.c. feed-through.

A sequence of 25 open and close operations of the disconnector was then carried out with sufficient time between operations to allow measurements to be recorded and inspected. A further 5 open and close operations were then carried out with both 50Hz voltage sources at 242kV rms in order to represent the most onerous condition for any substation layout.

TEST RESULTS

The instrumentation and records indicated that no flashovers to earth had occurred during the test sequence.

Detailed inspection of the interior of the disconnector showed it to be in good condition with only minor erosion of contact surfaces. No evidence of 'break out' of the disconnector arc during the test series could be found, nor were there any signs of breakdown in the attached GIS equipment.

The low frequency disconnector closing transients in Fig. 11(a) show the effect of trapped charge and a.c. feed-through voltage. The a.c. voltage can be seen to be offset by varying levels depending on the point-on-wave of V_4 at which the pre-strikes occur. The zero reference level for this closing transient is actually +0.2 pu (1 pu = 342kV) as indicated by the line above nominal zero.

This offset voltage was produced by an effective trapped charge of -0.2 pu which remained after the previous opening operation. The offset a.c. voltage can also be seen for an opening operation, in the test record shown in Fig. 11(b):- the final restrike, at t = 70 ms, left an effective trapped charge of +0.8 pu (274kV). (Note-actual trapped charge is +0.4 pu.). As the decay of trapped charge in gas insulated equipment is slow the offset a.c. voltage, with a peak of 1.7 pu (580kV), would persist for hours. Consequently the subsequent close operation during the test sequence had, for the first pre-strike, an initial peak voltage V_3 of +1.7 pu (580kV) to earth and a voltage (V_3 - V_4) of 2.7 pu (925kV) across the disconnector contacts.

An EMTP simulation, Fig. 11(c), shows a theoretical 'worst case' corresponding to an actual trapped charge of -1 pu remaining on the 'dead' side of the disconnector. This is equivalent to a trapped charge of -2pu relative to the nominal zero position of the a.c. feed-through voltage. The resultant waveforms show the a.c. voltage feed-through offset by the trapped charge with a peak approaching 3 pu (1026kV) which in turn produces, under the 'out-of-phase' condition, a voltage approaching 4 pu (1368kV) across the disconnector contacts (i.e. (V_3 - V_4)).

An examination of all of the test records revealed that the closing operations under 'out-of-phase' switching produced an average overvoltage of 1.5 pu (1.3 min. to 2.1 max.). Opening operations produced overvoltages in the range 1.4 to 1.7 pu. In addition, 74% of first pre-strikes occurred with the moving contact negative with respect to the fixed contact. The effective trapped charge left on the 'dead' side after opening operations was found to vary in the range -300kV to +300kV and was positive for 70% of the opening operations.

SUMMARY OF TEST RESULTS AND STUDIES

The tests and model studies have shown:

1. The amplitudes of the 50Hz overvoltages, resulting from the combination of trapped charge and a.c. feed-through from the circuit-breaker grading capacitors, greatly exceed those of the high frequency overvoltages.
2. Sustained 50Hz offset voltages, with peak values in the range 1.5 - 1.9 pu, were measured for the majority of the disconnector opening operations under asynchronous conditions.

3. The offset a.c. voltage produced by a previous opening operation resulted in a voltage which could exceed 2.5 pu across the disconnector contacts prior to a closing operation. The theoretical maximum is 4 pu.
4. Depending on the level and polarity of the offset the first pre-strike closing can occur some 900 ms before contact touch. The range of pre-arcing times observed during the tests was 460 - 912 ms.
5. Opening operations produced arcing times of typically 50ms. This shorter arc duration, in comparison with that of the closing operation, is attributed to the high speed of the 'flicker' contact used on opening in the particular design of disconnector under test.

CONCLUSIONS

The presence of grading capacitors in circuit-breakers allows 50Hz feed-through under open conditions and has been found to affect both the 50Hz and high frequency transients produced by disconnector switching on the "dead" side of the open circuit breaker.

No breakdown of the test rig insulation, which included gas-gap; gas-solid interfaces and solid insulation occurred. This indicates that the busbar insulation tested is adequate for the duties imposed by disconnector switching, including 'out-of-phase' switching.

CONCLUDING REMARKS

In operation, GIS substation insulation will be subjected to extremely rapid voltage transients arising from disconnector switching operations.

The ability of the insulation of such GIS bus sections and the associated equipment to withstand these transients has been experimentally demonstrated. The most onerous condition, the 180° 'out-of-phase' disconnector operation at rated phase voltage, was successfully withstood.

Good agreement was found between the transient magnitudes and waveforms predicted from TNA, EMTP and Bewley Lattice analytical studies and those measured experimentally on a full-scale test rig.

The forms and magnitudes of the transients propagated throughout a GIS, mesh-configured, 420kV substation as a result of over 100 different disconnector operations have been computed and the complex character of overvoltages have been demonstrated. The maximum predicted overvoltage amplitude is 2.58pu.

Two possibly significant features of the computed waveforms were, however, the magnitudes of the voltage "swings" predicted, up to 3pu, and the possibility of extremely high rate of change of the voltage. The maximum value computed was 38MV/μs.

The highest overvoltages occurred during off-mesh disconnector switching in transformer/reactor circuits. In general, these highest overvoltages occurred on the circuit being switched.

The amplitude distribution of the frequencies in the transient depends on the number and nature of the physical discontinuities in the "switched" circuit.

The amplitude of the lowest frequency component in the transient was a function of the overall busbar-mesh dimensions.

Currently GIS systems are tested to determine the withstand levels for standard lightning and switching impulses. The transients computed in the present study had voltage changes of almost 2pu which occurred in times as short as 20ns.

This considerable increase in the rates of voltage rise compared to those of present test waveforms must focus attention on the adequacy of such current test specifications.

REFERENCES

1. J.P. BICKFORD and P.S. DOEPEL "Calculation of Switching Transients with Particular Reference to Live Energisation". Proc IEE. 1967, 114, (4), pp.465 - 477.

2. J. OZAWA et al "Suppression of Fast Transient Overvoltage During Disconnector Switching in GIS". IEEE PES, Paper 86WM 138 - 2, Winter Meeting, New York, 1986.

3. CIGRE Working Group 13-04 "Requirements for Switching Tests of Metal Enclosed Switchgear". ELECTRA No. 110 1987 pages 7 - 46.

4. H.A. STUKLESS and M.A. HICK "Specification and Manufacturer Design Review for GIS".

   Paper presented at Symposium on GIS Technology and practice. TORONTO Sept 1985.

5. S.A. BOGGS, F.Y. CHU et al "Disconnect Switch Induced Transients and Trapped Charge in GIS" IEEE PAS Vol 101 198[illegible].

6. K. NAKANISHI, M. UEDA et al "Charging Current Switching by Disconnectors in GIS and some Laboratory Test Methods". CIGRE 1984, 13-06.

7. A. EDLINGER, G. MAUTHE et al "Disconnector Switching of Charging Currents in metal enclosed GIS at EHV" CIGRE 1984, 13-14.

8. O. BOSOTTI, W. MOSCA et al "Phenomena Associated with Switching Capacitive Currents by Disconnectors in Metal Enclosed SF_6 Insulated Switchgear" CIGRE 1982, 13-06.

9. W. WATSON, R.B. HOWIE, et al "Insulation Co-ordination of a 420kV SF_6 Insulated Substation in the UK". CIGRE 1984, 33-05.

10. N. FUJIMOTO, E.P. DICK, S.A. BOGGS and G.L. FORD "Transient Ground Potential Rise in GIS - Experimental Studies" paper 82WM 011-5 IEE PES Winter Meeting Jan 31 - Feb 5 1982.

ACKNOWLEDGEMENTS

The authors acknowledge the contribution made to this paper by colleagues within SSEB, NEI Reyrolle and University of Strathclyde.

International Conference on Large High Voltage Electric Systems

112, boulevard Haussmann — 75008 Paris

1988 Session — 28th August - 3rd September

33-12

O

Pref. Subj. 3

STUDIES OF VERY FAST TRANSIENTS (VFT) IN A 765 kV SUBSTATION

by

J. GRANDL, A. ERIKSSON*, J. MEPPELINK, K. FRÖHLICH

BBC Brown Boveri & Cie

(Switzerland)

C.v.d. MERWE

ESKOM

(South Africa)

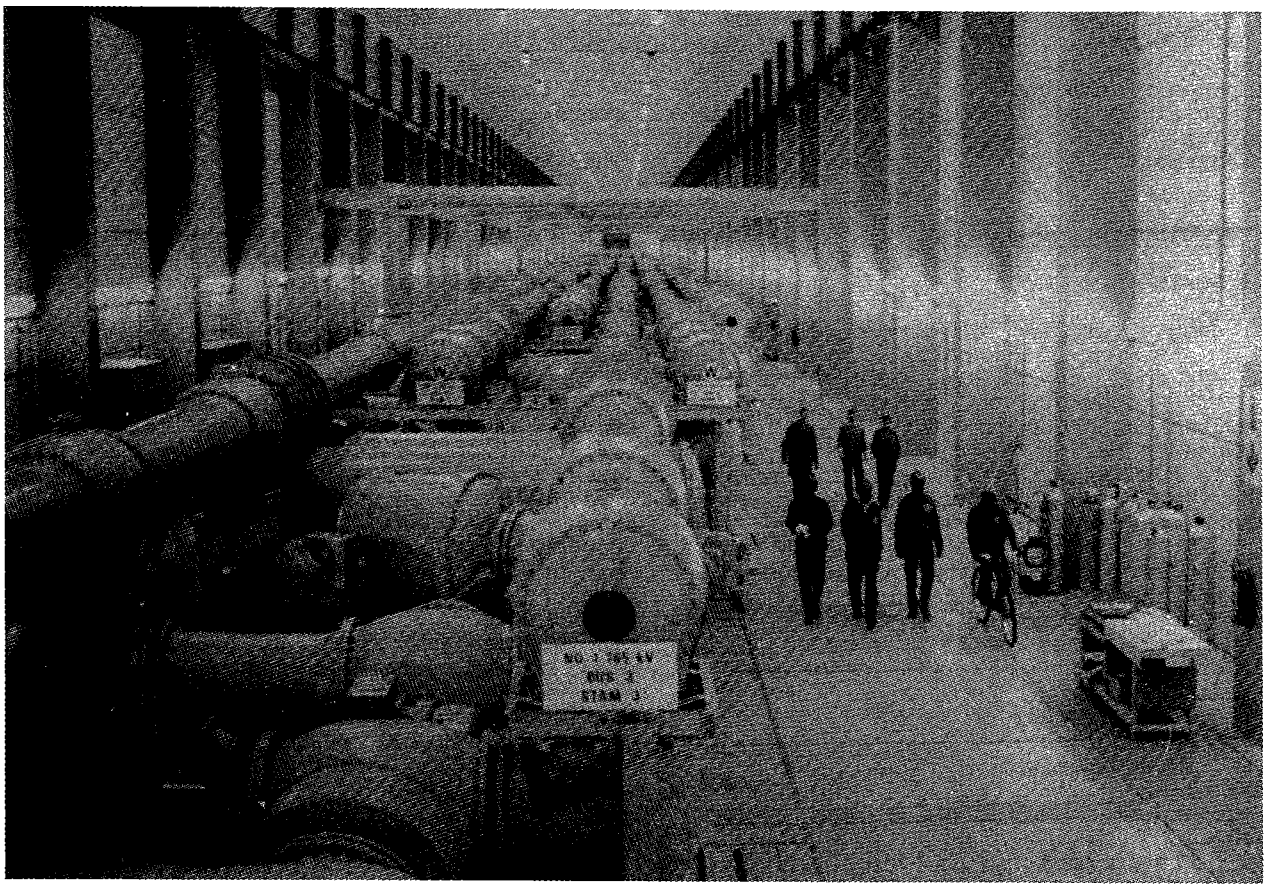

Figure 1: First 765 kV gas insulated substation ALPHA, South Africa

Abstract

The primary aim of this paper is to present a consistent approach to the study of Very Fast Transients (VFT) in Gas Insulated Substations (GIS); in this case illustrated by studies carried out as part of a comprehensive developmental project for a large 765 kV GIS. The techniques involved included both calculations (based on suitably optimised computational models of the GIS), as well as measurements in 765 kV GIS (using high speed pulse measurement techniques). In general, an evolutionary approach has been followed - ranging from basic circuit analysis and low voltage pulse response measurements on individual GIS components, up to full computerised analysis in the complete GIS - coupled with onsite VFT measurements in the 765 kV GIS.

* BBC Brown Boveri, ATX-ST, Postfach 8242, Zürich, Suisse.

Keywords

Very Fast Transients, GIS, Modelling, Calculation, Measurement

1. Introduction

It is well known, that rapid voltage collapses in SF_6 insulation, e.g. during disconnect sparkover, lead to steep voltage fronts with risetimes in the range of 5 ns. As a consequence, high frequency oscillations are excited in the related travelling wave process in the GIS geometry, giving rise to Very Fast Transients (VFT).

Their investigation has become a subject of research in high voltage technics for the past years. Especially at voltage levels greater than 300 kV, VFT were of interest and a lot of work has been done to cover parts of that topic. Measurements of VFT events have been carried out [2], the effects on equipment have been investigated [3] and calculations on some test configurations were undertaken [4].

With the installation of the 765 kV GIS in 1987, the opportunity arose to perform the first systematic, interdependend studies, ranging from developing models of single components, through to a complete simulation study of the gas insulated substation and concluded with onsite measurements.

2. Development of models

2.1 Basis

VFT events, excited by voltage collapses in SF_6, contain frequencies in the range 100 MHz down to 100 kHz. For calculation, it is necessary to develop equivalent computational models of the individual components making up a substation. These models must reproduce the GIS transient behavior in the corresponding frequency ranges as mentioned above.

A SF_6 insulated substation comprises an assembly of various geometric components, which are coupled, either directly, or via transmission line elements, such as:
busbar
insulator
voltage transformer
current transformer
metal oxide arrester
breaker
disconnector
bushing
power transformer
overhead line
line trap
capacitive voltage transformers

The basic references, normally available for modelling, are the design drawings. Careful analysis of the geometry allows development of equivalent circuits, or transmission line representations.

2.2 Low voltage step response

In the early stages of model development, analysis of the low voltage step response has become a common tool for purposes of model refinement, optimisation and ultimate simplification. A principle test configuration is shown in fig.2.

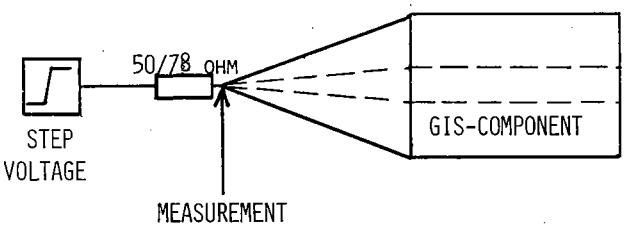

Figure 2: Test configuration for low voltage step response measurements

A low voltage source (about 5 V) injects a steep voltage pulse into the tested GIS compartment. A conical cylinder acts as geometrical impedance matching to the interconnecting coaxial cable. The surge impedance thus remains constant at the value for the test object, which is 78 Ω for a 765 kV busduct. To match the refraction from the 50 Ω output resistance of the pulse injection device into the 78 Ω test object, a 50/78 Ω impedance buffer is mounted between it and the pulse generator.

The tests were performed with a 4 ns risetime step, being typical of the front-times associated with voltage collapse in SF_6 insulated gaps. The step response of the GIS component can then be determined, using normal high-frequency oscillographic measurements, as carried out also, for example, in [5]. In the 765 kV project, such low-voltage measurements were carried out on all the main GIS elements for the 765 kV substation - as listed above. The first rough models, gained from the construction drawings, could then be progressively refined by analysing the measured step response.

Computational models, developed in such a manner, can be at various levels of complexity or detail. In practical applications, such as in very large substations, it is necessary to simplify the models to some extent, due to computer restrictions, but without losing primary information. This implies that important features of the overall transient response, such as peak amplitudes and main frequencies must not change significantly after simplification, whereas minor details, such as small spikes or deviations in shape, can be neglected.

General experience acquired in modelling networks has demonstrated the relative emphases in carrying out such simplifications. Overly complicated models of individual components and neglect of their integration in a complex installation, may lead to the most important features of the transient response being swamped in extraneous detail.

The "art" of modelling extended networks, such as those in the 765 kV substation, is thus to reduce the individual component

models to a practical level for computation purposes, but to retain the overall transient characteristics of the network, such that the overall transient response is correctly reproduced.

2.3 Low voltage measurements in the 765 kV pilot installation Betina

In order to perform developmental tests for the ultimate 765 kV substation, a pilot installation, named Betina, was erected in Switzerland. It comprised all the principal components of a practical substation. Fig. 3 shows the single line diagram of Betina.

In the 765 kV project, the first test of the models derived in the above joint process of circuit analysis and measured pulse step response, was through studies made in the 765 kV pilot installation. These studies also provided an unique opportunity to assess the effects of various computational model simplifications.

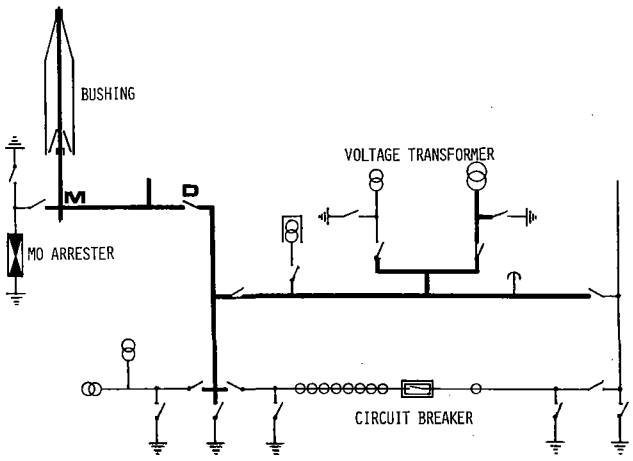

Figure 3: Single line diagram for the 765 kV pilot installation and tested configuration for HV investigations
D:operated disconnector for HV-tests
M:measuring point for HV-tests

As a first test of the primary models, a low voltage impulse was fed into a sample GIS configuration and the step response was measured in a manner similar to that employed during the earlier single component measurements.

The low voltage studies in the 765 kV pilot installation were aimed at three objectives. Firstly, to test and improve the models of the single components in an extended station. Secondly, to develop broader experience in calculating complex networks and to determine the main influencing parameters. Thirdly, to extend experience in understanding practical surge propagation characteristics - such as attenuation and travel time - in a representative substation.

For example, such investigations led to several primary conclusions. The concentrated capacitive effects of the dielectric spacers installed in the GIS, serve to reduce the propagation speed (to about 0,96 light velocity in average). This effect was also mentioned in former publications [4]. Furthermore the front of steep fast transients is sloped during travelling in GIS. For simplified calculations an effective compromise is to use an average fast transient risetime of 20 ns.

2.4 Low voltage calculations

In parallel with these pulse injection studies, the transient responses of the tested GIS configurations were also calculated and compared with the measurement results. Two different computational tools were used for these calculations; the well known EMTP (Electromagnetic Transients Program) and a PC program for travelling wave calculation. An example of such a measured and calculated low voltage transient is shown in fig. 4.

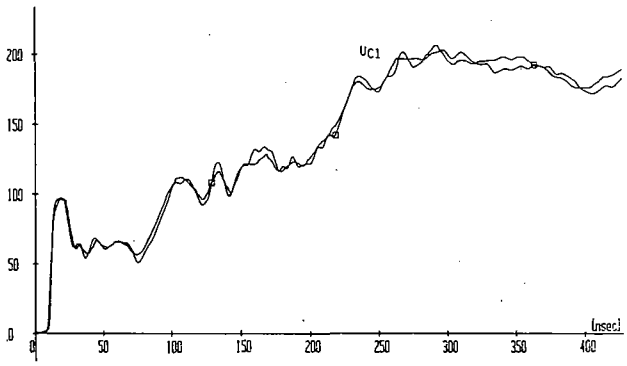

Figure 4: Measured and calculated low voltage waveforms for a configuration in the 765 kV pilot installation Betina

The figure shows an excellent agreement between measurement and calculation. It is clear that a very extensive model of the tested configuration was necessary to reach such a level of conformity.

3. High voltage measurements and calculations in the 765 kV pilot installation

3.1 Basis

The overall purpose of all these fast transient studies (including the previous low voltage tests, and the development of computational models), is of course to determine the practical overvoltages that may occur in GIS, or at connected equipment, during sudden voltage collapse in SF_6. As the main cause for such transients are disconnector operations, it is necessary to examine the latter in more detail.

When a disconnector switches an open ended busbar, a sequence of reignitions occurs across the contact gap. Typically, each reignition is at a different voltage level, depending upon the increasing or decreasing contact distance, and thus travelling waves of varying amplitudes but equal shapes are generated. A practical study of VFT voltages has to determine the principle shape (i.e. independent of reignition voltage) and the maximum voltages that can occur.

To reach that aim an effective strategy for a VFT study could involve the following:
- identify the main switching configurations
- develop a suitable computational model for each configuration
- calculate the resultant VFT voltages for disconnector operations at several points of interest in the substation
- determine maximum possible voltages, based upon trapped charge considerations
- determine the worst case configuration (i.e. where the highest voltages occur).

In order to achieve meaningful results, consistency must be demonstrated between simulation (i.e. computation) and practical experience (i.e. measurement) on defined events.

In considering disconnector operation, it is advantageous to take the first ignition of a closing operation onto an open ended busbar. The load side is considered to be discharged. The first reignition will generally occur at about the peak of the power frequency voltage (625 kV in this case), and, as a consequence, this value is equal to the reignition voltage across the gap. In general, the amplitudes of VFT voltages, generated by a disconnector operation, are directly dependent on the voltage differences developed across the contact gap.

The resultant calculated transient voltage for a specific configuration can be taken as a "system response". Based upon this, all possible amplitudes can subsequently be determined, depending on the relative voltages on both the source and load -side-contacts before a reignition. This allows determination of the maximum possible voltages for any arbitrary voltage composition (i.e. including trapped charge considerations), such as may occur during a disconnector operation, or any other voltage collapse in SF_6.

3.2 High voltage measurements

In the 765 kV pilot installation Betina, fast high voltage dividers were installed at several locations to measure VFT events. The measurement system covers a signal bandwidth up to 500 MHz [6]. Measurements across such wide bandwidths require careful EMI shielding measures for the complete measuring system in order to achieve a sufficient signal to noise ratio. Such measures include positioning of the equipment in a Faraday cage, routing of cables in metallic tubes - with low impedance grounding at both ends - and the use of power line filters for device supply.

Various switching configurations were chosen for detailed analysis, taking account of several aspects:
- determination of the influence of different components.
- identification of the highest voltages and evaluation of the determining parameters.
- test of the computational models as derived originally from circuit analysis and low voltage measurements.

VFT voltages were measured at the first ignition of a closing operation across a disconnector gap to a discharged busbar, as described above. The applied voltage was (800 kV/$\sqrt{3}$=) 462 kV line to ground.

For each configuration examined, VFT voltages were measured at several locations. Fig. 3 illustrates a sample tested configuration, showing the operated disconnector. The measurement location (M) is at the bushing. The corresponding oscillogram from is presented in fig. 5. Note, that the phase shift of the two curves is only for clearness.

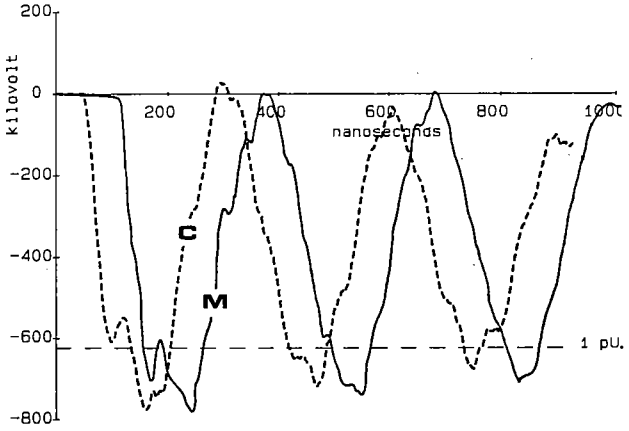

Figure 5: High voltage VFT measurements and calculations in a 765 kV pilot installation according to configuration of fig. 3
M: measured C: calculated

After an extensive series of parameter variations , including a variety of bus configurations, the highest measured VFT amplitude in the BETINA substation proved to be 1.32 pu (825 kV). Note, that all voltages in the pilot installation Betina were measured for the first reignition of the disconnector to a discharged load-busbar.

The maximum possible voltages are higher than the measured ones. Assuming the theoretical case of a trapped charge voltage of 1 pu at the load side before the reignition, the transient voltage amplitude will increase up to 1.64 pu (1025 kV). For further explanations of maximum possible voltages see chapter 4.2.

A component of particular interest during these tests was the metal-oxide surge arrester. In contrast to the other GIS components, where linear transient response is assumed across the voltage range, this element has to be investigated separately in the high voltage domain, because of its non-linear current/voltage characteristics. Computational models derived from low voltage measurements will only be valid in the non conducting state.

The measurements in the pilot installation Betina showed that all transient over-voltages remain well below the protection level of the installed metal oxide arrester, even under worst case conditions. So, according to the results of low voltage investigations, an MO arrester can be adequately represented by a capacitance of

some 100 pF, for virtually all transient events.

3.3 High voltage calculations

The aim of the comparative calculations that were undertaken in parallel to the measurements in Betina, was to confirm the reliability of the developed models and their associated parameters.

The calculation result shown in fig. 5 represents the transient voltage expected at the same position (see fig. 3) during the high voltage measurements. A comparison between measurement and calculation demonstrates overall consistency in representation of the main frequencies and amplitudes. Deviations in comparative amplitudes are less than 5%.

4. High voltage measurements and calculations in the 765 kV substation Alpha

4.1 Substation Alpha

All the preceding analyses found their primary application in the insulation coordination for the practical 765 kV SF_6 insulated substation, termed Alpha [1]. It contains 36 breaker poles, and is designed as a 2-busbar system. 2 power transformers, 3 reactors and 2 overhead lines are connected to the station at the present stage of operation. The length of the busbar is about 220 m. An overview of the GIS part of the station is shown in the photograph in fig 1.

4.2 High voltage calculations

A comprehensive series of VFT calculations was carried out for the Alpha 765 kV substation, as part of the overall overvoltage studies. A variety of different switching configurations was analyzed in a manner similar to that done in the BETINA pre-studies. As before, the calculations considered the first ignition across a disconnector gap from a transformer-fed source side busbar, to a discharged load side. Transient voltages were determined for different locations in the switchgear. Based on these results, the theoretical maximum overvoltages possible could then be derived.

As noted previously, analysis of the switching of a source voltage to a discharged load and investigation of the first ignition, is generally used because of its good reproduceability. In practical switching operations, however, the resultant transients can differ in amplitude from the above case, depending upon circuit conditions.

For example, switching to a load with trapped charge, or in the case of an "Opening" operation, the reignition voltage (i.e. the voltage difference across the gap) is higher than for the above analytical situation. In a VFT study therefore, it is important to determine the highest transient voltages that are possible. In the 765 kV analyses, three main situations were considered:

- A discharged load side busbar as applied for the measurements
- A DC voltage of 0.4 pu (i.e. 250 kV) on the load side, representing the average value of trapped charge voltage normally encountered.
- A theoretically possible "worst-case"; involving 1 pu pre-charge voltage (i.e. 625 kV) on the load side, with the 50 Hz peak value of 1 pu, but of opposite polarity, on the source side, prior to reignition across the gap. This corresponds to a voltage difference of 2 pu (1350 kV) across the contacts.

All switching configurations of practical interest were investigated in the entire substation. In the configuration yielding the highest overvoltages, the following VFT results were obtained:

"Closing" onto a discharged busbar; 1.68 pu (1050 kV)
"Closing" onto 0.4 pu trapped charge voltage; 1.95 pu (1219 kV)
"Closing" onto 1.0 pu trapped charge voltage; 2.36 pu (1475 kV)

In the majority of configurations analyzed, however, the calculated VFT amplitudes were mostly below 1 pu, and did not normally exceed a level of 1.5 pu - in accordance with general experience in a variety of investigations in other GIS installations [7].

For comparison: The LIWL (lightning impuls withstand level) of the 765 kV equipment is 2100 kV.

4.3 High voltage measurements

Following the above calculations of expected VFT in the substation Alpha, sample measurements were carried out on some selected configurations on site. The aim was to confirm the accuracy of the calculations, and thereby to substantiate the investigation of VFT events in an extended substation, through computation.

The measurements in Alpha were performed in a similar way to the earlier tests in the pilot installation Betina. Wideband HV dividers were installed at different locations to measure the transients, occurring at the first ignitions of disconnector closing operations. Fig. 6 shows a sample switched configuration. A power transformer fed source busbar is switched to a line, connected via an open breaker with grading capacitances. The bushing is linked via a line trap and capacitive voltage transformer to a 765 kV overhead line.

Fig. 7 shows the measured transient voltages observed at the load side close to the disconnector,(i.e. immediately before the open breaker).

The comparative reference calculation is presented in fig 8. In general, very good consistency is evident between the two sets of results. The observed differences in amplitude between calculation and measurement is 5%, thereby demonstrating the

effectiveness of the basic computational models and the calculation procedure.

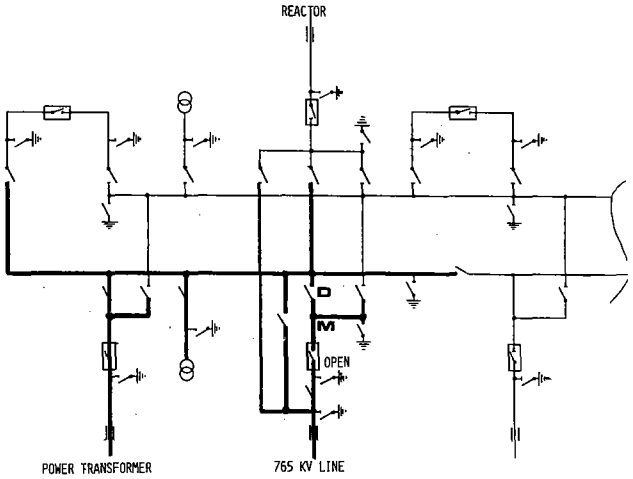

Figure 6: Part of 765 kV substation Alpha; measured and calculated configuration
D: operated Disconnector
M: Measuring point

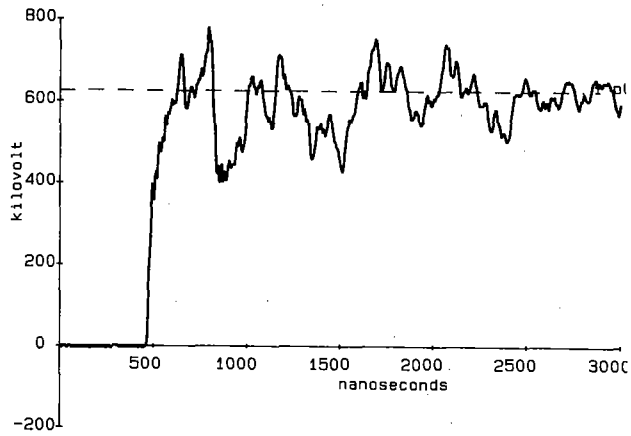

Figure 7: measured waveform for a sample configuration of 765 kV substation Alpha

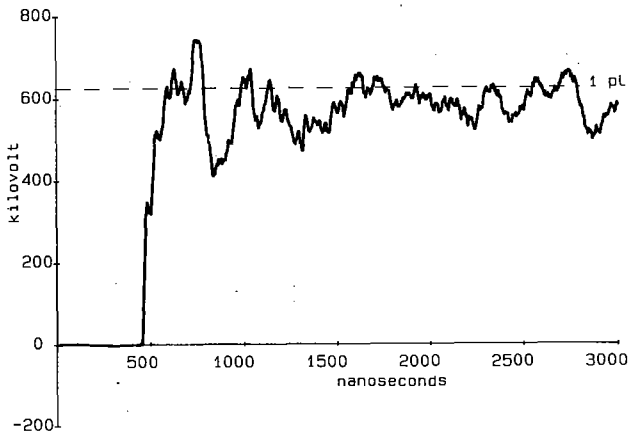

Figure 8: Calculated waveform for a sample configuration of 765 kV substation Alpha

Conclusion

Low voltage step-response measurements have proved to be a useful tool for developing models of GIS components in the MHz-domain, and for determining the transient behaviour of sample test configurations.

It is practical to calculate VFT events even in an extended 765 kV GIS substation. The resultant comparisons with measurements clearly demonstrates the reliability of the computations.

Suitable simplification of individual GIS component models to a practical level for calculation leads to a correctly reproduced overall transient response.

VFT amplitudes in the investigated 765 kV substation remain in many cases below 1 pu (625 kV) and normally do not exceed the level of 1.5 pu (940 kV). For the "worst case configuration" found, a transient voltage amplitude of 2.3 pu (1440 kV) was calculated, for the theoretical case of 1 pu trapped charge voltage prior to reignition across a disconnector gap.

Given the demonstrated linearity in VFT characteristics between the low voltage step response tests up to the practical studies carried out in the 765 kV GIS, the general method of approach presented here is thus applicable to VFT analyses over the full GIS range of operating voltage levels.

References

[1] **Lohmann, Brinzer:**
World's first 800 kV GIS substation
Brown Boveri Review, October 1987

[2] **Meppelink, Diederich, Feser, Pfaff**
Very Fast Transients in GIS
Submitted for IEEE WM 1988, New York

[3] **Meppelink, Remde:**
Electromagnetic compatibility in GIS substations
Brown Boveri Review, September 1986

[4] **Fujimoto, Stuckless, Boggs:**
Calculation of disconnector induced overvoltages in gas insulated substations.
Gaseous Dielectrics IV, Knoxville, Tennessee 1984

[5] **Witzmann:**
Fast transients in gas insulated substations-modelling of different GIS components.
5. international symposium on HV engineering, Braunschweig 1987.

[6] **Meppelink, Hofer:**
Design and calibration of a HV divider for measurement of VFT in GIS
5. international symposium on HV engineering, Braunschweig 1987.

[7] **Boeck, Witzmann:**
Main influences on the fast transient development in gas insulated substations.
5. international symposium on HV engineering, Braunschweig 1987.

International Conference on Large High Voltage Electric Systems

112, boulevard Haussmann — 75008 Paris

1988 Session — 28th August - 3rd September

O

33-06

Pref. Subj. 3

FAST TRANSIENTS IN THE EARTHING SYSTEM OF GIS

by

F. NOACK*, P. ZAHLMANN, R. BROCKE

Ilmenau Institute of Technology

J. SCHWARZ

VEB Transformatorenwerk Berlin

(German Democratic Republic)

ABSTRACT

Experimental studies in GIS under service conditions and in laboratories have been made to examine the effectiveness of the earth connections. For this currents in the enclosures and earth connections are measured. The configuration of GIS with cable connected feeders is under special conditions if the cables are longer than 30 m. The wave refracting at the cable/air termination and entering the GIS is not dangerous. The most effective measure to reduce the TGPR in this case is the shunting of discontinuities with varistors.

KEY WORDS : Earthing, Fast transient, GIS, Varistor.

INTRODUCTION

The transient ground potential rise phenomenon (TGPR) in GIS has been an important subject of research and discussions over the last few years [1-7]. The mechanisms are investigated and described and measures for limiting the phenomenon are proposed and applied.

With the introduction of electronic equipment with increased sensitivity, transient electromagnetic compatibility is a major concern. Unfortunately the physiological effects which might occur during disconnect switch operation require a reduction of the TGPR.

For this, the layout of the earthing system and other protective measures have a great influence on the reduction of these effects. The configuration of GIS with cable-connected feeders represents some special conditions for the propagation of waves and the protection of the equipment.

EXPERIMENTAL INVESTIGATIONS

Experimental investigations of the earthing grids of GIS have been made to examine the effectiveness of the earth connections when conducting surge currents. For this, measuring shunts and special dividers have been developed, permitting measurements up to frequencies of about 1 GHz.

The measure made under service conditions were supported by experimental studies in laboratories and by digital simulations. Systematic investigations at parts of GIS with earthing systems were conducted by means of a test generator. (Fig.1).

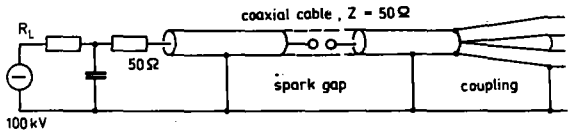

Figure 1. Cable generator.

The test generator with a laoding voltage of about 100 kV, generates electromagnetic pulses with peak values of about 50 kV, rise times of about 1 - 5 ns and pulse widths of about 1 - 2 µs. The relatively long pulse width was obtained by using long cables for the cable generator, (e.g. a loading cable of 120 m supplies a pulse width of 1.6 µs or 0.8 µs). With a specially developed SF_6 spark gap it is possible to realise the extremely rapid dielectric breakdown as in SF_6 disconnect switches and circuit breakers during operation. The pulses are coupled reflection-free in parts of the GIS system and thus correspond to the fast transients when switching.

Experimental studies were made to determine the inductance of earthing loops in GIS earthing systems by means of the current injection method.

By injecting a current pulse into a circuit the response of the circuit can be recorded. Measurement at many test points demonstrates the existence of very high frequency multi-frequency transients (200 kHz - 100 MHz) in the case of oscillation excitation.

These are caused by the electric and magnetic couplings between parts of the enclosures and earth connections. Figure 2 shows an example of a measurement at a test point between the insulated flanges of GIS.

*Ilmenau Institute of Technology, 6300 Ilmenau, (German Dem. Rep.)

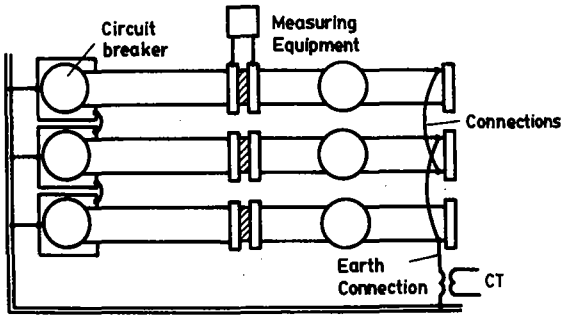

Figure 2a : Measurement equipment at a test point of the earthing grid of a GIS.

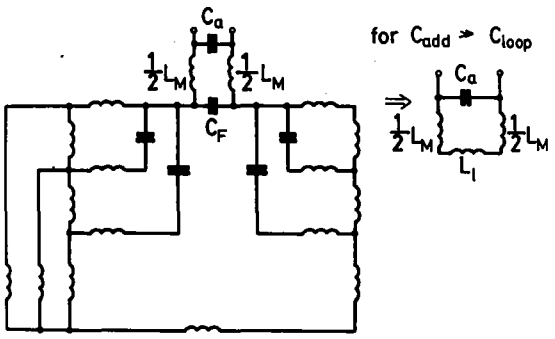

Figure 2b :Equivalent circuit of the earthing grid at a test point between insulated flanges.

If capacitors which are much greater than the effective capacity of the circuit are added, then only the oscillation determined by the effective inductance of the circuit and the added capacity will appear. The effective inductances of the earthing loops in GIS attain values in the range of 1 µH to 15 µH. By improving the earthing system (shortening the earthing loops at discontinuities) the effective inductance was reduced at best by only a few µH. The height of the enclosures above the earthing grid determines the minimum obtainable inductance.

CURRENTS IN THE ENCLOSURES OF GIS

The maximum value of the initial voltage wave within the enclosures depends on the kind of earthing of the neutral point and on the kind of switching operation. In the case of breakdowns in effectively-earthed networks, it will amount to $\sqrt{2}.U_n/\sqrt{3}$ and $\sqrt{2}.U_n$ in non-effectively-earthed networks. In the case of closing operation, one half of these values will be theoretically possible in the first front. In practice, repetitive restrikings in the opening and closing operations are inevitable and generate the characteristic overvoltages. These voltage waves also determine the currents in the enclosures. Measurements with a special shunt across the flanges of a 123 kV GIS resulted in current rises of :

$$\frac{di}{dt} \approx (1 \ldots 1{,}5)\ 10^{11}\ A/s\ . \qquad (1)$$

The use of the shunt at a GIS/cable termination is shown in Figure 3.

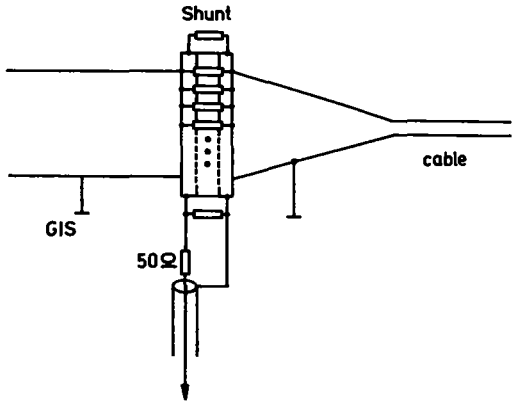

Figure 3 : Measurement equipment with pulse shunt at the GIS/cable termination.

Experimental investigations of disconnect operation induced overvoltages were carried out in GIS with a configuration as shown in Figure 4

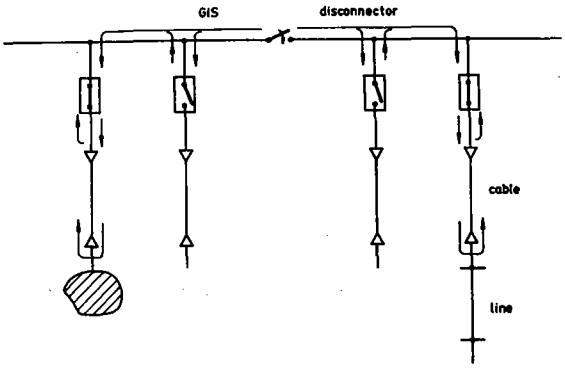

Figure 4 : Configuration of a 123 kV GIS with cable connected feeders.
Z_{GIS} = 60 Ω, Z_c = 18 Ω

All feeders of GIS are terminated with conventional cables. As the oscillogram of the initial behaviour of the pulse current shows (Fig.5), the current increases in steps lasting several nanoseconds each. This phenomenon results from the continuous refraction of the wave when passing the various feeders of the GIS.

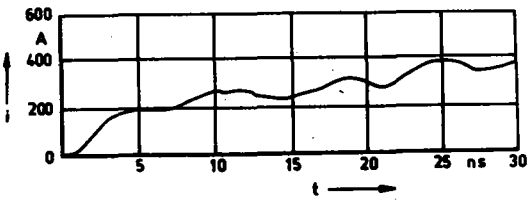

Figure 5 : Initial behaviour of the pulse current in the enclosure during disconnect switch closing operation.

The maximum theoretic amplitude of these steps will be :

$$i_{St} = \frac{U \cdot \sqrt{2}}{2 \cdot \sqrt{3} \cdot Z_{W\ GIS}} \qquad (2)$$

After charging the GIS (some 100 ns max.) the wave impedance of the connected cables determines the current behaviour.

$$i = \frac{U \cdot \sqrt{2}}{2 \cdot \sqrt{3} \cdot Z_{WC}} \qquad (3)$$

In 123 kV GIS values up to i ≈ 2.5 kA were measured. The further behaviour of the current is determined by the travel time of the wave in the cable :

$$t = \frac{2 \cdot l_c}{v_c} \quad , \; v \approx 1.5 \cdot 10^8 \text{ m/s} \qquad (4)$$

After time t, the refracted returning wave in the enclosure appears with reverse signs and is attenuated by the losses in the cable. An example of this behaviour is shown in Figure 6. The reflection point is given by the cable/air termination.

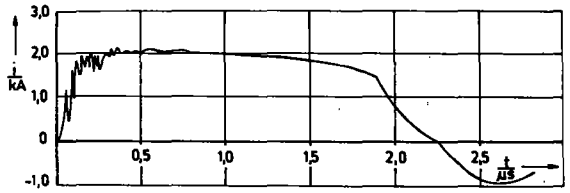

Figure 6 :Behaviour of the pulse current in the enclosure during disconnect-switch closing operation refracted at the cable/air termination.

At high frequencies of internally generated faults and disconnect switch induced transients, currents are constrained to flow along the surfaces of conductors. The electromagnetic field can emerge onto the external surface of the GIS at enclosure discontinuities, especially at insulation spacers between the flanges, at the GIS/cable termination and the GIS/air termination. At such a discontinuity i.e. an insulating spacer first coupled capacitively, the voltage increases until a flashover occurs, the arc voltage being at best some 100 V. The current rise is decreased by this.

THE EFFECT OF EARTH CONNECTIONS

It is well known that steep fronted travelling waves which couple from the internal coaxial GIS to the outside enclosure surface at the GIS/air termination cause the largest transient ground potential rise. TGPR occur also at other enclosure discontinuities. Some measures for limiting this phenomenon are proposed in [8,9].

Earth connections have a significant effect on the magnitude and wave shape of the TGPR. The two mechanisms are described in [10]. The length of the earth connections determined by the enclosure height above ground is the most relevant factor.

If the currents in the enclosures are to be conducted through an earth connection without inadmissible overvoltages, the maximum inductance of connections must be very small. With an inductance of L = 1 µH and a rate of current rise di/dt = 10^{10} A/s the difference is still u = 10 kV. It is however technically not feasible to realise inductances which are much smaller if the height above ground of the enclosure is given. It will not be possible to reduce the effects of the transient ground potential rise even if great efforts are made to improve the system. It proves much more effective to prevent electromagnetic energy from escaping from the enclosed system and to reduce voltage between the parts of the enclosure.

If the TGPR is created by the refraction of the travelling wave at the GIS/air termination then the most effective measure of limitation is the use of metallic conducting sheets between the bus enclosure and ground. Such shields bound to the GIS enclosure and to the earthing grid effectively reduce the transmitted wave.

Other conditions prevail if the feeders in GIS are terminated with cables. Conventional cables tend to have substantially more losses at high frequencies than GIS and thus attenuate the fast rise time of the travelling wave. The most significant transition point for the travelling wave is the cable/air termination and a refracted wave is also coupled onto the outside of the cable sheath. Both the configuration of the propagation path and the earth resistivity effectively attenuate the travelling wave. If the cables are longer than about 30 m the magnitude of the refracted wave entering the GIS is not dangerous. In this case, the GIS/cable termination are the significant sources of TGPR.

VARISTORS AS PULSE SHUNTS

Good results have been obtained with ZnO varistors suitably attached above the isolated parts of the enclosure. The limiting of the pulse voltage across these flanges to the small residual voltage of the varistors takes place without any noticeable time delay even in the case of extremely short voltage rises. Thus, the amplitude of the travelling wave coupled into the wave channel between enclosure and earth is substantially reduced and the secondary equipment is effectively protected. The low inductance arrangement of the varistors bridging the insulated flanges is important for the effective limiting of the overvoltage.

Figure 7 illustrates the measurement results obtained with a varistor set-up under both conventional and optimised conditions.

The choice of the rated voltage guaranteed that the varistor did not respond by power frequency events.

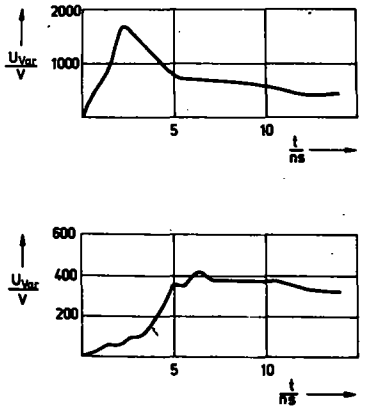

Figure 7 : Comparison of voltages at the varistors as a function of time during connect-switch closing operation. Upper curve : set-up with varistors under conventional conditions. Lower curve : set-up with varistors under optimised conditions.

Lifetime investigations at the varistors showed that even after 5000 pulses with u = 50 kV, i = 2 kA, no change of characteristics resulted within the range of very large pulse currents. The changes within the range of such small currents as those indicated in Figure 8 have no influence on the limiting effect.

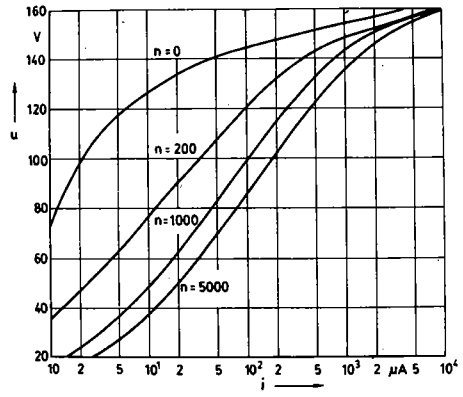

Figure 8 : Lifetime characteristics of ZnO varistors

When microelectronic devices and microprocessors are used in secondary equipment then these parts have to be provided with cascaded protective elements (varistors and capacitors).

The voltage at the input of the electronic circuits may be reduced to values smaller than 10 V by means of these elements. (Fig.9.).

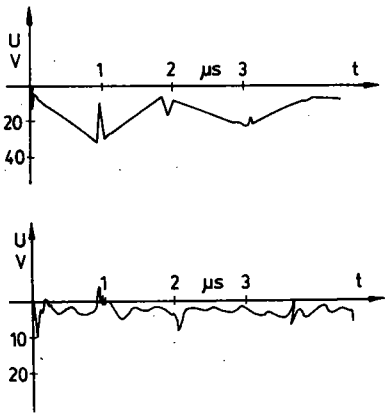

Figure 9 :Output voltages at the cascaded protective elements.

When the discontinuity is shunted by varistors, these will act as impressed voltage sources with changing signs due to the internal transients. (Fig.10).

The residual voltage of the varistors determines the currents flowing to the earth connections. These earthing connections act with their inductance for the steep front of the travelling wave. The current flows to the enclosures via the shortest path, without other connections in the earthing grid participating (Fig.11).

The rise of the earthing currents is essentially reduced by the effect of inductance and the small varistor residual voltage.

$$\frac{di}{dt} = \frac{u_v}{L} \qquad (5)$$

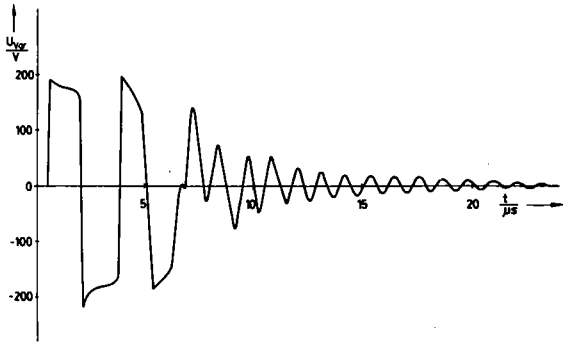

Figure 10: Residual voltage at the varistor as impressed voltage source.

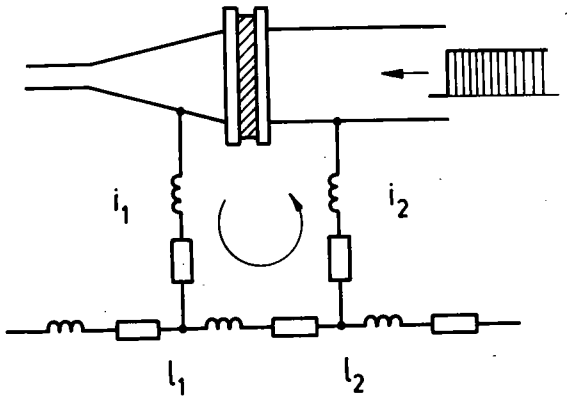

Figure 11 :Earthing loop at a varistor bridged discontinuity.

The values measured are :

$$\frac{di}{dt} = (10^7 \ldots 10^8)\ A/s \qquad (6)$$

The current increases during the travel time t linearly according to the following relation :

$$i = \frac{di}{dt}\,t = \frac{2u_v l}{L \cdot V} \qquad (7)$$

and decreases in the same way due to the returning wave. This results in a triangular current behaviour.

The results show that the approximation of earth connection through an inductance and a resistor is probably adequate for connections with a travel time shorter than the surge rise time. This model also makes clear the phenomenon of a d.c. component in the current behaviour expressed by the time constant

$$t = \frac{L}{R} \qquad (8)$$

The amplitude of the voltage in the earth channel is thus determined by the breakdown voltage at the insulating spacer and the varistor residual voltage.

If enclosures of GIS are divided into several sections each connected with the earthing grid by a corresponding earthing connection the resulting current distribution is in accordance with the values of the inductances of the earthing loops and by this, to their lengths (Fig.12.).

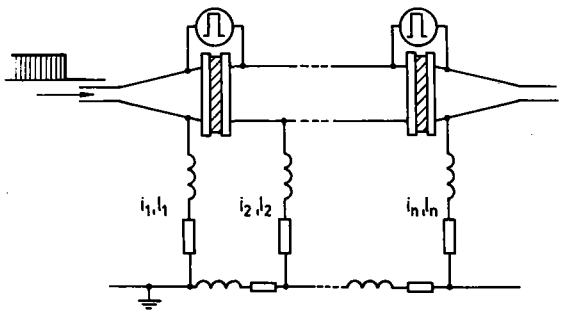

Figure 12 : Earthing loops at several parts of enclosures with varistor bridged discontinuities.

Figures 13 a and b illustrate two examples of different lengths of earth connections. If the earth connections are of the same length and the loops also have the same inductance, then the currents in the internal earth connections will be compensated and only the external earth connections will lead the currents.

In other cases all other earth connections are conducting.

It is necessary to note that the events in the internal GIS path are largely decoupled from the events in the external path between the enclosure and ground. This is caused by the non linear characteristic of the varistors. Only the frequency of the current oscillation depends on the length of the cables.

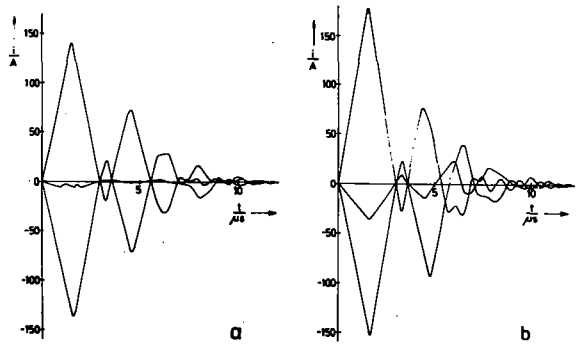

Figure 13 :Examples for current distribution in the earthing loops shown in Figure 12.
a) all earth connections are of the same length ;
b) earth connections are of different lengths.

CONCLUSION

On condition that the the feeders in GIS are terminated with cables the refracted waves entering the GIS are not dangerous. The cables must be longer than about 30 m.

In this case, the GIS/cable terminations and other discontinuities in the enclosure are significant sources of TGPR.

The most effective measure for reducing TGPR in this case is the low inductance shunting of the insulated flanges with varistors or other fast voltage limiters. The earth connections act with their inductance for the steep front of the travelling wave. The current flows to the enclosure via the shortest path, without other connections in the earthing grid participating.

If only one discontinuity is bridged with varistors then the earth connections must be close to the continuity.

REFERENCES

1 S.A. Boggs, N. Fujimata, M.Collod and E. Thuries
"The Modeling of Statistical Operating Parameters and the Computation of Operation - Induced Surge Waveforms for GIS Discomectors."
CIGRE Paper 13-15, 1984

2 G.L. Ford, S.A. Boggs and N.Fujimoto
"Transient Groundrise in GIS."
Transmission and Distribution, April, 1982

3 N. Fujimoto, S.A. Boggs, G.C. Stone
"Mechanisms and Analysis of Short Risetime GIS Transients."
CIGRE WG 33/13-09, 1986

4 J. Lalot, A. Sabot, J. Kieffer and S.W. Rowe
"Preventing Earth Faulting During Switching of Disconnectors in G.I.S. Including Voltage Transformer."
IEEE PES Summer Meeting, July 1985. Paper 85 SM 368-6

5 N. Fujimoto and S.A. Boggs
"Characteristics of GIS Disconnector Induced Short Risetime Transients Incident on Externally Connected Power System Components."
IEEE PES Winter Meeting, February 1987. Paper 87 WM 185-2

6 S. Ogawa, E. Haginomori, S. Nishiwaki T. Yoshida and K. Terasaka
"Estimation of Restriking Transient Overvoltage on Disconnecting Switch for GIS."
IEEE PES Summer Meeting, July 1985. Paper 85 SM 367-8.

7 G. Bernard, J. Massat, G. Ebersohl and G. Voisin
"Study of Electromagnetic Transients Due to Disconnector Switching in Metal Enclosed Substations."
Revue Generale de l'electricite - 11/83, p. 667-694, November 1983.

8 H. Aanestad, O. Deter, J. Lewis, H. Roehsler and A. Strnad
"Substations Earthing with Special Regard to Transient Ground Potential Rise - Design Aims to Reduce Associated Effects."
CIGRE WG 23-04, 1987.

9 E.P. Dick, N. Fujimoto, G.L. Ford and S. Harvey
"Transient Ground Potential Rise in Gas - Insulated Substations - Problem Identification and Mitigation."
IEEE Trans. PAS - 101, No. 10, October 1982.

10 N. Fujimoto, E.P. Dick, S.A. Boggs and G.L. Ford
"Transient Ground Potential Rise in Gas Insulated Substations - Experimental Studies."
IEEE Trans. PAS - 101, October, 1982

International Conference on Large High Voltage Electric Systems

112, boulevard Haussmann — 75008 Paris

1988 Session — 28th August - 3rd September

O

33-01

Pref. Subj. 1

SURGE PROPAGATION ANALYSIS : AN APPLICATION TO THE GRAJAÚ 500 kV SF_6 GAS-INSULATED SUBSTATION

by

P.C.V. ESMERALDO* F.M. SALGADO CARVALHO

FURNAS-Centrais Elétricas S.A.

(Brazil)

RÉSUMÉ

This paper presents the studies performed for the 500 kV Grajaú Gas-Insulated Substation related to lightning discharges and fast transient overvoltages generated by isolators operation.

From the results of these studies, considerations for the analysis of the failures occurred in the Grajaú GIS and its consequent modus operandi are discussed. Relevant aspects for new Gas-Insulated Substations specification are also brought to discussion.

KEYWORDS

Digital Computer Transients Modelling, Insulation Coordination, Lightning and Fast Transient Overvoltages, Isolators Operation, Gas-Insulated Substation.

1. INTRODUCTION

The Grajaú 500 kV Gas-Insulated Substation is situated in the metropolitan area of the city of Rio de Janeiro and about more than 50% of the total demand delivered to this city flows through it. During its initial operation, Grajaú Substation has experienced some failures as sparkover inside the enclosure, a 500 kV oil-impregnated paper bushing explosion and transformers failures.

Because the aforementioned failures, FURNAS-Centrais Elétricas S.A. decided to review the Grajaú surge propagation performance. Discussions with manufacturers, "in-site" and laboratory tests were conducted to help the explanation of those failures.

Peculiarities related to computer simulation and modelling for SF_6 substation in studies of lightning propagation and fast transients caused by the operation of isolators inside the GIS are presented. The simulations were done using the recognized digital computer program Electromagnetic Transients Program (EMTP) by Bonneville Power Administration. Modelling techniques used to represent the Gas-Insulated Substation components as bus ducts, spacers, corona shields, circuit-breakers, bushings, potential and current transformers and disconnector switches are analysed. The representation, in the Electromagnetic Transients Program (EMTP), of external components of the system connected to the Grajaú 500 kV Gas-Insulated Substation as transmission lines, towers, power and potential transformers and surge arresters are also detailed.

The overvoltages generated by both backflashes and shielding failures were investigated taking into account the application of metal oxide arrester compared with conventional gapped arrester. As the substation is fed by a 500 kV double circuit transmission line, 60 km long, it was observed that the phase circuit coupling plays an important role in the lightning overvoltages developed inside the GIS. In some cases, as in the open breaker configuration, the modelling consideration of coupling between phases of different circuits had caused significant reduction in the overvoltages calculated inside the Gas-Insulated Substation. This phenomenon was preliminarily analysed considering the modal analysis in conjunction with a lattice diagram.

Regarding the fast transient overvoltages generated by isolator operation a great number of possible network configurations in the substation were analyzed. Initially the studies were conducted considering a maximum 1.0 p.u. trapped charge. Later on, based on field measurements conducted by FURNAS, additional digital simulations were performed leading to 0.15 p.u., a typical manufacturer expected value which results in lower calculated fast transient internal overvoltages. The computed maximum values for this study are compared with insulation performance of the substation. The effectiveness of surge arrester vis-à-vis the fast transient overvoltages was also examined.

Based on the results obtained from the EMTP digital simulations and field experience, remarks and enhancements for future specifications are discussed.

2. SYSTEM MODELLING

2.1 Representation of GIS Components

2.1.1 Gas-Insulated Switchgear

As the GIS sections are a concentric cylinder type bus-bar, they were modelled in distributed parameter form by its surge impedance given by the formula $Z = 60 \ln D_2/D_1$, where D_2 is the inner diameter of enclosure and D_1 the outer diameter of conductor. The surge was considered to have a propagation in the light velocity (3×10^8 m/s).

2.1.2 Spacers

The main conductors are supported inside the enclosure by epoxy spacers which are responsible for a higher capacitive effect. The influence of the spacers can usually be neglected due to the low capacitance to be considered. However, to avoid

* FURNAS-Centrais Elétricas S.A. - Rua Real Grandeza, 219 - Rio de Janeiro - Brazil

cumulative differences in the calculations, the spacers were taken into account by an additional capacitance of 20 pF.

2.1.3 Circuit-Breakers

The circuit-breaker can be simulated by its surge impedance Z_c and its respective length ℓ_c, which can be estimated by the formula [1] $Z_c = \ell_c/C_c.v$ ohms, where ℓ_c is its length (in mm), C_c the internal capacitance of the circuit-breaker and v the velocity of surge propagation.

In this study, however, the circuit-breaker in the closed position was represented as an extension of the GIS bus-bar. In the open position, besides the above consideration a series concentrated capacitance (representative of grading capacitors) of 750 pF [2,3,4] was added in the model.

2.1.4 Bushings

The connection between the Gas-Insulated Switchgear and the aerial lines is done through bushings specially constructed for that purpose. They were represented by their surge impedance and length, plus an additional lump capacitance of 100pF [4]. It was also considered a 50% reduction of the surge propagation velocity inside the bushing over 2/3 of its total length, according to manufacturer information.

2.1.5 Potential Devices and Current Transformers

The potential devices were represented by lumped capacitance in the range of 1500 pF to 5000pF. The consideration of this model is important in the surge propagation within the GIS.

The current transformers are provided concentric to the conductor and the enclosure, and because of their small length they can be neglected.

2.1.6 Corona Shields

The corona shields can be represented using the same model of the spacers, i.e., small lumped capacitances of 20pF placed in their exact location.

2.1.7 Disconnector Switches

The disconnector switches in the closed position were represented as an extension of the gas-insulated bus-bar. In the open position the representation was an "open-circuit" and the length of the switch was also considered as an extension of the gas-insulated bus-bar. In the case of transients generation (i.e. the switch being operated) they were modelled by two stepwave current sources and a small resistance representing arc impedance. This representation was used because the switch restrike behaves as stepwave generator.

2.2 Representation of Other Components

2.2.1 Power Transformers

The power transformers were simulated by their surge capacitances. These capacitances range from 2 to 10 nF, depending on the transformer design. This representation, however, is not critical for the lightning overvoltage developed inside the GIS and approximated values can be used. For the Grajaú transformers 7 nF were used.

2.2.2 Inductive Potential and Capacitive Voltage Transformers

These equipments when located externally to the GIS can be represented by their own lumped surge capacitances.

2.2.3 Surge Arresters

As the surge arresters are the most important devices to establish the station insulation coordination, their representation requires reliable information from the manufactures. In the lightning overvoltage study was analysed the performance of both arresters, the conventional ones and the zinc oxide arresters. In this case their representation was assumed by using non-linear resistances taking into account different sparkover voltages and V x I characteristics according to the behaviour of the time-to crest of the incoming waves. In the fast transient study only the existing conventional arresters were modelled. Due to the lower overvoltage found their representation was not critical..

2.2.4 Transmission Lines

The lightning waves penetrate in the GIS through the transmission lines, so their representation must be very accurate. Usually this kind of study deals with a single-phase representation, which generally yields in conservative results. As the Grajaú feeding lines are consisted by one 500kV double-circuit, the coupling between two phases of the different circuits were considered, since the different velocity modes of propagation and differents rates of attenuation are responsible for the distortion experienced by the incoming waves travelling along the line.

The modal wave travel method used in conjunction with a lattice diagram gave an auxiliar analysis of overvoltage, where it could be observed that the building up voltages on the entrance of the station mainly depend on the distance between the point where the discharge hits the line and the station and the soil resistivity which affects greatly the ground mode velocity.

The analysis carried out with EMTP assumed two phase conductors, of different circuits, represented by their self and mutual impedances considering the Carson correction terms with appropriated soil resistivity. It is important to stress that higher resistivity values implies lower ground mode velocities, hence greater distortion. This aspect was carefully checked to assume a realistic soil resistivity.

2.2.5 Transmission Towers

In the backflashover study, data from tower models tests were considered to represent their surge impedance (Z_t = 120 Ω) and the surge propagation velocity having a reduction to 2 x 10^8 m/s. The tower footing resistance was obtained from field measurements in the near vicinity of the station. Regarding the insulator string, different withstand voltage taking into account the volt-time characteristics were considered according to the development of the voltage across the insulator string.

3. SURGE PROPAGATION STUDY

3.1 Description of Failures [5,6]

The first failure occurred during a thunderstorm when a sparkover took place on one phase of the 500 kV enclosure busbar.

After that, one oil-impregnated paper bushing exploded during normal operation, after being in service for less than two years. The next failures occurred on the transformers, the first one, immediately after the transformer had been re-energized it was tripped off by the operation of the differential protection and was observed a formation of combustible gas. A few months later, during normal operation, other banks were tripped off by the actuation of same protection and also of the pressure relief device. The third failure, two years later, was exactly in the same conditions as the first one.

Considering the failures mentioned before, FURNAS decided not only to review the lightning overvoltage study in a more conservative basis but also to investigate the high-frequency overvoltages related with fast transients generated by internal isolators during disconnect switching.

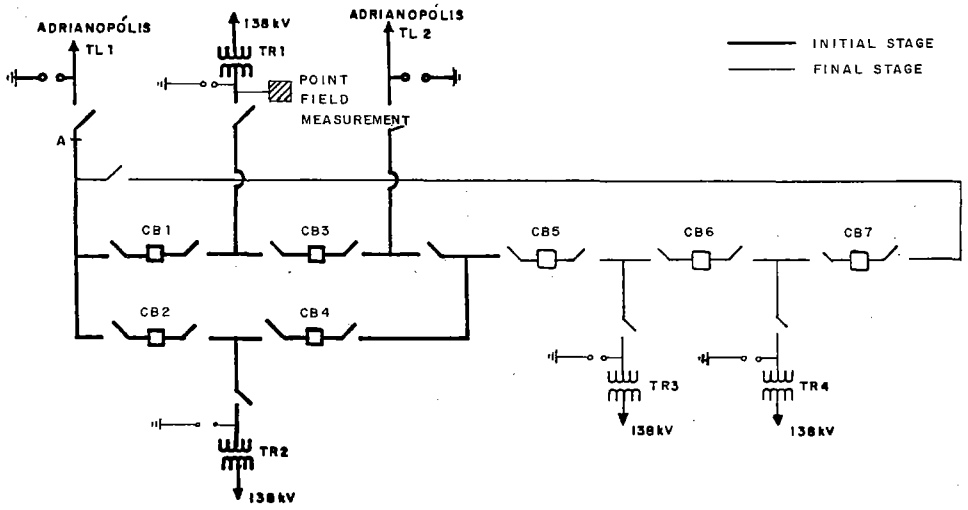

Figure 1 - Grajaú 500 kV Substation

3.2 Lightning Overvoltage Study

The lightning overvoltage study consisted in the determination of overvoltages generated due to direct strokes and backflashovers. The amplitude and the slope of the wave front of the discharges that reach the substation basically depend on the line insulation level, on the attenuation and distortion during propagation from the point of stroke to the substation entrance. The attenuation and distortion of the waves are essentially due to corona losses [7].

Of equal or more importance is the effect of coupling between conductors. The coupling of the 500 kV double-circuit lines connected to the Grajaú Substation plays an important role in the overvoltages developed inside the substation, since the multi-velocity wave propagation are responsible for significant reduction of surge voltages at the station entrance.

A sensitivity analysis was also conducted to assess the influence of certain parameters on the results, i.e. length of the arrester leads, grounding resistance, system voltage at the instant of the lightning stroke and soil resistivity.

Considering the aspects previously stated the conservatism imposed on this study was related to the incident truncated ramp wave having a crest time ranging from 0.5 μs to 1.0 μs, which means a substantial margin of pessimism. Also it was admitted the surge reaching the line about 100-150 meters from the substation, although this region is the most effective from the lightning protection point of view.

For the backflashover cases, both for discharges at the top of the towers or in the mid-span a maximum stroke current of 100 to 150 kA was assumed. In the case of direct discharges, the evaluation of the maximum current was based on the tower configuration. Through the electrogeometric model the maximum current that would reach the phase conductors and cause shielding failure, was calculated utilizing Whitehead's formula ($rs = 9.I_0^{0.65}$). This critical current was found of the order of 11 kA, which corresponds to a maximum voltage surge of approximately 2500 kV.

The lightning performance studies for the Grajaú Substation was developed in two stages. The first one analysed the substation during its initial operation and was used as a basis to clarify the first failure. Later, the expansion phases were studied from the start-up of the 3rd and 4th transformer banks (see Figure 1).

For the first stage of the Grajaú Substation the previous insulation coordination study indicated no need for enclosed arresters, but considering the failure occurred during a thunderstorn that possibility was carefully analysed again. The conclusions on this review not only confirm the prior conclusions but also did not indicate enclosed arresters for the substation future stages, even considering the long distances of the 2nd ring in SF6 ducts that feed the aforementioned transformers.

Cases were run with the substation configuration in normal condition and emergency conditions (line and transformers outages) with surges penetrating over both lines feeding the substation.

Analysis of the results

For the cases related to the initial operation stage, conventional arresters at the end of the line and the transformers entrance were considered. Later, the arresters installed at transformer entrances were replaced by zinc oxide arrester, taking into account the good performance of this equipment. Whereas the ZnO arresters showed themselves to be effective by improving the substation performance regarding lightning strokes, they were likewise recommended for the expansion stages.

Table 1 shows the maximum overvoltages due to direct strokes for the initial and future stages of Grajaú Substation, together with the lightning impulse withstand level (LIWL) of the equipment.

In the emergency cases were considered single, double and triple contingencies with lightning strokes coming from TL1 or TL2, considering line or transformers either permanently or temporarily out of service.

TABLE 1 - Maximum Overvoltages for Direct Stroke (Shielding Failure) Simulations

	LIWL (kV)	Max. Overv. (kV)		Max. Overv./LIWL (%)	
		Normal Condition (1)	Emergency Condition (2)	(1)	(2)
GIS	1550	1111	1329	72	85
Transf.	1425	1185	1310	83	92
Bushing	1675	1125	1297	67	77

The maximum 1310 kV overvoltages found in the transformer were due to a triple contingency and therefore have low probability of occurrence, i.e., TR1, TR2 and TL1 or TR1, TR3 and TL2 out of service (see Figure 1).

The maximum overvoltages recorded for backflashover simulations are presented in Table 2. Strokes hitting both the top of the tower or mid span are synthesized, considering the different parameters of the incident wave current, i.e.: (1) 0.5 μs/100 kA; (2) 0.5 μs/150 kA; (3) 1.0 μs/150 kA.

TABLE 2 - Maximum Overvoltages for Backflashover Simulations

	LIWL (kV)	Max. Overv. (kV)			Max.Overv./LIWL (%)		
		(1)	(2)	(3)	(1)	(2)	(3)
GIS	1550	1150	1290	1120	74	83	72
Transf.	1425	1200	1300	1250	84	91	88
Bushing	1675	1270	1541	1300	76	92	77

Open circuit-breaker configurations due to flashover to ground from a first lightning stroke were also simulated. Despite the lower values of the subsequent discharges, it was assumed that this open terminal would be exposed to a second stroke (multiple stroke) of same magnitude of the former, considering the pessimistic approach adopted for this study. It is seen that the maximum overvoltages did not remain within a safety margin of 10%, but neither did they exceed the equipment LIWL. Table 3 summarizes the maximum values obtained.

TABLE 3 - Maximum Overvoltages for Open Circuit-Breaker Configurations

	LIWL (kV)	Max. Overv. (kV)	Max. Overv./LIWL (%)
GIS	1550	1475	95
Transf.	1425	200	14
Bushing	1676	1449	86

Finally, as it had been stated, the importance of the coupling between the incoming lines can be verified through the comparisons between the oscillograms on Figures 2 and 3, where it is plotted the voltages at the station entrance and inside it (CB6). In this case, with lightning wave penetrating through TL1, with CB1, CB2 and CB6 opened the coupling representation can mean an overvoltage reduction of 20 to 30% (See Figure 1).

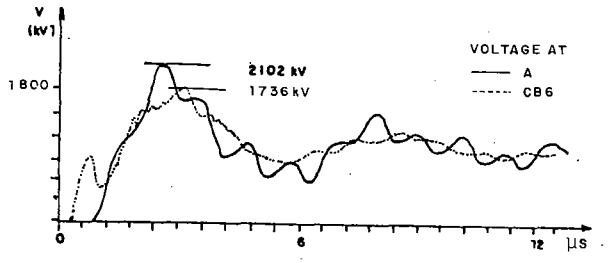

Figure 2 - Overvoltage Without Line Coupling

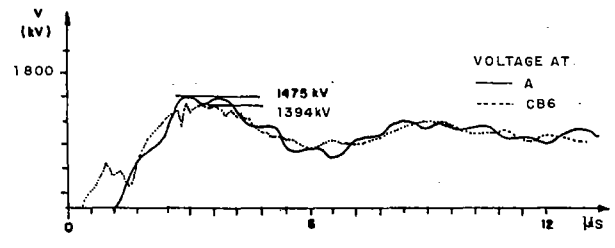

Figure 3 - Overvoltage With Line Coupling

3.3 Fast Transients Overvoltage Studies [2,3,8,9]

The studies performed to calculate the fast transients overvoltages considered that the Grajaú isolators are designed to interrupt charging currents of an electric circuit having two small SF_6 bus-bar sections and a circuit-breaker in the "open" position. The GIS isolator transients are generated by the intercontact arcing which occur during operation, both opening and closing. Several restrikes occur between contacts during a single operation. Each restrike generates a spark which equalizes the potential between the disconnector terminals.

These transients are characterized by a very high frequency in the range of MHz and magnitude depending on several factors such as disconnector characteristics, lay-out of the substation etc.

For the Grajaú substation, the effect of disconnect switch operation for various configurations was investigated. The computations carried out also considered the initial stage of the station. The study did not produce any voltages with very high values. The voltages were always lower than the values of the installed equipment insulation levels, i.e., the maximum overvoltages found were around 2.0 p.u.

The criteria adopted in the study were very conservative. Considering that the real value was unknown, it was assumed a trapped charge in the SF_6 bus-bar section to be switched of 1.0 p.u. The operation of the disconnect switch that generates the overvoltages was simulated when the voltage on the source side was at its positive maximum value (+1.0 p.u.) and on the other side, coming from the trapped charge, at its negative maximum value (-1.0 p.u.). In this way, at the instant of the switching, there was a voltage of 2.0 p.u. across terminals.

During the switching operation numerous other restrikes occur with the voltage across terminals at lower levels. Naturally, the overvoltages developed within the station are also of lower values. It should be remembered that there is no superposition effect of the successive restrikes.

Figure 4 shows one of the configurations analyzed for the Grajaú substation, and in Figures 5 and 6 some of the results obtained.

After the completion of the digital simulations, field measurements were conducted using techniques developed by ONTARIO HYDRO [3]. Because of the importance of Grajaú Substation to the Rio de Janeiro City energy supply, it was not possible to have it available for measurements during a reasonable time. However, valuable results were obtained and are detailed presented in [6]. The peak and the initial risetime values of the transient surge, generated by the disconnect switch operation when one of its terminals is under voltage, were measured for three basic configurations. The point of measurement was located near the power transformer which had suffered failures (see Figure 1).

Since at that time it was not possible to measure the trapped charge left at the floating part, a sensitivity analysis was made with the EMTP assuming values of 0.0, 0.15 and 1.0 p.u. The results obtained, both in the measurements and simulations, are presented in Table 4.

Although in these cases the overvoltages are not high it was possible to establish that the calculated values with 1.0 p.u. trapped charge has led to very conservative results. A good agreement between the field test and digital simulation was reached considering the trapped charge near 0.15 p.u.

It can be concluded that the EMPT allows the analysis of various operational configurations in order to determine the worst situation. It also gives flexibility when performing parametric studies.

The field tests are necessary in order to determine the effect of the switches design on the values of the trapped charge. They also give the possibility to check and to improve the digital models.

Planning studies performed in order to determine the equipment specifications of a SF_6 substation, may assume initially 1.0 p.u. for the trapped charge. If the results are not acceptable, it will be necessary to calculate the maximum allowable value and include this value in the disconnector specification. In this case, tests will be needed to prove the requirements.

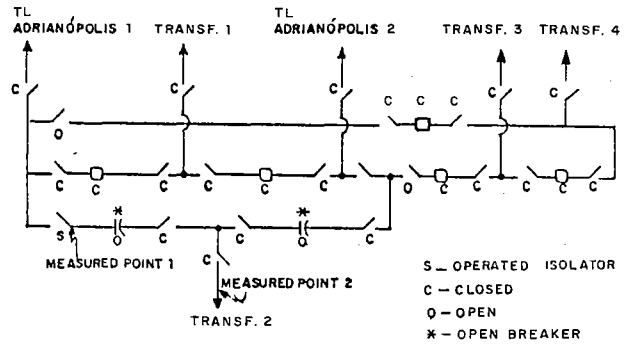

Figure 4 - Grajaú Typical Configuration Analysed

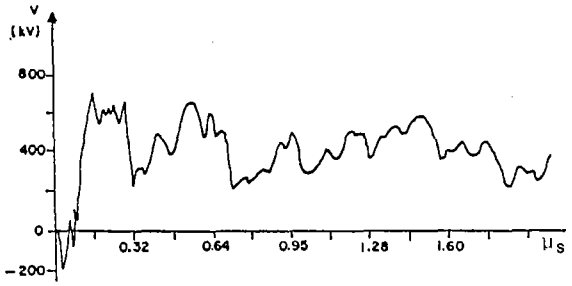

Figure 5 - Computer Calculated Overvoltage at Point 1

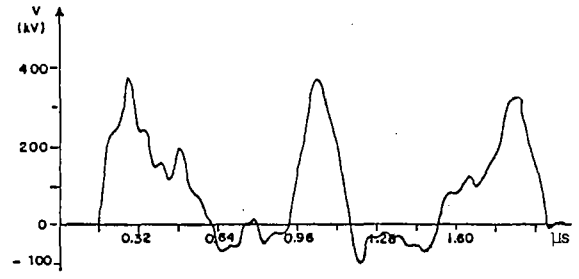

Figure 6 - Computer Calculated Overvoltage at Point 2

4. CONCLUSIONS

4.1 The results obtained in the lightning study have indicated values below the equipment lightning insulation withstand level (LIWL) for normal and emergency conditions of the station and open-circuit-breaker configurations. The minimum insulation margin remained around 10%.

4.2 The lightning overvoltage study showed the effectiveness of the ZnO arresters connected near the transformers when compared to the conventional. The study also showed that enclosed arresters are not required even for the substation expansion stages.

4.3 The coupling between the circuits of the 500 kV double line feeding the Grajaú Substation contributed significantly in the sense of reducing the overvoltages due to lightning at the entrance of the station. Some configurations bring about a reduction on the order of 20% to 30%.

4.4 The maximum high-frequency transients overvoltages due to disconnect switches operation were about 2.0 p.u. and the maximum oscillation frequency about 2.5 MHz. The overvoltages found are much less than the SF_6 bus-bar LIWL and other neighbouring equipment. Nevertheless, because equipment failures occurred [5,6] FURNAS is still proceeding to investigate the matter and, if necessary, additional measurements may be performed. Meanwhile, due to the importance and the necessity to have Grajaú in continuous operation, it was decided to avoid isolators operation under voltage. Only under some critical system operational conditions the isolators are allowed to operate.

4.5 The fast transient overvoltages did not lead the existing Grajaú conventional arrester to operate, because of their lower values. However, it was observed that the arresters would be incapable of limiting these overvoltages conveniently, because of their short wave fronts.

The capability of the arresters to protect a given length of the bus-bar (including the equipment installed along that section of bus-bar) is a function of the voltage wave fronts. Actually, the arresters can be helpful considering their performance with respect to lightning strokes which have longer wave fronts than those caused by the operation of disconnect switches.

4.6 Based on the result of the studies vis-à-vis the field reality, it seems that additional research and investigations, both theoretical and experimental, should be conducted to obtain further information on the behaviour of 500 kV Gas-Insulated Switchgear and related equipment when submitted to fast transients overvoltages. Future revisions of international standards should be stimulated to cover this subject.

4.7 When planning future applications of high-voltage gas-insulated substations, besides the analysis of the equipment submitted to lightning overvoltages, the insulation coordination studies

TABLE 4 - Measurements and Simulation of Transients During Disconnect Switch Operation-Table of Results

Case	Voltage at Point of Measurement Prior to Switch Operation(p.u.)	Measurements		EMTP SIMULATIONS					
				Trapped Charge: 0 pu		Trapped Charge: 0.15pu		Trapped Charge: 1.0 pu	
		Peak Value (p.u.)	Risetime (ns)	Peak Value (p.u.)	Risetime (ns)	Peak Value (p.u.)	Risetime (ns)	Peak Value (p.u.)	Risetime (ns)
A	0.13	0.46	20	0.33	18	0.41	18	0.90	18
B	1.00	0.30	6	0.29	21	0.33	21	0.72	21
C	0.14	0.44	20	0.39	18	0.50	18	1.11	18

shall include the determination of fast transients overvoltages "worst cases". The results obtained are to be used to prove equipment withstand and to achieve this, manufacturers collaboration is expected.

4.8 Regarding future specification the present study can give some directives concerning the impulse withstand level. When considering long SF_6 bus-ducts, with several sections and other equipment inside them, it seems that a section of a bus-bar tested separately in the manufacturer's site could offer lower insulation levels when they are assembled together in field. Special attention must be given to this matter that deserves some discussion by manufacturers and users.

REFERENCES

[1] BOECK, W. and PETTERSEN, K. - "Fundamentals and Specific Data of Metal-Enclosed Substations for the Insulation Coordination" - CIGRE 23-03, 1978 Session, Paris, August 30 - September 7.

[2] SCHLICHT, D.W., SCHMIDT W. and HEINELT. D. "Disconnect Switch Operation in SF_6 GIS" - IEEE: Canadian Conference on Communications and Power Montreal, October 15-17, 1980.

[3] BOGGS, S.A., CHU, F.Y., FUJIMOTO, N. KRENICKY, A., PLESSL, A. and SCHLICHT. D. - "Disconnect Switch Induced Transients and Trapped Charge in Gas-Insulated Substations" - IEEE: Winter Power Meeting, New York, February, 1982.

[4] BROWN BOVERI - "Surges in High-Voltage Networks", Plenum Press, New York, 1980.

[5] DIRENE, A. J., LEME, M.P. and NEVES, P. C. - "Failures in 500 kV and 138 kV Bushings Connected to Gas-Insulated Switchgear" - Doble Engineering Company Seminar, Boston, 1982.

[6] DIRENE, A.J., LEME, M.P., SICA, A.L. and FRANÇA, W.J. - "Investigation of the Effects of Switching Transients in Gas-Insulated Switchgear to 500 kV Bushings and Power Transformers" - Doble Engineering Company Seminar, Boston, 1984.

[7] CRONIN J.C., COLCLASER R.G. and LEHMAN R. F. - "Transient Lightning Overvoltage Protection Requirements for a 500 kV Gas-Insulated Substation" - IEEE PES Winter Meeting, N. York 1977.

[8] BARGIGIA, A., MAZZA, G., PIGINI, A., THIONE, L. and MAZZOLENI, B. - "Study of the Dielectric Strenght of SF6 Insulated Metal-Clad Substations and Application to their Design and Testing" - CIGRE - 33.12, Paris, 1982 Session, 1-9, September.

[9] BOSOTTI O., MOSCA, W., RIZZI, G., HASHOFF, L., LYNAST, E. and LÜHRMANN, H. - "Phenomena Associated with Switching Capacitive Currents by Disconnectors in Metal Enclosed SF6 Insulated Switchgear", CIGRE: 13.06, 1982 Session, Paris, 1-9 September.

International Conference on Large High Voltage Electric Systems

112, boulevard Haussmann — 75008 Paris

1988 Session — 28th August - 3rd September

O

33-04

Pref. Subj. 1

PURSUING REDUCED INSULATION COORDINATION FOR GIS SUBSTATION BY APPLICATION OF HIGH PERFORMANCE METAL OXIDE SURGE ARRESTER

by

T. KAWAMURA*
University of Tokyo

Y. ICHIHARA
The Tokyo Electric Power Co., Inc.

Y. TAKAGI
The Chubu Electric Power Co., Inc.

M. FUJII
The Kansai Electric Power Co., Inc.

T. SUZUKI
Central Research Institute of Electric Power Industry

(Japan)

Summary

This paper outlines the studies conducted in Japan on the insulation coordination of 500kV GIS substation.

Newly developed high performance metal oxide surge arrester and digital simulation of electrical transient phenomena make the good basis of reexamining insulation coordination for 500kV and 275kV GIS substation. By application of those surge arresters, lightning overvoltages within substation can be effectively reduced. To make the best use of these new technologies, we studied reducing the 500kV and 275kV insulation levels of GIS substation economically and reliably. Economical UHV insulation coordination is also studied on the same basis.

Keywords

Insulation coordination, GIS substation, Metal oxide surge arrester, Digital simulation, Lightning overvoltage, 500kV, 275kV.

1. Introduction

Considerable insulation reductions are essential for realization of economical GIS (SF6 Gas Insulated Switchgears) substation. In Japan the insulation levels of substation apparatuses, which were standardized by JEC-193 (Standard of Japanese electro-technical committee) [1] in 1977 primarily with consideration of high reliability, are considered to be higher than those in other countries. Newly developed high performance surge arrester and digital simulation of overvoltages make good basis of reexamining insulation coordination for 500kV and 275kV GIS substations.

For surge arresters, those of metal oxide type have been applied up to 500kV substation in these ten years. They have no series gap because of good non-linear characteristics, and can have lower residual voltage than conventional silicon carbide type ones with series gaps. Metal oxide surge arresters with more improved characteristics have been recently developed for practical use on these operational experiences. By application of them, lightning overvoltages within substations can be effectively reduced.

For digital simulation of overvoltages, an elaborate digital computer program (EMTP) was developed by BPA in the U.S.A. in 1970's. This program makes the analyses of transient phenomena more precise than analog calculations by TNA.

To make the best use of these technologies, we started to study reducing the 500kV and 275kV insulation levels of GIS substation economically and reliably. Economical UHV insulation coordination was also studied on the same basis.[2]

2. Techniques of analyses

Lightning overvoltages can be precisely analysed by the progress of computer analytical technologies. These techniques make it possible to simulate the facilities of transmission lines as well as substations and the physical phenomena of overvoltages. New detailed models were employed for the typical transmission line with double circuits and GIS substation in Japan. (Figure 1) These models, which employ new knowledge based on actual measurements, involve new model of transmission lines and backflashover model studied by the Institute of Electrical Engineers of Japan. [3], [4]

2.1 Program of analyses

The Electro-Magnetic Transients Program (EMTP), which was developed for transient phenomena simulation by Bonneville Power Administration (BPA) in the USA, was employed because this program was confirmed to be the most reliable one by many experiences in Japan and was highly esteemed in the world.

* University of Tokyo, 7-22-1 Roppongi Minato-ku Tokyo (Japan)

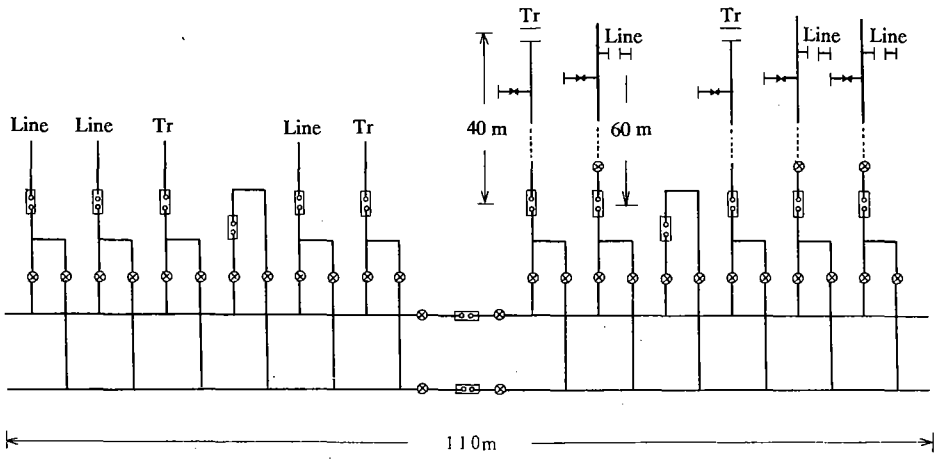

Figure 1 Typical Configuration of 500kV Substation

2.2 Model of transmission lines

Multi-section model of transmission lines with frequency dependent characteristics, eight phase Semlyen model, was used to faithfully simulate double circuit transmission line consisting of 8 phases (6 power lines and 2 ground wires), their mutual induction effects, and their frequency dependent line effects. [5]

For the simulation of double circuit tower, detailed tower circuit model was employed. This is the model divided into four circuits at the position where upper, middle, and lower arms are mounted. Each section of the model consists of lumped resistance, lumped inductance and distributed surge impedance. It was simulated to match with the surge response of waves measured across an arcing horn at the actual 500kV tower. (Figure 2)

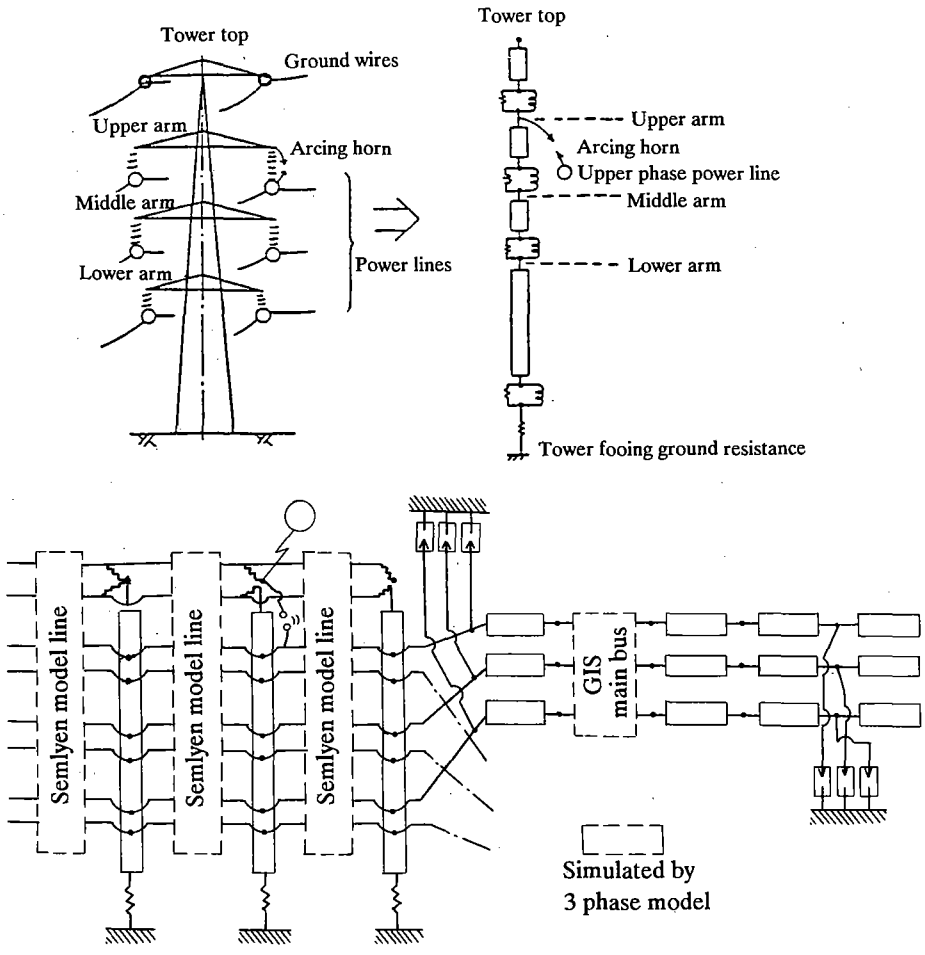

Figure 2 Model of Transmission line and Tower

2.3 Model of backflashover

The value of lightning surge entering into substations depends on the sharpness of the backflashover current. The observation of actual flashover phenomena at a long gap shows that the current sharpness is not so high as that obtained by the model by a single switch, because large discharge current flows before the flashover. Then we employed the new backflashover model in which time-dependent inductance is simulated in accordance with three stages such as leader stage, final jump stage, and arc stage. (Figure 3) [6], [7]

3. Conditions of analyses

3.1 Condition of lightning stroke

Lightning surges entering into substations include:

- Adjacent lightning surge with high sharpness and high value caused by backflashover on the first tower from the station
- Long distance traveling lightning surge with comparatively low sharpness and low value caused by lightning strokes on several kilometer distant tower from the station

For the security of substation, we studied adjacent lightning surge with severer sharpness and value. For the value of a lightning stroke, we chose 150kA for 500kV, and 100kA for 275kV in accordance with system security. For UHV system, 200kA lightning stroke, the highest current observed in Japan, was chosen. And 1/70 μs lamp wave was used for lightning current wave, which represents data observed in the past. [8]

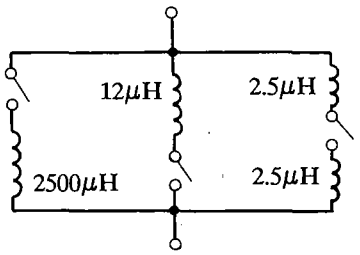

Figure 3 New Backflashover Model

(Example of the values)

3.2 Condition of substation configuration

For the condition of substation configuration into which lightning surge enters, three conditions were set up for the consideration of severity to GIS and a transformer. (Figure 4)

[I] of the Figure 4 is the severest case for transformer, in which lightning surge enters into the circuit under the condition that a single line and a single transformer are connected with the 1/4 main bus. [II] is the severest case for GIS at the line entrance, in which lightning surge enters into the circuit under the condition that a circuit breaker at the line entrance is opened. [III] is the severest case for GIS main bus, in which lightning surge enters into the circuit under the conditions that a single line is connected with the 1/4 main bus.

3.3 Characteristics of surge arrester

The drastic high performance of surge arrester was assumed for analyses. The newly developed metal oxide surge arrester has remarkable volt-ampere characteristic (V_{10KA} = 870kV), whose residual voltage is approximately 80% of the present metal oxide arrester in operation. Accompanying with reduction of v-i characteristic, this arrester has a higher energy absorption capability (250joules/cm^3) than energy absorbed in the temporary overvoltages. Its high performance can be realized by the improvement of the composition in zinc oxide elements and manufacturing method.

4. Results of analyses

The value of lightning overvoltages within a substation changes according to the number and location of arresters, or the length of GIS bus. In particular, the number and location of arresters are determined by the balance between performance and economy. The results studies show it effective to locate arresters at the line entrance as well as transformer terminal.

For 500kV substation, the maximum overvoltages are 1400kV for GIS and 1090kV for transformer. For 275kV substation, these voltages are 850kV for GIS and 640kV for transformer. For UHV substation, the maximum value is 2390kV for GIS and 1830kV for transformer under the condition that arresters are located in addition at the terminal of main bus because of economical reasons.

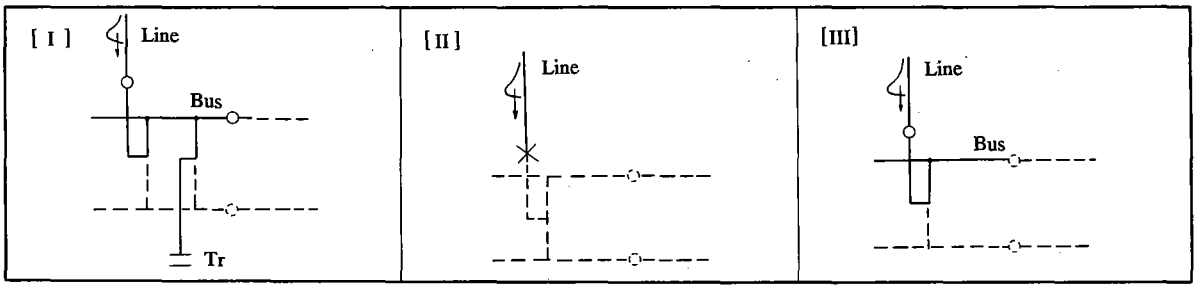

Figure 4 Conditions of Substation Configuration

Figure 5,6 shows the typical result of lightning overvoltage analyses in 500kV substations. It represents the analytical result in the configuration of a single line and a single transformer, with fifteen combinations of the following parameters by a distance of 10 meters.

- GIS bus length of L_1 = 20 to 60 m
- Transformer-primary cable length of L_2 = 20 to 40 m

For GIS, the maximum value of overvoltage is 1400kV at the section end of GIS main bus with the combination of L_1 = 30m and L_2 = 30m. For transformer, the maximum value is 1090kV at the transformer terminal with the combination of L_1 = 20m and L_2 = 30m.

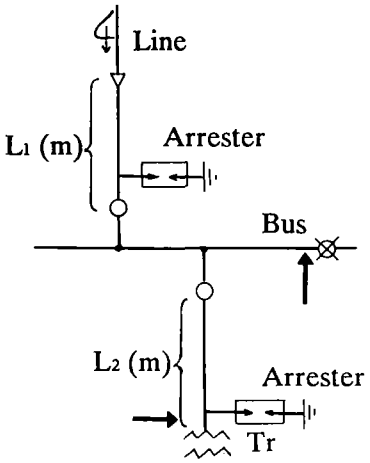

Table 1 Condition for Analyses of Lightning Overvoltages

Struck tower	No.1 tower
Stroke current	150kA
Wave shape	1/70 μs lamp wave
Substation configuration	1 line & 1 transformer connected
Power frequency voltage	Imposed
Characteristic of surge arrester	V_{10kA} = 870kV

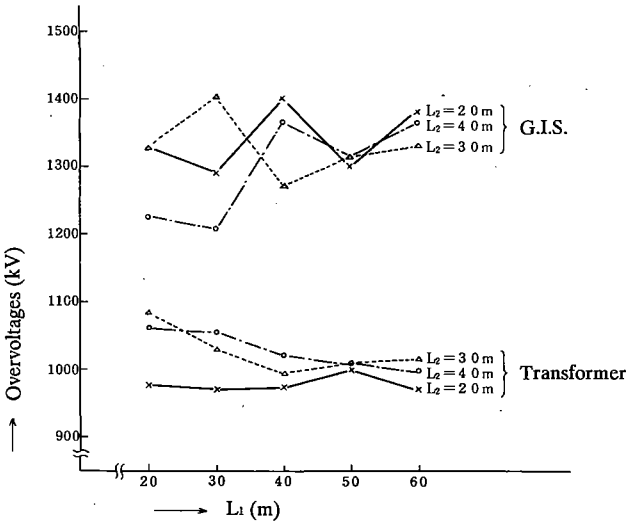

Figure 5 Results of Lightning Overvoltages with 15 Combinations of L1 and L2

5. Studies on Insulation Coordination

The values of maximum lightning overvoltages in the typical 500kV substation, are shown in Table 2; They are reduced by 30% from those based on the study of JEC-193.

The withstand voltages for substation apparatus , test voltage (LIWL), should be studied on the basis of the analytical result. For these purposes, it is necessary to determine carefully the margin between test voltage and analytical result.

The factors to determine the margin are listed as follows.

- Accuracy of analysed values
- Imposed power frequency voltage
- Disconnector switching overvoltage
- Shape of analysed overvoltage wave

The estimation of these factors is explained as follows.

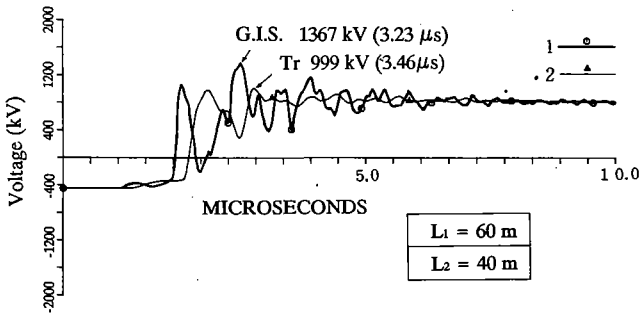

Figure 6 Typical Wave Form of Lightning Overvoltages

Table 2 Maximum Lightning Overvoltage

	Maximum Lightning overvoltage (kV)		N. B.
	Transformer	Others	
Analyses based on this paper	1090	1400	* Gas insulated switchgears * Analysed by EMTP
Analyses based on JEC 193	1530	1700	* Air insulated switchgears * Analysed by TNA

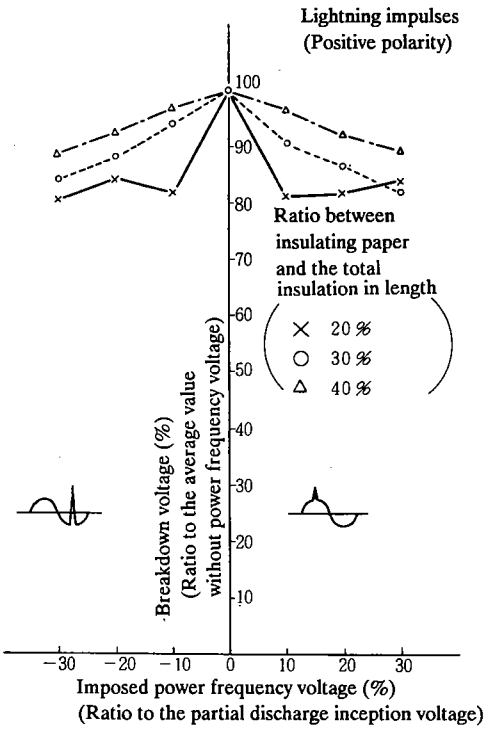

Figure 7 Effect of Imposed Power Frequency Voltage (transformer)

5.1 Accuracy of analysed result

The EMTP program which matches with actual phenomena, was employed in these analyses. In particular, for simulation, the newly developed precise model for transmission line and tower mentioned in clause 2.2 are employed. Furthermore, the conditions of lightning stroke and substation circuit configuration in these analyses are extremely severe and the lightning overvoltages are analysed under the imposition of power frequency voltages.

5.2 Imposed power frequency voltage

Whether the insulation strength of apparatuses changes on the condition of lightning surge with power frequency voltage from that of only lightning surge, or not, should be studied. The research on the part-model of GIS and transformer showed that:

(1) For GIS, the imposed power frequency voltage had no influence on the insulation strength if its value was 70% or less of the partial discharge inception voltage.

(2) For transformer, the imposed power frequency voltage had no influence on the insulation strength if its value was 20% or less of the partial discharge inception voltage. However, if the ration was larger, the strength was reduced by 10-20% in a certain construction ration of insulation paper to oil gap. (Figure 7)

Therefore imposed power frequency voltage actually has no influence on GIS insulation strength because the value of power voltage is not as high as that of lightning overvoltages. On the other hand, the strength of transformer is influenced by the imposed voltage in certain ratio. These phenomena are a new knowledge for the transformer insulation by the research of part- model. We are now studying how much they affect the insulation strength of full-size transformer. Therefore, the margin in this imposed power frequency voltage should be continue to be studied from now on.

5.3 Disconnector switching overvoltage

The value of steep front overvoltages caused by the operation of disconnecting switch was analysed by EMTP for 500kV substation. [9], [10], [11] Its maximum values are as follows:

- GIS: 1250kV
- Transformer: 600kV

Their effects on the insulation of transformers are not considered because their value is 60% as low as lightning overvoltages. On the other hand, their effect on GIS should be considered because they are 90% value of lightning overvoltage and occur frequently. However the strength within the spacer, which is mostly influenced by disconnector switching overvoltages, is designed by usual operation voltage and provides much stronger than that of lightning test voltage in Japan. Therefore it can be considered that GIS will not be influenced by disconnector switch overvoltage even if imposed by several thousand times of overvoltages with the 90% value of lightning overvoltage.

The strength of gas gap is also considered to have enough margin for extremely steep voltage such as disconnector switching overvoltage because insulation strength of short time v-t characteristic is higher than the level of lightning overvoltage. But there is another opinion that gas gap provided with small particles is influenced by this overvoltage. [12] So detail studies should be carried out from now on.

5.4 Shape of analysed overvoltage wave

The wave analysed in this study has an oscillating characteristic. The estimation of insulation characteristic between its wave and standard test wave 1.2/ 50 μs by area shows that standard test wave with the same peak value is equivalent to the analysed wave.

From studies of margins, we know that we have now two unknown factors, namely margin of imposed power frequency voltage and its disconnector switching overvoltage with small particles. These factors will continue to be studied eagerly from now on.

However, we can adopt two or three lower rank of the lightning test voltages in IEC Pub71-1 [13] than those at present in Japan, as shown in Table 3, because overvoltages are extremely reduced.

Table 3 Maximum Lightning Overvoltages and Test Voltages (LIWL)

	Maximum lightning overvoltage (kV)	Supposed value of LIWL (kV)	N. B.
Trans-former	1090	1175 - 1300	15-25% lower than present LIWL (1550kV)
GIS	1400	1425 - 1550	15-20% lower than present LIWL (1800kV)

6. Conclusion

We reached the following conclusions on the basis of the above-mentioned studies.

(1) By application of newly developed high performance metal oxide surge arrester and new digital simulation by EMTP, lightning overvoltages within substation can be remarkably controlled to 70% of those analysed in the study of the present test voltage.

(2) We can have a prospect to adopt lower test voltages by 15-25% than the present voltages for 500kV transformer and GIS.

These studies make the basis for reducing insulation of the 500kV GIS substation. From now on, we continue to evaluate such two factors as the effect of steep front overvoltages caused by the operation of disconnecting switch on GIS with small particles, and the effect of impulse impression under operating power frequency voltage on transformers.

Finally, we expect to realize the reliable and economical 500kV GIS substation.

References

1) The Japan Electrotechnical Committee, "JEC-193-1974, Standard for test voltage"

2) I.Miyachi et al., "Insulation Coordination for UHV SF6-Insulated Installations and Transmission Lines by Application of High Performance Metal Oxide Surge Arrester", CIGRE Paper No 33-03, 1984

3) The Institute of Electrical Engineers of Japan, "Statistical Approach to Insulation Design", Technical Report II-229, 1986

4) The Institute of Electrical Engineers of Japan "A New Method of Lightning Overvoltage Analyses in Power System", Technical Report II-244, 1987

5) J.Ozawa et al., "Lightning Surge Analysis in a Multiconductor System for Substation Insulation Design" IEEE Transactions on PAS-104, No.8, pp2244-2251, 1985

6) T.Sindo, T.Suzuki, "A New Caluculation Method of Breakdown Voltage-time Characteristics of Long Air Gaps" IEEE Transactions PAS-104, No.6, pp1556-1563, 1985

7) T.Sindo, T.Suzuki, "A Study of Predischarge Current Characteristics of Long Air Gaps" IEEE Transactions PAS-104, No.11, pp3262-3268, 1985

8) R.B.Anderson & A.J.Eriksson, "Lightning Parameters for Engineering Application", CIGRE ELECTRA, No.69, 65(1980)

9) S.Ogawa et al, "Estimation of Restriking Transient Overvoltage on Disconnecting Switch for GIS", IEEE Transaction on Power Delivery, Vol.PWRD-1, No.2, pp95-102, 1986

10) J.Ozawa et al, "Suppression of Fast Transient Overvoltage during Gas Disconnector Switching GIS" IEEE Transaction on Power Delivery, Vol.PWRD-1, No.4, pp194-201, 1986

11) S.Yoshizawa et al, "Fast Transient Overvoltage in GIS Caused by the Operation of Isolator", proc, of the 3rd International Symposium on Gaseous Dielectrics, 1982

12) Boeck.W et al "Insulating Behaviour of SF_6 with and without Solid Insulation in case of Fast Transients." CIGRE paper, 15-07, 1986.

13) International Electrotechnical Commission, "Insulation Co-ordination, Part1", Publication 71-1 1976

GROUPE 33
GROUP 33

SURTENSIONS ET COORDINATION DE L'ISOLEMENT
OVERVOLTAGES AND INSULATION COORDINATION

Rapports / *Papers*

33-13, 33-15, 33-09, 33-12, 33-06, 33-01, 33-04

A. SABOT (Subject Reporter) | K.H. WECK (Special Reporter) | G. CARRARA (President) | J. ELOVAARA (Secretary)

SUJET PREFERENTIEL 3 / *PREFERENTIAL SUBJECT 3*

Phénomènes transitoires rapides.

- Origine des phénomènes transitoires rapides en service (par ex. manoeuvres des sectionneurs ou autres causes). Problèmes impliqués dans la mesure des courants et tensions s'y rapportant.
- Distribution prévue des caractéristiques de courant et de tensions ayant une influence sur le comportement diélectrique des matériels (amplitude, paramètres de la forme d'onde, taux de répétition etc.) Précisions de calculs.
- Essais des matériels de ce point de vue (nouveaux circuits d'essais, amplitude et formes d'ondes des tensions d'essais , etc.)) à la fois en laboratoire et sur le site.

Fast transients

- origin in service of fast transient (e. g. disconnector operations or other causes). Problems involved in the measurement of the relevant currents and voltages.
- expected distribution of current and of voltage characteristics influencing the dielectric behaviour of equipment (amplitude, shape parameters, repetition rate, etc.). Accuracy of calculations.
- relevant testing of equipment (new test circuits, amplitude and shapes of test voltages etc.) both in laboratory and on site.

Questions 7 - 13

M. A. SABOT (France) - Subject Reporter

Two of the main topics for which we are here today in this meeting room are :
- restrike between contacts of a GIS disconnector,
- flashover to the enclosure within the disconnector.

This picture recorded in Laboratory is of course a worst case for the men in charge of the networks.

Briefly one can describe the phenomena involved in GIS during disconnector operations. The restrikes between contacts due to the voltage across the contacts ΔU generate voltage transients with steep front (voltage steps). Transmissions and reflctions of these initial steps superimpose to build up the so called Very Fast Transient (V.F.T.) Overvoltage. The V.F.T. overvoltage occur not only inside the GIS between phase conductors and enclosure but outside between the conductors and earth and between GIS enclosure and earth (so called Transient Enclosure Voltage).

During GIS disconnector operations, failures occured and were attributed to V.F.T. overvoltages. These failures took place within the disconnectors themselves but also in bus bar sections. Failures of transformers and capacitive bushings were also reported and attributed to GIS disconnector operations.

The main points that we have to clarify this morning are the followings :

- What can be the amplitude ΔU of the voltage across the GIS disconnector before restrike between contacts ?
- What is the amplitude S of the associated Very Fast Transient overvoltage generated by that previous restrike in GIS and outside GIS ? What are the times and frequency characteristics of these V.F.T. Overvoltages ?
- What is the dielectric behavior of all the equipments to the V.F.T. stresses compare to their behavior to the standard Lightning Impulse voltage (LI) ?
- How can be reduced the Transient Enclosure Voltages and their effects on secondary equipements ?

For the first point dealing with the amplitude ΔU of the voltage across the contacts of GIS disconnectors several values have been already mentioned. For report 33-13 of CIGRE WG.33/13.09. They ranged from 1.5 p.u. up to 2 p.u. This value is important both to determine the stresses on the disconnector contacts and the amplitudes S of the V.F.T. overvoltage so generated at restrike (S is more or less proportionnal to ΔU). To specify a test for disconnector it is important to know the possible ΔU. Report 33-15 states that ΔU can reach 2.5 p.u. and in report 33-09 ΔU can reach 2.7 p.u. and even 4 p.u. theoretically. All this matter should be clarified as far as possible this morning.

For the second point, the amplitude S of the V.F.T. Overvoltage generated by restrikes of disconnector the previous point is essential as S is more or less proportional to ΔU for a given GIS configuration. Taking a ΔU of 2 p.u., WG 33/13.09 in reports 33.13 states that S can reach 2.5 p.u. for severe case of GIS lay out but generally the value of S remains in the range of 1.5 to 2 p.u. If ΔU is greater than 2 p.u., S will be greater than those values. The maximal couple ΔU, S to take into account for an insulation point of view should be clearly stated. The main frequency of the V.F.T. overvoltage ranges in few MegaHertz with superimposed higher frequency oscillations (tens of MHz). Have these oscillations any influence on insulation strength ?

For the third point regarding the insulation point of view of GIS and other components up to now V.F.T. overvoltages are not considered in IEC or IEEE standards. Must we include such stresses in standard or LI test covers these V.F.T. For WG.33/13-09 in reports 33-13 only dielectric strength of switching disconnector must be tested with V.F.T. and a special test should be stated. For other components the LI test seems to be sufficient but transformer should be tested with LI chopped wave. But according to new test results the subject may be still open ?

Finally for the last point dealing with Transient Enclosure Voltage WG.33/13-09 gives the reasons for the generation of TEV and some guidance to avoid them. But calculations and measurements of such phenomena are very difficult. Such phenomena must be reduced as far as possible to avoid control or relay mis operation. Nevertheless in any case control and relay equipments must be carefully mounted in a fareday housing.

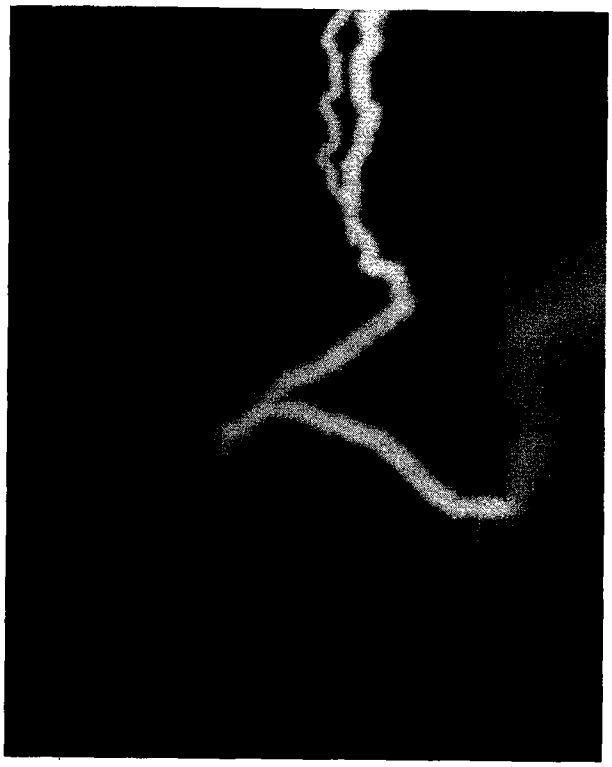

Mr. A. PIGINI (Italy)

The peak value of UFTO can be obtained by the following simple equation, with reference to either an opening, or closing operation:

$U_{FT} = DU*K-Uo$ 1)

with -DU voltage collapse (absolute value)
-Uo voltage existing before the restrike occurrence (absolute value)
-K overvoltage factor in the examined point

Tests performed on disconnectors of many types and varying many configuration parameters (see also report 33.15) have shown that:

- DU, Uo values (and their statistical distribution) depend basically on disconnector design and characteristics. They can be practically determined only through testing.

- The same is applicable for the Uo value after the last restrike relevant to an opening operation (residual voltage Ur). Tests have indicated that the maximum Ur value ranges from 0.4 to 0.9 depending on disconnector profile, operating velocity, etc.

- K value depends basically on the GIS configuration and changes along the configuration itself. It can be determined through testing or by calculation methods, once well calibrated. In particular typical K values for laboratory circuits, with stiff capacitance source side and small capacitance load side, are of the order of 1.8. A large K value range is applicable to field conditions (say 1.2 to 2).

-An estimate of the maximum overvoltage values can be made starting from Ur and K. As an example UFT values are reported as a function of Ur in Fig.1, with reference to K values of 1.2, 1.5 and 2. Depending on disconnector design, maximum overvoltage values result in the range from 2 to 2.5 p.u, at least with reference to the configurations usually considered for laboratory tests (K=1.8).

-The LIWL for the upper range of EHV and UHV is not much higher than UFTO, independently of the system voltage considered. Values of 2.76 p.u. have been standardised for 800 kV and 2.63 have been proposed for 1050 kV systems.

-The strength under very fast transients, without DC prestress, is close to that with standard lightning impulses.

-The strenght with actual very fast transients can be lower than that with standard LI, due to the presence of the residual voltage, which causes a DC prestress. This strength reduction is contributed for by particles, which can be present or form during operation, even in well designed GIS, which do not present major defects.
The estimated limit withstand voltage as a function of residual voltage for the case of a LIWL of about 2.7 p.u. (typical of 800-1050 kV systems) is reported in Fig. 1.

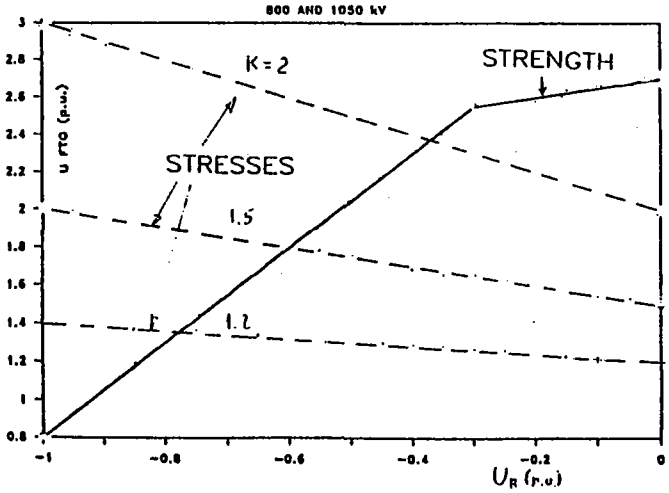

Fig.1 800-1050 kV GIS. Comparison of expected very fast transient overvoltage stress with expected strength characteristics.

-Comparing the curves of Fig. 1 it appears that, at least for GIS belonging to the upper range of EHV and to UHV, a series of possible combinations of Ur and K can occur and can lead to flashover during switching operation.
This is partly in contraddiction with the conclusions of the report 13 from WG 33/13 which suggest that, independently of the system voltage, fast transients generated during switching of capacitive currents are not a big problem for GIS, unless big defects are present.

M. G. VOISIN (France)

Mon intervention se réfère à la question 7 du Rapport spécial, relative à l'interdépendance entre variation de tension aux bornes du sectionneur, d'une part, configuration des postes et conception de l'appareillage, d'autre part.

Pour fixer les idées, soit ΔU, la tension maximale apparaissant entre les bornes d'un sectionneur, lorsque celles-ci ne sont pas reliées par un arc.

Si le sectionneur n'avait qu'à isoler ou mettre sous tension de simples conducteurs sous enveloppe métallique éventuellement isolés du réseau par un autre appareil de connexion (figure 1, cas (a)), on pourrait ignorer complètement la conception de l'appareillage. Le cas le plus défavorable serait en effet obtenu à la mise sous tension d'un élément laissé sous une tension continue résiduelle de 1 p. u. (par l'ouverture d'un disjoncteur, par exemple).

Le cas de l'isolement d'un élément comportant un transformateur inductif de potentiel (figure 1, cas (b)) est couvert par la même valeur de Δ U de 2 p. u.. Cette valeur représente effectivement un majorant pour la tension qui apparait aux bornes du sectionneur lors du régime oscillatoire de basse fréquence au cours duquel la capacité de l'élément de liaison se décharge à travers l' enroulement du transformateur de potentiel.

Mais le problème se complique dès que l'on doit prendre en compte les opérations dites "en discordance de phases" (figure 1, cas (c)). La présence, entre les bornes des disjoncteurs, de condensateurs de capacité très supérieure à la capacité naturelle entre contacts ouverts peut conduire à des tensions résiduelles sur un élément "isolé" où se superposent une composante continue et une composante à fréquence industrielle. La conception de l'appareillage (capacité de ce condensateur) et la configuration du poste (capacité naturelle entre conducteur et enveloppesde cet élément) influencent très fortement la composante à fréquence industrielle et les valeurs maximales de ΔU qui en résultent.

Dans les cas extrêmes, ainsi que le montre le rapport 33-09, on arrive d'ailleurs à des valeurs de ΔU qui avoisinnent théoriquement les 4 p.u. et dépassent donc sensiblement les conditions prévues par les normes pour les essais de tenue une minute à fréquence industrielle entre bornes des appareils de connexion ouverts.

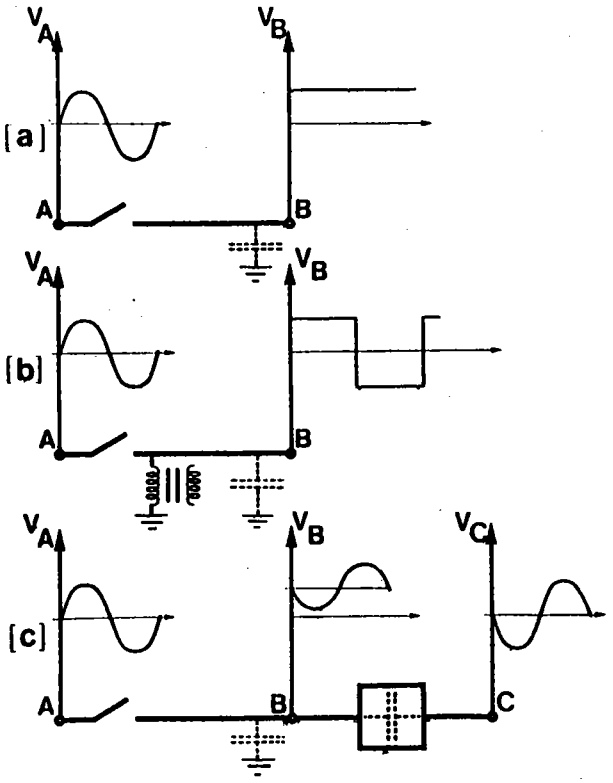

Fig.1: Manoeuvres de sectionneurs dans différentes configurations de réseau
a. Mise sous tension ou hors tension d'un conducteur
b. Isolement d'un élément comportant un transformateur inductif de potentiel
c. Manoeuvre en discordance de phases

Des ensembles d'appareils de conception différente peuvent se comporter différemment. Ainsi, nous avons mesuré récemment, au cours de 150 cycles de manoeuvres de sectionneur en discordance de phases (figure 2), un seul cas où ΔU à dépassé 2 p. u. (2,09 p. u.). Encore faut-il noter que le circuit d'essais utilisé conduisait à des conditions de discordance de phases excèdant légèrement 2 p. u. (2,1 p. u., comme indiqué sur la figure 2).

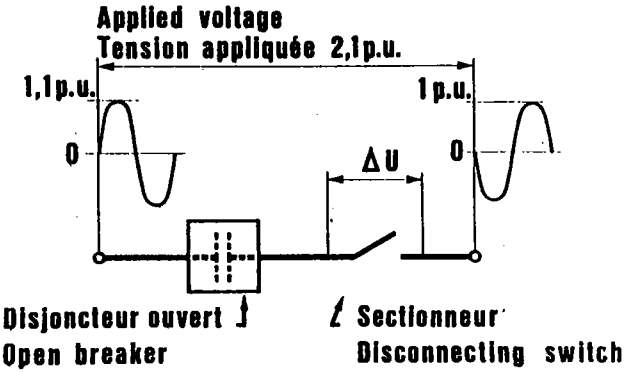

Fig.2: Schéma d'essai en discordance de phases

Il semble donc difficile de prendre en compte dans une recommendation unique des valeurs de ΔU dispersées dans une gamme de valeurs qui peuvent aller du simple au double à cause de la conception de l'appareillage et de l'arrangement des postes. Dans les cas où les opérations en discordance de phases sont possibles, une détermination du ΔU par le calcul et/ou les essais paraît nécessaire.

M. Ph. JOUCLAR (France)

Pour Electricité de France, les tensions entre les contacts du sectionneur provoquant l'amorçage ou le réamorçage entre contacts ne dépendent pas uniquement du sectionneur (vitesse, asymétrie des contacts,...). La configuration du Poste Sous Enveloppe Métallique et les conditions d'exploitation de ces postes interviennent tout autant que le sectionneur lui-même sur les tensions d'amorçage à la fermeture ou de réamorçage entre contacts à l'ouverture des sectionneurs.

Pour Electricité de France, il existe deux cas qui conduisent à des amorçages ou des réamorçage entre contacts pour une tension entre contacts atteigant deux fois la tension assignée du réseau (2 p.u.). Ces deux cas ne sont pas des cas d'école et sont réellement apparus sur le réseau 420 kV d'Electricité de France.

Le premier résulte de la fermeture d'un sectionneur sur un bout de barre précédemment mis hors tension par un disjoncteur. Dans ce cas le premier amorçage à la fermeture a lieu pour une tension entre contacts de 2 p.u.

Le deuxième cas peut se produire lors de l'ouverture par un sectionneur d'une portion de barre sur laquelle il y a un transformateur de tension de type inductif (1). Dans ce cas, les derniers réamorçages peuvent se produire pour des

tensions, entre contacts, voisines de 2 p.u. (figure 1). Ce deuxième cas, dû à l'asymétrie du sectionneur qui provoque la saturation du transformateur de tension, conduit à des distances de réamorçages entre contacts plus grandes que celles obtenues dans le premier cas relatif à une manoeuvre de fermeture, du fait de l'échauffement local du SF6 entre contacts provoqués par les réamorçages précédents (2). C'est ce dernier cas, le plus contraignant, qui a été considéré pour dimensionner les sectionneurs de P.S.E.M. d'Electricité de France.

(1) Lalot J., A. Sabot, J. Kieffer, and S.W. Rowe. "Preventing Earth Faults During Swichting of Disconnectors in GIS including Voltage Transformer". IEEE Trans on Power Delivery, Vol. PWRD-1, N° 1. Janvier 1986.

(2) Boggs, S.A., F.Y. Chu, N. Fujimoto, A. Krenicky, A. Plessl, and D. Schlicht. "Disconnect Switch Induced Transients and Trapped Charge in Gas-Insulated Substations". IEEE, Trans on Power Apparatus and Systems, Vol. PAS-101, N° 10, Octobre 1982

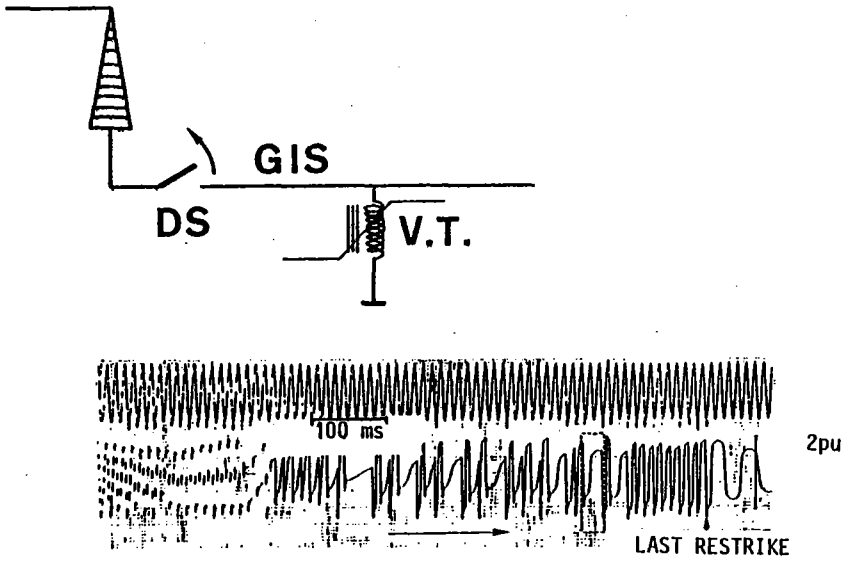

Figure 1 : Ouverture d'un sectionneur de Poste Sous Enveloppe Métallique lorsque la charge est un transformateur de tension inductif et un bout de barre : tension côté source en haut.

Mr. N. FUJIMOTO (Canada)

Very fast transient (VFT) phenomena in GIS has always been a topic of much discussion, primarily because the effects of ns-risetime transients on power system components were not well understood. VFT have been implicated in many several GIS failures, necessitating investigations into the phenomena. As the knowledge has increased, the importance of VFT phenomena can be put into perspective. The consensus now is that VFT, in general, should not pose a problem to GIS (paper 33-13). However, defects in the GIS (particles on spacers, protrusions, etc.) and marginal designs could be very sensitive to VFT overvoltages which occur during normal operating conditions. In order to evaluate new designs and because of the implications for testing (to locate the harmful defects), VFT phenomena and breakdown processes need to be fully characterized and understood. For these reasons, care should be taken in selecting parameters such as those which determine the voltage collapse across disconnectors (DS).

In principle, a single value for intercontact breakdown voltage does not adequately describe the important characteristics of fast transient phenomena in GIS. The use of an intercontact breakdown of 2 pu is often used as this might be considered as a "worst case" situation. However, for slowly operating DS switching small capacitive currents, an intercontact breakdown of 2 pu practically never occurs. Higher values of intercontact breakdown occur more frequently and 2 pu is possible for fast operating DS or DS operating in phase opposition. In addition, the simultaneous operation of DS on either side of a circuit breaker could result in an interaction through the breaker grading capacitance and result in an intercontact breakdown of slightly > 2 pu. The operation of a DS results in a series of transients, each of which is generated by each of the many intercontact arcs which occur. Consequently, the intercontact breakdown values and the transients generated will fall into a distribution; the probability of high values of intercontact breakdown will vary with the disconnector design and operating speed.

As a result of the great variability in intercontact breakdown, the usual approach is to consider VFT on a normalized basis. That is, VFT should be considered for an intercontact breakdown of 1 pu with no trapped charge. In this manner, the fast transient response of a station configuration to the excitation provided by the DS operation is characterized. These normalized responses are a function of operational configuration and location within the GIS. This approach allows the disconnector-specific parameters to be separated and considered independently. If the "worst-case" scenario of 2pu breakdown is desired, the VFT can be computed by the application of a simple algebraic relation which includes the normalized transient response, the intercontact breakdown and the initial conditions (voltage level prior to the transient). If a probabilistic approach is desired, the VFT

distribution can be fully considered once the statistical operating characteristics of the disconnector, including the distribution of intercontact breakdown, have been determined. This approach is described in papers 33-15 and 23-11. Statistical distributions generated by this approach were also demonstrated in paper 13-15 in the 1984 Session.

In principle, the nature of VFT phenomena is independent of the disconnector which only provides the excitation. For comparison purposes, normalized responses are best. In this manner, the salient features of the disconnector operating characteristics can be used to obtain the desired results. VFT is an inevitable feature of GIS, but proper characterization is essential to put the phenomena into perspective.

Mr. A.J. ERIKSSON (Switzerland)

As shown by various workers [1,2] and in Paper 33-13, the sparkover characteristics of a disconnect switch do depend on several factors - principally the disconnect design, and to a lesser extent, the circuit being switched (eg capacitive loads, or other).

The principal influences include

- the specific design of the contacts
- the degree of assymetry
- the contact speed

We favour a low contact speed (typically 0,1 m/s) and a moderate degree of assymetry (typically 15-30%). In that event, in contrast to high speed switches, the remanent trapped charges after an opening operation correspond to voltages in the range of only 0,1 - 0,5 pu., with an average of only about 0,3 pu. Under normal circumstances, the maximum restrike voltages during the actual opening sequence lie typically in the range of 1,1 - 1,5 pu., with a limiting value of about 2,0 pu.

In response to Questions 7 & 9, we certainly consider that measuring techniques are sufficiently developed to record all parameters of interest - both in the laboratory during disconnector evaluations, as well as on-site during measurement of VFT in practical GIS installations - up to the highest system voltage levels (765 kV).

Figure 1 depicts a sample set of results obtained during typical laboratory evaluation of a disconnect switch opening operation, using sensitive wideband measuring equipment. Applying modern techniques of automatic high-speed digital data capture and processing, the transient voltage differences prevailing across the disconnect during the reignition process may readily be determined, together with the corresponding restrike voltages.

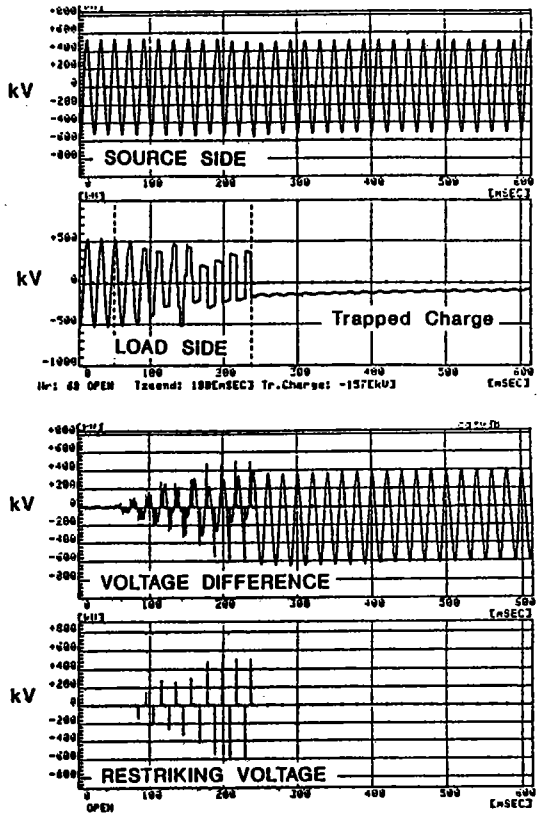

Figure 1: Laboratory Evaluation of a GIS Disconnect Switch - during an opening operation

Automatic repetition of such measurements over a large number of disconnect Open-CO operations leads also to the distribution of remanent trapped charges - as in Figure 2.

Based on extensive study of such disconnect operating features, (including a variety of load types), in analysing the expected VFT voltage characteristics of practical GIS configurations - as shown in our paper 33-12, we favour adoption of a trapped charge

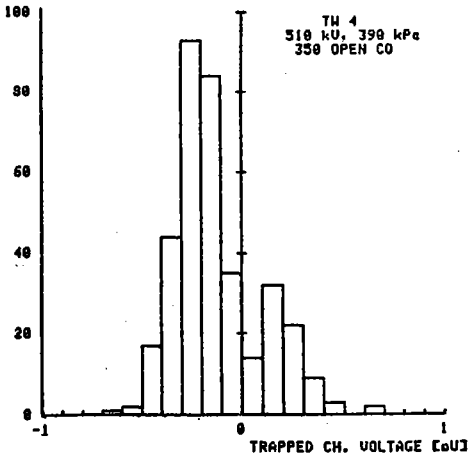

Figure 2: Sample Trapped Charge Distribution

level of 0,4 pu for normal engineering calculations (corresponding to a restrike voltage of 1,4 pu across our disconnector). In worst-case analyses, we extend this to a restrike voltage of 2,0 pu.

Dealing further with Question 9, we consider that the disconnect sparkover and subsequent VFT processes in practical GIS are now well understood. The related parameters of VFT overvoltages in GIS (eg. front-time, amplitude, frequency etc), may be readily characterised through either measurement or computation - as illustrated by the example of comparative disconnect VFT measurements and calculations shown in Figure 3 for a 765 kV GIS installation.

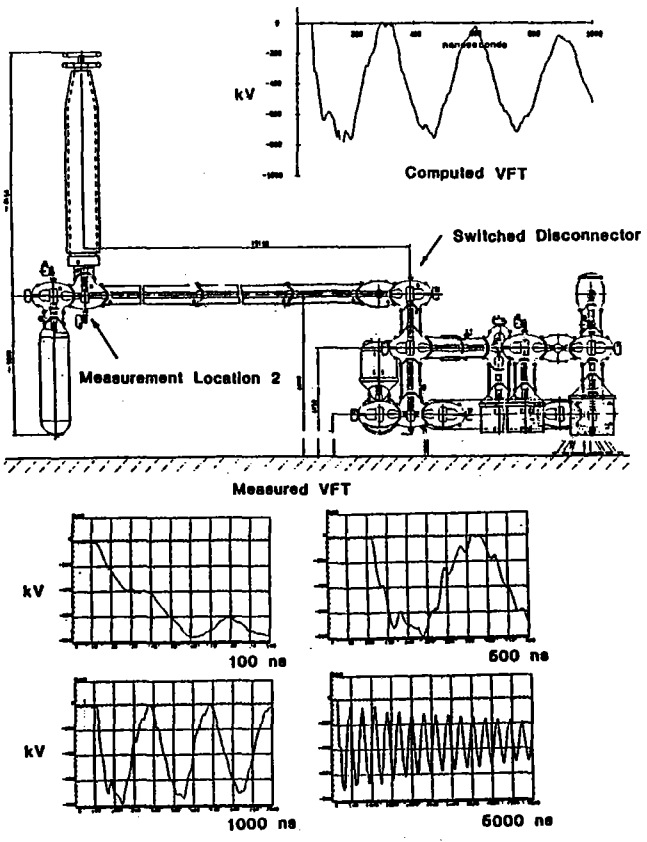

Figure 3: Comparative Measurement and Computation of disconnect switch VFT characteristics in a 765 kV GIS installation

Generalised values for such VFT parameters may only be given approximately however, since, in the end, they are determined by the nature of the GIS configuration involved. Based on our experience so far, localised VFT propagation effects rapidly reduce the front-times in EHV GIS to about 10-20ns, while peak amplitudes as high as 2,0 pu. are seldom attained. As noted in our paper 33-12, in an extensive computerised analysis of a broad variety of operating configurations in this large 765 kV GIS, the great majority of VFT did not exceed 1,5 pu. Primary oscillation frequencies are directly dependent upon the GIS layout involved, and the only practical generalisation is to associate these with about the 10 MHz range.

Where specific concern may arise regarding VFT stress upon individual equipment, we consider it more practical to apply the developed computation methods (as in 33-12) to characterisation of the specific VFT at the equipment concerned, and then to relate this to the equipment strength. As shown in 33-13 - and again in Figure 3 - comparisons between computed and measured VFT characteristics support a high confidence in the application of such computation methods.

[1] Boggs S., et al "Disconnect switch induced transients and trapped chagre in gas-insulated substations" IEEE Trans. PAS-101, No. 10 October 1982.

[2] Yanabu S., "Estimation of fast transient overvoltage in gas-insulated substation" IEEE PES Paper 88 SM 628-0, July 1988.

Mr. J.W. CHADWICK (United States)

In 1984, TVA conducted switching tests on a single-phase portion of 500-kV GIS BUS. Approximately 130 feet of bus, including three disconnecting switches (DS) and one magnetic voltage transformer (VT) were installed at and connected to our Wilson, Tennessee, 500-kV Substation which is of conventional air-insulated construction (see figure 1). Extensive tests of the DS were conducted to verify the adequacy of the switch to operate satisfactorily with the long bus sections associated with our busing arrangements and to investigate the effect of transients generated by the operation of the DS.

Measurements of the bus voltage were made using special capacitive voltage dividers installed in the ports of DS's in the GIS bus. High-frequency responses were captured using storage oscilloscopes while low-frequencies were recorded on light-sensitive oscillographs.

Without the VT installed, the bus voltage on the section of bus being switched by the DS exhibited the expected behavior as illustrated in figures 2a and 2b. With the VT installed, we observed a low frequency oscillation in the bus voltage as illustrated in figures 3a and 3b.

Oscillograms of the bus voltage and primary current in the VT revealed saturation of the VT and subsequent oscillations of energy between the capacitance of the bus and inductance of the VT (see figures 4a and 4b). These oscillations resulted in delta V on the bus of approximately 2 per unit during DS operation.

It should be noted that the VT saturation was observed for both close and open operations of the DS; it affected both the bus voltage and the VT secondary voltages; and the saturation occurred during the switching of 100 feet of bus and later 150 feet of bus (see figures 5a and 5b).

The total capacitance of the bus and VT being switched was calculated to be 2800 pF for 100 feet of bus and 3800 pF for 150 feet.

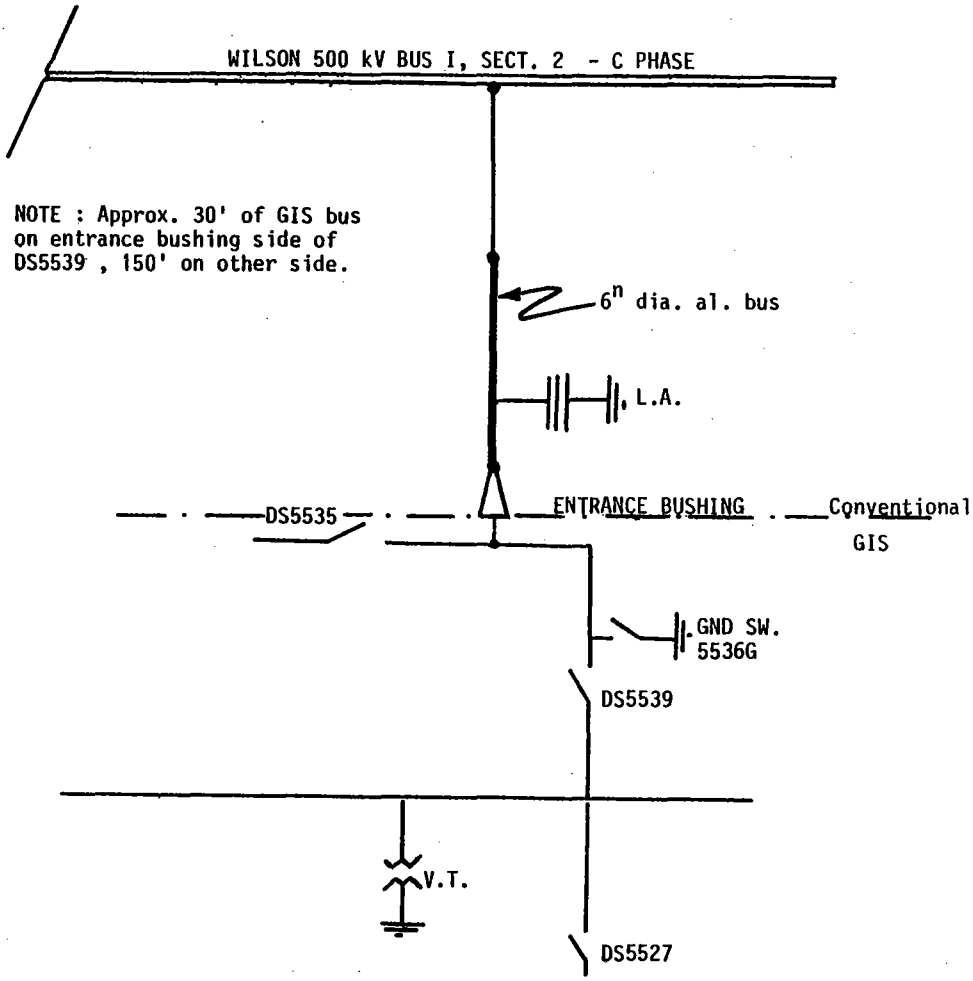

GIS Test Bus Configuration at Wilson, Tn. 500 kV Sub.

FIGURE 1

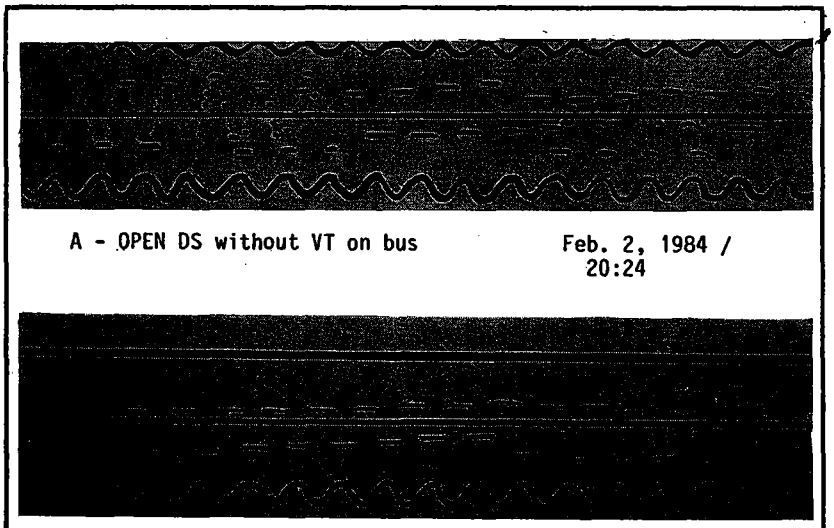

A - OPEN DS without VT on bus Feb. 2, 1984 / 20:24

B - CLOSE DS without VT on bus Feb. 2; 1984 20:14

TVA's Wilson Tn. 500 kV Substation - GIS Test

FIGURE 2

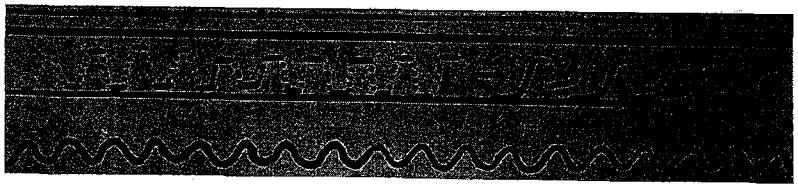

A - OPEN DS with VT on bus Nov., 13, 1984
10 :55

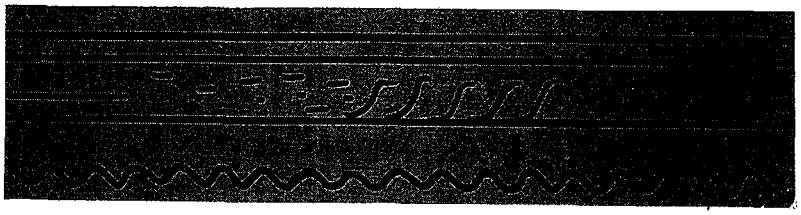

B - CLOSE DS with VT on bus Nov., 13, 1984
10:03

TVA4s Wilson Tn. 500kV Substation - GIS Test

FIGURE 3

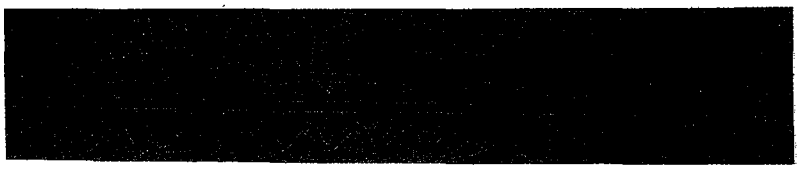

A - OPEN DS VT primary current , Bus voltage May, 24, 1984
10:01

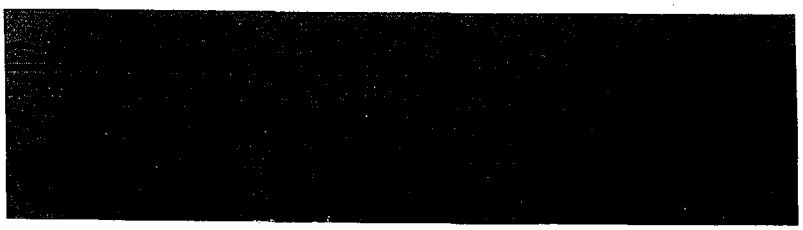

B - OPEN DS, VT primary current, Bus voltage May, 24, 1984
9:39

TVA's Wilson Tn. 500kV Substation - GIS Test

FIGURE 4

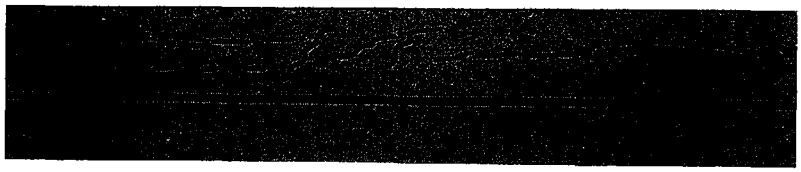

A - OPEN DS to drop 100 feet of bus March,16, 1984
VT Secondary voltage, Y_1-Y_3 14:51

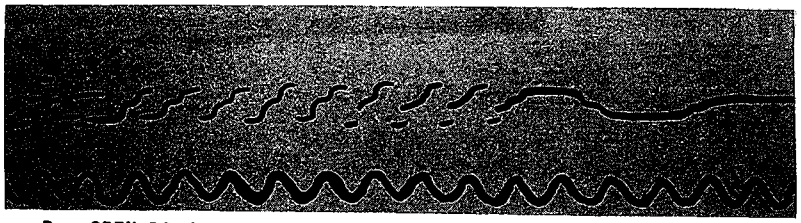

B - OPEN DS drop 150 feet of bus Nov.15,1984
VT Secondary voltage, Y_1-Y_3 10:51

TVA's Wilson, Tn. 500kV Substation -GIS Test
FIGURE 5

Mr. A.J. ERIKSSON (Switzerland)

Values of fast transient voltage collapse close to the GIS withstand levels - if these did occur in practice - would certainly be of concern to the insulation co-ordination, due to the likely amplitudes of the subsequent VFT which might develop at other locations within the GIS.

In practice, the aim of the overall GIS insulation co-ordination - as applied in the methods of 33-16, for example, - is to limit the amplitudes of any overvoltages penetrating into the GIS to levels well within the withstand level, such that GIS faults should not be caused at these voltages. Similarly, the VFT arising in practical GIS during disconnect switch operations (typically 1,5 - 2,0 pu.), are sufficiently far below the withstand levels not to stress the GIS insulation, and again, should not cause GIS faults.

A particular circumstance which could be of concern however, could arise during GIS on-site testing, especially if excessively high test voltages are involved. In the event then of a GIS fault - perhaps due to an assembly defect - the subsequent VFT and its development in other sections of the GIS could well lead to overvoltages outside the withstand levels. Concern regarding the effects of injudicious on-site testing has previously been expressed in sessions of SC 33 [1,2].

A practical example is depicted in Figure 1 - which relates to AC on-site tests within a particular test configuration in a large 550 kV GIS installation. Applying developed computerised procedures for analysing VFT characteristics (as in paper 33-12), the computed VFT are depicted which would ensue at a remote line bushing in this GIS, in the event of a site test flashover close to the point of AC voltage injection. At the AC test level of 570 kV (equivalent to 2.Un), the subsequent VFT approaches the GIS BIL at the remote locations - with consequent risk of secondary flashover at these positions.

Extrapolation of such analysis to the VFT which could follow such a secondary flashover, clearly leads to VFT which would be outside the BIL.

Bearing in mind that surge arresters are not usually connected during the primary on-site tests, it is important therefore, that GIS on-site test voltages and testing configurations be planned taking such aspects into account.

[1] Feser K., et al; "Dielectric field testing of GIS" CIGRE Paper 33-09, 1986.

[2] Diessner A., et al: "High voltage of SF6 insulated substations on site" CIGRE Paper 33-06, 1986.

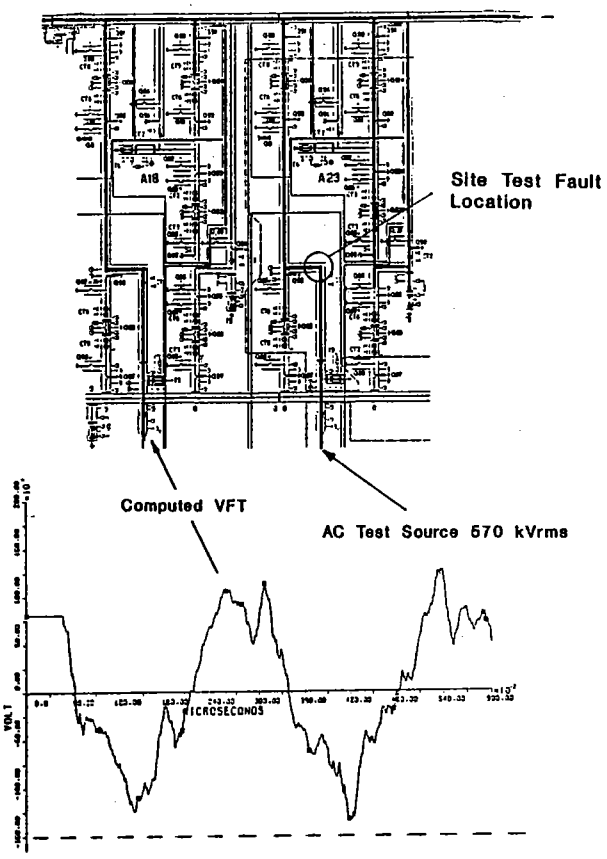

Figure 1: Evaluation of remote VFT arising due to site-test flashovers during GIS AC on-site testing. (550 kV GIS example).

Mr. W. MÜLLER (Fed. Rep. of Germany)

1. DS operation

For operation of disconnectors, breakers and earthing switches the working group on VFT gave an overvoltage factor up to 1,7 pu for most configurations and 2 pu for very specific cases. It was also mentioned that 2,5 pu can be reached.

In Germany one measured value of 2,8 pu was reported. This overvoltage might lead to damped oscillations up to 1,8 pu.

Regarding the resonance behaviour of transformers the considerations about tolerable resonance overvoltages hitherto are based on 1 pu excitation which could occur with overvoltage factors of 2 pu at DS and breaker operations.

As convener of the WG "Very Fast Transients in Transformers" of SC 12, I have following questions:

Are switching overvoltages of more than 2 pu realistic, and if so, is the probability of their occurance high enough to be taken into account in insulation coordination?

2. Insulation failure

The worse stress for the equipment could be an insulation failure within the GIS under rated conditions.

Some users claim that this breakdown could occur with a voltage equal to BIL of the GIS due to protection insufficiency of an incoming line and overswing of the line arrester. Moreover an underswing of 118 % after breakdown and consequently a peak - to - peak breakdown voltage of 218 % related to the BIL was measured.

It must be noted that this form of chopped wave is by far higher than the peak - to - peak voltage produced by the normal chopped wave test of transformers and reactors, where the underswing is limited to about 30 % and the peak - to - peak voltage to 130 % of BIL or chopped wave test level respectively.

Furthermore the breakdown is followed by a damped oscillation with about 4 pu amplitude according to the insulation level of the GIS in relation to the rated voltage.

I have the same questions as before:

Is a breakdown from full BIL level with an additional overswing of more than 100 % realistic and if so is the probability of its occurance high enough to be taken into account in insulation coordination.

Failures during the on site test are not to be taken into account because transformers and reactors should not be connected during this test.

Are there any breakdowns due to lightning stroke during normal service with BIL amplitude reported.

Mr. M.G. DWECK (United Kingdom)

This contribution is intended to show that calculations can be done which can provide satisfactory information on amplitudes and waveshapes of transients arising in gas insulated busbars. In the CEGB work has been done in recent years to assess these fast transients. Extensive calculations have been carried out. Some measurements have been done and the results used to confirm the calculation results.

In making the calculations use has been made of the CEGB digital computer program, BESS04. The program has been in use for 20 years and has been extensively validated by field tests. Wide experience has been gained in modelling for the solution of a variety of system problems. Many studies have been done on line switching; reactor, transformer and capacitor switching and lightning effects. Fast busbar transients, ferresonance and problems arising from load rejection have been studied. Problems arising on HV cables have been studied in specially bonded cable systems with the cable sheath and its earthing represented.

The program permits the representation of multiphase transmission lines in which travelling wave effects are calculated by the Bergeron method. Frequency dependence of line parameters can be simulated. The lumped element representation of capacitors, inductors and resistors can be included; the inductors and resistors may be non-linear. Transformer non-linear magnetising characteristics can be represented for single phase cores, and for 3 limb and 5 limb 3 phase cores. The program was modified in the 1970s when calculation techniques proposed by Professor Dommel and used in the EMTP program were introduced. The calculations have been compared satisfactorily with the results of a large number of system tests carried out over many years.

In the calculations of busbar transients a number of different circuit models have been used in order to assess the sensitivity of results to variations in the model.

In all the models busbars have been represented as transmission lines; sometimes with a full three phase representation of the busbars and the enclosure; sometimes as a single phase busbar with its enclosure and sometimes as a single conductor with the enclosure assumed to be at zero potential. Gas barriers between busbar sections were represented as lumped capacitances. The circuit breaker in the particular case considered was represented as a 4 unit circuit breaker with grading capacitors and with transmission lines to represent the connections between units. Voltage transformers and surge arresters were represented as capacitors.

400/275 kV transformers at the busbar terminations were represented as capacitances. The detailed representation of the busbars and other elements necessitated the use of lines as short as 3 metres in the model. A simplified circuit diagram is shown in Figure 1.

A number of studies were done to check the sensitivity of the results. An example of the responses at Point A from the use of a full 3 phase model and a single conductor busbar model is shown in Figure 2. As there are only small differences in the responses single phase modelling is adequate.

These results arise from a step voltage applied at the switch with a negative charge on the load side of the switch. The responses are such as could be obtained by a single restrike of a disconnecting switch.

Tests were also carried out at low voltage on the substation for which the calculations were made.

Two types of test were done. One where a d.c. charge of 60 V on the source side of the circuit-breaker was discharged into the line side by the circuit breaker. For this test the neutral connections for the transformers on the source side were connected to earth via a large capacitance which permitted the d.c. charge to be applied but which was a short circuit to high frequency transients. Other tests were done in which a d.c. step voltage of 30 V was applied to a point on the busbar and the responses measured.

Figure 3 gives an example of the test response compared with a calculated response.

There are some differences in the responses but, again, these are not sufficient to influence any conclusions which might be drawn from the calculation results.

In answer to question 9 our work indicates that values can be given, with good confidence, for amplitudes and rates of rise of voltage for specific switching or lightning transients in gas insulated busbars. Because of uncertainty in parameters it is necessary to carry out studies of sensitivity to variations in the uncertain parameters.

LINE DIAGRAM OF BUSBAR TESTED AND STUDIED

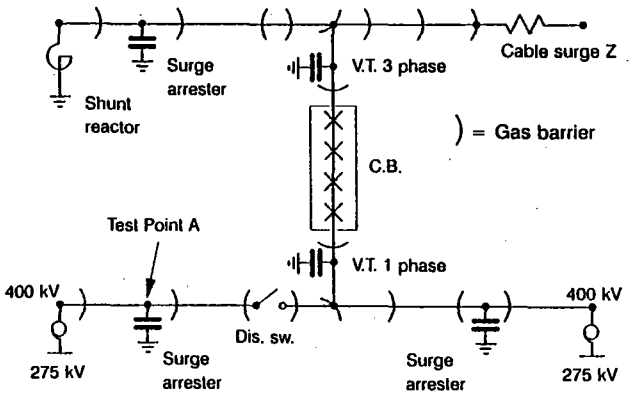

FIGURE 1

COMPARISON OF CALCULATED RESPONSES FOR 3 PHASE AND 1 PHASE MODELS

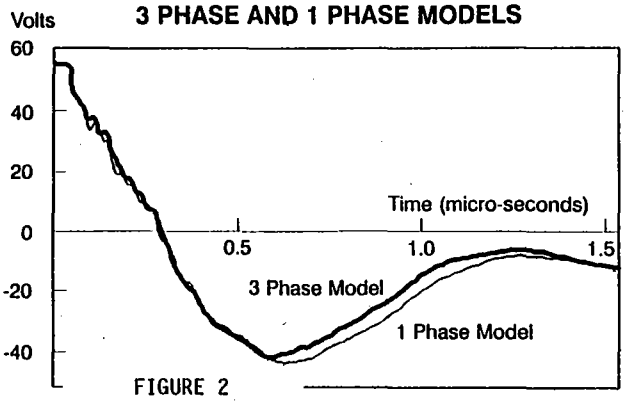

FIGURE 2

TEST AND CALCULATED RESPONSES

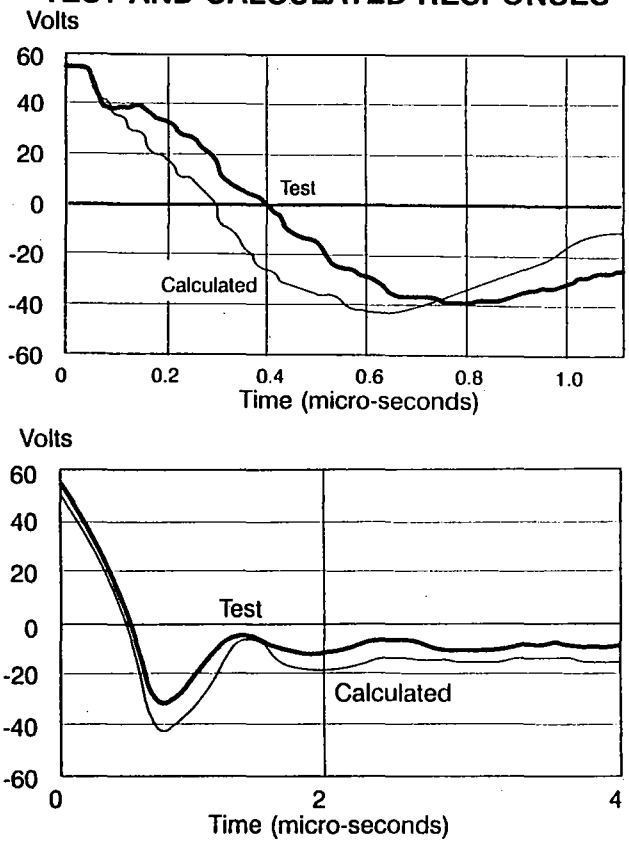

FIGURE 3

There is uncertainty in the type of surge which must be assumed to arise. The rate of rise of a lightning surge or the breakdown characteristic of an opening disconnector have to be determined from published statistical data or from tests on the equipment itself. The calculations are not highly sensitive to assumptions made about enclosure voltage. There was little difference between the results from a full representation of busbars and enclosure and the results when the enclosure was assumed to be at zero voltage.

Mr. Y MURAKAMI (Japan)

To investigate the very fast transient overvoltages (VFTO) phenomenon in GIS, it is important to measure its wave form precisely. The basic frequencies of the VFTO are mainly determined by the length and the layout of the bus bars. However, the higher frequency components up to 100 MHz arising from short surge impedance discontinuities such as spacers, disconnectors and short bus branches may possibly be superposed on the basic frequencies. Moreover, it is known that the rise time of step shaped traveling waves caused by restrike/prestrikes of disconnectors is within the range of 2-12 nano sec.

From these points of view, as a voltage sensor for VFTO, several 100 MHz frequency characteristics is necessary, and 1-GHz sensor (shown in Fig.1) was developed.

The disk electrode is coupled to the coaxial cable by utilizing a coaxial conical body. This structure enables potentials of the disk electrode to be detected in a wide area, and therefore, to be detected by the mean potential of the disk electrode, thus permitting the internal resonance mode of the low-voltage side capacitor to be averaged out. Diameter of the disk electrode was 15 cm; the low-voltage side capacitor, about 5 nF, was made from PTFE film 25 μm thick.

The step response time of this surge sensor was measured and it is clarified that step responce time of this sensor was about 350 pico sec (as shown in Fig.1(b)).

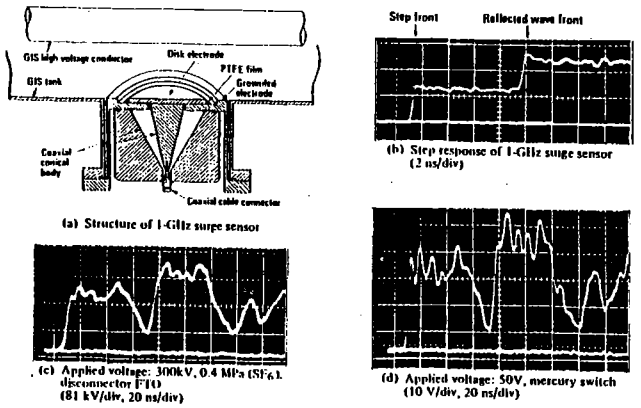

Fig. 1 1-GHz SENSOR AND ITS RESPONSE CHARACTERISTICS

The measured waveform was obtained and discussed by using this sensor into model GIS system. It is clear that measured waveform with 300 kV high voltage condition has very good agreement with 50 V low voltage measurement, having no noise problem (as shown in Fig.1(c)(d)). It was clarified that the small difference between these two waveforms depend on the spark collapse time of the disconnector gap..

As a conclusion, this new type sensor will be able to apply to VFTO measurement in an actual GIS.

Mr. N. FUJIMOTO (Canada)

The measurement of fast transients in GIS is generally well developed. Several laboratories possess the necessary technology which has sufficient bandwidth to record any possible parameter of interest (for example, [1,2]). However, the interpretation of the waveforms in terms of the "severity" of the voltage stress on insulation is another matter. From the information in the literature, the primary insulation concern with fast transients relates to defects in the GIS (paper 33-13), in which case, breakdown occurs in an inhomogeneous field situation and the dielectric strength can be substantially reduced. With VFT which include high frequency oscillations, the variations in voltage stress occur within the same time frame as that for growth of the breakdown (leader) channel in inhomogeneous fields. As a result, the high frequency oscillations of VFT could have a significant effect on breakdown level (paper 15-06). These interactions require further study to determine the proper combination of parameters which describe the waveform "severity" for the assessment of VFT. There is no reason why the peak magnitude of the VFT (by itself) should or should not be the best indicator of stress. Since the breakdown processes for VFT stress (especially with defects present or at the DS intercontact arc) will have a strong impact on equipment testing (and therefore on assuring reliability), further research in this area is encouraged.

1. Boggs, S.A. and N. Fujimoto. "Techniques and instrumentation for measurement of transients in gas-insulated switchgear." IEEE Trans. on EI, *EI-19*, No. 2, April 1984, p84.

2. Meppelink, J., P. Hofer. "Design and Calibration of a High Voltage Divider for Measurement of VFT in GIS" ISH Braunschweig 1987, paper 71-08.

Mr. K. FESER (Fed. Rep. of Germay)

The VFT overvoltages during disconnector operation were evaluated for a complex GIS installation. As an example the lay-out of the 420 kV substation Laichingen, EVS, Germany was used. The aim of this investigation was to get the maximum overvoltage factor of a certain arrangement and the main influencing factors on the overvoltage factor during a disconnector operation.

These comprehensive calculations to evaluate the maximum overvoltage factor for a given GIS arrangement result in the following main points for a voltage collapse of 2 p.u. across the disconnector:

- A complex circuit can be simplified for the determination of the overvoltage factor.
- The maximum overvoltage factor is evaluated at the bus ends.
- The main circuit can be simulated by the travel times and surge impedances. Important for the simulation are the capacitances at the line ends on the source side and the load side. Intermediate capacitances can be placed at the line ends. In Fig. 1 the equivalent diagram is shown.

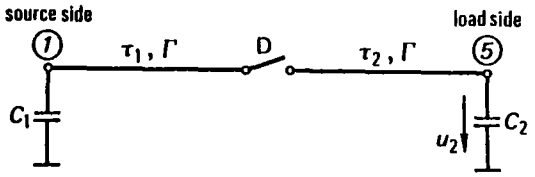

Fig. 1 Simplified equivalent circuit

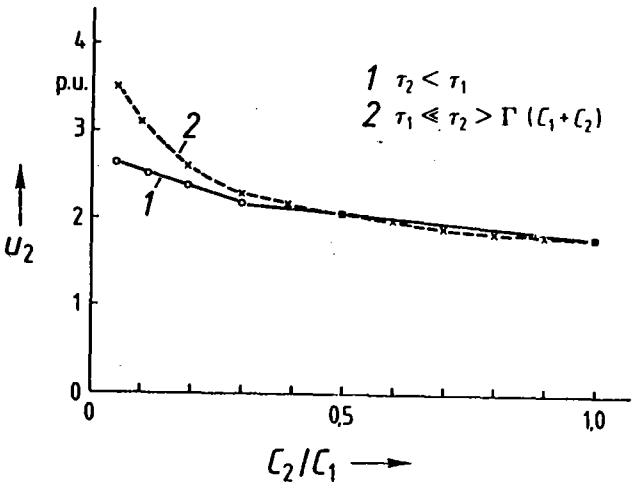

Fig. 2 Maximum overvoltage factor in function of C_2/C_1

- The overvoltage factor depends from the ratio of the capacitances at the load side C_2 and at the source side C_1. A low ratio results in a higher overvoltage factor. The overvoltage factor varies from 1.8 p.u. for C_2/C_1 = 1 to 2.7 p.u. for C_2/C_1 = 0,05 (Fig. 2). Small values C_2/C_1 are given in practice if at the source side a transformer is placed and. at the load side a piece of the bus is switched into the circuit.

Mr. C.J. JONES (United Kingdom)

It is our belief that it is yet not known, with any degree of certainty, what the effects of VFT are on GIS equipment in a normal 'in service' condition.

Insufficient data exists to establish how the multitude of combinations of factors i.e. rise time of front, peak value and frequency of transient, the level of trapped charge together with electrode and dielectric configuration etc... which will exist within a given substation environment can be assessed to establish their effect on the equipment.

Whilst it is know that the range of front times can be as fast as 1ns it has not yet been established what the effects of the resultant Giga Hz transients may be on the equipment. It is felt by us that the presence of these Giga transients cannot be ignored and that the only way to gain a full understanding is to have a measurement system capable of reccording the fastest possible wavefront.

To this end we have developed a measurement system (Fig.1) capable of capturing accurately 1 ns rise times and this will be used to estabilish transient overvoltages from disconnector switching in both the laboratory and service conditions.

Good agreement has been achieved between the shape of calculated voltage transient and measures transient using a relatively simple GIS rig (Fig.2) and conventional EMTP models The rig shown in Fig.2 consists of an accurate full size lightweight model of GIS ans an SF^6 filled spark gap to generate the controlled fast pulses.

However when the details of the responses are considered as shown in Fig. 3 it is apparent that differences do exist and it is now known that the level of EMPT model required is much more detailed than previously utilised.

The significance of the conventional model defiencies will become clearer when teh new measurement system has been applied to a full GIS installation and the influence of the very highfrewuency transients have been investigated.

The above work is part of a major programme being undertaken within the UK involving the close collaboration and support of CEGB, SSEB,CERL together with Strathclyde and Liverpool Universities.

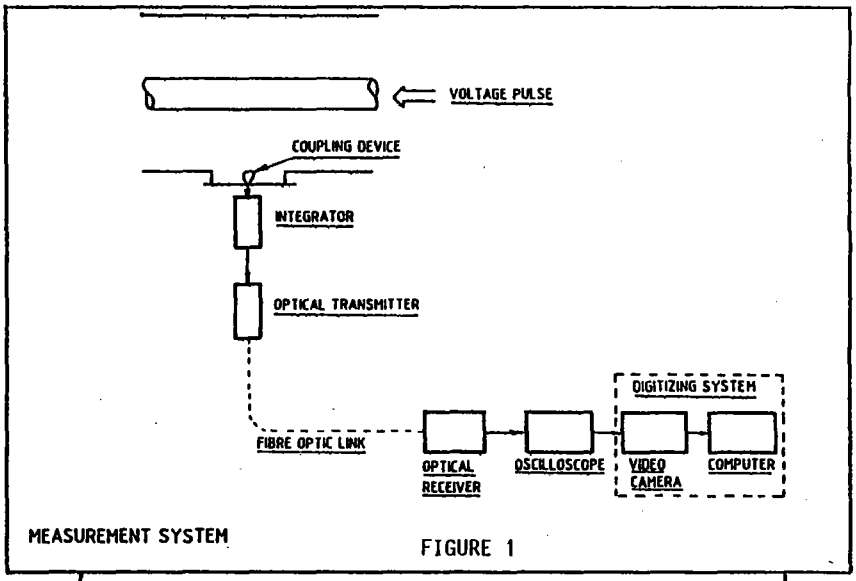

FIGURE 1

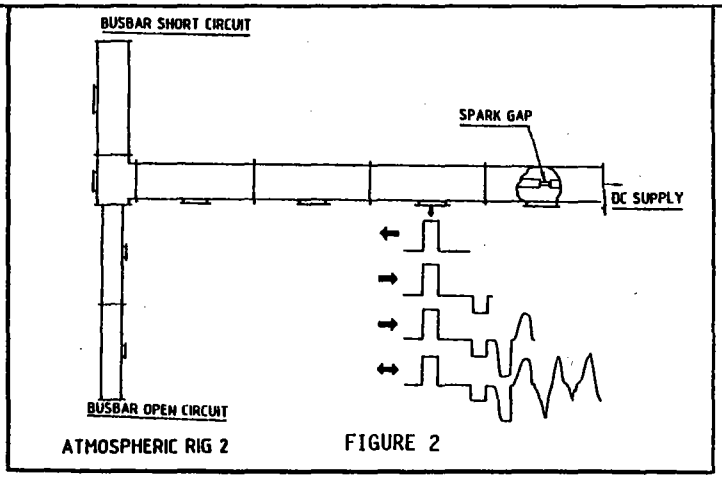

FIGURE 2

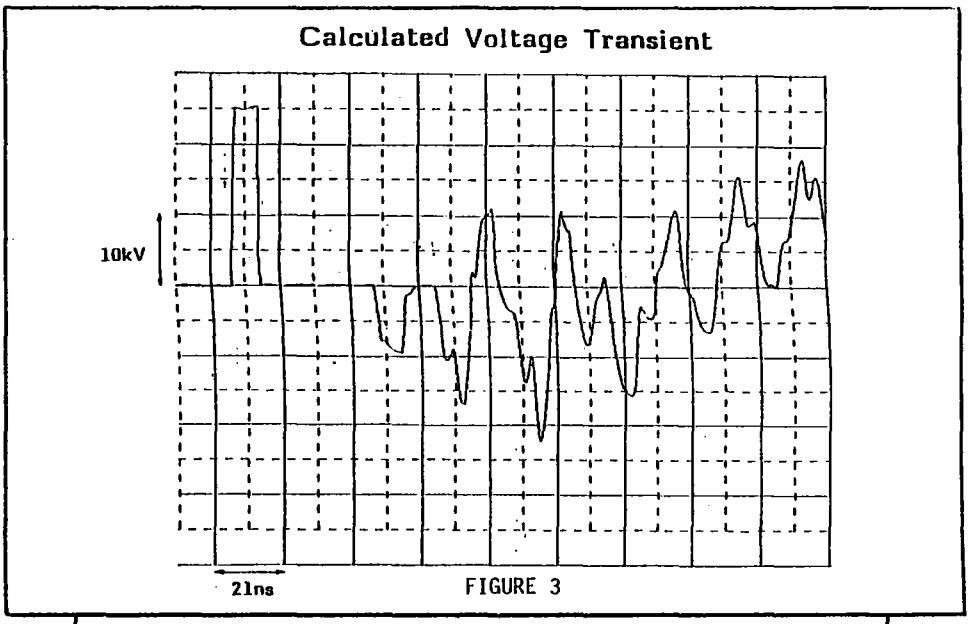

FIGURE 3

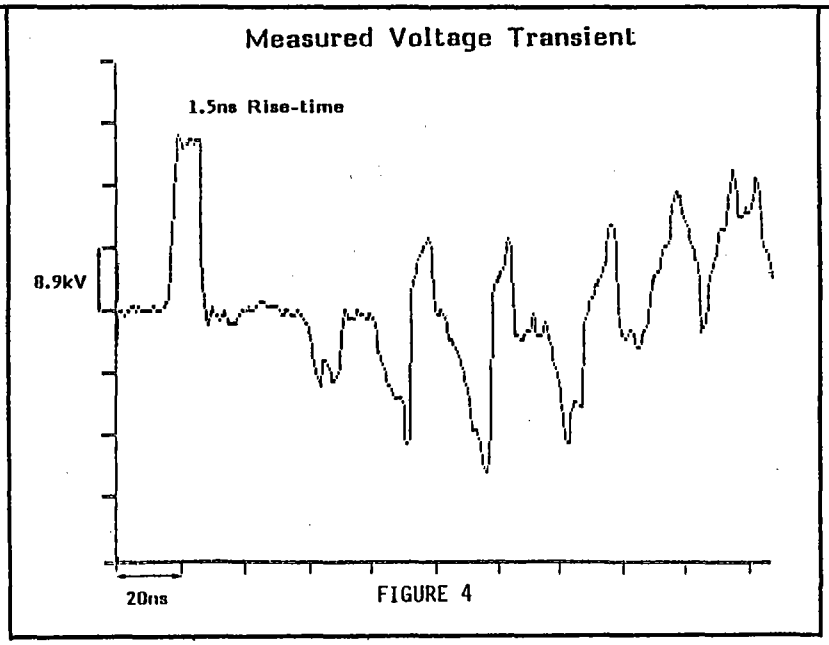

FIGURE 4

Mr. C. NEUMANN (Fed. Rep. of Germany)

Calculations of Very Fast Transients (VFT) in GIS can produce a good agreement with measurements. For this, the GIS being represented in modal quantities a frequency-depending damping of the modes HV-conductor to enclosure and enclosure to earth is to be considered and a voltage collapse across the disconnector according to Toepler's law must be taken into account.

Fig. 1 shows the behaviour of a calculation with and without frequency-depending damping assuming a square-wave voltage collapse. Due to the frequency-depending damping the maximum overvoltage is reduced from 1.4 pu to 1.3 pu.

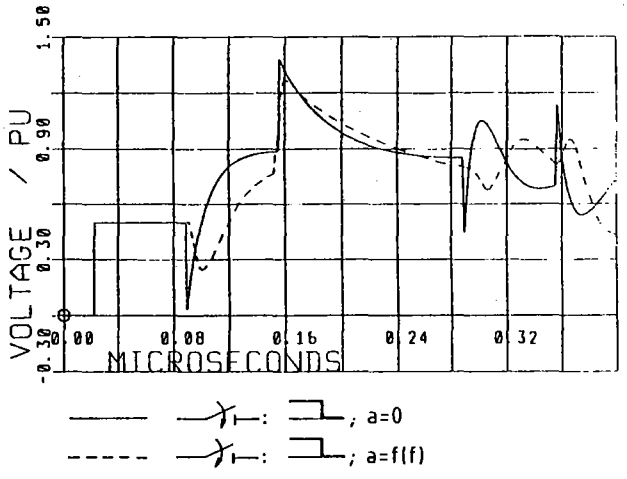

Fig. 1

The most realistic behaviour is obtained, when furthermore the voltage collapse across the disconector is taken into consideration with a time to breakdown of 20 ns according to Toepler's law, as shown in Fig. 2. In this case the maximum overvoltage reaches a value of 1.2 pu only.

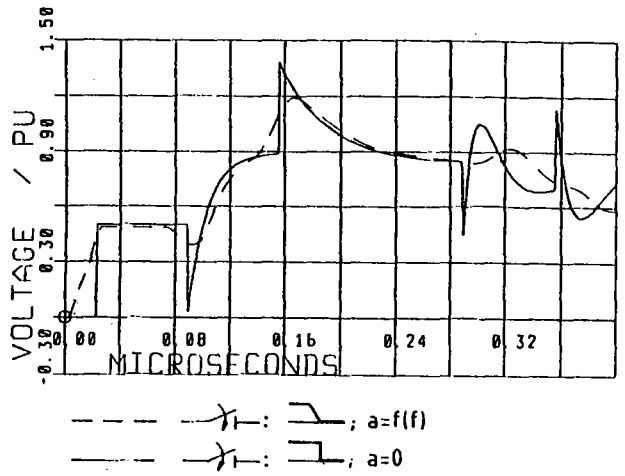

Fig. 2

Beyond that one can see from Fig. 2 that not only the maximum overvoltage, but also the time behaviour is strongly affected by these two assumptions. A correct time behaviour, however, is relevant for a realistic simulation of the overvoltage development in the us-range after various reflections and refractions have occured.

M. S.W. ROWE (France)

When defining the waveform parameters of importance for dielectric breakdown, in a given situation, the first step must be to determine the mode of discharge initiation and propagation.

For the specific case of disconnector (D.C) switching, photographic studies are difficult due to the intense light output from the main intercontact arc which masks the pre-breakdown propagation of the side branches.

In order to gain some information as to the leader propagation mode for fast oscillating voltages, we therefore undetook a series of experiments with a point-plane electrode system and a test circuit as shown in Fig. 1a.

In this circuit, two 600 kV transformers are connected such as to give complete phase-opposition across the operating D.C. Hence reproducing very severe transient conditions for the first strike. A second D.C. is mounted but is permanently closed and has a point electrode mounted in order to create a highly divergent field with respect to ground.

This circuit permits the generation of transient overvoltges having rise times from roughly 250 nS up to several microseconds. The peak voltages obtained can reach 2.6. p.U.

Having set up the circuit, and using disconnector closing to produce the transients required, we observed the predischarge propagation from the point electrode to ground with an Imacron camera in the framing mode at 5 x 10^6 images per second.

GROUND FAULTING

It should be remembered that on restriking, the electric field between the D.C. contacts rotates by 90° and the arc between contacts is thus subjected to a highly divergent, high frequency electric field to ground. Any side branches, which have developed in the quasi homogeneous inter-contact field, during initial streamer propagation, will now find themselves in a field tending to retrigger their propagation along the new field lines towards ground (1). If the D.C. dielectric design is insufficient, the local field may be high enough to allow propagation until a discharge path is formed from the intrcontact spark to ground (2). The rise times, fundamental frequencies and amplitudes of disconnector induced transients can have an almost infinite variety, depending as they do many practical parameters. However, the general form for the overall envelope can be described by the relation : $V = (A-B\cos[wt] \cdot \exp(-at)$, where for critical conditions of 1 P.U trapped charge, A = 1 and B = 2. This is not too extreme a simplification, except for specific cases, because the very high frequency components are usually rapidly damped out by various circuit parameters.
For relatively slow transient overvoltages, ground faulting is usually noted to occur at or near the first positive overall maximum value. However some are observed after several cycles at voltages well below the first peak value and even at apparently zero voltage (fig. 1 b).

Furthermore when rise times of the order of 300 nS are employed we have found that ground faulting always occurs after at least three cycles (1). If the SF6 pressure is reduced, the delay to ground faulting becomes increasingly long such that at 1 bar reproducible delays of five cycles are obtained for transients having rise times of 1.5 µs.

RESULTS

For our experiments, the general results were that, for transients with rise times of 1 µs and above, propagation appears "continuous", starting at a certain point on the wave front and leading directly to breakdown within roughly 250 ns. However, with rise times of about 300 nS propagation is "discontinuous" ; starting near the first peak but haulting as the voltage falls, with associated visible extinction of the leader channel. When the voltage rises again the channel reilluminates and propagation is retriggered, either following the general direction of the initial channel or branching differently (fig. 2). This renewed branching after an initial extinction suggests that the leader stem tip conditions are considerably modified during the "latent" period. This is thought to be due to space charge drifting with associated local electric field modification coupled with recombinaison within the leader channel and tip region.
Experiments were also conducted using transient overvoltages with roughly the same rise time and peak voltages but with much greater damping.

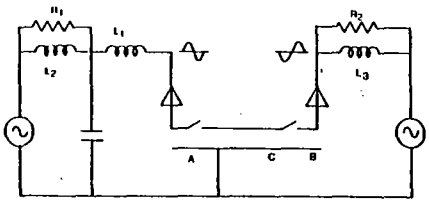

Fig.1a - Experimental test set up using full phase-opposition

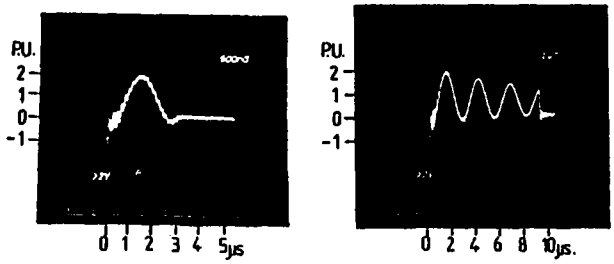

Fif.1b - Full scale D.C. ground faulting near zero voltage and after several cycles.

In these cases the breakdown voltage was notably increased because little or no propagation could take place after the first maximum. If as it is thought, a parallel can be drawn between propagation in this case and in that of an operating D.C., the waveshape can be seen to be of prime importance in determining the breakdown behavior for any D.C. The damping must clearly be taken into account.

These results also complet the picture of breakdown as surveyed by CIGRE Paper 15-06 where experimental data of propagation modes of leaders for very fast transients is lacking.

Finally, the propagation mode in real operating D.C. and hence the importance of the different waveform parameters also depends on the insulating gas composition and pressure. This is clear from Fig. 3 which indicates that only small proportions of gases in SF6 modify considerably the breakdown behavior at nominal pressure (3).

Given these results the importance of the various waveform parameters must also take account of the nature of the gas insulation.

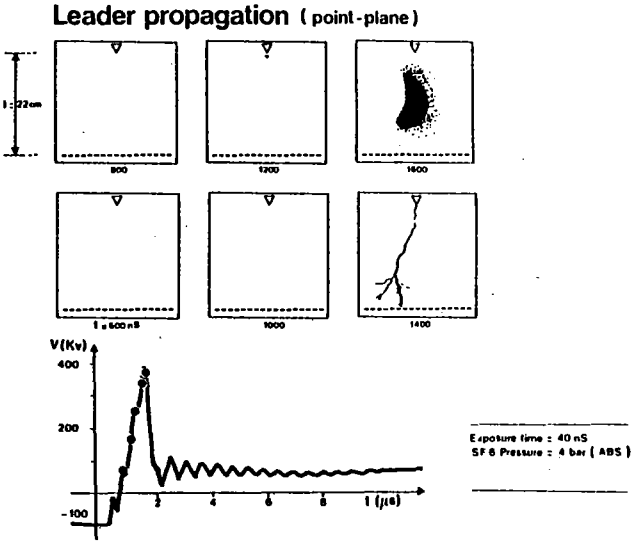

Fig.2a - Image convertor camera results of point-plane breakdown (t_m = 1,4 s).

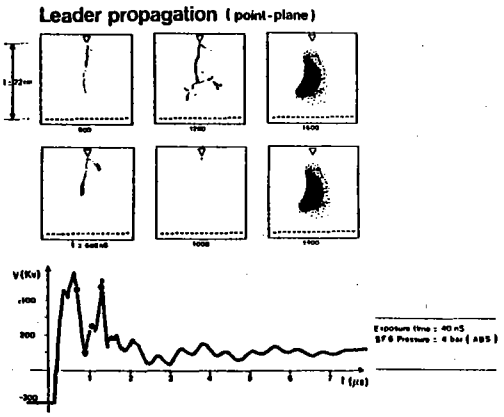

Fig.2b - Image convertor camera results of point-plane breakdown (t_m = 300 s).

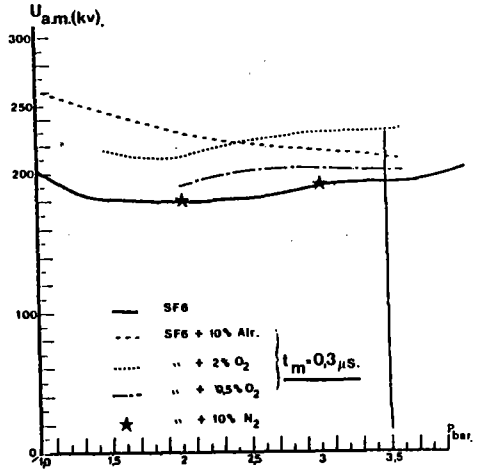

Fig.3 - Disconnector induced ground faulting (t_m = 300 nS) for SF6 and mixtures.

REFERENCES

(1) S.W.ROWE : "G.I.S. Disconnectors : A Physical Model for Ground Faulting" C.E.I.D.P., IEEE Electrical Insulation Society Annual Report.

(2) S.NISHIWAKI, Y.KANNO, S.SATO, E.HAGINOMORI, S.YAMASHITA and S.YANABU ; "Ground Fault by Restriking Surge of SF6 Insulated Disconnecting Switch and its Synthetic Tests", IEEE, Winter Meeting 1982, Paper 82 WM 187-3.

(3) S.W.ROWE : Improving G.I.S. disconnectors. I.E.E.E./C.S.E.E. Joint Conference on High Voltage Transmission Systems in China. Beijing, China. October 17.22, 1987.

Mr. G.C. DAMSTRA (Netherlands)

In the discussion on VFT most attention is given to the high frequency response of the measuring system. Upper bandwidth values of 100, 500 and even 1500 MHz are mentioned in many of the contributions. However it has to be realised that such systems, in particular in connection with light fiber transmission offer a limited low frequency bandwidth of 10, 50 or even 1000 Hz. This means that slower decaying processes or maybe the network frequency voltages cannot be presented correctly. The fast change of the voltage can be measured properly, but the correct absolute level of the voltage is lost during the measurement. In the discussion on question 7 emphasis have been laid on the importance of trapped charges for the value of the voltage jump and thus the VFT.

In order to measure the phenomena at both sides of the disconnector correctly, a prototype device has been developed to measure the voltage of an integrated capacitive divider with a risetime of about 10 nsec, but a quasi DC time constant of about one hour. So it is possible to measure the whole voltage waveshape correct and even to make O-C-O-test with proper DC offset due to the trapped charge of the previous opening. The device is fed by rechargeable batteries and use an analog fiber to the receiver connected to a two channel 100 MHz digitizing oscilloscope. The system is now in use for a 100 kV scale model disconnector.

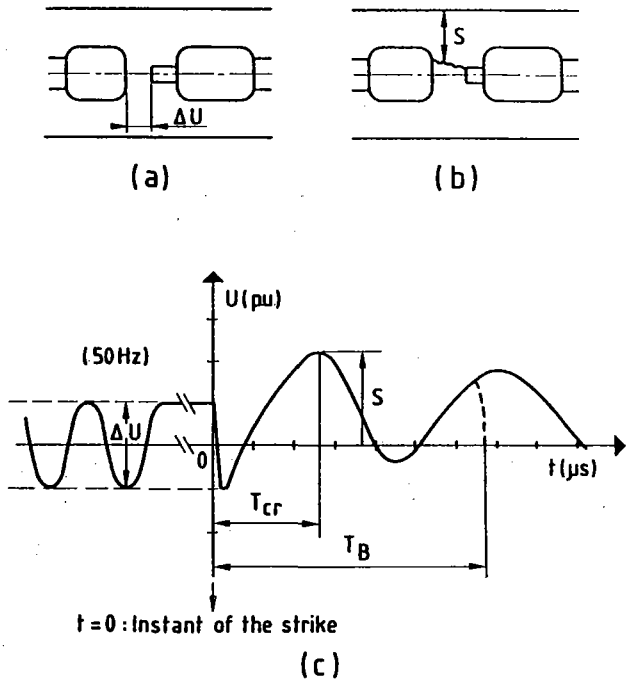

Figure. 1 :

a) Tension appliquée entre les contacts avant l'amorçage,

b) Surtension appliquée à l'étincelle entre contacts après l'amorçage entre contacts.

c) Définition des paramètres.

M. A. SABOT (France)

Je vais vous parler de la tenue diélectrique entre l'étincelle entre contacts d'un sectionneur de Poste Sous Enveloppe Métallique et la Cuve. C'est une configuration d'électrode à champ inhomogène particulière dont la tenue diélectrique a un comportement opposé vis-à-vis des Surtensions Transitoires Très Rapides à celui des configurations à électrodes fixes et à champ inhomogène tel que décrit dans le rapport 15.05. et précedemment par Mr. RIQUEL. En effet, pour ce cas particulier d'une étincelle entre contacts la tenue diélectrique décroit quand le temps à la crête de l'onde oscillante appliquée décroît. Ce résultat a été obtenu par des essais (Fig. 1) |1| où l'on a appliqué des ΔU entre contacts constants et des amplitudes de surtensions S constantes en faisant varier le temps à la crête (ou la fréquence) de la surtension (fig.2).

Donc pour deux couples ΔU,S gardés constants et trois valeurs de temps à la crête Tcr on a obtenu les probabilités d'amorçage à la crête suivante (fig. 3). On constate bien que la probabilité d'amorçage entre les étincelles entre contacts et l'enveloppe croît quant le temps à la crête de la surtension décroit. Autrement dit, pour ces cas particuliers d'électrodes, la tenue diélectrique décroît quand le temps à la crête décroît contrairement aux autres configurations à champ inhomogène ou homogène mais à électrode fixe |2|. Cette différence de comportement impose donc d'utiliser pour ce cas particulier, des ondes oscillantes à temps de crête court pour les essais de tenue diélectrique contrairement à tout le reste du Poste Sous-Enveloppe Métallique où l'on peut se contenter du choc de foudre.

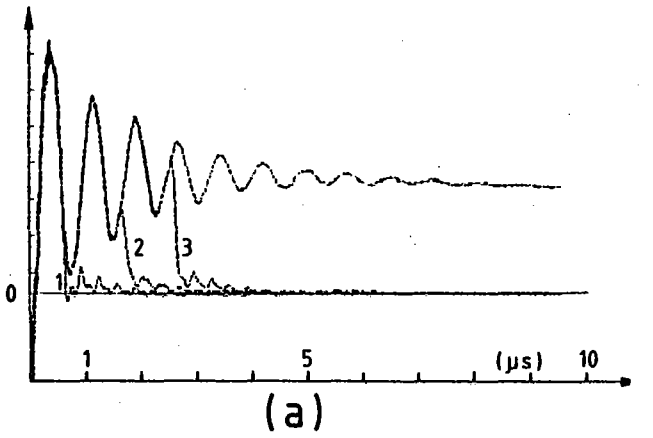

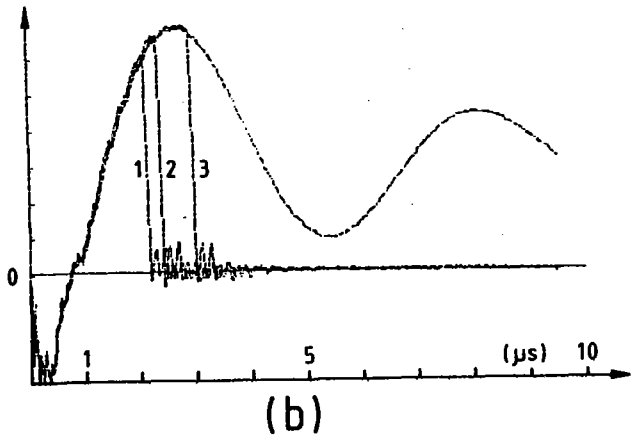

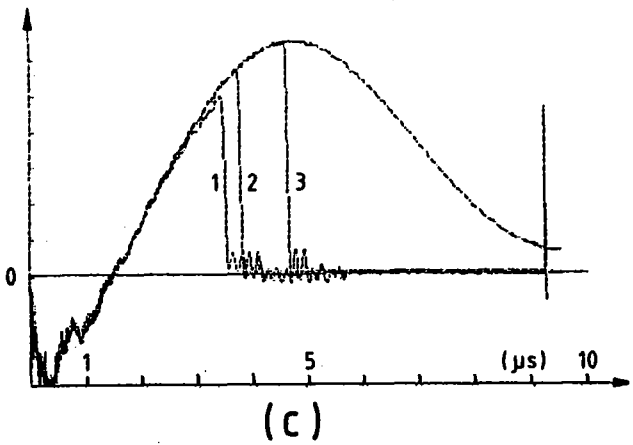

Figure 2 :

Formes des surtensions appliquées à l'étincelle entre contacts :

a) Tcr = 0,37 µs
b) Tcr = 2,7 µs
c) Tcr = 4,6 µs

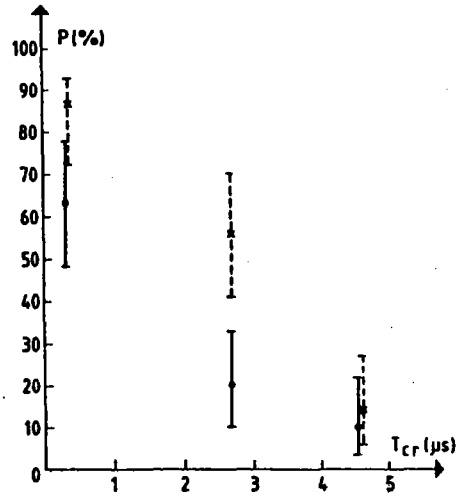

Figure. 3 : Variation de la probabilité d'amorçage entre les étincelles et l'enveloppe en fonction du temps de crête Tcr de la surtension S appliquée pour deux couples (ΔU,S) constants.

|1| J. Lalot, A. Sabot, J. Kieffer, "Dielectric Behavior of GIS Switching Disconnectors - Comparison of possible phase opposition Tests" IEEE Transactions on PWRD Nb 1 volume 3. January 1988, pp. 214-222.

|2| J. Lalot, A. Sabot, "Un arc peut en cacher un autre" Epure n° 13. Janvier 1987, pp. 27-35.

Mr. D.J. GLEESON (Ireland)

The withstand strength of GIS for very fast transient stresses appears in general to be adequate, except in the case of needle-shaped particles where some test results have indicated significantly reduced withstand levels, possibly even lower than the LIWL for the same conditions.

Modern trends to reduce LIWL for GIS and to optimise designs can only lead to a reduction in margins. There is increasing danger, therefore, of insufficient VFT withstand strength under conditions that can easily arise in practice.

It is clear that much work remains to be done in this area and it would accordingly seem unwise to advocate or agree to any reduction in rated values of LIWL for GIS, particularly in the EHV range, until a much clearer picture emerges regarding these phenomena.

Mr. M. DIETRICH (German Dem. Rep.)

According to the results presented in paper 33-15, in some operating conditions of SF_6 switchgear a stress on the insulation caused by a mixed voltage consisting of a d.c. voltage component and a VFT component may occur. If the VFT breakdown voltage is supposed to be about in the same order as the breakdown lightning voltage, the follwing conclusion can be drawn as a result of experimental investigations made at the Dresden University of Technology with mixed voltages consisting of d.c. voltage and lightning voltage:

1. SF_6 insulations without faults (slightly inhomogeneous field)

For this case it is generally known that the value of the breakdown mixed voltage $U_{d\Sigma} = U_{DC} + U_{LI}$ corresponds to the breakdown voltage at pure lightning voltage stress. Therefore, a test with pure lightning voltage whose value corresponds to the possible mixed voltage is sufficient.

2. Insulations with movable faults (particles)

In this case, theoretically, the breakdown mixed voltage may be much less than the breakdown lightning voltage. This would apply exactly to the case where the lightning impulse occurs at the moment when the particle is in the range of the inner electrode (provided that the d.c. component is so large that the particle is continuously moving). It was indeed possible to prove this effect for impulse voltages of longer duration (switching impulse voltages). However, as concerns the lightning impulse (and this applies even more to VFT) voltage the probability of such a constellation is so small that it is impossible to detect this effect of the reduction of breakdown voltage

3. Insulations with fixed faults

The breakdown mixed voltage of such an arrangement depends on the different types of superimposition possible (Fig. 1). The pure lightning voltage stress can be found on the ordinate and the pure d.c. voltage stress on the 45° line. In the case of equal polarity of d.c. and lightning voltage (ranges 1 and 3 in Fig. 1) the breakdown mixed voltage slightly rises with increasing d.c. voltage component as compared to the pure breakdown lightning voltage. The general characteristics of the breakdown mixed voltage and its components are shown in Fig. 2. Therefore, in these cases a test with pure lightning voltage is sufficient too. For this purpose, the value of testing voltage must be chosen according to the maximum possible sum of lightning voltage and d.c. voltage component. However, for the case of a different polarity of the components of mixed voltage (ranges 2 and 4 in Fig. 1) there is a falling tendency of breakdown voltage with increasing d.c. voltage stress. Considering the general characteristics of the individual components for this case, however, the breakdown mixed voltage decreases only at relatively high values of the lightning voltage component. Consequently, this combination can be regarded as uncritical as without a superimposed d.c. voltage the breakdown voltage would be much lower. From all this follows that a test with lightning voltage is sufficient even in those cases where a mixed voltage stress consisting of a d.c. voltage component and a lightning voltage component (or VFT component) occurs.
Furthermore, an on-site test, especially with oscillating lightning voltage can be carried out rather easily whereas the generation of mixed voltage requires a relatively expensive amount of equipment.

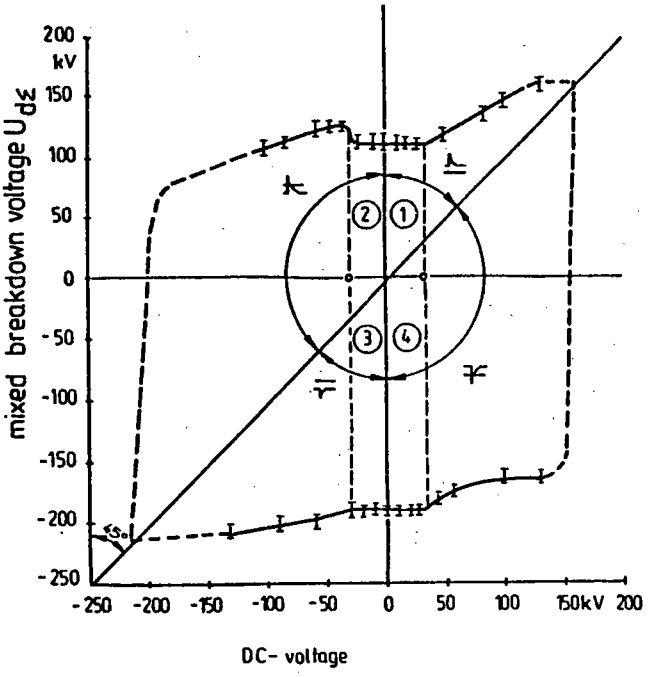

Fig. 1 Mixed breakdown voltage (superimposition of DC and LI voltages) for SF_6-insulation (gap distance 50 mm) with fixed defect (lengh 3 mm)

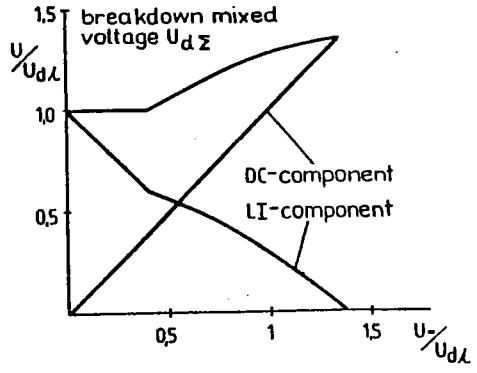

a) both components with the same polarity

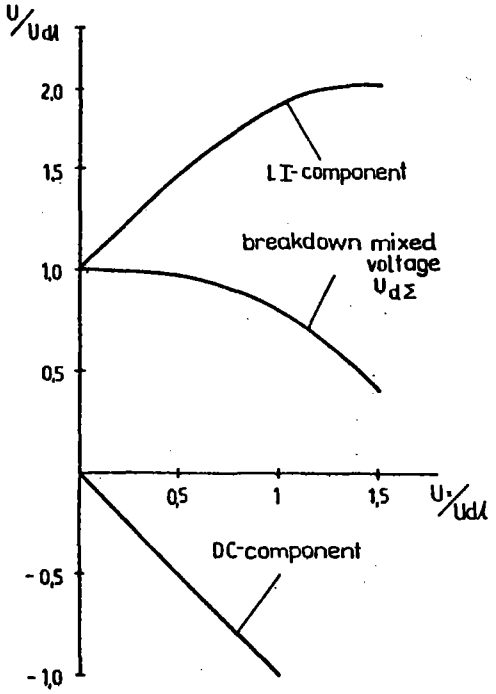

b) opposite polarity of the components of the mixed voltage

Fig. 2 Principle behavior of the mixed breakdown voltage U_d depend on the relation beetween the LI and DC components in relation to the pure breakdown LI voltage

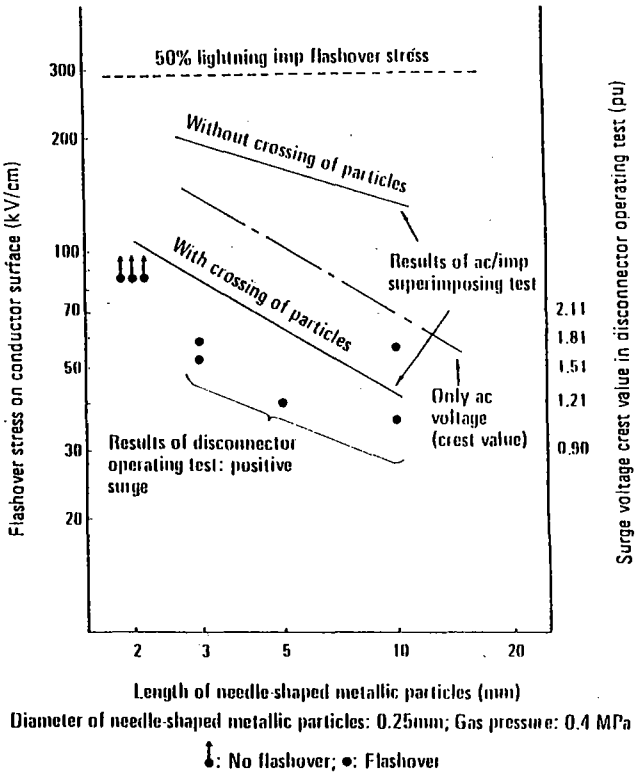

Fig. 1 TEST RESULTS CONCERNING FLASHOVERS IN 500 kV GIS MODEL

Mr. Y. MURAKAMI (Japan)

Insulation characteristics of gas insulated switchgear (GIS) that contained needle shaped metallic particles were investigated to solve problem related to disconnector restriking very fast transient overvoltages (VFTO). The metallic particles were included in GIS test model, and the disconnector was operated to generate multiple restriking surges. It was found that, in some conditions, flashover voltage (FOV) was extremely reduced (as shown in Fig.1).

In this case, 500 kV GIS test model was used, and under the normal operating voltage condition, that is $550/\sqrt{3}$ kV, the disconnector was operated. As a result, flashover stresses depend on the particle length and are smaller when metallic particles are longer. Flashover occurred with the particles of 3 mm, 5 mm and 10 mm length, however no flashover occurred with 2 mm-long particles. This is dependent on whether the particles cross the gas gap or not. It is presumable that the 3 mm length is a critical value against such a disconnector VFTO.

The level of 50% lightning impulse flashover stress without metallic particles is very high and is around 300 kV/cm (as shown in Fig.1). In contrast, if metallic particles exist inside the GIS, the flashover stress levels are reduced to one-sixth or less than this clean condition level. By expressing the stress as equivalent surge level, it is evident that flashovers were caused with 1.8 pu or less surges. From the surge level measurement on actual 500 kV GIS substation, 1.8 pu is the surge level that normally occurs.

To basically explain this reduction of flashover voltages, the disconnector surges were simulated with one-shot single or oscillating impulse voltages and flashover characteristics of metallic particles were obtained. In this case, metallic particle was set on the high voltage central conductor in GIS model.

In contrast to the result of clean condition which shows the incresing V-t characteristics of FOV along the short time range, FOV results with metallic particles show remarkable decreasing V-t characteristics, depending on the metallic particle length (as shown in Fig.2).

The reason of this FOV reduction will have the relationship with the corona stabilizing phenomenon around the small particle tips. The shorter the wave front of applied voltages is, that is, the higher the wave front steepness is, the smaller is the corona stabilizing effect and it will result in the FOV reduction.

Although the results of such FOV reduction with VFTO are remarkable, this

problem will be solved when the particles do not lift on or cross the gas gap to the high voltage conductor and, of course, when the particles are eliminated from the GIS.

Here attention must be paid to the electric field on the tank surface caused by ac voltage applied, as well as the presence of the metallic particles. To enhance the reliability of the VFTO insulation, ac tank surface stress must be suppressed under the particle crossing stresses.

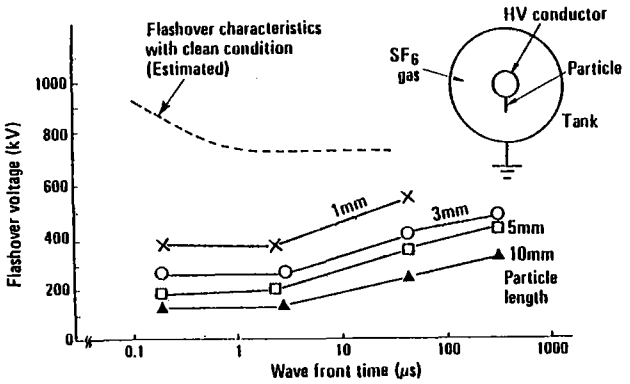

Fig. 2 V-T CHARACTERISTICS OF SF_6 GAS WITH METALLIC PARTICLE CONDITION (ONE-SHOT IMPULSE VOLTAGE APPLICATION)

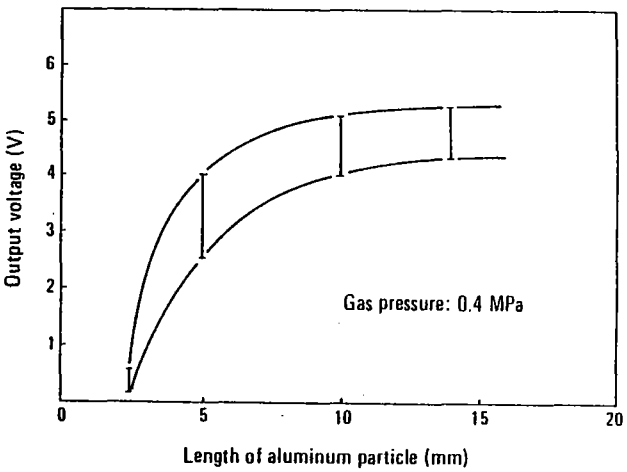

Fig. 3 RELATION BETWEEN OUTPUT VOLTAGE OF ULTRASONIC DETECTOR AND LENGTH OF ALUMINUM PARTICLE

The metallic particles can be eliminated by applying careful assembly procedure of GIS. For this purpose, the usage of clean room for assembly and the dust elimination technique by applying voltage in the factory will be effective. After the assembly of GIS, the metallic particles, even if these are small size, can be easily detected by the ultrasonic detector at site or by the partial discharge test in the factory.

The particle detection curve of such an ultrasonic detector, having around 200 kHz AE sensor, is obtained (as shown in Fig.3). According to this detection curve, particles with 3 mm length which will influence the VFTO flashover in GIS can be detected by this method at site. Once the particle is detected at site, GIS is opened and the particle will be eliminated. This technique has been already fully developed and is being practically used, finding no difficulty for detection.

Because of above procedure, we have no experience of particle initiated flashover caused by the disconnector VFTO in the field.

Mr. A.J. ERIKSSON (Switzerland)

Based on a broad range of laboratory testing experience with various GIS assemblies, we have no evidence that the oscillatory character of VFT has any particular influence on the GIS withstand strength characteristics. In consistency with the comments of papers 23-06 and 33-13, we also consider that the standard LI strength adequately represents practical GIS insulation withstand characteristics under VFT stress.

However, in response to the Special Reporter's remarks concerning "prestress", we do endorse the comments of paper 23-06 on the relative importance of composite stresses (i.e. VFT together with DC prestress), in the presence of particulate contamination.

Figure 1 depicts conceptually a laboratory test assembly which has been used to examine the combined effects of composite VFT stress and contamination on GIS dielectric strength.

The test object comprised a conventional conical spacer insulator which was subject to varying degrees of fine mixed dust

contamination. A DC prestress was applied via the HVDC generator, together with the secondary switch DS2 and a capacitor C (typical of a breaker grading capacitor). The VFT stress was supplied by allowing a normal disconnect switch to sparkover during the rising wave-front of a standard LI - the disconnect contact gap having been adjusted for this purpose. Various combinations of LI and DC polarity and relative amplitude were applied.

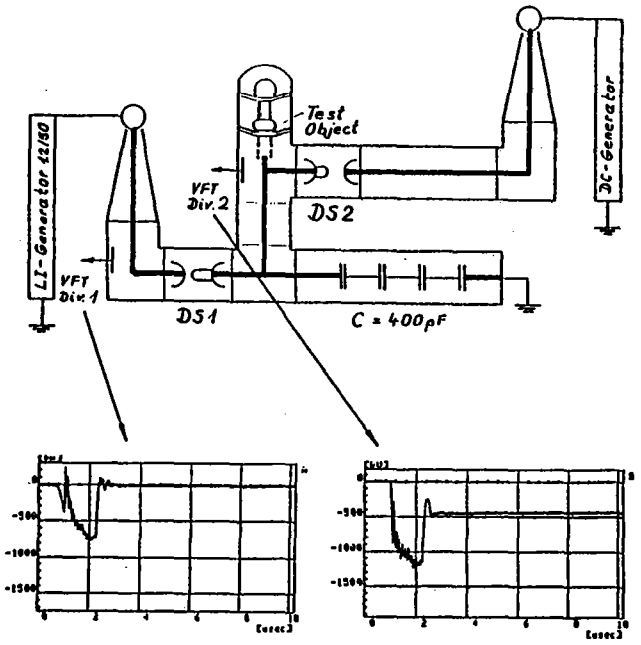

Figure 1: Laboratory testing of GIS withstand strength under the combined effects of composite VFT/DC stress and particulate contamination.

Figure 2 presents sample results in the relative strength quadrant -VFT/+DC. A decreasing withstand strength is apparent with increasing DC prestress over the equivalent trapped charge voltage range of 0,5-1.0 pu. for this particular GIS - in consistency with the results presented in paper 15-06.

The relative influences of dust quantity are also indicated, in that the test series 5/3 to 5/6 were made with 15mg, while 5/7 to 5/9 were made with 30mg contamination. The further reduction from 5/3 to 5/6 involved application of an AC preconditioning of the contaminated insulator, prior to application of the VFT compound stress.

In general, these results indicate that practical GIS elements are comparatively tolerant to the combined effects of compound stress and particulate contamination - in that relatively high levels of contamination were required to reduce the overall strength.

While it is clearly important that high grade quality control be ensured during GIS factory assembly and on-site erection, in order to avoid ingression of such degrees of contamination, in practice, we do not consider that correctly designed GIS is sufficiently sensitive to such VFT compound stress effects to warrant special purpose complex on-site tests.

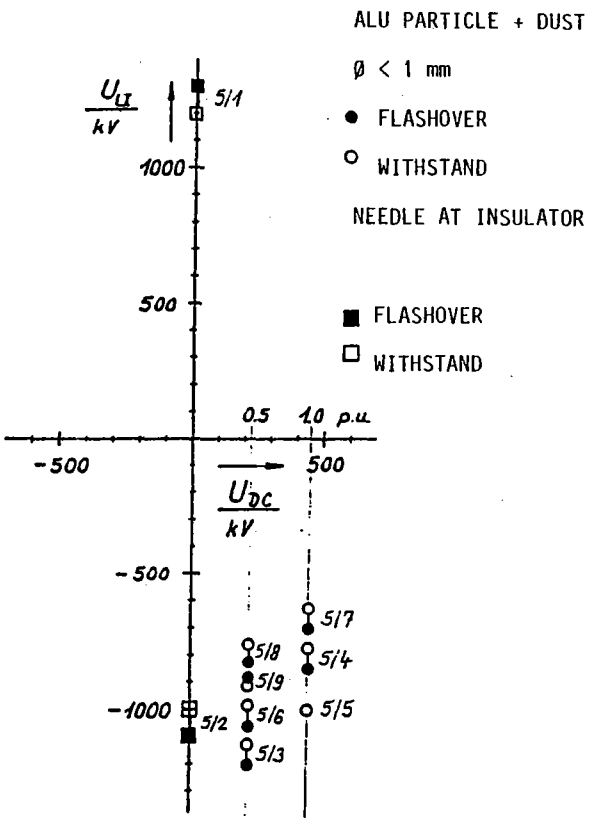

Figure 2: Effects of VFT composite stresses and particulate contamination on GIS dielectric strength (Sample results for horizontal spacer)

M. G. RIQUEL (France)

Lorsqu'on étudie l'influence de surtensions transitoires rapides (STTR) sur l'isolation dans les postes blindés on doit distinguer :

1). Les amorçages se produisant entre un conducteur et l'enveloppe.

2). Les amorçages se produisant dans les sectionneurs en cours de manoeuvre, entre l'arc entre contact et l'enveloppe.

Dans le premier cas de figure, du fait que l'amplitude maximale des STTR (~2,7p.u) est largement inférieure au niveau de tenue en choc de foudre (≈ 4 p.u.), seules les isolations fragilisées par la présence de défauts doivent faire l'objet d'une attention particulière.

En effet, en présence de défaut (pointe sur electrode, particule fixée...) l'hétérogénéité du champ qui en résulte provoque une chute considérable de la tenue au choc de foudre de l'intervalle. Par suite de l'effet stabilisant de la décharge couronne, ce type de défaut peut ne conduire à aucune réduction de tenue en 50 Hz.

Pour Electricité de France, ce risque est couvert par sa politique de contrôle diélectrique sur site qui préconise un essai au choc de foudre en complément de l'essai à fréquence industrielle.

La question que l'on se pose actuellement, est de savoir si l'essai au choc de foudre sur site peut également garantir la tenue sous STTR.

EDF a donc entrepris une série d'expérimentations visant à simuler des STTR (sous forme d'onde oscillante 0,7 - 13 MHz) et à étudier leur influence sur la tenue d'un intervalle comportant un défaut (pointe 4 mm) (fig. 1).

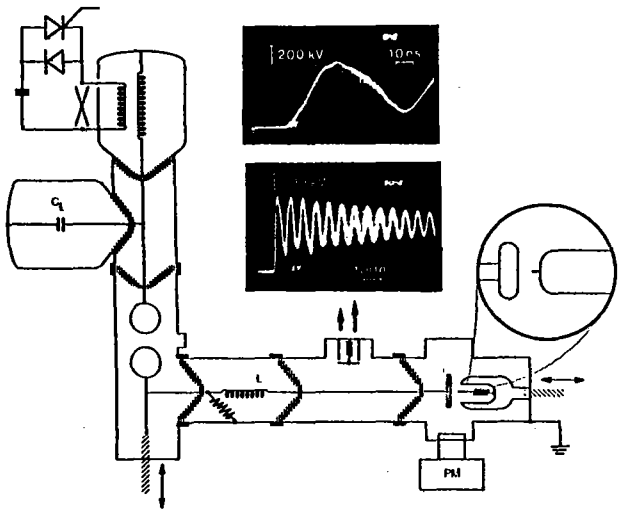

Fig. 1

Les premiers résultats montrent que l'onde de foudre s'avère toujours plus critique que les STTR simulées (fig. 2). Ils sont donc en parfait accord avec ceux présentés dans le rapport 15-05, et ceux du rapport 23-11 qui préconise d'introduire un essai au choc de temps de front inférieur à 10 µs.

Les divergences qui apparaissent avec certains résultats du rapport 15-06 seront discutées à la session 15.

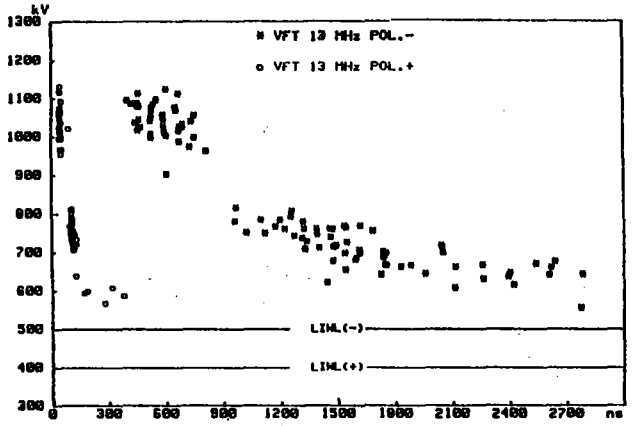

Fig. 2

Bien que les études se poursuivent, il exite d'ores et déjà un ensemble de preuves expérimentales qui démontrent la capacité de l'essai au choc de foudre à garantir la tenue sous STTR des intervalles à electrodes fixes.

Le cas de l'amorçage à la masse des sectionneurs en cours de manoeuvre, qui relève de phénomènes physiques différents, et présente une sensibilité accrue aux STTR, doit être couvert par un essai spécifique. Ce sujet sera discuté au cours des interventions suivantes.

Dans ma précédente intervention, j'ai indiqué que le comportement des isolations SF6 vis à vis des surtensions transitoires rapides était différent, selon qu'il s'agit d'une géométrie à électrodes fixes (cas général), ou d'une géométrie dont une électrode est constituée par un arc en formation (cas des sectionneurs en cours de manoeuvre).

Je voudrai vous présenter ici les raisons qui, à notre avis, expliquent ces différences.

Dans le cas d'un sectionneur qui manoeuvre la décharge se développe entre les contacts sous forme de canal ionisé (leader) comportant un certain nombre de branches latérales dont la racine commune se trouve sur le contact mobile (fig 1). Lorsqu'un de ces leaders atteint le contact fixe, et se transforme en étincelle, le champ électrique d'abord axial, devient radial (fig 2). En conséquence, le régime transitoire qui résulte de la connexion établie par l'étincelle provoque une surtension phase-masse.

Cette surtension peut réactiver les leaders latéraux en cours de désionisation et conduire à un amorçage entre l'arc entre contact et la masse (fig 3).

On assiste en fait à une course de vitesse entre la décroissance des branches latérales et la croissance de la surtension. Ainsi, plus le temps de crête est court, plus grande sera la probabilité de trouver une branche latérale susceptible d'être réactivée pour une amplitude de surtension donnée.

Par contre, dans une configuration à électrodes fixes, c'est l'inverse qui est observé :
La probabilité d'amorçage est d'autant plus faible que la contrainte est rapide à amplitude donnée.

Ceci est toujours vrai dans le cas des isolations saines.

Dans le cas des isolations fragilisées par la présence de défauts (pointe sur partie active), ce n'est vrai que pour des contraintes dont le temps de montée est inférieur à quelques µs , pour lesquelles le phénomène de stabilisation couronne n'apparaît pas /1/.

Ce comportement est dû au caractère fortement aléatoire de l'apparition des électrons qui permettent d'initier la décharge, et au temps, de propagation des leaders, qui varie généralement comme l'inverse de la tension appliquée.

En conclusion, l'essai au choc de foudre permet de garantir la tenue sous STTR des isolations "conducteur-enveloppe". Alors que le cas des amorçages à la masse des sectionneurs en cours de manoeuvre doit être couvert par un essai spécifique avec des ondes à temps de crête plus court.

/1/ I.D. Chalmers O. Farish S.J. Mac Gregor
"The effect of impulse waveshape on point/plane breakdown in SF6".
University of Stratchclyde GLASGOW. UK.

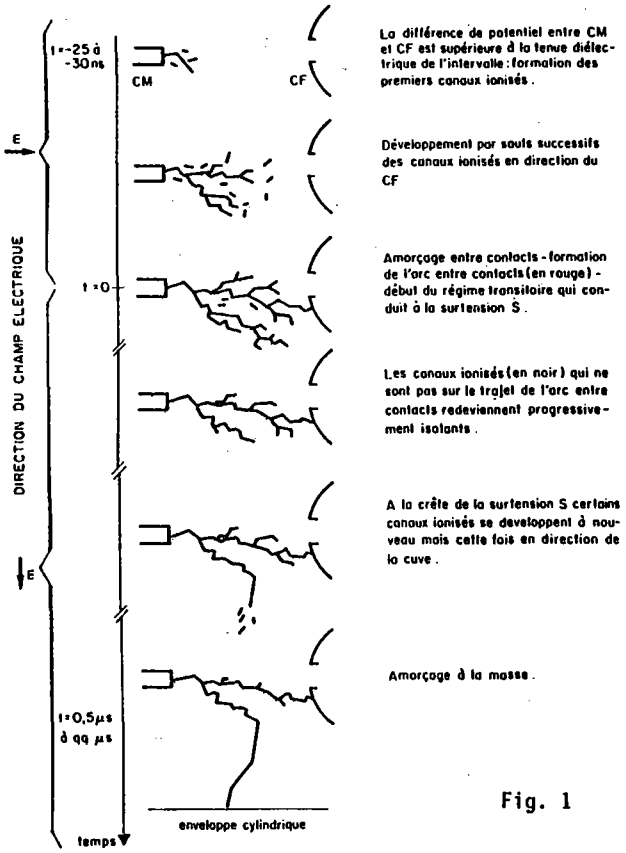

Fig. 1

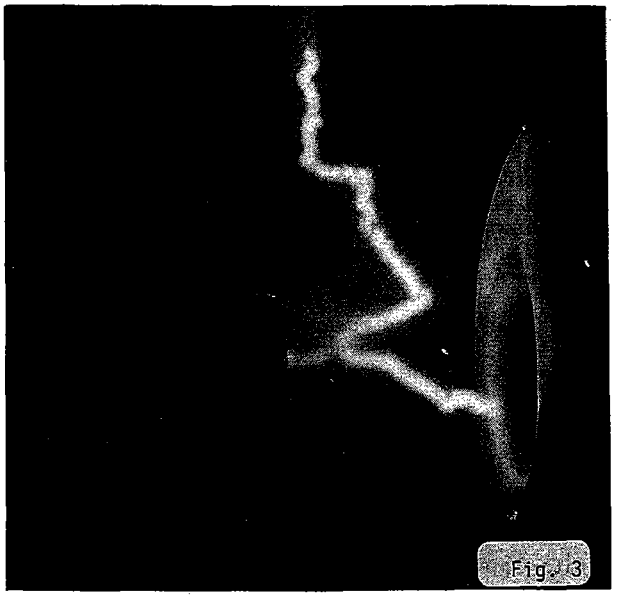

Mr. N. FUJIMOTO (Canada)

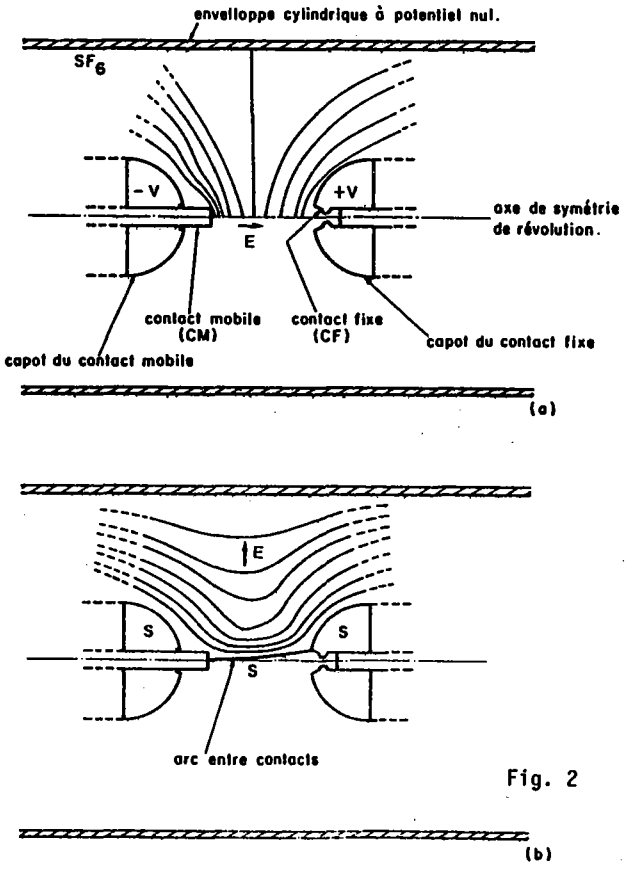

Fig. 2

The use of special tests using a variety of impulse waveforms have been proposed for ensuring the withstand of GIS against VFT overvoltages. The purpose of testing is to detect all the defects in the GIS which were introduced during assembly or shipping, which could result in problems, especially when exposed to VFT stress. However, as a result of the travelling wave nature, VFT waveforms cannot be used as to test GIS in a controlled manner. In addition, a large statistical scatter will exist for fast risetime stress, making the design of such a test difficult. Practicality dictates that an alternate waveforms be used. Normally, these will have risetimes in the range of 5-10µs to avoid problems with travelling wave reflections and are oscillatory to allow for higher peak voltages with portable impulse generators.

In order to assure the efficacy of testing, a relationship needs to be developed between the stress produced by VFT overvoltages under practical conditions which include the effects of trapped charge (for a range of possible defects) and the stress resulting from the test waveform chosen. This relationship allows the selection of the test levels necessary to assure that the VFT-sensitive defects will be detected. Sensitive (acoustic) PD measurements have also been suggested as a means of detecting the harmful defects (which are assumed to give off detectable corona under power frequency excitation) in lieu of an impulse waveform during on-site tests [1]. In this case, and for similar reasons as for impulse testing, a similar relationship is necessary between the measured PD level and the probability of that defect causing a problem when exposed to VFT. In either case, the important issue is that all defects which could cause problems during fast transients are detected during the test procedure. Although the characteristics of VFT are becoming well understood, further investigations are necessary before the most appropriate test techniques can be evaluated.

M. F. BURET (France)

Mon intervention se rapporte à la question n° 10 du Rapport Spécial, relative à la validité d'un essai en onde apériodique pour s'assurer de la tenue du matériel soumis aux tensions transitoires rapides.

Il faut tout d'abord remarquer que , d'une façon générale, les ondes de tension normalisées pour les essais, ne sont pas totalement réprésentatives des ondes appliquées au matériel en exploitation. Les ondes normalisées mettent les différents matériels dans des conditions d'essais comparables; la validité de l'essai n'est qu'une question de marge de sécurité par rapport aux conditions réelles de service.

Je vais tenter d'évaluer ce que peut être cette marge de sécurité à partir des essais présentés dans notre rapport 15-05. Nous avons montré que, pour des temps de front d'onde inférieure à quelques micro-secondes la courbe tension temps est continuellement croissante quand la raideur du front augmente.

Ceci implique que si la tenue du matériel est vérifiée par un essai en ondes de foudre, par exemple à 80 % de la tension d'essai de type, la tenue sera assurée pour toutes les ondes de tension transitoire rapide d'amplitude inférieure.

La figure montre une extrapolation des résultats obtenus en laboratoire, à du matériel 550 kV, d'un niveau d'isolement de 1550 kV crête. Des essais précédents ont montré que globalement, cette extrapolation est valable.

Si donc on considère la courbe tension temps qui passe par le point 80 % de la tension d'essai de type soit 1240 kV, (ce qui suppose une tenue très limite), la tenue en transitoires rapide, dont l'amplitude est inférieure à 2,5 pu, soit 1122 kV est largement assurée. Pour une durée de front de 0,2 pu, la tension d'amorçage est de 1751 kV, soit une marge de sécurité de 56 %.

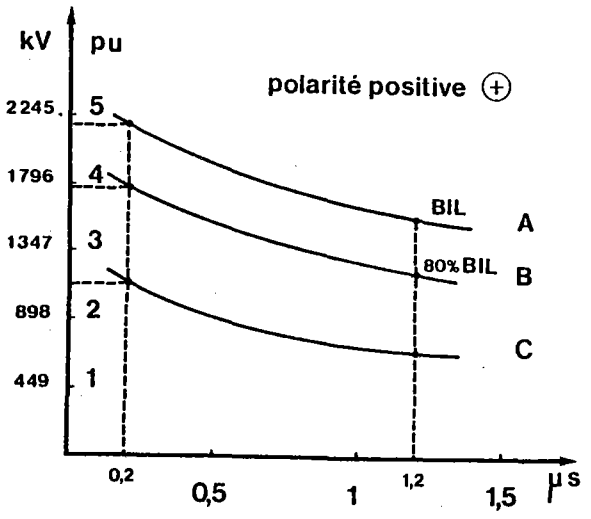

Figure: Courbes tension-temps
A.sans défaut
B et C avec défaut

D'après la courbe C, un défaut susceptible de produire un amorçage en transitoires raoides serait détecté par un essai en ondes de foudres à une tension aussi basse que 690 kV.

Ces chiffres ne sont évidemment que des ordres de qrandeur et demandent à être précisés. Il montrent cependant que la tenue aux transitoires rapides est largement assurée si le matériel a satisfait à un essai de tenue en ondes de foudre.

Ainsi des essais spécifiques en tension transitoire rapide ne sont pas justifiés.

Mr. M.G. DWECK (United Kingdom)

Transformers at the termination of GIS busbars may be subjected to fast transient voltages particularly following operation of disconnectors close to the transformer.

Using the circuit of Figure 1 a calculation was done of the transient voltage at the transformer HV terminals. It was assumed that the disconnecting switch was closed with 1 p.u. voltage on the transformer side and -1 p.u. voltage on the busbar side of the switch. This may occur during a closing or opening operation with repetitive striking in the disconnector. The response at the transformer terminals is shown in Fig 2.

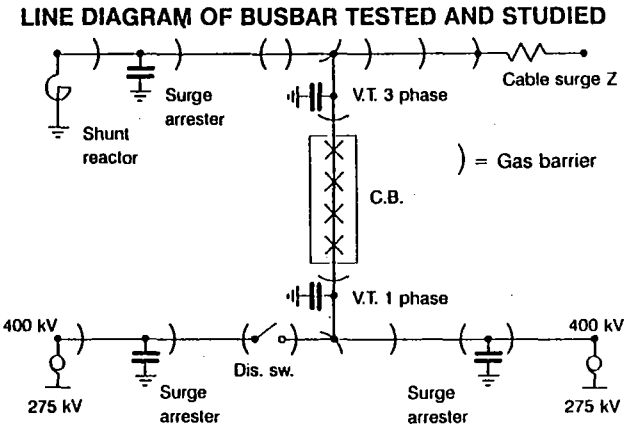

Fig. 1

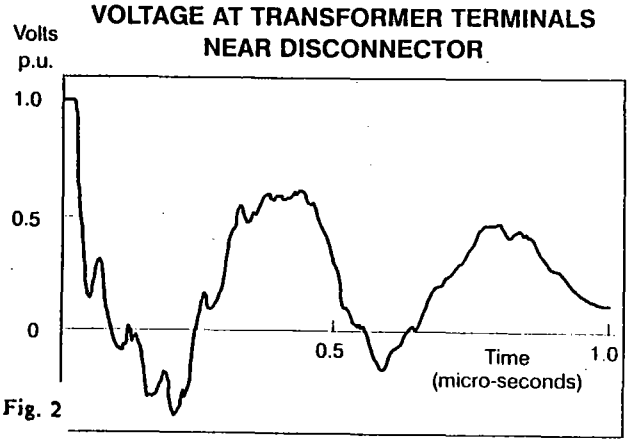

Fig. 2

There is a fast rising voltage having a highest peak to peak voltage of about 1.4 p.u. and a time peak to peak of about 0.2 us. This is followed by a damped response having a frequency of about 2.5 MHz.

Fig 3 shows the calculated voltage at the transformer with a standard 1425 kV double exponential 1.2/50 impulse wave superimposed. Although the amplitude of this typical applied voltage is low the initial rate-of-rise is higher than the double exponential impulse. However, it is felt that the full wave plus a chopped wave impulse test would be adequate to test for this condition.

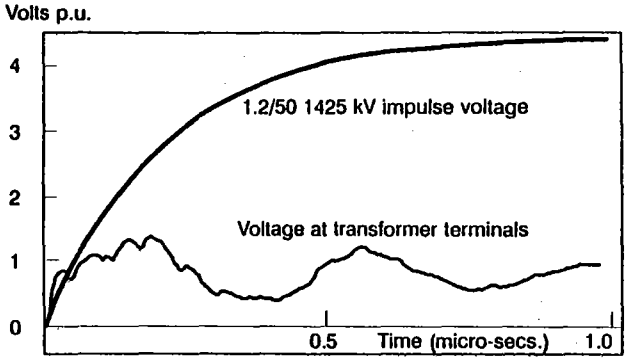

Fig. 3 **VOLTAGE AT TRANSFORMER TERMINALS COMPARED WITH IMPULSE VOLTAGE**

There is uncertainty about the transformer responses to voltages at the frequencies shown by the calculations and standard impulse tests may be inadequate to detect weaknesses here. There is some small risk of excitation of part-winding resonance in the transformer windings. There is some need to specify possible frequencies which may be generated and measures such as, for example, the fitting of varistors as mentioned in Paper 33.13 may be necessary.

Mr. A. STRNAD (Fed. Rep. of Germany)

There is a non-satisfying situation after more than 20 years of experience with GIS in HV networks: we still do not have standardized test procedures representing the stress that disconnector switching and flashovers in the GIS mean to connected components like transformers, cables etc. This situation should encourage both users and manufacturers to intensify the work on this topic.

Damage caused by disconnector switching to a transformer directly connected to a 420-kV-GIS of a neighbouring utility has made us very sensitive to VFT-effects. As a result we have adopted in a first step a VFT-test to a 420-kV-transformer. The transformer and its connection to the GIS, a 12-m-open air connection, have been rebuilt in the factory. The flashover in a GIS-test compartment has been initiated by an earth switch at a voltage of 1280 kV. It had not been possible to agree on a higher voltage with the manufacturer. The one-phase-test produced a 500-kHz-oszillation at the transformer. We measured the voltages in the GIS, at the transformer bushing, and at the top of the winding within the transformer.

Table I

	CHOPPED WAVE TEST AT 1640 KV	VFT TRANSFORMER TEST AT 1280 KV	VFT GIS MEASUREMENT REF. TO 1280 KV
MAX STEEPNESS	100 %	200 %	200 %
MAX VOLTAGE SWING	100 %	100 %	130 %
FREQUENCY	400 KHZ	500 KHZ	250 KHZ
DAMPING INCREMENT	100 %	90 %	25 %

ALL DATA VALID FOR VOLTAGES MEASURED WITHIN THE TRANSFORMER

In comparison to the standardized chopped wave test with 1640 kV - a standard test procedure in my country - this VFT-test produces within the transformer (Table I):

- doubled steepness
- a similar voltage swing
- a similar damping of oszillation.

The chosen test arrangement allows no proper simulation of the travel time between the flashover point within the GIS and the transformer; the corresponding frequency can cause additional stress in the transformer when it coincides with a resonance frequency of a winding.

Before commissioning we have performed tests on disconnector switching and initiated flashovers at a voltage level of 30 kV in a real 420-kV-GIS. To allow comparison the results have been converted to a breakdown voltage of 1280 kV.

Compared to the VFT transformer test the results of these measurements show (Table I):

- a similar steepness
- a higher measured voltage swing
- a less damped oszillation

Finally these results show that the steepness generated by GIS breakdown at the transformer is covered by the VFT transformer test; however, the voltage amplitude exceeds the values applied to the transformer.

We are going to discuss these results with the manufacturers.

Mr. G. PREININGER (Austria)

The question has been raised wether we need a new type of test to check the abilitiy of a transformer to withstand very fast transient overvoltages in service. The situation reminds me distinctly of the problem we dealt with in SC 12 some years ago, namely the resonance problem. Here as there the transformer designer has to face the fact that new arrangements in the electrical networks, new modes of operation or new kind of equipments create new kinds of stresses which have to be taken into consideration. Here as there only a few sporadic events give rise to concern, but soon one can hear demands for a new test, although nobody knows exactly how to perform such a test. First of all we

should better find out how these overvoltages could be exactly specified to provide the designer with a sound basis. We should also consider that new solutions may cost more money, not only for an improved insulation system or an elevated insulation level but also for a new test procedure. Our studies of the resonance problem showed that there are potential sources which could cause resonance in a transformer. But the studies proved also that a good deal of these sources in the networks could be avoided and that transformer designs could be modified to meet special requirements. For the remaining rest the probability of a resonance case is so low that the introduction of new costly test procedures seems not justified.

Most of the papers presented, dealing with VFT overvoltages, focus on disconnector switching as the principal source. Peak values up to 2.6 p.u. are mentioned. Accordingly a voltage change of 3.6 p.u. has been reported with a change rate of 3.3 MV/µs. This is still in the range of a chopped wave test performed with a multiple chopping gap. The voltage change in a 400 kV GIS would be approximately 1235 kV and is so well below a voltage change of 2180 kV during a choppped wave test with 30% underswing, assuming a BIL of 1425 kV. Steeper change rates occur associated with lower peak values. So it can be concluded that disconnector operations per se are no danger for the connected winding and need no specific consideration.

A different matter is the possibility of resonances in the MHz range. In paper 33-13 the frequency gain of a regulating transformer is shown with an outstanding q-factor at a frequency of about 1 MHz. In fact also we have observed such phenomena in a similar transformer, but also in smaller ones. Those frequencies are obviously caused by the dimensions of a transformer, the unavoidable lenght of leads and grounding connections. Protection by varistors seems the only practical solution for the time being. Again a special test to me is not practicable.

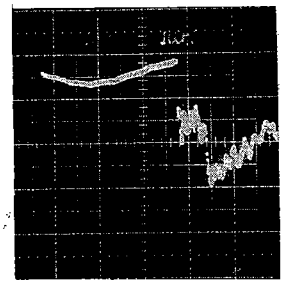

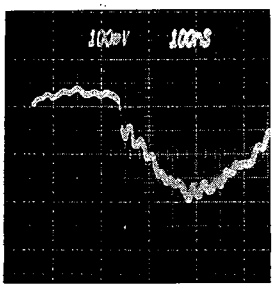

Figure 1a 100 ns/subdiv Figure 1b

There remains the flashover to ground inside a GIS, caused by an impinging lightning wave or an on-site test. Figures 1a and 1b show the voltages at the terminal of a 400 MVA transformer directly connected to a 400 kV GIS, developed by flashovers to ground in a distance of 10 and 19 m, resp. The measurements were performed by the Wiener Stadtwerke. The underswings are 50% and 83% and also here the lower voltage change is associated with the higher change rate. The voltage collapses to zero within 10 to 30 ns, the maximum of the underswing occurs after 140 and 300 ns, resp.. Figure 2 shows the flattening effect of the oil-SF6 bushing which is less than that of an oil-air bushing. The response at the connection between bushing and winding shows up to 50% the same steepness as the applied impulse. Then it becomes markedly flatter, obviously caused by the effect of

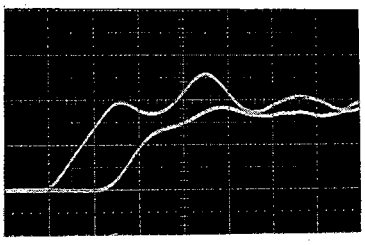

Figure 2 10 ns/div

the input capacitance of the winding. From this one can conclude that only a fraction of the voltage collapse is transferred to the winding with the full steepnes. Since the mechanism of the capacitive voltage distribution in an interleaved winding changes when the impulse becomes very steep, the resulting stresses within the winding can be higher than for a chopped wave. But peaks occurring at the very beginning have a very short duration and are presumably compensated by the increased insulation strength.

So the change rate is not the main reason for a new test. What we really have to consider is the value of the voltage before the flashover. A standard chopped wave test with 115% of the full wave and 30% underswing (related to the 115%) has a voltage change of 150% of the full wave. If we, e.g., assume a 20% safety margin in service and a possible underswing of 85%, the maximum permissible overvoltage would be 150x80/185 = 65% of the BIL. In a 400 kV GIS with a BIL of 1425 kV this would be 925 kV peak or 2.7 p.u.. If higher flashover voltages are required

- either because the protection level is not low enough and the probability of an impinging lightning wave is considered critical
- or on-site tests are performed with higher voltages and the transformer being connected

an additional clear requirement has to be stated in the specification. The value of the voltage change has an impact on the transformer design and may require reinforcement, at least of parts of the internal insulation system. An adequate test level can be obtained either by a higher BIL or an test loop with an appropriate underswing.

In any case, as additional costs and technical problems are involved, a thorough consideration of the real necessity of such a request is strongly recommended.

Mr. N. FUJIMOTO (Canada)

VFT have occasionally been implicated in failures of externally connected components, such as transformers. Statistics fail to show any apparent problems associated with VFT [1], implying that current test practices are adequate. However, the differences between VFT and chopped wave stress should be ap-

preciated. Measurements have indicated that the rate-of-rise of VFT impinging on transformers connected to GIS is similar to that of a chopped wave voltage stress, although the magnitudes and the waveform are totally different [2]. This seems to confirm the suitability of a chopped wave test for checking the transformer's ability to withstand VFT stress. However, a transformer subjected to a chopped wave test will usually see only a few limited applications of voltage. VFT generated by GIS disconnectors, on the other hand occur very frequently with many individual transients occurring with each DS operation. Consequently, one needs to consider the possibility of low probability breakdown or transient-related ageing which could occur with VFT but is not explicitly considered in the chopped wave test. Further investigations are required to establish the effect of fast transients on transformers in order that the ability to withstand VFT can be better evaluated and to avoid potential problems in the future.

Mr. D. KÖNIG (Fed. Rep. of Germany)

This contribution deals with transients occuring in switching circuits by making or breaking operations of GIS-disconnectors. By various studies it is well known that very fast transients such travelling wave phenomena with frequencies ranging far into the MHz-range may represent dangerous stresses for a gaseous insulation. However, up to now only few studies are concerned with low or medium frequent transients in the range of kHz up to some 10 or 100 kHz /1, 2, 3/. Phenomena, occuring in this frequency range, may be considered as "fast" transients, too, if compared with the low rated frequency of 50 or 60 Hz. This is especial-ly true for apparatus with windings like transformers, for which the parameter "frequency" is very important with respect to a correct function. Though the measured overvoltages at the terminals of power transformers in case of GIS-disconnector switching operations are comparatively small, local internal stresses due to the very complex internal structure of an apparatus with windings may be much higher and endanger the insulation system.

Measurements on site at two different locations using high voltage power transformers of different design as a voltage source lead to the result that in one case the low frequency oscillation of 3,5 kHz was superposed by a 24 kHz-medium-frequency transient, and in the other case the low frequency oscillation of 7 kHz was superposed by a 80 kHz-medium-frequency transient /2, 3/. Fig. 1 shows that these typical medium frequencies can be found as peculiarities in the measured curve of the impedance at the transformer terminals versus frequency /3/. However, a prediction which dominant medium frequency in case of a GIS-disconnector operation will appear at the transformer terminals based only on the measured impedance curve seems not to be possible up to now.

Two main methods in establishing an equivalent circuit for the simulation of the high frequency performance of a transformer are presently as follows:

The transformer design engineer uses a network simulation according Fig. 2a, which enables him to calculate the high frequency resonances and the voltage distribution inside the apparatus. This simulation method has been successfully applied up to frequencies of about 200 kHz /4/.

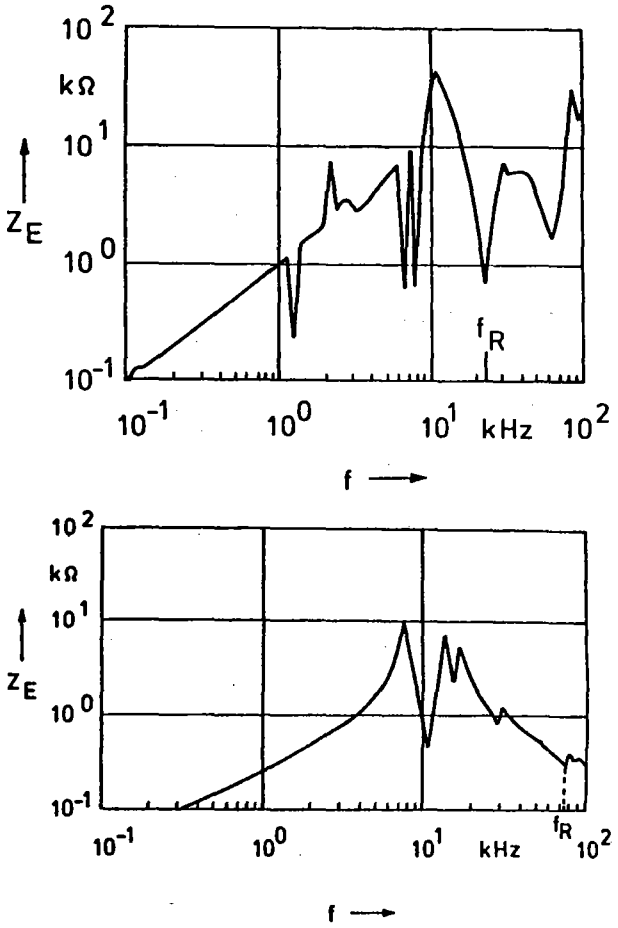

Fig. 1: Impedance measured at the terminals of two different high voltage power transformers versus frequency
f_R = resonant frequency, measured at on-site switching tests

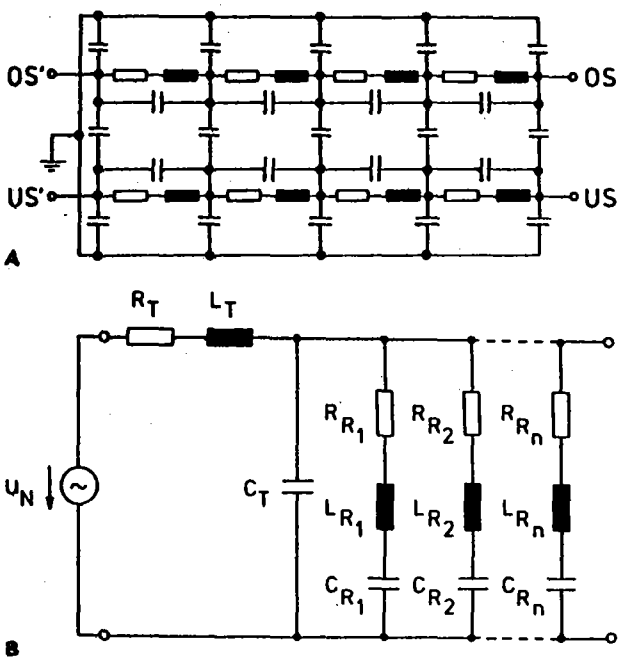

Fig. 2: Equivalent circuits of transformers
a) Network, able to oscillate
b) Series resonant circuits (modal-analysis)

On the other side the interaction of a transformer with the grid can be more or less easily described according Fig. 2b with the help of equivalent circuits with different resonant frequencies based on the modal analysis, but in that case only correlations between the stresses appearing at the terminals and the single equivalent circuit components are calculable /3/.

The interaction between a feeding transformer and the relevant load circuit, which both are connected by the load arc inside the GIS-disconnector, can be studied with the help of a synthetic three frequency test circuit according Fig. 3. Furthermore, the performance of GIS-disconnectors with respect to arc instabilities, reignitions and arc extinguishing can be investigated using this test circuit. Some recent results have been published this year /3/.

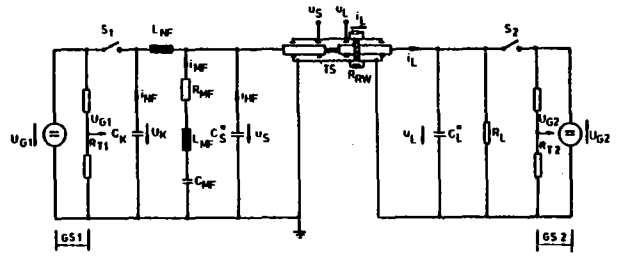

Fig. 3: Synthetic three-frequency test circuit for GIS-disconnectors

References:

/1/ D. König, G. Imgrund, C. Neumann, K. Maatz, L. Schiweck: Vorgänge beim Schalten kleiner kapazitiver Ströme mit SF_6-isolierten metallgekapselten Trennschaltern im 110-kV-Netz und ihre Simulation im Hochspannungslaboratorium, Elektrizitätswirtschaft, Jg. 85 (1986), S. 131 - 138

/2/ D. König, G. Imgrund, J. Meppelink, D. Schlicht: Performance of GIS-disconnectors under laboratory and network conditions. Gas-Insulated Substations - Technology and Practise, Ed. S.A. Boggs and coworkers, Pergamon Press Canada Ltd., 1986, pp. 75 - 85

/3/ G. Imgrund: Untersuchungen zum Schalt- und Löschverhalten SF_6-isolierter metallgekapselter Hochspannungstrennschalter im 110-kV-Energieversorgungsnetz und im Hochspannungslaboratorium. VDI-Fortschrittsberichte, Reihe 6/Nr. 219, VDI-Verlag GmbH, Düsseldorf (1988)' (Dissertation TH Darmstadt, 1988)

/4/ E. Buckow: "Berechnung des Verhaltens von Leistungstransformatoren bei Resonanzanregung und Möglichkeiten des Abbaus innerer Spannungsüberhöhungen", Dissertation TH Darmstadt, 1986

M. M. LOUIS (France)

Je voudrais vous présenter les raisons qui ont amené Electricité de France à choisir un schéma d'essai en opposition de phase (Fig.1), pour vérifier la bonne tenue diélectrique en cours de manoeuvre des sectionneurs 400 kV de Poste Sous Enveloppe Métallique (PEM).

Les conditions d'exploitation

Pour EDF, comme l'a rappelé Monsieur JOUCLAR précédemment, c'est l'opération d'ouverture d'un transformateur de tension qui a été jugée la plus contraignante [1].

Bien que la différence de potentiel entre contacts du sectionneur pour les derniers réamorçages est limitée à 2 p.u., comme l'essai est fait à la fermeture il n'y a donc pas ionisation et échauffement du gaz qui réduit la tenue diélectrique entre contacts [2].Pour palier cet inconvenient, on a choisi après essai [1] (fig. 2) d'appliquer entre contacts une différence de potentiel de 2,2 p.u. pour provoquer l'amorçage ; ceci répond, je pense, aux préoccupations exprimées dans le rapport 23-11.

En ce qui concerne le choix de la forme et de l'amplitude de la surtension appliquée à l'étincelle entre contacts et l'enveloppe (2,1 p.u., temps de crête compté depuis l'instant du réamorçage entre contacts 0,3 à 0,5 µs) il y a deux raisons [3] :

- l'amplitude de 2,1 p.u. et le temps de crête se rapprochent plus de la réalité des surtensions générées dans des PEM,
- une telle onde est plus facile à générer en laboratoire qu'une onde à temps de crête plus longue.

La limitation à une seule étincelle entre contacts par manoeuvre a été voulue pour bien maîtriser pour chaque essai la différence de potentiel entre contacts et l'amplitude de la surtension appliquée comme on le fait lors des essais au choc de foudre. En effet des conditions de différence de potentiel non représentatives pourraient entraîner des trajets de leaders entre contacts n'ayant rien à voir avec la réalité (champ électrique initial irréaliste, ceci répond, j'espère, aux préoccupations exprimées dans le rapport 23-11).

Enfin le nombre élevé de fermetures (50), s'il peut paraître "fastidieux" à certains (rapport 23-11), n'en est pas moins nécessaire pour s'assurer de la bonne tenue diélectrique du sectionneur si le nombre d'amorçages à la masse est inférieur à 2. En effet, une telle exigence peut paraître a priori très sévère comparée aux 2 amorçages sur 15 chocs permis lors d'essai de matériel autorégénérateur, mais là encore cette exigence est nécessaire vu les grands écarts types [3] rencontrés sur les deux paramètres d'influence. En fait 1/50 est statistiquement moins contraignant que 2/15.

[1] J. Lalot,, A. Sabot, J. Kieffer, and S.W. Rowe. "Preventing Earth Faults During switching of Disconnectors in GIS Including Voltage Transformer". - IEEE Trans on Power Delivery, Vol. PWRD-1, N°1. Janvier 1986 .

[2] S.A. Boggs, F.Y. Chu, N. Fujimoto, A. Krenicky, A. Plessl, and D. Schlicht. "Disconnect Switch Induced Transients and Trapped Charge in Gas-Insulated Substations" - IEEE, Trans on Power Apparatus and Systems, Vol. PAS-101, n°10 Octobre 1982.

[3] J. Lalot, A. Sabot, J. Kieffer. "Dielectric Behavior of GIS Switching Disconnectors - Comparison of possible phase opposition Tests - IEEE Transaction on PWRD Nb 1 volume 3. January 1988, pp. 214-222.

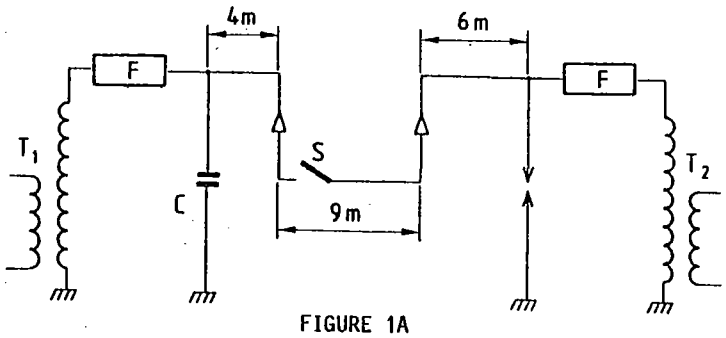

FIGURE 1A

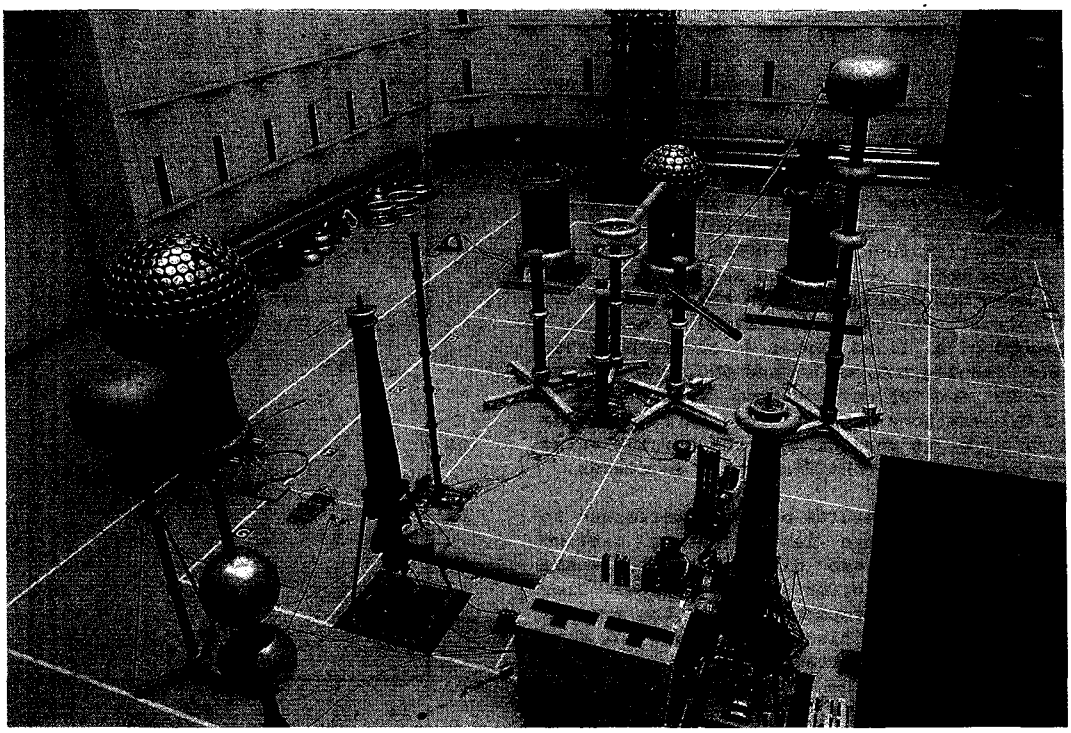

FIGURE 1B

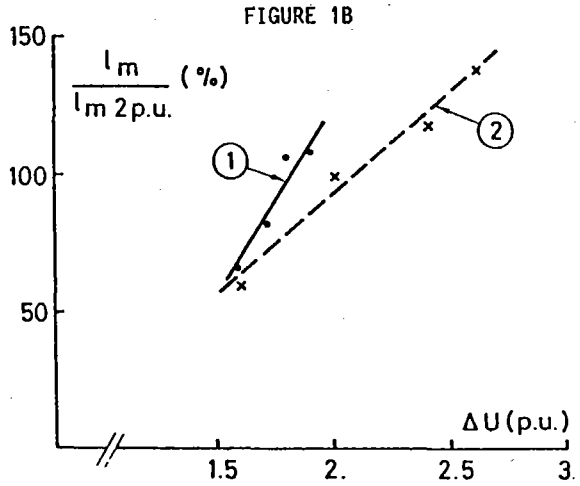

Variation of the mean length between contacts l_m at restrike versus ΔU in percent of the average length for ΔU = 2 p.u. at closing in phase opposition (l_m 2 p.u.).

1 - at the opening of a VT (full line)
2 - at the closing in phase opposition (dotted line)

FIGURE 2

Mr. A. BARGIGIA (Italia)

- The voltage collapse DU depends on the characteristic of the testing circuit and on the disconnector design (contacts profile, speed ect...), as an example the maximum value of DU increases increasing the ratio Cs/Cl (capacitance source side /capacitance load side), decreases increasing the asymmetry degree of the withstand voltage between contacts and decreasing the speed contact.
  The peak overvoltage, during an opening or closing operation, can be evaluated for each arc by means of:

  $$Ufto = U0 + K*DU \qquad (1)$$

  The maximum value of the overvoltage does not coincide, generally, with the last restrike in opening or with the first restrike in closing operation but depends on the worst couple of value U0, DU. Using a computer simulation of the disconnector it was derived that, in first approximation, the maximum overvoltage can be calculated putting in (1) U0=1-DUmax and DU=DUmax instead of the worst couple of U0 and DU.
  Using the same computer simulation the values of DU and Ur (residual voltage) were derived simulating 8 times groups of a fixed number N of disconnector operations ranging between 13 and 800. The maximum values of DU and Ur derived from each of the 8 groups of N operations were reported in figure 1 as a function of N. It results that the average value increases with N, while the dispersion decreases.

- Figure 2 shows the results of test performed to compare the maximum arc length during closing operations feeding the two disconnector terminals with AC-AC (out of phase) or AC-DC voltages. Time of closing operation (proportional to the maximum arc length for the same disconnector and the same testing condition) is reported as a function of the total strength between the contacts. In the same figure a comparison with the "static characteristic" of the disconnector is proposed.
  The results shows that AC-AC supply is equal or slightly more critical than AC-DC supply at least from the point of view of the maximum length of the arc between the contacts.
- Composite stresses (DC+ Fast Transient) decrease the withstand voltage of a GIS. A limit curve was derived from tests on several different GIS. A companion discussion relevant to question 7 shows some practical cases that can lead to flashover during operation. The probability to have such a cases increases increasing the nominal voltage of the considered system.

- Mainly on the the base of such a considerations ENEL prepare a test specifications concerning the metal-clad disconnector. The tests listed for disconnector, in addition to the ones specified from the relevant Standard, are the following:

  -Opening and closing operation feeding one terminal at the phase to earth voltage (see figure 3a). The voltage should not be removed between opening and closing operations. Two hundred cycles (O-C) should be performed. The voltages at both terminals of disconnector should be recorded during the operations, maximum DU and Ur determined. The value of the source side capacitance should be at least 15 times the value of the load side capacitance. The voltage should be applied at the terminal giving the maximum arcing time.

-Closing operation feeding one terminal with AC at phase to earth voltage and the other with DC of negative polarity at the peak value of the phase to earth voltage (1 p.u.) see figure 3b. One hundred closing operation should be performed in this conditions and one hundred operations should be performed inverting the supply of the two terminals. The voltages at both terminals of disconnector should be recorded, to measure the time of closing operation. The value of the AC side capacitance should be at least 15 times the value of the DC side capacitance.

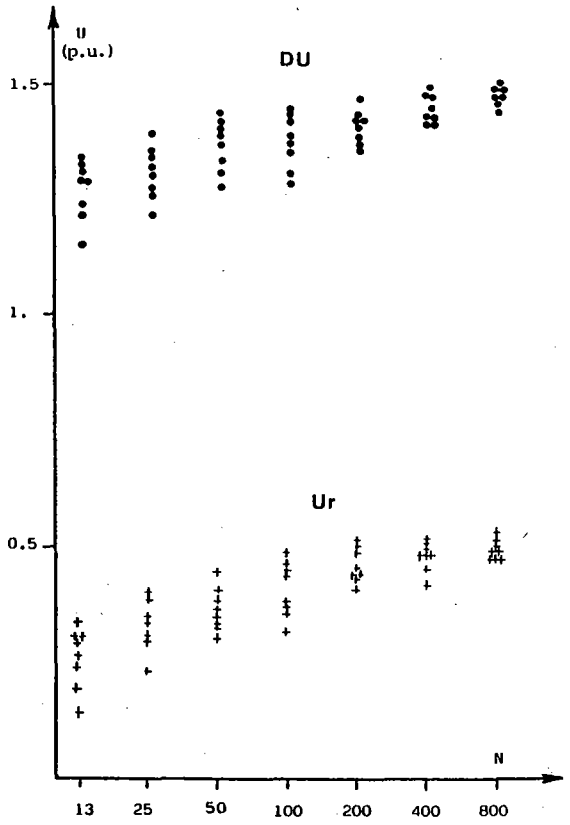

Figure 1: Maximum values of DU and Ur obtained by simulating 8 times groups of the given number N of disconnector operations.

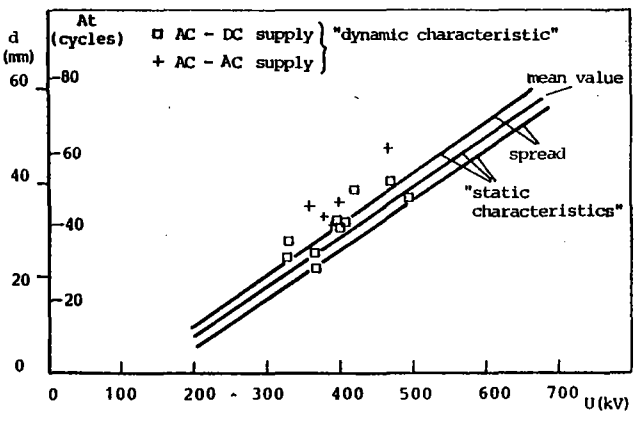

Figure 2: Maximum arcing distance when closing disconnectors as a function of the total strength between the contacts. The "dynamic" characteristic is compared with the "static" one.

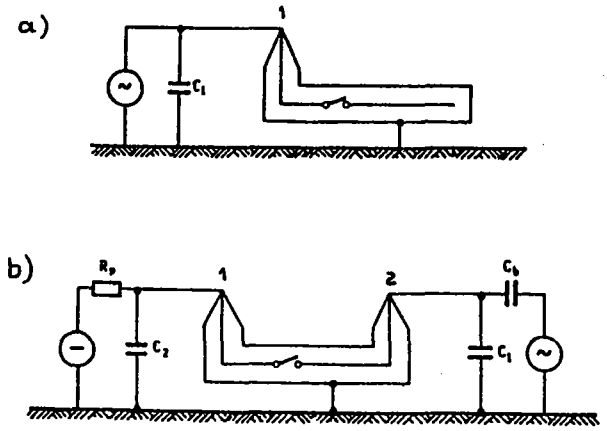

Figure 3:

Testing circuits proposed for additional tests on metal clad disconnectors: a) AC supply, b) AC-DC supply.

Mr. D. KÖNIG (Fed. Rep. of Germany)

This contribution deals with the switching behaviour of GIS-disconnectors. It aims to draw your attention to the circumstance that a GIS-disconnector should not only be regarded as a source for the generation of very fast transients but as a switching device characterized by a sophisticated interaction between the circuit elements and the load current arc, too. Depending on the time window under consideration load arc currents occur in the kA-range during the travelling wave stage and in the some A-range during the medium and the low frequency oscillation stage. Arc instabilities and the properties of the voltage source as an important part of the network are to be taken into account. In case of power transformers according to our findings at least one dominant resonant frequency in the some 10 kHz-range, i.e. in the medium frequency range exists.

Studies on this subject have been performed at the High Voltage Laboratory of the Technical University of Darmstadt since a couple of years /1-4/ and have been comprehended in a recently published thesis /5/.

Our studies aimed at first to establish a suitable simulation of the circuit conditions, including the peculiarity of the voltage source "power transformer" simulated with the help of the modal-analyze, and to investigate theoretically the characteristics of the relevant switching circuits by means of EMTP. Fig. 1 shows as an example one set of the obtained voltage and currents curves. From the latter one it is evident that an extinguishing of the arc can be expected only at current zeros. If reignitions will take place or not depends on the TRV and on the dielectric recovery strength of a gap with unblasted SF_6. Fig. 2 shows a measuring result of a making operation of a 123-kV-GIS-model-disconnecting switch with slow motion in the grid, demonstrating a multiple frequency transient load arc current flow with two reignitions, each after a short current zero interval.

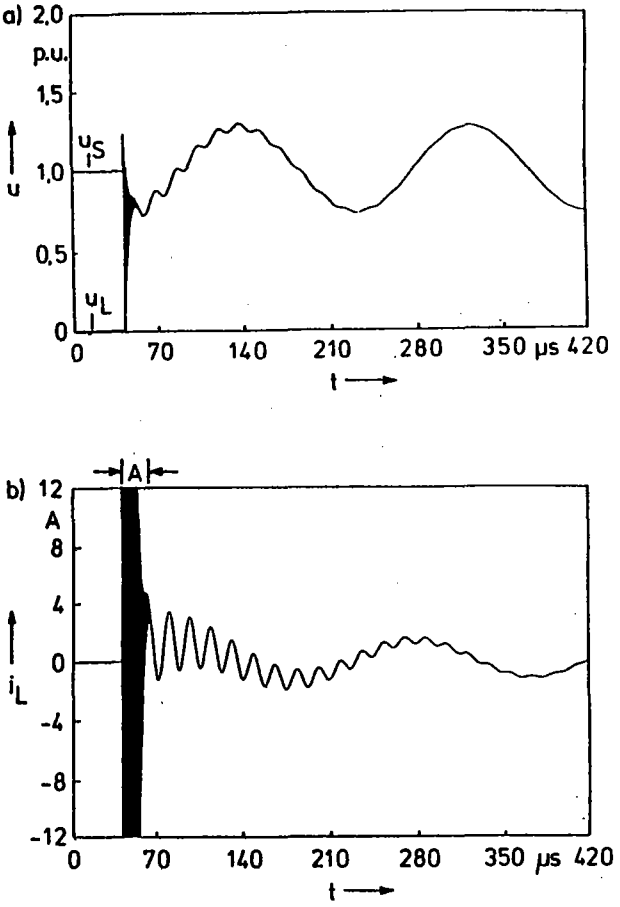

Fig. 1: EMTP-Simulation of a GIS-disconnector making operation:
High (time interval A), medium and low frequency transients in a three frequency circuit
u_s = source side voltage
u_r = load side voltage
i_r = load current

The second aim was to get more knowledge on the time dependence of the dielectric recovery strength of a prestressed unblasted SF_6-gap. A typical measuring result is shown in Fig 3.

The third aim of our studies was to design and to study synthetic test circuits, which allow to simulate the low and the medium frequency transients occuring under network conditions even in a laboratory. This work might be understood as a fundamental contribution to the impending standardization of switching test conditions of GIS-disconnectors by IEC.

References:

/1/ D. König, K.H. Fellmann: Beitrag zur Frage des Schaltverhaltens von metallgekapselten SF_6-isolierten Hochspannungstrennschaltern. etz-Archiv, Bd. 2 (1980), S. 161 -168

/2/ K.H. Fellmann: Untersuchungen zum kapazitiven Schaltverhalten von Trennschaltern in SF_6-isolierten metallgekapselten Schaltanlagen. Dissertation TH Darmstadt, 1983

/3/ D. König, G. Imgrund, J. Meppelink, D. Schlicht: Performance of GIS disconnectors under laboratory and network conditions. Gas-Insulated Substations - Technology and Practise, Ed. S.A. Boggs and coworkers, Pergamon Press Canada Ltd., 1986, pp. 75 - 85

/4/ D. König, G. Imgrund, C. Neumann, K. Maatz, L. Schiweck: Vorgänge beim Schalten kleiner kapazitiver Ströme mit SF_6-isolierten, metallgekapselten Trennschaltern im 110-kV-Netz und ihre Simulation im Hochspannungslaboratorium, Elektrizitätswirtschaft, Jg. 85 (1986), S. 131 - 138

/5/ G.Imgrund: Untersuchungen zum Schalt- und Löschverhalten SF_6-isolierter metallgekapselter Hochspannungstrennschalter im 110-kV-Energieversorgungsnetz und im Hochspannungslaboratorium. VDI-Fortschrittsberichte, Reihe 6/Nr. 219, VDI-Verlag GmbH, Düsseldorf (1988) (Dissertation TH Darmstadt, 1988)

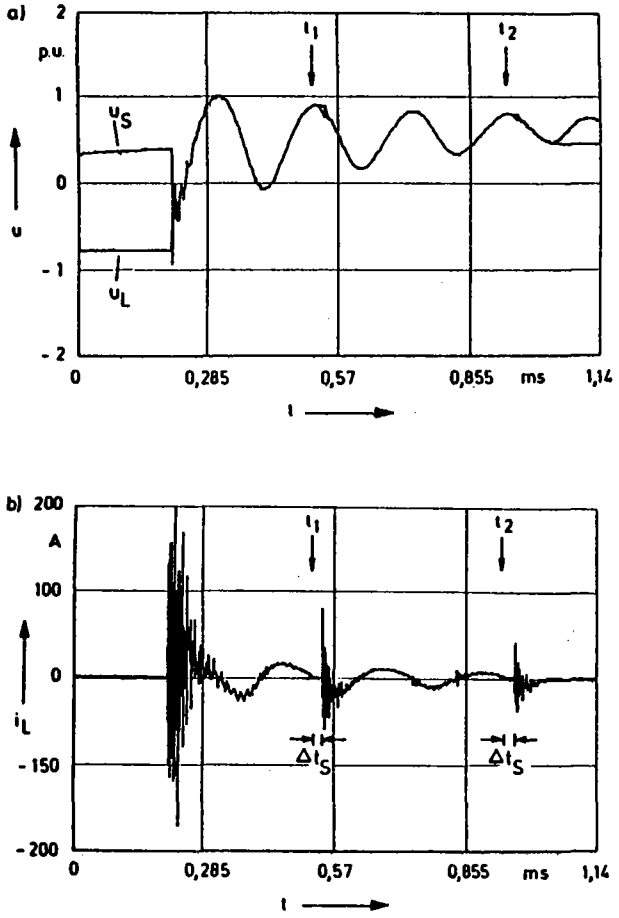

Fig. 2: Measurement of transients during a GIS-disconnector making operation in the grid (limited resolution of high frequency transients)
u_n = source side voltage
u_L = load side voltage
i_L = load current
t_1, t_2: instants of arc extinguishing
Δt : intervall without load current

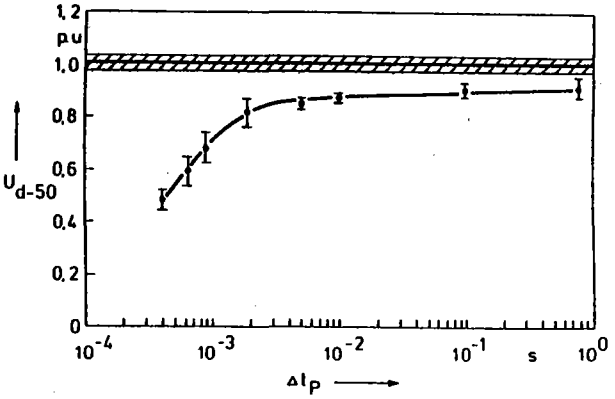

Fig. 3: Dielectric recovery strength of a SF_6-insulated rod-plan-test arrangement, stressed by double lightning impulse voltages
Δt_p = time intervall between the impulse voltage
1 p.u. = dielectric strength without prestress

Mr. N. FUJIMOTO (Canada)

In order to test the DS to characterize VFT overvoltages, a test should be performed which characterizes (statistically) the number and magnitude of the breakdown arcs which occur across the contacts. These are necessary to assess the distribution of VFT which occurs for that DS in a particular environment. A simple measurement of the "arcing pattern" or the variation in load side voltage during DS operation usually yields the necessary information by examining the voltage transitions in the recording. The source side voltage should be kept slightly higher than normal in order to extend the data to longer than normal contact separations. From these records, the variation in intercontact breakdown voltage as a function of time can also be determined, from which a model for DS operation can be developed. Such models are useful in investigations of DS and VFT behaviour in other situations such as for a different operating speed and for a slightly different operating voltage. These factors are discussed in paper 23-11.

Tests for DS withstand are necessarily different. Disconnectors are required to operate under a variety of conditions and disconnectors, depending on the design, operate differently. For instance, some DS are required to operate under phase opposition situations whereas others do not. Some disconnectors, as a result of a slow operating speed, might be prone to low probability failure events because of the many restrikes which occur. Rapidly operating DS generate few restrikes but with generally higher intercontact separations. As a result, the appropriate withstand test should be tailored to the required duty, the DS characteristics and its most likely mode of failure. A test for a slowly operating disconnector should address the statistical

aspect resulting from the large number of restrikes. This could be accomplished by a test involving a large number of restrikes or a test under more severe conditions to compensate for a reduced number of restrikes. With regard to a rapidly operating disconnector, a synthetic test involving a single intercontact arc under "worst case" conditions might be more appropriate.

1. Lalot, J. "On-Site Acoustic Detection of Abnormalities in Metal-Clad Substations." Proc. International Symposium on Gas-Insulated Substations, Technology and Practice, Toronto, 1985.

2. Fujimoto, N. and S.A. Boggs. "Characteristics of GIS disconnector-induced short risetime transients incident on externally connected power system components." Paper presented at the 1987 IEEE PES Winter Meeting (New Orleans), Paper 87WM185-2.

Mr. G. HATVANI (Hungary)

In Hungary we have in operation 420 kV outdoor SF_6 gas isolated metalclad equipment since the year of 1977. During operation of this, as early as the very beginning, the operators have experienced phenomena at switching actions of isolators - like sparks, noise effects, etc... - which were referring to the occurrence of potential differences between the grounded components. In the feeding circuits of the monitoring, controlling, and protective system non-explained trippings took also place at several times. Only as a result of a longer observation it could be found out, that these trippings always occurred at operations with disconnectors. The short-circuits, inducing these outages had a momentary character, and their places could be discovered only by systematic investigations, in general at device terminals.

The cladding is grounded cca. every 4 meters, and the length of the grounding leads are 2.5 to 5 meters, according to the height of the equipments. Due to these circumstances it was from the beginning clear, that these could have only been occurrences with shorter wavelengths than the dimensions of above, and so of very high frequencies. Investigations performed by oscilloscope and measuring spare-gaps revealed these transient potential rises to be damped oscillations with frequencies much more than 10 MHz, and amplitudes over 10 kilovolts, between certain grounded points.

During these investigations we also made attemps to find solution of the problem we had to control by all means, since this problem could eventually prevent the operation of the protection system. For the first time we endeavoured to modify the grounding system by increasing the number of the grounds, but a notable improvement was not achieved, as it could be envisaged by the constrained length of grounding leads. It seemed, the problem could have been settled at the existing equipments only by symptomatic treatment, by increasing the capacities in the system. To perform countermeasures, we developed a plan of several steps, consisting of the followings:

1) Every monitoring, and controlling cable on the equipment cladding must be replaced with shielded cable, and the shielding has to be connected to the cladding at both ends.

2) The non-live wires in the cables must be grounded at their ends, to increase the ground capacity, respectively to protective factor.

3) When this would not be enough, in the monitoring and controlling circuits, every endangered, weakly insulated points must be provided with condensers of cca. 10 nano-farads in capacity, connected between the wires, as well as between the wires and the ground (enclosure, or device compartment) very near the points exposed to danger.

According to the measurements and operating experiences the problem at the "weak" points has been settled by the items No. 1. and No. 2. for the monitoring and controlling cables, because the potential differences decreased from the original value of some kilovolts to a value of a few hundred volts, therefore there was no need more for the above mentioned condensers. Since that time the applied measures have become an integral part of our specifications for design and construction.

Mr. N. FUJIMOTO (Canada)

In principle, transient enclosure voltages (TEV - also referred to as Transient Ground Potential Rise, TGPR) are an extension of the internal VFT voltages. As a result, many of the characteristics, such as the risetime, frequencies, etc. are common and the same general approach to their calculation should be taken. However, with TEV, further considerations are necessary in addition to those for internal VFT. Internal fast transients are normally amenable to calculation because coaxial GIS, generally, forms an excellent distribution network for short risetime transients. Propagation losses are normally ignored and signal distortions usually come from impedance discontinuities, such as breakers, short bus sections, etc. Propagation external to the GIS is another matter. The propagation mode must consider eddy current losses in the ground and impedance discontinuities are more difficult to model. Measurements indicate that in an actual station, TEV signals attenuate at the rate of about 0.3 db/m [1]. Grounding straps, support structures, scaffolding will all influence the TEV voltage waveform. Although many of these can be approximated with transmission line sections, the development of the model can sometimes stretch the imagination. Such calculations are normally used for order-of-magnitude estimations and to assist in analysis of the phenomena and mitigation techniques [2]. TEV is, overall, a subset of the VFT phenomena in GIS. But, as a result of the different environment, modeling and calculation is corresponding more difficult than for internal transients.

1. Fujimoto, N., E.P. Dick, S.A. Boggs and G.L. Ford. "Transient ground potential rise in gas-insulated substations - Experimental studies." IEEE Trans. on PAS, *PAS-101*, No.10, October 1982.

2. Dick, E.P., N. Fujimoto, G.L. Ford and S. Harvey. "Transient ground potential rise in gas-insulated substations - Problem identification and mitigation." IEEE Trans. on PAS, *PAS-101*, No.10, October 1982.

Mr. R. MALEWSKI (Canada)

Among the measures of mitigation of the transient enclosure potential rise which have been indicated in the paper 33.13 by the WG 33/13-09, there was no mention of the resistive coating of the GIS outer surface near the bushing.

Although at present, there are no industrial applications of this technique, a laboratory investigation has confirmed its feasability. Essentially, the resistive coating of some 5mm thickness and a magnetic permeability of at least 100 is applied on the outer surface of the GIS enclosure tube in the section 1 to 1,5 m adjacent to the bushing flange. The travelling wave propagating between the outer surface of the GIS enclosure and the ground is attenuated by approximatively 2 orders of magnitude by this resistive coating.

15-00

PART OF SPECIAL REPORT FOR GROUP 15

(Insulating Materials)

by

C.W. REED*
(Special Reporter)

PREFERENTIAL SUBJECT 1

Preferential Subject 1 addresses a topic covered previously at the 1986 SC15 General Session, namely the performance of SF_6 gas when subjected to fast voltage transients. Two papers (Papers 15-05 and 15-06) addressed this topic directly and will therefore be discussed together.

Gas insulation (usually SF_6 gas) in metal-clad substations is subjected to a large variety of transient overvoltages, arising primarily from lightning strokes on overhead lines and the actuation (operation) of cut-off (disconnect) equipment. The latter (disconnect) operation produces a range of fast or very fast transients (VFT) which the SF_6 gas (with or without solid insulating spacer) must be able to withstand. A wide variety of such transients are produced, as traveling surges originate from the disconnect operation and are reflected by different GIS components. The shape and magnitude of the transients depends on GIS design and the overall system configuration.

The major components in the transients that can be identified include: transients with frequencies below some hundreds of kHz (— these are limited in amplitude and therefore not very detrimental); VFT with oscillation frequencies up to 50MHz, normally caused by surge development in the GIS (— these produce the largest overvoltages and are therefore of major practical importance); and oscillations with frequencies up to 200 MHz, caused by reflections between adjacent internal GIS components (— usually their magnitude is low). These different components superimpose upon one another as the disconnect operates; they are also superimposed on the applied ac or dc voltage.

Until now, such high frequency overvoltages have been accommodated by operating the GIS equipment with high overvoltage factors, determined from prior service experience. However, for EHV GIS equipment the safety margins are less and, in the future, it is anticipated that additional optimization of GIS design will take place. Hence, there is a strong interest in CIGRE and other organizations in understanding the nature and effect of VFT on the performance of SF_6 gas insulation.

Paper 15-05 covers an experimental investigation of steep leading edge and oscillating voltage waves on SF_6 performance in coaxial electrode geometries, relative to normal lightning impulse waves; the corresponding V-t curves are thus generated and discussed. Paper 15-06 is an up-date on a comprehensive research investigation of VFT in SF_6 gas, in coaxial geometries with and without solid spacers, and with and without deliberately-added field non-uniformities; the effects of VFT superimposed on ac and dc stresses are described and a model is presented involving discharge development under fast rising pulses, coupled with computer calculations, that enables many of the observed breakdown phenomena to be predicted.

Two test arrangements are used in Paper 15-05 involving a coaxial arrestor to represent the bus bar set in a metal-clad substation. The first test arrangement was used to generate oscillating waves with a 200ns leading edge; in the second arrangement, a preflashover gap was used in order to achieve fast transient waves with rise times of 20-90ns. Tests with these waveform were then compared against tests with reference lightning impulse waves (1.2/50 μs) in the same coaxial electrode system. With the second test configuration, additional tests were conducted with a deliberately-added needle protruding 5mm from the center electrode. (The needle protrusion, which produces a significant localized field non-uniformity, is variously referred to as a "peak type fault," "form fault," or "superficial fault.") A nice account is provided of the circuitry and precautions needed to measure the applied waveforms and the corresponding breakdown voltages. The breakdown waveforms were then transformed to V-t curves (using IEC Standard 60.2); such data are presented for both positive and negative waveforms over the time range 20ns to 1 μs.

As found by other investigators of this region of breakdown in SF_6 gas (e.g. Paper 15-06), Paper 15-05 finds that the V-t curve increases continuously as the wave front duration decreases. The presence of the added needle causes the V-t curve to drop significantly but its shape stays basically unaltered, leading the authors to conclude that steep leading edge waves have comparable sensitivity to electrode field enhancement to that of lightning waves. As normally found with non-uniform field breakdown in SF_6 gas, breakdown is significantly less with posi-

*GENERAL ELECTRIC COMPANY, CORPORATE RESEARCH & DEVELOPMENT, PO BOX 8, SCHENECTADY NY 12301, UNITED STATES

tive polarity than with negative polarity. The authors cautiously conclude that their results need confirmation on industrial equipment and that there is a need to take into account steep leading edge waves in decisions on future on-site testing of HV metal-clad equipment.

Paper 15-06 provides an up-date on research activities described in Paper 15-07 at the 1986 CIGRE Session but now extended to include work at four separate laboratories (two in the Federal Republic of Germany, one in Italy, and one in Switzerland). As in the previous paper, this is concerned with the breakdown of SF_6 gas due to VFT waveforms in coaxial electrode geometries (a common GIS component) with and without solid insulators, and with and without a deliberately-added field inhomogeneity—a metallic needle attached to the inner electrode. V-t curves are generated and used to assess performance. Many of the details of their experimental set ups and the results of preliminary investigations associated with this work have been described elsewhere and should be examined if possible. Focus of the present paper is on a very perceptive analysis of past and present data, some by other researchers, and a mechanistic treatment of several aspects of VFT breakdown in SF_6 gas. In the absence of a prestress, the VFT breakdowns in SF_6 gas with or without spacers show very similar withstand levels to those obtained with lightning impulse waves, though in a defect-free system they are always distinctly higher. With deliberately-added defects (10mm needle), not only are the V-t curves lowered (as was also found to be the case in Paper 15-05), but the data indicate that the withstand strength is lower for VFT than for lightning impulses. (There was no indication of a similar lower VFT withstand with (5mm) needle protrusions on the inner electrode in Paper 15-05; hence it will be of interest at the 1988 General Session to try to establish the reason for this difference.)

When VFT are superimposed on dc stresses, a large reduction in breakdown occurs, which is considered to be largely due to the presence of particles; the behavior is very similar to that seen with lightning impulse waves. Interestingly, in the absence of particles, solid insulating spacers did not cause a reduction in VFT strength. Similar effects were not present with ac stresses unless very large particles were present.

Two other topics are also included in Paper 15-06: a problem caused by VFT in SF_6 gas caused by the generation of potential differences between different locations connected electrically—the potential differences give rise to "sparking" discharges which have no affect upon the V-t behavior but can cause damage to adjacent insulating materials; and a discussion of how discharge development caused by VFT affects GIS breakdown for both positive and negative polarities. The latter discussion outlines the underlying physical phenomena and shows how computerized breakdown models, coupled with experimental observations, can be used to rationalize why the minimum breakdown voltages with VFT stresses will be greater than or equal to those with lightning impulses or step pulse stresses. Paper 15-06 concludes by stressing that its purpose is to help to explain many of the technical features of VFT behavior. With these two interesting papers, the stage appears to be set for a detailed discussion of VFT effects at the 1988 CIGRE Session, including their relevance to equipment performance and testing procedures.

Question 1. Can additional results on VFT behavior in SF_6 gas insulated structures by the authors of the two papers or by other experts be given? Have results been attained which differ from those discussed? Are there data available on the effect of deliberately-added particles (effect of length, shape, and position) that shed light on the differences in V-t curves with field inhomogeneties found in Papers 15-05 and 15-06?

Question 2. In view of the generally superior performance of VFT noted in both Paper 15-05 and 15-06 (i.e. the higher withstand voltage compared to lightning impulse waveform) is there any need for VFT testing on equipment in addition to normal lightning impulse tests? If so, will the purpose of VFT tests mainly be for quality control; for example, to identify unwanted/unexpected field inhomogeneties?

Question 3. Do experts have additional contributions on the model for discharge development and streamer and leader formation in SF_6 gas subjected to VFT voltages, described in Paper 15-06 or on the computer model for breakdown? Are there alternative models which should be considered? Can the authors up-date us on further refinements of their model or its application?

International Conference on Large High Voltage Electric Systems

112, boulevard Haussmann — 75008 Paris

1988 Session — 28th August - 3rd September

O

15-06

Pref. Subj. 1

RECENT RESEARCH ACTIVITY ON THE DIELECTRIC PERFORMANCE OF SF_6, WITH SPECIAL REFERENCE TO VERY FAST TRANSIENTS

Paper presented on request of the Chairman of Study Committee 15, Th. Praehauser

by

G. LUXA*, E. KYNAST
Siemens AG

W. BOECK, H. HIESINGER
Technical University of Munich

A. PIGINI, A. BARGIGIA
CESI ENEL

S. SCHLICHT, N. WIEGART, L. ULLRICH
Brown, Boveri Ltd.

Summary

The report presents recent research activities on the dielectric performance of SF6 with special reference to very fast transients (VFT). The transients caused by switching operations in Gas Insulated Substations (GIS) are considered and the insulation behaviour with and without solid insulation is described. Special attention is paid to composite stresses: transients superimposed to AC- and DC-voltages. The effects of the transient potential rises on shielding elements are shown. A theory of physical discharge development is described and applied to the VFT breakdown phenomena.

Keywords

SF6 - very fast transients - GIS - disconnector - vt-curve - sparking - composite stress - discharge development

1. Introduction

During switching capacitive currents by disconnectors many strikes occur and the voltage across the disconnector gap collapses within a few nanoseconds. The actual time value depends on the disconnector design, the instantaneous gap distance and the gas pressure. Due to the subsequent travelling surges originating from the disconnector and their reflections at different GIS components, a multitude of transient phenomena is generated. The shape and amplitude of these transients depend on the GIS design and on the overall system configuration.

Among the overvoltages generated various components can be distinguished. Overall transients with frequencies below some hundreds of kHz are normally caused by oscillations of the whole system consisting of the GIS and connected adjoining apparatus, e.g. transformers. Their amplitude is generally rather limited and does not usually determine the insulation design.

Very fast transients, with oscillation frequencies extending up to 50 MHz, normally due to the surge development within the GIS, are superimposed to overall transients. They constitute the most important component of the overvoltage and play a fundamental role for insulation design.

Further oscillations with frequencies up to 200 MHz, caused by reflections between adjacent internal GIS components are superimposed to VFT. Usually their amplitude is comparatively low.

It has to be considered that all mentioned overvoltages are normally superimposed to AC or DC voltages. Details of the previously mentioned overvoltages about their magnitudes and effect on various GIS components are given in [1].

The rated withstand voltages specified for GIS belonging to HV and to the lower range of EHV consider high overvoltage factors. This is in agreement with the service experience of more than 20 years, which has proved the reliability of well designed GIS. For GIS belonging to the upper range of EHV, a larger attention should be paid to these stresses, due to the reduced safety margin involved in the specified withstand levels, and especially taking into account the present trend to optimize GIS design.

In the following, main attention will be paid to the dielectric strength under the above mentioned overvoltages with the aim to indicate the present state of the art and the needs for further research activity.

* SIEMENS AG, Schaltwerk Hochspannung, Nonnendammallee 104-107, 1000 BERLIN 13

2. Insulation behaviour of SF6 with and without solid insulation

The results with VFT are still rather limited. Most of the results in literature refer to lightning impulse (LI). Nevertheless some typical features of VFT breakdown in comparison to lightning impulse breakdown can be explained.

2.1 Insulation behaviour of the correct insulation system

In a correct insulation system of common GIS designs a weakly inhomogeneous field distribution is given. The most common GIS components are coaxial electrode arrangements with and without spacers. For such components extensive laboratory tests have been made. The results can be considered as representative for the typical insulation of a correct insulation system.

Regarding the gas first, the typical breakdown development for positive and negative polarity is shown in Fig. 1. In case of positive polarity the breakdown normally occurs in the initial steep front. It can be considered as a pure streamer breakdown with an extremely short formation time for the breakdown channel. The resulting breakdown delay time is therefore extremely short, the corresponding VFT voltage-time characteristic is very flat (Fig. 2). Depending on the design and the VFT shape the minimum values of VFT are 10 to 20% above [2,3] or close to the LI withstand level [4,5].

In case of negative polarity breakdown develops after longer formative time lags. As a consequence low probability VFT breakdowns occur up to some hundred nanoseconds delayed on the subsequent oscillation. Therefore, there is a distinctly up-turning trend of the corresponding voltage-time curve (Fig. 2) with higher breakdown values [5], sloping down to a minimum value close to that of positive polarity. In any case the very short time to breakdown leads to an extremely high scatter [2,3,6].

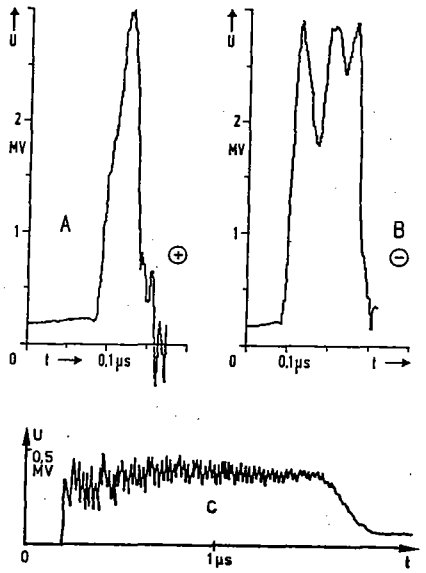

Fig. 1 Typical VFT breakdown development for positive (A, positive type front VFT breakdown) and negative (B, negative type tail VFT breakdown) polarity in case of a correct insulation system and VFT breakdown development of an insulating system with a long needle shaped protrusion (C).

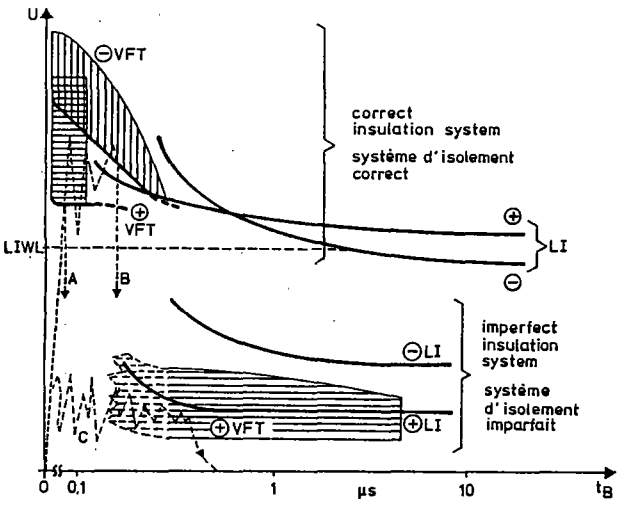

Fig. 2 Voltage-time characteristic for LI (lower boundaries) and VFT overvoltages (range of results) for a correct (see chapter 2.1) and an imperfect (see chapter 2.2) GIS insulation system. The voltage curves A, B, C are related on Fig. 1.

For comparison in Fig. 2 the principal patterns of the voltage time characteristics for normal LI are additionally shown with the well known less pronounced up-turning trend and lower breakdown values in the long time range for negative polarity [3,6,7,8]. Therefore, for VFT and steep LI the positive polarity has to be considered as more critical, whereas for standard LI and SI the negative polarity is decisive.

In case of spacer flashover the up-turning trend in the short time range is considerably reduced in case of LI. This is caused by a reduction of the formative time lag due to a promoted breakdown channel development caused by insulation surface effects. Some laboratory tests have shown that such an effect seems not to be given in case of VFT breakdown at least for the spacer tested. Mainly the field distortion by the spacer and its electrodes for mounting and field grading is important. The spacer of Fig. 3 with its special mounting devices is an especially suitable example to prove these characteristic properties. In Fig. 4 the test results are compiled for the gas breakdown and the spacer flashover.

The spacer (Fig. 3) was tested in the same coaxial cylinders of 520/150 mm diameter of the GIS bus in which the pure gas was tested. At the inner conductor the maximum field strength in the gas is not enhanced by the spacer. This is achieved by a field grading electrode embedded in epoxy resin in region A. At the external electrode the maximum field is enhanced by the mounting

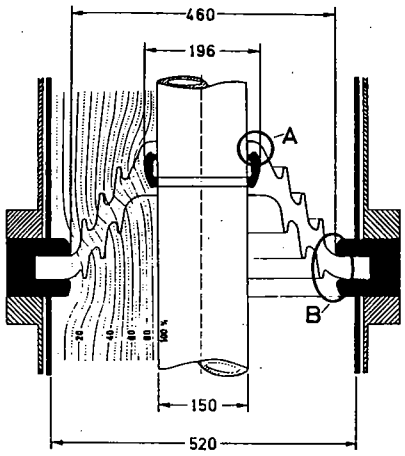

Fig. 3 Tested gas insulated coaxial system with spacer

ring in region B resulting in a maximum field above that at the inner conductor (about 15%). Regarding LI first, the lower boundary of the voltage-time curves in the long time range - marked by the broken lines - for positive polarity exceeds that for negative polarity as proved by comparison of Fig. 4a and 4b. Due to the effect of the grading electrode in region A (Fig. 3) almost the same lower boundary is given in Fig. 4b and 4d. In Fig. 4c the field enhancement at the external mounting ring in region B with critical negative polarity results in a decreased lower boundary of the voltage-time curve with respect to Fig. 4d. Furthermore 4c and 4d show in comparison to 4a and 4b the characteristic reduction of the up-turning trend in case of spacer flashover.

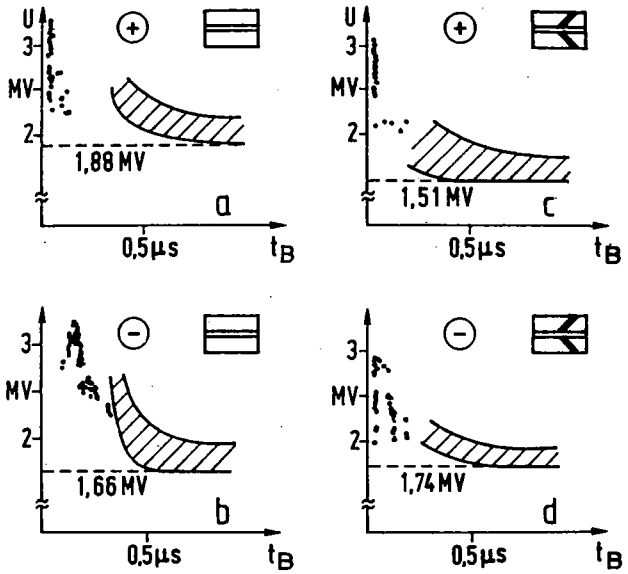

Fig. 4 Breakdown behaviour of the coaxial system of Fig. 3 without (a,b) and with (c,d) spacer for positive (a,c) and negative (b,d) polarity (SF6 pressure 0.3 MPa).
Matched curves: vt-characteristic for LI (0.4/50)
Dots: VFT breakdowns (Front time 50 ns, oscillation frequency 10 MHz)

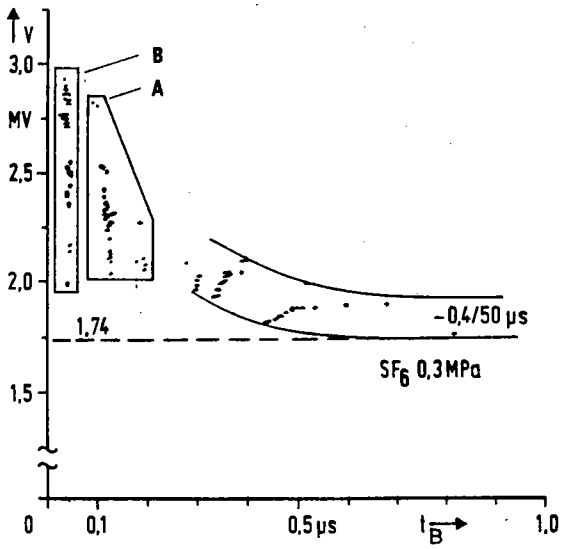

Fig. 5 Breakdown behaviour of the coaxial system of Fig. 3 with spacer and negative polarity at the inner conductor according Fig. 4d
A - Negative type tail VFT breakdown originating from region A of the spacer or the inner conductor
B - Positive type front VFT breakdowns originating from region B of the spacer

Regarding the VFT breakdown results the generally given big scatter range and in case of pure gas the extremely short time to breakdown for positive polarity (Fig. 4a) and the up-turning trend of the lower boundary of the voltage-time characteristic for negative polarity (Fig. 4b), both with minimum values can be easily recognized. In case of spacer flashover and positive polarity shown in 4c most breakdowns are originating from the inner conductor due to the extremely short formative time lag for positive polarity even if the maximum field at the external negative mounting ring is slightly higher. Only the delayed breakdowns seem to be caused by the negative external mounting ring. In case of spacer flashover and negative polarity (Fig. 4d) in a similar way some breakdowns are originating at the positive external mounting ring some are originating from the inner negative conductor. As shown in Fig. 5 these different types of flashover values can easily be separated. Due to the higher field at the external mounting ring the minimum VFT breakdown value in Fig. 4d is below that of 4c.

As indicated by this example the VFT insulation behaviour seems to be mainly influenced by the maximum field in the gas and the belonging electrode polarity even in case of spacer flashover.

2.2 Insulation behaviour of an imperfect insulation system

Regarding extremely inhomogeneous fields caused by irregularities of the insulation system, like needle shaped protrusions, the VFT breakdown values are considerably reduced in accordance with the downturning trend of the corresponding voltage-time

characteristic for increasing front steepness (Fig. 6). The upper curves represent the test results for both polarities under correct conditions. The lower curves show the test results of the bus duct section with a 10 mm needle in a corner of the center conductor. The latter voltage time characteristics have the opposite slope to those of the correct arrangement, and the positive polarity is lower than the negative, which is the opposite of the behaviour of the correct arrangement [9,10,34,35]. Both effects are mainly caused by the decreasing corona stabilization and changing leader inception conditions. Details of the mechanism are given in chapter 5.

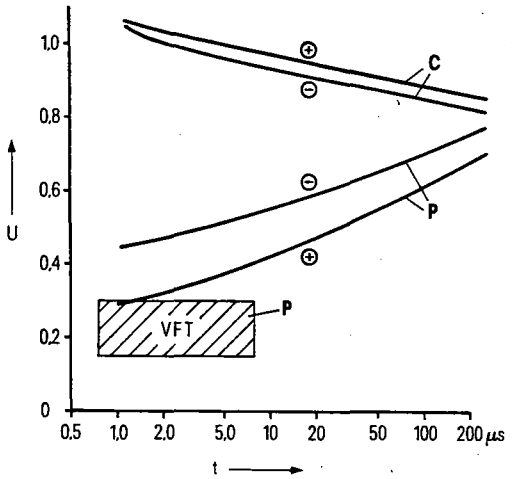

Fig. 6 Relative voltage U versus time to crest or to breakdown t
Impulse withstand voltages for various shapes
C - in a correct insulation system
P - with needle shaped protrusion
VFT - Range of VFT-breakdown voltages versus time to breakdown, caused by disconnector operation due to needle shaped protrusion (oscillation frequency 40 MHz)

In the short time range (Fig. 2) the up-turning trend of the LI voltage-time curve is caused by the formation time for the leader development and the resulting breakdown delay.

Theoretically such an up-turning trend must exist for VFT voltage too, but it could not be experimentally proved. Due to the rare results the corresponding VFT voltage time characteristic can only be roughly indicated (Fig. 2; 6). The breakdowns occur late on the oscillating tail (Fig. 1C) with a big scatter. The positive breakdown values are somewhat lower than those for negative polarity. Due to the big scatter the breakdown probability is very low for low VFT amplitudes and increases with the oscillation frequency and the degree of the field inhomogeneity. For 40 MHz and a needle length of 10 mm a breakdown probability of 1% had been found during disconnector switching operation at rated service voltage in a 420 kV GIS which was successfully tested beforehand with oscillating switching impulse of 100% switching impulse withstand level [3]. Such VFT breakdowns had been observed very rarely and only in the neighbourhood of disconnectors, where the breakdown level is extremely reduced by high VFT oscillation frequencies for 40 MHz and more [11,12,13]. A similar but much less pronounced decrease of the breakdown voltage has to be expected for more conceivable irregularities like particles and edges with lower field distortion effects.

3. Behaviour of GIS-components under impulses superimposed to AC and DC voltages

Superposition of overvoltages and AC voltage is a very typical stress condition for GIS-components intended for AC application. Overvoltages superimposed to a DC voltage are to be considered as typical stress conditions when DC applications are considered. This stress condition may occur also for GIS for AC application, due to operation of disconnectors.

When switching on/off busbar sections of a GIS by disconnectors, the operation occurs through several restrikes, leading to 'fast' overvoltages. Furthermore after opening, a DC voltage (due to residual charge) is left on the open side [1,14,15, 16]. Consequently when closing the disconnector, the stress to ground, on the load

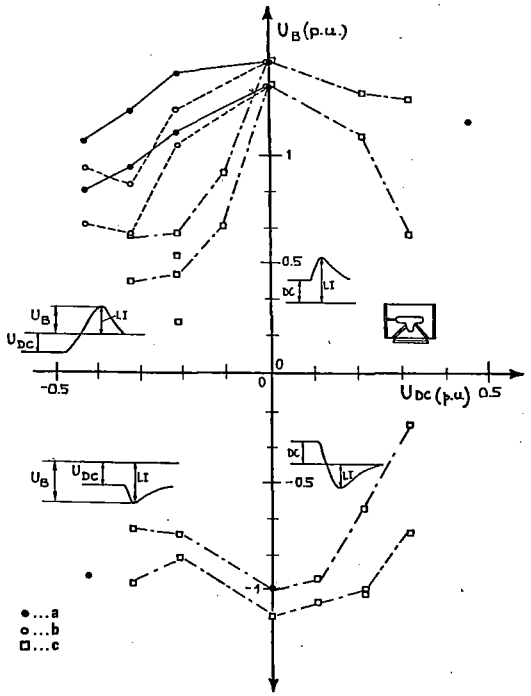

Fig. 7 Tests with composite stresses (LI+DC). Breakdown voltage (total voltage to ground at breakdown), versus the value of the applied DC component
(1 p.u.: minimum observed breakdown voltage under negative LI without DC prestress)
a - Clean condition with preconditioning
b - Clean condition without preconditioning
c - with particles without preconditioning
1g weight, 0.5mm max. length, aluminium

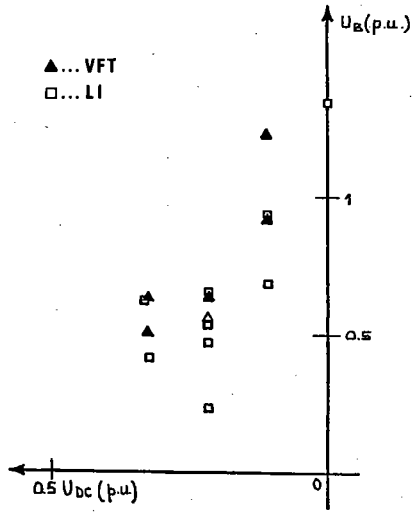

Fig. 8 Tests with composite stresses. Breakdown voltage with VFT (total voltage to ground at breakdown) versus the value of the applied DC component. Comparison with results obtained with LI
(1 p.u.: minimum observed breakdown voltage under negative LI without DC prestress)

side, is characterized by a fast transient superimposed to a residual DC prestress applied for a relatively long time.

The performance of SF6 insulated components under overvoltages superimposed on AC and DC voltages was widely investigated [17,18, 19,20,21,22,23].

Taking care of the investigations performed the following indications may be derived:

- Large reduction of the impulse strength may be caused by the presence of the DC prestress. Important reductions were observed only in the condition of DC and impulse having opposite polarity. Similar reductions were not observed with AC prestress unless very large particles were involved [22,23].

- Large reductions of the strength are not directly caused by the presence of spacers, as shown by tests with and without spacers in extremely clean conditions [17]. They are mainly related to the presence of free particles, as shown by tests with different degrees of contamination (Fig. 7) [18].

- The reduction is present for all impulse types: SI, LI, and VFT. Particular tests have shown that the strength under VFT may be well represented by that with LI, also in presence of a DC prestress (Fig. 8) [18].

- Tests have been repeatedly made on GIS configurations in 'industrial clean conditions', after having verified the absence of partial discharges, the compliance of the withstand levels with IEC specifications and after suitable conditioning. The reduction of the strength with a DC prestress was found very spread, ranging from negligible to very high values, and the results are poorly repeatable. Again it is thought that the reduction is caused by small particles, which may not be fully avoided, and their presence may not even be checked by usual dielectric and partial discharge tests.

- The influence of the DC prestress on the dielectric strength was found for GIS of various types and manufacturers [19].

- The influence of the DC prestress seems to increase for higher gas pressure, as expected for a field enhancement type effect [19], as shown in the example of Fig. 9.

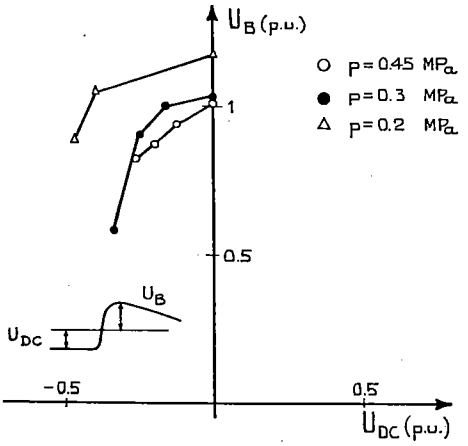

Fig. 9 Tests with composite stresses (LI+DC). Minimum observed breakdown voltage (total voltage to ground at breakdown) obtained after a large number of tests repetitions, versus the value of the applied DC component
(1 p.u.: minimum observed breakdown voltage under negative LI without DC prestress at the examined pressure)

As far as consequences for design are concerned, only the stress condition related to switching of capacitive currents will be examined in the following; by the way this is a good example about the critical stress. In particular the characteristics in Fig. 10 are considered which report the lowest curves measured with composite voltages of the type LI + DC on 'industrial clean conditions'. They are taken, as a first approach, as representative of all GIS configurations. In particular, in Fig. 10, a comparison is made between the strength under LI (representing also VFT) and the stress (amplitude of the overvoltages reported versus the pre-existing DC component value) measured during switching of capacitive current tests (closing operations). Tests of this type were performed on various GIS, with many testing arrangements: in the figure only examples of the results obtained on some test conditions are given. The figure suggests that the flashovers observed during switching operations with overvoltage values lower than the expected strength with LI only, may be well accounted for the strength characteristic under composite voltages. On the other hand the coexistence of flashover and withstand cases above the reference strength characteristic confirms the spread

of the strength under the considered overvoltages. As a conclusion the strength under composite voltage of the type VFT+DC is very important in design and may constitute a limit when thinking of compact solutions.

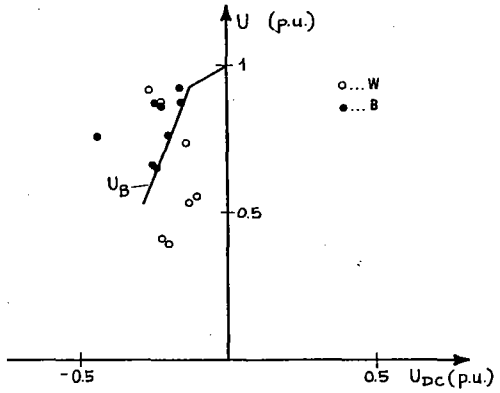

Fig. 10 References characteristic for LI+DC composite voltage (representing also FT+DC). Comparison with possible stresses measured on actual GIS when disconnecting capacitive currents (closing operations) (1 p.u.: minimum observed breakdown voltage under negative LI without DC prestress)
W - Withstand cases
B - Breakdown cases

4. Influence of transient potential rises on conductor connections to shielding elements

The well known effects of VFT are the increased stress of the insulation to ground, the transient potential rise of ground systems and the influence on measuring and control cables. Beside these there are effects inside of the GIS components, which can lead to problems when they are neglected during the design stage.

Transients can lead to potential differences between parts, which are conductively connected together. For sufficiently high frequencies and peak values, discharges can be observed between the parts. In the following these discharges will be described as sparking. Similar effects occur when the electrical contact between shielding parts is not sufficient.

4.1 Sparking between shielding elements

During development tests of several GIS types [14,24] phenomena like these were observed between parts as well on the high-voltage side as on the grounded side inside the housings.

An obvious example for sparking geometry is a shielding sleeve which is connected to the conductor mechanically and electrically on one side only (Fig. 11). The sparking occurs in the small gap between the conductor and the not connected open end of the sleeve. The current of the travelling surge is - due to the high frequency character - restricted to the surface of conductor and sleeve. Following the surfaces, along the inner diameter of the sleeve and the small conductor inside of the sleeve, the inductivity of the loop and the steepness of the current determine the voltage across the gap. Exceeding the insulating strength of the gap, it is bridged by discharges. The dependency of sparking on the area of the current loop was proved by varying the diameter of the inner conductor and the length of the configuration.

The arrangement of the gaps under sufficiently high frequencies may be treated like a three electrode problem similar to the configuration in a disconnector. But the leader breakdown mechanism of the disconnector gap cannot be transferred to this kind of gap because the gap width is only in the range of one millimeter. For this distances leader development is not possible. Streamer development initiated by the corona at the most inhomogeneous point is more likely the breakdown mechanism of the small gaps. Breakdowns to the earthed housing by sparking can be excluded for this arrangements because leader development and branching are not possible.

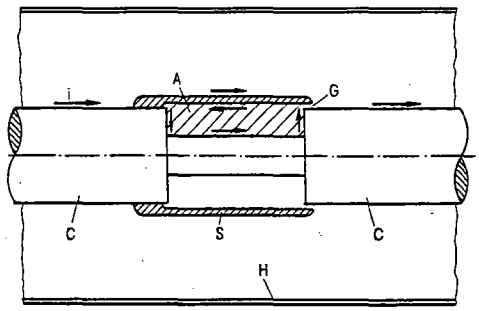

Fig. 11 Example for sparking effects inside the housing (H) of GIS:
Gap (G) between conductor (C) and open end of the sleeve (S)
A - Area determing the voltage across the gap
i - current path on the surface of conductor and sleeve

This fact was shown in a test configuration which is extremly 'bad' in comparison to normal GIS design: Two sleeves standing against each other with the gap at the outer diameter so that the sparks are not covered by a sleeve (Fig. 12). With a gap of 1 mm sparking began during switching operation at 80% of the system power-frequency voltage to ground of a 420 kV system. Up to 200% no flashover occurred.

Sparking phenomena can also occur at the grounded parts inside of the GIS. An example is the insulating gap in the shielding electrode of current transformers, which is necessary for avoiding current loops around the cores. The voltages to ground for tests concerning capacitive switching of disconnectors were increased up to two times the normal service voltage with high-frequency overvoltage factors in the range of 1.5 to 2.0 times of the peak value of test voltage. No triggering effect of the sparking was observed.

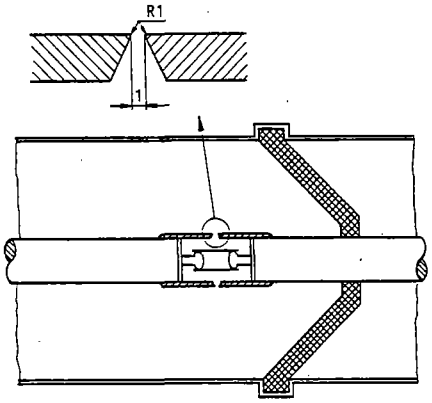

Fig. 12 Test arrangement with 'badly' designed shielding sleeves to investigate the triggering effect of sparking

4.2 Effect on solid insulation and conductors

Although the sparking does not trigger flashovers between conductor and housing it should not be neglected, especially if the gap is filled with or built by solid insulating material. In this case the material can be damaged or even completely destroyed by the sparking, so that it cannot fulfill its mechanical or electrical purpose anymore. Furthermore for unfortunate choices of the materials it is possible that it burns off and produces soot which can reduce the insulating strength of spacers.

It is not always possible to renounce of solid insulation in the gaps and sparking cannot be avoided. Therefore in any case the design of the gaps is important. The dielectrically weakest point between the shielding parts should be a pure gas gap as a protection gap for the solid insulation.

Each discharge in a gas gap leads to melting and vapourisation of a small amount of conductor material. But due to the small energy this will not lead to problems.

Sparking effects seem to be more important at badly mounted or even badly designed electrical connections, for example springs with unsufficient contact pressure. The contact points can melt and the connection becomes worse. Because the melting points of aluminium do not weld together, the parts may have not contact any longer. This leads to partial discharges already at power-frequency voltage and further destruction by erosion. To avoid this, a sufficient number of solid electrical connections are necessary, depending on the geometry of the parts.

5. Discharge development in SF6: Corona development, streamer and leader formation

5.1 Survey of discharge phenomena in SF6

In the past the discussion of VFT in GIS has been focused mainly on the origin and numerical modelling of transient overvoltages. Also numerous experimental investigations have been devoted to the effects of transients on the dielectric performance of GIS, but comparatively little effort has been made to understand the underlying physical effects although such an approach is likely to enable a systematic assessment of the role of VFT in GIS reliability.

Recently considerable progress has been achieved in the fundamental knowledge of discharge phenomena in SF6. In fact it is now possible to compute breakdown voltages in arbitrary geometries under almost arbitrary voltage waveforms for both positive and negative polarity. Not only does the numerical model serve as a valuable design tool, but also can it help to assess testing efficiency or to predict GIS performance under VFT.

In the following, the sequence of events in discharge development (in non-uniform fields) is briefly sketched out for different time regimes: As mentioned above (Fig. 2; 6), the most striking effect of

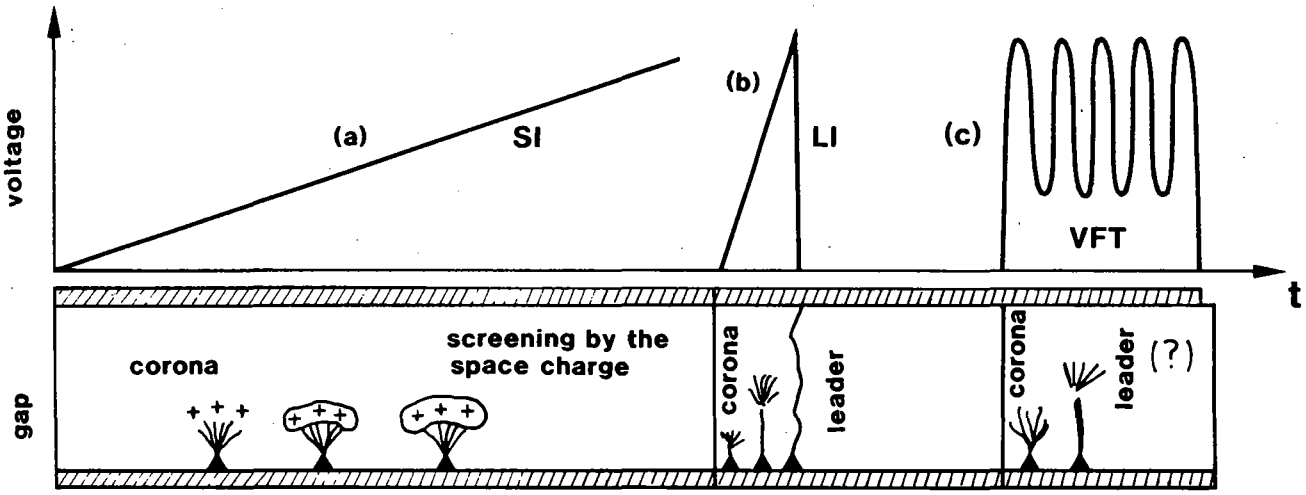

Fig. 13 Qualitative picture of discharge development under a: slowly rising voltage (e.g. SI); b: fast rising voltage (e.g. LI); c: VFT

different rise times can be found in the case of irregularities in a GIS associated with strong field inhomegeneity. Fig. 13 (a;b) elucidates the picture that has been developed: At rise times greater than about 10 µs ion drift induced corona stabilization becomes important. After a corona has been launched at roughly the streamer inception voltage, ions have sufficient time to leave the corona region before the minimum leader inception voltage is exceeded (Fig. 13a). The space charge thus built up by a series of corona discharges will reduce the field at the electrode. Leader inception level and breakdown voltage are thus raised compared to cases where characteristic ion drift times are much longer than the voltage rise time (e.g. under LI stress, Fig. 13b).

It also becomes clear that in correct condition of the insulating system, i.e. under quasi-uniform field conditions, the ion screening is of negligible influence: the corona inception level equals the breakdown level, i.e. when the corona is launched, the leader inception condition is fulfilled simultaneously, and the streamer to leader transition takes place before ion drift can distort the field.

Under VFT conditions, the picture is completely different. The gap voltage and the electric field may change in very short times compared to characteristic times of discharge development (Fig. 13c), leading to substantial changes of the withstand capability. For a discussion of these additional effects, the statistical delay time, the corona formation time, the leader stepping time, and the time to breakdown in relation to the oscillation period and the total duration of the VFT have to be considered.

To achieve a profound understanding of the relevant physical mechanisms, an approach has been used where the phenomena involved were investigated separately. As a first step, SF6 breakdown in different inhomogeneous geometries under unipolar step pulses was investigated for positive and negative polarity. The resulting numerical model allows the prediction of breakdown voltage as a function of pressure for arbitrary geometries with an error of less than 10% for step and lightning pulses [25,26,27]. Research efforts now focus on effects of fast transient over-voltages, with some important results being already available. Finally, to refine the modelling of leader branching behaviour, theoretical studies have been carried out [28].

A problem of great practical importance is to understand the mechanism of flashover to ground in a disconnector during switching operation. After it had become clear that the radial flashover is a consequence of the leader branching during the preceding axial strikes [29,36], (Fig. 14), the theoretical modellings can be applied very successfully. This is also valid for the sparking between busbar and shielding sleeve (chapter 4.1) or the case of irregularities occurring in GIS like e.g. needle shaped protrusions (chapter 2.2).

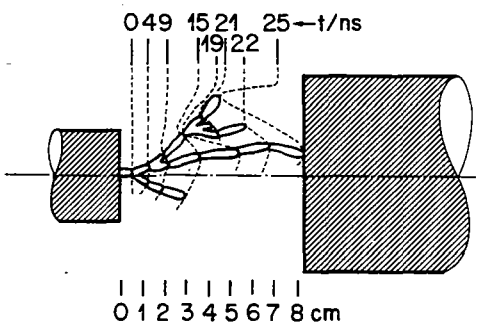

Fig. 14 Spatio-temporal development of the axial discharge in a disconnector reconstructed from streak and still photographs [5]

5.2 Discharge development under fast rising step pulses

The process following the production of an initial electron is the development of a streamer corona. Note that there is no 'streamer guiding field' in SF6. Due to the strong electronegativity SF6 streamers always require an average applied field equal to the critical field 89 kV/(mm*MPa).

Above a certain voltage, streamer to leader transition can occur involving a novel phenomenon, for which the term 'leader precursor' has been coined [30]. Fig. 15 gives an impression of the stepped propagation of a leader in SF6. Voltage and current are displayed on the same time scale. After the corona expansion has stopped, a dark period is followed by renewed ionization activity ('precursor') at the corona boundary. Once the channel is connected to the anode, a new corona is generated further into the gap, which coincides with a significantly reduced voltage drop along the channel ('leader'). The same sequence of events is observed in the subsequent leader steps, but with additional reilluminations of the leader channel in between steps.

Breakdown voltages and probabilities can be predicted with a computer model of breakdown [25,27], consisting mainly of four parts: a modified volume-time law (initiatory electron production [31,32]), the critical field concept for corona extension and corona charge, a critical charge criterion for leader inception derived from precursor theory and a leader channel modelling [33], which supplies the leader voltage drop. Breakdown voltages can be predicted to within about 10% for arbitrary electrode configurations with inhomogeneous fields under both polarities. A comparison between experimental and theoretical data is given in Fig. 16.

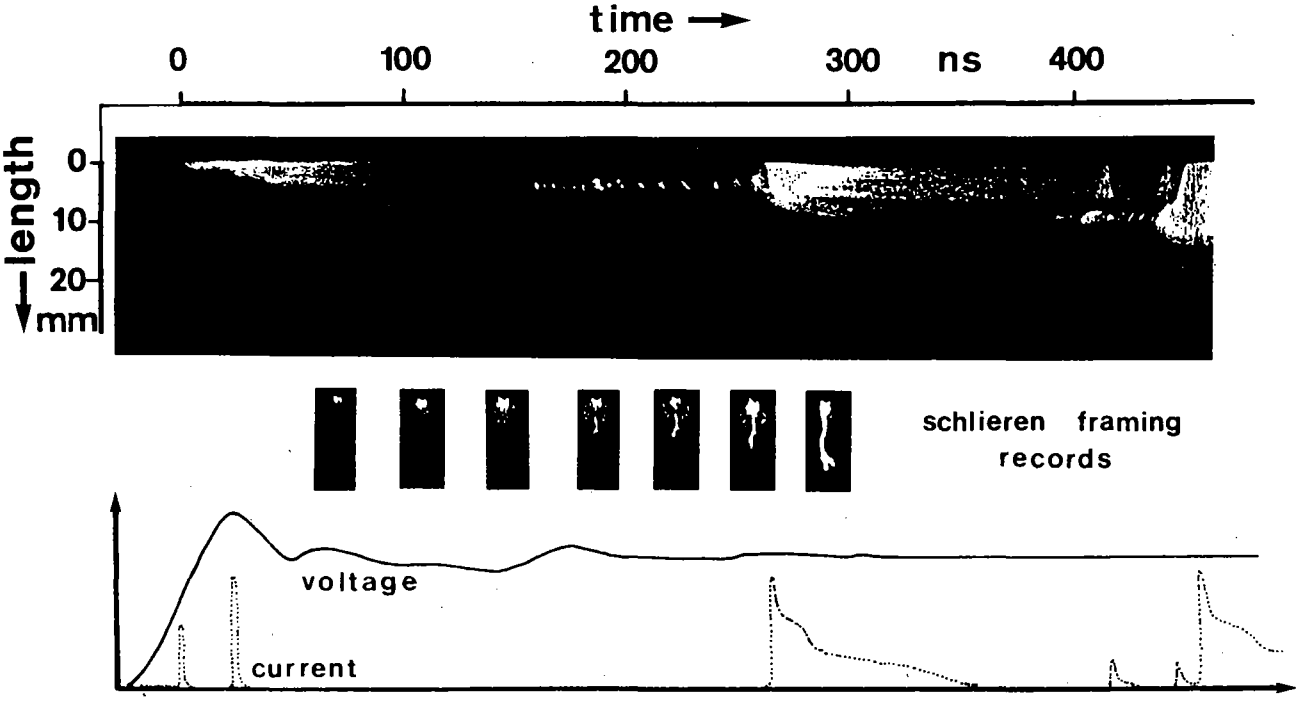

Fig. 15 Fast streak record of stepped leader propagation with corresponding voltage and current signals (rod plane gap with 1 mm rod diameter and 65 mm gap spacing; 0.15 MPa SF6; positive polarity, step pulse, 200 kV)

5.3 Discharge development under fast oscillating voltage superimposed on a step pulse

As outlined in the preceding chapters, conditions are quite complex in practical cases, making direct comparisons of different experimental results very difficult. Nevertheless, a classification of the effects of VFT according to physical mechanisms is possible on the basis of the knowledge presented in chapter 5.1 and 5.2: The stepwise propagation of a leader discharge under constant voltage U and pressure p is characterized by the stepping time {tau} that is given by the fit function (1)

$$\{tau\} = \frac{375\ ns}{(U/kV) * (p/MPa)^2} \qquad (1)$$

as well as by the time to breakdown $t_B = d/v_L$, where d is the gap spacing and v_L the mean leader propagation velocity. These time scales have to be related to the characteristic time scales of VFT, namely the period 1/f of the oscillating voltage and the duration T of the transient voltage.

Let us now consider an overshooting step pulse (a) as shown in Fig. 17a, and a weakly damped periodic sinusoidal pulse (b) as shown in Fig. 17b.
- In the case of pulse (a) and 1/f > {tau} (above 0.15 MPa) few leader steps can occur during the overshoot, but the breakdown is completed at the constant voltage after the overshoot. If the breakdown voltage is expressed in terms of peak levels, it is higher than with the pure step pulse by roughly a factor of 2 (Fig. 17a).
- For 1/f < {tau} (below 0.15 MPa) the overshoot produces a big corona. The charge of it screens the electrode at later times, thus leading to an increased breakdown voltage.
- With pulse (b) applied and pressures above 0.3 MPa, several leader steps occur within a half period. As the leader decay time is in the range of us, the channel can

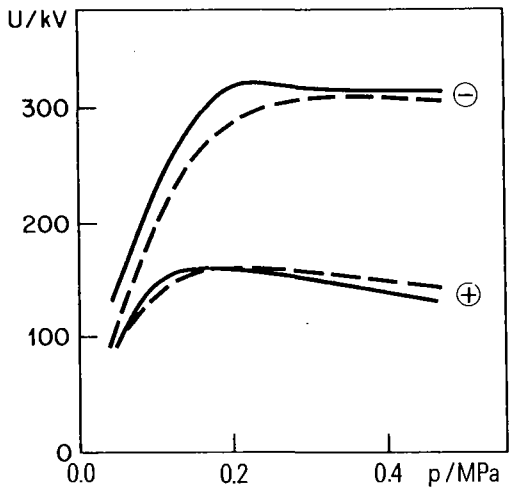

Fig. 16 Leader inception voltage versus pressure in SF6 under both polarities (dashed lines: Experimental data; solid lines: model predicitons; rod plane gap with 1 mm rod diameter and 48 mm gap spacing)

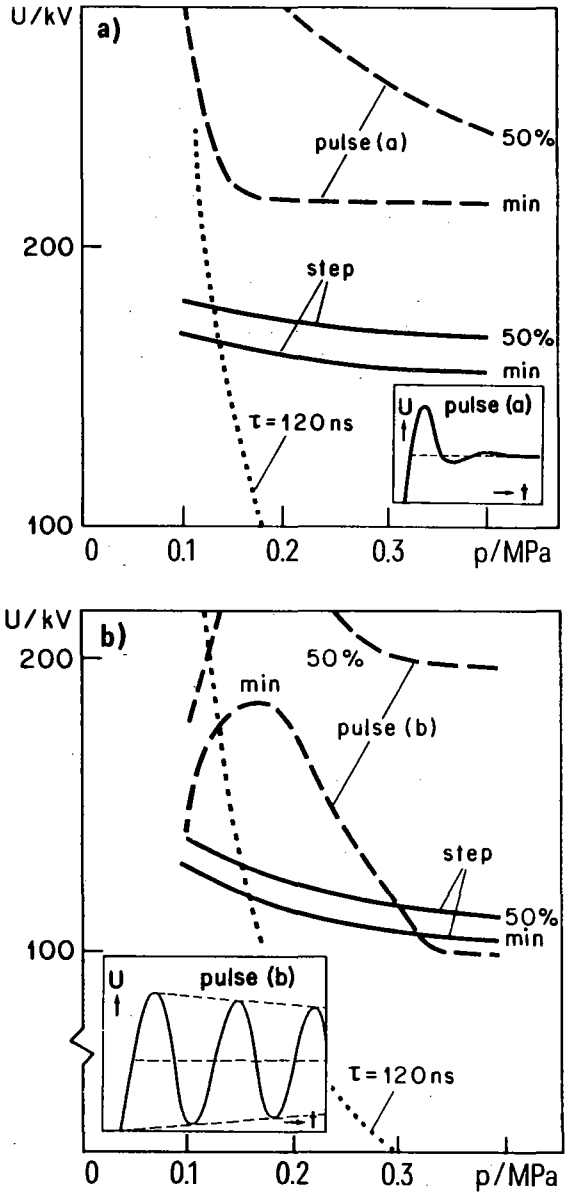

Fig. 17 Experimental breakdown curves for three different pulse shapes; positive polarity; SF6; rod plane gap with 1 mm rod diameter. Curve with {tau} = 120 ns added; left of it: {tau} > 120 ns
right of it: {tau} < 120 ns.
a) 210 mm gap spacing; step and shape (a) pulses
b) 69 mm gap spacing; step and shape (b) pulses

survive the low voltage half periods. Therefore step pulse and pulse (b) lead to equal minimum breakdown voltages above 0.3 MPa (Fig. 17b).
- Under both pulse shapes (a) and (b) and for stepping times {tau} close to 1/f, breakdown voltages are raised drastically compared to step pulse application.

A comparison of measured 50% breakdown curves for step pulse and pulse shapes (a) and (b) are also given in Fig. 17a and 17b.

The statistical distribution of breakdown voltages is considerably distorted by the presence of transients, and the distortion is different for shapes (a) and (b).

In technical applications, the condition that the leader stepping times are shorter than the period of the oscillating voltage is fulfilled in many cases. To apply the results given above, one has to take into account that the field configurations are similar to rod-plane concerning the inhomogeneity for disconnector failure or conducting particles in GIS. Other problems like determining the breakdown from a busbar or a shielding sleeve with a certain surface roughness to earth are somewhat different because of the lesser degree of inhomogeneity. In such cases, the leader crosses the gap in only a few steps with short resulting breakdown times. In the limit of a uniform field no leader propagation will occur; at the streamer inception level a streamer will cross the gap in one step and complete the breakdown.

In spite of their preliminary character, the theoretical and experimental results summarized above exhibit a high degree of understanding of the phenomenology of VFT effects described in the preceding chapters. It was found that the minimum breakdown voltages under VFT stress are always greater than or equal to those obtained under LI or step pulse stress.

In the case that the VFT are superimposed to a DC voltage, the discharge development does not differ much from that described above, provided that the DC voltage is sufficiently below the streamer inception level. However, because of the influence of the DC voltage on the ion concentration in the gap, the statistical properties will be completely different. If there are free particles in the gap, these cause additional effects, which are described in chapter 3.

Note that, as the time scales of voltage variation are comparable to leader propagation times, the voltage at the instant of breakdown becomes meaningless. The quantitative results given above arose from a more qualitative understanding in the part: For VFT periods shorter than the leader stepping time, the voltage is averaged over the time to breakdown, whereas in the case of VFT periods much longer than the stepping time, the peak voltages are the relevant ones in the dimensioning procedure. If both the times are nearly equal, the dielectric strength of the gap tends to increase, anyway. To make use of these rules, an idea of the frequency limits of the VFT spectrum is required as well as the maximum amplitude.

Concluding one can say that the investigation of the basic physical mechanisms has lead to a state of knowledge that can be applied to technical problems very satisfactorily.

6. Conclusions

The design of GIS is generally based on the LI voltage withstand level. Therefore most information is available for LI and much less data are published for VFT stress. Due to this situation the strength of VFT has been systematically related to LI strength.

Considering pure VFT (neglecting the influence of prestress) almost the same withstand levels as for LI are given for a correct GIS insulating system.

In the presence of defects, for example a needle-shaped defect, some results indicate a possible lower withstand value which deserves further investigation.

When the VFT are superimposed to DC large strength reduction can occur in the presence of particles. Similar effects were not observed in case of AC prestress.

Small sparking caused by VFT potential differences between conductively connected parts in GIS have no effects on the insulation withstand levels.

A theory of VFT breakdown mechanism is presented by which many of the mentioned effects can be explained.

Further investigations are necessary in the fields of VFT phenomena including physical modelling.

References

[1] WG 33-09
Very fast transient phenomena associated with gas insulated substations
CIGRE Report 33-.., Paris 1988

[2] Taschner W.
Voltage-Time Curves of SF6-Insulation for steep fronted Impulse Voltages below 1 µs
Gasdischarges and their Application Conference , Oxford England, 1985

[3] Boeck W., Taschner W., Gorablenkow J., Luxa G.F., Menten L.
Insulating behaviour of SF6 with and without solid insulation in case of fast transients
CIGRE Report 15-07, Paris, 1986

[4] Reynders J.P., Meppelink J.
Characteristics of disconnect switch transients and control of the consequent electromagnetic interference
CIGRE - Open Conference on EHV Transmission System, paper 6
Johannesburg, 1987

[5] Reynders J.P., Modry R., Meppelink J.
Volt-time curves of disconnector generated fast transients inside GIS
5th Int. Symp. on Gas. Diel.,
Knoxville, 1987

[6] Taschner W.
Dependency of vt-curves on the front steepness of testing voltages in SF6, measuring method and definitions
Gas discharge Conference Edinburgh S.172, 1980

[7] Taschner W.
Stoßkennlinien einiger grundsätzlicher Anordnungen in SF6 bei verschiedenen Schlagweiten und Drücken
ETZ-a Bd. 97 (1976), H2 S.118-120

[8] Pigini A., Rizzi G., Bargigia A., Mazza G., Mazzoleni B.
Dielectric strength of SF6 insulation under very fast overvoltages
4th ISH paper 32-12, Athens, 1983

[9] Diessner A., Luxa G.F., Mosca W., Pigini A.
High voltage testing of SF6 insulated substations on site
CIGRE Report 33-06, Paris 1986

[10] Izeki, N.
Voltage-time characteristics of SF6 Gas
Electra Nr. 101, July 1985

[11] Boeck, W., Witzmann, R.
Main influence on the fast transient development in Gas Insulated Substation (GIS)
5th ISH paper 12-01, Braunschweig, 1987

[12] Reisinger F., Muhr M., Diessner A., Schenner H.
Field measurement of fast transient voltages in the 420 kV-GIS Wien Süd
CIGRE SC 15 Symposium, Vienna, 1987

[13] Witzmann R.
Fast transients in gas insulated substations (GIS) - Modelling of different GIS components
5th ISH paper 12-06, Braunschweig, 1987

[14] Kynast E., Lührmann H.M.
Switching of disconnectors in GIS, laboratory and field tests
IEEE 85 WM 176-3, 1985

[15] Bargigia A., Mazza G., Pigini A., Thione L., Mazzoleni B.
Study of the dielectic strength of SF6 insulated metal enclosed substations and application to their design and testing
CIGRE Report 33-12, Paris, 1982

[16] Bargigia A., Porrino A., Rizzi G., Santagostino G., Mazzoleni B.
Contribution to the choice of the dielectric withstand levels of SF6 gas insulated substations
CIGRE Report 33-13, Paris, 1984

[17] Bargigia A., Brambilla R., Pigini A., Rizzi G.
Influence of solid insulation on the dielectric performance of SF6 configurations
4th Int. Symp. on Gas. Diel.,
Knoxville, 1984

[18] Bargigia A., Mazza G., Bertazzi A., Mosca W., Pigini A.,
The dielectric strength of SF6 configurations under impulses superimposed to DC voltages. Impact on the design of AC insulated substations
IEEE Int. Conf. on Prop. and Appl. of Diel. Mater., Xian China, 1985

[19] Bargigia A., Mazza G., Pigini A., Rizzi G.
Strength of typical GIS configurations with special reference to composite and combined stresses
5th Int. Symp. on Gas. Diel., Knoxville, 1987

[20] Dessouky E., Mosch W., Speck J., Hauschild W., Jahn JH.
Particle initiated breakdown of SF6 insulations at DC and AC voltages superimposed with switching impulse voltages
4th ISH paper 33-01, Athens, 1983

[21] Hauschild W.
CIGRE - Discussion to question 2.2 of subject 2, Group 14, Paris, 1986

[22] Kindesberger J., Taschner W.
Impulse voltage breakdown in SF6 with AC and DC BIAS voltages
Symposium on Gas Insulated Substations Technology and Practice, Toronto, 1985

[23] Kobayashi S., Yamagata Y., Nishiwaki S., Okubo H., Kawaguchi Y., Marakami Y., Yanabu S.
Particle-initiated flashover caused by disconnector restriking surges in GIS
5th ISH paper 12-03, Braunschweig, 1987

[24] Gorablenkow J., Kynast E., Lührmann H.
Switching of capacitive currents by disconnectors in gas insulated substations
IEEE 83 SM 499-1, 1983

[25] Wiegart N., Pinnekamp F., Boggs S.A., Boeck W., Kindersberger J., Morrow R., Niemeyer L., Zaengl W., Zwicky M.
Corona Stabilization to Testing of Gas-Insulated Switchgear
Report for the Canadian Electrical Association, CEA No. 153 T 310, 1985

[26] Wiegart N., Niemeyer L., Pinnekamp F., Boeck W., Kindersberger J., Morrow R., Zaengl W., Zwicky M., Gallimberti I., Boggs S.A.
Inhomogeneous Field Breakdown in GIS - the Prediction of Breakdown Probabilities and Voltages
IEEE-PES WM, New Orleans, 1987

[27] Gallimberti I., Ullrich L., Wiegart N.
Experimental Investigation of the Streamer to Leader Transition in SF6 under Negative Polarity
5th Int. Conf. on Gas. Diel., Knoxville, 1987

[28] Niemeyer L., Wiesmann H.J.
Modelling of Leader Branching in Electronegative Gases
5th Int. Conf. on Gas. Diel., Knoxville, 1987

[29] Edlinger A., Mauthe G., Pinnekamp F., Schlicht D., Schmidt W.
Disconnector Switching of Charging Currents in Metal-Enclosed SF6-Gas Insulated Switchgear at EHV
CIGRE Report 13-14, Paris, 1984

[30] Gallimberti I., Wiegart N.
Streamer and Leader Formation in SF6 and SF6-Mixtures under Positive Impulse Conditions, Part I: Corona Development, Part II: Streamer to Leader Transition
J. Phys. D: Appl. Phys., 19, pp. 2351-2379, 1986

[31] Wiegart N.
A Model for the Production of Initial Electrons by Detachment of SF6-Ions
IEEE EI-20 (3), pp. 587-594, 1985

[32] Kindersberger J.
The Statistical Time Lag to Discharge Inception in SF6
Doctoral Thesis, Technical University Munich, 1986

[33] Niemeyer L.
A Model of SF6 Leader Channel Development
8th Int. Conf. on Gas Discharges and their Applications, pp. 223-227, Oxford, 1985

[34] Hauschild W., Mosch W.
High voltage field testing of GIS from the viewpoint of failure mechanism
Proc. of Int. Sympos. on GIS, Toronto, Canada, part 4, pp.185-194, Sept.1985

[35] Pflaum E.
Discussion on testing of GIS
Proc. of Int. Sympos. on GIS, Toronto, Canada, part 4, pp.194-196, Sept.1985

[36] Bosotti O., Mosca W., Rizzi G., Hashoff L., Kynast E., Lührmann H.
Phenomena associated with switching capacitive currents by disconnectors in metal enclosed SF6 insulated switchgear
CIGRE Report 13-06, Paris, 1982

International Conference on Large High Voltage Electric Systems

112, boulevard Haussmann — 75008 Paris

1988 Session — 28th August - 3rd September

T

15-05

Pref. Subj. 1

DIELECTRIC WITHSTAND OF SF_6 STRESSED BY STEEP FRONTED WAVES

by

Ph. AURIOL, F. BURET

Ecole Centrale de Lyon

G. HELLE, S.Z. MA

Alsthom

(France)

Abstract

This report presents a survey conducted in the field of steep and oscillating waves. The survey studies SF_6 behaviour by means of two test arrangements employing a coaxial gap, the geometry of which is representative of a busbar set in a metal-clad substation. The tests were performed with fast transient waves (20 to 90 ns rise time), oscillating waves (200 ns rise time) and lightning impulse (1.2/50 µs) in the case of a faultless geometry and with a needle type fault on the central conductor. These tests permitted the tracing of flashover voltage time curves in the SF_6 for SF_6 absolute pressure of 0.1 MPa. The results demonstrate that fast transient waves are less constraining than the lightning impulses.

Key-words

SF_6, Fast transient, Oscillating wave, Voltage time curve.

1. Introduction

Gaseous insulation metal-clad substations are subjected in operation to a large variety of transient overvoltages.

These disturbances originate mainly from lightning impulses on overhead lines and operations of cut-off apparatuses.

These overvoltages display highly differing temporal characteristics for standardised waves which are bi-exponential in form, i.e. they decrease slowly and regularly.

In particular, overvoltages generated by the operation of a circuit-breaker in a HV metal-clad substation display very short rise times (ten or so to several tens of nanoseconds) with large amplitude oscillations on the wave tail and for which the fundamental frequencies might be clearly greater than 10 MHz [1] (Fig.1).

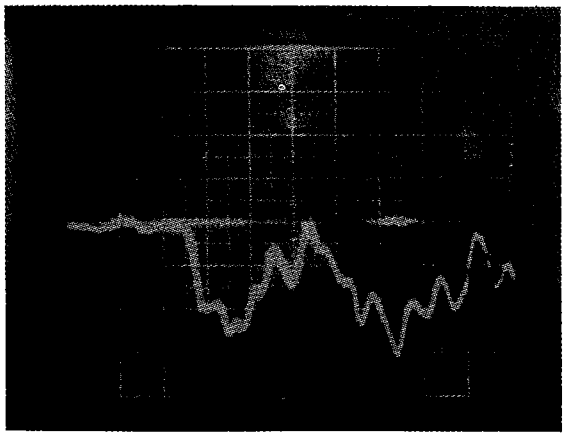

20 ns per square

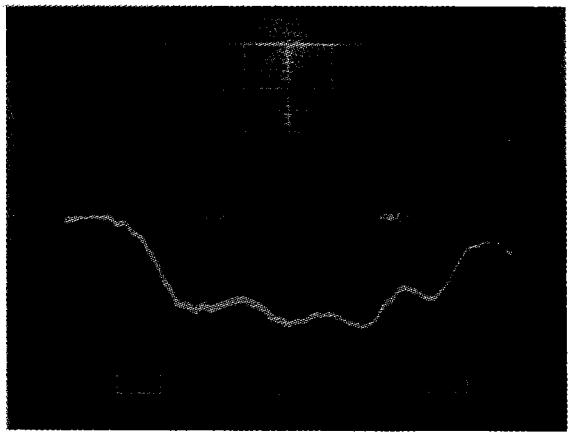

5 ns per square

Figure 1. Transient voltage obtained in an experimental arrangement reconstituting a circuit-breaker in a small sized metal-clad substation.

Alsthom, 130 rue Léon Blum, 69100 Villeurbanne, France

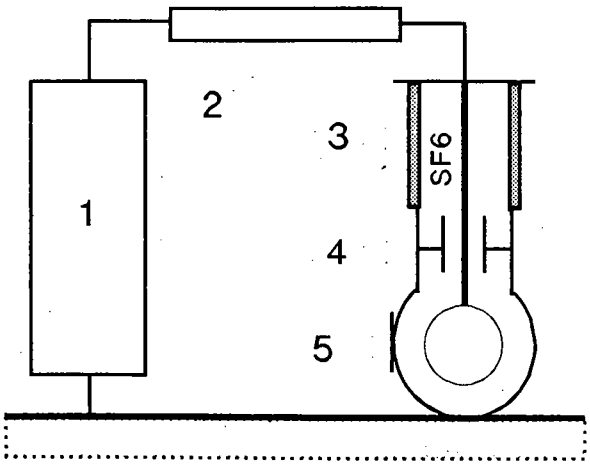

Figure 2. Test system No.1.

1 Generator, Marx type 1 MV - 50 kJ
2 200 Ω resistive braid
3 245 kV bushing
4 Coaxial gap (45/120 mm)
5 Capacitive probe

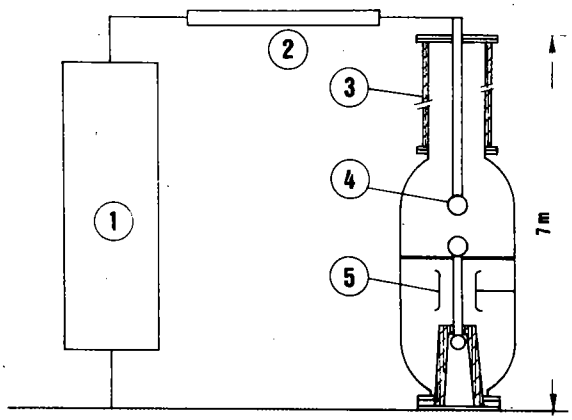

Figure 3. Test system No.2.

1 Generator, 1 MV - 17 kJ
2 Resistive braid
3 245 kV bushing
4 Pre-sphere gap
5 Coaxial electrode (80/210 mm)

It is therefore important for the reliability of such equipment to study the behaviour of the different components constituting its insulation under this type of stress and most particularly gaseous insulation.

Numerous test results have already been obtained with standardised wave shapes leading to higher breakdown times to the microsecond [3]. They are rarer in the rapid transient field and most particularly in the case of non homogeneous fields.

This report presents the results obtained during tests performed on representative electrode models of metal clad substations and intended to specify the dielectric withstand of SF_6 under fast transient voltage stress, in the presence or not of a form fault on an electrode.

2. Test Layout

The behaviour of SF_6 has been studied in a coaxial configuration for which the field utilisation factor (E average/E maximum) is approximately 0.6 which corresponds to that of an industrially produced set of busbars.

Two arrangements differing in concept were made :

The first one (Fig.2) contained an impulse generator (1 MV, 50 kJ) connected by means of a 200 Ω resistor to a test chamber which constituted a low-value load capacity (200 pF). The voltage application bushing is an out-sized type so as to eliminate flashover at this level. The wave obtained displays thanks to the natural oscillation of the circuit an overvoltage factor of 1.4 p.u. with a typical transition time (between 10 and 90 per cent of the amplitude) of 200 ns.

The second test circuit (Fig.3) contains a pre-sphere gap, below the voltage application bushing and as a result is not subjected to transient voltages. This arrester is located in a separate compartment of the coaxial system designed so as not to modify the breakdown conditions by irradiation.

Thus thanks to the weak formative time of the SF_6 (formation time for the ionised channel), it is possible to obtain below the pre-sphere gap transient waves for which the rise fronts are found to be between 20 and 90 ns. The reflections, that occur inside the chamber introduce high-frequency oscillations on the wave tail.

This layout does a good job of simulating the type of wave that might be generated in a metal clad substation during operation of a disconnector, the phenomena being identical (breakdown between the electrodes of the disconnector).

The first circuit, which did not display this advantage, is on the other hand capable of producing a wave repetitive in form and amplitude and thus facilitates interpretation of results.

3. Measurement means

The voltage waves applied, for which the amplitudes are limited to approximately 900 kV, have been measured using a capacitive probe having a pass band of 300 MHz constructed in accordance with [4].

Figures 4 and 5 show two characteristic recordings of the waveforms obtained.

Transient voltage acquisition was performed by digital oscilloscope (Philips PM3311-125 Hz, Tektronix RTD710-200 MHz, LE CROY4900-125 MHz) which facilitated analysis of the measurements. However, a minimum of precautions must be taken to obtain correct operation of this type of equipement in a highly disturbed environment.

Indeed, during a SF_6 breakdown the current variation rates and the voltage in the discharge circuit reached extremely high values. The induced currents in the measurement circuit ground as well as the radiations produced might greatly disturb the recording.

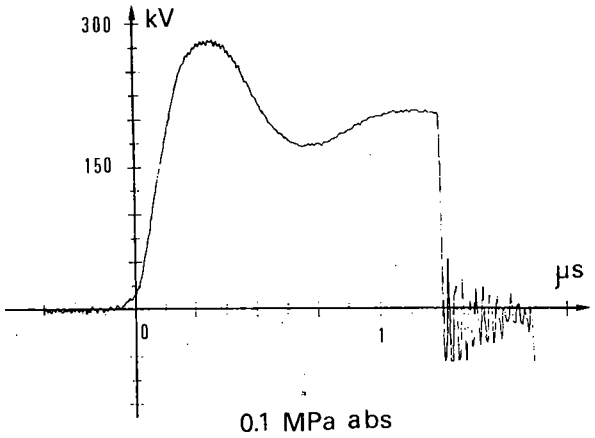

Figure 4. Wave form obtained with the first test layout.
Breakdown in negative polarity.

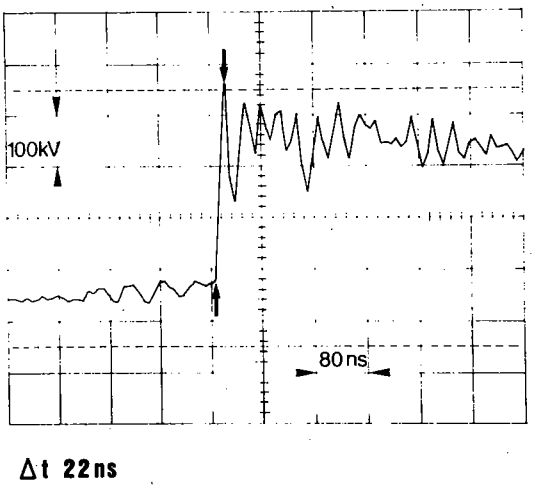

Figure 5.Wave form obtained with the second test layout.

The solutions adopted consisted in the use of a cable with a very high recovery rate (multi-sheath cable) so as to display high immunity to radiations.

It is imperative that the recorder be placed in a metal-clad cage connected to the measurement ground and to make the assembly operate at a floating potential. It is thus possible to suppress a major portion of direct radiation on the measuring equipment as well as the currents induced in the coaxial cable ground. The connection between the recorder and the computer is performed by means of an optical fibre.

4. Results

The tests were performed on the two test layouts in a homogeneous field (faultless electrodes) and on the second layout in a non-homogeneous field (needle on the voltage side electrode). The behaviour of the SF_6 in these configurations is compared with that it displays with a lightning impulse which remains for the time being the reference shock wave to determine insulation levels for metal clad substations in the short-time field.

The results are translated in the form of voltage time curves defined in conformity with IEC Standard 60.2 (Fig.6). In other words, flashover points are defined by flashover time and :

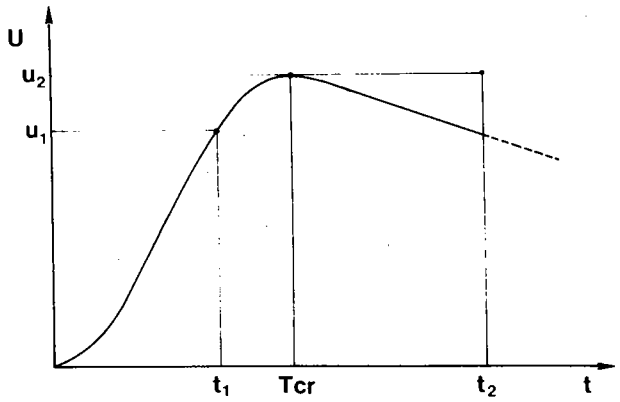

Figure 6. Definition of v-t curve according to IEC Standard 60.2.

- the amplitude of the maximum wave peak if flashover occurs on the wave tail (U_1,t_1).
- the amplitude corresponding to flashover if the latter occurs on the wave front (U_2,t_2).

Each of these voltage time curves have been established by applying between 500 and 1000 impulses.

4.1. Homogeneous field : configuration without fault

4.1.1. Arrangement No.1

The test results are given in Figures 7a and 7b. They represent the compilation of the breakdown points obtained with lightning impulse as well as on the oscillating wave fronts for which the front times are approximately 200 ns.

4.1.2. Arrangement No.2

The test results are given in Figures 8a and 8b. They represent the compilation of the breakdown points obtained with lightning impulse as well as on the front and tail of steep fronted waves for which the front times lie between 20 and 90 ns.

4.1.3. Comments

The results demonstrate that when the steepness of the impulse increases, the breakdown voltage level also increases. In other words, the resistance to a steep fronted wave is greater than that for a lightning impulse. This confirms previous research efforts [5] and [6].

This observation remains valid when one also takes into account the breakdown points on the wave tail (Figs. 9a and 9b).

4.2. Heterogeneous field : configuration with fault

4.2.1. Arrangement tested :

These tests were performed with arrangement No.2.

A form fault is simulated by means of a calibrated needle (Fig.10) implanted on the central electrode, protruding by 5 mm.

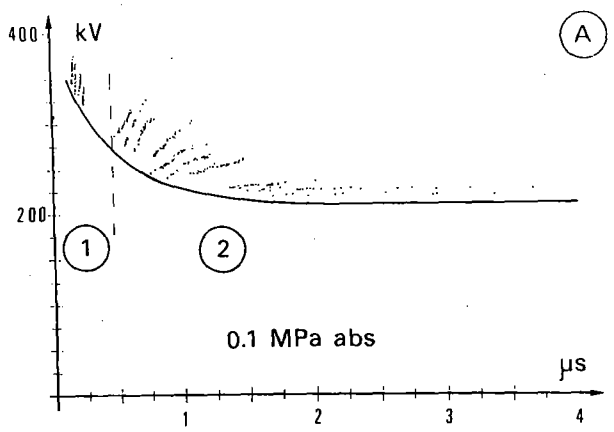

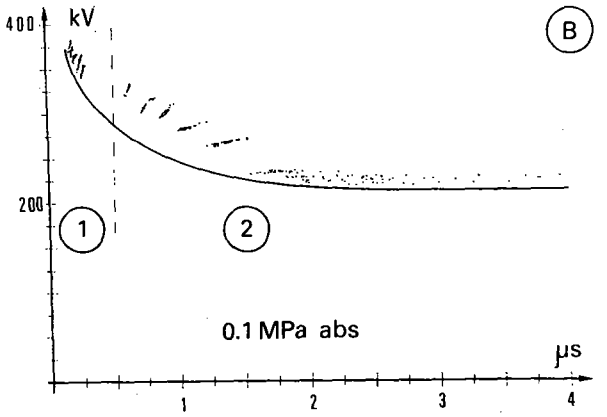

Figure 7. Influence of front steepness (arrangement No.1).
A - positive polarity
B - negative polarity
1 Oscillating wave front
2 Lightning impulse

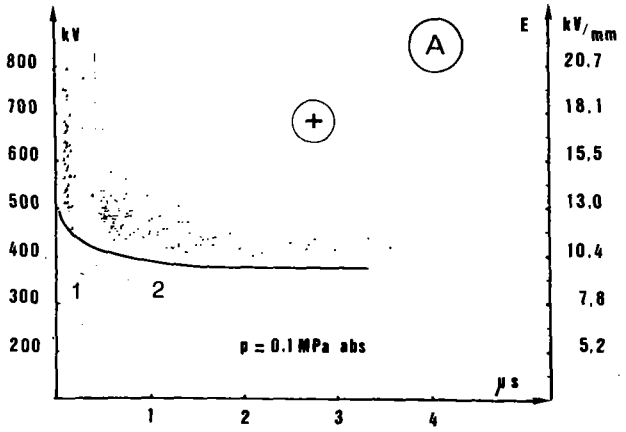

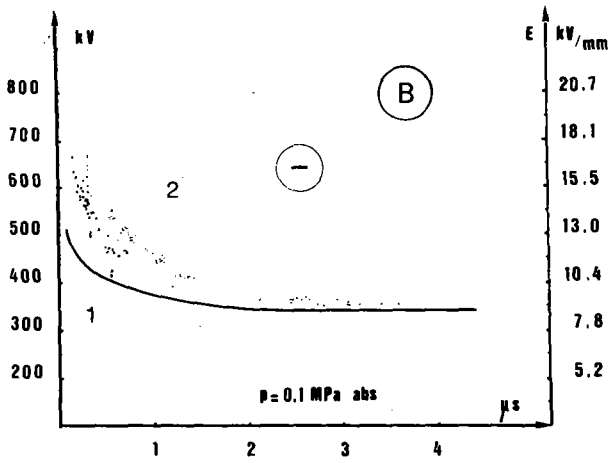

Figure 8. Influence of front steepness (arrangement No.2).
A - positive polarity
B - negative polarity
1 Oscillating wave front
2 Lightning impulse

The tests were performed with a steep fronted wave and for a front time lying between 20 and 90 ns.

The test results are given in Figures 11a and 11b.

The comparison of the v-t curves obtained with and without fault is given in Figure 12.

4.2.2. Comments :

It is to be noted that in the presence of a fault, the voltage withstand is greatly diminished as against the previous case.

The + wave withstand is less than the - wave withstand in conformity with what occurs in heterogeneous field structures.

One also observes that the dielectric withstand also increases with the steepness of the wave.

It can therefore be concluded that in the arrangements we have tested in inhomogeneous fields, the resistance to steep fronted waves is greater than resistance to lightning impulses.

5. Conclusion

The laboratory tests performed on models representative of metal clad equipment have shown that the v-t curve, characteristic of the dielectric withstand of SF_6 as a function of the front time of the applied voltage wave, is an increasing and continuous curve when the duration of the wave front decreases from 1 μs to 20 ns.

When the under voltage electrode displays a superficial fault, the flashover voltages are reduced but the v-t curve displays the same appearance : the flashover voltage grows when the steepness of the front increases, thus confirming the fact that steep fronted waves are not more sensitive to electric field concentrations than lightning impulses.

The number of impulses we applied is sufficient to give the tests statistical significance and that the probability of having a flashover at a value less than the voltage-time curve is very slight.

The results indicate that very steep fronted voltage waves display a sensitivity to form faults (heterogeneity of electric fields) comparable to that obtained with lightning impulses.

These conclusions, which await confirmation by studies on industrial equipment, should be given consideration in the thinking now going on as regards the possible taking into account of steep fronted waves for the definition of new on-site testing of HV metal-clad equipment.

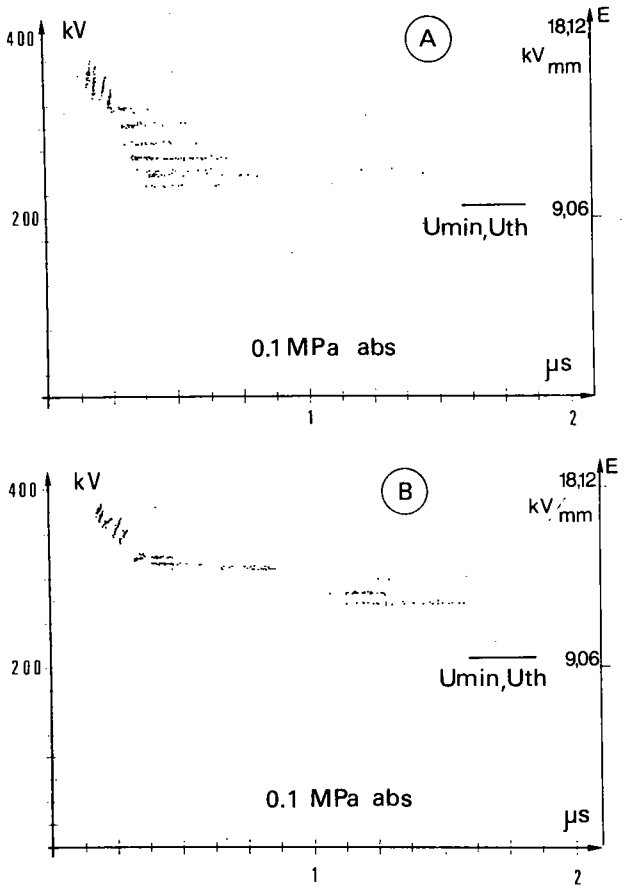

Figure 9. Breakdown obtained with oscillating wave.
A - positive polarity
B - negative polarity
U_{min}: Minimum breakdown voltage with a lightning impulse
U_{th} : Theoretical threshold voltage (calculated)

For more than 250 ns, the flashovers occur on the tail of the oscillating wave.

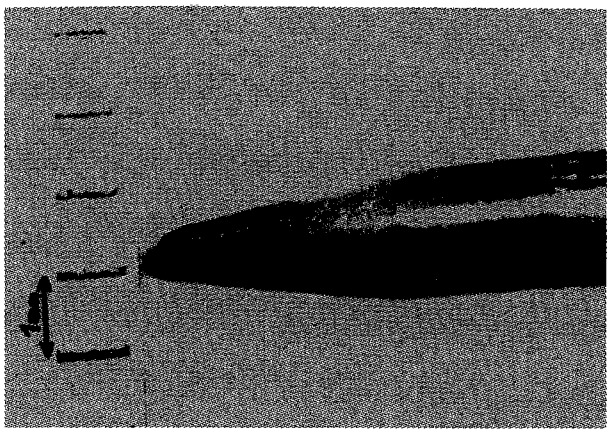

Figure 10. Calibrated needle.

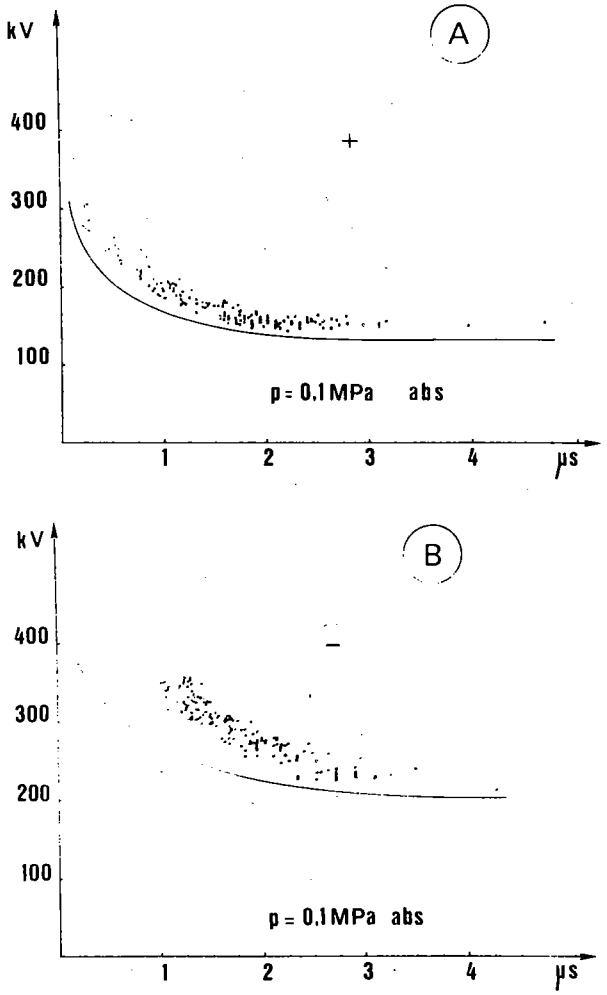

Figure 11. V-t characteristic of arrangement No.2 with pointer on central electrode.
A - positive polarity
B - negative polarity
· - Lightning impulse
. - fast transient

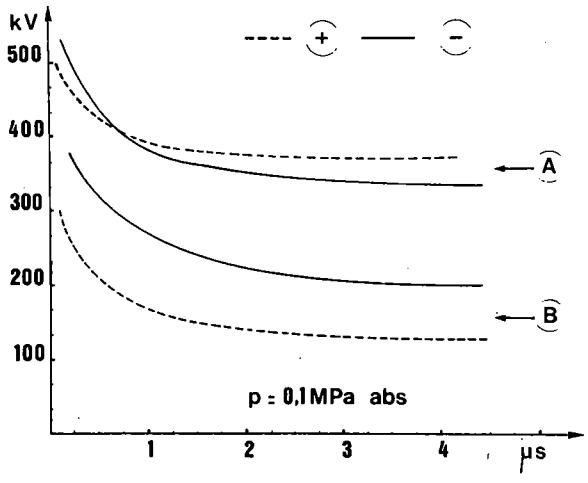

Figure 12. Comparison of the two geometries
A: geometry without fault
B: geometry with fault (needle)

6. Bibliography

[1] S.A. BOGGS, N. FUJIMOTO, M. COLLED, E. THURIES - The modeling of statistical operating parameters and the computation of operation induced surge waveforms for GIS disconnectors - CIGRE 1984 report 13-15.

[2] F. BURET - Study on SF6 voltage withstand with fast oscillating waves - Doctoral thesis at INPG, Grenoble, 6 November 1986.

[3] IZEKI - Voltage-time characteristics of SF6 gas - ELECTRA no. 101, July 1985, CIGRE report of group 15-03, pp 41-59.

[4] S.A. BOGGS, N. FUJIMOTO - Techniques and instrumentation for measurement of transients in gas insulated switchgear - IEEE Trans. on E.I., vol. 19, no. 2, April 1984, pp 87-92.

[5] W. BOECK, W. TASHNER, J. GORABLENKOW, G.F. LUXA, L. MENTEN - Dielectrical properties of SF6 when faced with rapid transients with and without solid insulation - CIGRE 1986, report 15-07.

[6] A. STEPKEN - Investigation of the leader development in SF6 for impulse voltages - 5th ISH, Braunschweig (FRA), 24-28 August 1987, report 13-07.

GROUPE 15
GROUP 15

MATERIAUX ISOLANTS
INSULATING MATERIALS

Rapports / *Papers*

15-06, 15-05

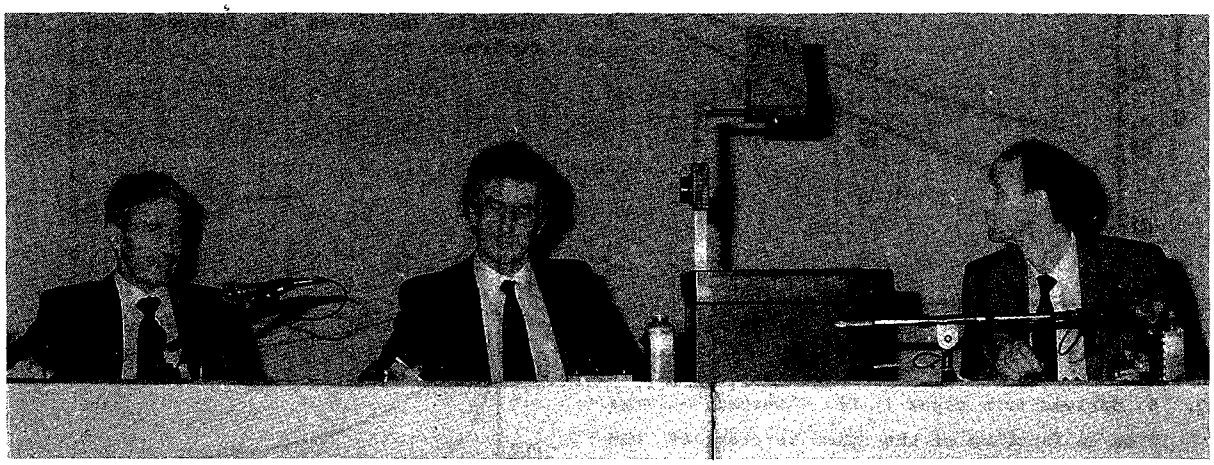

Th. PRAEHAUSER (President) — C.W. REED (Special Reporter) — E.ERIKSSON (Secretary)

SUJET PREFERENTIEL 1 / *PREFERENTIAL SUBJECT 1*

Nouveaux travaux relatifs au SF_6 et autres gaz à grande rigidité, particulièrement en présence de phénomènes transitoires rapides.

New work with SF_6 or other high strength gases, especially in the presence of fast transients.

QUESTIONS 1 - 3

Mr. A. PIGINI (Italy)

My comment is related to the volt time characteristics of non uniform configurations and, in particular, I would like to stress the differences between Fig. 2 and Fig. 6 of the report 15-06, which maybe, do not appear clearly from the paper.

Fig. 2 reports sketches of the volt time characteristic, obtained with the same impulse shapes, giving, as foreseen in the present IEC standards, the breakdown voltage (maximum voltage reached before breakdown) as a function of the time to breakdown.

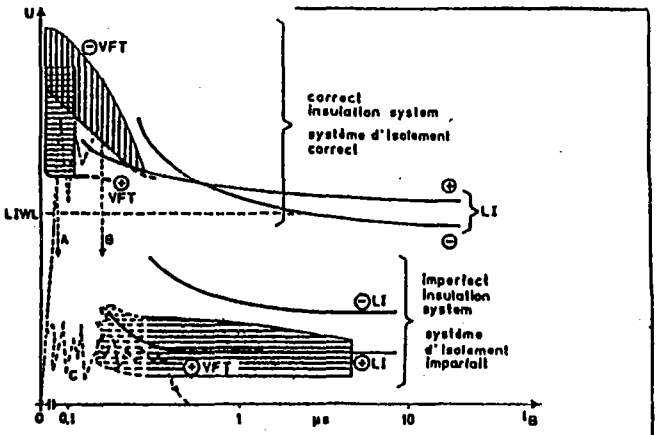

FIGURE 2 - derived from paper 15-06.
EXAMPLE OF VOLT-TIME CURVES, FOR GIVEN IMPULSESHAPES.

The curves are generally limited to time of interest for LI (1-10 s). From the curves, it appears that, for a given impulse shape the breakdown voltage decreases with the time to breakdown, even for non-uniform configurations (e.g. configurations with defects), in agreement with that reported in Paper 15-05.

Fig. 6 reports examples of characteristics relating to peak value and the time to crest of the applied voltage, and have been obtained with different impulse shapes. They can be used mainly for the comparison between LI and SI strength. From the curves, it appears that when considering different impulse

shapes, the withstand voltage for non uniform configurations (e.g. configurations with defects) increases with the same time to crest of the applied impulse.

Both representation can be useful to derive interesting consequences for design and testing. However, a mixture of the two representations could give rise to some confusion.

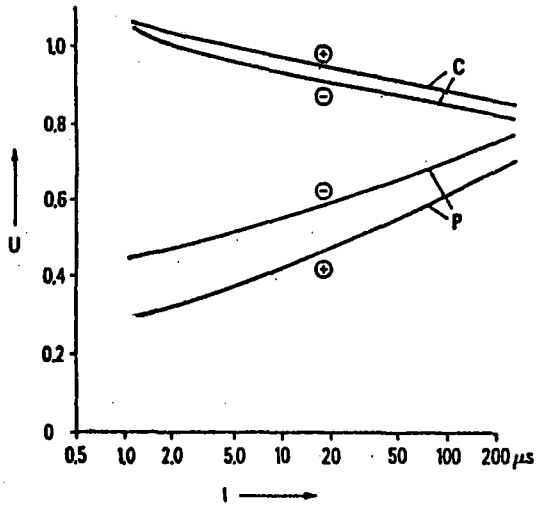

Fig. 6 derived from paper 15.06. Withstand voltage as a function of the time to crest of the applied voltage

M. F. BURET (France)

Mon intervention se rapporte à la question n° 1 du Rapport Spécial, relative à la comparaison des courbes tension-temps en champ inhomogène publiées dans les rapports 15.05 et 15.06.

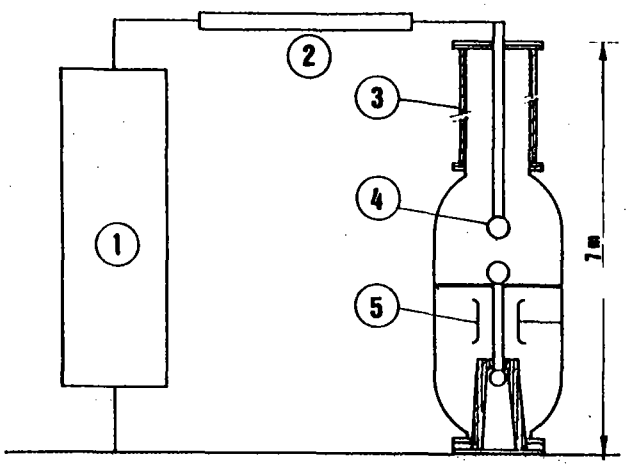

Fig.1: Dispositif d'essai
1.Générateur 1MV-17kJ
2.Tresse résistive
3.Traversée 245kV
4.Electrode de préamorçage
5.Electrode coaxiale (80/210 mm)

Les courbes du rapport 15.05 ont été tracées après des séries de 500 à 1000 chocs de tension appliqués à un système d'électrodes coaxiales (fig. 1). Un éclateur auxiliaire intégré dans l'enceinte permet d'obtenir des ondes de tension transitoire dont le temps de front est de 20 à 90 nanosecondes.

Chacune des courbes de la figure 2 est l'enveloppe inférieure des points d'amorçage. Les courbes A sont obtenues avec l'éclateur coaxial sans défaut.

Les courbes B sont obtenues après avoir placé une aiguille de 5 mm de longueur sur l'électrode centrale.

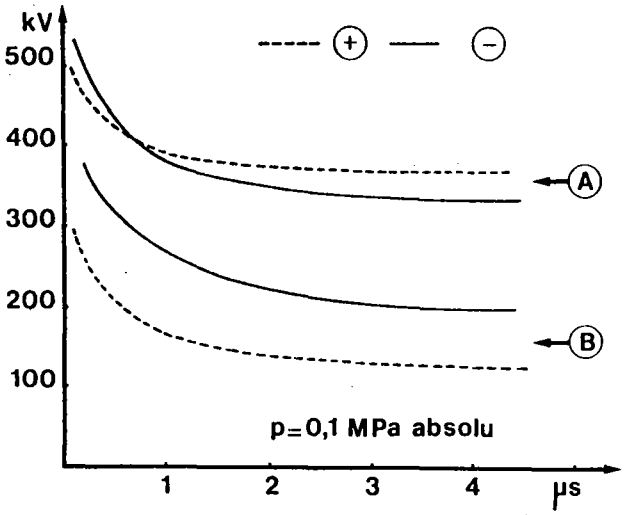

Fig.2: Courbes tension-temps
A-----Géométrie sans défaut
B-----Géométrie avec défaut

La comparaison de ces courbes avec celles de la figure 2 du rapport 15.06 ne montre pas de différence fondamentale dans leur allure générale. En particulier, dans les deux cas, la courbe tension-temps tend à croître lorsque les temps de front deviennent inférieurs à 1 microseconde, en champ homogène comme en champ inhomogène.

Ces différentes études montrent bien que la tenue en tension transitoire rapide est meilleure qu'en choc de foudre, pour des temps inférieurs à une dizaine de microsecondes.

Pour des temps plus longs, de quelques dizaines à quelques centaines de microsecondes, la figure 6 du rapport 15.06 montre que la tenue diélectrique diminue quand la raideur du front augmente. Nous avons nous-mêmes constaté ce phénomène d'ailleurs bien connu, mais nous avons volontairement limité notre étude aux temps de front inférieurs à une micro-seconde.

Il n'y a donc pas de contradiction fondamentale entre les résultats publiés dans les deux rapports.

Je souhaite apporter en outre un complément au rapport 15.05.

On connait bien l'efficacité des parafoudres à oxyde métallique pour réduire le niveau des surtensions en ondes de foudre, avec des temps de front de l'ordre de la microseconde.

La question se pose de savoir quelle peut être l'efficacité d'un tel parafoudre vis à vis des surtensions transitoires très rapides, compte-tenu du temps de mise en conduction du parafoudre, temps qui est forcément non nul.

Nous avons effectué des essais en adaptant au second montage décrit dans le rapport un parafoudre à oxyde de zinc dont la tension résiduelle est de 132 kV sous 10 mA (fig. 1). Les essais ont été effectués dans les mêmes conditions que précédemment.

La figure 3 montre une image de la tension résiduelle sur le parafoudre soumis à une onde à front raide. Le temps de montée de la tension est toujours supérieur à 40 nanosecondes; cela est dû à ce que le parafoudre présente un comportement capacitif avant sa mise en conduction.

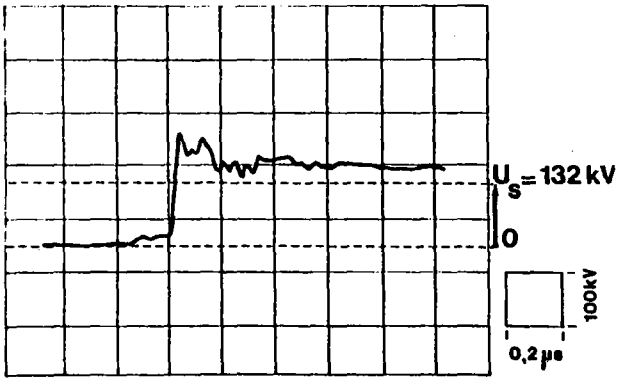

Fig.3 Tension résiduelle sur le parafoudre soumis à une onde à front raide

La figure 4 montre que, dans le domaine des tensions transitoires très rapides, le parafoudre réduit sensiblement le niveau des ondes incidentes, même s'il présente une efficacité plus faible qu'avec les ondes de foudre.

Ceci permet de répondre à la question qui se posait de savoir si le temps de mise en conduction n'était pas trop important pour enlever tout efficacité au parafoudre dans le domaine des tensions transitoires très rapides.

Le parafoudre à oxyde de zinc apparaît donc comme un moyen propre à réduire le niveau des tensions transitoires générées par les manoeuvres des sectionneurs des postes blindés. Néanmoins, ces résultats ne sont obtenus que sur des montages d'essais en laboratoire. Il reste à vérifier l'efficacité des parafoudres avec des matériels industriels et à résoudre le délicat problème de leur localisation dans les postes blindés.

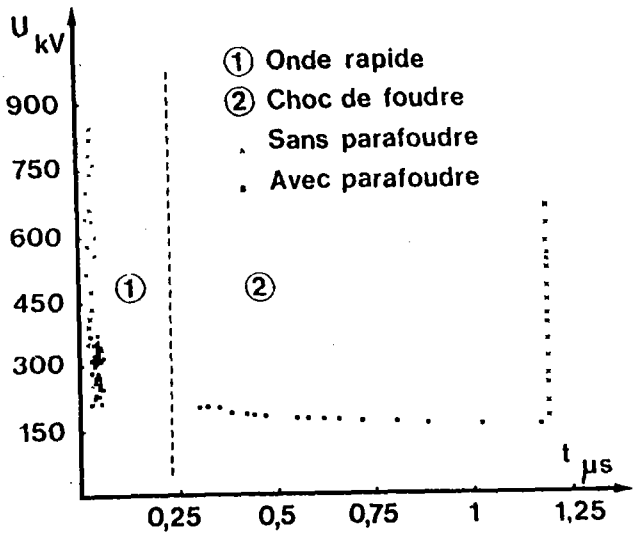

Fig.4 Réduction du niveau de surtension par le parafoudre

M. J.M. DELCOUSTAL (France)

Mon intervention se rapporte à la question 2 du Rapport Spécial, relative à l'intérêt que peut présenter un essai sous tension transitoire très rapide.

Les études présentées précédemment confirment que la tenue diélectrique du matériel blindé sous tension transitoire très rapide est meilleure que la tenue sous onde de foudre; en présence d'un défaut, la diminution de la tenue est du même ordre. Il est alors évident qu'un essai sous transitoire rapide n'ajoute rien aux informations données par l'essai en ondes de foudre. Cet essai est inutile, là ou l'essai en choc de foudre est pratiqué.

Néanmoins, la question n° 2 envisage le cas où cet essai serait jugé utile et demande s'il devrait constituer un essai de contrôle-qualité.

Pendant plusieurs années, nous avons soumis nos matériels blindés à des essais en usine comportant l'essai normalisé à fréquence industrielle suivi d'un essai en ondes de foudre. Nous avons constaté que ce dernier essai n'apportait pas d'information significative quant à la qualité du matériel. En effet les conditions d'assemblage en usine sont telles que la probabilité d'avoir un défaut détectable par l'essai en onde de foudre après un essai à fréquence industrielle est très faible et nous avons renoncé à ce type d'essai. Il en serait de même avec un essai sous transitoires rapides qui ne ferait qu'apporter des sujétions complémentaires sans améliorer la qualité du matériel.

Le problème peut être vu différemment si on considère les essais sur site avant mise en service, alors que les conditions de transport et de montage, souvent difficiles, ont pu introduire des défauts. Les essais diélectriques effectués doivent donner l'assurance de la bonne tenue diélectrique en service, y compris vis à vis des tensions transitoires rapides. Mais il n'est pas du tout évident que cette garantie passe nécessairement par un essai en transitoires rapides, difficile à effectuer sur site et difficile à définir du fait que les formes des ondes de tension dépendent de la configuration du poste.

Pour l'instant, nous n'avons pas de réponse définitive à apporter à ce problème et des reflexions sont encore nécessaires. Néanmoins nous pensons que parmi les essais réalisables simplement sur site, il en existe certainement qui doivent permettre de garantir la tenue en transitoires rapides.

La plupart des amorçages constatés en cours de manoeuvres de sectionneurs ont probablement eu pour origine la présence de particules. Le développement des méthodes acoustiques devrait permettre d'améliorer cette situation non seulement en permettant d'éliminer les particules existantes au moment de la mise en service mais aussi (et peut-être surtout) celles qui sont susceptibles d'apparaître en service.

M. G. RIQUEL (France)

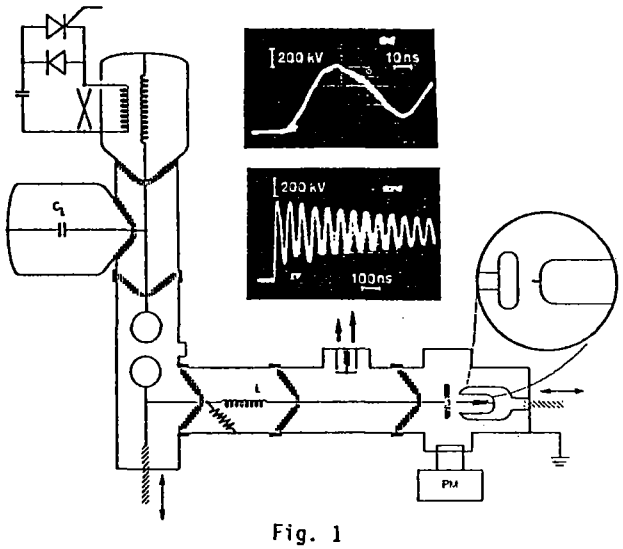

Fig. 1

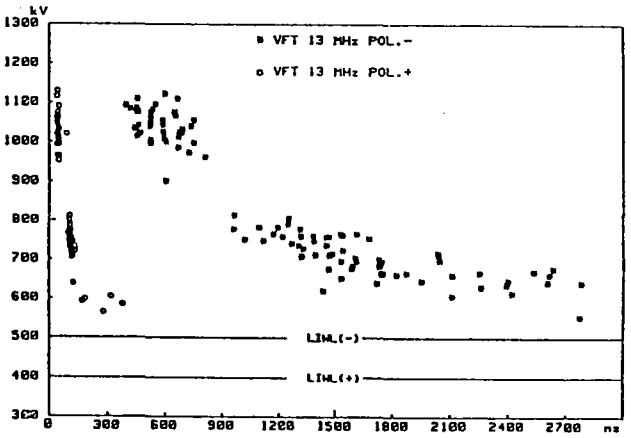

Fig. 2

Electricité de France pratique depuis de nombreuses années une politique de contrôle diélectrique sur site des Postes Sous Enveloppe Métallique (PSEM) qui préconise l'essai au choc de foudre en complément de l'essai à fréquence industrielle.

Ceci permet de couvrir le risque d'amorçage dans le cas de défaut de profil d'électrode (pointe sur partie active, particule fixée...). En effet, ce type de défaut provoque une forte inhomogénéité du champ électrique qui réduit considérablement la tenue au choc de foudre. La tenue en 50 Hz n'est généralement pas altérée du fait de la stabilisation couronne.

La question que l'on se pose actuellement est de savoir si l'essai au choc de foudre peut également garantir la tenue vis à vis des surtensions transitoires rapides (STTR). Electricité de France a donc entrepris une série d'expérimentations visant à reproduire en laboratoire des STTR réalistes et à étudier leur influence sur des isolations fragilisées par la présence de défaut.

Les STTR simulées sont des ondes oscillantes dont la fréquence peut varier de 0,7 à 13 MHz ; le défaut est simulé par une pointe de longueur ajustable fixée sur une des électrodes d'une géométrie à champ homogène .Fig. (1).

Les premiers résultats obtenus à 0,45 MPa (pression de service des PSEM) avec des ondes de 4 et 13 MHz et des pointes de 4 et 10 mm montrent que les STTR s'avèrent moins contraignantes que l'onde de foudre, quelle que soit la polarité . Fig. (2).

Ces résultats sont en accord avec ceux présentés dans le rapport 15/05 , obtenus à partir de conditions expérimentales différentes ; ce qui tendrait à prouver leur généralité.

Les divergences qui apparaissent avec certains résultats du rapport 15/06, notamment ceux présentés à la figure 6 où la tenue sous STTR s'avère pus faible qu'en choc de foudre, seraient imputables, à notre avis , à la forme particulière de l'onde utilisée, (fig. 1-C du 15/06) .

Il s'agit en effet d'un échelon de tension de temps de montée de l'ordre de 10 ns , se prolongeant au-delà de 2 µs , et sur lequel se superpose une oscillation àhaute fréquence (40MHz) d'amplitude relativement faible. Par conséquent , la durée pendant laquelle la tension appliquée se trouve au dessus du seuil d'initiation de la décharge est nettement supérieure à celle correspondant à une onde de foudre de même amplitude. Donc, si l'on se réfère au concept de volume critique, l'amplitude de la STTR sera plus faible que celle de l'onde de foudre à probabilité d'amorçage donnée.

En conclusion, et pour répondre à la question 2 du rapporteur spécial, je dirai qu'il existe d'ores et déjà un ensemble de preuves expérimentales qui démontrent la capacité de l'essai au choc de foudre à garantir la tenue sous STTR, et qu'un essai plus spécifique ne semble pas utile.

Mr. W. BOECK (Fed. Rep. of Germany)

Two different breakdown mechanisms caused by switching operation are described in paper 15-06 and were discussed by different speakers. Of course both are important and have to be considered.
Extremely low breakdown values were observed by the VFT-breakdown in case of needle shaped protrusions at the inner conductor as reported in paper 15-06. But in some publications and contributions of the podium discussion a much smaller reduction of the breakdown voltage in case of VFT overvoltages has been reported. By brand new research results /1/ this seemingly contradictory statements can be easily explained.
The breakdown in SF_6 is normally caused by a stepwise propagating leader channel with a pressure depending stepping frequency. In case of a VFT overvoltage besides the amplitude the frequency of the oscillation seems to be of importance for the breakdown. This oscillation consists of many components due to the manifold surge reflections and refractions at different components of the GIS. Expecially all those oscillation components seem to promote the leader channel development which exceed the leader stepping frequency. For low gas pressures and the belonging low leader stepping frequencies there are more VFT oscillation components beyond this stepping frequency than for higher pressures. Extremely low VFT breakdown values are therefore either given for VFT overvoltages with extremely high oscillation frequencies or in case of low gas pressures. Taking into account this general coherency there are no contradictions at all between the different results reported.
Additionally many VFT phenomena can be explained satisfactorily.

1. If there are only negligible VFT oscillation components with frequencies beyond the stepping frequency as it is often given for normal gas pressures between 4 and 5 bar the VFT oscillation becomes ineffective for the leader channel promotion and the VFT breakdown voltage equals the breakdown voltage of the not oscillating LI. The LI is therefore well adapted for testing.
2. Due to the reflections at the adjacent components high VFT oscillation frequencies (Fig.1(1)) are mainly observed in the vicinity of the operated disconnector (DC). As experienced in practise the lowest breakdown values are therefore given in this part of the GIS. In the main part of the GIS (Fig.1(2)) due to the refraction process at an internal component (CB) the oscillation frequencies are reduced. A much higher reduction takes place at the bushing (B) leading to a considerably reduced oscillation frequency (Fig.1(3)) of the external transients.
3. During tests at site secondary breakdowns are sometimes caused due to VFT. In case of breakdown during tests VFT are generated in a similiar way like during disconnector operation. At special locations of the GIS i.e. open ends especially high VFT amplitudes are caused which may lead to such a secondary breakdown. Even more than one subsequent breakdown was observed. Especially in case of resulting non restoring insulation faults the test procedure may be much complicated. In order to reduce these effects the at site testing voltage should be restricted to at least 80% of the belonging withstand level.

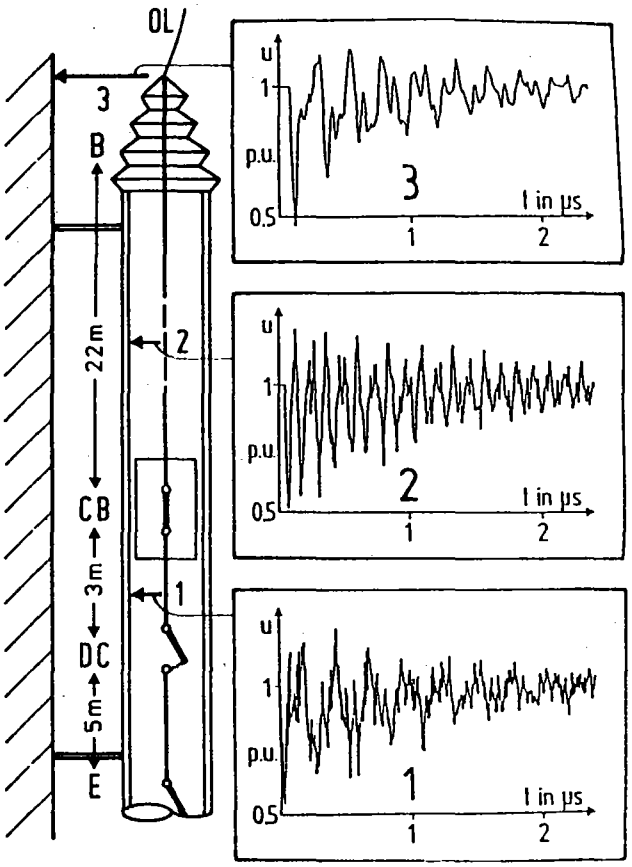

Fig.1 VFT development
1 In the vicinity of the disconnector (DC)
2 In the main part of the GIS
3 External VFT at the overhead line (OL)

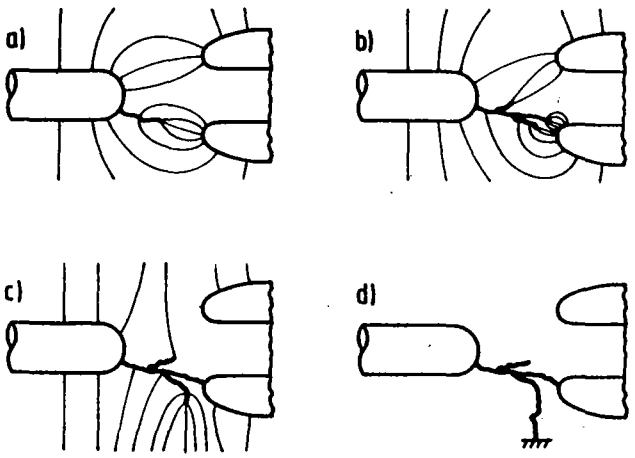

Fig. 2 Flashover to ground due to leader branching during disconnector operation

4. During switching operation flashovers to ground out of the striking spark were observed. These phenomena are caused by leader branching during the spark development (Fig. 2b). When one of the leader branches reaches the opposite electrode (Fig. 2c) the prevailing axial field changes over to a radially directed field and a side leader may act like a leader out of a needle shaped protrusion. By the simultaneously created VFT overvoltage this leader is promoted to ground (Fig. 2d). Since the VFT overvoltages have their highest oscillation frequencies in the operated switch itself this leader promotion is very effective and may even lead over big distances to a sparkover to ground as experienced in practise.

5. It has to be emphasised that in case of an adequate disconnector design and a correct GIS insulation system there are no problems at all caused by this VFT breakdown mechanism. The VFT breakdown value in this case equals the LI breakdown voltage. Therefore, the comparetively low VFT stress of normally less than 2 p.u. cannot endanger the insulation. The breakdown caused by the combined VFT and DC stress due to trapped charge, too, is mainly promoted by particles. These problems can therefore be solved in the best way by a sufficient quality during production and installation mainly in the vicinity of the switches, where the insulation level in case of particles and protrusion will be especially reduced.

Alltogether our present knowledge of VFT phenomena allows reasonable explanations of many effects experienced in practise and helps to find methods to prevent them.

/1/ H. Hiesinger, R. Witzmann: Very fast transient breakdown at a needle shaped protrusion. In: GD 88, IX International Conference on Gas Discharges and their Applications, P. 323-326, 19th - 23rd September 1988 in Venedig

Mr. G.F. LUXA (Fed. Rep. of Germany)

In general good agreement between reported tests of V-t characteristics is obtained. Some contradictory results are mainly due to differences of test arrangements and kind and position of irregularities and of VFT frequencies.

Test on GIS equipment with an unintended surface defect (protruding particle) show little influence on AC and switching impulse withstand but strong influence on VFT breaking voltage, all in consistency with experimental results.

A comparison of the results of impulse voltage tests and the range of breakdown voltages for very fast transients is given in Figure 1 for the cases of correct condition and with a protruding irregularity.

Curve 1 and Range A present the well known characteristic in the case of correct condition with increasing withstand values for shorter times to crest. The irregularity for curve 2 and Range B was due to the protruding irregularity. In this case the slope is contrary to that of the correct arrangement. The withstand values reach remarkably low values and go down to 25% of the full lightning impulse voltage.

The investigations have shown that a steep fronted voltage test could prove the absence of any such dangerous irregularities and will lead to a further increase of reliability. These results are the background for improved site testing with additional impulse tests with a front time of about 10 µs.

As VFT withstand normally is superior to lightning impulse (LI) withstand no specific VFT test is proposed as standard. LI-test should be kept without reduction of the present voltage factors. A more complexed testing may be justified for the disconnector as VFT stresses are most critical in the vicinity of this equipment.

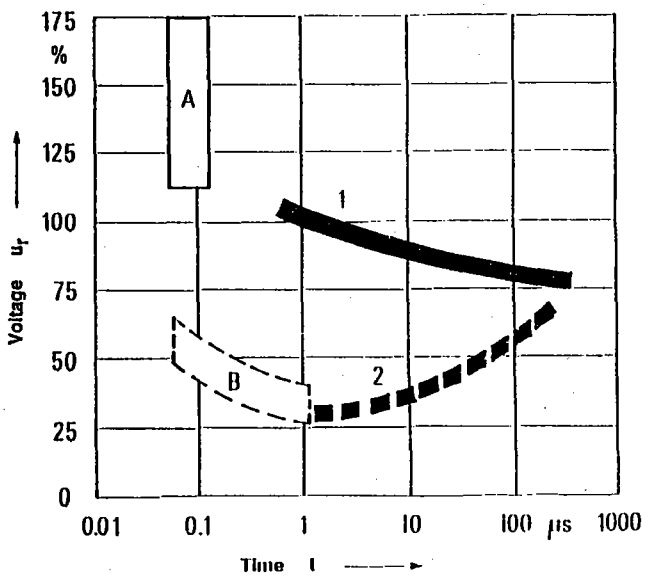

Fig. 1 Relative voltage u_r dependent on time to crest or to breakdown t of SF_6-insulated bus duct section, influence of protruding irregularity

Impulse withstand voltages for bus duct section
1 correct condition
2 with protruding irregularity

Range of breakdown voltages for very fast transients
A correct condition
- streamer breakdown
B with protruding irregularity
- leader breakdown

23-00

PART OF SPECIAL REPORT FOR GROUP 23

(Substations)

by

F. SCHERER *
(Special Reporter)

1.2 Preferential Subject 2:

Grounding and earthing in substations and power stations needs a special attention to match the earth fault currents and their danger to operators and secondary circuitry. Additionally the effects of fast transient voltages caused by switching phenomena, especially in connection with GIS, and lightning strokes can affect secondary equipment especially if electronic devices are used.

Preferential Subject 2 is defined as follows:

"Grounding and earthing in substations and power stations. Effective avoidance of unpermissible induction voltages of low and high frequency on primary components and auxiliary systems. System neutral grounding techniques."

3.2 Questions to Preferential Subject 2

"Grounding and earthing in substations and power stations. Effective avoidance of unpermissible induction voltages of low and high frequency on primary components and auxiliary systems. System neutral grounding techniques."

As the subject fast transient overvoltages is to be discussed in a separate combined session during the 1988 Conference, we limit ourselves to two questions on the phenomena of transient ground potential rise and its attenuation which are of special interest for the practical substation designer.

Attenuation of the Transient Ground Potential Rise

Question 2.1

The optimum remedy for attenuation of the transient ground potential rise (TGPR) and associated effects changes often with the substation configuration and type (GIS, AIS) and depends on factors such as type of secondary installation (i.e. electromechanical or electronic control and protection), system voltage etc. What are the considerations that arise in choosing the optimum ratio between effectiveness and cost of the necessary measures? Is a probabilistic approach appropriate? Is the actual knowledge of TGPR and associated effects sufficient to establish the necessary remedial measures in all practical configurations? Can delegates comment on the measures proposed in papers 23-06 and 23-10 or do they have other suggestions?

Question 2.2

Optimization of remedial measures pre-supposes some quantitative knowledge about the reduction of very fast transients (VFTs). Dependent on the measures applied paper 23-10 shows a digital computational procedure to forecast crest values and curves of VFT on enclosures and earthing systems of GIS. What accuracy may be obtained with such computer models? Are there other computer programs available which are able to handle generally applicable models? How much can such computer programs contribute to a proper selection of remedial measures for the reduction of the TGPR and associated effects? Where are the limits?

---

* Sprecher Energie AG, 5001 Aarau, Switzerland

International Conference on Large High Voltage Electric Systems

112, boulevard Haussmann — 75008 Paris

1988 Session — 28th August - 3rd September

O

23-06

Pref. Subj. 2

SUBSTATION EARTHING WITH SPECIAL REGARD TO TRANSIENT GROUND POTENTIAL RISE DESIGN AIMS TO REDUCE ASSOCIATED EFFECTS

Paper presented in the name of Study Committee 23 (Substations)

by

H. AANESTAD, O. DETER, H. RÖHSLER**,
J. LEWIS, A. STRNAD*

Abstract: This paper presents practical hints to the substation engineer on how to reduce transient ground potential rise (TGPR) and associated effects. The measures reported concern both the lay-out of the earthing system and the secondary installation; they are supplemented by recommendations on how to improve the secondary equipment in order to avoid maloperation caused by TGPR.

Keywords: transient ground potential rise - earthing - switching - lightning - shielding - coupling - secondary installation - secondary equipment - test procedure

1. Introduction

In recent years the transient ground potential rise phenomenon has become a more and more important subject of discussions and studies /1/. It was the broad application of gas-insulated substations (GIS) and associated experience with TGPR-problems that intensified the work in this field; the introduction of electronic equipment in substations has also led to an increased sensitivity of secondary devices.

Though the keyword "TGPR" is associated especially with GIS breakdown phenomena this paper will additionally cover ground rise effects in air-insulated substations (AIS).

Recommendations and measures to reduce TGPR and its influence on secondary equipment have been given in previous papers /2,3,4/. It is the aim of this paper to review TGPR-problems occuring in relation to the lay-out of the earthing system and to summarize recommendations on how to reduce TGPR and the associated effects.

To receive detailed information a questionnaire has been sent out to the members of Study Committee 23; it has been answered by 60 respondents from 18 different countries. The great number of respondents that answered the questionnaire and the detailed information represents a great interest in the topic of TGPR.

The result of this questionnaire is the basis for the investigation presented.

* The authors wish to thank the members of WG 23.03, WG 23.04, and WG 23.05 for their assistance in the preparation of this paper

2. Origin and consequence of TGPR

TGPR is caused by high frequency events; the mechanisms associated with these phenomena differ significantly from those to be observed with power frequency events. Sources of TGPR can be

a direct lightning strokes to earthed components
b operation of lightning arresters
c phase to ground insulation faults
d discharges between switch contacts during switch operation

These events are associated with currents fed into the earthing system. For occurrences a, b these currents will have rise times of up to 100 ns and amplitudes in the range of some kA to some 100 kA depending on the lightning parameters. A breakdown of the insulation (c, d) whatever the cause, has rise times up to 50 ... 200 ns for air insulation and 3 ... 20 ns for SF_6-insulation; depending on these rise times steep currents will be fed into the earthing system.

The radiation of electromagnetic waves caused by insulation breakdown is not a topic of this paper; however, GIS travelling waves may cause severe TGPR as soon as they leave the enclosure, e.g. at the GIS/air-bushing /2/. This effect is most pronounced with GIS disconnector operations.

The high frequency currents cause local transient potential rise in the earthing system due to

- high impedance of the earthing grid
- high impedance of the earth connection from the device to grid, the inductance comes up to approx. 1 μH/m
- short rise times of the events and a travel speed of 0,3 m/ns giving high voltage differences in short travel distances.

An earth connection of 1 m length has an impedance ωL of about 60 ohms for frequencies of 10 MHz and has been observed to give rise to high TGPR.

The consequences of TGPR are wide-spread; as local potential differences cause currents in cable screens and cabinets they are able to affect the screened circuits. Earthed components may have potential differences that in excess can result in flashovers between these components.

** EVS, POSTFACH 158, 7000 STUTTGART 1, REP. FED. D'ALLEMAGNE

These effects may reduce the overall reliability of substations and that is why special measures to avoid TGPR related disturbances are necessary.

Whilst an adequate lay-out of the earthing system will reduce TGPR, a total elimination is not possible. Therefore measures at the earthing system have to be supplemented by measures in the installation in order to reduce the coupling into secondary circuits. A proper lay-out will guarantee TGPR related secondary voltages that do not exceed those transmitted via the measuring transformers directly into the secondary cables.

Lastly, as the effect of the disturbance can be estimated, the withstand capability of the secondary device can be specified thus avoiding destruction and maloperation of secondary equipment due to TGPR effects.

3. Experience with transient ground potential rise

More than one third of the contributors that answered the questionnaire reported experience with transient ground potential rise.
The problems reported are mainly related to switching events in GIS and atmospheric events in air-insulated substations. There were also contributors that reported effects similar to TGPR, but were unable to verify the problems due to lack of evidence.

The experiences collected by the questionnaire are described in the following sections and also the solutions that have been adopted by the contributors to eliminate disturbances.

3.1 Lightning phenomena

There was only a minor number of respondents who reported experience with TGPR problems caused by lightning strokes in AIS. The experience concerned strokes to earthed components in substations, i.e. lightning protection facilities.

TGPR due to strokes to earthed components in AIS and its consequence ranges from maloperation of alarm indicators and direct intertripping to the damage of sensitive equipment and control circuits. First and most important measure adopted is an improvement of the earthing of lightning protection devices, structures, lightning poles, and radio towers which reduces TGPR at its origin. Additionally secondary equipment subject to maloperation has been desensitized using voltage limiting devices.

It has also been reported that potentials transferred by a control cable between neighbouring substations resulted in damage to control equipment. This problem has been solved by two buried earth wires in parallel to the cable which take over the greater part of the current from the control cable screen and reduce the induced voltages.

The described measures reduce TGPR and its effect on the equipment. When adopting a measure of this type there is no knowledge about the quantitative reduction that is achieved because atmospheric events are non-recurring phenomena, unlike switching events. However it is possible to estimate the transient secondary voltages caused by lightning phenomena for a given substation by a combination of measuring techniques and mathematical methods. For further information see Appendix.

3.2 Switching phenomena

Most TGPR effects have been observed during switch operation and GIS disconnecter switching gives rise to severe and frequent TGPR.

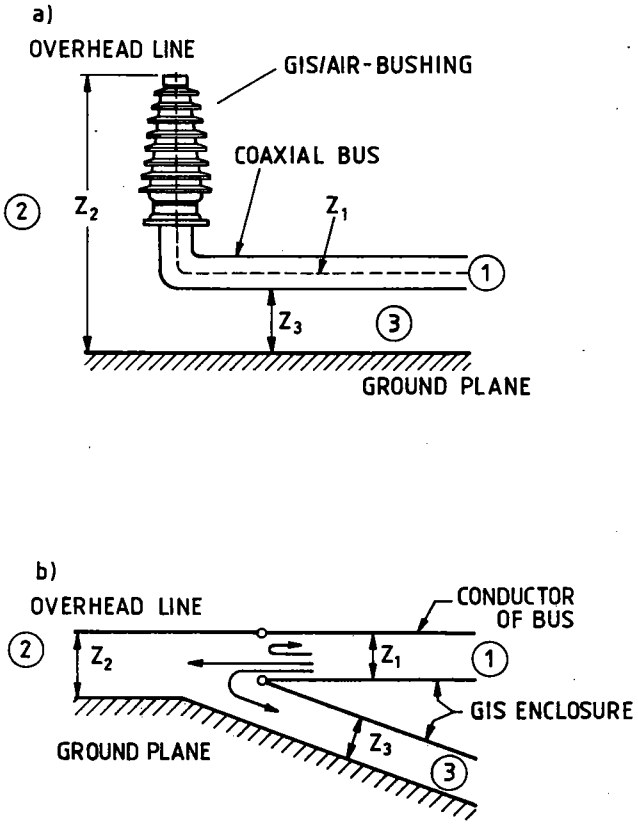

Fig. 1: GIS/air-bushing and bus modelled as transmission lines /2/

a Configuration investigated
b Schematic model

Z_1 Surge impedance of GIS bus duct
Z_2 Surge impedance of overhead line-ground system
Z_3 Surge impedance of enclosure-ground system

During one operation of a disconnecter there are up to 100 discharges between the switch contacts of which the most critical follow eachother in not more than 10 ms. The maximum restrike voltage between contacts is twice the phase to ground voltage and the risetime of the breakdown can be as fast as 50 ... 200 ns for air-insulation and 3 ... 20 ns for SF_6-insulation. It is this short risetime and the low damping within the coaxial system that causes problems particularly with GIS. It has also been suggested to provide small insertion resistors for the disconnectors to reduce switching related TGPR; however this measure is up to the manufacturer rather than the user.

Switching related TGPR phenomena occur as soon as the waves travelling from the switching contacts along the GIS are able to leave the enclosure; insulating flanges, SF_6/cable terminations and the GIS/air-bushing are typical locations, the latter showing the most significant sheath discontinuity. As shown in Figure 1 the wave leaving the enclosure moves on between ground plane and enclosure and between ground plane and overhead line. It is the refraction of the waves from the initial coaxial bus to the enclosure-ground system that defines the basic mechanism of TGPR.

One effective measure adopted is the use of metallic conducting sheets placed between enclosure and ground at the GIS/air-bushing (Figure 2); the sheet, well bonded to the enclosure and to the earthing system, offers a low impedance connection to the refracted wave. Compared to a single earth wire from enclosure to earth this sheet obviously shows an improved performance due to better geometrical arrangement to the refracted wave. Fig. 2 illustrates that the refracted wave is kept out of the substation by the shield and the currents associated do not affect the earthing within the GIS. A contributer reported that TGPR is reduced to about 25 % of its original values by this method.

In general and especially with GIS the adoption of short straight earth connections with low impedance is necessary; this is emphasized by many respondents reporting about TGPR problems that were solved by simply improving earth connections that had been performed in a less favourable way.

Connections between enclosures, e.g. at a GIS/transformer interface, have been performed by 6 to 8 strips arranged circumferentially to avoid voltage differences and discharges. Where a connection was not possible due to other reasons (circulating currents, isolated cable screens, etc.) an effective measure was to bridge by voltage limiting devices, if necessary arranged circumferentially at the enclosure. It has been reported that the devices adopted were preferably of the varistor type, i.e. devices without spark gaps.

4. Lay-out of the earthing system and the secondary circuits with special regard to ground potential rise effects

In one way or another TGPR has influenced the lay-out of the earthing system and the secondary circuits. The respondents reported improvements that are based on experience with ground potential rise and that have proved to reduce the effects occurring. Measures have also been reported that have a preventive character and have been derived from theoretical considerations.

The measures concern three areas:

- the source
  while events causing TGPR cannot be avoided a reduction of the ground rise associated can be achieved by proper measures
- the coupling
  local potential rise in the earthing system may be coupled into secondary circuits and the coupling factor can be reduced by measures in the installation

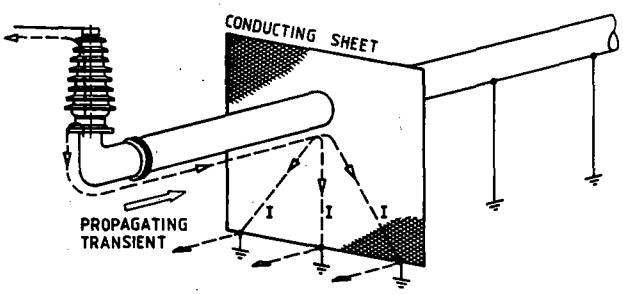

Fig. 2: Adoption of conducting sheet at the GIS/air-bushing

I currents caused by refracted wave

- the drain, i.e. the secondary device
  desensitizing the secondary equipment by adopting it to the special electromagnetic environment in substations including a proper test

The detailed description given by the contributors concerning

- the lay-out of earthing grid and earth connections
- the lay-out of the installation
- the experience with ground potential rise effects

allows us to summarize practical hints and recommendations in order to avoid harmful experience. A summary is given hereafter.

4.1 Measures to reduce TGPR - the source

4.11 Air insulated substations

The measures recommended for lightning phenomena in AIS may also be valid for air-insulated facilities at GIS, for instance open-air arrestors at the GIS/air-bushing, etc.

There are general measures required for insulation coordination that also have a beneficial effect on frequency and severity of lightning stresses to substation earthing:

- HV overhead lines are generally equipped with one or more shielding wires according to the requirements of insulation coordination. Line shielding has the advantage that high current strokes collected by the lines are fed to earth via the shielding wires and the towers and affect the substation earthing to a lesser extent. TGPR problems caused by strokes to the line are therefore kept away from the substation earthing to a great amount.
- Direct strokes to the conductor are limited in amplitude by line shielding and this reduces arrestor operations. Consequently the frequency and severity of TGPR caused by arrestor operation within the substation is also reduced.

  For the protection of the HV substation itself lightning poles and/or shielding wires are installed. It is an advantage of the shielding wires fixed to structures that lightning stroke currents are fed into the earthing system via multiple injection points. For lightning poles all the stroke current is fed into the earthing grid at one concentrated point, offering less favourable conditions with respect to ground rise.
- To achieve a low earthing impedance arrestors, structures, poles, etc. are connected to the earthing grid by at least two connections. It has also been reported that especially in the area of arrestors and lightning poles a narrow meshing of the earthing grid is adopted. This earthing is occasionally improved by additional rods driven into earth.
  A good measure is to bond the device into the earthing grid at a crossing point of earth conductors, thus getting four links or to form additional meshes by the links (Fig. 3).

Special care should be devoted to the earthing grid below VT, CT, etc. It has been reported that earthing grids have sometimes been improved by adding interties and/or driven rods to achieve low earthing impedance at these locations.

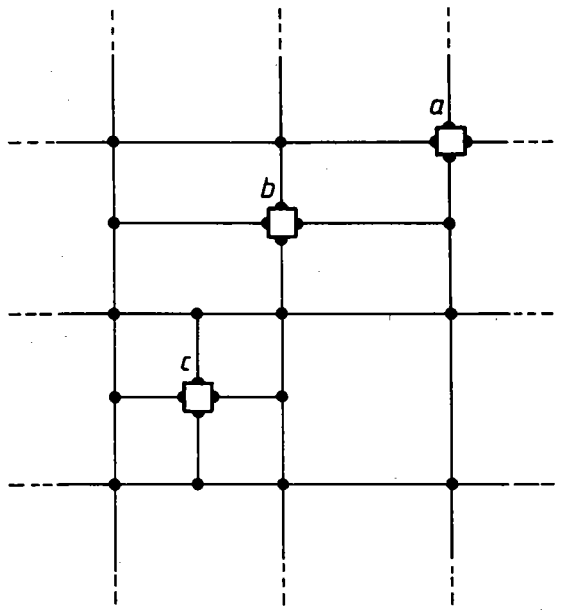

Fig. 3: Connection of equipment to the earthing grid: insertion at a crossing point (a) or by additional interties (b, c)

4.12 Gas-insulated substations

The measures recommended in the following are valid for GIS related TGPR. For air-insulated facilities (see 4.11) it must be emphasized that improved line shielding - adopted with respect to insulation coordination - significantly reduces TGPR within the substation caused by strokes to the lines.

4.121 Earthing technique

Steps to reduce ground potential rise in GIS are generally dependant on the earthing philosophy of the substation. Multiple point earthing of the enclosure is a favourable technique with respect to TGPR. When power frequency currents have to be suppressed, insulating flanges may be needed and sparking across the flanges can occur during disconnector switching. Theses sparks may need to be suppressed. Single point earthing to avoid circulating current and for example to facilitate fault monitoring is a configuration more sensitive to TGPR but has been applied successfully.

General measures having a beneficial effect on the ground potential rise are:

- straight earth connections from enclosure to grid
  The length of the earth connections, determined by the enclosure height above ground, favours low constructions with respect to TGPR. Increasing the number of earth connections is beneficial as soon as their length exceeds the spacing between the leads. Metallic supports can often be used to achieve proper earth connections.

- dense earthing grid below the GIS
  To allow proper attachment of the various earthing connections a dense earthing grid is recommended, if possible connected to the reinforcement of the concrete.

4.122 Shielding technique

The term "shielding technique" in the context of GIS denotes measures that prevent breakdown initiated electromagnetic waves from leaving the enclosure and stressing the enclosure-ground system.

- Shielding at the GIS/air-bushing (Fig. 2); for enclosures led through walls a shield can be adopted economically by bonding circumferentially by 6-8 strips to the enclosure. In addition it should allow multiple connections to the earthing grid. The thickness of the shield is only a mechanical problem due to the small skin depth for the frequencies in question. Experimental studies /2/ indicate that steel, aluminium and copper sheets , 0.5 mm thick, worked well.

  For GIS not installed in a building it is advantageous to use the support of the GIS/air-bushing to achieve a similar shielding.

- Connections between enclosures, if not directly interconnected e.g. at the GIS/transformer interface, have to be performed by 6-8 strips arranged circumferentially and kept as short as possible.

- Where a direct interconnection of the enclosure is not possible (isolating flanges, isolated cable screens, external current transformers) the insulation is to be bridged by 6-8 voltage limiting devices of the varistor type instead. Careful choice of the characteristics must guarantee that the varistor is not affected by power frequency events; sufficient energy absorbtion capacity is important for devices mounted at the GIS/cable interface.

The described bridging is a special kind of shielding applied to insulated flanges because it keeps the electromagnetic wave initiated by breakdown within the enclosure. For varistor bridged flanges the energy leaving the enclosure is determined mainly by the clamping voltage of the voltage limiting devices, when installed with negligible effect of lead wires.

4.2 Measures to reduce the coupling

Reducing the coupling by measures in the installation has a beneficial effect for both TGPR and ground potential rise caused by lightning. It has to be emphasized that the recommendations given in this chapter are restricted to coupling mechanisms initiated by ground potential rise.

The general measures that produce favourable conditions are

- use of shielded secondary cables (low coupling impedance, low screen resistance)

- separating secondary cable routes from interfering sources

- additional earth wires laid in cable trenches connected to the earthing network at the two ends and additionally, if possible, at a few points along their route

- shielding techniques can be applied to operation rooms and buildings. An economic shielding is achieved by connecting the concrete reinforcement to the earthing grid. Overall shielding of rooms (floor, walls, ceiling) by metallic sheets is an expensive measure and requires that special care must be given to internal noise sources (lights, etc.). For secondary equipment designed for use in HV substations overall shielding of rooms is not necessary.

4.3 Measures taken on secondary equipment

The equipment in HV substations has to operate in a special electromagnetic environment. Test procedures that are able to simulate the stresses allow equipment to be constructed with an adequate withstand capability thus avoiding destruction and maloperation e.g. by TGPR

effects. However, such test procedures are not generally applied to secondary equipment though the adoption of voltage limiting devices to desensitize equipment is common.

- Best way of ensuring the withstand capability of secondary devices is to apply adequate test procedures that simulate the real stress over the whole frequency range. IEC test procedures like IEC 255 cover only a part of these stresses; an adequate test procedure has been presented in /4/. The necessity of testing the withstand capability grows as more sensitive electronic equipment is installed in substations. However, tests generally have to be applied in the design stage, when an economical solution can be achieved. Consequently a certain withstand capability has to be fixed when commissioning.

- For modifying equipment in service the application of voltage limiting devices is common. The limiting devices should be of the gapless type and be mounted at the inlets, with short connections and sufficient energy absorbtion capacity.

5. Summary and conclusions

This paper gives practical hints to the substation engineer on how to design future substations and to modify substations in service in order to avoid problems with transient ground rise effects. The measures summarized are based on the experience collected by an international questionnaire and cover the typical problems. They include measures in the secondary installation to reduce the coupling effects and on the secondary equipment as the drain of the disturbances.

Experience has shown that it is a proper lay-out of both earthing system and secondary installation that achieves the most economic solution.

These measures are to be supplemented by an adequate withstand capability of the secondary equipment. However, the standards available cover only a part of the real stresses; that is why there is still a need for an agreed test procedure that covers the real stress over the whole frequency range. The introduction of electronic equipment in substations and the increased sensitivity of such devices creates an urgent need to overcome this deficiency in the standards.

References:

1. R. Boersma: Transient ground potential rise in gas insulated substations with respect to earthing systems. ELECTRA No 110, January 1987

2. E.P. Dick, N. Fujimoto et.al.: Transient ground potential rise in gas insulated substations - experimental studies, problem identification and mitigation. IEEE Trans. PAS 101, Oct. 1982, pp. 3603 - 3619

3. H. Röhsler, A. Strnad: Noise sources and interference values in High Voltage Substations. Conference on Electromagnetic Compatibility, Zürich 1985

4. A. Strnad, C. Reynaud: Design aims in HV substations to reduce electromagnetic interference (EMI) in secondary systems. ELECTRA No 100, May 1985

5. M. Fischer, A. Strnad: Bestimmungen der bei Blitzeinschlägen zu erwartenden transienten Überspannung in Sekundärkreisen von Hochspannungsschaltanlagen. Elektrizitätswirtschaft 82 (1983) 87 - 91

Appendix

Estimation of transient secondary voltages caused by strokes to earthed components

It is possible to estimate the transient secondary voltages caused by lightning phenomena for a certain substation by a combination of measuring technique and mathematical methods /5/: When discharging a charged overhead line into the earthing system of a substation the discharge current and the voltages at selected points of the secondary circuits can be measured (Fig. A). The knowledge of these signals allows the transient response of the system to be computed.

The maximum transient voltages caused by lightning strokes at the selected measuring points can then be calculated by bringing in the lightning parameters. When regarding the distribution of the lightning strokes the result will show the noise voltages at the selected points depending on the frequency of occurrence. Fig. B shows the result of such an investigation; for this example the points M1 and M2 at either side of an isolating auxiliary relais have been chosen for the examination. At the measuring point M1 the voltage of 2700 V is exceeded once in ten years, the corresponding value for M2 is 560 V.

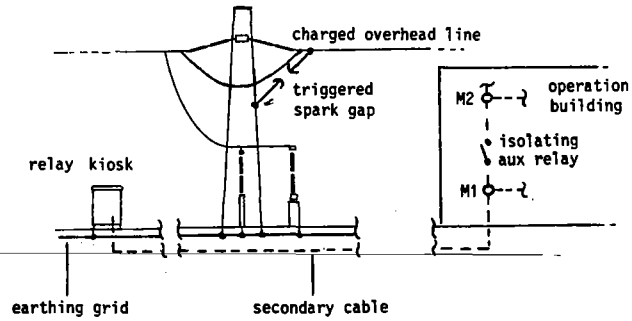

Fig. A: The arrangement

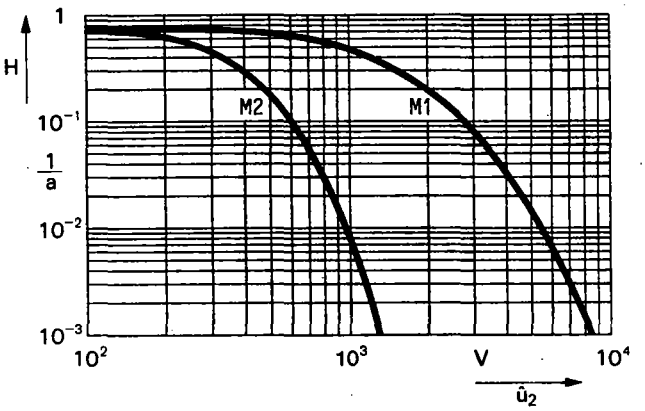

Fig. B: Noise voltages $\hat{u}_2$ in a 420/123 kV air-insulated substation caused by lightning strokes to earthed components

H frequency of strokes producing a noise voltage which exceeds $\hat{u}_2$

M1, M2 measuring points

International Conference on Large High Voltage Electric Systems

112, boulevard Haussmann — 75008 Paris

1988 Session — 28th August - 3rd September

O

23-10

Pref. Subj. 2

ATTENUATION OF FAST TRANSIENTS IN GIS EARTHING SYSTEMS

by

W. BUESCH*, H. STEPHANIDES, T. HEINEMANN

Sprecher Energie Ltd.

(Switzerland)

Abstract

Fast transient overvoltages occurring outside enclosures during switching operations with gas insulated switchgear (GIS) were investigated for system voltages from 72.5 to 245 kV. A programme was developed using special modelling techniques to compute transient phenomena in waveguide systems. Overvoltage behaviour and crest values were then computed at specific points in earthing systems and in the secondary circuits of instrument transformers. For comparison purposes measurements were also made.

Various methods for limiting overvoltages at GIS extremities (i.e. GIS/cable transitions and SF6/air terminations) were simulated and their effectiveness evaluated. The digital computing procedure developed yielded useful supplementary information and led to enhanced assessments of the cost optimisation of the various remedial methods tested.

Key words:

Substation, GIS, switching transients, discontinuities, earthing.

1. Introduction

Over the last 20 years, gas insulated switchgear (GIS) has been used for a wide range of applications. Earthing systems have usually been designed for step and touch voltages on the basis of the earthing failure conditions covered by IEEE 80 or VDE 0141 standards, that is, for phenomena at power frequency and slow transients.

The long practical experience with GIS substations has shown that the above method of earthing system design is inadequate owing to the occurrence of high frequency transients most often caused by the operation of disconnectors and circuit breakers [1,2,3]. The possible consequences of such transients may include non-destructive flashovers in standard type 50 Hz earthing systems and unacceptably high overvoltages in secondary circuitry. Hence it has become necessary to extend 50 Hz earthing systems in order to limit GIS transient overvoltages [4]. Adequate measures are mainly related to GIS discontinuities. In recent years numerous papers have been published on this subject, e.g. [5,6] and suitable remedial measures recommended [7,8,9].

The use of electronics and micro-processors in GIS substations makes further efforts necessary because electronic components and systems are much more sensitive than conventional electro-mechanical designs.

Although numerous measures are successfully applied, the difficulty remains however to choose the optimal remedy technically and economically for an installation already at the design stage.

This contribution shows the method of modelling electrical circuit elements, the estimation of optimal solutions and the comparison with on-site measurements.

2. Computer simulation of fast transient overvoltages in GIS systems

The transient phenomena caused by disturbances and GIS switching operations affect several regions including those within enclosures and sheathing, earthing systems and air insulated conductors and HV cables. The phenomena occurring in all these regions are interrelated at discontinuity points and must therefore be computed simultaneously. To consider their influence without excessive effort, they are only calculated at well-defined points, above all at the ends of the conductors on the nodes of the network. At these terminals only two variables may be exactly defined: the currents i in the conductors and an electromotive force (EMF) e,

* Sprecher Energie Ltd., Power Distribution Projects, 5001 Aarau, Switzerland

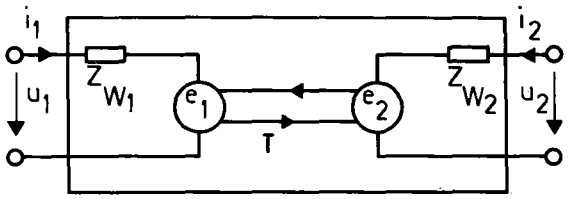

Fig. 1: Equivalent circuit of waveguide element

which effectively represents the influence of all waves in the surrounding field.

The computer program utilized [10] was developed to calculate these currents i and EMF e in an optimum approximation. The use of modern distribution theory [11] achieved high computational stability. Each system of interacting conductors between such terminals is modelled by a waveguide represented by the equivalent circuit shown in Fig. 1. In the present state the EMF in this circuit is approximated as follows:

- the main components are calculated applying the theory of travelling waves in multi-conductor systems;
- additional effects including the attenuation of the waves along the conductors and the interaction between the conductors by intermediate coupling waves are considered in impulse responses; the current curves of all waves are convoluted with such impulse responses.

In this approximation the waveguide is defined by:

- the number n of conductors,
- the matrix of characteristic impedances Z_w for the n-conductor system,
- the propagation time T for each mode of the resultant wave,
- the distribution of the wave currents over the conductors in each of these modes, and
- the impulse responses for each mode of the wave.

Since the voltages u are not directly calculated they are defined by the formula:

$$u = Z_w . i + e$$

Lumped resistors are inserted between the terminals of these waveguides and the nodes representing the ohmic resistance of conductors. Thus arbitrary connections may be modelled. Nodes with terminals of the same waveguide are grouped together. Solving the node equation all interactions between such nodes are considered.

The examples given in Section 3 are waveguides simulated as outlined above using the conductor systems involved, viz.:
- HV conductor submitted to the applied voltage,
- enclosures for the three phases,
- equivalent conductor representing neighbouring earthed structures.

The standard GIS element consists of five conductors in parallel. Rather more complicated multi-conductor waveguides can be used to model items like cable transitions and current transformers. They then comprise additional parallel conductors as illustrated in Section 3.

In the case of the earthing system all conductors are simulated. Parallel conductors a long way from each other, e.g. parts of the earthing system at opposite walls, and conductors or conductor sytems located vertically above each other are simulated individually. On the other hand, coupling is taken into account in the case of conductors that are close together. Flat conductors are replaced by equivalent round conductors. In certain cases the bundle conductor formula is applied.

3. Application: GIS discontinuities

The program outlined above is used to compute fast transient overvoltages such as those occurring at GIS discontinuities. Overvoltages of this kind are essentially caused by electromagnetic waves leaving the SF6 enclosure at discontinuities. The main discontinuities are the GIS/cable transition, the SF6/air termination and the instrument transformers of the GIS. The effects of these sources of disturbance are considered below.

For the present investigation a segregated-phase 110 kV GIS, installed indoors with a double busbar system and 6 bays is considered. The simplified single line diagram (Fig. 2) shows the busbars BB1 and BB2, the coupling bay E1 and the bays E3 and E6. The end of E3 can be either a GIS/cable transition or an SF6/air termination.

Fig. 3 shows schematically for one GIS bay how the system in Fig. 2 was simulated. All elements consist either of one of the 5 conductor systems described in Section 2, or of a similar but more complicated system of conductors. The simulation diagrams for a GIS/cable transition, an SF6/air termination and an instrument transformer with its secondary circuit will be described below.

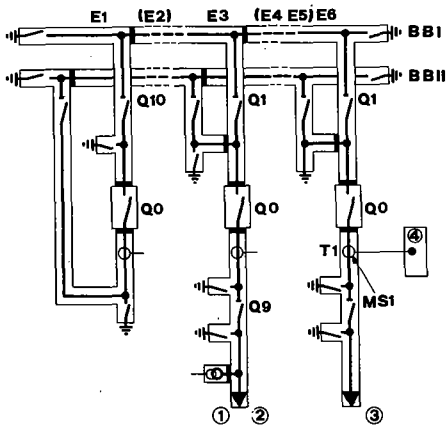

Fig. 2: Simplified single line diagram of 110 kV GIS, segregated phases
MS1 Measurement point in current transformer terminal box
(1) GIS/cable transition, (2) SF6/air termination, (3) HV test transformer, (4) control cubicle

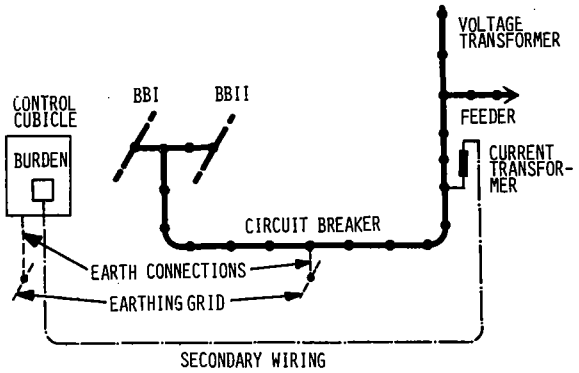

Fig. 3: Single line simulation of a GIS bay
GIS elements

The calculations performed in all cases embrace the entire system, and overvoltages are in principle computed at all points in the earthing system simulated.

All transient voltages u calculated are referred to the reference voltage U_o, this being the voltage between the contacts of the disconnector before sparking over. When sparkover occurs at the crest of the sine wave with a residual voltage of 10 % on the switched busbar, U_o may be assessed to be 1.1 phase-to-earth crest voltage. For the 110 kV system, U_o is thus approximately 100 kV.

GIS/cable transition

Two similar circuits meet at GIS/cable transitions. One is the GIS conductor with current return path along the inside of the enclosure; the other is the cable conductor with current return path along the inside of its sheath. If the enclosure is not coaxially linked to the sheath, a non-enclosed conductor section will inevitably appear between the two enclosed portions. At such discontinuity, transient currents must find their return path through the earthing system giving rise to high overvoltages. As a consequence, flashovers which must be prevented may even occur in extreme cases between the GIS enclosure and the cable sheath.

Fig. 4 shows the cross-section of a GIS/cable transition schematically. The simulation of the corresponding equivalent waveguide system is presented in Fig. 5. The discontinuity appears between the GIS enclosure and the cable sheath. In this example it is bridged by 4 parallel connectors uniformly distributed at the enclosure circumference.

As wave propagation velocities are not the same inside and outside the insulator on the GIS side shown in Fig. 4, this first section of enclosure is simulated by a system of 3 concentric conductors. It is assumed that the intermediate conductor has an extremely high ohmic resistance.

A second section including the end of the stress control cone of the cable is also simulated by a 3 concentric-conductor system.

The third section is the discontinuity itself. The conductor, the stress control cone and the

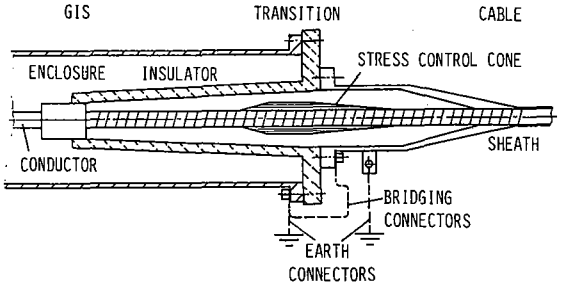

Fig. 4: Cross-Section of a GIS/cable transition

outside of the insulator constitute 3 concentric conductors. They form with the 4 bridging connectors a system of 7 coupled conductors. The radial connector sections are allowed for, as also are the current from these sections inside the enclosure and the cable sheathing in additional independent waveguides. The characteristic impedances of the waveguides were computed for these models using the standard formulae for the self and mutual inductions and the earth and mutual capacitances.

The model was completed by adding the enclosures and the cable sheaths of the two other phases, and also the connections to the earthing grid. Physically, these connections are copper strips 1.5 m long and 20 x 2.5 mm in cross-section.

Using this model for the above 110 kV GIS the transient overvoltages occurring at the GIS/cable transition of feeder E3 were calculated. The system is supplied from the feeder E3 with Q0 open. The short conductor section between Q9 and Q0 is switched with the disconnector Q9. Such switching is likely to produce the highest transients at the GIS/cable transition in service. Simulated transient voltage curves u/Uo occurring at the 110 kV GIS/cable transition between GIS enclosure and cable sheath are shown in Fig. 6 for 2 typical cases. At the open discontinuity, the crest voltage $\hat{U}$ is as high as 0.73 U_o or approximately 73 kV. Flashover may well occur because the dielectric strength of the insulating system incorporated in the GIS/cable transition drops considerably with frequency. Overvoltages in this situation must be reduced.

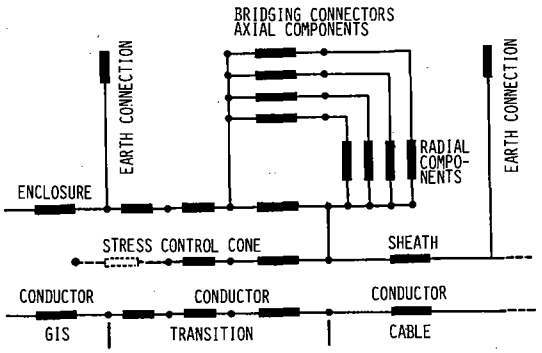

Fig. 5: Single line waveguide simulation of the GIS/cable transition presented in Fig. 4
Waveguide
Boundary between regions with differing dielectric constants

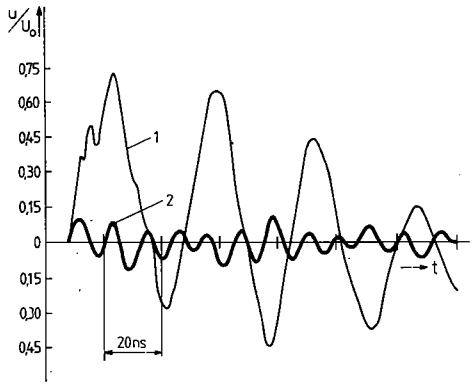

Fig. 6: Simulated overvoltages u/U_o at 110 kV GIS/cable transition between GIS enclosure and cable sheath
1, Discontinuity not bridged but earthed on both sides
2, Discontinuity bridged with 4 flat connectors, length 300 mm, cross-section 20 x 2,5 mm

Additional earth connectors would attenuate such overvoltages only if their inductances were extremely low. In this situation, reducing the connector lengths from 1.5 m to 0.6 m on both sides of the discontinuity would reduce overvoltages by only 4 %, which is quite inadequate. To reduce transient overvoltages in the GIS earthing system, bridging the discontinuity with several connectors is a frequently applied solution.

Fig. 7 illustrates the effect on the crest overvoltages $\hat{U}$ of the number and width of flat connectors. The two curves show that:

- A single connector reduces the crest voltage to approximately one third of that of the open discontinuity;
- The improvement due to adding further connectors gradually diminishes as their total number increases;
- The width of connectors has little effect.

If it is not possible to link the GIS enclosure directly to the cable sheath, the bridging connectors should be replaced by varistors. When calculating overvoltages in this case on the basis of the equivalent circuitry, the non-linear characteristic of the resistors must be considered.

SF6/air termination

When a GIS is connected directly to overhead lines, the transient currents circulate on the one hand between the air insulated HV conductors and the earthing system, on the other hand in the GIS between the HV conductor and the inside of the enclosure. When the disconnector is operated transient overvoltages appear in any case at this discontinuity.

It is often difficult in practice to estimate the overvoltages likely to occur at SF6/air terminations, and this is particularly true when special earthing arrangements have been made.

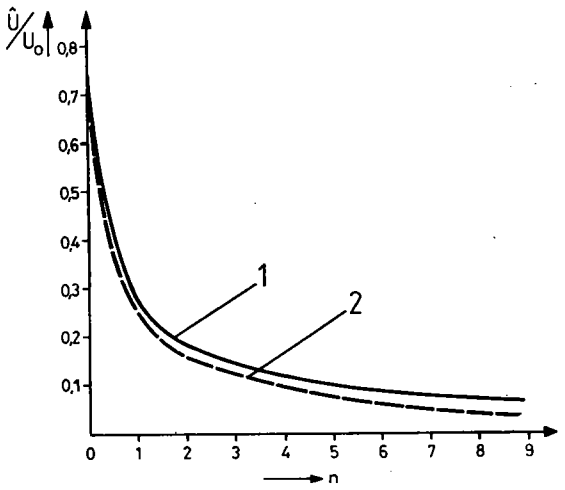

Fig. 7: Effect of the number n of flat connectors on the crest voltage $\hat{U}/U_o$ of transients at the GIS/cable transition for two conductor widths
1 20 x 2.5 mm 2 60 x 2.5 mm

The example in Fig. 8 shows how special earthing systems may be simulated. The figure depicts a 3-phase equivalent circuit simulating an SF6/air termination. A metallic plate has been added at the penetration of GIS enclosures through the wall just ahead of the SF6/air bushings (Table I, Case IV).

The SF6/air termination given in Fig. 8 is simulated as follows:
- the metallic plate by a waveguide with a short propagation time and a low characteristic impedance (a),
- the 4 flat connectors in parallel between the plate and the enclosure by a single waveguide whose characteristic impedance is 25 % of that of each conductor (b),
- the capacitance between the plate and a bushing by a conductor section earthed at one end and coupled to a line element (c).

In addition, the earthing system of the installation was extended to comprise three

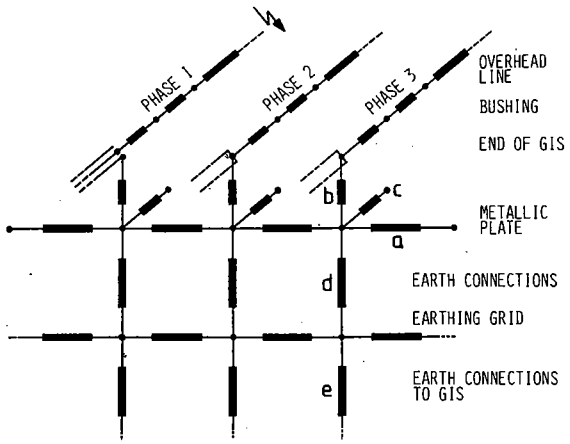

Fig. 8: Three-phase waveguide circuit equivalent to an SF6/air termination with a metallic plate

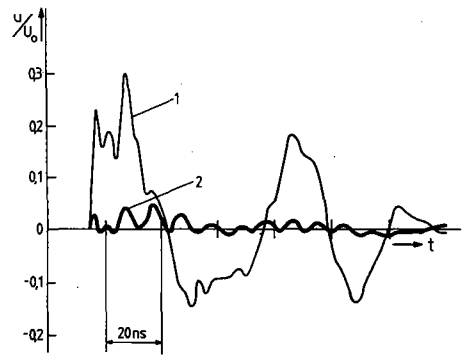

Fig. 9: Simulated transient overvoltages u/U_o at the 110 kV SF6/air termination
1, No additional earth connectors (Case I)
2, With large metallic plate (as Case IV)

additional 60x2 mm copper earth connectors between the plate and the earthing grid (d) and between the earthing grid and the circuit breaker (e).

With reference to Fig. 2 the feeder of bay E3 is now terminated with an SF6/air bushing placed outside on the building wall. Again Q9 is switched and Q0 is open.

The following earthing system arrangements are considered:

Case I: No additional earth connectors;
Case II: Broad connector plates between phase enclosures;
Case III: Connection of ends of phase enclosures including connection with earthing grid;
Case IV: Large metallic plate connected four times to each phase enclosure and three times to the earthing grid.

Table I and Fig. 9 summarize the results of calculation. The voltage values u are related to an ideal earth potential.

The following conclusions may be drawn from the given results:
- Without additional earth connectors, the crest voltage $\hat{U}$ rises to about 30 % of U_o (Case I);
- Inserting broad connector plates between the phases (Case II) or connecting these enclosures to the earthing grid (Case III) limits the crest voltage $\hat{U}$ to approximately 15 % of U_o;
- Maximum overvoltage reduction to less than 10 % of U_o is obtained by inserting a number of parallel earth connectors from the bushings to the earthing grid and a large metallic plate (Case IV).

The values stated above may be used to judge the effectiveness of the various remedial measures. At the lower end of the range of voltage ratings, i.e. 72,5 kV-245kV, more simple and therefore more economical solutions will usually be sufficient (e.g. Cases II, III).

Current transformers and secondary circuit

Instrument transformers in GIS systems represent a further source of fast transients that will propagate outside enclosures. The overvoltages generated depend on the design of the transformer

CAS/CASE	$\hat{U}/U_o$
I 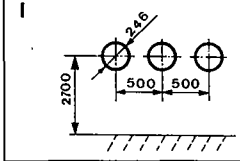	0,33
II 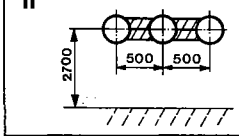	0,15
III 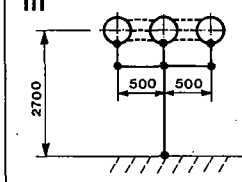	0,17 0,10[1)]
IV 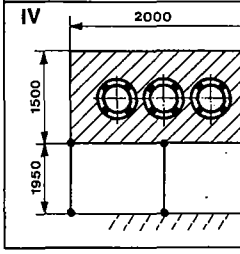	0,06

Table I: Effect of various arrangements on crest voltages $\hat{U}/U_o$ of transients at the 110 kV SF6/air termination
1) With additional broad connector plates for Case II

and the associated secondary circuitry, including the earthing system provided.

The simulation example also comprises the secondary circuit with the burden Z. The equivalent waveguide system used is shown in Fig. 10. The secondary winding lies between a metallic screen and the surrounding enclosure. Its self-capacitance and also the capacitances with the metallic screen and the enclosure are simulated by a waveguide. The inductance of the winding is simulated by another series-connected waveguide. Both are connected via conductors to the measuring circuit. This contains two wires connecting the load Z in the control cubicle. One of the wires is earthed in the cubicle. The sheath of the measurement cable is earthed via short conductors at both ends. The secondary is not earthed in the transformer itself.

The factors determining the transient overvoltages occurring in the secondary circuit are essentially:
- The voltage induced in the winding by the conductor. This is a low frequency component generated by the inherent oscillations of the conductor current;
- Voltage transients at high frequencies transmitted to the measuring circuit by the voltage divider, which consists of the metallic screen, the winding and the enclosure.

The simulation described above was used for calculating transient overvoltages appearing in

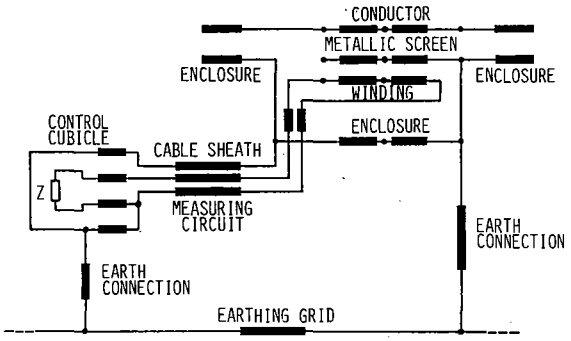

Fig. 10: Single-line waveguide equivalent to a current transformer with secondary circuit

the secondary circuit of a current transformer. In addition measurements on site were carried out in a 110 kV GIS and the results compared.

The GIS shown in Fig. 2 was single-phase-fed from the feeder of bay E6 using an HV metal enclosed test transformer. The circuit breaker Q0 was closed and busbar BB1 connected through disconnector Q1/E6. The transient overvoltages appearing in the secondary of current transformer T1/E6 were measured at point MS1 and also computed. The results are shown in Fig. 11. The supplied voltage was 42 kV rms, that is, approximately 2/3 of the installation's phase-to-earth rated voltage. The measurements indicated the existence of an almost linear relationship between overvoltage amplitude and supply voltage. Therefore, the measured overvoltage of 500 V crest value corresponds to 760 V at the system rating of 110 kV.

From Fig. 11 it can be seen that the calculation provides a remarkably good approximation to the oscillations measured. Initially, the high frequency components predominate, but after about 300 ns their attenuation is such as to permit the appearance of lower frequency oscillations of the system. The essential transmission mechanisms may thus be observed.

Comparing the two curves shows that it is difficult to predict the occurrence and extent of isolated peak voltages of a few nanoseconds duration. Such peaks usually result from the superimposition of voltages from the conductor and natural oscillations generated inside the current transformer. The amplitudes of the voltage peaks may be affected considerably by small variations in transformer circuit parameters, viz.: capacitance and inductance of measuring cables, load resistance and inductance, inductance of the connections between winding and measuring cable wires and between enclosure, cable sheath and control cubicle earth connectors.

Despite these difficulties, the current transformer model described enables adequate estimates to be made of the main effects of the transformer, measuring cable, load and earth connectors on the transient overvoltages appearing in the secondary circuit.

The examples presented in Section 3 demonstrate that the investigated simulation technique is

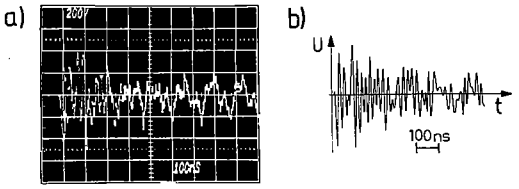

Fig. 11: Transient overvoltage (common mode) at current transformer's secondary terminal (MS1, Fig. 2) during switching operation
a) measured b) calculated

quite useful to estimate the effects of many possible measures in GIS earthing systems, thus enabling an optimisation between effectiveness and cost.

4. Conclusions

The computer results and long practical experience with gas insulated switchgear in the 72.5-245 kV voltage range lead to the conclusions set out below:

The proposed computational procedure and modelling technique can in principle be used to simulate and evaluate most methods of transient overvoltage attenuation in GIS earthing systems. The accuracy of the results will depend on the care taken to simulate the system. In many cases, estimates accurate enough for practical use may be obtained quite simply. This is especially true of GIS feeders with their transition to cables and overhead lines.

System configurations vary considerably and quite often may need to be simulated individually. This is the case of earthing systems. Standardization amongst manufacturers and users of the methods used for overvoltage limitation would be highly desirable. An important contribution in this respect can be made by computer models, as is shown in this paper.

GIS/cable transition

The discontinuity between the GIS enclosure and the cable sheath should always be bridged by at least one flat connector. Without bridging, the transient overvoltages caused by switching operations may reach crest values resulting in unacceptable flashovers.

If direct bridging is not allowed, the flat connectors should be replaced by varistors.

SF6/air termination

With phase-segregated GIS and unless special preventive measures are taken, transient overvoltages at this GIS discontinuity may be about a third of the rated voltage of the installation. Recommended remedial action includes the provision of:

- broad connectors between GIS phase enclosures at their feeder ends,
- additional earth connectors from the bushings to the earthing grid.

In critical situations a large metallic plate multiple earthed and installed at the penetration of GIS feeders through the building wall is most effective.

The following general rules can be identified:

- In the absence of preventive measures, overvoltages at the GIS/cable transition will in general be higher than those at SF6/air transitions;
- At SF6/air terminations overvoltages are strongly moderated by the use of additional connectors to the earthing grid. On the contrary, the effect of such connectors at SF6/cable transitions is rather small. Bridging connectors between the GIS enclosure and the cable sheath are the most important;
- The desirable reduction in overvoltage transients will depend on the type of secondary system in use (i.e. electro-mechanical or electronic control and protection circuitry) and also on the system voltage;
- Further investigations are necessary in order to establish safe and nevertheless economical solutions for reliable system operation in all configurations.

5. References

[1] Bernard G., Massat J., Ebersohl G.,Voisin G.: Study of electromagnetic transients due to disconnector switching in metal enclosed substations; R.G.E., pp 667-694, 1983

[2] Koenig D., Imgrund G., Meppelink J., Schlicht D.: Performance of GIS disconnectors under laboratory and network conditions; Proceedings of Intern. Symp. on gas-insulated substations: Technology and practice, pp 75-85, Toronto, 1985

[3] Haug O., Menten L., Röhsler H., Strnad A.: Transiente Spannungsbeanspruchung von Betriebsmitteln an gasisolierten Schaltanlagen; Elektrizitätswirtschaft, Heft 4, S 109-113, 1987

[4] Boersma R.: Transient ground potential rises in gas insulated substations with respect to earthing systems; Electra, No. 110, pp 45-54, 1987

[5] Dick E.P., Fujimoto N., Ford G.L., Harvey S.: Transient ground potential rise in gas-insulated substations - Problem identification and mitigation; IEEE Trans. PAS, vol. 101, pp 3610-3619, 1982

[6] Jshikawa M., Oh-hashi N., Ogawa Y., Ikeda M., Miyamoto H., Shinagawa J.: An approach to the suppression of sheath surge induced by switching surges in a GIS/power cable connection system; IEEE Trans. PAS, vol. 100, pp 528-538, 1981

[7] Strnad A., Reynaud C.: Design aims in HV substations to reduce electromagnetic interference (EMI) in secondary systems; Electra, No. 100, pp 87-107, 1985

[8] Aanestad H., Deter O., Röhsler H., Lewis J., Strnad A.: Substation earthing with special regard to transient ground potential rise: Design aims to reduce associated effects; Cigré SC 23, 23-87 (WG04) 12 IWD, Meeting in Johannesburg, Okt. 1987

[9] Meppelink J.: Elektromagnetische Verträglichkeit bei SF6-gasisolierten Schaltanlagen; Bull. SEV, Bd. 77, S 1497-1500, 1986

[10] Stephanides H.V.: Optimierung des Ueberspannungsschutzes elektrischer Anlagen; Bull. SEV, Bd. 75, S 1400-1406, 1984

[11] Schwartz L.: Théorie des distributions; 2me édition, Hermann, Paris 1966

International Conference on Large High Voltage Electric Systems

112, boulevard Haussmann — 75008 Paris

1988 Session — 28th August - 3rd September

O

23-11

Pref. Subj. 3

DEVELOPMENTS IN IMPROVED RELIABILITY FOR GAS-INSULATED SUBSTATIONS*

by

N. FUJIMOTO (1), F.Y. CHU, S.M. HARVEY, G.L. FORD

Research Division, Ontario Hydro

(Canada)

S.A. BOGGS
Underground Systems Inc.
(Canada)

V.H. TAHILIANI
Electric Power Research Institute
(United States)

M. COLLOD
Alsthom
(France)

Abstract

The reliability of gas-insulated substations (GIS) has been a matter of active discussion for the past several years. As a result, a great deal of research has been undertaken during the past several years. This paper reviews the recent GIS reliability-related research carried out at Ontario Hydro and discusses the practical implications for the improved reliability and operation of GIS. In particular, substantial effort has been devoted to problems arising from the operation of disconnectors. Investigations of disconnector operational characteristics have revealed the parameters which influence the probability of failure and have facilitated the design of more reliable GIS. The characteristics of disconnector operation induced short risetime transients have also been studied and techniques for waveform computation developed. Disconnector transients cause a wide range of problems which include: transient overvoltages which have been implicated in GIS failures; transient high voltages on the grounded enclosures of the GIS; and problems of electromagnetic compatibility with control wiring and associated equipment. In addition, the sparking which occurs in disconnectors (as well as in the case of a fault) causes the decomposition of the SF_6 gas into toxic byproducts. The various byproducts and their formation rates have been characterized; these data assist in failure diagnosis and in establishing the appropriate safety precautions during maintenance. To address the problems of transient induced failure, the efficacy of various test techniques in assuring reliable operation has been assessed.

Keywords

GIS; Reliability; Disconnector; SF_6 Byproducts; Fast Transients; Testing

1.0 INTRODUCTION

Gas-insulated substation (GIS) technology has gained widespread acceptance throughout the world and has found application to 800 kV. Although the overall performance of GIS has been quite good, the technology has not been without its problems, especially with the early designs for EHV voltage classes (345kV and above). The perceived need to improve reliability has motivated a great deal of research over the past several years.

The problems which have occurred often take the form of unexpected (and often unexplained) in-service failures of the GIS or its relaying systems. Such failures often occur concurrent with disconnector operation and take the form of failure within a disconnector during operation, failure of adjacent switchgear during switching, or failure of relaying as a result of the generated transients. These problems have also increased the emphasis on maintenance and repair, giving greater prominence to the concern, common to all utilities operating GIS, for personnel safety during maintenance. With a new technology, new safety criteria were necessary.

This paper summarizes a research program which was undertaken as a result of the problems which Ontario Hydro and other utilities have encountered with GIS technology. A more complete description of this research is available from the Electric Power Research Institute [1]. The research program includes five projects:

1. Methods to determine the reliability-related operational characteristics of GIS disconnect switches.
2. Methods for calculating the magnitude of internally-generated transients.
3. Methods for mitigating transients on control wiring to improve relaying reliability and facilitate the use of electronic equipment in GIS.
4. Improved high voltage commissioning test techniques to assure surge integrity.
5. Methods for safe handling and disposal of solid and gaseous decomposition byproducts during maintenance.

* Research funded by the Electric Power Research Institute, the Canadian Electrical Association and a consortium of utilities under the Ontario Hydro GIS Reliability Research Programme.

(1) Ontario Hydro Research Division, 800 Kipling Avenue KR151, Toronto Ontario M8Z 5S4, Canada.

Of the five projects, four were related to various aspects of disconnector operation. Disconnector-generated transient overvoltages are a more common cause of GIS failure than externally-generated surges (lightning, conventional switching surges, etc.) Knowledge of the nature and magnitude distribution of such surges is, therefore, very important to any attempt to investigate the dielectric characteristics of GIS for fast (disconnector-generated) transients. Such investigations are necessary in order to specify appropriate testing to assure the integrity of the switchgear for such surges. The design of the disconnector and GIS, along with the fundamental dielectric characteristics of SF_6, determine the nature of the transient (risetime, etc.) The statistical operating characteristics of the disconnector determine the statistical distribution of transient magnitudes as a function of position within a GIS. Disconnector transients may also induce false information on control wiring and are consequently relevant to the investigation of electromagnetic compatibility and the associated mitigation techniques. These are necessary to improve relaying reliability and facilitate the use of solid state circuitry in relaying systems.

2.0 DISCONNECT SWITCH-RELATED RELIABILITY

Failures of GIS disconnectors during operation usually occur as a result of the branching of intercontact sparks to ground [2,3]. The probability of such failure is related to the time-varying field distribution from the intercontact spark to ground which depends on the transient overvoltage waveform at the switch, the operating voltage and the details of the contact geometry. As a general rule, an increase in the maximum contact separation at which intercontact arcing begins (on closing) or persists (on opening) correlates with the increased failure probability. Research has indicated that the maximum contact separation is highly correlated with the maximum trapped charges which a disconnector can leave on the load side during opening operations. Although trapped charge *per se* may not be of great importance, the concept is useful in view its correlation with important measures such as the maximum contact separation at which arcing occurs and the transient overvoltage level.

2.1 The Arcing Pattern and Trapped Charge

Disconnectors can be characterized by recording the pattern of arcing (i.e. the load side voltage) during operation on a capacitive load [4,5]. The pattern of voltage transitions as a function of time (the "arcing pattern") gives an indication of the variation of intercontact breakdown voltage as a function of contact position (or time) for both polarities. The difference in breakdown voltages for the two polarities indicates a dielectric "asymmetry", which, in general, varies with contact position. An asymmetry which is large compared to the statistical variance in breakdown voltage produces a systematic pattern near the end of the arcing sequence (for opening operations, or near the beginning of the arcing sequence for closing operations - figure 1). For opening operations, a systematic arcing pattern causes the load side voltage to fall into a "stable" region from which neither positive nor negative breakdown can occur [5]. This occurs soon after the stable region develops and results in clearing at a relatively small contact separation, a systematically small trapped charge, and reduced transient overvoltage magnitudes. As the intercontact breakdown voltage is statistical, the final residual voltage (trapped charge) has a distribution which is usually centered at about 0.3 pu and ranges from 0 to 0.5 pu. For a hypothetical switch with no dielectric asymmetry, a systematic pattern does not develop and the trapped charge probability density distribution is nearly uniform from +1 to -1 pu (figure 2). As the dielectric asymmetry of a disconnector is usually a function of contact separation (figure 3), a disconnector which demonstrates systematic operation at one operating voltage (for example, clears in the region of V_1 as shown in figure 3) may not do so at another operating voltage (V_2).

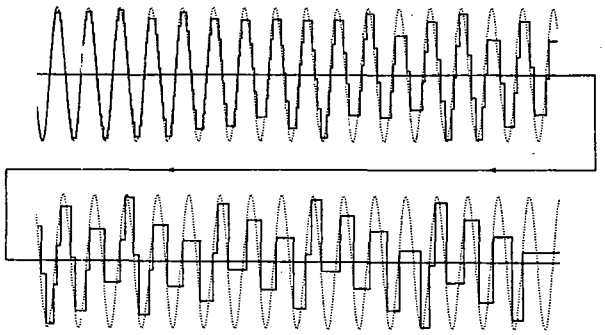

Figure 1 - Typical load side voltage ("arcing") pattern for a disconnector opening operation, leading to a small trapped charge on clearing. Closing operations have similar, but reversed patterns. The difference in the breakdowns in the upward and downward direction (asymmetry) leads to the systematic pattern near the end of the pattern and a consistently small trapped charge.

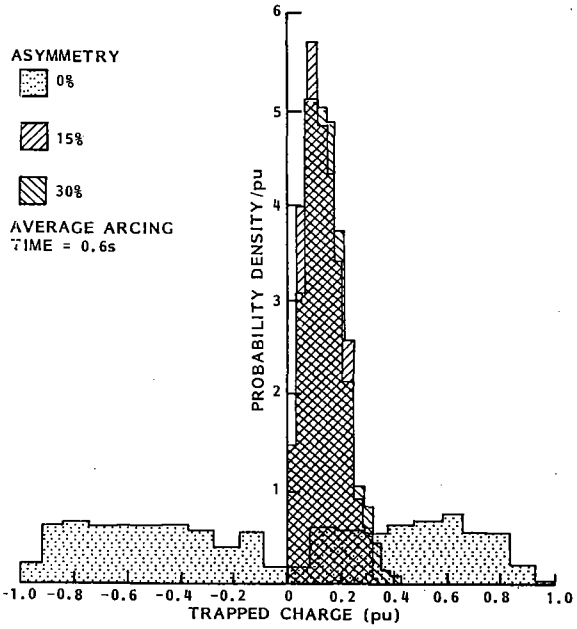

Figure 2 - Computed trapped charge distributions for disconnectors with varying asymmetries in intercontact breakdown voltage.

This results in different characteristics with, possibly, statistically larger trapped charges which correlates with larger contact separation at clearing and the generation of higher magnitude transient overvoltages (figure 4). As a result, a GIS operated at a higher voltage level, at which the disconnector has little asymmetry in the region of clearing, can suffer from a probability of failure disproportionate with the increase in operating voltage.

The asymmetry characteristics, including the statistical variation in intercontact breakdown (measurements indicate a standard deviation in the range of 5% to 10%), were incorporated in a Monte Carlo simulation of disconnector operation. Results from such simulations correlated very well with the measured probability density distribution of a disconnector during several thousand operations [5]. Simulations can be used to determine disconnector operating characteristics prior to design and type tests, so that worst-case conditions can be simulated to assure reliability. In addition, such analysis gives a better indication of

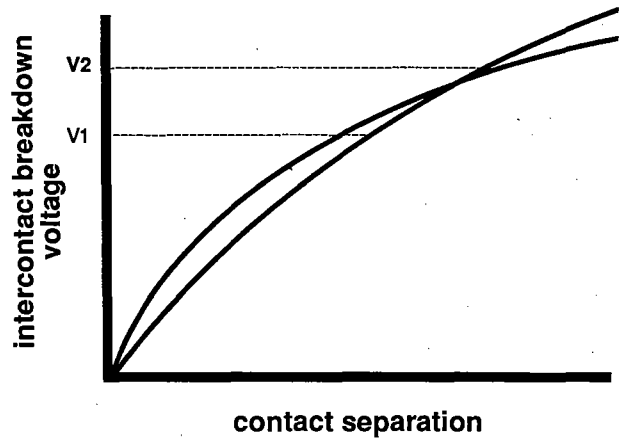

Figure 3 - An example of the variation in intercontact breakdown voltage as a function of contact separation for both polarities. The dramatic change in asymmetry could result in very different operational characteristics depending on the operating voltage. The example shown is characteristic of some but not all 1550 kV BIL disconnectors.

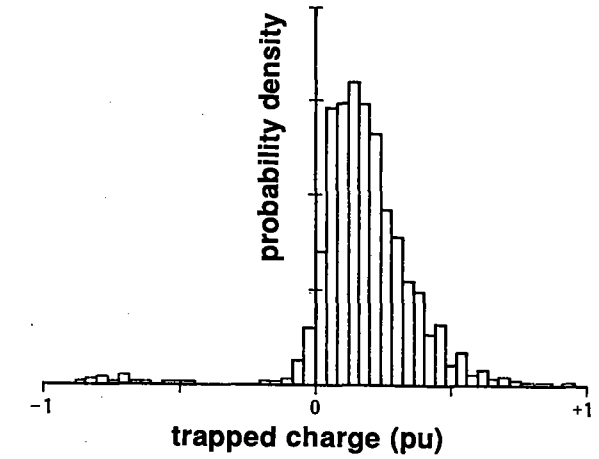

a) operation at 420 kV system voltage

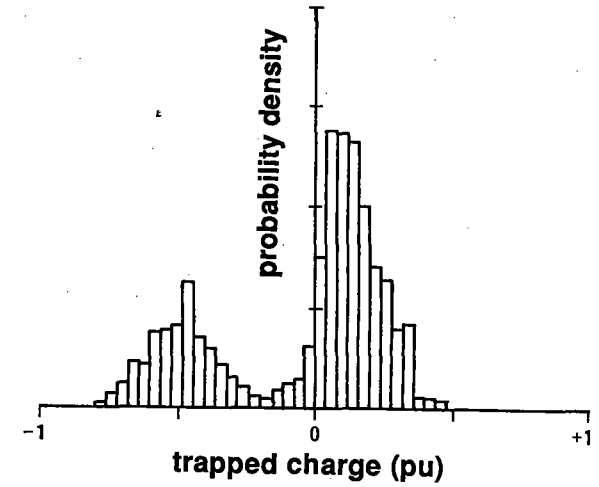

b) operation at 550 kV system voltage

Figure 4 - Trapped charge distributions computed by modeling a 1550 kV BIL disconnector (with characteristics similar to that of figure 3), in a simulation at operating voltages of 420 kV and 550 kV.

the degree to which test conditions are more onerous than normal operational conditions. The effect arising from operation at a different operating voltage and the effect of mechanical operating speed on switch characteristics are other parameters which can be evaluated through simulations. In general, the faster the disconnector, the broader the distributions for trapped charge and arcing time, as a result of a less systematic arcing pattern.

Another use of disconnector analysis is the evaluation of low probability operational characteristics. For example, simulations might indicate that a disconnector has a generally narrow distribution of arcing time and trapped charge but has a low (but finite) probability of a long arcing time and high trapped charge. This suggests that tests should be undertaken to assure the reliability of the switch at the higher intercontact separations which might occur on a low probability basis.

A third use of simulations is to provide a basis of evaluating transient overvoltages on a statistical basis. As each intercontact spark during operation generates fast transients, the statistics of intercontact breakdown are also a factor in the statistics of transient overvoltage magnitudes [5]. A complete evaluation of transients also involves the effect of substation configuration, as discussed subsequently in section 3.

2.2 Disconnector Testing

In general, the conventional "statistical" factory tests, involving thousands of operations under conditions representing normal operation, may not replicate low probability failures which occur during actual use. Additional special tests are necessary to assure reliable operation.

The "one-minute arcing test", has proven useful in revealing low probability failures which could not be reproduced by a manufacturer during more than a thousand normal operations in a test arrangement. In this test, the switch is left to arc continuously for approximately one minute at the maximum contact separation at which arcing can be sustained at or slightly above the normal operating voltage. In this manner, several thousands of intercontact sparks occur near the most onerous contact separation, which tends to reveal low probability phenomena. However, this test has often been criticized as being overly onerous as a result of the excessive heating and ionization of the intercontact gas.

Another test method requires the operation of a disconnector connected to two out-of-phase test sources energized at slightly above the normal operating voltage. Such out-of-phase operation provides a realistic simulation of what occurs during generator synchronization, saturation of a magnetic PT on the load side of a disconnector during disconnector opening [6], or disconnector clearing in a contact separation region of small asymmetry resulting in an intercontact breakdown approaching 2 pu. In one particular phase opposition switching test [6], the disconnector is closed under conditions of phase opposition in a circuit configuration which results in transient overvoltages in the range of 2.5 pu. The transformer primaries are shorted at the first prestrike in order to limit the power dissipated in the prestrike arc. Such phase opposition testing results in a long prestrike arc, which substantially increases the probability of failure to ground relative to that during operation under all but the most onerous conditions. In this form, an out-of-phase switching test does not simulate the effects of SF_6 ionization and heating during operation (which may extend the contact separation during opening). In addition, only a single spark is obtained with each disconnector operation, making statistical testing very cumbersome. On the other hand, the test is apparently sufficiently severe that a disconnector which passes such a test should be reliable in service.

Both the phase opposition and "one-minute" arcing tests appear to be practicable and have been used by some manufacturers to study the low probability failure of disconnectors. While other tests may be effective in assuring disconnector reliability, the challenge facing the industry is to develop a relatively simple and effective test which can be carried out by any reasonably equipped test laboratory. Although the arcing and/or phase opposition tests meet these criteria, tests universally accepted by users and manufacturers should be developed. This is a challenge which faces the industry and which should be addressed in the near future.

3.0 INTERNAL TRANSIENT OVERVOLTAGES

Disconnector operation induced transient overvoltages represent the largest stresses in GIS under normal operating conditions. In addition to the fast (5-15 ns) risetime, these overvoltages are characterized by the high frequency of occurrence and the relatively short duration (typically microseconds to 10's of microseconds). A single operation of a slow disconnector (total arcing time of 0.1 - 1.0 s, typical for most North American and European equipment), will generate 10's to 100's of individual transients (caused by each of the prestrikes). As disconnectors are operated routinely in many substations, GIS components may be exposed to a large numbers of transients. However, the magnitude of transient overvoltages tends to be relatively low (typically 1.5 to 2.0 pu), although values in the range of about 2.5 pu can occur in some instances [2,3,6].

In order to understand fully the mechanisms of transient overvoltages, computer modeling and simulation techniques were developed. As a result of the fast risetime, models used in conventional studies were inadequate, and new transmission line-based techniques were necessary.

3.1 Calculation of Transients

For the purpose of modeling, GIS can be viewed as a network of unmatched low-loss coaxial transmission lines. When the network is stimulated by a high frequency traveling wave, such as generated by the intercontact spark during disconnector operation, the network resonates as a result of various reflections at impedance mismatches within the station and at the terminations. As a result, the primary resonant frequencies depend on lengths of bus within the GIS. A second class of lower frequencies may be the result of the resonance of external devices, such as capacitive voltage transformers, with the GIS. The superposition of these two classes of resonances results in the overall waveform of the transient. The relative magnitude of the two types of resonances depends on the configuration of the GIS and the location within the GIS at which the measurement is taken. Models which properly account for both classes of resonances are necessary for accurate simulations.

As a result of the short risetime of the traveling wave stimulus, transmission line (distributed parameter) concepts must be incorporated into GIS models. In general, all nonidealities or subcomponents within the GIS which result in appreciable reflections or waveform distortion with ~5 ns risetime (approximately 100 MHz bandwidth) stimulus must be modeled accurately. As the primary frequencies of the resonances depend on bus lengths, the electromagnetic propagation time delay in component models becomes important; the use of transmission line-based models is the most efficient way to accommodate the time delay.

In general, accurate results in computer simulations requires the use of detailed models. However, while detailed models may be suitable for specific applications such as modeling a simple arrangement for the testing of disconnector, system studies on a large GIS which incorporates many components requires simple but accurate components models to achieve an overall GIS model of a manageable size. Using the techniques described in [5,7], generalized models for bus duct, circuit breakers, GIS to air bushings, and some other typical GIS components, including the effects of damping, have been developed. Figure 5 illustrates a computer simulation in comparison with a measurement performed for a full scale GIS configuration. The measurement was performed with wide bandwidth capacitive sensors installed in the GIS [8]. The relatively good agreement indicates the validity of the modeling technique. The lack of precise agreement of the fine detail is a result of simplifications used the overall model. The inclusion of more details in the simulation, such as representation of each spacer, can result in more detailed agreement [9], at the expense of greater complexity in the overall model.

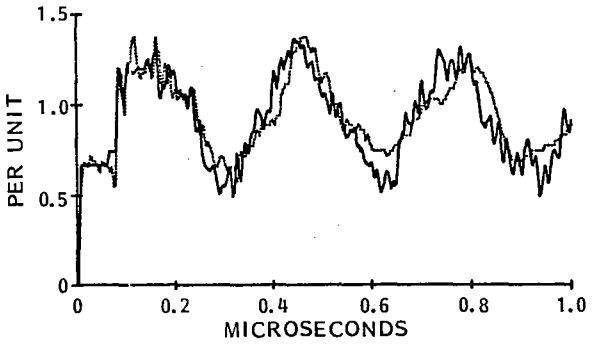

Figure 5 - A comparison of a computer simulation and an actual measurement of a DS induced transient overvoltage waveform in a 138 kV GIS. Details are given in [7]. The measured data are plotted with the dotted line and the computed data are plotted with a solid line.

3.2 Statistical Characteristics of Transients

Computer simulations of transient characteristics are performed on a normalized basis by assuming the intercontact spark which generates the travelling waves occurs from 1 pu on the source side to ground potential on the load side. The resulting simulation characterizes the normalized response of the GIS arrangement to the stimulus (the intercontact spark at the disconnector). This simulation also characterizes the (normalized) variation in transient waveform as a function of position within the GIS. In an actual disconnector operation, many intercontact sparks occur, each of which generates a time varying overvoltage pattern which is a scaled version of the normalized response. This response is superimposed on whatever conditions, such as a momentary dc voltage on the load side, existed prior to the spark which generates the transients. If $K(t,s)$ is the normalized response of the GIS configuration as a function of time t and position s, U is the intercontact breakdown voltage and Q the preconditions, the transient overvoltage (also a function of t and s), $V(t,s)$ is:

$$V(t,s) = U \times K(t,s) + Q$$

In general, U and Q are random variables which depend on the disconnector operating characteristics. Q is the voltage prior to the transient at the point of interest, which could be, for example, the momentary dc voltage (trapped charge) on the load side immediately prior to an intercontact spark which occurred with an intercontact voltage of U. In this case, $V(t,s)$ is also a random variable which characterizes the transient overvoltages as a function of time and position within the GIS. The application of this approach to determine distributions of peak transient overvoltage magnitudes was demonstrated in [5]. The above equation can also be used to estimate certain worst case values. For

example, if the peak magnitude of a normalized response, K_{max} = 1.7 pu and U = 2 pu (which is the worst-case situation which occurs if the trapped charge Q = -1 pu) then the peak transient can be calculated as $V_{max} = 2 \times 1.7 - 1 = 2.4$ pu.

4.0 TRANSIENTS ON CONTROL WIRING

Transient voltages exist on GIS control wiring because of imperfect shielding between the control circuit conductors and the high voltage conductors. The frequency content of GIS transients often extends to the 100 MHz range, although the bulk of the high frequency energy is found in the 1 to 30 MHz range. As a result of the high frequencies and short cables in these compact substations, greater care is necessary in shielding and interference control than in conventional stations.

Electromagnetic compatibility (EMC) can be influenced by substation configuration, switchgear design, control wiring practices and the vulnerability of electronic equipment. Improvements in the first two areas will produce a generally more benign electromagnetic environment in the GIS with substantial benefits in terms of control system transient immunity specifications and operating practices. In many cases, improvements in the effectiveness of shielding which already exists within the GIS equipment, in the frequency range from 1 to 30 MHz, is all that is required. In the area of equipment vulnerability, further investigations are required to establish appropriate transient withstand capability standards which take into account both the broadband nature of GIS transients and the special needs of new instrumentation technology. Changes in the remaining area, control wiring practices, can be highly beneficial and cost effective particularly when integrated into an overall electromagnetic compatibility design package. Appropriate wiring practices suggested in this study are as follows:

- Use shielded control cables. Copper tape shields are recommended for all applications; however, braided shields can be used for short runs, where installation is difficult, and/or where highest performance is not required.

- Enclose all equipment to be mounted on or near the switchgear and bushings in cabinets or housings which provide effective high frequency shielding.

- Ground cable shields at both ends. Grounding connections should be as short and direct as possible and should terminate at the point of cable entry to cabinets or housings. Connections should have a current capacity equal to that of the cable shield (unless a fusible connection is required). Coaxial type ("zero impedance") shield connections are highly effective and are preferred at all cable terminations.

- Use effective high-frequency electromagnetic shields in current and voltage transformers.

- Install cables as much as possible in electrically continuous cable pans or below grade trenches. Maximum advantage should be taken of any available structural or other shielding provided by the substation architecture.

- Run exposed sections of cable as close as possible to grounded structures, including grounding bars and the electrically continuous aluminum sheath. Loops should be avoided where cables enter sheath mounted devices.

5.0 IMPROVED HIGH VOLTAGE TEST TECHNIQUES

The objective of this research was to determine the tests necessary to assure the dielectric integrity of gas-insulated switchgear under the full range of stresses encountered in service. The purpose of testing is to reveal defects in design, manufacturing and field assembly. As a result, testing-induced flashover in GIS often occurs under inhomogeneous field conditions. Recent developments indicate that breakdown mechanisms in inhomogeneous field gaps in SF_6 are now well understood for rectangular waveforms of positive polarity [10]. One of the factors which determines breakdown is the availability of a discharge-initiating free electron at an appropriate location in the insulation system. The primary source of such free electrons is collisional detachment from negative ions. Knowledge of the ion production rates, loss mechanisms, and field-dependent electron detachment probability permits the computation of breakdown probabilities under inhomogeneous field conditions.

The understanding of inhomogeneous field breakdown allows a more complete evaluation of existing test methods in terms of their relative usefulness and efficacy in achieving their intended function and demonstrates that test criteria and selection can be determined on a scientific basis, which results in greater assurance of reliability. Although much of the research is theoretical in nature, the resulting understanding has very important practical implications for all forms of testing.

5.1 Design and Type Tests

The purpose of design and type tests is to assure that the basic design of the apparatus meets the required specifications and design criteria, including reliability criteria. For this purpose, design tests should normally be undertaken to determine the margin of safety, while type tests must be sufficiently rigorous to provide reasonable assurance of dielectric integrity under in-service conditions.

Research in breakdown mechanisms indicates that impulse waveforms of less than 10 μs risetime should be included as part of such tests. As (positive voltage) breakdown probability is correlated with negative ion density, consideration must be given to the time between applications of impulses during which negative ions form from natural causes. Although a period of six minutes has been determined as the time required for ion densities to reach equilibrium conditions [10], the best time interval should be optimized to maximize test effectiveness [11]. In general, the value of design and type tests can be improved through more careful control of test procedures, including those which ensure a consistent negative ion density in the gas.

5.2 Factory Tests

The purpose of factory testing is to detect errors in manufacture. A power frequency test with a crest voltage of about 66% of the BIL in combination with sensitive partial discharge detection has become conventional. However, such a test may not assure the BIL of the equipment as shipped, and might suffer from a lower sensitivity to a small stress enhancement than is provided by a positive impulse voltage. However, the alternative of a surge test in addition to the conventional test is often criticized as a result of its high cost and limited value. Given that the switchgear will be shipped and installed after factory testing, the factory test provides very little assurance that the installed equipment is defect free. Therefore, a more rigorous field test is probably more cost effective than a more rigorous factory test.

5.3 On-Site Field Tests

At the lower voltage levels, most manufacturers and utilities consider a power frequency field test to be adequate. This philosophy is the result of a number of factors including large shipping sections which reduces the work required for field assembly and relatively large safety margins between operating voltage and BIL (BIL is taken as a general measure of equipment dimension). Most GIS has been designed with a "safety factor" (BIL/Crest Operating Voltage) in the range of 4.5 or

greater, with the exception of the 345 kV, 1050 kV BIL and the 550 kV, 1550 kV BIL switchgear installed in North America. The experience with both of these classes of GIS has been much worse than for the equipment with a higher safety factor.

The above "safety factor" is relevant, as far more failures of GIS occur during disconnector and breaker operation than occur as a result of lightning, and the safety margin between disconnector transient overvoltage magnitudes (which are proportional to operating voltage level) and the BIL is correlated to the safety factor. As transient overvoltages can, in theory, occur with magnitudes as high as 3 pu, a low safety factors in the range of 3.5 (as for 550kV, 1550kV BIL equipment) leaves very little margin for degradation of the BIL with age, installation, etc. With these reduced safety margins, rigorous field testing becomes more important. Although opinions on the best test method vary, the use of both impulse and power frequency site tests for low safety factor installations is often suggested. Recent results concerning the effect of positive surge risetime on the breakdown voltage caused by a small needlelike stress enhancement indicate that a surge test with a waveform risetime <10 μs is necessary. These investigations have indicated that the breakdown voltage for a surge of 100 μs risetime can be a factor of ***two*** greater than for a surge of 10μs risetime for such a defect [12]. The 10μs risetime appears optimal, as shorter risetimes can cause unwanted overvoltages as a result of reflections within the station.

6.0 HANDLING OF SF_6 ARCING BYPRODUCTS

During maintenance or repair of SF_6-insulated equipment, the handling of gaseous and solid arcing byproducts has become a matter of concern. Previous research indicates that byproducts can represent a health hazard [13,14] and that the insulating strength of the equipment can be affected [15,16]. The objective this research was to gather the necessary information to provide a scientific basis for formulating safe procedures for handling byproducts. The approach taken was to (1) identify the byproduct species, (2) estimate the quantities formed, and (3) obtain knowledge of the toxic properties and the allowable exposure level for workers. The identification of byproduct types, their properties, and their formation rates was undertaken through literature search and experiments. Byproducts were generated experimentally under power arc, switching arc and partial discharge conditions to simulate the various conditions encountered in actual GIS. Field samples from Ontario Hydro's in-service faults were obtained to supplement the laboratory samples. Highly sensitive analytical instrumentation was developed to identify the species and measure the quantities formed in a high background level of SF_6. This information was used to estimate the levels of byproducts which would be produced under the typical conditions which might require maintenance in actual GIS (i.e. current interruption, fault, disconnector operation and partial discharge). These levels were then compared with existing "safe" exposure limits, such as Threshold Limit Values (TLV) for workers to establish safe handling procedures. The reaction of the byproducts with cleaning agents and solvents were also studied and the effectiveness of the cleanup and removal processes was examined.

6.1 Byproduct Formation

The formation rates for SOF_2, SO_2F_2 (the primary gaseous byproducts) and the solid arcing byproducts for power arc, switching arc and partial discharge have been measured and the results given in [14]. Aluminum electrodes generate the highest level of byproducts as a result of the exothermic reaction between aluminum and SF_6. In a power arc, the formation rate of SOF_2 is about 20,000 μl/l per kJ at STP conditions. Since other electrode materials have lower formation rates and SOF_2 is the dominant species, this formation rate can be used for worst case estimation of arc byproduct exposure levels.

The existence of adsorbed gas on the surface of the solid particles was confirmed in this project by the vacuum gas extraction technique. Previous research [17] has shown that the average size of the particles is about 1 μm which leads to effective surface areas as high as 10 m^2/g. The presence of the surface adsorbed gas completely changes the characteristics of the solid and the toxicity of the particulate may be determined by the adsorbed gas instead of the solid itself.

An unsuccessful attempt was made to search for the highly toxic species S_2F_{10} in partial discharge samples. While this species is unlikely to be sufficiently stable to affect safety, previous research on its existence produced conflicting results [18]. Future research should be conducted to confirm or deny its existence under practical arcing conditions in quantities close to the TLV. Any indications of its existence in stable form may affect the validity of the handling procedures developed to date.

6.2 Safe Work Practice

In general, respiratory protection from gaseous and solid byproducts is recommended during GIS maintenance and byproduct handling. Because of the abundance of SOF_2 relative to the other decomposition products and its relatively low permissible exposure criteria, SOF_2 dominates the respiratory protection requirements. The procedures (published elsewhere [14]) discuss the various levels of respiratory protection ranging from full face mask with supplied air respirator to half face gas mask with combination organic vapor-acid gas chemical cartridge. For short term (up to 10 minutes) inspection and cleanup after the gas has been removed, a cartridge filter gas mask is usually adequate.

Contaminated SF_6 gas should be treated before reuse or disposed. Field experience at Ontario Hydro indicates that common scrubber materials such as 13X molecular sieve is adequate for the removal of the arced gas after a major fault. However, the saturation levels of the molecular sieve should be checked before removal of a substantial amount of arced gas, or new scrubber material should be used for each removal.

The major conclusion which can be drawn from the study is that with adequate protection and precautions, the level of exposure to workers handling faulted GIS equipment can be reduced to values acceptable by industrial hygienists and by law.

6.3 Investigation of Effects on Materials

Another aspect of the SF_6 byproduct research is the study of the effect of byproducts on the dielectric and mechanical integrity of GIS. Samples of spacer material were exposed to high levels of arc byproducts and the change in dc surface resistivity and impulse withstand strength were measured. Analysis of the degradation mechanisms was carried out.

Evidence from actual GIS and laboratory experiments indicates that epoxy spacers with silica fillers are subject to attack by arc byproducts which can severely degrade the dielectric integrity of the spacer. Experiments using alumina-filled spacer materials indicated mixed results. The attack is associated with visible changes on the surface, lowering of the impulse withstand strength and a corresponding drop in the dc surface resistivity. An attack mechanism by hydrofluoric acid (HF) by diffusion through the epoxy to the filler site is suspected. HF is a common byproduct generated in secondary reactions of the primary gaseous byproducts with moisture. The reuse of insulating materials which have been exposed to arced gas should be undertaken with caution. Details of this research are described in [19]. In view of the importance of material compatibility, aging and reusability in influencing GIS reliability, a systematic study will be undertaken.

7.0 GENERAL CONCLUSIONS

Problems with early EHV GIS designs emphasized the need to understand GIS components at an analytical level and has led to extensive research efforts at Ontario Hydro and many other laboratories. Advances in understanding of the operational characteristics of disconnectors, the transient overvoltages, control wiring EMC and test requirements have contributed to a new generation of more reliable equipment. Research into SF_6 decomposition mechanisms has lead to the development of well-documented safety procedures for the efficient maintenance of GIS. Although some issues related to standardized test techniques and some technical issues are left unresolved, most major problems are now sufficiently understood on a fundamental level.

Many of the major concerns which have been addressed were symptomatic of a new and improving technology. As the problems have become understood, better, more reliable GIS has evolved. Although modern GIS is more reliable, end-of-life issues need further investigation. As a result, the focus of reliability-related research has shifted to issues of long-term reliability, ageing and improved diagnostics.

8.0 REFERENCES

1. "Gas-Insulated Substation Reliability Research Program." EPRI final report EL5551, Vol.1 & 2, Dec. 1987.

2. Narimatsu, S., K. Yamaguchi, S. Nakano, and S. Maruyama. "Interrupting Performance of Capacitive Current by Disconnecting Switch for Gas Insulated Switchgear." IEEE Trans on Power Apparatus and Systems, *Vol. PAS-100, No.6*, June 1981.

3. Edlinger, A. G. Mauthe, F. Pinnekamp, D. Schlicht, and W. Schmidt. "Disconnector Switching of Charging Currents in Metal-Enclosed SF_6-Gas Insulated Switchgear at EHV." 1984 CIGRE, paper 13-14,

4. Boggs, S.A., F.Y. Chu, N. Fujimoto, A. Krenicky, A. Plessl, and D. Schlicht. "Disconnect Switch Induced Transients and Trapped Charge in Gas-Insulated Substations." IEEE Trans on Power Apparatus and Systems, *Vol. PAS-101, No.10*, Oct. 1982.

5. Boggs, S.A., N. Fujimoto, M. Collod, and E. Thuries. "The Modeling of Statistical Operating Parameters and the Computation of Operation-Induced Surge Waveforms for GIS Disconnectors." 1984 CIGRE, paper 13-15.

6. Lalot, J., A. Sabot, J. Kieffer, and S.W. Rowe. "Preventing Earth Faults During Switching of Disconnectors in GIS Including Voltage Transformer". IEEE Trans on Power Delivery, *Vol. PWRD-1, No.1*, Jan. 1986.

7. Fujimoto, N., H.A. Stuckless and S.A. Boggs. "Calculation of disconnector induced overvoltages in gas-insulated substations." In L.G. Christophorou & M.O. Pace (Eds.) *Gaseous Dielectrics IV*, Pergamon Press, New York 1984.

8. Boggs, S.A. and N. Fujimoto. "Techniques and Instrumentation for Measurement of Transients in Gas-Insulated Switchgear." IEEE Trans on Electrical Insulation, *Vol. EI-19*, April 1984.

9. Witzmann, R. "Fast Transients in Gas Insulated Substations (GIS) - Modeling of Different GIS Components." 5th International Symposium on High Voltage Engineering (ISH), Braunschweig, FRG, 1987. Paper 12.06.

10. Wiegart, N., et al. "Inhomogeneous Field Breakdown in GIS - The Prediction of Breakdown Probabilities and Voltages." Three companion papers presented at the IEEE PES 1987 Winter Meeting, New Orleans. Paper No. 87 WM 190-2; 191-0; 192-8.

11. Discussion and closure of reference [10].

12. Diessner, A., G.F. Luxa, W. Mosca and A. Pigini. "High Voltage Testing of SF_6 Insulated Substations on Site." CIGRE 1986 paper 33-06.

13. Boudene, C., et al. "Identification and Study of Some Properties of Compounds Resulting from Decomposition of SF_6 Under the Effect of Electric Arcing in Circuit Breakers". Rev. Generale de Electricite-Numero Special, June 1974.

14. Chu, F.Y. "Decomposition in Gas-Insulated Equipment", IEEE Trans on Electrical Insulation, *Vol EI-21, No 5*, October 1986.

15. Tominaga, S., et al. "Gas Analysis Technique and its Application for Evaluation of Internal Conditions in SF_6 Equipment". IEEE Trans on Power Apparatus and Systems, *Vol PAS-100*, Sept. 1981.

16. Samuelsson, R. "Corrosion and Surface Resistivity Changes in Different Insulating Materials Caused by Decomposed SF_6 and Moisture". ASEA Journal, *Vol. 52, No. 6*, 1979.

17. Chu, F.Y. and C.K. Law. "Effects of Power Arc Fault in GIS". Proc. of Sixth International Symposium on Gas Discharges, IEE Publ. 189, 1980.

18. Pettinga, J.A.J. "Full Scale High Current Model Tests on Bus Bar Constructions for GIS". Proc. of CIGRE Symposium High Current in Power Systems, pp.506-585, 1985.

19. Chu, F.Y., et al. "GIS Spacer Surface Degradation Analysis", Final Report to the U.S. Electric Power Research Institute, Project 1360-10. To be published.

GROUPE 23
GROUP 23

POSTES
SUBSTATIONS

Rapports / *Papers*

23-06, 23-10, 23-11

J.J. O'NEILL (Assistant) | F.SCHERER (Special Reporter) | Th. YKEMA (President) | R.OTT (Secretary)

SUJET PREFERENTIEL 2 / *PREFERENTIAL SUBJECT 2*

Mises à la terre dans les postes d'interconnexion et de centrales. Suppression effective des tensions induites de fréquences basses et élevées dans les composants primaires et les réseaux auxiliaires. Technique de mise à la terre du neutre.

Grounding and earthing in substations and power stations. Effective avoidance of unpermissible induction voltages of low and high frequency on primary components and auxiliary systems. System neutral grounding techniques.

QUESTIONS 2.1 - 2.2

Mr. H. RÖHSLER (Fed. Rep. of Germany)

Referring to question 2.1 of the Special Reporter I want to give a short comment on Paper 23-06. The topic of this Paper, transient ground potential rise (TGPR), has led to a cooperation of the Working Groups 03, 04, and 05. It has been the aim to make TGPR-effects understandable to the substation engineer and to help with problem identification and solution. To get an overview a questionnaire has been sent out to the Members of SC 23 to collect experience with TGPR. The numerous response by 60 contributors from 18 countries has shown that there is a great interest in this topic and that solutions have been achieved to overcome problems with TGPR. It is this experience that has led to recommendations on how to design future substations and how to modify substations in service in order to avoid problems with TGPR-effects. These recommendations concern on the one hand the source, the potential rise, that can be reduced by proper earthing and shielding facilities; on the other hand it also deals with reducing the coupling effects and improving the withstand capability of the secondary equipment.

I am very glad to hear from colleagues who already have adopted measures described in this paper and have succeeded in uprating the GIS in a way that the disturbing TGPR-effects disappeared.

Coming back to Question 2.1 of the Special Reporter the experience collected by our questionnaire allows a clear statement:
Whatever is the cause of TGPR related disturbance - it is the problem identification that is of great importance and the identification determines the measures to be adopted. If once correctly identified the problem can be solved often by only minor modifications. That is why more sophisticated models that allow to balance effectiveness and cost seem to be neither applicable nor necessary; a probabilistic approach for instance would require input data not known to the user.

Concerning the design of future substations there is a similar situation; however, in the design stage measures to avoid TGPR problems, like e.g. shielding facilities, can be adopted at still lower cost.

In my utility many years of experience with AIS and GIS up to 420 kV has shown that a proper lay-out as recommended in Paper 23-06 allows service without TGPR related disturbance.

Mr. W. BÜSCH (Switzerland)

We refer to question 2.1 of the special report in particular to the necessary measures avoiding unacceptably high transient enclosure voltages (TEV) in GIS installations.

The aim of all the measures applied should be the attenuation of TEV to an acceptable level, so that the following troubles do not occur:
- flashovers in the earthing system including GIS enclosure,
- damage of secondary equipment, or
- maloperations.

A complete elimination of TEV is not possible.

A great number of possible measures are presented in the papers 23.06, 23.10 and 33.06. To obtain an optimum ratio between effectiveness and cost, the measures have to be selected considering also the level of the system voltage.

On the one hand, it is known that the crest value of TEV increases approximately proportional with the system voltage. On the other hand, insulation distances between adjacent earthed structures do not change essentially. The selection of the necessary measures are strongly related to the system voltage.

For higher system voltages expensive measures may be frequently necessary, such as
- large metallic screens at SF6/air terminations,
- integration of reinforcements to the earthing grid,
- complete screening of all control circuits, etc.

For lower system voltages frequently the proven economic design of the earthing system of GIS may be successfully applied, e.g.
- low-inductive bridging of discontinuities on the enclosures,
- additional connections between adjacent enclosures,
- short, low-inductive connections between enclosure and earthing grid.

Therefore, we are suggesting different recommendations for the voltage ranges

$U_m \leq 300$ kV and
$U_m \geq 300$ kV.

Mr. T. NITTA (Japan)

Fighting with TGPR has a long history ever since the first GIS was introduced about 20 years ago. Now, to my understanding, it is not a serious problem as far as proper countermeasures are applied to the GIS.

TGPR appears only when the sheath of the GIS is not continnous. There are four kinds of discontinuities in normally designed GIS, shown in Fig 1.

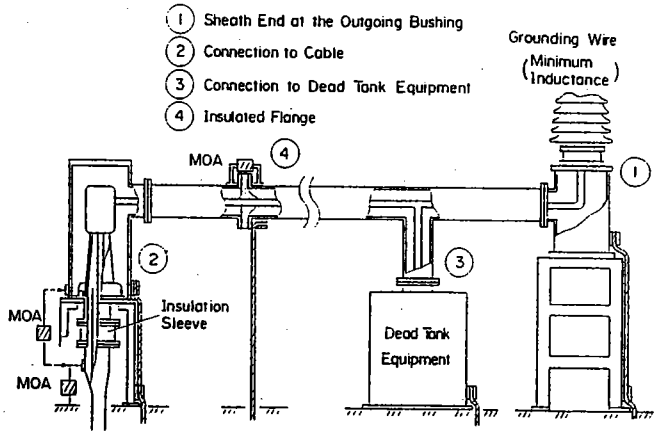

Fig.1 Four Kinds of Discontinuity of GIS Sheath

The first type of discontinuty is at an outgoing bushing to aerial line. The sheath is usually grounded at this point with minimal residual inductance. However, unless the end of the bus is not very close to the ground, the peak of the TGPR is highest at this point due to the residual inductance in the grounding connection. In wiring low voltage circuit of the GIS, care must be taken not to be interfered by the high TGPR. With this precaution, the TGPR at the point is harmless.

The second type of discontinuity is at the cable connection. Because of the low surge impedance of the cable and its shearh, the TGPR at the point is not so high as that at the bushing. However, if the TGPR produce an internal breakdown in the pot head, it will be a cause of a serious failure at the cable connection. The insulation has to be protected in coordination with the TGPR by a metal oxide arrester placed either between the sheath of the cable and the ground or across the sleeve insulating the sheath of the cable and the GIS.

The third type discontinuity in GIS sheath is a termination at a deal tank type equipment in the GIS. Since the high voltage part is completely enclosed in the grounded tank, TGPR at the discontinuity is not appreciable in this case.

The fourth kind of discontinuuity is at the insulating flange in a bus. The insulating flange is used in some GIS designs to apply external CT in the bus and/or to limit the current in the grounding circuit and the sheath. TGPR at the discontinuity appears at the sheath and across the flanges on both sides of the insulation. The TGPR can be suppressed effectively by puting a plural number of metal oxide arresters or spark gaps across the flanges. The picture in Fig 2 shows an example of such metal oxide arrester.

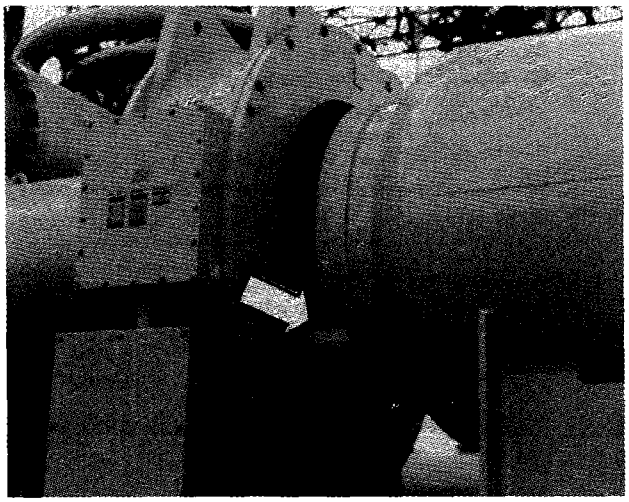

Fig.2 Example of MOA Surge Absorber at the Insulated Flange

The TGPR generated at these four kinds of discontinuities of GIS sheath can be limited to harmless levels with the precautions stated above. From safty point of view, high frequency peak of TGPR whose time to crest is less than 0.1μs is not even sensible with bare hands as shown in the curve in Fig 3.

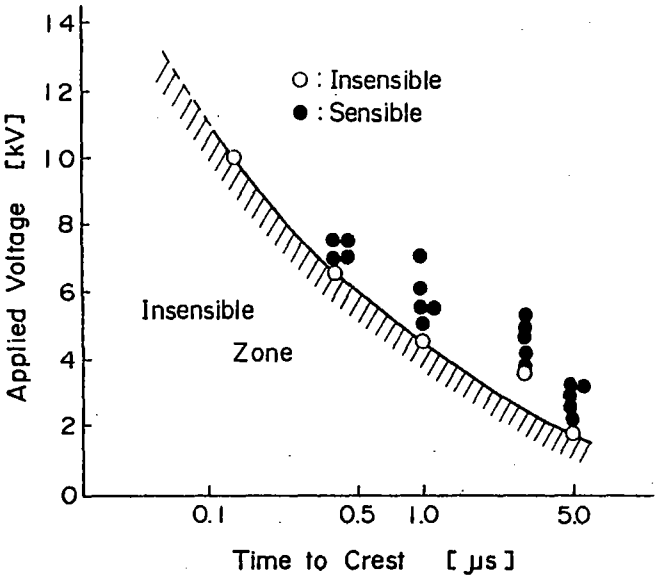

Fig.3 Sensible Zone of Impulse Voltages

Mr. M.J.M. VAN RIET (Netherlands)

Summary
Very fast transient voltages cannot be avoided and will, in case of gas-insulated substations (GIS), always keep occurring. With an appropriate earthing system, however, these voltages are entirely controllable. Relatively sensitive process-computers

can then be applied up to some meters from the installation. Of course such computer equipment should meet the IEC class 3 in respect of sensitivity to transient voltages.

In fact the very fast transient voltages (VTF) are not new, but normal switching overvoltages which, as appears from the study committee 33, mostly have an amplitude of approx. 2 pu (see paper 33-12). New is the extremely high frequency and, consequently, the steepness of these overvoltages. The solution for the control of these voltages should be found in a good earthing system. In that case the transient voltages do not matter, but the transient currents produced do. Or, as professor Van der Laan of Eindhoven Technical University rather poetically words: 'chercher le courant'.

Installation of a good earthing system is often based on details. An example of same is given in figure 2 in paper 23-06, added to this text as figure 1:

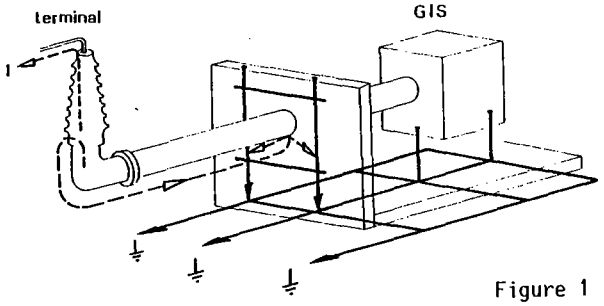

Figure 1

The transient current at the inner side of the enclosure (with a penetrating depth of some 0.1 mm) must return to the building at the foot of the terminal via the outer side of the enclosure; a detour of several meters. This creates a very big potential difference between earth and phase behind the terminal.
A far better earthing is described in figure 2, in which the two transient currents have to go about the same distance either through the phase conductor or at the inner side of the enclosure to the earthing system.

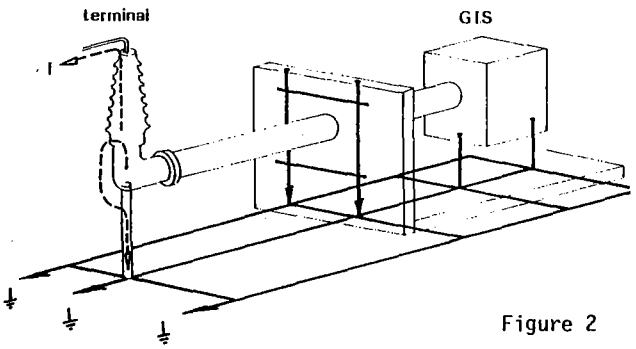

Figure 2

Consequently the coaxial behaviour of the enclosure is hardly interrupted. For the secundary cable work it is essential that it consists of a shielded two-side earthed cable, mounted directly to the enclosure and in a well-conducting cable channel.

The transient voltages that might still arise after all efforts, can easily be measured by KEMA by means of the 'sparking' test; see figure 3.

"Sparking" test

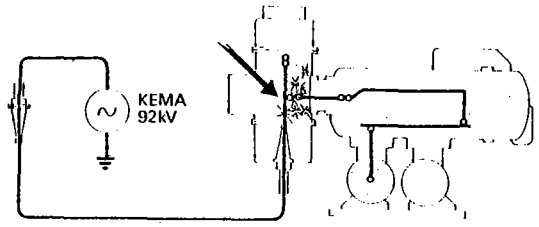

Figure 3

In such a situation a continuous 'burst train' is produced in the SF6-compartment in which a seperator is about 1.0 mm open. Then the TGPR phenomenon will appear permanently.

This test has been made by PGEM both with a GIS and an AIS. The results showed that in both cases the amplitude of the transient voltages measured steadily came to some hundreds of volts in the secundary cables. In case of a GIS the frequency varied from 100 to 300 MHz, whereas up to 50 MHz was measured in an AIS.

So the fully automatized GIS in Ulft has been in trouble-free operation during one and a half year already, in spite of the fact that process-computers are situated at a distance of only 2 meters from the installation.

M. P. CLARENNE (France)

Il faut remarquer en préambule que l'appellation MTTT (montée en tension transitoire des terres) fait croire à une montée en tension de l'ensemble du réseau de terre par rapport à la terre lointaine, comme cela se passe en cas de défaut d'isolement.

En fait, les réamorçages entre contacts du sectionneur en cours de manoeuvres engendrent des courants HF qui circulent dans les enveloppes des postes et se déversent dans le réseau de mise à la terre aux entrémités de ces enveloppes.

Dans ces conditions, le réseau de terre n'est plus équipotentiel et je préfèrerais plutôt parler des "différences de potentiel transitoires" qui apparaissent sur ce réseau.

Approche probabiliste

La valeur maximum de la différence de potentiel transitoire entre deux points donnés du réseau de mise à la terre ne s'évalue pas par des méthodes probabilistes, car elles sont calculables.

- Dans le cas où le poste comporte au moins une traversée SF6/air par phase, cette différence de potentiel transitoire dépend :

  . de la tension U du réseau,

  . de l'architecture de l'ensemble : poste blindé - réseau de mise à la terre, qui définit un coefficient de transfert k inférieur à 1 (voir réponse à la question 2.2).

La valeur maximum de la différence de potentiel atteint :

$$2.\frac{U\sqrt{2}}{\sqrt{3}}.k$$

- Dans le cas où le poste ne comporte aucune traversée SF6/air la valeur maximum que peut atteindre la différence de potentiel transitoire est définie par la tension de conduction des résistances non linéaires qui réunissent :

  . les enveloppes du poste aux gaines des câbles et

  . les enveloppes du poste aux cuves des transformateurs.

Optimalisation des mesures de protection

Les fréquences des différences de potentiel transitoires se situent dans la plage 10 - 200 MHz.

Les seuils de susceptibilité dans cette plage de fréquences des équipements à courants faibles sont généralement mal connus et de toute façon inférieures aux valeurs prescrites pour 1 ou 2,5 M.Hz, par les normes en vigueur.

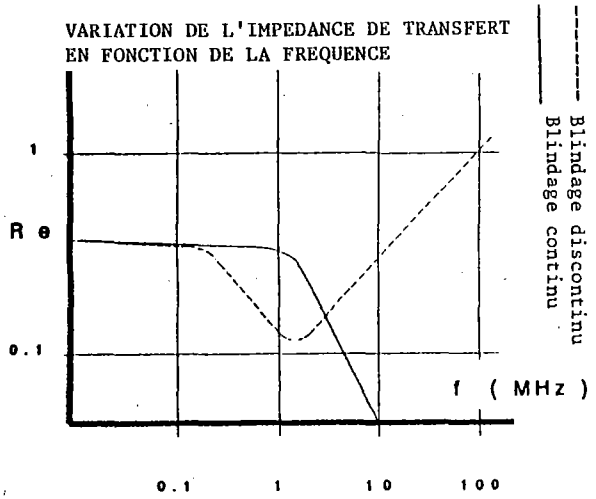

Dans ces conditions, même si la différence de potentiel est limitée à quelques centaines de Volts par des résistances non linéaires, il est prudent actuellement de protéger dans tous les cas les circuits à bas niveau par un blindage continu relié au réseau de mise à la terre à ses deux extrêmités par des connexions de faible impédance en H.F.

Le blindage continu est indispensable, car seule cette technique permet d'attribuer une valeur faible à l'impédance de transfert, dans la plage des fréquences considérées.
L'optimalisation ne peut donc porter actuellement que sur des techniques de blindages individuels (par câbles) ou collectifs (tuyaux, goulottes) et sur les accessoires de mise à la terre.

Mr. N. FUJIMOTO (Canada)

Transient Ground Potential Rise (TGPR, also referred to as transient enclosure voltage - TEV) is, in general, a nuisance problem which has always plagued GIS. Although TGPR is common to all GIS, the many GIS in existence today, for the most part, have not suffered adversely as a result of TGPR. Despite the lack of precise medical knowledge, there have been no incidence of serious shock injury by personnel exposed to TGPR. Nonetheless, the phenomenon is real and should always be given consideration in the design, operation and maintenance of GIS. In order to assess the requirement for mitigation techniques, one needs to assess its effects and importance in each specific situation.

With the knowledge and understanding available today regarding the mechanisms and nature of TGPR, GIS designs can be made, subject to other design constraints, "resistant" to the effects of TGPR at relatively little additional cost. For example, principles such as maintaining a low profile on line entry bus, use of frequent grounding connections, special bonding techniques at support structures, the use of shielded control cable with shielded connectors, careful routing of cabling, etc. can be incorporated in the station design at an early stage to minimize the TGPR and its effects. In many cases, these measures will be sufficient to control TGPR to acceptable levels.

Measures in addition to those above can be used to meet specific needs. Additional grounding and shielding can be applied at additional cost if required for specific applications, such as to facilitate the use of electronic devices in the GIS. Additional measures might also be necessary to meet certain minimum requirements, especially if the some of the simple measures are not possible because of other design constraints.

Special attention should be given to the insulated flange at direct cable to GIS connections. As suggested in paper 23-10, cases in which the insulated flange cannot be bridged (to limit circulating current or to provide galvanic corrosion protection) definitely need to be protected with varistor elements. Although TGPR-induced sparking resulting from switching operations are usually inconsequential and results in little or no damage, similar sparks by fault-induced TGPR provide paths for power frequency fault current directly across the flange, possibly resulting in significant damage [1]. Properly sized varistors are necessary in this case to prevent the formation of the transient spark and control the flow of fault current.

Question 2.2

TGPR, as an extension of the internally generated very fast transient (VFT) phenomena, shares many of the characteristics in terms of risetime, dominant oscillation frequencies, duration, etc. As a result, calculational techniques which are employed should utilize the same philosophy as for the calculation of VFT, i.e. modeling with distributed components. Computer programs which are normally used to compute VFT voltages, such as the EMTP, can be used successfully to simulate TGPR, provided that proper modeling is possible. One key idea which needs special attention is the lack of a common ground reference for travelling waves. For instance, to model the GIS/air termination by the three transmission line network requires that an ideal transformer be implemented, when using the EMTP, to account for the proper connection of the three transmission lines and the discrepancy in ground reference (figure 1).

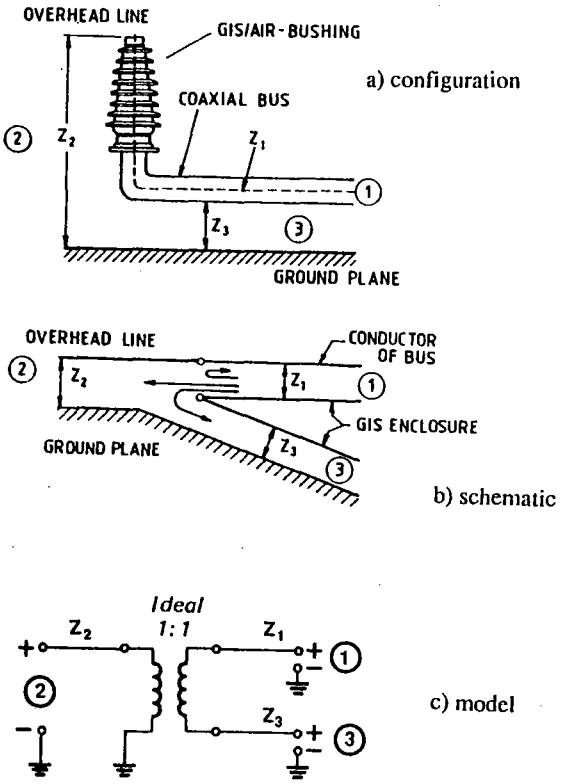

Figure 1 - Modeling of the GIS/air termination with an ideal transformer to account for proper coupling of TGPR.

VFT modelling has resulted in excellent agreement between calculated and measured results, primarily because good models of the well-controlled internal GIS geometry are possible. Modeling of external components for TGPR offers additional challenges and uncertainties. Propagation is lossy and the eddy current losses in the ground should be considered. Measurements in actual GIS indicated an overall attenuation of TGPR in the range of 0.3 db/m [2]. Every ground lead and support structure affects the TGPR signal and influences the waveshape. Precise modeling is extremely difficult although reasonable results might be possible in simple, well-controlled geometries. Otherwise, computer simulations should be used for order-of-magnitude calculations to assist in the analysis of phenomena and evaluate the effectiveness of mitigation schemes. In critical situations, direct measurements in the station environment might be prudent.

When these computer techniques are used in concert with a good fundamental understanding of the TGPR phenomena, various mitigation techniques can usually be developed for almost any practical situation. This approach will often result in order-of-magnitude solutions but can be achieved with relative ease. More precise results requires greater modelling accuracy which, in all but the simplest configurations, is probably not feasible, especially when effective solutions are available by the other approach.

1. Fujimoto, N., S.J. Croall and S.M. Foty. "Techniques for the protection of gas-insulated substation to cable interfaces." Presented at the IEEE PES Summer Meeting, July 1987. Paper 87 SM 530-9.

2. Fujimoto, N., E.P. Dick, S.A. Boggs and G.L. Ford. "Transient ground potential rise in gas-insulated substations - Experimental studies." IEEE Trans. on PAS, *PAS-101*, No.10, October 1982.

Mr. W. BÜSCH (Switzerland)

1) Accuracy of computer models integrating the GIS surroundings

The space inside a GIS enclosure is defined rather exactly. In general, a high level of accuracy may be obtained with reasonable effort.

The configurations in the surroundings of a GIS, e.g. complex conductor grids, screens and dielectrica, are more unsymmetrical and variable. Modelling these surroundings is therefore more difficult.

The accuracy of such digital computations depends on the following factors:
- the way in which the technical circuit is modeled by the applied equivalent circuit,
- the accuracy of the constants and curves defining the characteristics of the elements of the equivalent circuits,
- the computer time available for the calculation.

From a practical perspective similar accuracy to the one achieved for circuits inside the enclosure may not be possible for GIS surroundings without an extremely high computational effort.

A resonable compromise between accuracy and computational effort must be found. In practice errors of some 10 % seem to be tolerable.

2) Contribution of computer programs to a proper selection of remedial measures

In order to avoid expensive remedial measures after commissioning of installation, it is important to incorporate appropriate measures at the design stage. Suitable computer programs should be a good tool for that.

In many cases some possible measures have to be compared. To eliminate the uneconomic measures, frequently a rough estimation of the effectiveness of the solutions is sufficient.

For such a comparison only the difference between the considered cases is relevant. Thus the most effective and economic measure only may be selected for a specific case.

3) Where are the limits?

Crest values of overvoltages are calculated with some uncertainty.

The limits of such computations are given by
- the knowledge about the characteristics of the elements of the outer circuits, and
- the allowed economic effort.

In principle, it is possible to improve the accuracy of the results by:

- modelling the GIS and its surroundings using a higher number of elements and considering additional interactions,
- improving the accuracy of the input data by executing additional tests on simplified arrangements.

M. P. CLARENNE (France)

La simulation n'est intéressante que pour les postes équipés de traversées SF6/air qui présente une grande discontinuité d'impédance. Son principal intérêt réside dans la nécessité d'expliciter clairement les couplages entre conducteur HT et réseau de mise à la terre dans la zone étudiée

Cette simulation conduit vers des agencements qui réduisent les valeurs des différences de potentiel transitoires en fixant des valeurs aux inductances propres des éléments du circuit tels que : connexions de mise à la terre des traversées et des diviseurs capacitifs, géométrie du réseau de terre de la terre de travée...

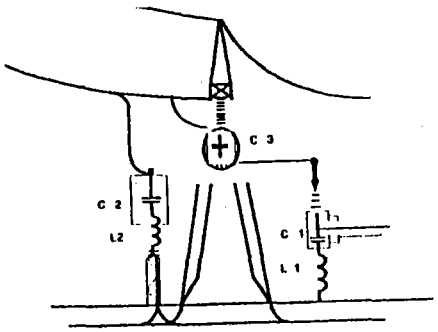

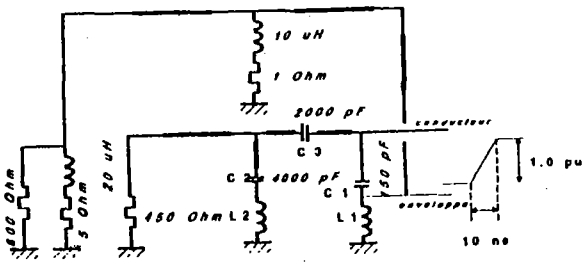

FIGURE 1 - SCHEMA DE LA SIMULATION

L 1 = 10.8 u H L 2 = 7.0 u H	12.1 7.8	3.7 8.1	3.8 7.8
L 1 = 6.8 u H L 2 = 3.8 u H	7.8 4.8		
L 1 = 4.8 u H L 2 = 3.1 u H	7.8 4.8	3.1 5.1	2.85 4.8

La précision des simulations dépend de la fidélité des modèles et de la précision sur les valeurs des paramètres. Toutefois :

- les modélisations : . de la source (zone en amont de la transition étudiée)

  . de la forme de l'onde génératrice du phénomène,

- les évaluations des inductances propres des constituants du circuit dans la plage des 10 - 200 MHz,

sont incertaines et les données telles que celles de la figure 1 ne sont que des approximations.

Malgré ces approximations, la simulation définit un coefficient de transfert :

$$k = \frac{\text{différence de potentiel transitoire}}{\text{amplitude de l'onde génératrice}}$$

d'une configuration donnée et toutes choses égales, permet de rechercher la plus avantageuse.

L'analyse des paramètres montre que pour réduire le coefficient de transfert, il est souhaitable:

. de réduire la distance entre la base de la traversée et le réseau de terre,

. de réduire l'impédance en HF du réseau de mise à la terre (méplats en faisceaux - grands rayons de courbure...).

. d'utiliser au mieux la voie de refermeture pour les courants HF que constituent les diviseurs capacitifs,

. de réduire la surface de la boucle : conducteur HT - traversée - réseau de terre - diviseur capacitif. (voir Figure 2)

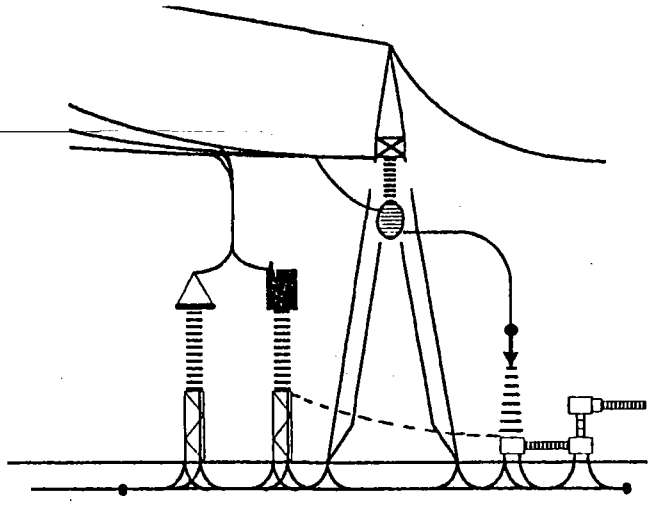

FIGURE 2

En utilisant le logiciel EMTP avec les éléments de la figure 1, puis en jouant sur la disposition des appareils et la conception du réseau de terre, nous avons obtenu les coefficients de transfert ci-dessous :

La limitation aux valeurs tolérables des tensions de pas et des tensions de contact, exige d'enterrer une certaine longueur de conducteur constituant l'électrode de terre. Plutôt que d'implanter arbitrairement le maillage, il est avantageux de disposer la longueur nécessaire de manière à ce que les inductances propres des éléments du réseau de terre mentionnés plus haut soient minorés, ce qui en définitive n'a qu'une très faible incidence sur le coût.

DISPOSITION	BUSHING			
	SUR CHASSIS STANDARD		SUR CAILLEBOTIS	SUR CHASSIS SURBAISSE
	CIRCUIT - BOUCHON POSE	CIRCUIT - BOUCHON SUSPENDU	CIRCUIT - BOUCHON SUSPENDU	CIRCUIT - BOUCHON SUSPENDU
CLASSIQUE	0.87	0.52	0.45	0.36
ADAPTEE	0.38	0.55		
LIAISON DIRECTE	0.36	0.42	0.32	0.25

$$k = \frac{\text{Différence de Potentiel Transitoire}}{\text{Amplitude de l' Onde Génératrice}}$$

Mr. C. NEUMANN (Fed. Rep. of Germany)

Transient Ground Potential Rise (TGPR) or according to the new CIGRE-terminology Transient Enclosure Voltage (TEV) leads to overvoltages in the secondary equipment of GIS caused by different coupling mechanisms. With regard to the increasing application of electronic- and microprocessor-based secondary equipment, the knowledge of TEV and of measures to reduce these voltages takes on increased significance.

Digital computer programs can help to study the fundamentals and to reduce the testing expenditure considerably.

The following examples may demonstrate which fundamental physical phenomena of GIS must be taken into account for such calculatory investigations. The calculations were performed with the well-known EMTP. The configuration considered is similar to the SF_6/air-termination described in

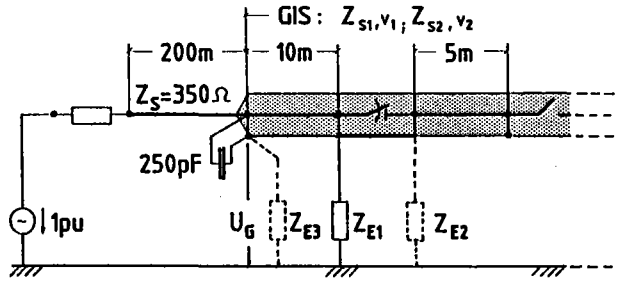

Fig. 1 : Equivalent circuit for the simulations

Report 23-10. Fig. 1 shows the corresponding equivalent circuit. The GIS-elements are represented in modal quantities, i.e. for a single-phase enclosed switchgear exist two modes per phase.

Furthermore, a frequency-depending damping and a voltage collapse with a time to breakdown according to Toepler's law is taken into account.

Fig. 2 a shows the transient voltage u_G at the SF_6/air-termination with and without frequency-depending damping. The voltage collapse across the disconnector is assumed to take 20 ns.

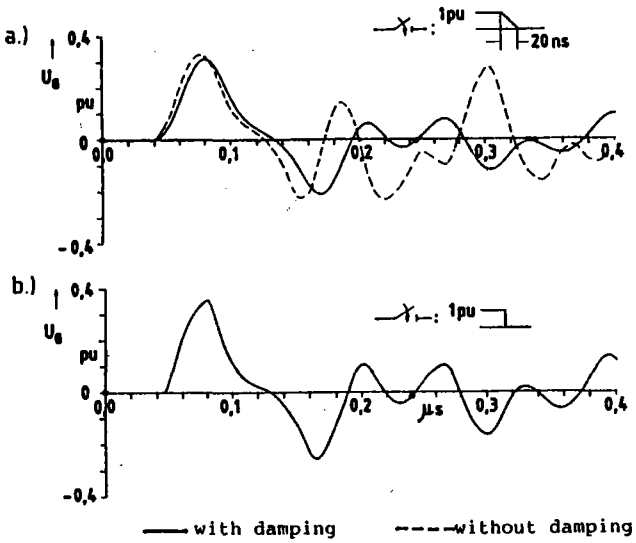

Fig. 2 : TEV at the SF_6/air-termination according to different assumption

One can find a maximum overvoltage of about 0.3 pu. Taking damping not into consideration the value is about 5 % higher. Since in this case the surge impedance and the velocity of the ground mode must be assumed for a constant frequency, the time behaviour differs from that with frequency-depending damping.

Fig. 2 b shows calculation results for a simulation with frequency-depending damping, but the voltage collapse across the disconnector is assumed to be a square-wave voltage step.

One can see that the maximum overvoltage is only poorly affected by the different assumption. This is in contrast to results of calculation of VFTO in GIS, where the maximum overvoltage shows a strong dependence on the voltage collapse, i. e. on the time to breakdown assumed. This can be explained by the fact that the voltage collapse is coupled on the enclosure and generates in this way an oscillation in the earthing circuit producing the TEV.

The assumption of a frequency-depending damping in the calculation leads to a more realistic time behaviour, particularly in the region of the second peak of the oscillation. This may be of importance when considering damping measures.

To gain realistic values, therfore, our further studies took into account frequency-depending damping. For the same model could also be applied for simulations of VFTO in GIS, a voltage collapse with a time to breakdown of 20 ns was assumed, too.

With this model investigations were performed with the aim to reduce the TEV, e. g. the TEV at the SF_6/air-termination.

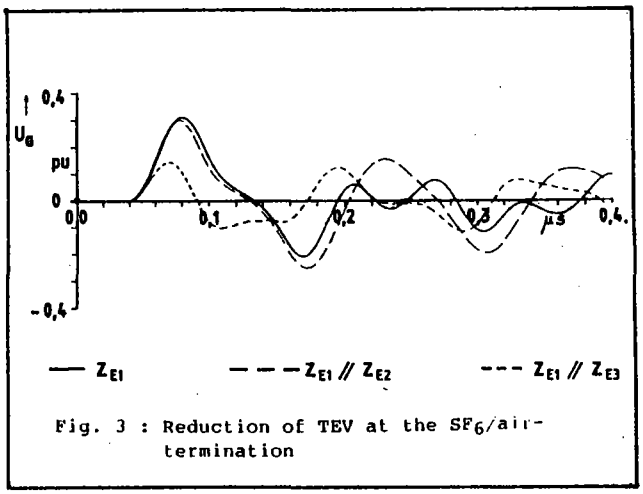

Fig. 3 : Reduction of TEV at the SF_6/air-termination

From Fig. 3 can be taken that the transient overvoltage at this point cannot be reduced by decreasing the impedance of the main earth connection simulated in the calculations by an additional impedance Z_{E2}. However, an additional earth connection between the bushing flange and the earthing grid - represented in the calculations by the impedance Z_{E3} - can limit the overvoltage to 0.1 - 0.15 pu.

The results are in good correspondance with the values calculated in Report 23 - 10.

Mr. A.J. ERIKSSON (Switzerland)

As noted also in papers 23-06 and 33-13, we emphasise that a great deal of work has now been done in this field - and that there is no particular mystique still involved.

TGPR arising in GIS through disconnector switch initiated VFT are well understood, well defined (through either measurement, or computation), and are readily controlled.

Practical TEV have amplitudes up to about 10% of the originating VFT, but longer rise-times (some 50-200 ns), and are principally influenced by

- the nature of the GIS interface, or discontinuity (such as an AI bushing)
- the GIS geometry, layout, and earthing
- the spacing and geometry of grounding connections

In response to the Special Reporter's questions concerning optimised design considerations, we fully endorse the measures outlined in 23-06 and 23-10, having applied similar concepts to good effect in many GIS. In practice, we follow a deterministic approach - based on consideration of worst-case VFT characteristics - and feel it important that such "remedial" measures be incorporated from the beginning, as part of an integrated engineering design.

In consistency with modern principles of electromagnetic compatibility (EMC), an integrated approach should include the following aspects:- [2]

(a) Control of the TEV at source, through;

- appropriate disconnector design
- modular design / layout of GIS components, thereby tending to standardise the GIS geometry and reducing the profile
- standardised layout of GIS bonding and grounding connections - in order to avoid empirical on-site "solutions"
- primary shielding and bonding, through integration with building metallic screens

(b) Minimisation of coupling, through, eg

- meshed earthing systems
- effective shielding of secondary circuits (ie. design of cable shields / connectors)
- correct cable shield and secondary circuit grounding principles
- mains supply filtering, and transient overvoltage control

(c) Tertiary shielding of secondary equipment, through, for example;

- design of appropriate housings
- layout and segregation of circuits
- high attenuation interfaces with isolation (including fibre-optics)

The overall aim should be to ensure that any disturbance voltages due to TEV are reduced to well within the final electronic equipment tolerable levels.

Although TEV do not present any direct hazard to persons, co-ordinated implementation of such measures will also ensure the absence of visible sparking and will avoid any disturbance of personnel.

We have successfully applied such an integrated approach in the design of GIS installations up to the highest voltages (765 kV), in combination also with modern microprocessor based control and protection systems in the switch bay environment. [2]

In response to question 2.2 concerning analysis of relative VFT and TEV control measures using computerised simulations, Figures 1 and 2 illustrate comparative measurements and computer-based analyses of the TGPR adjacent to a practical 765 kV GIS installation. Simplified travelling wave analyses were used to examine the effects of the various grounding measures employed, (based on modelling in the equivalent frequency domain, up to about 10 MHz).

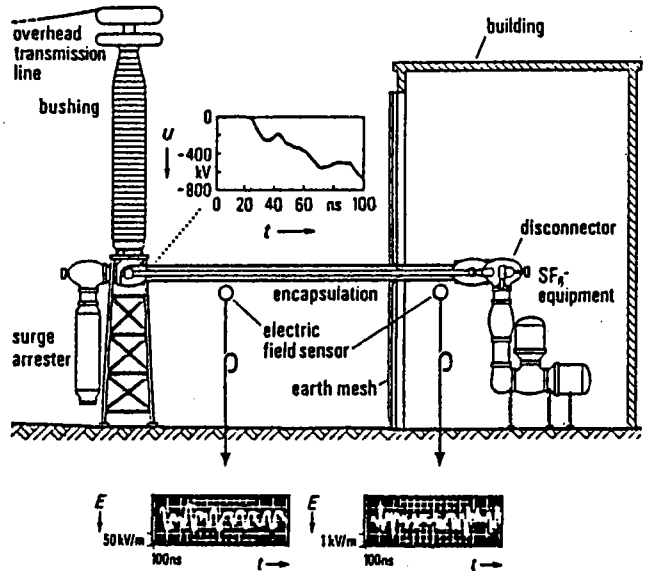

Figure 1: Comparative measurements of TEV - inside and outside the building mesh - for a 765 kV GIS installation

In this example, direct flanging of the GIS bus-duct to the building reinforcing steel mesh - coupled with appropriate grounding at the building and at the GIS bushing/MO surge arrester interface, ensured about 30 dB attenuation of the TEV arising inside the building during disconnector "Close" operations. As seen in Figure 2, the travelling wave representations of the grounding measures correctly reproduce the observed characteristics of the measured TEV - and the relative attenuation inside the building.

Coupled with the use of relatively standardised GIS modular layouts, we regard such simplified modelling procedures as suitable for the assessment of effective TGPR control measures in practical GIS installations.

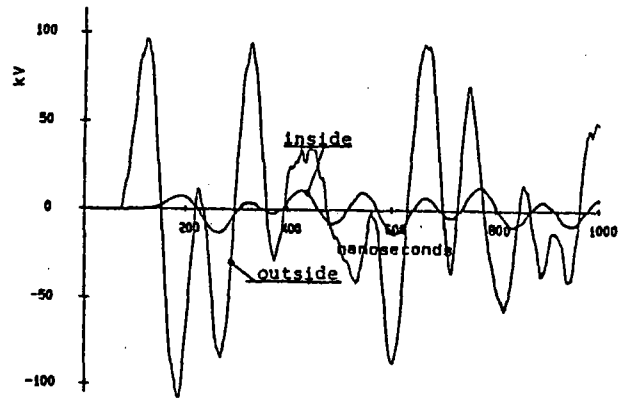

Figure 2: Comparative computation of the TEV - inside and outside the building mesh - using a simplified travelling wave model.

[1] Meppelink J., et al; "Very fast transients in GIS" IEEE PES Paper 88 WM 114-1.

[2] Meppelink J., et al; "Electromagnetic compatibility in GIS substations". BBC Review No 9-1986.

M. P. CLARENNE (France)

Les résultats qui viennent d'être présentés de deux séries de simulations effecutées indépendamment, fond apparaître des coefficients de transfert minima de 0,1et 0,25.

Cette différence confirme que les résultats dépendent étroitement des modèles. Ainsi par exemple dans ces deux cas, les durées de montée de l'onde génératrice du phanomène étaient respectivement de 20 et 10 ns. Quelle est-elle réellement ?

La simulation est surtout intéressante pour définir la disposition optimum. Néanmoins si ce genre d'études devait se développer, il serait souhaitable de convenir des valeurs à donner à la durée de montée du front d'onde, à l'impédance de la source, aux impédances caractéristiques de la ligne et du réseau de garde, afin de pouvoir comparer des choses comparables.

36-00

PART OF SPECIAL REPORT FOR GROUP 36

(Interference)

by

W. JANISCHEWSKYJ*
(Special Reporter)

Introduction

Traditionally, the purview of CIGRE Study Committee 36 included the "interphase" between two vital industries of a country. This "interphase" is formed by "interference" between installations of power utilities and those of communication companies. Solution of problems occurring within this "interphase", naturally, requires efforts on the sides of both industries, and, from the standpoint of a country as a whole, a haphazard approach is unacceptable, since a technically sound as well as economically optimal solution must be seeked (1).

With the advent of modern information processing equipment, performance capabilities of power systems and those of communication networks have been highly enhanced, however, at the same time the need for compatibility between the two has much increased. In this context one thinks of the electromagnetic compatibility aspect of communication as well as control equipment operated near or within power utility facilities. This equipment is exposed not only to capacitively coupled high-frequency electromagnetic noise, but also to inductively and conductively coupled electromagnetic influence down at power frequencies and at their harmonics. Susceptibility of such equipment to extraneous noise and need for its immunity constitute present day's questions that must be answered satisfactorily by manufacturers as well as by users of such equipment (2). Two preferential subjects for the 1988 Session were chosen by the CIGRE Study Committee 36 with this background in mind.

There is, however, one more area of "interference" with installed equipment that falls within interests of our Study Committee and is also addressed by one of this year's preferential subjects. Ground currents are found in the vicinity of power installations and they may harm buried metallic parts of industrial installations. Sheeths of cables, metallic pipes, ground rods and similar objects may be consumed by electrically enhanced galvanic corrosion. Equipment in question may belong to power industry itself, it may be part of communications industry or it could be operated by other industries such as suppliers of oil or gas.

Concerns about induced voltages and associated ground currents as well as their long-range corrosion effects resulted in placing this topic as the *first* preferential subject. Rationel for selection of the second discussion topic relates to previous work of our Study Committee on power line noise below 30 MHz. As may be seen from the present CISPR standard (3), such questions as passive interference or influence of electromagnetic noise upon instrument landing systems and upon communication between land mobile vehicles still remain unanswered. These, together with the capacitively coupled interference at frequencies above 30 MHz have been lumped together and posed as the *second* preferential subject. Finally, electromagnetic compatibility (EMC) problems related to power plants and substations constitute the *third* preferential topic for the 1988 Session of CIGRE Study Committee 36.

On topics of the three preferential subjects of the present Session, a total of ten papers was received; a very satisfying response from the technical community. Papers are reasonably distributed among the three preferential subjects. Three reports discuss questions related to the *first* preferential subject, two papers report on measurements relevant to the *second* subject, and five contributions focus on various aspects of the *third* topic.

Some aspects of preferential subjects have been treated at the June 1987 Colloquium of Study Committee 36 held in Montreal. On that occasion there was an especially suitable opportunity for the exchange between the Northamerican viewpoint and opinions of experts throughout other parts of the world. When appropriate, reference will be made to ideas expressed in Montreal.

PREFERENTIAL SUBJECT NUMBER 3:

Electromagnetic compatibility problems and protection methods, especially with regard to local instrumentation networks (including optical fiber transmission) in power plants and substations.

The third preferential subject seems to have captured the attention of experts throughout the world and attracted a total of five papers (36-01, 36-02, 36-05, 36-07 and 36-10). All five papers discuss the different coupling mechanisms involved and their relative weights within various frequency ranges. Of these, a total of four papers tackle primarily the question of immunity to electromagnetic radiation, and only one paper (36-02) deals in detail with questions of potential rise caused by ground currents.

* UNIVERSITY OF TORONTO, DEPARTMENT OF ELECTRICAL ENGINEERING, TORONTO, CANADA M5S 1A4

Electromagnetic Noise and Immunity

The four papers (36-01, 36-05, 36-07 and 36-10) authored on opposite sides of the globe, have a lot in common, although each deals somewhat differently with the influence of electric power installations upon delicate electronic equipment on premises of power utilities or in their vicinity. All papers analyse the sources of "noise" and the various modes of their "interference" and focus on electromagnetic compatibility of communication equipment in this "environment". While intermediate steps and even some observations are different (eg. the question whether peak values of radiated fields caused by switching operations in gas insulated installations are larger or smaller than in air insulated substations), there are some observations and conclusions that are the same. All papers agree that radiated fields in gas insulated stations, because of the difference in geometry and layout, have a much wider frequency bandwidth reaching into the range of tens of MHz. Also, economical solution to the electromagnetic noise problem was normally found through reduction of incident noise, eg. by increased shielding, rather than through raising, by changes in design, the immunity level of electronic equipment. It is most satisfactory, however, to see that observations and reasoning of experts from different countries produce a complementary picture of a very complex, and so timely problem.

Question 3.1

It would be interesting to hear from other experts in the field that may have a different approach to resolution of the perennial problem of choice between higher immunity levels of communication equipment and lower noise generation by power plant.

Would local economy in some parts of the world require a solution opposite to that adopted by the above four papers, i.e. where special equipment with increased immunity levels would be preferred?

Question 3.2

In reading the four papers one cannot help to notice that in tackling the same problem, each paper refers to a different set of specifications. Are such specifications, existing in different parts of the world, compatible with each other or is there, as suggested by paper 36-07, a need, for special specifications in this area? Will one set of such specifications do or must there be different specifications for each type of electronic equipment?

Question 3.3

Paper 36-05 suggests that it is the task of the power utility to achieve "compatibility" of sensitive communications equipment with the "environment" created by the power installation. Are there other views to the resolution of this question? Should manufacturers of electronic equipment be responsible for achieving the needed level of "immunity"?

Potential Rise of Underground Conductors

Interference effects of ground currents are treated under the first preferential subject. As mentioned previously, it was decided to treat the potential rise caused by ground currents under the third preferential subject only.

All five papers (36-01, 36-02, 36-05, 36-07 and 36-10) touch on the question of ground currents in substations and on the associated potential rise of cable sheeths and control circuits. However, only paper 36-02 provides a comparison between computed and measured values of cable sheeth potential rise following a fault on the high voltage side of a substation. Good correlation is shown between computed and measured results, and both indicate dangerously high voltages. It is surprising, however, that in accordance with practice in Canada and USA, as reflected by IEEE Standards No. 80 (8) and 367 (9), voltage rises shown in the paper are excessive. Two questions should therefore be asked:

Question 3.4

Why is there a difference between data shown in the paper and those found in Northamerican specifications?

Question 3.5

What should be done to protect personnel and equipment from dangerous overvoltages?

Authors of paper (36-05) discuss in detail methods of grounding that are especially appropriate for high frequency. It would be of interest, however, to compare quantitatively the low frequency performance of their grounding associated with a fault similar to that discussed in paper (36-02).

Question 3.6

Is the potential rise of ground used in paper 36-05 similar to that shown in paper 36-02, or would the authors of paper 36-05 find their performance closer to that of IEEE Standards 80 and 367?

In paper (36-10) effects of electromagnetic fields associated with transient processes such as switching operations and occurrence of lightning were studied in detail. Effects of low-frequency earth currents associated with these processes were only touched upon in discussion. At the same time resultant potential rises were not determined but may be equally important. The situation is especially severe when in very large stations, islands of potential rise can occur. As a result, large currents flow over the bonding conductors and are responsible for large induced voltages in communication and control circuits.

Question 3.7

How would one evaluate the large currents flowing in bonding cables connected to several grounding grids?

Question 3.8

Can the authors of paper (36-10) elaborate on the magnitudes of fault currents produced in their chosen example? Again, how do these compare with results of paper (36-02)?

REFERENCES

[1] D.M. Hinton, W. Janischewskyj, "Power and Communications: Partners and Adversaries", COPIMERA (Panamerican Congress of Mechanical and Electrical Engineering and its Allied Branches), Montreal, Canada, October, 1982.

[2] Gerry A. Jackson, "International EMC Cooperation - Past, Present, Future", Keynote speech, 1986 International Symposium on Electromagnetic Compatibility, Symposium Record, pp. 1-3.

[3] CISPR, Publication 18, "Radio Interference Characteristics of Overhead Power Lines and High Voltage Equipment" Part 1: Description of Phenomena (1982), Part 2: Methods of Measurement and Procedure for Determining Limits (1986), Part 3: Code of Practice for Minimizing the Generation of Radio Noise (1986).

[4] W. Janischewskyj, A.M. Hussein, N.H.C. Santiago, "Performance and Analysis of a Micro-Gap Discharge Circuit", IEEE Transactions Paper, No. 86 SM 408-9, IEEE/PES Summer Meeting, Mexico City, Mexico, July 20-25, 1986.

[5] Cortina, R., et al., "Results of Measurements of Corona Effects (Loss, RI, Audible Noise), on Large Conductor Bundles and Large Diameter Tubes", CIGRE, Paris, 1980, Report No. 36-06.

[6] W. Janischewskyj, E.B. Harvey, M.G. Comber, "Power Line Interference and Assessment of Television Picture Quality", IEEE Transactions on Power Apparatus and Systems, vol. PAS-102, No. 5, May 1983, pp. 1039-1049.

[7] R.G. Olsen, V.L. Chartier, "Recent Advances in Modeling and measurement of Electromagnetic Interference From Electric Power Lines", Paper presented at the CIGRE SC 36 Colloquium, Montreal, Canada, June 8-9th, 1987.

[8] R.C. Madge, "Effect of Large Metallic Structures on AM Radio Broadcast Patterns", Paper presented at the CIGRE SC 36 Colloquium, Montreal, Canada, June 8-9th, 1987.

[9] "Guide for Safety in AC Substation Grounding", ANSI/IEEE Standard 80-1986.

[10] "IEEE Recommended Practice for Determining the Electric Power Station Ground Potential Rise and Induced Voltage from a Power Fault", IEEE Standard 367-1987.

International Conference on Large High Voltage Electric Systems

112, boulevard Haussmann — 75008 Paris

1988 Session — 28th August - 3rd September

T

36-05

Pref. Subj. 3

PROTECTION OF MICROPROCESSOR BASED DISTRIBUTED CONTROL UNITS IN GAS INSULATED SUBSTATIONS AGAINST ELECTROMAGNETIC INTERFERENCES

by

F. CHEVALLEY*
Services Industriels de Genève

H. SAUVAIN
EMC Fribourg

(Switzerland)

Summary

This paper presents the measures to be taken to protect sensitive equipment such as microprocessor based distributed control units in gas insulated substations (GIS) against electromagnetic interferences.

First the paper explains the set of problems associated with electromagnetic interference (EMI) by dividing them into EMI source, its victim and the couplings between them.

Then it presents results of disturbance measurements taken in high voltage substations and of immunity tests on a microprocessor based control unit.

Finally constructional measures are proposed. They refer to the construction of the buildings, of high voltage equipment, of sensitive equipment and to the grounding grid.

Key words

substation - electromagnetic compatibility - microcomputer - network operation

1. Objective

The regional transmission networks 220/130 kV and the distribution networks 18 kV as well as their generation plants are operated by means of a remote control system including the dispatch center equipped with process computers and the remote control units in the substations. All the relevant network components are remotely monitored and operated.

In order to facilitate the transmission of information to the dispatch center, the power utility presently modifies their local control equipment by installing microprocessor based distributed control units near to the high voltage apparatus of their substations and plants.

The control functions of these units are feeder oriented and are connected to the central unit, where the remote and local control functions are integrated.

The operation of such sensitive units within the zone of high voltage GIS SF6 equipment, which is strongly disturbed, requires the investigation of electromagnetic compatibility.

2. Electromagnetic interferences (EMI)

2.1 The Electromagnetic compatibility (EMC) concept

Regarding EMC the EMI source is connected to its victim by four couplings of different type: galvanic, capacitive, inductive and radiated coupling.

The concept also includes means of protection associated with the emitter and/or receiver, and with the couplings [1].

2.2 The EMI source

The operation of high voltage isolators or circuit - breakers produces heavy electromagnetic disturbances, which are much more pronounced in gas insulated substations, compared to open air substations.

When an isolator or a circuit-breaker is operated in a GIS SF6 substation, electromagnetic impulses with a steep wavefront are generated by the internal electrical arc. Additionally, these impulses are reflected at the ends of the metallic casings (line and/or cable feeders). The frequency spectrum ranges from low frequencies up to some tens of Megahertz. These predominantly electrical (E) field impulses are initially restricted to the interior of the metallic casings which represent a very good shielding. However, electromagnetic waves propagate outside at line and cable feeders, since at these critical places there is a discontinuity in the characteristic impedance and an opening in the shielding [2].

Also the measuring sensors (voltage, current etc.) within the insulated substation provide preferred paths for the propagation of the disturbances.

* Services Industriels de Genève, Service de l'Electricité, Case Postale, 1211 Geneva 11,

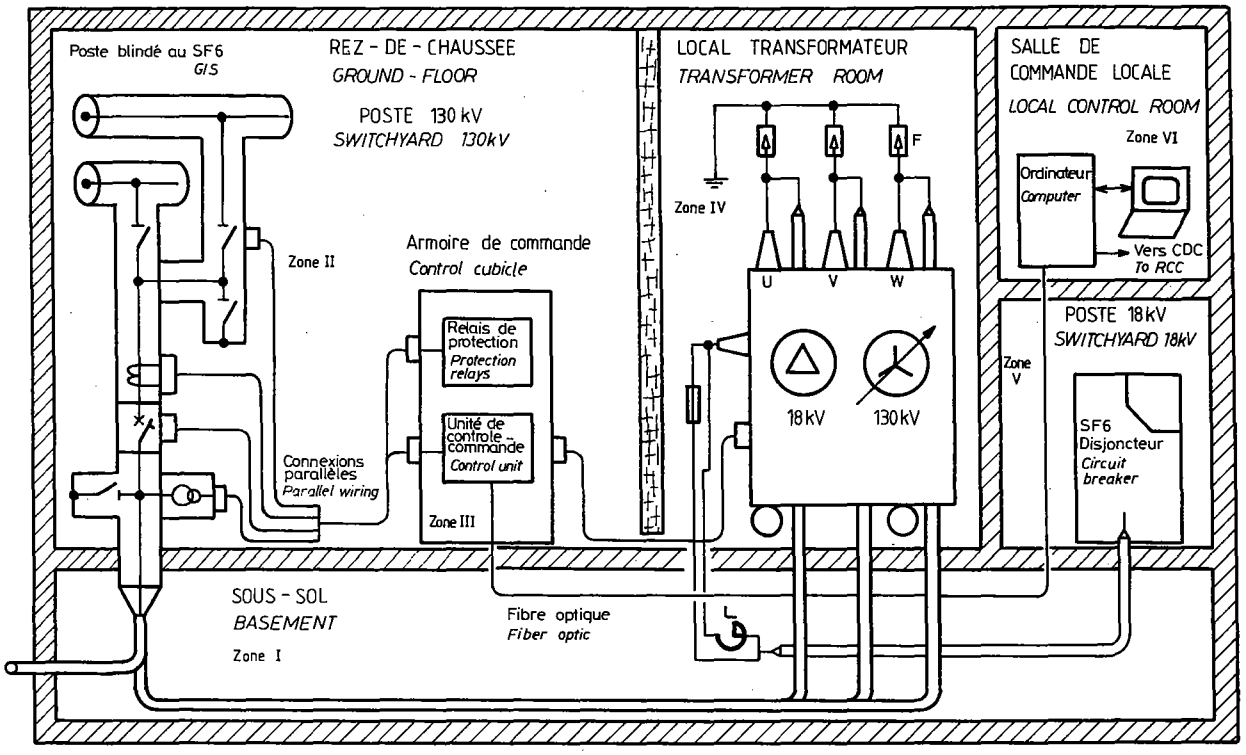

Fig.1: Cross-section of the substation and arrangement of the EMC zones.

2.3 Couplings

The electric field produced by a current can be defined mathematically by its three components: electrostatic, induction and radiation, as it is shown in formula (1) in the simplified case of a dipole model. For an electrical impulse with a frequency of 10 MHz (wavelength λ = 30 m) (Fig. 2) the radiation component becomes very important for a distance r from the source as it is given in formula (2).

$$(1)\quad E(t) = \frac{2h}{4\pi\varepsilon_0}\left[\frac{1}{r^3}\int_0^t i(t)\,dt + \frac{1}{r^2 c}\,i(t) + \frac{1}{rc^2}\,\frac{di(t)}{dt}\right]$$

$$c = \frac{1}{\sqrt{\mu_0 \varepsilon_0}} = 3.10^8 \text{ m/s}$$

$$(2)\quad r \geq \lambda / 2\pi \cong 5\,\text{m}$$

Thus a simultaneous protection in the conducted mode (filters, spark gaps, varistors etc.) and in the inducted and radiated modes (shielding) becomes necessary [3].

For the auxiliary lines and the grounding network the lengths involved are often near to a quarter of the lengths of the disturbing waves. The following parameters: characteristic impedances of the line or feeder, propagation, reflection, antenna effect, are indispensable in a protection study. A grounding network designed only for 50 Hz is no longer sufficient, because its impedance at high frequencies is too large [4].

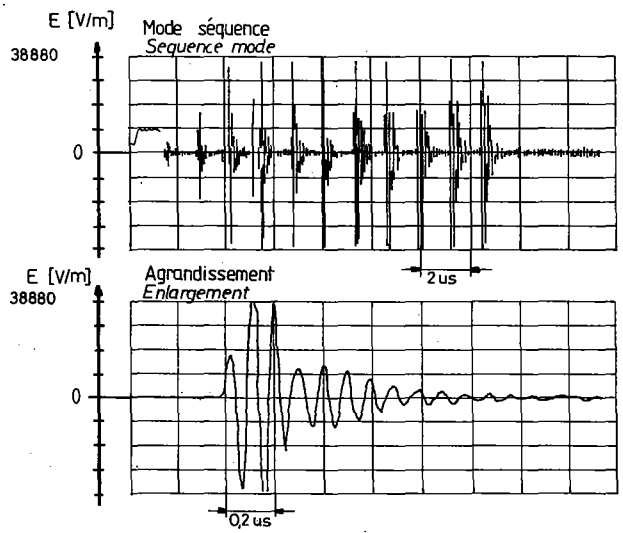

Fig.2: Electrical field (vertical polarisation) generated in a GIS SF6 220 kV substation on opening an isolator (in sequence mode, the time interval between 2 impulses is not significant).

2.4 The EMI victims

In the case of conducted interferences, the standards related to the protection of electronic equipments against electromagnetic disturbances, such as the standard IEC 255 [5], are insufficient in view of the disturbance phenomena found in GIS SF6 substations. Standards applicable to industrial processes and not to substation equipment, recently issued or in preparation, such as IEC 801 [6], cover these phenomena much better.

In the cases of radiated and induced interferences, tests performed according to IEC 801 have shown that microprocessor based control units, exposed to a permanent electromagnetic field, sometimes form unfavourable weak points in immunity. The example in Fig.3 shows a deficiency at 10.8 MHz.

Thus an incompatibility can be expected since the impulse electromagnetic field measured in the GIS SF6 substations reaches the maximum value of 38.8 kV/m exactly at 10 MHz (Fig.2). Because it has an amplitude which is several thousands of times bigger than the permanent field used in the test, it will produce more important disturbing effects.

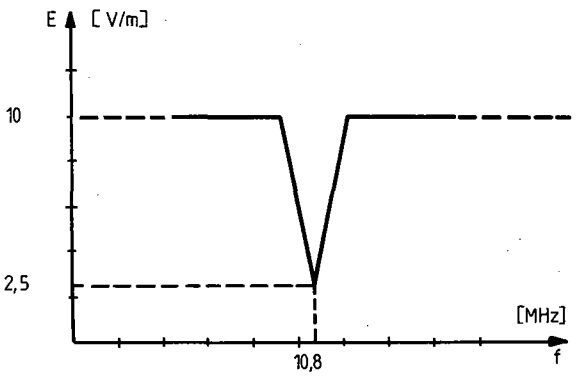

Fig.3: Immunity of a microprocessor based control unit exposed to a permanent electromagnetic field according to IEC 801-3.

3. Results of measurements

3.1 Measuring arrangement (in impulse mode)

The conducted interferences are measured in terms of:

- voltage u(t)
- current i(t)
- power u(t) * i(t)
- energy $\int_0^t u(t) * i(t)\, dt$

The radiated (and induced) interferences are measured in terms of:

- electric field E(t)
- magnetic field H(t)

The measurement arrangement (Fig.4) uses passive and active sensors (Fig.5) and allows for the following parameters: power, energy, differential value. A shielded cage protects it against the intensive electromagnetic environment.

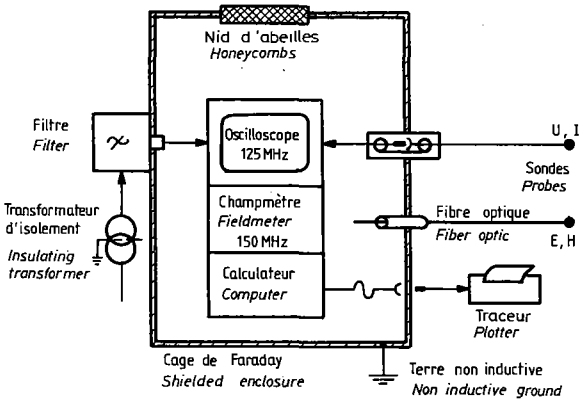

Fig.4: Measuring arrangement.

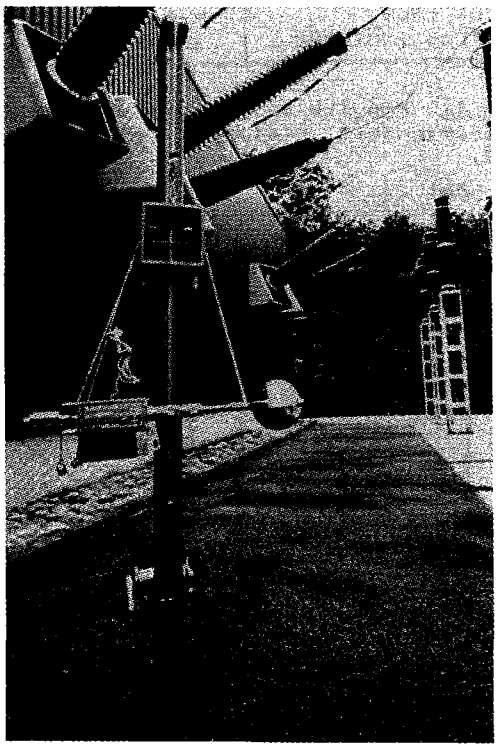

Fig.5: Measuring of the electrical impulse field in open air, outside a 220 kV GIS SF6 substation.

3.2 Characteristics of the disturbances

The electric (E) and magnetic (H) fields measured in the GIS SF6 substation Foretaille and in four other open air substations are displayed in Table I. The maximal electric field measured (Fig.2) reaches 38.8 kV/m in the 220 kV GIS SF6 substation, against 1.1 kV/m in the open air insulated 130 kV substations (Fig.6).

Action Place of measurement	Type of substation	E (V/m) H (A/m)	
Opening changeover isolator Substation building 5 m from feeder	220 kV SF6 indoor	38 880	<1
Closing changeover isolator Substation building 5 m from isolator	130 kV air indoor	1 150	2
Opening changeover isolator Under air isolator 4 m from isolator	130 kV air outdoor	940	3
Closing changeover isolator Marshalling kiosk armed concrete 20 m from isolator	130 kV air indoor	3	<1
Opening isolator Relaying kiosk 6 m from isolator	130 kV air outdoor	3	<1
Opening isolator Control room 50 m from isolator	130 kV air indoor	<1	<1

Table I: Results of measurements of impulse electromagnetic fields, radiated and induced.

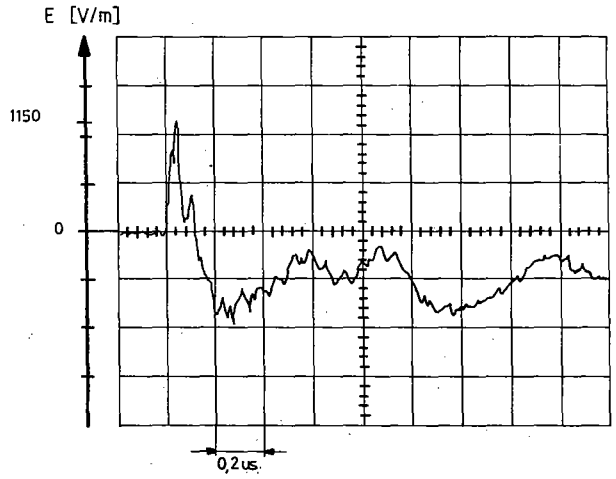

Fig.6: Electrical field (vertically polarized) measured in an open air 130 kV substation when closing an isolator.

The voltages and currents induced into the auxiliary lines in the five substations are measured at different places: HV substation, relaying kiosk, cubicles in the HV substation, marshalling board, load dispatching center; they are recorded in the common and differential modes. Fig.7 shows the voltage and the current on a +24 V telecommunication line in Foretaille within a limited time, which signals the 220 kV isolator position when being closed. In this case the measured oscillation frequency of the current reaches 31 MHz. Table II gives an abstract of the measurements in the common (CM) and differential (DM) modes for the Foretaille substation.

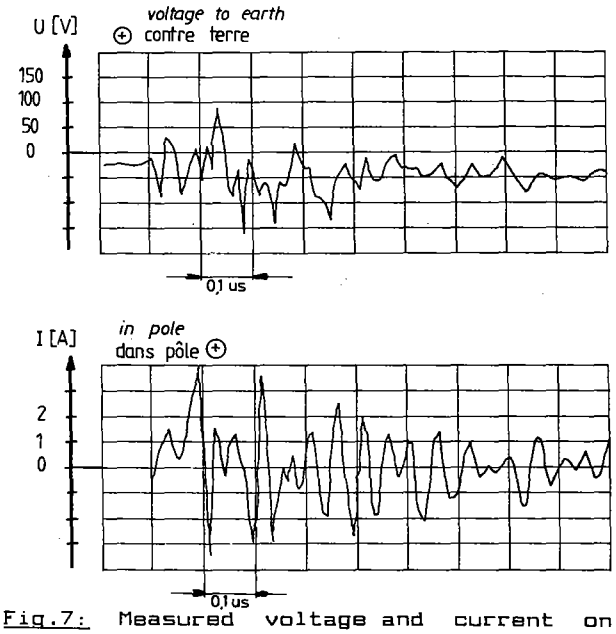

Fig.7: Measured voltage and current on a telecommunication line in a 220 kV GIS SF6 substation when an isolator is closed.

Auxiliary circuit Transmission level	Voltage [V] CM	Voltage [V] DM	Curr. [A] CM
Isolator communication line 110 V DC	1 750	-	5
Isolator signalling line 24 V DC	110	-	8
Isolator signalling line 48 V DC and 110 V DC	200	-	3
Power telemeasuring line 5 mA DC	-	-	4
Energy telecounting line 48 V AC	40	10	-
PT measuring line 200 V AC	400	-	6
CT measuring line 5 A AC	-	-	5
Auxiliary supply line 220 V AC	400	210	-
Auxiliary supply line 110 V DC	180	20	-

Table II: Results of the measurements of conducted interferences in auxiliary circuits (distance = 10 m) of a 220 kV GIS SF6 substation when operating an isolator.

Summarizing the measurings performed, the most difficult constraints to overcome originate mainly from:
- the high frequencies (10 to 30 MHz)
- the amplitudes of the currents induced into telemeasuring circuits (for example in a 5 mA loop a current of 28 A has been measured)

The amplitudes of the overvoltages are generally lower than values from standardized tests. The measured energies do not pose problems for the spark gaps, varistors or separating relays etc.

3.3 Sensitivity of electronic and communication equipment

Numerous tests of immunity against electromagnetic interferences performed on remote and local control equipment show a good behaviour of these equipments, provided that comparatively small frequencies (impulse 1.2/50 us, damped oscillation of 1 MHz etc.) and long term standardized tests are applied. However, when exposed to a volley of quick high frequency transients, their overall behaviour is less satisfactory.

Table III presents a summary of results of immunity tests performed on a local process control unit.

Radiated interferences	Sensitivity	Classification Qualification
Electrical field	2.5 V/m 10.8 MHz	Class 1 IEC 801-3 sensitive
Conducted interferences	**Sensitivity**	**Classification Qualification**
Transient overvoltage 1.2/50 us	CM: > ± 1 kV DM: > ±800 V	IEC 255.4 good
Bursts of fast transients on supply circuits	2 kV	Class 2 IEC 801-4 moderate
Bursts of fast transients on control circuits	2 kV	Class 3 IEC 801-4 moderate
Voltage interruption	V = 110 V DC -100% 100ms	good
Electrostatic discharges	2 kV	outside class IEC 801-2 bad

Table III: Immunity tests on a microprocessor based control unit.

4. Constructional measures

4.1 General principle

Referring to electromechanical compatibility, a GIS SF6 substation forms a loop consisting of (Fig.8):

- the high voltage part (metallic casings, sealing ends of cables and/or lines)
- the sensors and auxiliary cables
- the control cubicles
- the grounding circuits

For compatibility generally two precautions have to be taken:

a) To open the loop by separating the EMI source from the victim by galvanic means (transformers, transducers, relays, optocouplers, fiberoptics etc.)

b) To create a very low impedance ground plane on which the whole system is based

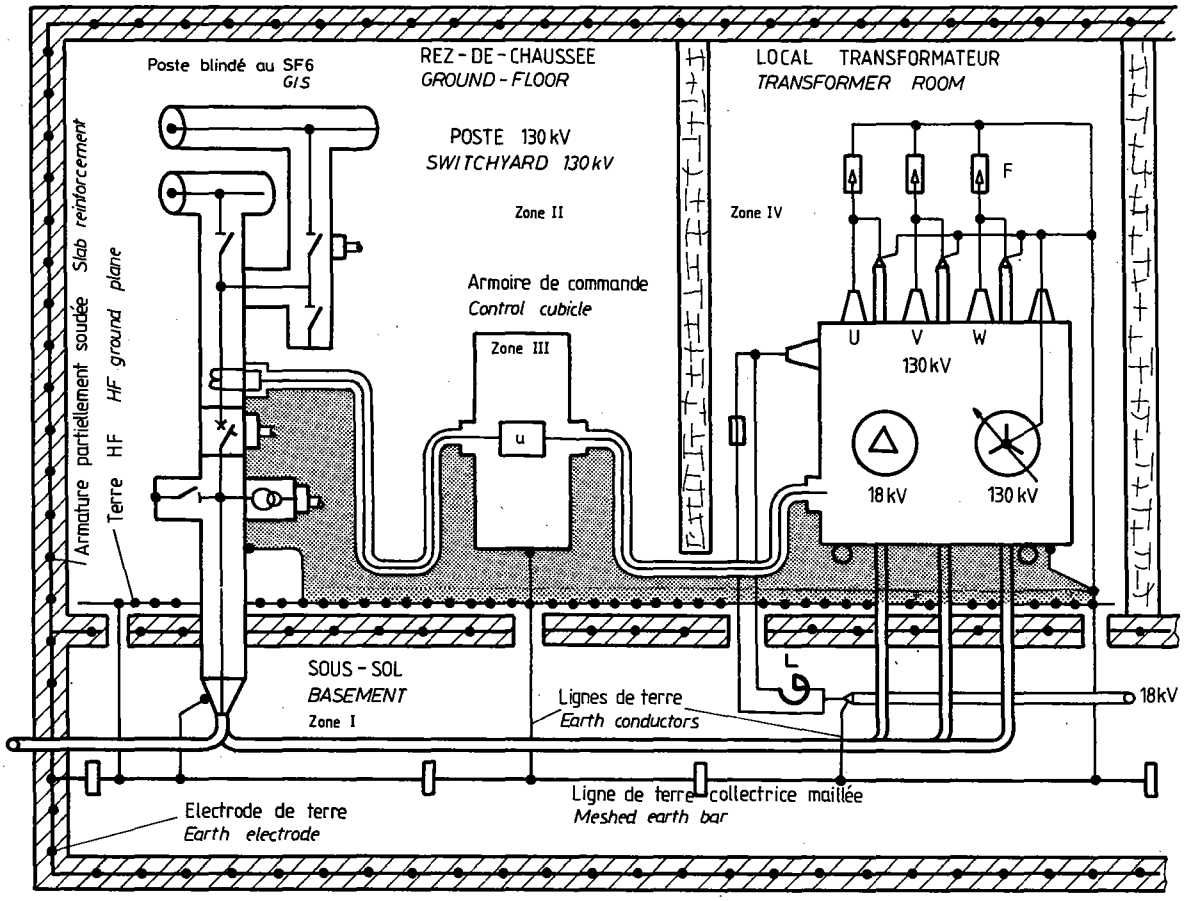

Fig.8: Grounding principle.

The solution a) allows to reduce the loop current. However, the radiating component of the electromagnetic field of the EMI source and the difficulty to obtain and to install galvanic separators suitable for high frequencies make this solution very difficult, due to the increased number of connections to be protected.

The solution b) allows to reduce the voltage between the frame of the high voltage part and the cubicles by applying a ground plane whose impedance stays low also at high frequencies. This solution [2,4], which is easier to realize provides the additional advantage of using the ground plane as shielding and as a separation of zones (Fig.8).

4.2 Zones

The surrounding of cable and line ends forms zone I, which is most exposed to the impact of electromagnetic fields. This zone is located in the basement for the cable sealing ends (Fig.9) or outside the substation for the overhead line ends. In case of line ends also the electromagnetic impact on the surroundings has to be taken into account. The grounding impedance of the ends should be restricted to a low value by means of short and multiple connections.

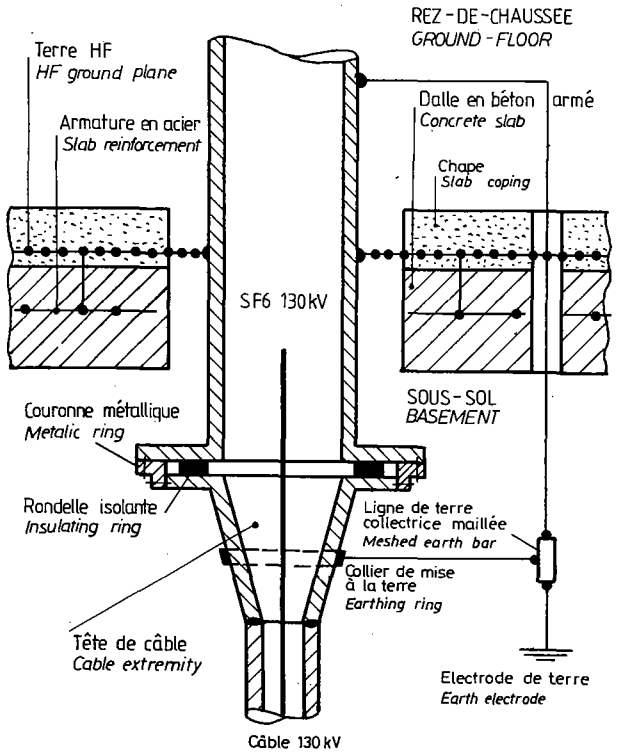

Fig.9 : Detail of cable end

A first barrier which is defined by appr. 20 dB [7] and which consists of the ground plane and of the concrete reinforcement of the floors or walls, separates the zone I from zone II where the high voltage substation and the control cubicles are installed. The auxiliary cables connecting the high voltage parts to the cubicles are shielded and grounded at both ends. Their transfer impedance [8] must be sufficiently small (appr. 2 mOhm/m).

A second barrier which is defined by appr. 40 dB (for a 130 kV substation) and which consists of the walls of the control cubicles, protects the sensitive microprocessor based equipments against the direct electromagnetic radiation and against the currents circulating in the shieldings of the auxiliary cables. Thus it forms a zone III. The supply of the cubicles should be specially protected against the common mode disturbances by means of, for example, interposing transformers with a low parasitical capacity. The disturbing currents which circulate in the common mode in the conductor pairs (specially in current measuring circuits) will be damped out in this mode in a similar way.
For the serial links between the individual control cubicles and to the central unit of the dispatch center fiberoptics transmission is exclusively used.

A third barrier with respect to hardware (for example: interposing relays connected in series, internal tests) and software (for example: antivalent logic, duplicate storage of indications etc.) [9] protects, as a last line of defense, the sensitive equipment in zone III.

4.3 Grounding (Fig.8)

Special attention must be given to the design of the grounding network. In the special case of an underground transformer substation in an urban area the cast walls of the building and their reinforcement form an earth electrode with a very low impedance at 50 Hz.

An earth bar is installed there and passes through the whole lower part of the building. To this bar all earth conductors are connected.

An intermeshed network grounding the high voltage equipment is designed according to the rules known for security grounding 50 Hz [10]. The above-mentioned arrangements allow to cover the scope of protection of both material and persons. They contribute as well to the decrease of the overall impedance of the earthing network.

For the protection against electromagnetic disturbances a close - meshed ground plane provides a unique and equal ground potential with a low impedance at high frequencies.
The earth conductors which are connected to the earth bar are short and have a low impedance at high frequencies. The necessary installation techniques have been the subject of publications in Switzerland, specially in the field of civil protection [11].

4.4 Specifications for sensitive equipment

A specification containing the prescriptions for the electromagnetic compatibility of microprocessor based control units is worked out and given to the suppliers at the time of invitation to offer. The compliance with the specification together with the quality of the second and third barriers are verified by tests on substations with a similar arrangement, possibly preceded by factory tests [12] and followed by the final on site tests.

This procedure of tests on substations with a similar arrangement offers the advantage of covering possible gaps in the standards relative to the radiated interferences in a high voltage substation.

4.5 Other systems to be made compatible

The research for compatibility by means of, for example, the definition of an influence matrix [13] is also applied to the following equipments:

- digital protection relays (For example in medium voltage circuit-breaker compartments)
- installations for remote counting
- voltage regulators
- digital transients recorders
- units controlling the ventilation and fire protection
- computer peripherals and terminals
- etc.

5. Conclusions

The manufacturer of GIS SF6 substations guarantees the availability and security etc. of the high voltage system. The manufacturer of microprocessor based control units guarantees immunity against electromagnetic disturbances according to the existing standards.

In general it is left to the power utility to guarantee the electromagnetic compatibility because they usually lead the construction of the substation. Exactly at this level the best gains in the task of separating EMI sources from victims are obtained. It is the power utility who study, specify and apply the appropriate means, such as:

- the realization of an equipotential and intermeshed grounding network and of low impedance earth conductors
- the choice of materials used for the construction of the buildings
- the general layout with respect to the local arrangement of very high voltage equipment, of line and cable endings, and the definition of the interference zones
- the coordination of shielding elements and electromagnetic protection of the control circuits (cubicles, connectors, cables, transducers etc.)
- the specification of microprocessor based control unit equipments

In their endeavour to control the electromagnetic interferences in high voltage substations, the power utility also desire that studies should be made as how to limit the phenomena at their sources. The manufacturers of GIS apparatus and substations should take them into account.

The urgency of the problems of electromagnetical compatibility in high voltage substations has caused the utilities operating the transmission and distribution networks in the French speaking part of Switzerland to create a working group in order to study the problems arising in this field.

References

[1] Aguet M., Blech Ph., Ianoz M., Sauvain H. Perturbations électromagnétiques dans les réseaux électriques de distribution (Bulletin ASE/UCS 69 (1978) 24, p. 1310..1314)

[2] Meppelink J., Remde H. Compatibilité électromagnétique de postes à SF6 (Revue Brown Boveri, 73 1986 (9), p. 498..502)

[3] White Donald R.J. Electromagnetic shielding materials and performance (Don White Consultants, Library of Congress 75-16592, 1975, p. 1.1..1.8)

[4] Champiot G; Guillery P. Pour avoir un bon réseau de terre : des règles simples pour respecter la physique de base (Revue Générale de l'Electricité, RGE No 10, Nov. 1986)

[5] IEC International Electrotechnical Commission. Single input energizing quantity measuring relays with dependent specified time. (Publication 255-4, 1976)

[6] IEC International Electrotechnical Commission. Electromagnetic compatibility for industrial process measurement and control equipment. (Publication 801 - 1 to 5, 1984).

[7] Sauvain H., Chung Chi Lin Atténuation des ondes électromagnétiques de choc par l'acier des armatures de béton (Publication EPFL No 189, 1980)

[8] Blech P., Dijamatovic Y., Ianoz M. Mesure de l'impédance de transfert en régime impulsionnel (Bulletin ASE/UCS 78 (1987) 9, p. 488..492)

[9] Brand K.P., Kopainsky J., W. Wimmer Verrouillage assisté par ordinateur d'installations de couplage avec disposition quelconque de jeux de barres (Revue Brown Boveri 74, 1987 (5), p. 261..268)

[10] IEEE Guide for safety in AC substation grounding Std 80, 1986

[11] Département Fédéral de Justice et Police, Office fédéral de la protection civile Instructions techniques pour l'installation de protection EMP de l'alimentation en énergie électrique des constructions de protection civile (Publication 1750.00/77, 1985)

[12] Hirschi W., Sauvain H. Elektromagnetische Verträglichkeit bei EDV-Anlagen (Design & Elektronik 146, Ausgabe 25, Dez. 1986)

[13] Bundesamt für Wehrtechnik und Beschaffung Elektromagnetische Verträglichkeit, Programme und Verfahren, Verfahre für Systeme (VG 95374 Teil 4, Dez. 1981).

International Conference on Large High Voltage Electric Systems

112, boulevard Haussmann — 75008 Paris

1988 Session — 28th August - 3rd September

O

36-07

Pref. Subj. 3

PROTECTION OF DATA COMMUNICATION SYSTEMS AGAINST ELECTROMAGNETIC INTERFERENCE IN HIGH VOLTAGE STATIONS

Paper presented in the name of Study Committee 36 (Interference)

by

R. ANDERS and D. McGRATH*

RESUME

This paper is based on the reports of some of the members of CIGRE WG 36-04, namely Messrs. Anders (Sweden), Bondia (Spain), Champiot (France), Pelligrini (Italy) and two non members, Messrs. Bergman and Nirs (Sweden). Although their reports contain much useful information on the performance of specific data communication systems in harsh electrical environments this paper gives a general overall review of the protection of such systems from electromagnetic interference. Different types of system configurations are described and protection requirements, particularly cable installation and equipment test requirements are discussed.

KEYWORDS

High Voltage - Interference - Computer - Auxiliary Cabling - Power Station - Substation - Tests - Fibre Optics.

1. INTRODUCTION

The development of the microprocessor has given rise to a revolution in many areas, especially in the areas of office automation and industrial process control systems. The necessity for reliable communication between microcomputer units, especially remote terminal units and central computers has led to the development of standardised data transmission links and networks. These standard systems were originally designed for use in office systems. However, on account of their reliability and relatively low cost they are being increasingly used in various process control systems. The obvious major advantage of such standards is the resulting compatibility between the various systems.

2. PRESENT DATA COMMUNICATION STANDARDS

The most commonly used standards today are the Electronic Industries Association (EIA) RS 232 and RS 422 standards [1, 2] and the relatively new ANSI/IEEE 802.3 and ANSI/IEEE 802.4 standards [3, 4]. The RS standards were originally used for communication with computer peripherals at low data transmission speeds (RS 232) and for high speed communication between computer units in environments where a higher level of protection against electromagnetic interference is required (RS 422).

The ANSI/IEEE standards are used for high speed data communication in distributed systems - the 802.3 standard is for office type administrative computer systems while the 802.4 is for industrial process control systems.

Systems which are designed in accordance with the ANSI/IEEE standards have a much higher immunity to electromagnetic interference than systems designed to either the RS 232 or the RS 422 standards. The IEEE 802.3 standard evolved from the Ethernet system while the IEEE 802.4 has its origins in the IEC Data Proway system and the Manufacturing Automation Protocol (MAP), the proposed communication standard generally associated with a well-known American car manufacturer.

Components and protocols specified in these four standards are often used in process control local area networks (LANs). However, the system hardware is often modified in systems which are designed to the RS standards. On the other hand very little modification of the hardware is possible in systems which are designed to the ANSI/IEEE standards.

* Electricity Supply Board, Transmission Department, 41 Merrion Square, Dublin 2, Ireland.

3. THE ELECTROMAGNETIC ENVIRONMENT

It is well known that computers are sensitive to electromagnetic interference. Consequently, they need to be protected against maloperation. Common protection methods are the use of specially designed power supply units, special earthing techniques and relay suppression. In general air conditioning, especially humidity control, is necessary to protect against electrostatic discharge (ESD) between operators and computer equipment. The most sensitive components of a computer installation are the data communication links between the various computers and terminals - along these links extremely low level signals are transmitted at very high speeds. Typical transmission speeds range from 10^4 to 10^7 bit/s. Protecting transmission links by installing signal filters is very difficult and in general impractical.

3.1 Office Installations

In a large office building power frequency potential differences of a few volts may exist between different locations of a computer system under normal operating conditions. Higher potential differences are possible on the occurrence of a power frequency earth fault. In addition to this type of possible interference other sources of interference, notably switching transients, and static electricity must be considered - both these are often more difficult to protect against than power frequency interference.

It is well known that, as well as causing a maloperation in data transmission, electromagnetic interference can affect sensitive internal circuits inside a computer itself. There are various ways in which the interference can appear on internal wiring. For example, it can be conducted along a transmission line or via a power supply unit of the computer. Alternatively, the interference may be caused by radiation from a nearby source, for example, a 'walkie-talkie' radio. The operation of a computer terminal, or the computer itself, in a large office system may be affected by such interference. Fortunately, maloperation is often acceptable in office systems provided the systems can be re-activated without delay.

3.2 Installations in Substations and Power Plants

The most serious electromagnetic compatability (EMC) problems are found in high voltage stations, both of the open-air and GIS design [5, 6, 7, 8]. In general, the low voltage control circuits and equipment installed in these stations have a good insulation withstand level - up to 2.5kV for 50Hz AC and 5kV for impulse voltage. Despite these relatively high levels several incidences of equipment damage caused by excessive interference voltages have been reported. A common method of limiting such overvoltages is to use screened cables, with the screen earthed at both ends, for all signal and control circuits. Measurements of interference voltages in open air substations have indicated that voltages of up to 10kV are possible if unscreened cables are used. Higher voltages are possible in GIS. Another interference source is the operation of relays and contactors in the low voltage control wiring itself - the frequency of the interference voltage lies in the 0.1-10MHz range. A third possible source of interference is lightning. Finally interference voltages may also be caused by a high voltage earth fault inside the station,

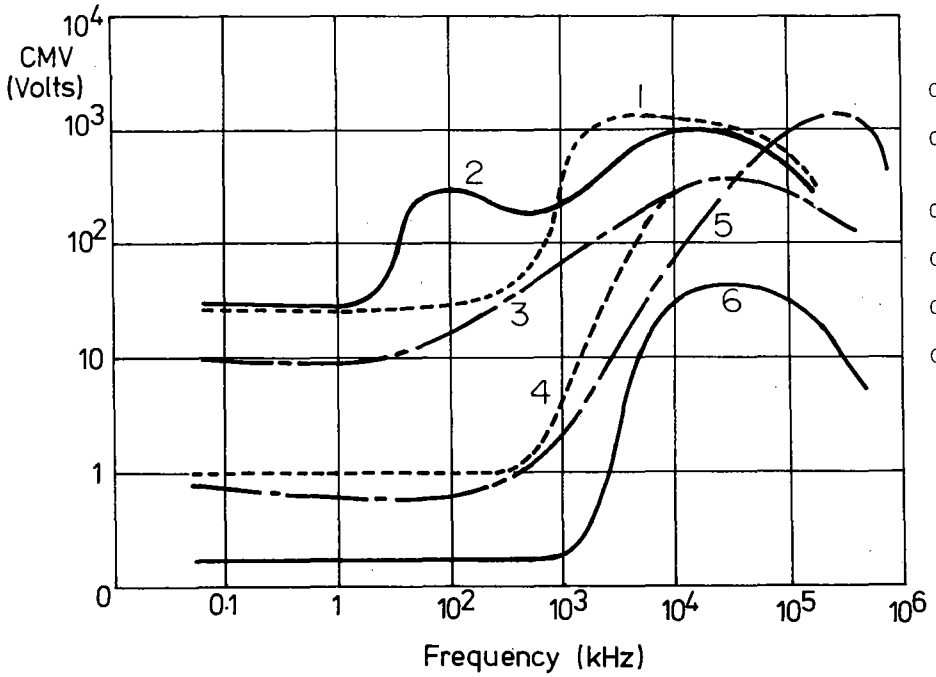

Curve 1: Open Air Substation

Curve 2: Series Capacitor Bank

Curve 3: Power Plant

Curve 4: Control Building

Curve 5: GIS Station

Curve 6: 'Protected' Control Room

Figure 1: Maximum values of interference Common Mode Voltage (CMV) vs. frequency for various installation environments.

e.g. flashover across high voltage insulation, when potential differences of up to several hundred volts may exist between different locations in the station. Typical maximum values of interference common mode voltages which can occur in the frequency range up to 100MHz are shown in Figure 1. It is seen that the maximum voltage varies with frequency and with the type of installation environment - these voltages are typical of the voltages measured on a circuit which is earthed at one end. However, it is possible to reduce these voltages considerably by good installation practice such as cable layout and earthing. The voltages in the lower frequency range are caused by high voltage power frequency earth faults. The most common source of the high frequency voltages are the operation of high voltage switchgear and the switching of low voltage relays in station control rooms.

4. PROTECTION OF DATA TRANSMISSION SYSTEMS

In general data communication systems use balanced input/output signals at the transceiver. Therefore, all interference voltages which appear at the terminals of a transceiver are common mode voltages which can be of the order of 10,000 volts. In sharp contrast, signal voltages (which are differential mode) are considerably smaller - generally less than 1 volt. However, both interference and signal voltages can be in the same frequency range.

Data lines and networks must be designed to operate correctly under these conditions. Generally, this is achieved by installing well screened cables, and by protecting the equipment by transformers, opto-couplers, or by fibre optic cables. Other requirements are often necessary, particularly where serial data transmission is used. For example, in a remote control system where the availability of the system must be guaranteed in the event of a component failure redundancy of the system is often used, i.e. a duplicate system is installed with the facility for automatically switching from the 'faulted' to the 'standby' system. In other cases, two separate methods of signal transmission may be used, e.g. by cable and by radio. In order to ensure the security of a system fault detection codes and repetition procedures should be built into it. However, as the philosophy of system design is such a large area it will not be discussed in this paper.

4.1 Fibre Optic Cables

One of the most effective methods of counteracting possible electromagnetic interference is the use of fibre optic cables instead of conventional cables. As is well known today, fibre optic systems are immune to electromagnetic interference and are well suited for communication between locations which are at a relatively high potential difference with respect to one another (e.g. control circuits for capacitor banks). Also, it is quite common for fibre optic cables to be used in long telephone transmission circuits - these fibre optic cables are generally provided with steel wiring for mechanical protection and with conventional wiring for the power supply circuits to the repeaters installed along the circuit route. However, for applications in H.V. stations where a high potential difference may exist the ideal solution is to install fibre optic cables which have no metallic wires. Also, in order to protect the fibre optic cable against damage from corona discharge in areas of high potential it is advisable to immerse the cable in insulation oil.

A major advantage of modern fibre optic cables is their relatively small losses and the fact that they can, therefore, be used in very high frequency transmission systems, over long distances (e.g. tens of kilometres). On the other hand these advantages are of only minor importance in applications such as high voltage stations where cable distances are relatively short (hundreds of metres). For such applications fibre optic cables are still fairly expensive. In addition, station installation and maintenance personnel will require intensive training in the installation of fibre optic technology.

The use of fibre optic cables is on the increase. To date, they have not been used in simple 'multidrop' systems (i.e. a system in which a number of transceivers are connected to a common 'data' busbar or line). On the other hand, it is quite common for optical repeaters to be used in all transceivers.

4.2 Conventional Cables

Conventional screened cables are generally used for all types of electrical transmission over long distances - in the telephone industry screened cables, which are well designed to ensure balanced signal circuits, are used. In most applications high frequency cables which have low losses in the high frequency range must be used - a notable exception is low frequency transmission where the RS 232 standard is acceptable. The length of the transmission cable is limited by the signal transmission speed - for speeds of 150 kBit/s the cable length can be of the order of one kilometre which is normally sufficient for local data systems. However, for high transmission speeds (e.g. 10 mBit/s) specialised expensive coaxial cable must be used if cable lengths of some hundred metres are required.

Providing cables with shields which are earthed at both ends will reduce the values of the common mode voltage. The effectiveness of a shield is often quantified by a parameter called 'The Reduction Factor'. This is simply the ratio of the common mode voltage on a cable with and earthed shield to that of an unshielded cable. It can vary from 1 for a cable which provides no screening against interference voltages down to 0 for a theoretically perfectly shielded cable.

It is essential that cable shields should be of either a braided or braided/metallic foil design. Also the shield resistance should be less than approximately 5 ohms/km. This is necessary to ensure that the cable has good screening and also to ensure that signal attenuation along the cable is acceptable.

Another important point to note when installing a cable is that although the cable itself may have a very good (i.e. low) reduction factor the actual type of arrangement used for connecting the cable shield to earth can have a significant effect on its value, particularly at high frequencies. The effect of the type of earthing

arrangement on the reduction factor can be seen by comparing curves 1a and 2a with curves 1b and 2b respectively in Figure 2. The ideal arrangement is for the shield to be connected concentrically around the terminating connector if possible. Alternatively, the shield should be clamped directly to the transceiver chassis to ensure a low 'high frequency' impedance.

For cables using twisted pairs the shield should be directly earthed at both ends of the cable and also on all transceivers. For coaxial cables it is not possible to earth the screen at both ends because this will give rise to a signal-ground loop. Instead earthing via a capacitor is recommended at all transceivers to ensure reliable protection against high frequency interference. Secondary overvoltage protection equipment such as varistors or gas-arrestor tubes should be installed on the unearthed end of the cable. In high voltage substations the cables should be installed in well earthed metallic conduit tubes to minimise common mode voltage interference. The reduction of the common mode voltage, which appears on the signal input terminals, when the cable screen is earthed at both ends, is shown in Figure 2. It is seen that the reduction factor for normally shielded cables improves with frequency up to the Megahertz range after which it starts to increase in value. Also shown is the very significant improvement in the value of the reduction factor which can be achieved with metal conduit.

4.3 Isolation of Signal Circuits

It is necessary to use isolated input and output circuits in all transceivers. The only exception to this is where fibre optic cables are used. In general non-isolated data transmission circuits, which have a limited common mode voltage tolerance range (in standard components the maximum voltage is often only a few volts), should onle be used in environments which are relatively interference-free, e.g. in control rooms in which a good earthing system is installed.

In addition, there are a variety of isolation methods available. For example, transceivers with an ungrounded reference zero can be used in systems which use low data transmission speeds. Opto-couplers may be used to provide isolation, particularly in point-to-point systems. At higher speeds and in multidrop systems high frequency protection is often provided by installing small well-balanced transformers which have small interwinding capacitances.

A sketch showing how a multi-drop bus coaxial cable can be protected is shown in Figure 3.

5. SYSTEM CONFIGURATIONS

The earliest systems were designed for point-to-point communication. Other designs quickly followed, e.g. the 'star point' designs in which many units are connected radially from a common central processing unit (CPU). In recent years a system design known as a 'multidrop system' has become increasingly common - in this system a number of units are directly connected to the same cable. The advantage of the system is that it allows direct exchange of information between all units. For example, a typical design for a data communication system in a high voltage substation is shown in Figure 4. In this example it is seen that three different types of standardised units, i.e. D1, D2, D3 are used to obtain information about the operating status of high voltage equipment. Note the data system allows for communication with a remote control centre. In supervisory and process control systems various transducers, relays, etc., are connected to different units which themselves are

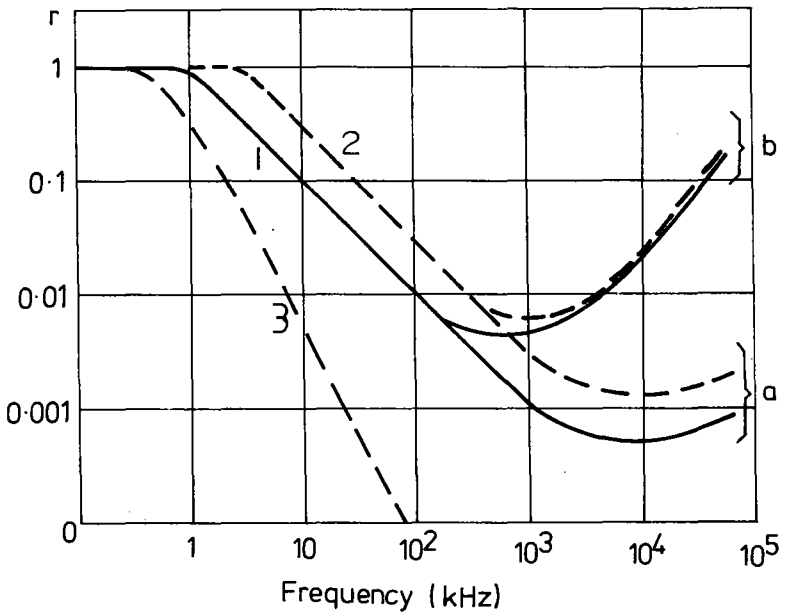

$$r = \frac{Z_r}{R' + jwL'}$$

where Z_r = transfer impedance of cable.
R' = Resistance of cable shield per metre
L' = inductance of cable shield per metre.

Curve 1: R' = 4 mΩ/metre
L' = 1 μH/metre

Curve 2: R' = 13 mΩ/metre
L' = 1 μH/metre

(a) 10mm shield earthing connection
(b) perfectly concentric shield earthing connection.

Curve 3: Typical metal conduit.

Figure 2: Reduction Factor (r) vs. Frequency (f) for different Cable Shields and Earthing Connections

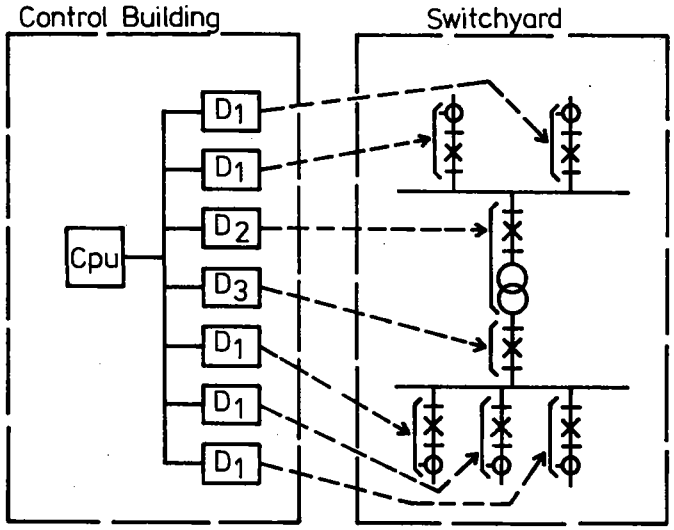

Figure 3: Typical earthing & Protection requirements in a Multidrop Bus System.

interconnected via the transmission busbar transceivers.

The complexity of systems has increased in recent years with many present systems using both the 'point-to-point' and 'multidrop' designs. Examples of the various types of system designs are shown in Figures 5(a) to 5(h).

6. REVIEW OF SYSTEMS IN OPERATION AT PRESENT

Details of data communication systems, which are known to members of WG 36-04 are given in Table 1. In all twelve systems from four countries - France, Italy, Spain and Sweden - are described. Four of the systems were specially designed for operation in high voltage stations - two of these use fibre optic cables while the other two use conventional cables and relatively high signal levels. Eight of the systems are based on the standards discussed in Section 2 of this report - however in the majority of these systems modified well protected transceivers are used.

In general, the type of cabling used in the systems is either multipair or coaxial. In systems which can be exposed to a high level of interference, e.g. systems no. 4, 5, optic fibre cabling is often used. However, it should be noted that there is a technical limitation to the use of optic fibre cables - at present data transmission via fibre optic cables is only possible in point-to-point systems. It is not yet possible to connect several transceivers to the same cable. Therefore, for an interconnected system, e.g. a multidrop system a complex design

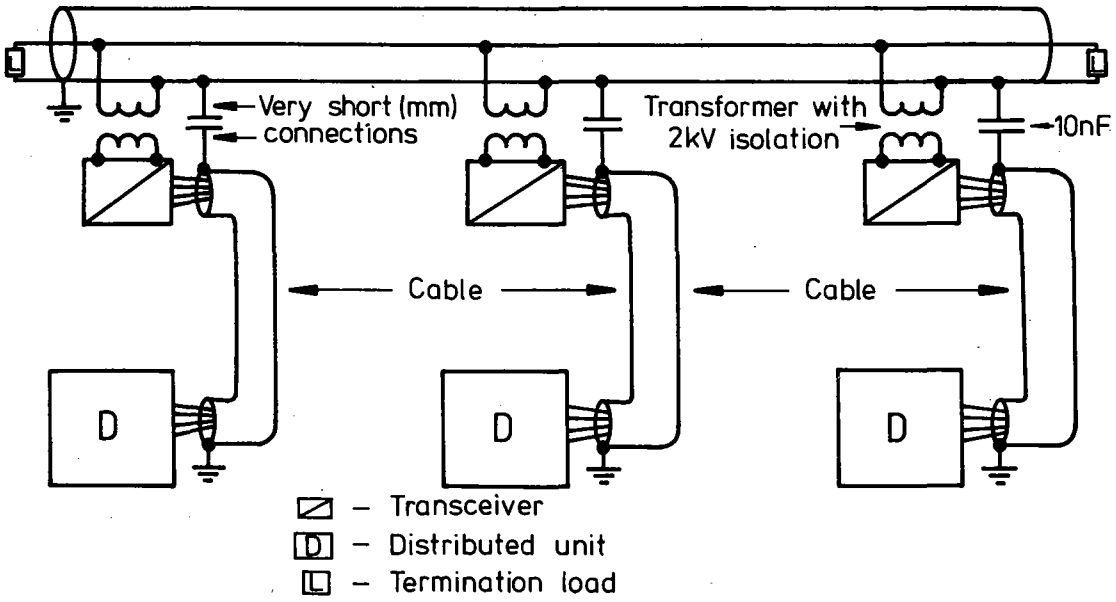

Figure 4: Typical design of a Data Communication System in a High Voltage Substation.

(a) Point-to-Point System
(e.g. System No. 10 in Table 1)

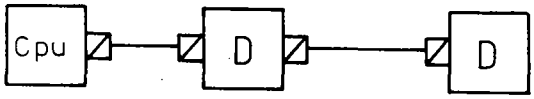

(b) Point-to-Point System
(e.g. No. 6)

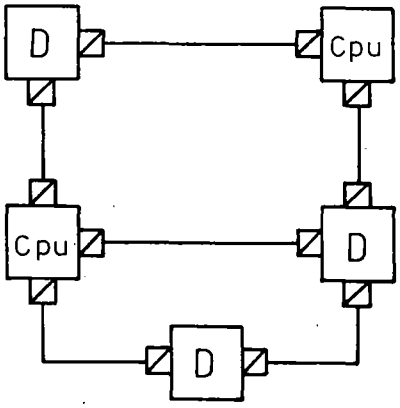

(e) Network of Point-to-Point Systems
(e.g. No. 3)

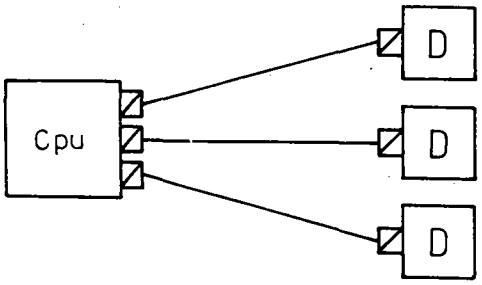

(c) Star-Point System
(e.g. Nos. 2, 7)

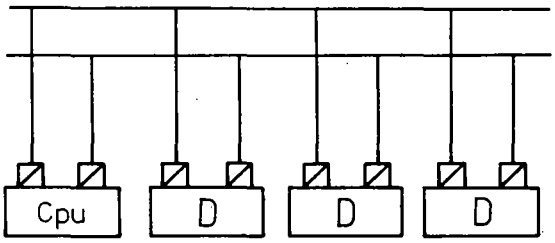

(f) Multidrop System with Duplication of
Connections for Redundance
(e.g. No. 12)

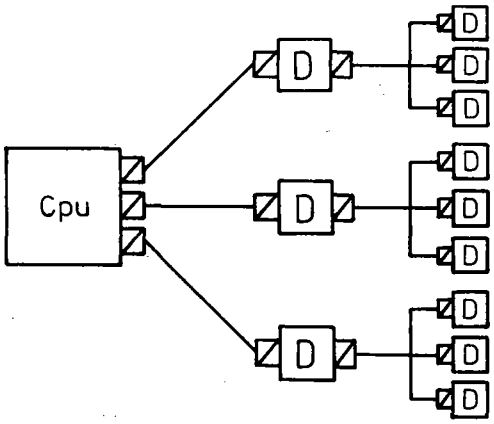

(d) Star-Point Multidrop System
(e.g. Nos. 5, 9)

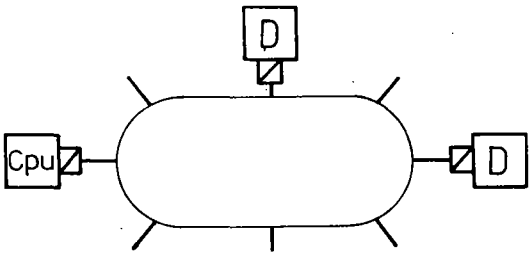

(g) Multidrop System with Ring Configuration

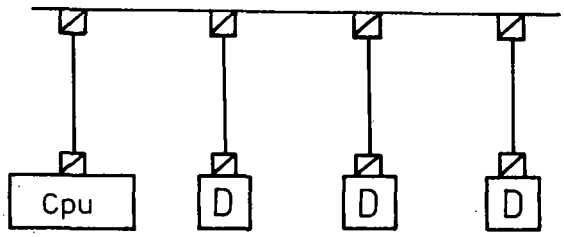

(h) Multidrop Point-Point System
(e.g. Nos. 8, 11)

— TRANSCEIVER

Cpu — CENTRAL PROCESSING UNIT

D — DISTRIBUTED UNIT

FIGURE 5: VARIOUS SYSTEM CONFIGURATIONS USED FOR DATA COMMUNICATIONS

is required - this often involves the use of repeaters with built-in time delays and sophisticated computer software. In comparison it is relatively easy to design an interconnected system which uses conventional twisted pair or coaxial cabling. However, in designing these conventional type systems immunity against electromagnetic interference is of paramount importance. Such immunity must be verified by interference testing. The various relevant immunity interference tests are discussed in Section 7 of the report.

A brief description of some of the systems detailed in Table 1 is as follows:-

System No. 1:

This is an optoelectronic system for a series capacitor bank and is actually the replacement for an older version (System No. 6). However, it is not really a data communication system but rather a system which uses optical transmitters on all current transformers. A major point of interest is that the electrical power to the small transmitters is supplied via fibre optic cables.

System No. 3:

This system was designed for installation in harsh electrical environments in which fibre optic cables have significant advantages, e.g. prevention of accidental explosive ignition from short circuits or electromagnetic interference and also for applications which require very high data transmission speeds, e.g. various applications in nuclear power stations and on oil drilling platforms. In the nuclear power station the system is used for the acquisition of station operational data and meteorological data. In all fourteen computers and approximately 230 microprocessors are interconnected by the system.

System Nos. 4 & 9

Both these systems were designed to the ANSI/IEEE 802.3 standard. System No. 4, which used fibre optic cables for data communication in a high voltage substation, had been in service for test purposes for a few years. System No. 9, which is installed in an industrial plant uses coaxial cables - these cables would need to be enclosed within metallic conduit if they were to be routed through a harsh electrical environment such as a high voltage open-air substation. Various interference immunity laboratory tests, which are required for protection/control equipment in high voltage substations, were carried out on the system.

System No. 5:

This system allows data communication via fibre optic cables between the control room and the

SYSTEM NO.	USER	TYPE*	CABLE TYPE	AREA OF INSTALLATION (YEAR OF INSTALLATION)	BASED ON STANDARD	TYPE OF NETWORK	NUMBER OF UNITS	MAX. CABLE LENGTH (M)	TRANSMISSION SPEED (kBIT/S)
1	SSPB,* Sweden	Optoelectr. protection	Optic fibre	Series capacitor station (1987)	-	Starpoint	Many	500	10
2	SSPB, Sweden	MB 200 L	Optic fibre	Nuclear power station between plants (1984)	RS422	Starpoint	4	1200	153.6
3	SSPB, Sweden	Delta X	Optic fibre	Nuclear power station station area (1983)	-	Network (point-point)	230	2100	6000/12000
4	EDF, France	Pandor	Optic fibre	Substation with kiosks (1985/87)	IEEE 802.3	Network	5	-	10000
5	FECSA, Spain		Optic fibre/ twisted pair	Substation with kiosks (1986)	RS232C	Starpoint/ multidrop	-	-	19.2/9.6
6	SSPB, Sweden	Optronic protection	Optic fibre/ twisted pair	Series capacitor station (1974)	-	Point-Point	2	500	50
7	SSPB, Sweden	MB 200 L	Coaxial	Inside nuclear power plant (1985)	RS422	Starpoint	Several	300	153.6
8	ASEA, Sweden	MB 300 L	Coaxial	Industrial Steel Plant (1988)	IEEE 802.3	Multidrop	$\leq$ 45	500	10000
9	SSPB, Sweden	MFB/ MB 200 L	Twisted Pair/ Coaxial	Substation with kiosks (1988)	RS422/ IEEE 802.4	Starpoint/ Multidrop	3/5	300/30	153.6/2000
10	ENEL, Italy		Twisted pair	Between power plant and substation (1972)	-	Point-point	2	1200	100
11	SSPB, Sweden	MB 200 L	Twisted pair	Substation control building (1983)	RS422	Multidrop	8	30	153.6
12	SSPB, Sweden	MB 200 S	Twisted pair	Inside instrument room of nuclear power plant (1984)	RS422	Multidrop	10	50	153.6

*The master BUS 200 (MB 200) system is used in many installations of the Swedish State Power Board (SSPB). However various types of modems and transceivers are used. The 'short distance' (S) version of the system (e.g. MB 200 S) is only used inside local control rooms. In other types of installations (e.g. nuclear power plant) the 'long distance' (L) version is used - generally twisted pair or co-axial cable connections are used, but fibre optic cables are often used in harsh electrical environments.
For completeness two MB and MFB (i.e. Master Field Bus) systems which are being commissioned at present are listed - these systems are of interest because they are based on new system standards.

TABLE 1 - CHARACTERISTICS OF VARIOUS DATA COMMUNICATION SYSTEMS

marshalling kiosks in a high voltage switchyard. The various units within each marshalling kiosk are connected via a multi-drop bus connection. A relatively low data transmission speed is used. Both the local system and the shields of the 'bus' cables are earthed at one point only. Overvoltage protection is provided on the unearthed end of the cable shields. Prior to it being put into service the system underwent interference immunity testing.

System No. 6:

This is the old optronic protection system which was used for series capacitor banks [9]. All data was collected in 'data acquisition' units which were installed in a high potential location and transmitted via short fibre optic cables to corresponding units which were at earth potential. At these second units the optical signals were reconverted to electrical signals for transmission to the station control room via shielded cables. In fact the cables were provided with two shields - the outer shield was earthed at both ends, while the inner shield was only earthed at the 'control room' end. This design was decided on only after tests and measurements showed that high interference voltages were possible at relatively low frequencies (e.g. 10kHz). At these low frequencies a single cable shield has a reduction factor of approximately 1, i.e. it provides minimal protection against interference. Another reason for the design was the high attenuation in the fibre optic cables available at the time. These allowed signal transmission only over a very short distance - of the order of 10 metres.

System No. 11:

This is a multi-drop bus system which is installed in a 400kV GIS/220kV open air substation. At present a total of eight units are connected to the bus - the number will be increased when a proposed extension of the open-air substation is completed. The system uses a 'long distance bus', as distinct from a 'short distance bus' which is generally only installed in control rooms. By design the 'long distance bus' has a higher interference immunity than the 'short distance bus' Interference tests were carried out to ensure the reliability of the system. To date the system has been in service, without any occurrence of maloperation, for over four years.

System No. 12:

This 'point-to-point' system was installed in 1972 to enable data communication between a power plant and an adjacent 400kV substation. In all 16 parallel links are provided between the two 'points' which are 1.2 kilometres apart. To ensure reliability of operation the system was designed and tested to withstand both the effect of high voltage equipment switching transients and of lightning strikes to an underground 400kV cable which was routed in parallel with the data communication cables over a distance of approximately 600 metres.

Measurements and calculations of common mode and differential mode voltages were carried out for both these sources of interference. From these results the system design was optimised. Since its installation no maloperation of the system has been caused by electromagnetic interference.

	Immunity Requirements for System No.			Immunity Requirement in Standard			
	12	7, 8, 9	5	RS 232 C	RS 422 and RS 485	IEEE 802.3	IEEE 802.4
Power Frequency Breakdown Voltage	15V	2kV	2kV	15V	15V	250V	-
Common Mode Voltage (50Hz)	5V	500V	-	3V	7V	-	-
Impulse Voltage (1.2/50 uS)	1kV	5kV	5kV	-	-	-	-
1MHz Interference Voltage	1kV	2.5kV	2.5kV	-	-	-	-
Fast Transient Voltage	2kV	4kV	-	-	-	-	-
Transient $\left(\frac{dV}{dt}\right)$ Rise Time	100V/ns	200V/ns	-	-	-	1V/ns	-
Radiated Interference	10V/m	10V/m	-	-	1V/m	2V/m* 5V/m	2V/m* 5V/m

* The values of 2V/m and 5V/m are for the frequency ranges 10kHz-30MHz and 30MHz-1GHz respectively.

1. No values are given in standard IEEE 802.4

2. The values given in standard IEE 802.3 are very small and much lower than values which can be present in harsh electrical environments such as high voltage stations.

TABLE 2 - TEST IMMUNITY REQUIREMENTS

7. IMMUNITY INTERFERENCE TESTS

As mentioned in Section 6 it is essential that systems which use conventional cables are adequately designed for protection against electromagnetic interference.

Some systems which have been installed for many years (e.g. system nos. 3, 6, 10 in Table 1) were not designed in accordance with any specific interference standard. However, in general, realistic interference simulation tests were carried out by equipment manufacturers. Today, systems are tested in accordance with standards though most of these standards are not very realistic for harsh electrical environments. It is interesting to compare the test values used for some of the systems described in Table 1 with the standard test values - this comparison is shown in Table 2. The obvious conclusion from Table 2 is that realistic immunity test requirements for systems installed in harsh electrical environments are lacking in the existing standards. Therefore, modification of existing standards or development of specific standards for high voltage station type environments must be given serious consideration.

The various levels of the common mode interference voltages for different types of installation environments were shown in Figure 1. It is essential that the interference tests simulate the coupling mechanism by which these voltages appear on communication cabling. For example, the test voltage should be applied between a cable shield and earth, e.g. cabinet chassis. Also, the type of circuit earthing to be used on site, e.g. a floating or solid earth connection, should also be used in testing.

8. CONCLUSION

Today, there is an increasing use of computerised data communication systems in harsh electrical environments such as high voltage stations. Some of the systems, which are reviewed in this paper, have been installed in recent years and have taken advantage of the interference immunity characteristics of fibre optic cables. Fortunately, experience with older systems, which use conventional cables has been satisfactory. Indeed, the most common form of interference protection still used today is the adequate isolation of signal inputs to transceiver units and well designed cable shields.

Perhaps, the most convenient solution in the near future for a data communication/control network is a high voltage substation which has distributed units, e.g. local relay centres, is as follows. The network should be of a starpoint/multidrop design similar to system no. 5 in Table 1. Two different types of cabling should be used - fibre optic cables should be used for the long and potentially vulnerable (to electromagnetic interference) data communication lines between the starpoint itself (i.e. the CPU which is normally located in a control building) and the distributed units throughout the substation. Conventional coaxial or twisted pair cables should be used in the distributed and relatively unexposed local multidrop networks. The most relevant standards for such a system are the ANSI/IEEE 802.4 for the multidrop networks and the ANSI/IEEE 802.3 and 802.4 for the starpoint network - however some modifications are required. On the other hand networks which have been loosely based on the EIA RS 422 standard have the big disadvantage that neither the frequency nor the type of coupling used in the transceiver is standardised. Consequently, it is not generally possible to connect different units, transceivers, etc., which have been based on, but nonetheless modified from, this standard.

Although new standards for data communication systems have appeared in the last few years no specific standards for systems which are to be installed in harsh electrical environments have been published. Given the growth expected in digital technology in power systems it is imperative that such standards are developed.

REFERENCES

[1] Electronic Industries Association (EIA) Standard RS 232 Interference Between Data Terminal Equipment and Data Communication Equipment Employing Serial Binary Interchange.

[2] Electronic Industries Association (EIA) Standard RS 422 Electrical Characteristics of Balanced Voltage Digital Interface Circuits.

[3] ANSI/IEEE Standard 802.3 Local Area Networks: Carrier Sense Multiple Access with Collision Detection (CSMA/CD) (1985).

[4] ANSI/IEEE Standard 802.4 Local Area Networks: Token - Passing Bus Access Method (1985).

[5] Anders, R., Campling, A.C. - Investigations into Interference in Substation and Power Station Auxiliary Cabling. CIGRE 36.09 (1976).

[6] CIGRE Working Group 36.04 - Interference Problems on Electronic Control Equipment in Power Plants and Substations - Installation and Interference Tests. (1980).

[7] Ford, G.L. - Study of Fault-Produced Overvoltages as Related to Grounding Practices for SF6-Insulated Substations. CEA, Contract No. 071T101 (1982).

[8] CIGRE Working Group 36.04 - Interference Problems on Electronic Control Equipment The Influence of Recent Technical Developments (1984).

[9] Andersson, J. and Anders. R. - Optronic Protection System for Series Capacitor Platforms. CIGRE SC 36 Colloquium, Toronto (1977).

EVALUATION OF THE ELECTROMAGNETIC INTERFERENCES ON THE POWER PLANT AND SUBSTATION AUXILIARY EQUIPMENT

by

R. CORTINA, L. PANDINI, G. PELLEGRINI *

ENEL

(Italy)

Abstract

The paper considers the problem of electromagnetic compatibility in electrical installations (power stations, substations, control centers, etc). In particular, with reference to some typical configurations of these installations, the paper describes the methods developed by ENEL for evaluation of induced voltages and currents on auxiliary circuits, due to various primary sources of electromagnetic interference (lightning strokes on buildings, earth-wires and H.V. circuits; switching of H.V. isolators and circuit-breakers; switching of L.V. circuits; ground faults; electrostatic discharges; etc.). These methods, based on simplified mathematical models and on the results of experimental investigations, consist in the following main steps: analysis of the layout of the system; characterization of the primary interference sources (frequency of occurrence, wave-shape, frequency spectrum, etc.); calculation of the induced interferences, taking into account the various coupling, attenuation and shielding effects. Examples of calculations for some typical plant configurations are given, together with design criteria of the auxiliary equipment of power installations with reference to electromagnetic compatibility.

Keywords

Auxiliary equipment, control center, coupling, frequency spectrum, electromagnetic compatibility, electromagnetic interference, immunity, induced current, induced voltage, power station, shielding, substation, wave-shape.

1. Introduction

The problem of electromagnetic compatibility between electronic control, protection and supervision systems, and power systems in electrical installations (power stations, substations, etc.) has been under consideration by ENEL for many years [1] [2]. On the basis of the results of systematic investigations dealing with the various aspects of the problem, general criteria for the design of the auxiliary systems of these installations have been defined.

These criteria generally include the following main phases:

- Assessment of the electromagnetic environment in which the auxiliary systems have to be installed.
- Evaluation of the interferences (voltages, currents, electric and magnetic fields) acting on the circuits and equipment of the above systems.
- Assessment of adequate safety margins between interference levels and immunity levels of equipment.
- Definition of suitable laboratory test methods to duplicate the various types of interference.
- Study of possible corrective actions (shielding, filtering, earthing, etc.) to control the levels of interference.

Obviously, all these phases are interdependent and the final design of the auxiliary system in respect of electromagnetic compatibility is the result of technical and economic analyses, which consider the reciprocal incidence of the cost of reducing interferences and that of improving equipment immunity.

A fundamental phase of the above-mentioned criteria is that relating to the evaluation of the interferences acting on circuits as a consequence of the primary sources and of the various coupling mechanisms. The paper aims to make a contribution to this problem through a brief description of the methods generally used by ENEL, pointing out the possible limitations of these methods for certain applications and presenting some investigations in progress to improve and refine the methods.

2. Primary sources of interference

The most typical sources of interference that may affect the auxiliary systems of electrical installations are the following: switching operations in H.V. electrical circuits; fault current flow in earth circuits; electrical transients due to insulation discharges or to surge-diverter and spark-gap sparkovers.

* ENEL - Centro Ricerca di Automatica - Via A. Volta 1 - 20093 Cologno Monzese (Milano) - Italy

Another source of interference that is also present in other installations, but that takes on particular importance in electrical installations due to the presence of tall earthed structures, is lightning. Finally, other interferences that are generally present in all installations are the following: fast transients due to switching operations in L.V. equipment, electrostatic discharges, high frequency fields of radio transmitters, and conducted and radiated interferences from other pieces of equipment or from power supply.

The information available on the characteristics of the above interferences is considered sufficient in most cases [3] [4]. This information can be summarized as follows:

- Switching of H.V. isolators produces multiple sparkovers across the contacts during the operating interval. The corresponding voltage transient is a train of damped oscillating waves with amplitudes up to two times the phase-to-ground voltage; the rise times are in the range of some tens of nanoseconds for open-air substations and one order of magnitude lower for gas-insulated substations (G.I.S.); the fundamental frequency of the oscillation depends on the circuit length and the propagation time (several tens of kiloherz to some Megaherz for open-air substations and up to some tens of Megaherz for G.I.S.). Single oscillating phenomena, involving, in general, lower frequencies are produced by circuit-breaker operations. Insulation flashover, and spark-gap or surge-arrester operation also produce H.F. oscillations, followed by the power frequency short-circuit currents in the earth grid of the electrical installation.

- Statistical distributions of lightning current parameters (amplitude, duration, rise time steepness) are available from systematic investigations [5] [6] [7]: amplitudes up to about 400 kA have been recorded in upward positive flashes, while the maximum steepness values (200 kA/μs) have been obtained for downward negative flashes (subsequent strokes); times to crest range from 0.2 to 20 μs for negative flashes and from 2 to 400 μs for positive flashes; times to half value range from 5 to 200 μs for negative flashes, and from 80 to 1000 μs for positive flashes. Reference values of lightning current parameters are considered for each installation with reference to a defined probability limit; e.g. a probability limit of 95% is generally covered by current amplitude of 80 kA and steepness of 60 kA/μs.

- Electrical fast transients produced in switching inductive loads by relays are characterized by a series of spikes with some nanoseconds rise time and durations from some microseconds up to some tens of microseconds. The time interval between spikes ranges from 10 to 100 μs, and the duration of the burst is generally some milliseconds. The voltage amplitude at the source (switching contacts) can reach 5 kV peak.
  Switching by contactors may produce higher levels.

- Electrostatic charges give rise to voltages with amplitudes in the range of a few hundred volts up to 20 kV. Discharge current pulses have a rise time of the order of a few nanoseconds and can reach values of several tens of Ampères, depending on the voltage level and the circuit parameters.

- Portable transceivers generally used in electrical installations are characterized by an operating frequency in the 146-174 MHz and 420-470 MHz bands and a power rating up to a few watts; the generated field strength is up to 10 V/m in close proximity of the antenna.

- Emission levels of other equipment or the power supply are taken from the relevant documents [8] [9] stating interference limits.

In principle, all the above-mentioned primary sources of interference should be considered for the various types of installation. However, the relative importance of each kind of interference is very different for the various installations, due to the different coupling factors between the circuits of the auxiliary system and those of the electrical power system. For example, the interferences caused by switching operations in the H.V. circuits are very critical in the case of a substation, given the proximity of the circuits of the auxiliary equipment to the sources of interference (see Fig. 1). Another example is shown in Fig. 2, where the different effect on the auxiliary circuits due to lightning strokes on a control building is qualitatively indicated for three different situations: buildings with a dedicated lightning protection grid insulated from the reinforcement and metal structures of the building itself (possible situation in control centers); buildings with the lightning protection grid inside the wall of the building itself (possible situation in nuclear power stations); buildings without a dedicated lightning protection system, in which the presence of earthed tall structures, such as earth wires, power lines or metereological towers and chimneys, ensures a certain degree of protection against direct strokes on the buildings (possible situation in substations).

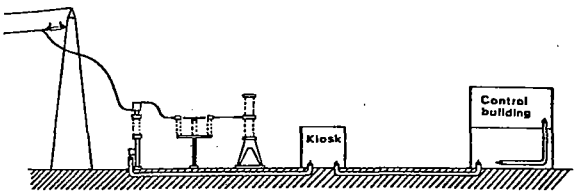

Fig. 1 - Typical layout of H.V. substation, showing control circuits very close to sources of interferences (switching on H.V. circuits)

In describing, in the next section, the general methods of evaluating the interferences induced on auxiliary circuits, an attempt will be made to assess, more quantitatively, the influence of the configuration on the effect of a lightning stroke on the control building.

3. Evaluation of the induced interferences

Starting from the characteristics of the primary sources, evaluation of the interferences induced on auxiliary circuits should involve the following other steps:

- Identification and characterization of all possible circuits layouts: in Fig. 2 shows some typical layouts.

- Assessment of the prevailing coupling mechanisms (common-impedance, inductive, capacitive, and radiation couplings) for the various interferences.

- Calculation of the induced currents and voltages (common-mode and differential-mode) at the equipment terminals, taking into account the propagation, attenuation, and shielding characteristics of the cables.

- Calculation of the fields on the equipment, taking into account the shielding characteristics of the building walls and of the cabinets.

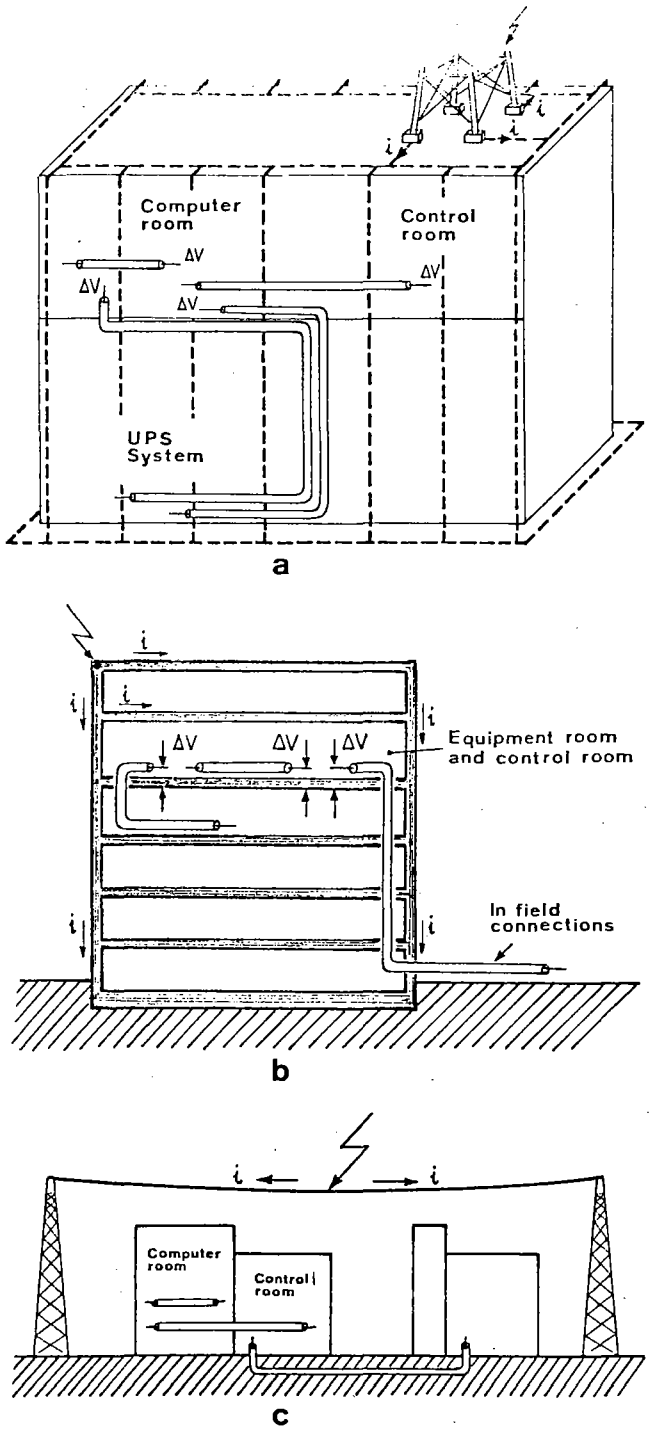

Fig. 2 - Different situations of control buildings with reference to lightning strokes:

a) building with dedicated lightning protection grid insulated from reinforcement and metal structures
b) building with lightning protection grid inside the reinforced structures
c) building with indirect protection against lightning strokes

A purely analytical approach is, in general, very complex, and requires knowledge of some of the electrical parameters of the circuits that are difficult to assess. At ENEL, at present, a semi-empirical approach is considered, consisting in the use of simplified analytical models, supported by experimental checking. This approach is described in detail for a reference configuration and a reference interference (configuration in Fig. 2b and interference produced by lightning strokes on the building); the choice is justified by the fact that this configuration, albeit not very common, presents, in respect of lightning interference, many specific problems. For other configurations and other types of interference, an attempt will be made to point out the differences in respect to the chosen reference condition.

3.1 Reference condition

Fig. 2b shows three basic auxiliary circuits:

- circuits connecting pieces of equipment on the same floor of a building;

- circuits connecting pieces of equipment on different floors;

- circuits connecting pieces of equipment inside a building with measuring devices outside it.

This current flow, in fact, produces voltage drops along the structures of the building and, consequently, by common-impedance and capacitive couplings, induced voltages on the active conductors of the cables, and currents on the screens. The magnetic field produced by the currents in the structures also gives rise, by inductive coupling, to additional induced voltages on the cables and on equipment circuits; due to the different coupling factors for the three types of circuits, the levels of induced interferences are also different.

Calculation of the above induced interferences requires, first of all, evaluation of the number and distribution of the lightning strokes on the structures; subsequent determination of the distribution of the lightning currents into the various paths within the walls of the building; consequent calculation of voltage drops along these paths and of the electric and magnetic fields inside the building. For evaluation of the number and distribution of the strokes, use is made of a physical model, developed by ENEL and CESI [10], that takes into account the ceraunic level of the area, the main parameters of the lightning current, the geometrical characteristics of the building under examination and of the other structures in the vicinity.

Determination of the distribution of currents and evaluation of the corresponding voltages and fields are the most difficult phases, inasmuch as they require sophisticated mathematical models and some assumptions on the electrical behaviour of the metal structures and their connections. Fig. 3 shows the results of calculations of voltage drops along the various paths of the structure, performed using a simplified model, which considers lumped-parameters electrical circuits, given parameters of the lightning striking the building and a given striking point. The results of some experimental investigations (Fig. 4) conducted by injecting a transient current into the structures of a building under construction, with an H.V. impulse generator, were used to calibrate the model.

Research is in progress to refine the analytical approach for a more accurate evaluation.

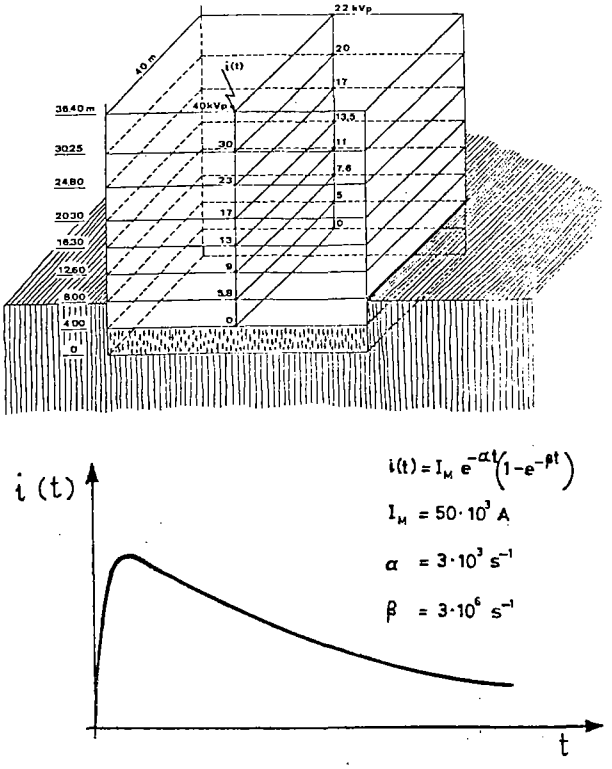

Fig. 3 - Voltage drops on the structures of a building (configuration of Fig. 2b), caused by a direct lightning stroke with given characteristics

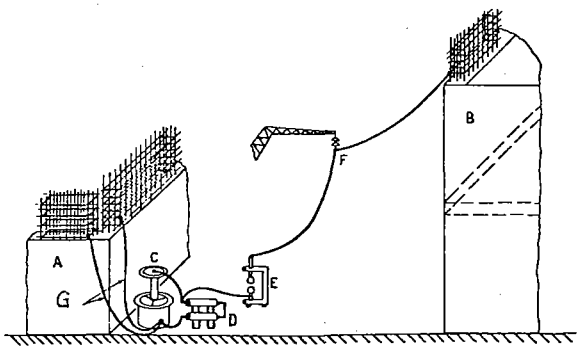

A: auxiliary building
B: control building
C: H.V. power supply
D: energy storage capacitor bank
E: H.V. spark-gap
F: insulated connection
G: ground connection

Fig. 4 - Test set-up for simulation of a lightning stroke on a control building

Starting from the voltage drops along the structures and from the fields around them, the induced interferences in the cables are evaluated as follows:

a) Common-impedance coupling

The common-mode voltage induced on a cable circuit is evaluated in the most critical case, in which one terminal of the circuit is grounded and the other one is floating (Fig. 5). As indicated in the figure, this situation is quite realistic, due to possible insulation defects, low impedance terminations, presence of filters, etc.. However, in other cases, the common-mode voltage is intermediate between the maximum value calculated as above and half this value (case of equal impedances at the two terminals). In addition, the induced voltage is first calculated by ignoring any shielding effect, and is therefore assumed equal to the voltage drop in the building structure along the length of the cable; the attenuation due to screens, conduits, and trays, earthed at both ends, is then considered on the basis of equivalent circuits (for example, as in Fig. 6). The same equivalent circuit is also considered in calculating the induced current in the cable screen. From this current the common-mode voltage can be also calculated, using the transfer impedance concept.

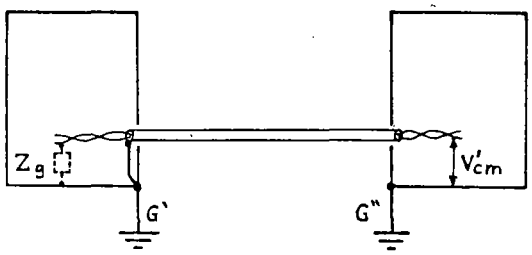

G',G": connection to local ground network
V'cm: common-mode voltage
Zg: impedance of active conductor to ground

In the worst case $Zg \simeq 0$ due to:

- *filters on input/output circuits of equipment*
- *surge arresters, transient suppressor, etc.*
- *galvanic connection to ground of a conductor*
- *low isolation resistance, stray capacitance*

Fig. 5 - Common-impedance coupling mechanism

$$\frac{V'_{cm}}{V_{cm}} \cong \frac{1+j\omega L_s/R_s}{1+j\omega L_g/R_s} \quad (\text{for } L_s \gg L_g)$$

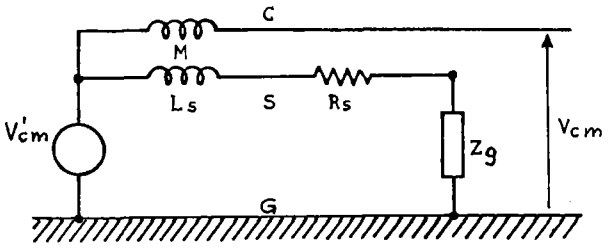

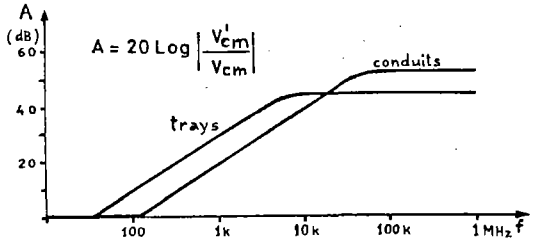

C: active conductor
Ls: shield inductance
S: shielding device
Rs: shield resistance
M: mutual inductance shield-active conductor
Zg: ground connection impedance of the shield ($Zg \simeq Lg$)
V'cm: ground potential rise (equivalent generator)
Vcm: common-mode voltage on conductor C

Fig. 6 - Equivalent circuit for evaluation of the shield attenuation and example of calculation

The differential-mode voltages are evaluated according to Fig. 7, in which complete unbalance is considered in order to obtain the maximum expectable value. Balanced signal lines are affected by lower differential-mode voltages, depending on their rejection to the common-mode voltages.
Table I summarizes the results of calculations made according to the above methods and with reference to the parameters assumed for the lightning current.

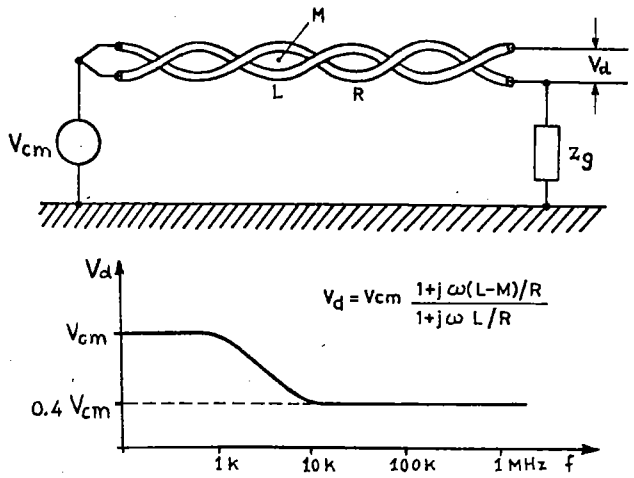

L: conductor inductance
R: conductor resistance
M: mutual inductance between conductors
Zg: impedance of a conductor to ground (worst case: Zg=0)
Vcm: common-mode voltage (equivalent generator)
Vd: differential-mode voltage

Fig. 7 - Evaluation of differential-mode voltage due to different common-mode voltages on two unbalanced conductors

b) Inductive coupling

Fig. 8 shows the mechanism of the inductive coupling on a cable layed down on a ground structure. In this case, too, the common-mode voltage is first obtained by calculating the magnetic field due to the current flow in the structures, ignoring the shielding effects, and then applying the attenuation factors produced by the screens, the conduits, etc.. Experimental results of attenuation values as a function of the frequency are given in Fig. 9.

The differential-mode voltages are determined, with reference to the above-mentioned Fig. 7, considering, again, the unbalance of the two active conductors and, in addition, the residual loop determined by two active conductors, due to insufficient twisting.

The above-mentioned Table I gives indications of the common-mode and differential-mode voltages due to inductive coupling.

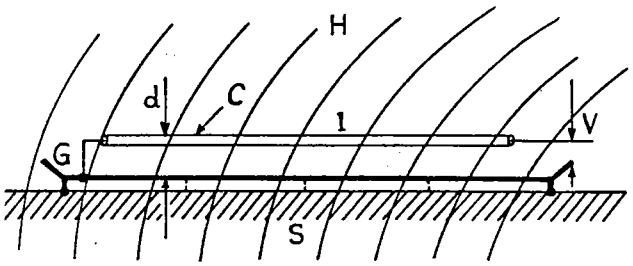

C: active conductor of length l
S: reference structure (ground conductor, cable tray, etc.)
d: exposition distance to magnetic field
H: magnetic field
G: reference to ground
V: common-mode induced voltage

Fig. 8 - Simplified model for the inductive coupling analysis

c) Capacitive coupling

Capacitive coupling may produce common-mode voltages that are maximum in the case of conductors floating at the two extremities; in this case the induced voltages are about half the maximum values determined by the common-impedance coupling.

3.2 Other conditions

For other configurations (for example those in Fig.s 2a and 2c) and for other types of interference, the general procedure for evaluation of induced interferences is essentially the same. However, the various coupling factors and, consequently, the induced interference levels may be substantially different. For example, with reference to the configuration in Fig. 2a, in which all the auxiliary circuits have been considered inside the building, only the inductive coupling in respect of lightning current flowing in the dedicated grid is relevant; common-impedance coupling may be ignored, being the building structures not involved by lightning currents.

Table I - Example of evaluation of the maximum values of the voltages induced in the auxiliary circuits of a power plant, due to lightning strokes on the control building (Fig. 2b).

Typical circuits	Common-mode voltage (V)		Differential-mode voltage (V)	
	Common-impedance coupling	Inductive coupling	Common-impedance coupling	Inductive coupling
Inside control room	60	10	25	5
Between rooms at different floors	300	50	120	20
Between control building and field	320	60	130	25

Similar considerations apply to the configuration in Fig. 2c, when the lightning strikes the protection structures. In this case, the inductive coupling is strictly dependent on the parallelism lengths between interfering and victim circuits; when the configuration in Fig. 2c is used in substations, with auxiliary circuits connecting the peripheral equipment in the kiosks to the main central building (see also Fig. 1), these circuits are subjected, not only to inductive coupling, but also to common-impedance coupling, due to circulation of the lightning current in the substation earth grid; similar effect occurs for strokes on a power line, due to capacitances to ground of voltage and current tranformers.

$$A = 20 \log\left(1 + \frac{2\mu d}{3 r_e}\right)$$ for power frequency and harmonics

$$A = 0.13\, d \sqrt{f \sigma \mu}$$ for higher frequencies

(μ = relative permeability: 500; f = frequency in Hz; r_e = equivalent radius; σ = conductivity: for Cu 0.17 S/m; d = screen thickness)

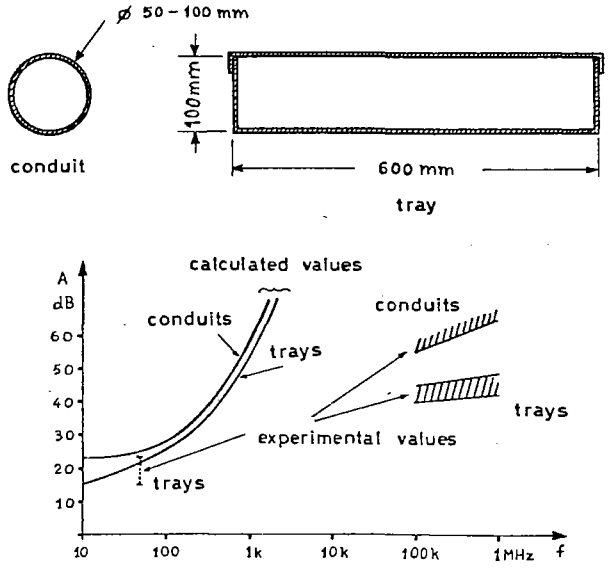

Fig. 9 - Example of evaluation of magnetic field attenuation due to trays and conduits

As regards the other types of interference, those due to switching operations on HV circuits, or other similar transients, are very critical, as already mentioned, in the case of a substation (Fig. 1). In this case, in fact, the sources of interference are very close to some peripheral equipment in kiosks and, therefore, induce in this equipment and in the circuits connected to them severe interferences by common-impedance, inductive and capacitive couplings. The prevailing coupling is determined by the circuit configuration and by the frequencies involved.

The interferences due to circulation of fault currents is mainly determined by common-impedance and inductive couplings. Their severity depends on the short-circuit current levels, the earthing system configuration, the lengths of parallelisms, etc.. For these interferences, the shielding effect of screens, conduits and trays is quite limited (see Fig.s 6 and 9).

Fast transients due to switching operations in L.V. circuits mainly produce interferences in other L.V. circuits by capacitive coupling: this coupling may take place between circuits of the same cable, between circuits of different cables in the same cabinet, between circuits in different cabinets. Determination of induced interferences requires assessment of electrical models for the various configurations; at ENEL simple formulas for the various capacitances involved are used, together with results of systematic measurements of the various parameters of the circuits.

Induced interferences by electrostatic discharge are of difficult evaluation, being determined by the currents associated with a direct discharge on the equipment.
Studies are in progress for evaluation of the effects of the various parameters of this particular type of interference.

Induced interferences to radio-transmitters are evaluated by using empirical formulas which express the electromagnetic field in the proximity of the equipment as functions of radiated power, distance from the antenna, antenna factor and attenuations involved.

Conducted and radiated interferences from other pieces of equipment are established, as already mentioned, assuming as maximum levels the limits prescribed by specific standards on the various types of equipment.

Interferences from power supply are generally expressed in terms of voltage fluctuations, voltage dips, harmonics, etc..

4. EMC design criteria of auxiliary circuits in electrical installation

In the previous sections a general procedure for evaluation of induced interferences is presented. For pratical reasons, however, the design of auxiliary circuits, with reference to electromagnetic interference, is not developed for any possible configuration that may be meet in electrical installations. At ENEL a classification of the various circuits has been established in terms of severity levels [11], defined with reference to the immunity requirements of the equipment connected to the above circuits: these requirements are obtained from the predicted interference levels adding adequate safety margins. The choice of the environmental class (at present 4 classes are considered, plus one special class for exceptional cases) and the associated immunity level derives from technical and ecomical analyses and is based on the electromagnetic environment obtainable with the installation practice adopted for the various auxiliary circuits; the choice is applicable to dedicated and general-purpose equipment. An example of this classification with reference to some typical circuits and some kinds of interference is given in Table II.

The verification of the equipment immunity in respect of the various interferences is made with laboratory tests, performed according to standardized procedures, developed by ENEL, taking into account international recommandations.

5. Conclusions

Design of auxiliary circuits of electrical installations in respect to electromagnetic interference requires an accurate assessment of the electromagnetic environment and suitable criteria for the evaluation of the electromagnetic interferences.

Sufficient information is generally available on the main parameters of primary sources of interferences present in electrical installations.

Simplified models, supported by experimental investigations, as those presented in the paper, are considered adequate for evaluation of induced interferences on auxiliary circuits for the most common configurations. For particular cases, involving special reliability requirements, some refinements of the analytical models are considered appropriate and research in this field are in progress at ENEL.

Design criteria based on classification of the electromagnetic environment, which take into consideration various kind of plants, installation practices and mitigation methods, and laboratory qualification tests activities have been developed at ENEL and adopted on a vaste scale with satisfactory results.

References

[1] G. Pellegrini, A. Raimo, C. Reynaud: "EMC problems in H.V. substation" - IEEE International Symposium on Electromagnetic Compatibility - Washington, July 1976.

[2] G. Pellegrini, A. Raimo: "EMI protection of the electronic equipment to be installed in the control center of a large electric network" - 1st Symposium and Technical Exibition on Electromagnetic Compatibility - Montreux, May 1975.

[3] A. Bodini, L. Pandini, G. Pellegrini: "In field recording and analysis of electrical transients with computerized system for EMC diagnosis of H.V. substations and power plant control equipment" - 2nd Symposium and Technical Exhibition on Electromagnetic Compatibility - Montreux, June 1977.

[4] A. Natale, L. Pandini, G. Pellegrini, C. Reynaud: "Le interferenze elettromagnetiche ed i sistemi di automazione degli impianti elettrici: diagnostica e prevenzione" - Annual conference of the Italian Electrotechnical Association - 1979.

[5] Working Group of Italian Electrotechnical Committee Technical Committee 81: "Lightning protection of structures" - L'Energia Elettrica, Vol. 61, 1984 and Vol. 62, 1985.

[6] K. Berger, E. Garbagnati: "Lightning current parameters - Results obtained in Switzerland and in Italy" - URSI - September 1984.

[7] R.B. Anderson, A.J. Eriksson: "Lightning parameters for engineering application" - Electra n. 69, 1980.

[8] CISPR Publication 22: "Limits and methods of measurement of radio interference characteristics of information technology equipment" - 1985.

[9] CISPR Publication 14: "Limits and methods of measurement of radio interferences characteristics of household electrical appliances, portable tools and similar electrical apparatus" - 1985.

[10] R. Cortina, L. Dellera, E. Garbagnati, A. Pigini, W. Serravalli, L. Thione: "Some aspects of the evaluation of the ligtning performance of electrical systems" - Report 33.13 - CIGRE, 1980.

[11] L. Pandini, G. Pellegrini: "Criteria adopted at ENEL for the design of electromagnetically compatible systems" - 7th International Zurich Symposium of Electromagnetic Compatibility - March 1987.

Table II - Example of environmental classification of electrical installations in respect of electromagnetic interferences. Common-mode voltages due to lightning strokes and switching of H.V. isolators.

Plant	Auxiliary circuit	Class	Immunity requirements (V)	
			Lightning strokes	Switching of H.V. isolators
Substation	from H.V. equipment to kiosks	4	4000	2500
	from kiosks to control building	3	2000	1000
	inside control and auxiliary building	2	1000	500
Power station	between different buildings	2	1000	500
	between rooms of the same building	2	1000	500
	inside control room	1	500	-

International Conference on Large High Voltage Electric Systems

112, boulevard Haussmann — 75008 Paris

1988 Session — 28th August - 3rd September

O

36-01

* Pref. Subj. 2

EXPERIENCES IN THE INFLUENCE OF PRIMARY PLANT OPERATION ON SECONDARY PLANT AND PROCEDURES TO MINIMISE ITS EFFECT

by

J.M. HAYDON*

SECV

(Australia)

RESUME

The introduction of compact, high technology Gas Insulated Switchgear (GIS) and increasing the amount of co-located electronic equipment in modern power transmission networks requires a new awareness of Electromagnetic Interference (EMI). This paper presents an overview of EMI experiences associated with GIS and conventional switching plant. It discusses various mechanisms of interference, measures appropriate to dealing with such interference and testing techniques. As a consequence of these experiences, a number of attitudes and rules of thumb have enriched the EMI awareness of this organisation.

KEYWORDS

Electromagnetic Interference - Switching Transient - Gas Insulated Switchgear - Shielding - Radiated Interference - Conducted Interference - Telecommunications Equipment.

INTRODUCTION OF GIS

In 1968, the State Electricity Commission of Victoria (SECV) commissioned its first 500 kV transmission lines. Switching stations for these early lines were air insulated and consequently spacious. Communications systems (the major early user of electronics) associated with these early lines were built around power line communications for both voice and protection signalling functions.

The first GIS switching stations (also for 500 kV transmission) were introduced into SECV service in the early 1980s. By this time, electronics for communications services in particular were far more sophisticated. Equipments chosen for communications services were of a design intended for telecommunications authority application. This ensured continuity of supply of compatible equipments and modern, proven designs well removed from prototype serial numbers.

Development of the 500 kV transmission network accelerated in the late 1970s and the early 1980s, saw the commissioning of three new stations and associated lines. All of these stations used GIS and two were fully enclosed. At two of these sites (Moorabool and South Morang Terminal Stations), the major telecommunications plant was physically separated (200-300 metres) from the switchyard but, in the third (Sydenham Terminal Station), the distance between primary plant and secondary plant, especially telecommunications plant, was 20-50 metres. This installation provided the first EMI experiences.

THE FIRST EXPERIENCES

GIS switching stations have a number of advantages for power transmission networks. Fully enclosed stations are compact and it is this feature rather than the use of GIS which brings secondary plant into near proximity with primary plant and its attendant high, switching generated transient electromagnetic fields. Sydenham Terminal Station in the outer north-western suburbs of Melbourne is such a station.

To support the communications needs of this station and other stations of the network, a microwave communications system was established to Sydenham and Moorabool stations and integrated with existing systems. The microwave system was commissioned in advance of GIS station completion and operated without disturbance or malfunction for six months.

Upon station completion, its commissioning program was marred by repeated teleprotection equipment alarms. Of particular concern was the "Blocking" teleprotection function. The equipment chosen for the function was such that upon detection of an impulse or other signal disruption that could result in false output command, it "squelched", i.e. ignored input signal for a preset duration. It only provided an output signal when input signal conditions were such as to reduce the possibility of false command to very low levels.

* Transmission Development Department, State Electricity Commission of Victoria, 15 William Street, Melbourne Victoria 3000, Australia.

Under such conditions, if local protection plant were to detect a line fault which required that a "Block" signal be sent to the far end of line segment, that "Block" signal was in danger of not being detected at the far end before secondary protection at the far end activated its local line switching equipment, resulting in unintended loss of power transmission.

At the Sydenham Terminal Station, the microwave radio site and the station control buildings are on opposite sides of the switchyard. The microwave radio site on the southern side of the yard originally housed all Frequency Division Multiplex (FDM) equipment. However, when the station was commissioned, channel multiplex equipment was relocated to the station control building. Standard "groups" of 12 voiceband channels (to CCITT recommendation G732) were connected by shielded, balanced cables laid directly through the switchyard to higher order multiplex equipments which were retained in the microwave building.

Investigations revealed that this architecture had a number of deficiencies:

a Some of the equipments were adversely affected by the high transient fields caused by local switching.

b Although the balanced, shielded cabling between the buildings provided a high level of rejection of these transient fields, it was not adequate for this installation.

c End to end cable performance was degraded by room cabling and earthing at each end, particularly the channel multiplex end which also housed the main distributing frame.

Two principal mechanisms of interference effect were noted in these early tests:

a Impulse noise in the protection signalling channel.

b Disruption of the modulating carrier supply for the FDM equipment.

IMPULSIVE NOISE IN THE CHANNEL

Layout of the Sydenham Terminal Station is such that the teleprotection equipment is some 30 metres distant from the FDM channel termination and channel multiplex equipment. Interconnecting cables were balanced, twisted and shielded and earthed at one end only. Signal level was set to around -6 dBm in 600 ohm (approx 0.37 V r.m.s.). Isolator operation was observed to produce impulsive disturbances on the teleprotection signal. These impulses had peak amplitudes between -10 and -20 dB relative to the signal. For the less protected telephone service cabling, much higher levels were observed.

Impulse noise was also observed to be coupled directly into the channel level multiplex and into the group level multiplex. Higher order (super group and baseband assembly) equipments and the microwave radio equipment were not observed to contribute significantly to the signal path degradation. These higher order equipments were fully enclosed and earthing structures within the equipment were such that the signal path earth was isolated from the chassis (although small capacitative coupling must be acknowledged).

DISRUPTION OF THE MODULATING CARRIER SUPPLY

Frequency Division Multiplex provides multiple channels for signalling, etc, by modulating the voice band signals into a contiguous sequence of frequency domain "blocks". For each of the contiguous blocks, one or more modulating frequencies is required. Loss or absence of these modulating frequencies results in the cessation of existence of the frequency domain block(s) supported by that modulating or carrier frequency.

In the Sydenham experience, the generator for these carrier frequencies was a number of phase locked loops (PLL) referenced to an accurate 4 kHz signal. Each PLL provided one of the required carrier frequencies. for reliability the carrier supply module was duplicated.

Upon detection of loss of even one carrier frequency, the primary carrier supply was automatically disconnected and the standby unit substituted.

During primary plant switching operations, one or more of the phase locked loops in either the primary or standby carrier supply was observed - both in the field and laboratory - to be disrupted. This resulted in the loss of individual carrier frequencies which was not corrected by changeover to the standby unit because it suffered the same problem. These carrier frequencies once lost through loss of lock in the PLL, would be unavailable for periods of 0.1 to 0.5 second, corresponding with the time required for the PLL to regain lock to the reference supply. For most of the protection schemes operating out of this site, such delays are intolerable.

CORRECTIVE MEASURES

To overcome the effects of impulsive pick up on cables, the signal to noise ratio was enhanced. This was achieved by:

a Where terminal equipment had adequate drive capability, the transmit signal was set to the highest practicable level. To be part of this category, equipments had to be able to provide more than 0 dBm (in 600 ohms, approx 0.77 V r.m.s.). Reception of such signals for input to the next system component invariably required attenuation of signal (and noise) which was carried out as near as practicable to the input point.

b Where terminal or intermediate equipments were not able to provide the necessary drive, amplifiers were used. For voiceband, 600 ohm signals, a special termination printed circuit card was developed which provided both amplifier and attenuator. For the case of group band signals (60-108 kHz), commercial group extenders were used which achieved the same function as the voiceband device.

One aspect of the group extender installation was the wide band width of such devices which were installed without a band limiting filter. The lack of this band limiting filter enabled the high level but low frequency components of the impulsive noise to be presented to the receiving unit. These out of band signals then saturated or overloaded the input stages and thus indirectly continued to disrupt the signal pattern. Installation of the band limiting filter corrected this problem.

In order to eliminate or contain the equipment disruptions - both direct coupling of impulsive noise into the signal path and PLL disturbances - all susceptible equipment was enclosed in shielded cabinets. Prior to this last resort action, considerable study was undertaken to harden the equipments against the transient fields, however, within the limits of reasonable resource expenditure and time, shielding proved to be the more appropriate solution.

Shielding required was determined by measuring the local transient fields in the switchyard and equipment rooms and in the laboratory measuring the field required to disrupt the equipment. Allowing a safety factor of 15 dB for the uncertainties, the cabinet shielding required was around 50 dB at 1 MHz. Because magnetic fields were observed to be high, the cabinets were designed for both electrical and magnetical shielding. Magnetic shielding level adopted was 40 dB at 1 MHz.

EFFECTS UPON CO-AXIAL CABLES

In three cases, this authority has experienced significant disturbances on co-axial cable systems. The experiences all relate to microwave radio base band cables in different environments as follows:

a At a GIS (not fully enclosed) station where a buried co-axial cable connected a multiplex equipment room and a 400 metre distant radio room.

b At an air insulated switching station where the co-axial cable followed a partially buried, partially cable trench route of 400 metres from a multiplex equipment room to a radio room within an adjacent distribution (22 kV) switchyard on a separate earth mat.

c Within a large power station where the co-axial cable connects a radio equipment room to a multiplex equipment room by a 250 metre, cable tray route.

In all of these instances, the signal interface to the radio equipment supports a band width of approximately 1.3 MHz at approximately -40 dBm in 75 ohm (approx 0.087 V r.m.s.).

At the GIS station (case (a)), direct pick up in the co-axial cable was such that for any 4 kHz block, the peak impulse level was about equal (within 6 dB) to the maximum channel signal level (test tone level). In such instances, the signalling system could not satisfactorily operate.

To overcome this limitation, the co-axial cable was abandoned and communication between the two rooms rearranged. Higher order multiplex (group, supergroup and baseband assembly) equipments were transferred to the radio room and group extenders identical to the units used at Sydenham installed for high level (0 dBm) communications between the rooms.

The second co-axial cable experience (case (b)) appeared initially as a failure of signalling channels during a fault on a line which did not actually terminate at that site. Very shortly afterwards (days), a fault on a 22 kV feeder out of the distribution substation which contained the radio room caused large neutral current to flow and reproduced the results of the previous line fault. After the first incident, data logging equipment had been installed and it captured the data of the second fault.

Mechanisms identified were -

a a large increase in noise (assumed impulsive) in the signal path;

b coupling of impulse noise onto control signal lines, causing automatic changeover to a non-existent standby radio.

Elimination of the changeover was achieved by simply disconnecting the drive to the changeover relay and effectively locking the signal connection to the one existing radio. However, the second mechanism required further study.

Subsequent testing of the co-axial cable signal path showed -

a current flowing in the outer screen of the co-axial cable which was tied to the local earth mat at either end;

b high frequency (100 kHz to 10 MHz) components - which occur during system faults - of the outer screen current coupled into the separate signal path (inner screen and central conductor); this mechanism is quantified in terms of the Transfer Impedance of the co-axial cable.

The mechanism described for case (a) above was also assumed to be a contributor to signal path noise. However, because of the earthing of the cable at both ends, the extent of this effect would be diminished, but would become significant upon unearthing one end. For this reason, the solution adopted at this site was similar to that for case (a); viz, supergroup extenders operating on balanced signal cables were used between the two equipment rooms.

In the last instance, case (c), communications services at the power station were required prior to completion of the communications equipment rooms. To provide the necessary services, a small room approximately half way between the communications room and the antenna was provided. This served as the initial communications room and, upon commissioning of the planned room, all equipment except the radio (because of antenna cable difficulties), was relocated to that room. Signalling between the radio room and the equipment room was via double screened co-axial cable.

At the time of commissioning of the communications equipment rooms and later the first generator of power station, the system performed to specification. However, as the subsequent generators were commissioned and the amount of secondary electrical machinery increased, so also did the noise in the communications system, eventually producing alarms in terminal equipments. In this case, the noise in the signal path is continuous and so far only an interim solution of separating the co-axial cable from other cables where possible in the cable tray. The proposed solution for this case is the installation of video bandwidth amplifiers and suitable attenuators to raise the signal level on the co-axial cable and, hence, improve the signal to noise ratio.

POWER LINE CARRIER EFFECTS

Power line carrier signalling is generally very reliable, however, experiences have demonstrated its susceptibility to EMI. One example will be cited related to the design of the matching unit which interfaces the Capacitor Voltage Transformer (CVT) to the power line carrier co-axial conductor.

This experience occurred with the unintended loss of a 500 kV transmission line between two GIS stations (Sydenham and Moorabool).

In this incident, a circuit breaker operation at Sydenham resulted in the disruption of a power line protection signalling system which was transmitting a "block" signal to Moorabool. The lack of this block signal resulted in the unintended operation of the 500 kV circuit breaker.

Investigation showed that the cause was deficient line matching equipment design. In the units installed at the subject site, the LMU drain coil was designed to be 45 mH (14 ohms reactance at 50 Hz). Protective gas gap devices were installed across the drain coil.

During the operation of a circuit breaker associated with another line segment, but sharing a common bus, transient voltages of several kV peak amplitude and 10-50 nSec rise time are presented to the CVT and ultimately to the protective gas gap. The gas gap correctly limits the voltage across the drain coil and the coupling transformer. However, once ignited, the gas gap resembles a low impedance and series voltage source. The relatively high value of drain coil inductance then sustains the gas gap for a period of time related to the instantaneous current through the coil at the time of gas gap ignition($t = L/R$, $L = 45$ mH, $R = 1$-5 ohms). For the duration of the gas gap ignition, the output of the coupling transformer, the powerline carrier signal is short circuited to ground and transmission fails.

Post incident investigations produced short circuit durations of between 1 and 10 msec and, on occasions, repeated a number of times for the one switching event. Initial corrective measure was to replace the gas gaps with zinc oxide VDRs. This limited the outage time to an observed maximum of 2 msec which, because of the integrating action of the output relay drive, would not be extended.

Final corrective action was to replace the 45 mH drain coils with units of 3 mH which is adequate for reliable signal coupling, but drammatically reduces the time constant of the drain coil - VDR system.

Because this was the first record of such a powerline carrier failure, a supplementary study of several GIS and air insulated switching stations was carried out. The study sought to assess and characterise the peak value and frequency characteristics of voltages presented at the LMU transformer, i.e. across the drain coil. The study examined 220 kV and 500 kV switching stations. Results of the study showed some differences in the peak value of drain and voltages, but a considerable difference in the frequency components of these transients. GIS stations showed frequencies between 4 and 10 times greater than for air insulated stations. Source impedance of these transient voltages was calculated and found to vary, depending on switchyard configuration at the time of switching operation. Lowest value was 55 ohms and highest value was 240 ohms. Median was 155 ohms. Of particular interest in this program was the repeatability of the waveshape captured by the high speed oscilloscope.

RADIATED ELECTROMAGNETIC FIELDS

Much of the EMI experience with GIS and conventional stations related to equipment and system susceptibility to radiated transient electromagnetic fields which occur during switching of primary plant. A number of studies were carried out to measure these radiated fields and their spectral distribution.

Investigations were made using frequency domain measurement techniques and equipment intended for US.MIL STD 461/462 applications. They were aimed at measuring field intensities in equipment rooms, near switchyard boundaries and at locations along the line, but at some distance from the switching plant. Because they were related to interference in FDM systems, they were generally limited to frequencies below 5 MHz.

Figures 1 and 2 below show sample results from this program. Figure 2 shows the results from a 220 kV air insulated station with measurements taken at the station boundary. Figure 1 is the result of measurements approximately 50 metres from the line, but 24 kms distant from the location of the actual switching of 500 kV GIS.

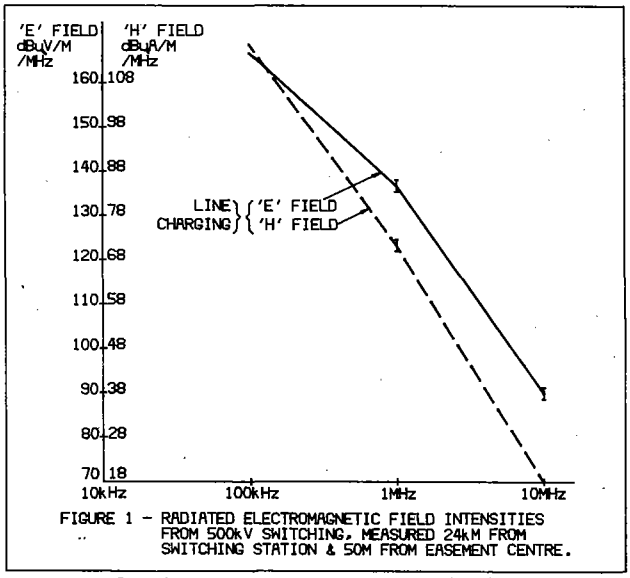

FIGURE 1 - RADIATED ELECTROMAGNETIC FIELD INTENSITIES FROM 500kV SWITCHING. MEASURED 24kM FROM SWITCHING STATION & 50M FROM EASEMENT CENTRE.

Results of this program may be summarised as follows:

a The peak amplitude of the transient field produced by the switching operation is comparable for both GIS and air insulated stations of similar working voltages.

b The frequency spectrum of the GIS transient field extends to considerably higher frequencies than for comparable voltage air insulated stations.

c The maximum intensity transient is produced by the circuit breaker operation which charges the line segment. Peak intensities for line charging are some 10 dB greater at 1.0 MHz than disconnect switch operation.

d The radiated field persists for some considerable distance from the actual switching plant, although the high frequency components of such transients dissipate more rapidly than low frequency components.

e The majority of the radiated energy from switching operations is concentrated at the lower end of its spectrum. For air insulated stations, the peak intensity is between 10 kHz and 100 kHz.

MEASUREMENT TECHNIQUES

For both radiated and conducted interference effects in switchyards, very special care is required as the transient field intensities in the vicinity of the switchyard are very great. Work for EPRI (ref 1), cites 3000 V/m, and studies referred in this report measured 1600 V/m. Under such conditions, ordinary instrumentation is unusable. Early attempts by the author resulted in oscilloscope traces sweeping backwards and occasionally producing loops on the screen.

The series of conducted transient voltage measurements was carried out using a high speed storage oscilloscope which was mounted inside a transformer tank (approximately one metre cube). Cables to the oscilloscope were enclosed inside flexible iron conduit for as much of their length as was practicable or safe. The oscilloscope sweep trigger was set and the oscilloscope sealed inside the tank which had only one aperture - a small viewing window approximately 20 mm diameter. Upon conclusion of the switching operation, the tank was opened and the storage screen photographed.

Radiated field measurements were carried out using frequency selective instrumentation and calibrated antennae. As all measurements were near field, both electric and magnetic intensity were measured. To produce a spectral plot of the radiated field, it was necessary to repeat a switching operation many times.

A more efficient approach to the measurement of transient fields in the time domain approach. This was the technique used in the EPRI study and a shielding exercise by Ontario Hydro Power Station (references 1 and 2 respectively).

Time domain methodology produces a measurement result that is the peak field intensity. Further, the result from a time domain approach more closely represents the signal that will be coupled into any susceptible cable or equipment. Where the interference measurement is related to a digital signal (i.e. wide frequency range and wavefront related), the time domain approach produces the most readily useable results. Reference 2 describes simple antennae systems and techniques that are suitable for this approach. However, the low sensitivity of such equipments limits its application to fields greater than about 1 volt per metre.

Attempts by this organisation to establish time domain measurement technology have had mixed success. The low sensitivity of the receiving antennae was accommodated by use of amplifiers and high gain oscilloscopes. However, such equipment has to date been so affected by the radiated field as to render the result unuseable. Nevertheless, time domain measurements with subsequent conversion to the frequency domain is believed to be the most suitable technique for measurement of transient radiated and conducted interference and will be pursued toward successful application.

INTERFERENCE CONTAINMENT

A wide range of techniques for the reduction or containment of interference have been applied in this organisation's efforts to provide secure and reliable communications. The most successful approaches to date have been:

a Elimination of actual or potential earth loops by isolating signal paths from chassis or station grounds and use of transformers or optocouplers for equipment isolations.

b Use of single point earthing. This represents a tradeoff between the high level transient interference and the low level, continuous background interference, and recognition that for high frequencies it is difficult to provide an adequate earth. Single point earthing must be used in conjunction with signal path isolation from chassis earth to be effective.

c Use of balanced signal paths in general, but not universal preference to unbalanced (co-axial) paths (refer to figure).

d Preference for wrapped metal tape shields for cables over braided shields. Tape shields result in lower transfer impedance (i.e. lower coupling into the signal path).

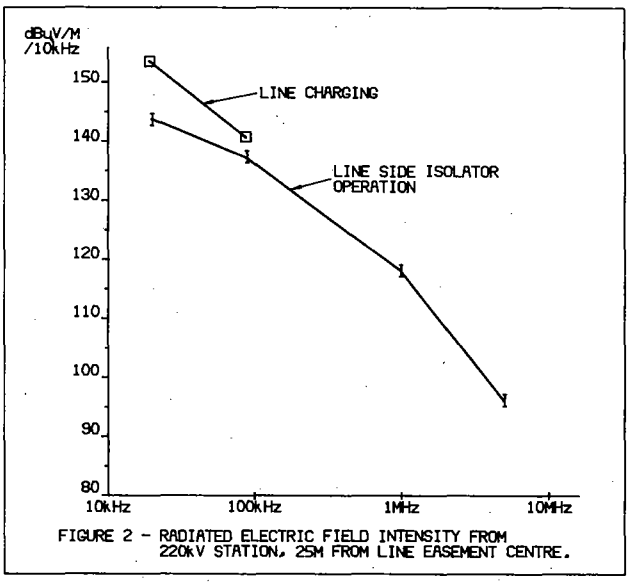

FIGURE 2 - RADIATED ELECTRIC FIELD INTENSITY FROM 220kV STATION, 25M FROM LINE EASEMENT CENTRE.

Shielding of equipment or cable paths is generally the last resort, especially if required after installation of equipment. Some success has been achieved in conversion of open equipment racks into closed cubicles, and thus minimally disrupting the installation or its operating equipments.

For new installations, shielding is established as a matter of course. Such shielding is one or two tiered, depending on the nature of the site. The first tier is architectural shielding for the rooms which will house sensitive equipment. Should the location of the building be a particularly hostile environment such as in the near vicinity of a power line or switching equipment, then equipment cubicles of known shielding performance and fully enclosed iron cable conduits are also installed.

Such practices allow more flexibility in the choice of equipments for installation and reduce the demands on staff in that environment for observance of limiting or constraining work practices. Further, the proper designing of architectural shielding overcomes the wide variations which have been observed in existing sites. Measured building shielding effectiveness at 1 MHz varies between 5 and 15 dB, whereas the general building goal should be 30 dB for low threat sites and 50 dB or more for hostile sites.

PROVIDING PROTECTED ENVIRONMENTS

The level of shielding required is clearly dependent on -

a the intensity of interfering field;

b the susceptibility of the potential victim system;

c contractual arrangements.

Whilst (a) and (b) are self-explanatory, the last may not be obvious. Many equipment manufacturers, computer systems in particular, are becoming aware of the consequences to warranty costs of EMI. Consequently, many are stipulating environmental conditions under which their equipment is warrantied. Should the environment fail to conform to these conditions, the vendor may void the warranty.

Susceptibility of equipment is a largely unresolved issue because only a small fraction of potentially useful equipment is rated in its capacity to withstand EMI. In the near future, however, the voluntary standards presently developing in the USA under the patronage of the Electronics Industries Association offer some understanding of manufacturer viewpoints. Suggested maximum EMI fields vary from around 0.1 volt per metre to 1.0 volt per metre. This conforms generally with US-MIL-STD 461/462 and recent CIGRE studies. These suggest that most equipment should be operable up to 1 volt per metre and only very special equipments are expected to operate in fields of more than 10 volts per metre.

These considerations indicate that equipment environments should be established to limit internal field intensity to 1.0 volt per metre across the spectrum from 10 kHz to 10 MHz. provided the location for such an equipment room can be chosen such that the maximum external field intensity does not exceed 100 volts per metre, then shielding required is 40 dB. Establishing this level of shielding is not trivial, but it is reasonably achievable without large additional costs during construction.

Provision of such a protected environment for equipment is the preferred approach of this organisation. The alternative is to limit the selection of equipments to those which are able to withstand the natural hostile environment. The preferred approach permits the use of commercial equipment which is manufactured for a much larger user base. This means that it is readily available, well supported and of low cost. further, being essentially commercial equipment, it will have far more user appeal than equipments developed for small production runs. Finally, maintenance works or subsequent equipment alterations are unlikely to result in degradation of the system. To this end, all new installations are assessed for EMI containment requirements. As far as practicable, such measures are designed into the structure.

REFERENCES

1 EPRI EL2982 - Measurement and Characterisation of Substation Electromagnetic Transients. Prepared by Texas A&M University.

2 Electromagnetic Sheilding of a System Computer in a 230 kV Substation - S M Harvey and W J Ponke
IEEE Transactions on Power Apparatus and Systems PAS-95 No 1
January/February 1976

GROUPE 36
GROUP 36

PERTURBATIONS
INTERFERENCE

Rapports */Papers*

36-05, 36-07, 36-10, 36-01

G. BONNARD (Secretary) — M. MEYNAUD (Secretary Assistant) — M. SFORZINI (President) — W. JANISCHEWSKYJ (Special Reporter)

SUJET PREFERENTIEL 3 / *PREFERENTIAL SUBJECT 3*

Problèmes de compatibilité électromagnétique et méthodes de protections, en particulier pour ce qui concerne les réseaux d'instrumentation locaux (y compris les transmissions par fibres optiques) dans les centrales et les postes.

Electromagnetic compatibility problems and protection methods, especially with regard to local instrumentation networks (including optical fibre transmisssion) in power plants and substations.

Questions 3.1 - 3.8

Mr. R. CORTINA (Italy)

I have no particular additional information on paper 36-10.
I would only like to say that the simplified model adopted in the paper for the calculation of the lightning current distribution on the structures containing the electronic equipment has recently been improved.
A new analytical model, based on lumped-element circuits, but that uses a more complete simulation of the various components of the structures, is already at a final stage.
Another model, to be used for very tall structures, that could involve propagation phenomena of the electromagnetic wave for the maximum frequencies involved by lightning current, is under consideration.
This new model will also take into account non-linearity phenomena that could be present in the actual structures, generally made of steel-reinforced concrete.

M. F. CHEVALLEY (Suisse)

Lors de la construction du poste blindé SF6 130 kV mentionnée dans notre rapport, nous nous sommes efforcés de réduire le couplage des interférences, par une disposition favorable de l'équipement haute tension, par la mise en place d'un plan de terre haute-fréquence et en apportant une attention particulière à toutes les connexions de mise à la terre.

De plus, ayant constaté que les essais d'usine, selon les normes CEI actuelles citées sous références 5 et 6, ne permettent pas de conclure à l'immunité des microcalculateurs exposés à des perturbations électromagnétiques HF, nous avons décidé de procéder à des essais d'immunité de ces équipements en les soumettant à ces phénomènes sur site hautement perturbateur. En l'occurrence, nous les avons installés dans un poste blindé SF6 220 kV en service à l'endroit le plus perturbé, directement sous les têtes de câble 220 kV, comme le montre la Figure 1.

Ces essais ont montré clairement que seuls les équipements de contrôle-commande installés avec des précautions particulières tels que découpage galvanique des entrées-sorties, blindages des armoires et des

modules, mises à la masse équipotentielle, filtrage de l'alimentation, etc., fonctionnent correctement près des travées haute-tension.

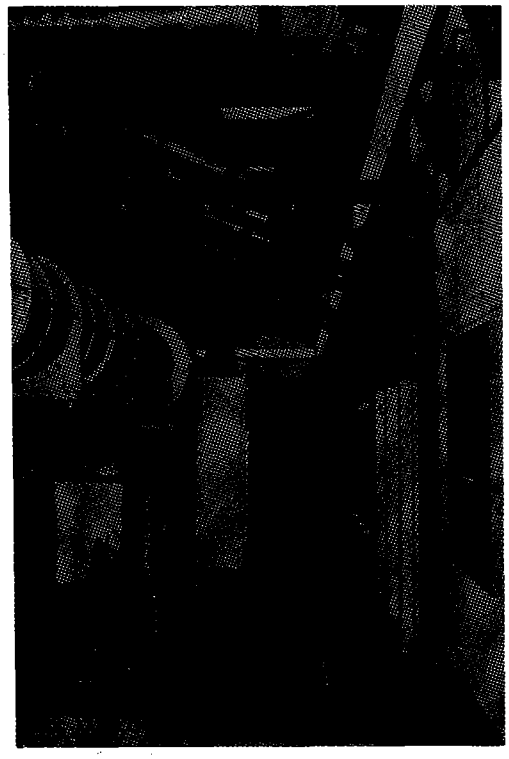

Figure 1.- Essais d'un équipement de contrôle-commande installé dans un poste blindé SF6 220 kV.

Mr. H. SELJESETH (Norway)

Q 1 & 2

Different classes of interference immunity are necessary for electronic equipment to satisfy compatibility requirements in different interference environments. The IEC-801 series publications apply four different immunity classes. However, it would certainly be possible to reduce the number of test classes to two or three because it is normally possible during installation to apply separate measures to improve the environment or the immunity of the equipment.

I feel that the most economic solution will appear when the user selects among equipment available on the market and at the design stage it may even be preferable to improve the environment to be able to use electronic equipment with a lower class of immunity.

The main demand for immunity testing and environment classification is that standardization exists and that a sufficient selection of tested equipment is commercial available.

Q 3

Big power utilities are normally able to handle compatibility questions but not always small utilities. The same conclusion applies to equipment manufacturers. Big manufacturing companies delivering both power installation and instrumentation and control equipment can take the responsibility for achieving compatibility. Therefore big power utilities can use small manufacturers. Small companies should normally prefer big manufacturers.

M. H. SAUVAIN (Suisse)

1.- Normes actuelles et en préparation

Pour exiger une immunité suffisante des équipements de contrôle-commande à microcalculateurs à installer dans un poste blindé SF6, l'entreprise d'électricité responsable de la construction a dû étendre l'utilisation des normes et des spécifications en matière d'interférences électromagnétiques.

La norme CEI 255-4 (Relais de mesure à une seule grandeur d'alimentation d'entrée à temps dépendant spécifié) utilise la tension de choc 1.2/50 μs et l'onde oscillante amortie 1 MHz.

La norme CEI 801-4 en préparation (Compatibilité électromagnétique pour les matériels de mesure et de commande dans les processus industriels - Quatrième partie : Exigences en matière de transitoires électriques rapides) prescrit des interférences plus réalistes (50 MHz), puisqu'elles sont du même ordre de grandeur que celles mesurées dans les postes blindés SF6 (jusqu'à 50 MHz).

NORME	CEI 255-4	CEI 801-4
F	1 MHz	50 MHz
SF6	50 MHz	

2.- Essais de rayonnement électromagnétique

Un essai supplémentaire a été imaginé et appliqué: différents équipements informatiques ont été placés sous une antenne à lignes parallèles, connectée à un générateur de transitoires électriques rapides.

Les premiers résultats ont montré que l'immunité au rayonnement électromagnétique en mode sinusoïdal permanent (référence CEI 801-3) était environ 10 fois plus petite que celle en mode impulsionnel répétitif (référence CEI 801-4).

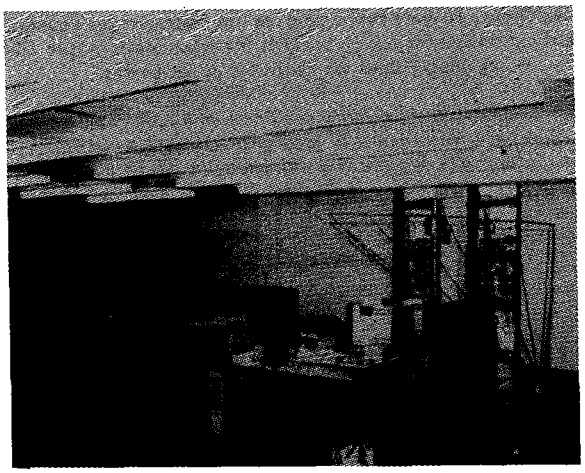

Mr. H. SELJESETH (Norway)

National safety standards on grounding are based on slightly different research results and very different assumptions. Some standards are based on approximately worst case, e.g. that an exposed person is at the most critical point at the critical time and has a rather low resistance to ground.

Others may be based on risk probability and thus accept much higher rise of earth potential and touch voltages (see touch voltages Fig.1, curve 3a and 3b, 4 and 5).

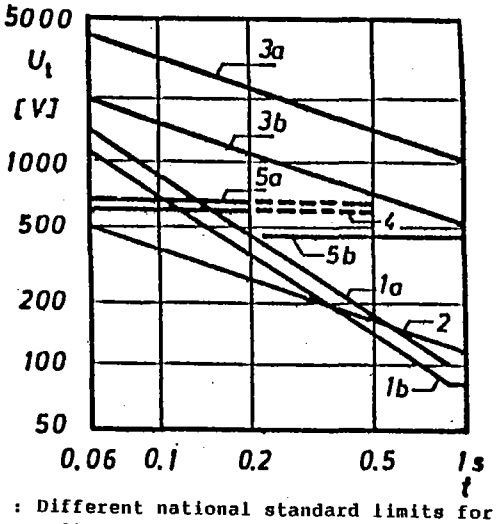

Fig.1 : Different national standard limits for touch voltages as a function of exposed time.
Electra No.71, 1980 p.52

Experience, i.e. existing knowledge about accidents seems to indicate that the existing standards are very safe. In my country no fatal accident is known due to people touching correctly grounded equipment. Such accidents with ground involved were always caused by wrong connection or missing/broken earth conductors and in a few situations when broken phase conductors have dropped to the ground from overhead distribution lines (systems with ungrounded neutral and no earth fault protection).

In Norway we have no mandatory limits for short time ground potential rise and touch voltages. Fast earth fault protection is considered to be a sufficient alternative. On the other hand many precautions are taken to reduce ground potential rise and touch voltages by systems with grounded neutral, e.g. use of equipotential grounding grids, grounded conductors buried around fences and particularly application of two shield wires with high conductivity at the transmission lines. By this arrangement about 60% of the earth fault current (I_f) will be kept in the shield wires due to induction (share (1-r) in Fig.2). The main part of the earth current (I_e, about 40%) will flow to ground through the tower footing ground electrodes. In areas with very poor earth conductivity the current flowing to earth through the local grounding system of a substation or power station may be much less than 10% of the total earth fault current. Thus the low current density to earth from the station's earth which is caused by the shield wires will limit touch voltages.

Q 6
In my opinion a meaningful comparison between power frequency, earthing and high frequency earthing is not possible because :

- power frequency earthing is mainly a question of limiting difference of potential in the earth,
- high frequency earthing is a question of limiting potential difference in the earth conductor system.

For instance in an area with very high earth conductivity it may be possible to achieve sufficiently low earth resistance and touch voltages with only a few conductors and/or rods in the earth. However if the the physical size of the system is large, the high frequency performance may be very bad but can be improved by increasing the number of rods and/or conductors.

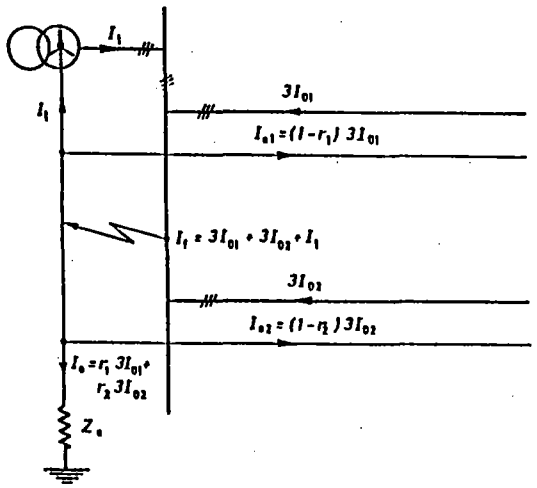

Fig.2 : Example of earth fault current distribution with earth fault in a substation with two trans mission lines.
Electra No.77, 1980 p.54

If the earth conductivity is very low, problems are usually more difficult but high frequency performance can still be improved by increasing the number of conductors. However, the problem of power frequency earth potential rise is not solved in this way because a small meshed (earthing) grid, necessary for high frequency earthing, has a very poor effect as earthing electrode. However, it will solve possible touch voltage problems within its area.

Consequently, high frequency earthing is mainly a question of getting short earth conductor connection to reasonable good potential reference systems and must be regarded as a supplement to the earthing system necessary to satisfy safety standards.

Mr. R. CORTINA (Italy)

In answering to the question of the special reporter, I wish to point out that the intention of our paper 36.10 was to give general methods of evaluation of electromagnetic interferences, which are similar for the various types of interferences. Of course, transient processes involve a wide range of frequencies and, therefore, the analytical models that have to be applied for the determination of the interferences are more complicated. For this reason in the examples reported in paper 36.10, transient interferences are mainly discussed. The methods to be applied to the analysis of 50 Hz phenomena, like overvoltages due to the circulation of short-circuit currents, can be easily derived by the more general methods applicable to the transient processes.

The two main coupling mechanisms are in this case : the common-impedance coupling and the inductive coupling, with the relevant shielding efficiency.

The first one may produce, as pointed out by the special reporter, disturbances up to the ground potential rise. According to our experience, however, if this potential rises are limited in order to assure the safety values for the personnel, by an appropriate design of the earthing grid, the induced interferences on the electronic systems are generally sufficiently lower (less than 50-100 V), than the immunity levels of the equipment.

In particular cases, where the installation is made of different parts insisting on separate earthing systems (as, for example an hydroelectric power plant with a remote control system), the induced voltages caused by 50 Hz fault currents could be critical (values up to several hundred volts were recorded). Our practice in these cases to reduce the disturbances within acceptable values considers the following mitigation methods :

- use of low-impedence ground conductors installed in close proximity of the signal cables ;

- use of galvanic separation devices, as insulation transformers, relays, optical isolators, etc.

In paper 36.10, three typical examples of installation have been considered :

- the control system of the nuclear island of a nuclear plant;

- the control system of a conventional power station;

- the control system of a substation.

In the first case, the H.V. substation was fairly distant from the nuclear building and, therefore, the effect of a fault in this substation on the circuits in the power station were considered as non-relevant.

The short-circuit currents used for the calculation were those of the M.V. distribution systems : considering the importance of the plant, the short-circuit current due to a double fault to earth was considered (40 kArms). The corresponding maximum overvoltages in the electronic circuit were only 20 Vrms due to the presence of high density of metallic structures in the installation.

For the other cases (conventional power stations and substations) the short circuit currents assumed may range from 10 to 40 kA. As already mentioned, the corresponding values of the common-mode interferences are generally kept below 100 V, in the case of circuits insisting in the same earthing system ; in other cases, as that reported by paper 36.02, higher values may be reached; of course, (as already mentioned in the previous discussions), in these cases, suitable mitigation method should be adopted.

M. B. JACQUET (Belgique)

(SUJET PREFERENTIEL 1)

Mon intervention concerne les problèmes d'optimum économique dans la maitrise des perturbations dans les postes à haute tension. Les travaux effectués en Belgique ont montré que l'optimum était obtenu en répartissant judicieusement les efforts entre d'une part, la conception du poste et de sa filerie et d'autre part, la réalisation des équipements.
Il est en effet apparu qu'en adoptant à la construction des postes, des mesures simples et peu coûteuses, on pouvait réduire les perturbations à un niveau acceptable pour des équipements conçus en respectant les règles élémentaires de protection contre les perturbations, sans exiger de prouesses particulières des constructeurs. Ces mesures simples concernent :
- la conception du réseau de terre (réseau maillé destiné à assurer une certaine équipotentialité même en HF
- le trajet des câbles auxiliaires
- l'utilisation de câbles blindés
- la mise à la terre du blindage en plusieurs points - au minimum aux 2 extrémités - et si possible en des points supplémentaires.

Je sais que cette philosophie des mises à la terre multiples des blindages ne fait pas encore l'unanimité, certains craignant des circulations importantes de courants BF dans les blindages. Cette crainte n'est plus du tout justifiée dès l'instant où tout s'articule autour d'un réseau de terre consistant et bien maillé.
On réduit ainsi pratiquement les sollicitations HF maximales entre fils et terre à quelques centaines de volts, que ce soit lors des manoeuvres, de défauts ou de coups de foudre.
On complètera ces mesures par des spécifications modérées d'immunité aux perturbations pour les équipements. Ces spécifications s'appuieront utilement sur les nouvelles normes CEI de la série 801.

Mr. L. LAGOSTENA (Italy)

I wish to make a few remarks on the definition of "environment". The Special Reporter, at Question 3.3, speaks of environment created by the power installation, i.e. the electrical lines, the circuit-breakers, the switches, wich are the origin of disturbances. This is a quite common opinion. I think that this concept should be better clarified to avoid misunderstandings.

For many people, and myself among them, the environment must take into account also the communication channels (that is, in a power station, the auxiliary cabling such as the shielded cables , optical fibres when used, grounding etc...) and not only the power circuits.

This is quite logical : for an apparatus the world, the environment, is constituted by its box and connections to the other pieces of equipement.

If we take this wider definition of the environment, each piece of electronic equipment (relay protections, micro-computers, amplifiers etc...)can be chosen according to three or four classes of rnvironment (each class characterized by a set of maximum admissible disturbances, ranging from low frequency disturbances like voltage dips and harmonics, to high frequency disturbances) : the basic environment is that of the low-voltage socket that is present in our houses or in commercial premises. The other environment will be characterized by higher levels of disturbances.
What is important to stress with this definition of the environment is that : for the same industrial or electrical station it is possible to fix different classes of environment for the equipment connected thereto depending from the type of auxiliary wiring or grounding or protective measures taken against the disturbances produced by the power system.
Another point to be stressed is that the class of environment depends from the type of disturbance : that is the class of environment does not depend only from the type of plant.
A GIS (Gas Insulated Station)can be harsh for fast transient and problems involved, (radiated field etc.) but a plant with AC/DC conversion (very common for railway conversion stations or for industry) can be harsh for the high level of harmonics : both plants, GIS and AC/DC conversion plants require a project for a very harsh environment, but for a quite different type of disturbances.

Mr. H. LORKE (C.C.I.T.T.)

CCITT has recently drafted new recommendations concerning disturbances in digital telecommunication installation. Although those recommendations are intended to be applied to public telecommunication networks they might be useful for the design and operation of privately owned or local area networks, too. In particular the draft recommendation mentioned cover the following subjects :

Rec. K.22 - Overvoltage resistibility of equipment connected to an ISDN T/S bus.
This recommendation relates to any terminal equipment which

is intended to be connected to the 4-wire T/S bus of an ISDN installation and specifies the overvoltage conditions and the test procedure taking into account relevant IEC Publications (i.e. 664, 801 -2, 950)

Rec. K.23 - Types of induced noise and description of noise voltage parameters for ISDN basic user networks. This recommendation describes the various sources of induced noise, it categorizes the required equipment performance and classifies the induced voltages concerning amplitude, frequency and wave-shape.

Rec. K.24 - Method for measuring radio frequency induced noise on telecommunication pairs.
This recommandation is an approach in standardizing measuring methods concerned and, among other things, gives advice of termination networks, reference earth point, recommended bandwidth and electric field immunity.

Mr. P.O. PERSSON (Sweden)

First, I want to thank you Mr. Chairman in the same way that Mr. Lorke, CCITT, has already done for the useful and close cooperation between SC 36 and CCITT. Similar cooperation has also started with IEC in EMC questions. Similar questions have been treated in CCITT for more than 60 years but the name EMC was not invented. It is important to harmonize CCITT recommendations with the need of EMC specifications. I will thank IEC and amongst others Mr. Goldberg, Chairman of TC 77 present today in SC 36 session for that.

Concerning the different questions treated earlier this day, I want to make some comments to question 1.2, because for private reasons, I was not able to do so in the morning. The question concerns CCITT and is experienced by my work in the Swedish Telecom Administration.

In Sweden, we have now two HVDC installations, the Kontiscan link to Denmark and the Gotland link. The third one is under construction between Sweden and Finland and has been mentioned by colleagues from Finland.

The existing links in Sweden have had problems with corrosion and harmonic disturbances in the adjacent telecom network. But I will also mention a new type of interference observed in connection with increasing the power in the link between the island of Gotland and the mainland. High DC earth potentials happened in the mainland local area telecom region. Because of the use of DC signalling between some local telecom centrals not too far from each others, the signalling in one direction were blocked through DC potential differences sometimes in the order of 10-25 volts between the centrals. New signalling AC systems had to be installed in some centrals, a relative expensive procedure.

Similar events has not earlier been experiences in HVDC projects. The disturbances like these are probably very rare. In Sweden the soil resistivity is very high, in this case up to 20-300000 ohms and it may be the reason for the high earth potential differences.

Mr. W. JANISCHEWSKYJ (Canada)

My comments pertain to "compatibility" of equipment with its electromagnetic "environment". "Immunity" of electronic equipment consists in its ability to operate satisfactorily in the presence of "noise". As far as substation control and communications equipment are concerned, electromagnetic field and the inductively, conductively and capacitively coupled interference, both originated by power plant, constitute such objectionable "noise". In general, however, radiation from a source electromagnetic energy, even when operating in its normal frequency range, i.e. while being "signal" of the given installation, may represent "noise" to another piece of equipment. Well known incidences of opening automatic garage doors by low overflying aircraft may be used as the cases in point.

Last year, Canadian Standards Association, through its Steering Committee on Electromagnetic compatability, constituted an Advisory Task Force on Electromagnetic Environment. The purpose of this Task Force is to identify conditions under which electromagnetic compatability of various classes of apparatus must be specified. It is our intention to document electromagnetic steady-state environment of all important classes of equipment, including radio stations and power lines, and to develop an envelope of the resultant frequency spectrum extending from DC to 300 GHz. It is an ambitious task in itself. We realize, however, that it will be necessary for us to also make a statement on electro-magnetic noise caused by transients. That task is much more involved in view of the fact that no comprehensive theory on transient processes in non-linear media exists at this time. In spite of these obstacles, we hope to bring our task to an end in another year.

6. CLOSING REMARKS

GIS sources of VFTO are:

(i) disconnector and circuit breaker switching operations,

(ii) line to enclosure faults.

A typical voltage collapse time, generating the VFTO, is in the range of 10 nanoseconds.

The VFTO components have frequency range of 1 to 40 MHz with an overall duration of the order of 10 microseconds, due to persistance of oscillations below 10 MHz. The frequencies above 10 MHz are only significant for the first 2 microseconds of the transient.

The general form of VFTO may be calculated by digital simulation with a 10% accuracy by relatively simple modelling. Nevertheless the accurate simulation of very high frequencies (over 10 MHz) requires more complex models of the individual GIS components.

Adequate VFTO measurements can be achieved using measuring systems with a 100 MHz bandwidth.

For the VFTO due to line to enclosure fault their amplitude can be dangerous for insulation mainly during on site testing and can reach twice the applied voltage at the instant of failure.

For disconnector switching, when the voltage collapse between contacts at restrike is 2 p.u., the peak value of the VFTO can reach 2.5 p.u. for very severe cases of GIS lay-out but generally the peak value remains in the range of 1.5 to 2 p.u. For most cases the voltage collapse between contacts is lower and the associated peak value of VFTO is below 1.5 p.u.

During the normal operation of GIS, switching of disconnectors is the major cause of VFTO. The speed and asymetry of the disconnector contacts affect the maximum magnitude of the voltage collapse between contacts at restrike. This voltage collapse can be in the range 1.2 up to 2.0 p.u. according to the switched load (pure capacitive, inductive) and the system configuration. The voltage collapse between disconnector contacts at restrike can exceed 2.0 p.u. on rare occasions when switching disconnectors under out of phase conditions.

It is generally accepted that for defect-free and uncontaminated GIS, at least up to 525 kV, the VFTO breakdown level is not lower than the Lightning Isulation Withstand Level (LIWL) defined according to IEC standard 517.

Any defects or contamination leading to an enhancement of the electric field, especially at the high voltage conductor, may reduce the VFT breakdown voltage to below the L.I. breakdown level. However for defects investigated so far, the differences are comparatively small at the usual operating pressures.

The breakdown developement under VFTO appears to be influenced by oscillations in the waveform, but further work is needed to determine the precise mechanism for the different types of defect which might be found. In particular it should be noted that a free particle may have a greater effect if it is displaced by an AC or DC field.

The presence of residual voltage due to the charge trapped on the load side, after disconnector opening, may modify the insulation strength but investigation is still in a preliminary state and need to be continued.

In an operating disconnector a branch from the intercontact leader can be driven by the VFTO and lead to a radial breakdown. This phenomenon is generally avoided today by a proper design of the disconnector. Suitable test procedures for disconnector are under consideration within IEC.

The final dielectric integrity of installed GIS with respect to VFTO is presently checked by either on site lightning impulse test or acoustic and partial discharge tests at power frequency.

In transformers, switching operations within the GIS may excite internal circuits with resonant frequencies in the range of some ten kHz to few MHz. Thus, even for applied voltage oscillation at the transformer terminals lower than 1 p.u., localized overvoltages in the transformer may appear due to part winding resonances with high overvoltage factors. For the lower frequency range (up to hundred kHz) a properly design of the transformer winding system can master these stresses. For the upper frequency range (over 500 kHz, VFTO domain) the application of surge arresters and varistors or other damping elements may be recommended as for example in the case of resonances at the tap changer leads.

Steep front overvoltages originated by switching operations or insulation breakdowns within the GIS also appear at the transformer terminals. In case of switching GIS disconnectors, VFTO have p.u. values less than 2.5 p.u. and do not exceed the protection level of the transformer arrestors. The type of connection (directly by SF6/oil bushing, indirectly by SF6/air bushings and air/oil bushings) influence the propagation of the VFTO into the transformer. VFTO, when passing the bushing, lose steepness, but increase their amplitude by about 30 per cent. The relevant overvoltages in the winding depend mainly on the winding design. Maximum voltage stresses appear at the entrance turns of layer windings and at the entrance coils of coil windings.

Research work on the influence of VFTO on transformers and their specific insulation system is going on.

Nevertheless, up to now, on one hand it seems that at least the present IEC LI chopped wave test should be performed on transformers and inductive voltage transformers connected to GIS to cover the disconnector switchings provided suitable requirements are introduced on the steepness of the chopping at the transformer terminals. On the other hand, transformers are not connected to GIS during on site testing and the probability in service condition of a line to ground fault in GIS at a voltage near the BIL is very low, if the GIS is correctly designed and tested. Therefore, line to ground fault in GIS should not be taken into account for insulation coordination of transformers connected to GIS.

Transient Enclosure Voltages (TEV) are phenomena of very high frequency, short duration transient voltages, which appear on the earthed enclosure and supporting structure of the GIS, principally during disconnector switchings. These TEV are responsible also of Electro-Magnetic Compatibility problems (EMC).

TEV magnitudes can be in the range of 0.2 p.u. but the overall duration is of the order of microseconds. Modelling for computer calculations must utilize distributed component concepts as for the calculation of internal VFTO. However the modelling of external connections and components is more difficult and resultant calculations should only be used for order of magnitude estimations. These calculations can be used for qualitative analysis of TEV characteristics and the assessment of mitigation techniques.

Physiological effects of TEV on personnel have not been investigated extensively, but there are no reported cases of injury from this cause. Secondary effects, for instance a fall arising from an unexpected, but otherwise harmless TEV shock, can be minimized by a suitable operating procedure.

The EMC aspects from TEV and radiated noise are best solved by the use of proper shielding techniques. Guidelines for appropriate actions are summarised in papers 23-06 and 36-07. Study Committee 23 will issue a brochure covering the earthing of GIS which will include special measures for the effects of TEV for both primary and secondary equipment. With these procedures EMC can be assured and TEV effects minimized. Measures are especially important when solid state electronic equipment is being applied.

Tests for EMC are not yet fully standardized and activity in this field should be pursued.

With the current knowledge of TEV phenomena the effects can be well controlled. Better calculation methods could assist the further refinement of assessment and mitigation measures. When standard test methods for EMC are established all TEV and radiated noise problems can be said to be adequately addressed.

Reproduction photomécanique
IMPRIMERIE LOUIS-JEAN
BP 87 — 05002 GAP
Tél. : 92.51.35.23
Dépôt légal : 577 — Juillet 1989
Imprimé en France